North Sea FLOW Measurement Workshop

1997

North Sea FLOW Measurement Workshop

1997

Paper No	Paper Title	Author Details	Company	Page
15	On-Line Quality Control of Ultrasonic Gas Flow Meters	R Sakariassen	Statoil/K-Lab	240
16	Gas Well Flowline Measurement by Ultrasonic Flow Meter (UFM)	J B Argricola	Nederlandse Aardolie Maatschappij B.V.	255
17	Testing of Noise Supression System for Multipath Ultrasonic Gas Flow Meters	B D Kristensen	Kongsberg Offshore as	270
18	Dry Calibration of Ultrasonic Gas Flow Meters	G de Boer	Instromet Ultrasonic B.V.	284
19	Performance Testing of Ultrasonic Flow Meters	T A Grimley	Southwest Research Institute	302
20	Diagnostic of Industrial Gas Flows by Ultrasonic Tomography	J Demolis, P Gajan and A Stzelecki	ONERA	324
21	Liquid Correction of Venturi Meter Readings in Wet Gas Flow	H de Leeuw	Shell International E&P	335
22	Wet Gas Testing with The V-Cone Flowmeter	S A Ifft	McCrometer	354
23	European Intercomparison of the Calibration of Gas Density Meters and an Introduction to a Guideline to the Determination of Density	M Tambo and T Søgaard	The FORCE Institute	364
24	Disturbed Flow Profiles and the Effect on Gas Meter Behaviour – Systematic Investigations and Practical Conclusions	G Wendt, B Mickan, R Kramer and D Dopheide	Physikalisch-Technishe Bundesnstalt PTB	418
25	Quality Assessment of Gas Metering Stations by Means of a Portable and Retractable Inspection Probe	S Larsen, J Bosio and A S Sivertsen	Statoil/K-Lab	445
26	Computation of Flow Through Venturi Meters	J A Sattary, P Johnson and M Reader-Harris	NEL	453
27	Wet Gas Sampling and Analysis	T F Welker	Welker Engineering	473
28	Evaluation of On-Line Chromatograph Performance	C J Cowper and R P Mounce	EffecTech Ltd	480
29	MFI WaterCut Meter – A Fiscal Meter	S Nordborg and T Børslid M Hebnes	Statoil Multi-Fluid ASA	492
30	Coriolis Flowmeter in LPG Custody Transfer – Petrobras Test	V A Rezende C Aplle	Strack Consultoria Micro Motion	502
31	Master Meter Method	C Michel and P Dupuy	Faure-Herman	511
32	Test Results Krohne 8” Ultrasonic Flowmeter	A Boer W Volmer	Krohne Altometer NMI Certin BV	523
33	Factors Affecting the Performance of Ultrasonic Flowmeters	G J Brown and S I Fletcher	NEL	533

NSFMW.97

North Sea FLOW Measurement Workshop

Paper ~~1~~ – 1.1

COMPARING PERFORMANCE OF MULTIPHASE METERS
«How to see the woods for the threes?»

Authors:
Chris J.M. Wolff, Shell International Exploration and Production b.v.
The Netherlands

Organiser:
Norwegian Society of Chartered Engineers
Norwegian Society for Oil and Gas Measurement
Co-organiser:
National Engineering Laboratory, UK

Comparing performance of multiphase meters
How to see the wood for the trees?

Chris J.M.Wolff

Shell International Exploration and Production b.v.
The Netherlands

SUMMARY

A method is presented to condense the results of multiphase meter performance evaluations into one or at the most a small number of characteristic values. Ranking of these allows easy performance comparison of different meters. One important characteristic is the fraction of the data points that satisfies a certain (in-)accuracy criterion, which is called the "yield". Another one is the width of the error distributions, for which the standard deviation appears to be unsuitable due to the large number of outliers. More workable numbers for the widths are obtained when at either side of the distribution 10% of the data points are discarded and the width between remaining extreme errors is selected (the 80% width). The approach also demonstrates that expressing the measurement errors in terms of relative oil and water flow rate errors produces results which give an unnecessary poor impression, due to the fact that without separation of the phases, the relative error of a quantity close to zero is bound to be large. Using the relative errors for gas and liquid and absolute errors for BSW gives more consistent and more useful results. Finally it is shown that the often heard statement: "the multiphase meters investigated, generally satisfied the 10% accuracy criterion" cannot be supported using the conventional 95% confidence limits.

INTRODUCTION

Various comparative tests of multiphase meters (Porsgrunn 1 & 2, Multiflow 1 & 2 at NEL, Texaco JIP at Humble) have invariably produced large quantities of data, which are usually presented in a large number of scatter graphs. The result is that the observer is inundated with information and it has become virtually impossible to assess or compare the performance of the different meters. For comparison of meter performance one would really need a means of ranking the meters. To allow ranking it is required that the performance is condensed in a single figure (a scalar performance indicator). In this article four different methods of calculating such a performance indicator will be introduced and their usefulness discussed. It will also be shown that statements of overall performance of meters are very dependent on which of these four performance indicators is actually used. Usually this specification is not included in the statements. It is needless to say that a performance indicator always applies to a certain operating envelope or test data set, hence it must not be used without that being defined.

Very often engineers will want to know why the performance of a meter is as it is and they want to analyse the test results. To facilitate this process some further key parameters are suggested. Their number should be as small as possible to allow easy comparison.

Finally, it is shown that the method of converting the three-dimensional measurement results in a scalar can be used to identify the area in the operating envelope where a meter has its worst performance. By excluding this area from the recommended operating envelope it should be possible to arrive at an improved performance indicator of the meter for the remaining area. It is hoped that meter suppliers will adopt this method to sharpen up the specification of their meters performance.

DIFFERENT PERFORMANCE DEFINITIONS

The first performance criterion to be considered is based on the accuracy requirement as formulated by the users of the information, which is usually:
"The relative uncertainty of oil, water and gas flow rates should be better than a certain percentage, for which often 10% is taken.".
Rather than the word "uncertainty", one often uses "inaccuracy" or even just "accuracy". In real life the distinction between these is not always adhered to. That may even apply to the rest of this article.

The above requirement means that for one measurement consisting of three components (oil, water and gas) none of the three relative errors must be larger than the 10% criterion. In mathematical formula:

$$MAX\left(ABS\left(\frac{\Delta O}{O}\right), ABS\left(\frac{\Delta W}{W}\right), ABS\left(\frac{\Delta G}{G}\right)\right) \le Cri \qquad (1)=M\sim OWG$$

The criterion value (Cri) can be 10% or any other agreed number.

A different interpretation of the verbal requirement statement is also possible. And it would appear that in practice, people discussing the performance of multiphase meters rather use that different definition. This is usually not clearly defined, but it is stated here that in practice one seems to consider the relative errors of oil, water and gas separately.
In formula

$$ABS\left(\frac{\Delta O}{O}\right) \le Cri.$$
$$ABS\left(\frac{\Delta W}{W}\right) \le Cri. \qquad (2)=S\sim OWG$$
$$ABS\left(\frac{\Delta G}{G}\right) \le Cri.$$

It will be shown that this difference in definition results in a completely different "yield" of data points satisfying the criterion.

A different formulation of the requirements was presented by Slijkerman et.al. [1] in 1995 on behalf of authors from Statoil, SAGA, Norsk Hydro, BP and Shell. It presents the following general requirements:

5% to 10% relative accuracy in total liquid flow rate (L);
5% to 10% relative accuracy in gas flow rate (G)
2 % absolute accuracy in water cut measurement (B)

In the mathematical formulation introduced above this would become either

$$MAX\left(ABS\left(\frac{\Delta L}{L}\right), ABS\left(\frac{\Delta G}{G}\right), p * ABS(\Delta B)\right) \le Cri \qquad (3)=M\sim LGpB$$

or

$$ABS\left(\frac{\Delta L}{L}\right) \le Cri$$

$$ABS\left(\frac{\Delta G}{G}\right) \le Cri \qquad (4)=S\sim LGpB)$$

$$p * ABS(\Delta B) \le Cri$$

The criterion value (Cri) can be taken 5%, 10% or any other value. The weight factor p has been introduced to allow a more stringent criterion to be applied to the water cut accuracy. When a relative accuracy of 5% is used for liquid and gas, and 2% absolute accuracy for water cut, then p is 2.5. In this article a default value for p of 2 will be used throughout.

A numerical example to illustrate the above has been calculated using the data set produced by one of the multiphase meter evaluation in the course of 1996. The data set comprised 120 measurement points at different flow rates, compositions and pressures. The yield of data points satisfying the criterion has been calculated and expressed as a percentage of the total number of data points. For definitions (1) and (3) this was straight forward. For definitions (2) and (4) the three errors constituting one measurement point were taken separately, as if the data set comprised 360 independent points. To obtain some insight in how the yield (of "good") points depended on the criterion value chosen, the latter was varied between 0 and 50%, resulting in a kind of cumulative error distribution. The result for one of the meters submitted to the test is shown in Fig.1.

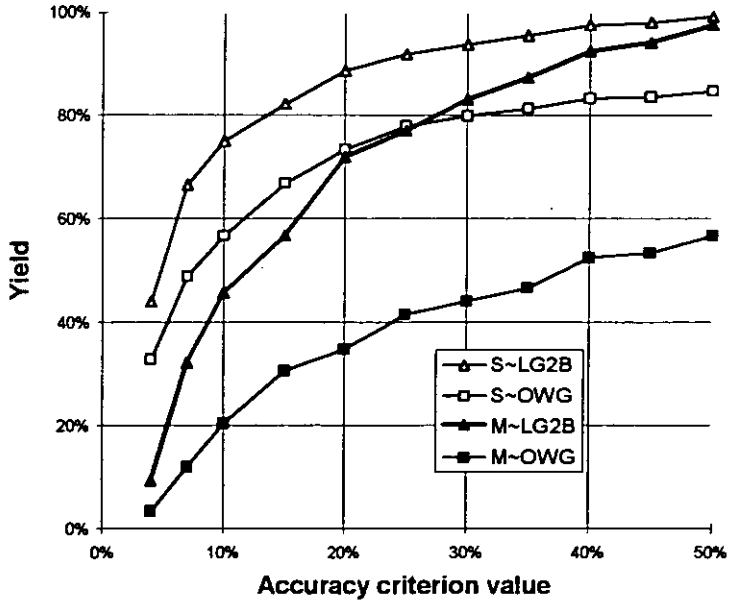

Fig.1 Typical cumulative error distribution curves (or yield curves) for an arbitrary meter submitted to a test and for four different accuracy definitions M~OWG, M~LGpB, S~OWG and S~LGpB as defined in the text.

Table 1 Yields of six meters (M1 - M6) during final test series at Porsgrunn 2

		M1	M2	M3	M4	M5	M6
Yields when Cri=10%; p=2							
	M~OWG	17%	7%	20%	15%	13%	10%
	M~LG2B	30%	21%	45%	42%	14%	24%
	S~OWG	52%	35%	57%	52%	50%	35%
	S~LG2B	69%	51%	75%	68%	64%	57%
Yields when Cri=20%; p=2							
	M~OWG	37%	25%	34%	34%	64%	29%
	M~LG2B	82%	54%	71%	68%	66%	48%
	S~OWG	75%	54%	73%	68%	82%	57%
	S~LG2B	93%	73%	88%	84%	89%	75%

Table 2a Ranking of Porsgrunn 1 meters on 10% criterion (1 is best, 5 is worst)

meter:	M1	M2	M3	M4	M5
M~OWG	5	1-2	1-2	3	4
M~LG2B	5	3	1	2	4
S~OWG	5	4	2	3	1
S~LG2B	5	4	2	3	1
AVERAGE	5	3.1	1.6	2.8	2.5

Table 2b Ranking of Porsgrunn 1 meters on 20% criterion (1 is best, 5 is worst)

meter:	M1	M2	M3	M4	M5
M~OWG	4	3	1	2	5
M~LG2B	5	3	1	2	4
S~OWG	5	4	2	3	1
S~LG2B	5	4	2	3	1
AVERAGE	4.8	3.5	1.5	2.5	2.7

Notice that at the accuracy criterion value of 10% the yields range from 20% to 75% depending on the accuracy definition used. E.g. only 20% of the data points satisfy the criterion if the worst (rel.) error of oil, water and gas is used (M~OWG). But, on the other extreme, if the liquid, gas and BSW are used as parameters and the errors considered separately (S~LG2B) 75% satisfy the 10% criterion value. This illustrates the drastic influence of the definitions used on the yields and hence on our conclusions about overall performance. The definitions acknowledging the three dimensional character of the measurement and using the worst accuracy of the three elements as the determining factor (M~OWG and M~LG2B) are clearly much more stringent than the definitions that treat all measurement errors separately (S~OWG and S~LG2B). In addition the oil, water gas definitions produce a much lower yield than the liquid, gas, BSW ones. This is also understandable since the relative error of a small fraction of any phase is bound to be large and this occurs more frequently when the pair of oil and water are considered than with the pair of liquid and BSW. This was actually the reason behind the formulation of the requirements presented by Slijkerman et.al. [1].

The author is of the opinion that for a proper characterisation of the performance of the multiphase meters the maximum type accuracy definitions should be used, i.e. either M~LGpB or M~OWG. Of these two, on practical grounds the liquid, gas, BSW definition (M~LGpB) is preferred, in line with Slijkerman et.al.

COMPARISON

Calculation of the yield curves for different meters submitted to the same test points, allows the performance of the meters to be compared. For ranking of the meters one only needs to calculate the yield figure at an agreed accuracy criterion value and do a ranking based on that single performance figure. According to Slijkerman et.al. the criterion values should be taken at 5% or 10% with p=2.5 resp. 5. However 5% produces such low yields in the data sets of the evaluations available (Porsgrunn 1995, Porsgrunn 1996 and NEL), that it was considered practical to standardise for the time being on 10%, with 20% as a back-up. The weighting factor p has been taken to be 2, as mentioned above.

As example, in Fig.2 the percentage data points satisfying a 10% accuracy criterion value (Yields) are given for the five meters of the Porsgrunn 1 test data set (340 data points) for each of the four different accuracy definitions as introduced above. In Fig.3 the same is done applying a 20% criterion value. In table 1 similar information is given in numerical form this time for the six meters tested in the Porsgrunn 2 trial. Whether graphical or tabular presentation should be used, is a matter of personal preference. For that reason an example of either form is presented in this paper.

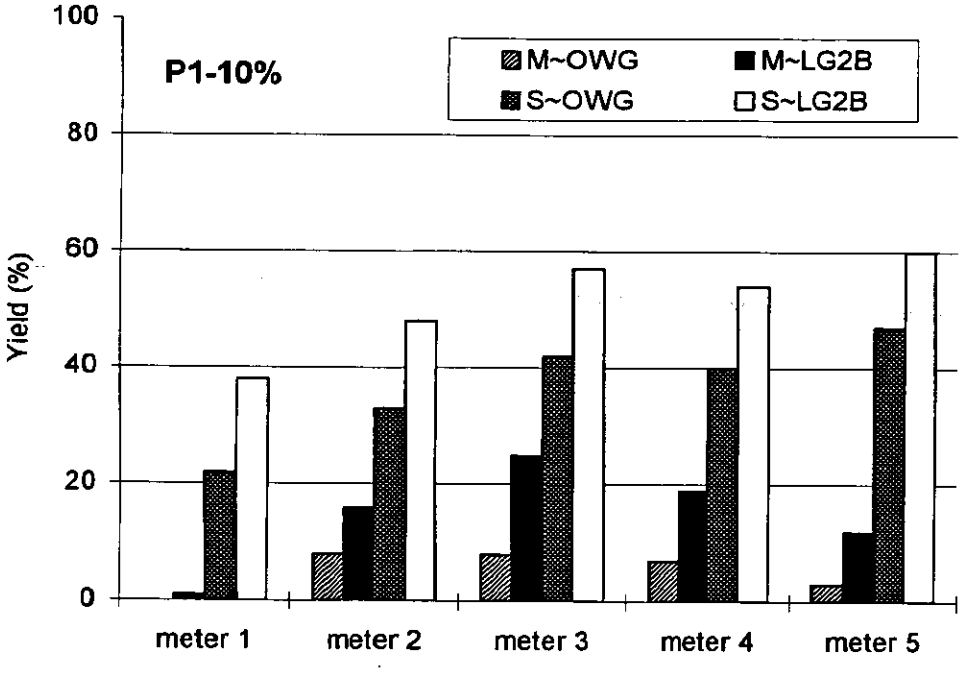

Fig.2 Percentage data points (Yields) for five meters used at Porsgrunn1 trial satisfying 10% accuracy criterion value

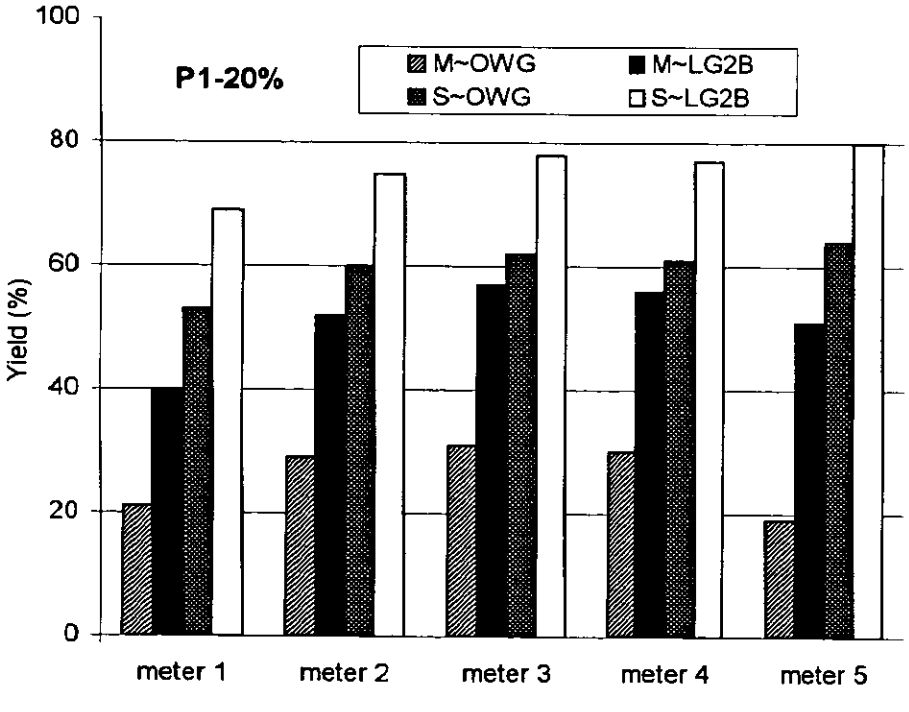

Fig.3 Percentage data points (Yields) for five meters used at Porsgrunn1 trial satisfying 20% accuracy criterion value

It is possible to do a performance ranking of meters submitted to the same test points. As an example the result of ranking the Porsgrunn 1 meters (yield data of Fig.2 and 3) is shown in table 2a and 2b. It appears that the ranking is hardly dependent on the criterion value used (10% or 20%)
Another rather surprising result from this exercise is that the ranking order is not too dependent on the choice of accuracy definition applied either, with one exception which is discussed below. Certain meters always rank high (or low), regardless the definition used. Hence the ranking method allows one to home in on the better performers. Meter 3 ranks clearly very high.
Note meter 5, which is the best if the three components of the measurement are taken separate, but is almost the worst if the three-dimensional character of the measurements is taken into account. With this meter apparently always one of the three components has a larger error.

However, a ranking does not tell us whether the better meters also satisfy our needs. For that we need a quantitative assessment. In the following paragraphs it will be shown that quantitative assessment is possible, but not as straight forward as it might seem to be at first.

In table 1, one can see that even for the best meter of the Porsgrunn 2 evaluation only 75% of all data points satisfy the S~LG2B<10% criterion and only 45% satisfy the M~LG2B<10% criterion. The better yields for the 20% criterion are 93% and 82% respectively.

Now, before trying to conclude on a typical accuracy level achieved, it has to be pointed out that the mathematical/statistical basis of this subject is not simple. Note that we are dealing here with both one-dimensional and three-dimensional error distributions. With single phase meters one would usually require that 95% of all data points satisfy the accuracy criterion, and assumes that the plus/minus 2-sigma range of the error distribution corresponds with a 95% confidence level. But for multi-dimensional normal distributions the relationship between the width of a distribution and the confidence levels is not the same as for one-dimensional normal distributions. As is shown in table 3 for a three dimensional distribution, the plus/minus 2 sigma envelope corresponds with only a 74% confidence level and not the 95% that we are used to. It would seem that for a fair assessment of the performance of multiphase meters one should take a 95% confidence level (and yield) target for the one dimensional error distributions (S~OWG and S~LG2B accuracy definitions), but use the 74% confidence level (and yield) target as an equivalent for the three-dimensional distributions (M~OWG and M~LG2B). The author would like to invite people better skilled in statistics to express their opinion on this. For the time being it suffices that this mathematical phenomenon is highlighted.

Table 3. Confidence levels for one-, two- and three-dimensional gaussian distributions with equal standard deviations in all directions

	One-dimensional (%)	Two-dimensional (%)	Three-dimensional (%)
+/- 1 σ	68	39	20
+/- 2 σ	95	86	74
+/- 3 σ	99.7	98.9	97.0

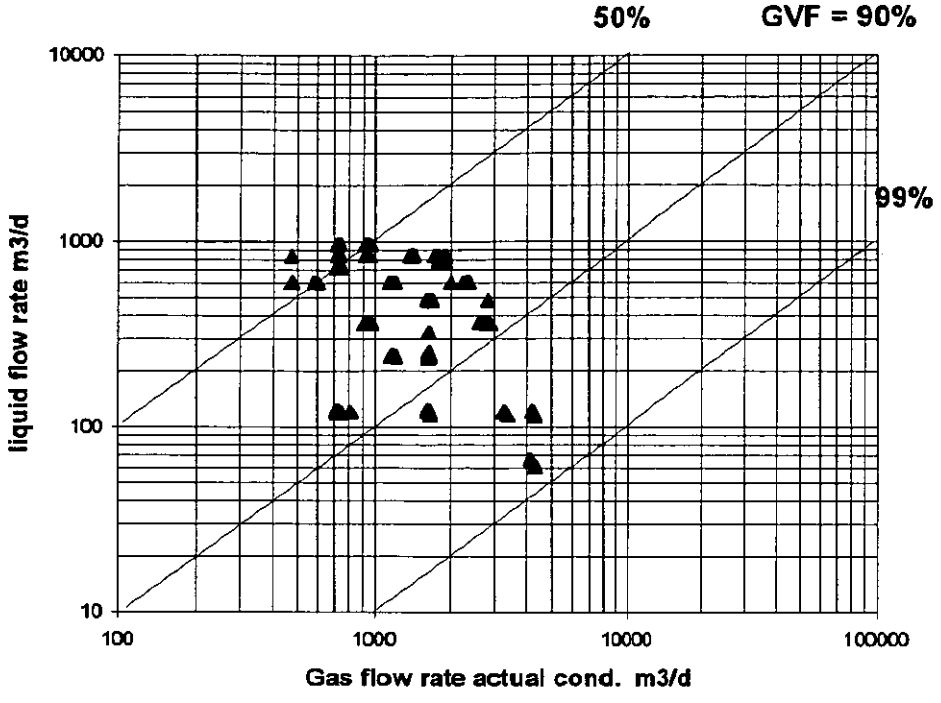

Fig.4a Example of graphical representation in the two-phase map of set of measurement points used

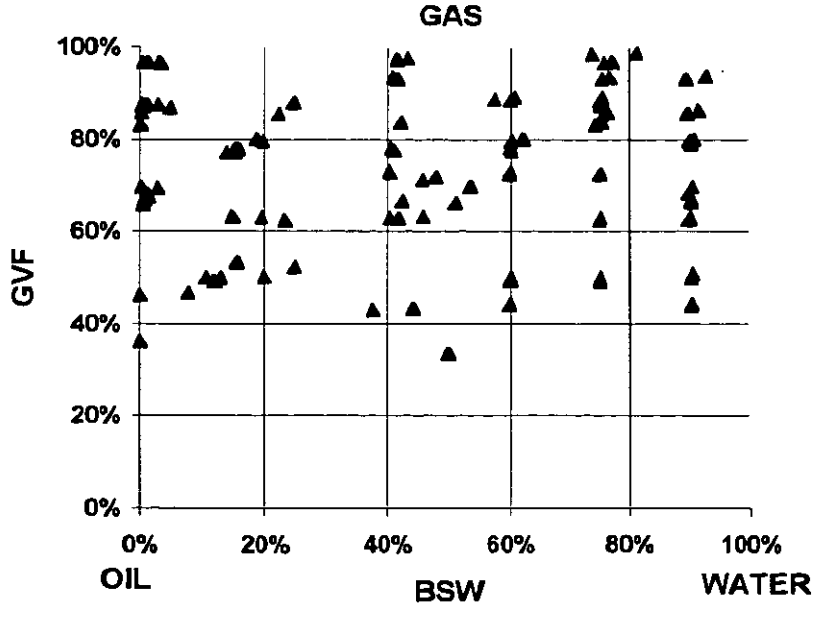

Fig.4b Example of graphical representation in the composition map of set of measurement points used

Assuming that the above mathematical reasoning is correct, then for an overall meter performance of 10% accuracy, the S (separate) criteria should produce a yield of more than 95% and the M (maximum) criteria more than 74% . This has not been achieved so far. (See Figs 2 and 3, and Table 1). A 20% accuracy (for the entire data sets) seems closer to the reality. For a reduced operating envelope better accuracies may apply. This will be addressed later.

The method proposed allows to compare performance of multiphase meters, however as mentioned earlier, this requires that the test data set to which the performance figures apply is known and well defined. Therefore this test set (the test envelope) must be presented together with the performance results. It is suggested that the reference measurement set is presented in graphical form, as shown in Fig.4 a&b, comprising of a standard two-phase map and a composition map (GVF vs. BSW). Tables would in principle give the information as well, but the quick insight one gets from a graphical representation is often preferred.

WIDTH AND MEDIAN OF DISTRIBUTIONS

Whilst the yield figures give a basic measure of the performance of a meter demonstrated during a test, they give little insight in the underlying strong points or shortcomings of the meter. Such insight can be achieved by looking at the error distributions of the individual measurement components. The components recommended for consideration are:

$$\Delta O/O,\ \Delta W/W\ ,\Delta G/G,\ \Delta L/L,\ \Delta B$$

Notice that the GVF is excluded. The reason for this in the nature of the quantity, which is strongly non-linear. E.g. a 1% error at GVF 50% has a different impact than the same error at e.g. GVF 98%. It would for that reason make sense to work with a gas-liquid ratio at line condition rather than the GVF. But this is not usual and will not be introduced in this article.

It has been investigated whether average values of the (rel.) errors would be a useful characteristic value, but it appeared that the averages are too strongly influenced by the many extreme outliers. The **median** of the error distribution works much better. The median is the data point with 50% of the data points having a smaller value and the other 50% having a larger value.

Similarly the standard deviation of the error distribution was adversely affected by the outliers as well. A more robust measure of the width of a distribution appeared to be the maximum and minimum errors when 10% worst error data points at either side had been discarded. The result has been called the 80% width. In a one-dimensional normal distribution this would correspond with the range from -1.28σ to $+1.28\sigma$. To allow direct comparison with the accuracy criterion value as used in the yield graphs (Fig.1) rather **half the 80% width** will be used. (The "half 68%-width" would correspond with 1σ)

Initially the width between the upper and lower quartiles was considered, but this would leave only 50% of the data points covered in the range. This was felt to be too low.

Only the width of the gas, liquid and BSW error distribution appeared to be meaningful in general. The oil and water relative error distributions contained too many very extreme values. This is simply due to the fact that oil and water flows approach zero too frequently. The same reason as was behind the proposal to express meter performance in terms of gas, liquid and BSW.

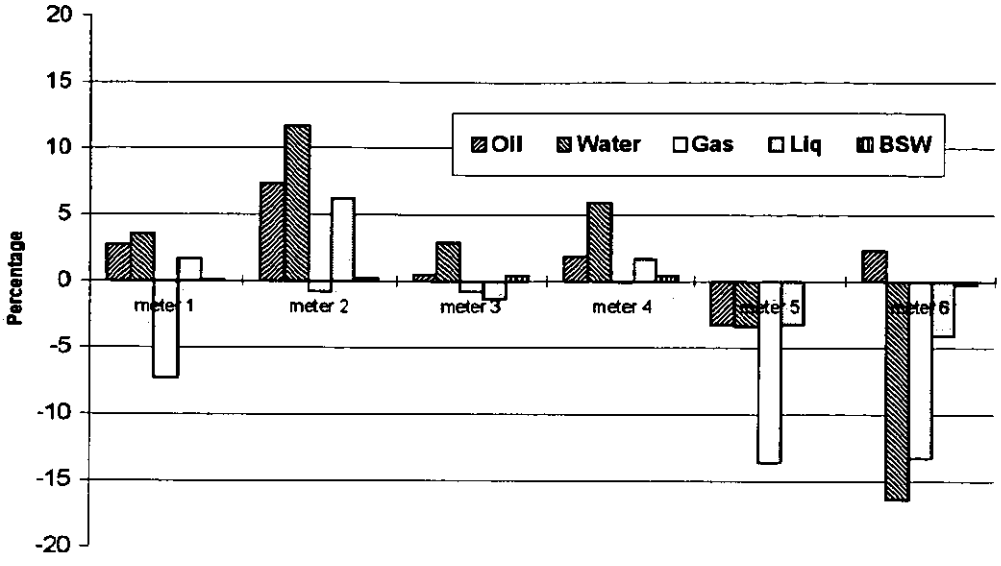

Fig.5 Medians of the error distributions of components for six different meters

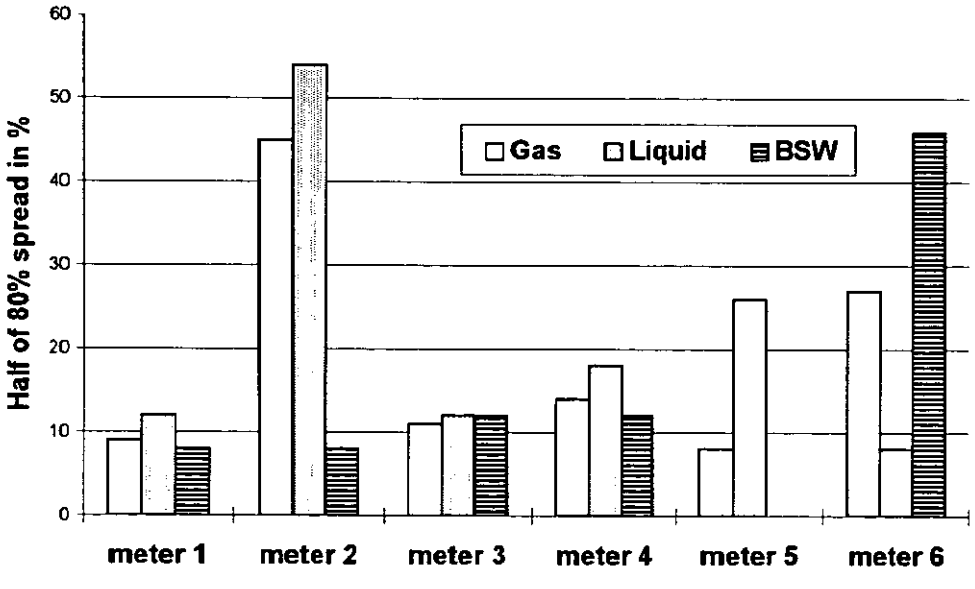

Fig.6 The width if the error distributions of compnents expressed as half the distance between the extreme error values when 10% of the data points at either end of the distribution have been discarded.

As an example the medians and half 80%-widths of the error distributions of the Porsgrunn 2 trial are depicted in Fig 5 and 6 respectively. The most remarkable features to be seen in the graphs are:
1) Meter 2 sticks out with half widths of the gas and liquid error distributions around 50%.
2) The half width of the BSW distribution of meter 6 is about 45%.
3) Meter 1 has a small width of the gas distribution combined with minus 8 % median. Hence the gas measurement is "well defined" but there seems to be a systematic error in the model used. Here seems to be scope for improvement through a better model for converting the raw measurements into reported quantities.

Using the width of a distribution and its number of points an estimate can be made of the uncertainty of the mean. With 120 points in the distribution and a width of plus or minus 10%, the reliability interval of the mean is approximately 1% (10% divided by square root 120). When the width of the distribution is plus or minus 40% the reliability interval of the mean is still only +/- 2%. The author has simply assumed that what applies to the mean also applies to the median.

In general it would appear that whilst the "yield" is a good measure for the observed performance of a meter, the "widths of the error distributions of the components" are a very useful indication for its potential, more so than the median.

SUPPLIER GIVEN SPECIFICATION

The yield method can also be used to check how many of the test data point actually satisfy the supplier given meter specifications. It is suggested that the suppliers do this themselves. The accuracy definitions used could be either MAX(O,W,G) or MAX(L,G,p*B) or both of them. It would give the clients a good measure of the level of confidence that can be attached to the specification.

STANDARD REPORT

The above analysis of the available test results suggest that the summary of the evaluation of a meter should consist of

Minimum:
1a) graphical representation of the test set (Two-phase map and composition map)
1b) Number of data points in the test
2) 10% (5%) yield figure according to M~LG2B
3) Yield percentage according to manufacturers own specification

To gain more insight this minimum could be expanded to an example characterisation as given in Table 4. As can be seen from the data for this particular meter, the gas measurement seems to be the weak spot for this meter (minus18% median), but the width of the gas distribution (only 8%) is good enough to enable improvement through better modelling.

SELECTING BEST OPERATING ENVELOPE

Suppliers could also improve their "score" by narrowing down the operating envelope of their

Table 4. Example of full set of numbers characterising the performance of a multiphase meter during a test. (Values are taken from a real meter evaluation comprising about 210 points. The corresponding data set is not presented)

Yields	10% accuracy	20% accuracy
M~OWG	0%	16%
M~LG2B	3%	30%
S~OWG	38%	69%
S~LG2B	55%	83%
	Median	**half 80% width**
Oil	2.9%	19%
Water	-0.4%	61%
Gas	-18.0%	8%
Liquid	0.3%	8%
BSW	-0.2%	6%

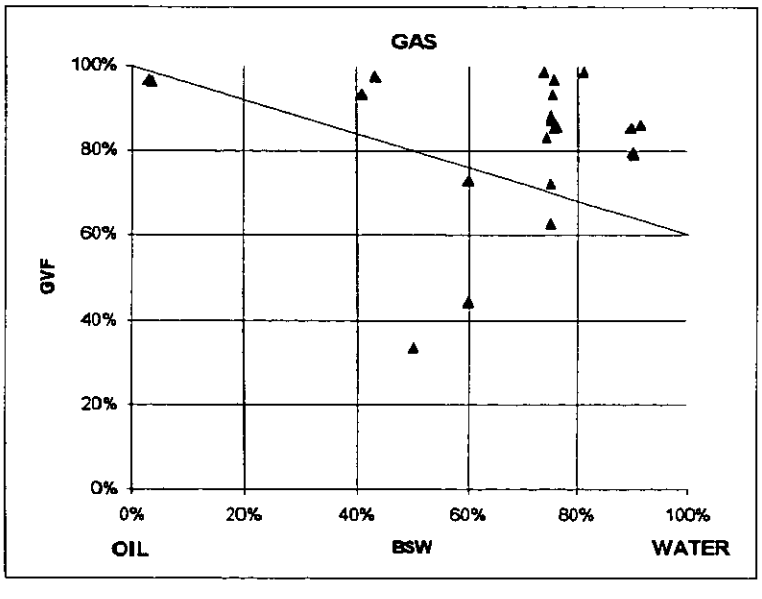

Fig.7 Twenty percent worst data points for one of the meters plotted in the composition map. It won't surprise that the points are concentrated in the corner of high BSW and high GVF. Line is GVF = 1- 0.4 * BSW

meter to the area where the meter performs best. One way of determining this optimum area is by chopping the area(s) of worst performance. As an example this has been done for one of the meters out of the available data sets. For each data point the maximum of the liquid, gas and 2*BSW errors were calculated (M~LG2B). The points were ranked on this value and the 20% worst points were plotted in a composition map. The result is shown in Fig.7. One sees that as could be expected these "worst" performance points are concentrated around the high GVF, high BSW area. The next step was to reduce the specified operating envelope by excluding compositions with high GVF and high BSW. The split was made according to the line

GVF> 1 - 0.4*BSW

This was an arbitrary choice, just to demonstrate the method. For the remaining data points the yield figures were calculated again. The results are shown in table 5.

Table 5 Comparison of yields for one of the meters. Old is total data set and New is after removal of the high BSW, high GVF points.

	Old	New		Old	New
Cri	10%	10%		20%	20%
M~OWG	15%	19%		34%	44%
M~LG2B	42%	55%		68%	84%
S~OWG	52%	57%		68%	73%
S~LG2B	68%	77%		84%	91%

CONCLUSIONS

A method is presented that allows the results of multiphase meter evaluation tests to be condensed into no more than a small number of characteristic values. The prime parameter is the yield figure which is the percentage of data points satisfying a certain accuracy criterion.

Provided the evaluation is done on the same or at least a comparable reference data set, the performance of meters can be ranked based on these yield figures. The yield figures can also be used as a general qualification of meter performance if the reference measurement set is not explicitly defined but considered to be typically applicable for that meter.

Based on the test data available and the definitions introduced in this paper, it should be concluded that the overall accuracy of multiphase meters is closer to 20% relative for liquid and gas and 10% abs for BSW, than to 10% and 5% respectively.

The method can be used to demonstrate experimentally the confidence level one can attach to vendor supplied accuracy performance specifications of multiphase meters.

The method can also be used to identify the operating envelope corresponding with optimum performance of a certain meter.

REFERENCE

[1] Slijkerman, W.F.J. et.al. "Oil Companies Needs In Multiphase Flow Metering" NSFMW, Lillehammer 1995, paper 23.

NSFMW.97

North Sea FLOW Measurement Workshop

Paper 2: 1.2

THE PORSGRUNN 2 TEST PROGRAMME OF MULTIPAHSE METERS

GENERAL RESULTS AND EXAMPLES OF DIFFERENT METER PERFORMANCE

Authors:
S.A. Kjølberg, Norsk Hydro ASA, and H. Berentsen, Statoil, Norway

Organiser:
Norwegian Society of Chartered Engineers
Norwegian Society for Oil and Gas Measurement
Co-organiser:
National Engineering Laboratory, UK

Research Centre
Porsgrunn

STATOIL

The Porsgrunn 2 Test Programme of Multiphase Meters

General Results and Examples of different Meter Performance

S.A.Kjølberg, Norsk Hydro ASA, Norway
H.Berentsen, Statoil, Norway

1. The Summary

Use of multiphase meters has a large economical potential, especially in development of satellite fields. During the last 10 years several development projects of multiphase flow meters are supported by the oil industry and multiphase meter experience is gained through different testing and field trial programs. Among these are tests in the Multiphase Flow Loop at the Hydro Research Centre in Porsgrunn, Norway.
This presentation gives examples of observations made during the "Porsgrunn 2" test programme carried out in 1996.
This test programme was carried out on meters from Fluenta a.s, Framo Engineering A.S, ISA Controls Ltd., Kværner Process Systems A.S and Multi-Fluid International A.S. Sponsoring oil companies were: BP Exploration, Conoco, Elf, Esso, Phillips, Shell, Saga, Statoil and Hydro.
The Porsgrunn test programs are carried out in The Multiphase Flow Loop (MPFL) at Norsk Hydro, Research Centre Porsgrunn. The MPFL is a circulating test loop for hydrocarbon liquid (crude oil or condensates), hydrocarbon gas and formation water operating up to 110 bar and 140 °C. The flow loop has a length of 120 meter and a diameter of 3 inch (77.9 mm).
The test programme consisted of pressure levels from 30 to 90 bar, of watercuts from 0 to 90 % and of gas volume fractions up to 98 %. Fluids were: Formation water, hydrocarbon gas and crude oil, all recombined to Oseberg oil field specifications
Results are presented as examples of performance of two meters, one operating on the basis of cross-correlation only and one with only venturi based velocity measurements.
The results show that the accuracy and the distribution of liquid and gas flowrates of a multiphase flow meter having velocity calculations based on cross-correlation only are well up to the level of the venturi based meter tested.
Studying flow regimes and fluid continuity as possible factors for making influence on multiphase meter performance we found that even if the test programme covered several flow regimes, non of these were found to have any influence on the accuracy of the two specific multiphase meters. Watercut was, however, found to be a parameter that made significant influence on the composision measurement of one of the two meters.

2. The acknowledgement

Acknowledgement is given to the following oil companies which attended as clients to the "Porsgrunn 2" test programme. The authors would like to express their gratitude for the interest and support given by the clients during the test programme and for the permission to use test program results as a basis for this presentation.

BP Exploration, Sunbury
Norske Conoco AS
Elf Petroleum Norge AS
Esso Norge AS
Phillips Petroleum Norge AS

Saga Petroleum AS
A/S Norske Shell
Statoil
Hydro

3. The multiphase flow meters included

The following multiphase meters were installed in parts of, or in the complete, test programme:

Fluenta MPFM 1900VI
Framo Multiphase Meter
ISA Multistream Meter
Kvaerner Process Systems Meter
MFI MultiPhase Meter

4. The test facility

4.1 General

The Multiphase Flow Loop (MPFL) at Norsk Hydro, Research Centre Porsgrunn is a circulating test loop for hydrocarbon liquid (crude oil or condensates), hydrocarbon gas and formation water operating up to 110 bar and 140 °C.
The fluids used are recombined to specified composition.
The pressure in the loop is controlled by a gas accumulator. The flow rates of the individual phases are measured by flow meters and controlled by variable capacity pumps. The circulation capacity of liquid is maximum 60 m^3/h, while the maximum gas capacity is 205 Am^3/h.
The temperature of the fluids are controlled prior to mixing of liquid and gas. All equipment, including all pipes, have electric heat tracing ensuring stable temperature.
A simplified flow diagram is enclosed in the appendix.
After establishing three phase flow the fluids enter the test loop. The loop has a length of 2 x 60 meter with a pipe having a internal diameter of 77.9 mm. At the end of each of the two loop lengths there are test sections. At the end of the first length is the test section used for the multiphase flow meter test and at the end of the second length a test section area equipped with several types of instrumentation adapted for multiphase technology measurements. Downstream the instrumentation area the fluids enter the separator before being recirculated.

4.2 The test section

48 meters (approximately 600 pipe diameters) downstream of the mixing point of the three fluids, the test section used for the test of multiphase flow meters was connected as a parallel flow line. A photo showing the flow loop including the test section is shown in the appendix.
In the test section which have the same diameter as the flow loop the multiphase flow meters were installed, three in series, two in parallel. Each meter installation was thoroughly discussed with the suppliers before making the test set-up.

In separate meetings with each vendor prior to the testing, installation arrangement and assistance, meter documentation's and calibration procedures were thoroughly discussed and settled.

4.3 The reference flow meters

The reference meters were calibrated with representative fluids at operating conditions. Calibrations are traceable to national or international standards and are carried out by accredited laboratories.

Oil flowmeter :2" PD meter Kral & L/M OMX68.01147, 0.6 - 42 am3/h,
Water flowmeter :2" turbine meter Daniel 2"-1406-1P, 2 - 51 am3/h,
Gas flowmeter :80 mm turbine meter Instromet SM-RI-G160-80-150-G, 5 - 250 am3/h

Water concentration in crude oil leaving the separator was continuously determined by a MFI Water Cut Meter. Also regularly manual sampling and analysis were carried out on both liquid phases leaving the separator.
Net liquid flow rates were calculated on the basis of fluid concentrations.

5. The test fluid

The MPFL was filled with fluids according to Oseberg oil field specifications. (90 bar data: Oil density: approx. 800 kg/m^3, gas density: approx. 70 kg/m^3 and water density: approx.1000 kg/m^3). Crude oil was taken from the Oseberg A test separator and brought to Porsgrunn without any air contamination. Pentane, butane, propane, ethane and methane were used to recombine the crude to Oseberg specifications and to make the correct hydrocarbon gas composition. The water phase was artificially made formation water, also according the Oseberg specification.

6. The test program

The test program consisted of three test periods and was organizied to provide information from both installation and operation. Between the first and second test period the vendors were alowed to make meter adjustments.
The test temperature was kept at 60 °C and the pressure changed between 30, 60 and 90 bar.
Gas superficial velocities were from 0 to 12 m/s and liquid superficial velocities from 0.1 to 2.5 m/s implying watercuts from 0 to 90 % and GVFs from 0 to 99 %.
The data presented in this paper are mainly taken from the third test period.

7. The test results

As a basis for this presentation we have focused on two different types of multiphase meter outputs; one with only venturi measurements as basis for velocity calculations and one with the velocity calculations only based on cross-correlation. In addition to the presentation of examples of results and observations from testing of these two

types of meters we also present some observations made on reproducibilty of a multiphase meter.
General knowledge of multiphase meters point out fluid continuity (oil- or water continouos fluid) and flow regime to be factors that most probably make influence on multiphase meter performance. This presentation is focused on possible differences between the two types of multiphase measurement caused by these operating conditions.
Figure 1 and figure 2 give an ordinary presentation of meter performance; a graph showing multiphase meter reading versus reference meter reading.

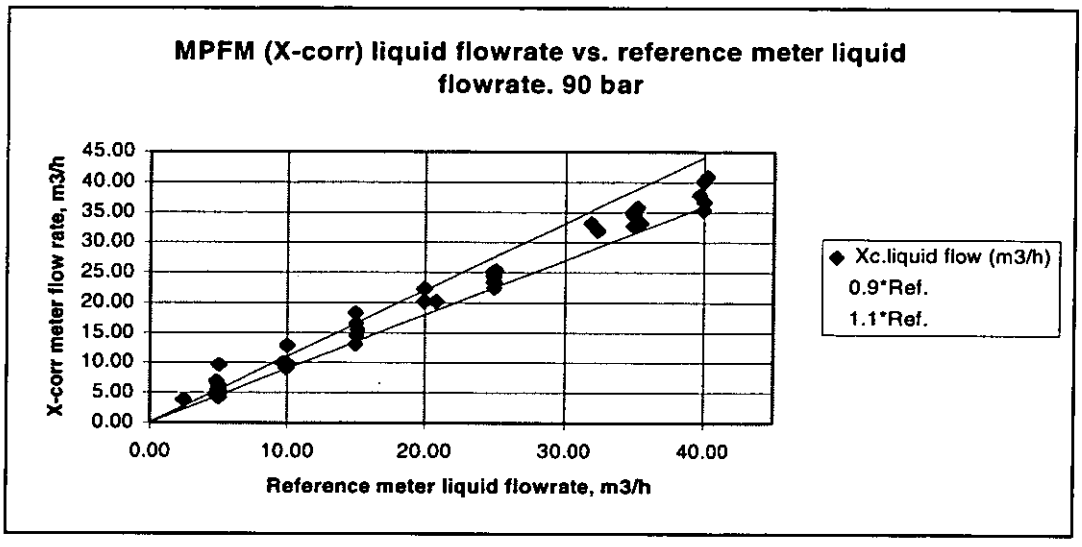

Fig 1. Cross-correlation based liquid flowrate vs. reference flowrate

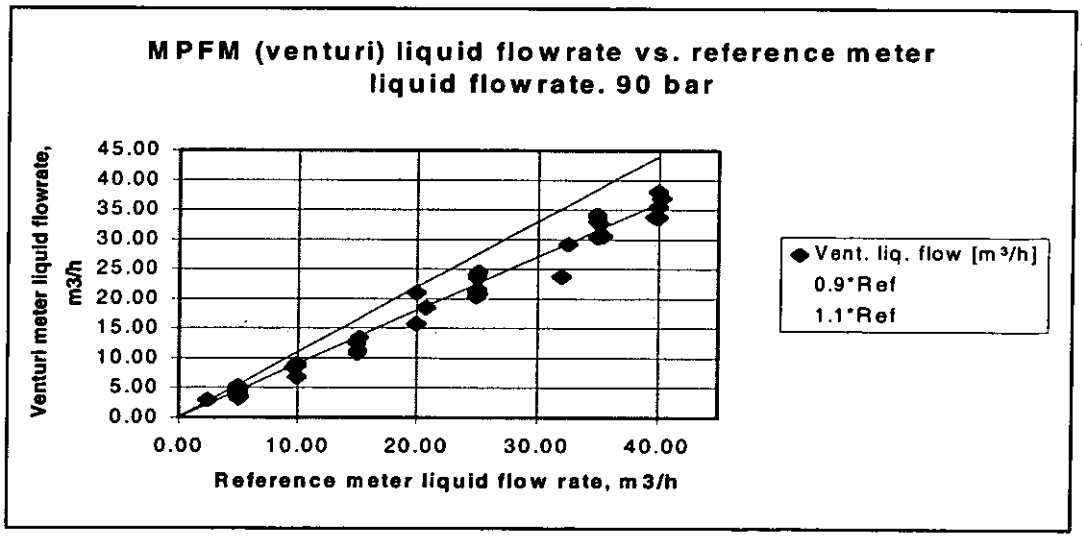

Fig.2 Venturi based liquid flowrate vs. reference flowrate

The main observations made from the graphs presented in figures 1 and 2 are:
- Some under-estimation of the venturi based liquid flow rate.
- The distribution of the different measurements are of the same order of magnitude.

Consequently we can conclude that the liquid velocity measurements of this specific cross-corelation based system is well up to the level of a venturi based system.

The results of gas flowrate measurement are presented in figures 3 and 4.

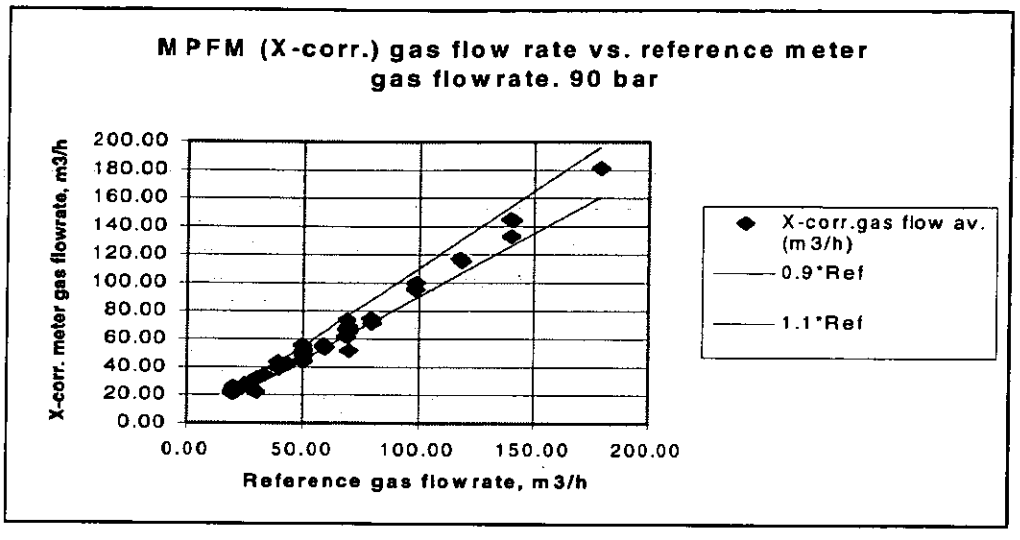

Fig. 3 Cross-correlation based gas flowrate vs. reference gas flowrate

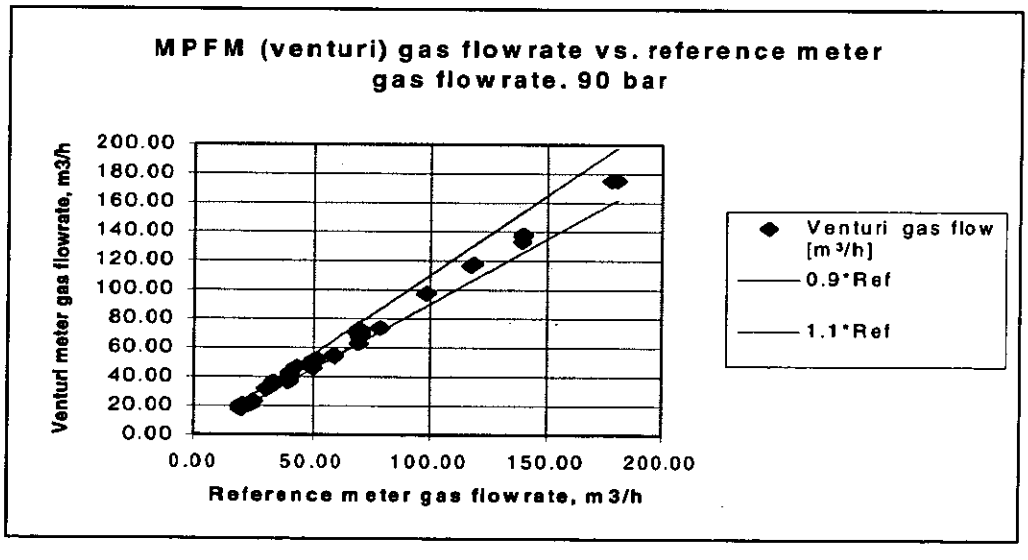

Fig. 4 Venturi based gas flowrate vs. reference gas flowrate

Nor for the gas flowrate are we able to observe any significant difference between the two types of velocity measurements.

To look for other possible differences in the performance of the two types of meters we will look into the composition measurements, here presented as outputs of meter oil rate versus reference oil rate.

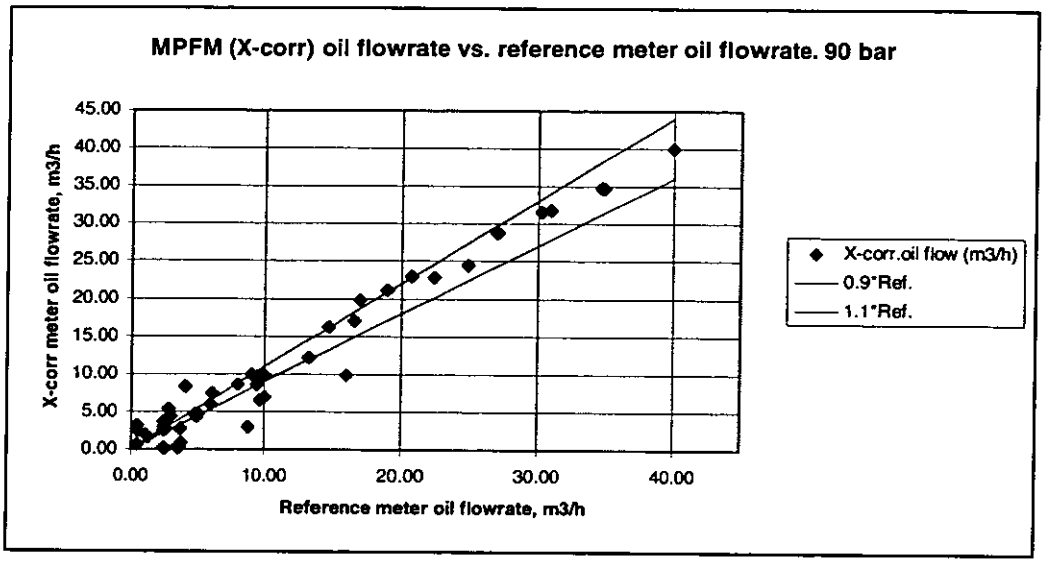

Fig. 5 Cross-correlation based oil flowrate vs. reference flowrate

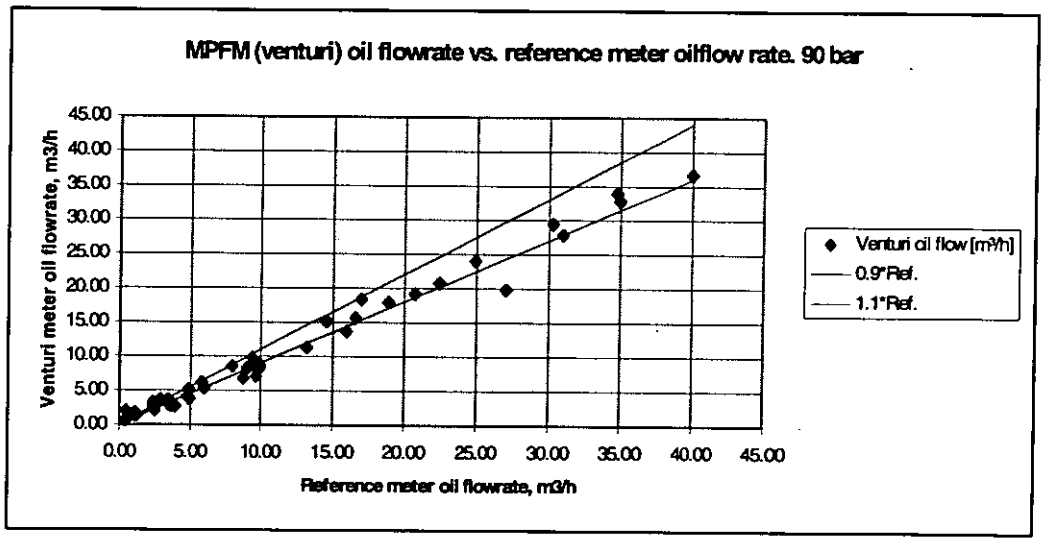

Fig. 6 Venturi based oil flowrate vs. reference flowrate

For the venturi based meter we find some under-estimating of rate. However, for the cross-correlation based meter we find a significant wider distribution of the readings of low flowrates of oil.

We will look into the possible effects of operating conditions to search for relationships that would explain the difference of the oil flow measurement.

7.1 The flow regimes

One parameter most probably making influence on the meter performance is the type of flow regime. Figure 7 shows meter performance presented as error of liquid flow measurement vs. flow regimes (as indentified in a horizontal pipe).

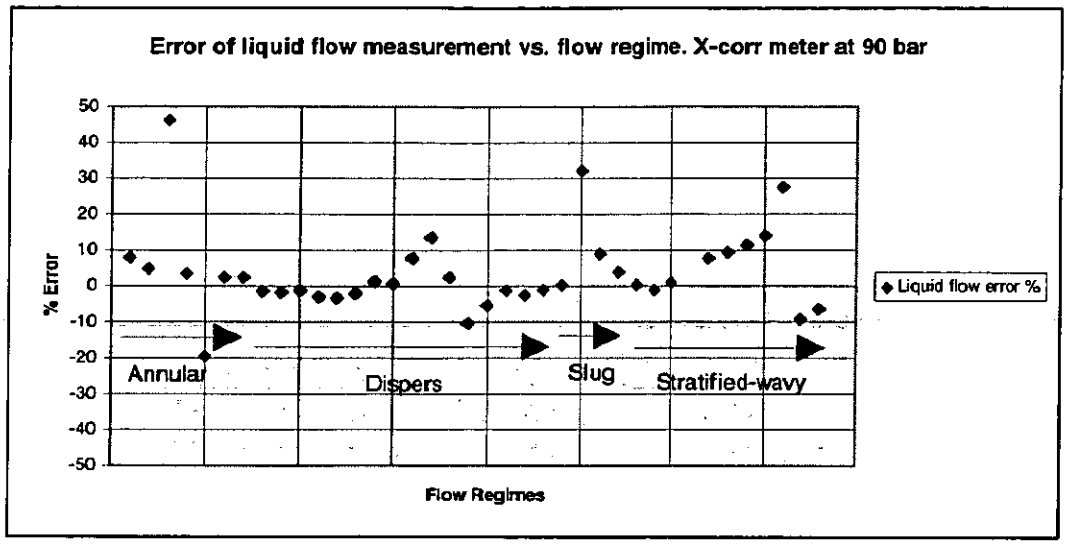

Fig. 7 Cross-correlation based liquid flowrate vs. flow regime

The data presented in figure 7 confirm the conclusion drawn on the basis of results presented in graph no. 1; it is not possible to observe any effect of flow regime on the quality of the liquid flowrate readings.
The same presentation made on oil flowrate is showed in figure 8.

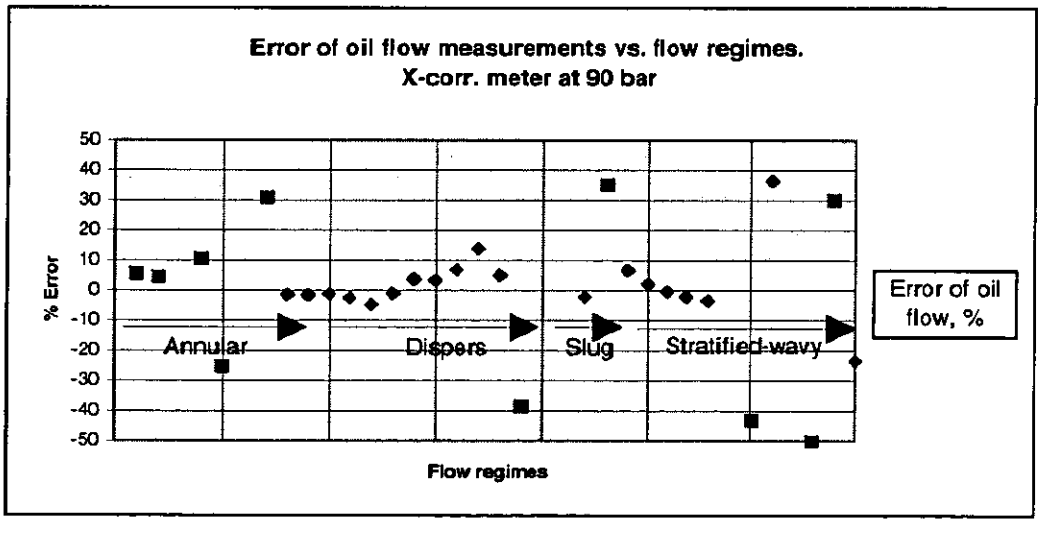

Fig. 8 Cross-correlation based oil flowrate vs. flow regime

In figure no. 8 all data points representing low oil flow (< 7 m^3/h) are showed as squares , all other datapoints as diamonds. It is observed that the low flow data points represent the measurements having the far greatest error. However, nor for these low flowrate data points there can be observed any relationship between flow regime and error of measurement.

Venturi based measurements:

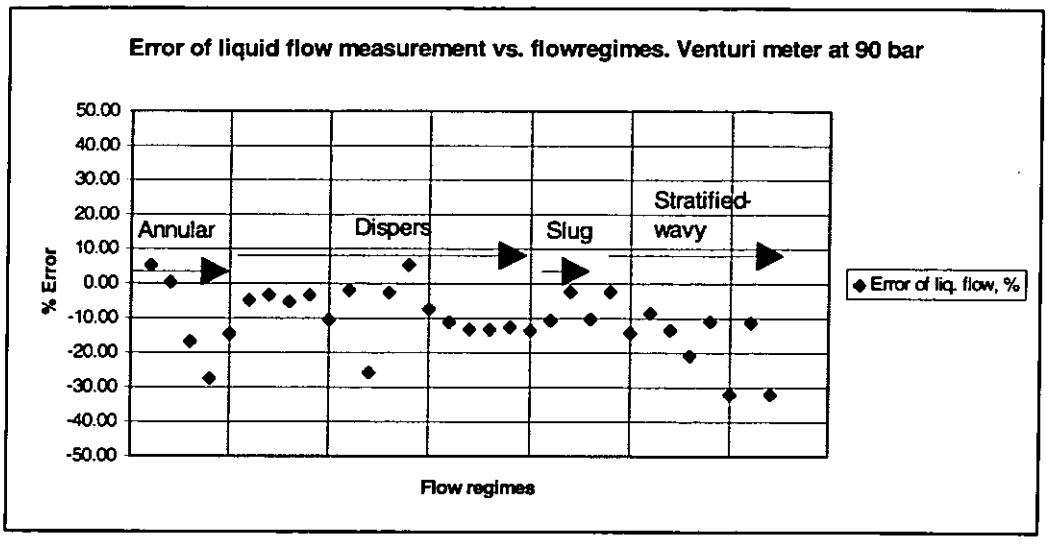

Fig. 9 Venturi based liquid flowrate vs. flow regime

Nor for the venturi based measurement we observe any significant relationship between error of liquid flow measurement and flow regimes. We only observe the same under-estimate of liquid flow as presented earlier.

From these graphs we can conclude that none of these two specific meters are influenced by flow regimes. For the venturi meter we find the under-estimated liquid flowrates as observed in the basic data in figure 2, the under-estimation can, however, not be linked to any specific flow regime.

7.2 The continuity (I.e. The watercut)

General knowledge of multiphase flow meters will also indicate water concentration as a parameter that will make influence on meter offsets.
A presentation (figure 10 and 11) showing the error of liquid rate measurement vs. continuity shows that the composition measurement of the cross-correlation based meter definitily is affected by the liquid continuity. The error of liquid rate measurement is significant higher in a water continouos fluid.
For the venturi meter, however, the conclusion is not that clear, but some influence from the watercut is observed.

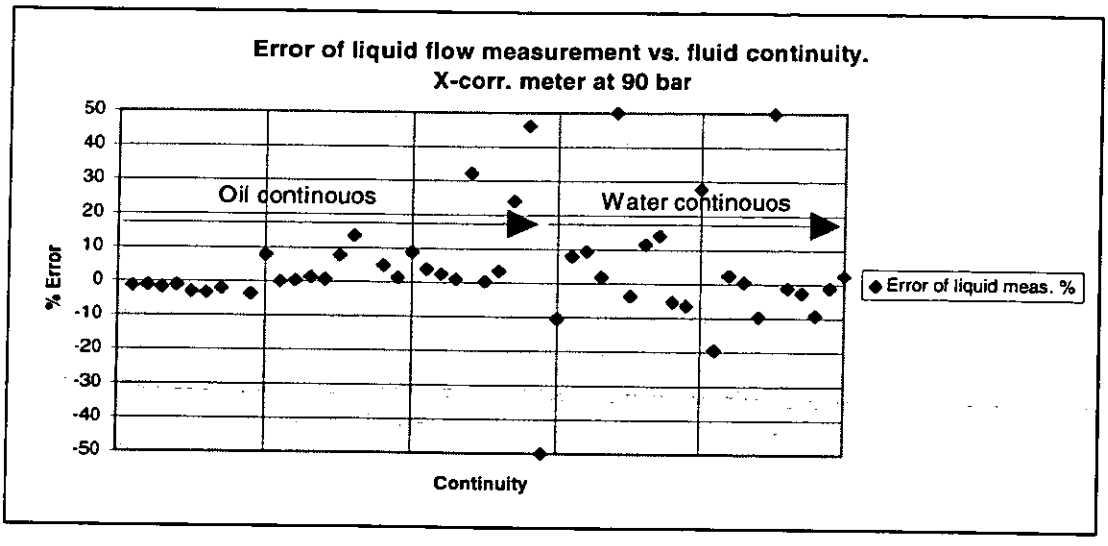

Fig. 10 Cross-correlation based liquid flowrate vs. fluid continuity

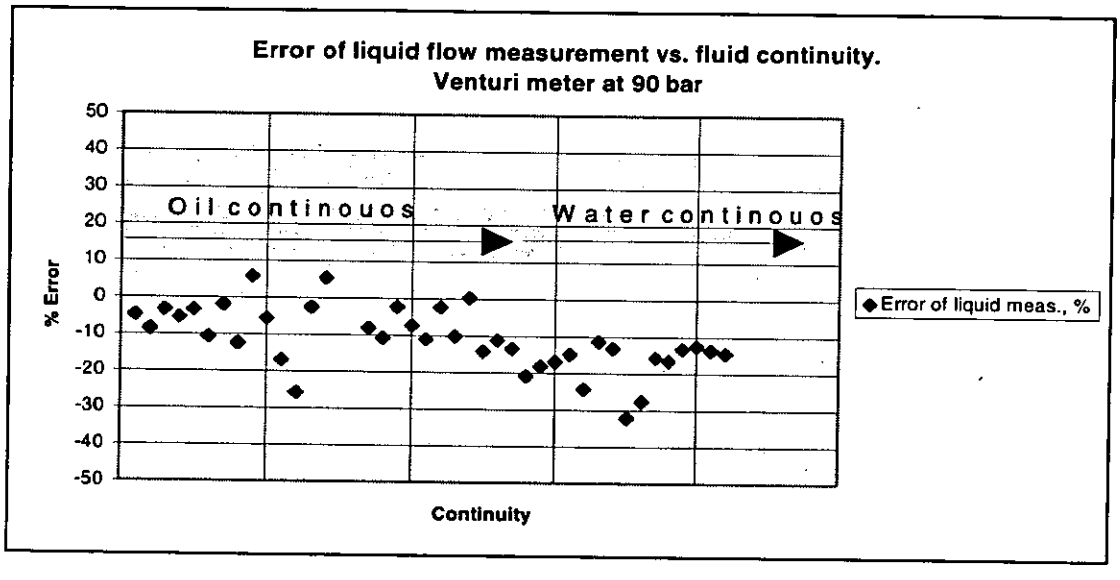

Fig 11 Venturi based liquid flowrate vs. liquid continuity

In order to investigate the effect of presence of water more thourogly we may look at the watercut calculated by the meters. Figure no.12 and no. 13 show watercut as presented by the meters versus reference watercut. Once again we observe the influence of water on the composition measurements of the cross-correlation based meter. The meter readings show a much wider distribution at watercuts of 60 % and higher.

For the venturi based meter the picture is not that clear; we find distribution in the watercut area of 40 - 75 %, however, at the 90 % level the readings are well located in a narrow distribution.

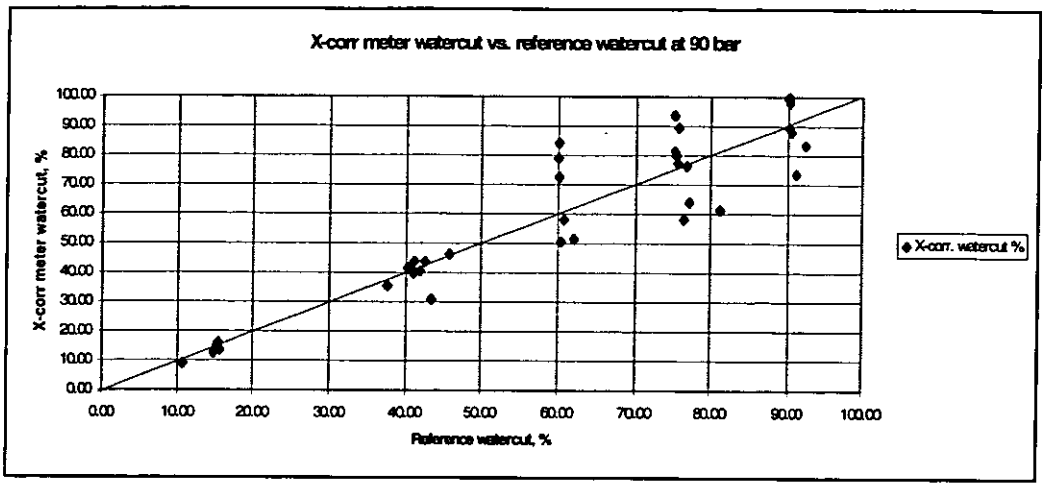

Fig. 12 Watercut presented by cross-correlation based meter vs. reference watercut

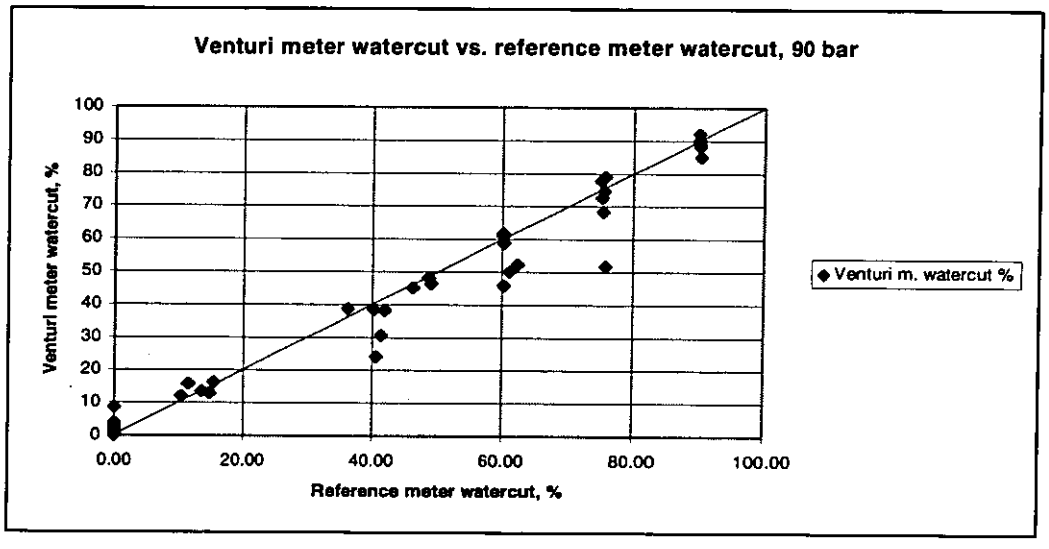

Fig. 13 Watercut presented by "Venturi meter" vs. reference watercut

7.3 Reproducibility

In cases when having a good reference system the possible offset of a multiphase meter could be compensated by making meter adjustments. Consequently it wil be most important to have a meter reproducing the readings at equal operating conditions with a high degree of accuracy.
The reproducibility of the cross-correlation based multiphase meter was evaluated. Since the concentration of water has been found to have influence on the meter accuracy the same parameter is used as a basis for reproducibility evaluation. The following figure shows reproducibility versus watercut.

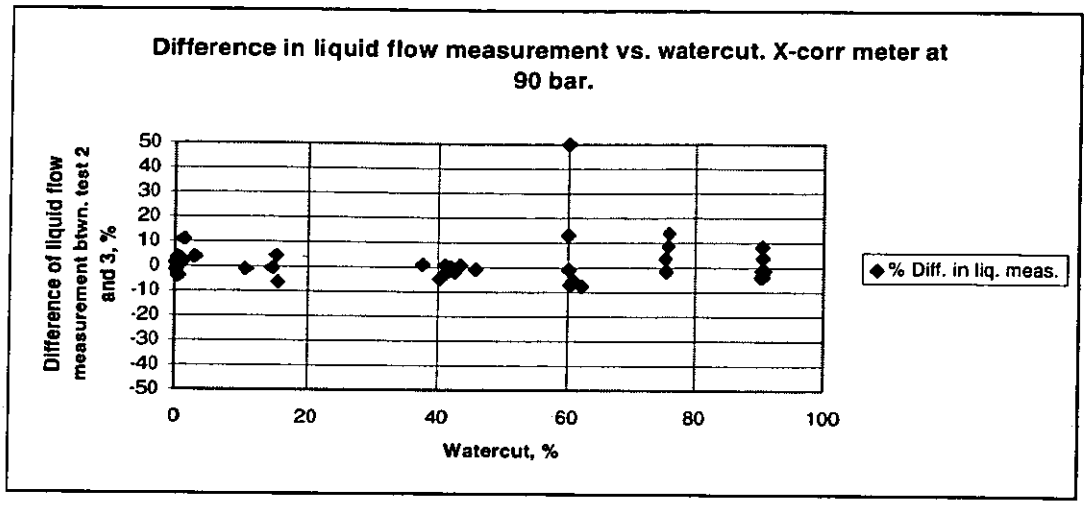

Fig. 14 Reproducibility presented as difference between the readings of two equal test points in two differents test series.

The data points do not show any significant watercut influence on the reproducibility. Consequently systematic errors caused by weakness in the liquid composition measurement can be corrected.

8. The conclusions

The results from testing of a multiphase flow meter having velocity calculations based on cross-correlation only show that the accuracy and distribution of the liquid and gas flowrates are well up to the level of the venturi based meter tested. Studying flow regimes and fluid continuity as possible factors for making influence on multiphase meter performance we found that even if the test programme covered several flow regimes, non of these were found to have any significant influence on the accuracy of the two specific multiphase meters. However, we found watercut to be a parameter that made significant influence on the composision measurement of one of the two meters.

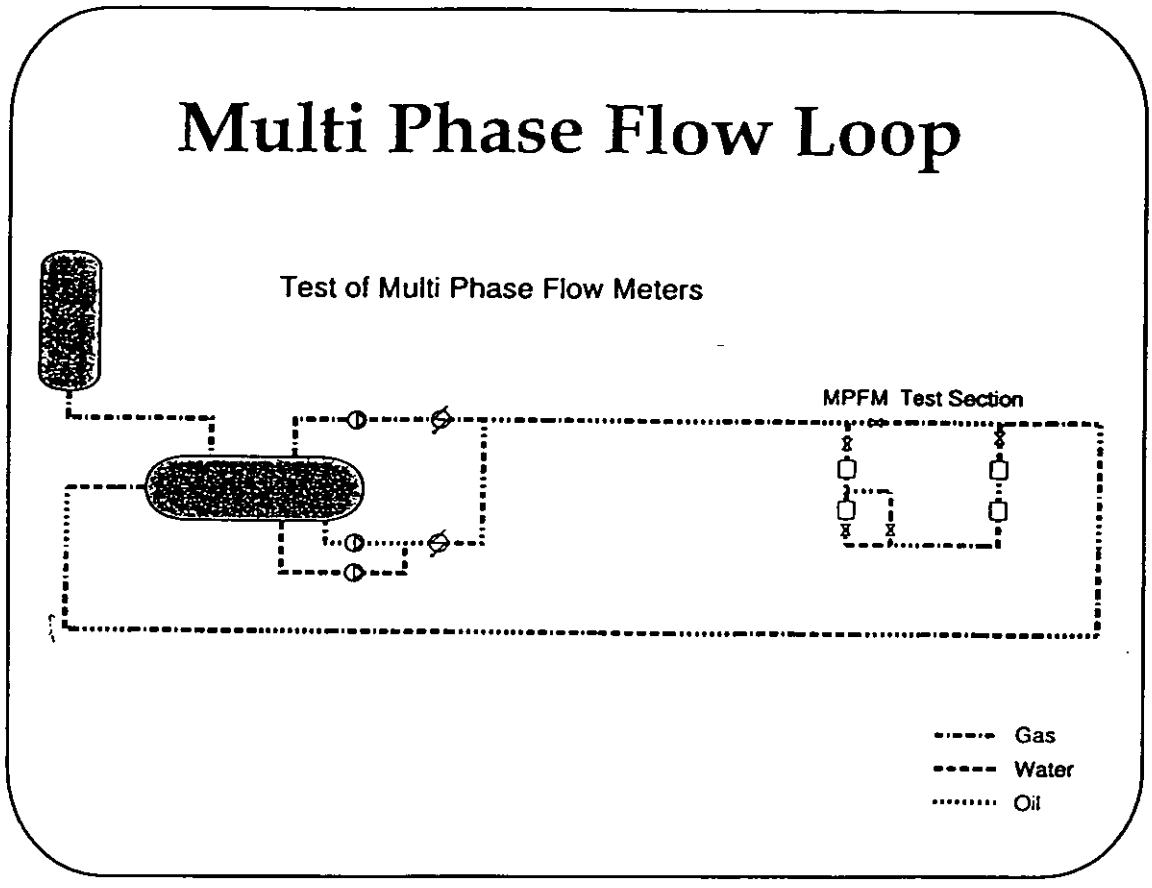

Simplified flow diagram of the Multiphase Flow Loop

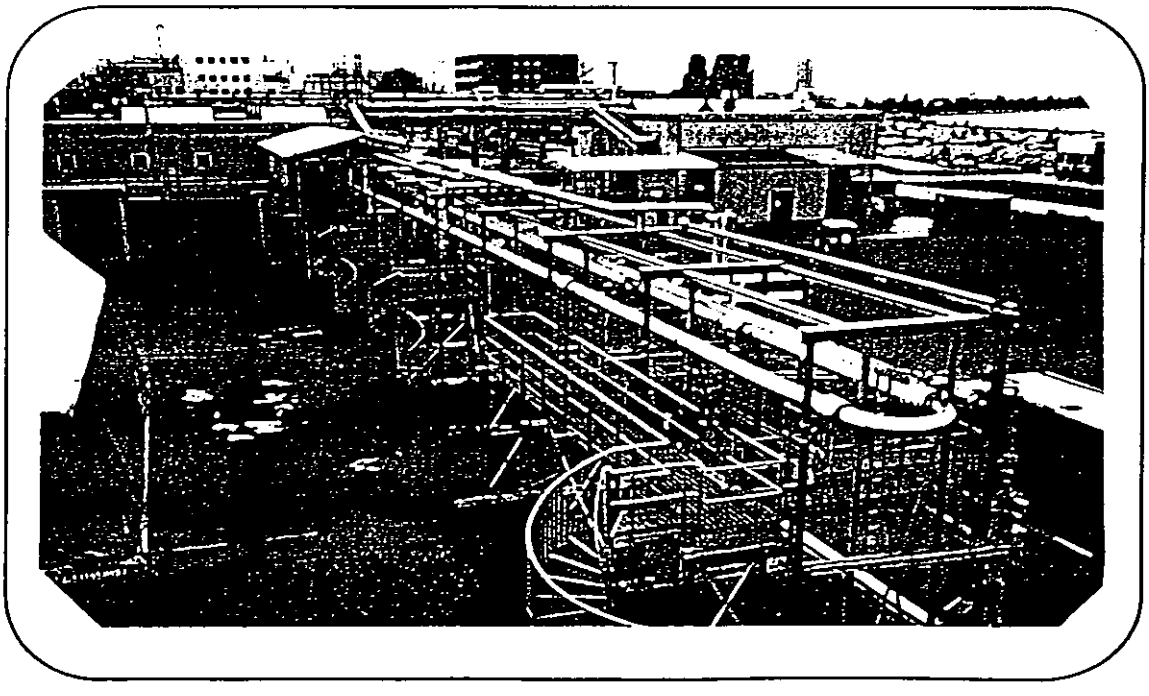

Photo of the loop including test section

NSFMW.97

North Sea FLOW Measurement Workshop

Paper 3: 1.3

TOPSIDE AND SUBSEA EXPERIENCE WITH THE FRAMO MULTIPHASE FLOW METER

Authors:
B.H. Torkildsen, P.B. Helmers and S.K. Kanstad, Framo Engineering AS
W. Letton, Daniel Industries Inc.

Organiser:
Norwegian Society of Chartered Engineers
Norwegian Society for Oil and Gas Measurement
Co-organiser:
National Engineering Laboratory, UK

NORTH SEA FLOW MEASUREMENT WORKSHOP 1997

TOPSIDE AND SUBSEA EXPERIENCE WITH THE FRAMO MULTIPHASE FLOW METER

By
Bernt H. Torkildsen, Framo Engineering AS, Winsor Letton, Daniel Industries, Inc.
Per B. Helmers, Framo Engineering AS and Stig K. Kanstad, Framo Engineering AS

ABSTRACT

Multiphase flow meters have been in regular service onshore and offshore for several years, and operators are achieving some level of comfort with the technology. A significant amount of experience has been gained with the Framo Multiphase Flow Meter both topside and subsea. Typical applications are well testing, well management and allocation metering.

For topside applications, the principal advantage of the meter remains the elimination of the test separator and all it's associated hardware and maintenance. For subsea applications, the advantage is even greater as separate test lines and in some cases even entire platforms can be eliminated.

The Framo Multiphase Flow Meter concept which combines the Framo Flow Mixer with a Multi Energy Gamma Meter and a Venturi Meter offer the optimum in precise estimation of oil, water and gas flow rates and has at the same time proved to be a particular robust concept. True reproducibility and high accuracy combined with built-in features such as simple calibration and a separate gas and liquid sampling arrangement solve many of the operational problems that are encountered with alternative methods.

Operational experience with Framo Multiphase Flow Meters installed around the world, both topside and subsea, will be reviewed. Special attention will be paid to the difficult issues peculiar to subsea meters, such as their remote installation, retrieval, calibration, and maintenance.

Finally, future trends in multiphase metering will be explored, particular will the challenges of introducing this technology into more routine applications be addressed.

BENEFITS OF MULTIPHASE FLOW METERS

When the developments of multiphase flow meters started for more than twenty years ago, one of the main aims was to develop low cost flow metering systems, which could accurately measure the flow rates of oil, water and gas in difficult multiphase flow regimes including emulsing and foaming conditions, where conventional metering systems based on phase separation have great difficulties. With the Framo Multiphase Flow Meter this aim has been achieved, as the meter is capable of measuring the individual flow rates of oil, water and gas without being affected by any multiphase flow regime or whether the liquid is oil- or water- continuous.

Resent years experienced have however taught us that the benefits of multiphase flow meters reach fare beyond this. Even when conditions are present for efficient separation in conventional metering systems, (**Fig. 1a)** the advantage of being able to continuous or near-continuous monitor each well stream (**Fig. 1b and 1c**), is so great that although the multiphase measurement is fundamentally more difficult than a single phase measurement, the performance from multiphase flow meters is often comparable and even better than what is normally achieved with conventional metering systems. In addition, whereas a conventional testing system might take hours to become stable for measurement, a multiphase flow meter could yield good test results minutes after a well is switched in.

Elimination of test separator, manifold and/or flow lines is ordinarily the single most important reason for choosing to use a multiphase flow meter (**Fig. 1**). Not only are test separators and their associated metering equipment expensive, but their bulk requires also additional platform space in offshore topside installations. In the case of satellite fields, running a test line back to a test separator on a platform is also a non-negligible expense.

Because well-designed multiphase meters must be virtually maintenance-free it they are to be used subsea or on unmanned platforms, their application will significantly reduce operational expenditures (OPEX) over conventional test separation systems.

The reservoir engineers requirement for representative fluid samples is well accommodated by the Framo Multiphase Flow Meter as it has a built-in feature which allow individual sampling of gas and liquid in a very efficient manner. Numerous other advantages of multiphase measurement could be listed, but what is shown above should be sufficient to convince any potential user that they deserve consideration. Having crossed this threshold, whether through one's own experience or that of others, it is apparent that if one chooses to use a multiphase meter, then a test separator is no longer needed.

CHALLENGES OF MULTIPHASE FLOW MEASUREMENT

Multiphase flows exhibit many complex phenomena, and by its very nature, metering of it is extremely complex and fraught with subtle problems. Some of these will be

explained here.

Flow Regime Effects
Different distributions of oil, water and gas in space and time within a pipe are classified in flow regimes, **Fig. 2**. However, flow regimes vary depending on operating conditions, fluid properties, flow rates and the orientation and geometry of the pipe through which the fluid flow. Characteristic for well streams is that flow regimes are changing, and dramatic changes can occur rapidly or as part of a more gradual process, however in most cases prediction of it is extremely difficult. Slijkerman *et al* 1995 /8/ showed several real-world examples of how wells can drastically change their production characteristics over their lifetime, changes that cause the flow to span three or four different flow regimes. For the same flow rates, different flow regimes will result in changes in phase hold-ups, in phase velocities (slip) and in local transient characteristics of the flow.

Since a flow regime can never be exactly simulated or reproduced, verification of multiphase flow meter performance in a laboratory is very difficult, and has only limited value unless the meter is insensitive to different flow regimes, a feature that however is essential for a true multiphase flow meter.

Sensor Dependence
Some sensors are more strongly dependent on the relative physical distribution of the oil, water, and gas in the pipe than others. Particularly sensitive are electromagnetic measurements. Fairly insensitive is gamma attenuation, so long as the attenuation path is through a representative sample.

Oil-Water emulsions can cause severe problems on certain electromagnetic sensors, especially when making the transition from oil-continuous to water-continuous, or the reverse. Gamma attenuation on the other hand is not influenced by whether the oil and gas has formed an emulsion or in that case whether the liquid is oil- or water- continuous (Rafa, Tomoda, Ridley 1989 /1/).

Both electromagnetic and nuclear sensors exhibit changes in their response when confronted with a change in water salinity. Slijkerman *et al* 1995 /8/ showed the relative watercut sensitivities to salinity for conductivity and gamma attenuation methods, **Fig. 3**. This sensitivity can be further reduced for the gamma attenuation method by careful selection of gamma energy levels.

FRAMO MULTIPHASE FLOW METER

The Framo Multiphase Flow Meter consists of three primary components: (1) a static Flow Mixer to homogenize the flow and eliminate flow regime effects; (2) a Venturi Meter to measure the composite or bulk flow through the meter; and (3) a Multi Energy Gamma Meter imbedded in the throat of the Venturi. Each of these will be discussed individually.

FRAMO Flow Mixer

The purpose of the Framo static in-line mixer is to provide stable, homogeneous multiphase flow conditions through the measuring section, independent of upstream conditions. It is the means whereby the Framo meter can make the claim of always having a common velocity through the device for all three component phases. It is comprised of a cylindrical compartment with a gas/liquid diverter, an injection pipe, and a gas/liquid ejector, as shown in **Fig. 4**.

When arriving in the flow mixer the liquid phase is continuously drained to the bottom of the compartment and through the ejector. The gas phase is diverted to the top section of the compartment and via the injection pipe to the ejector. In the ejector nozzle, a turbulent shear layer is generated. Minimum associated pressure loss is achieved by utilising this turbulent shear layer mixing process.

As shown in **Fig. 10**, parts for taking liquid and gas samples from the most advantageous points in the mixer are standard features of both topside and subsea designs. These will be discussed in more detail later.

The Framo Multiphase Flow Meter has three methods for addressing the problem of salinity variations over time. The first is by simply taking a liquid sample from the bottom of the mixer, as shown in **Fig. 10**, and analysing the separated water for salt content. The second is through a new method for salinity determination derived from an analysis of the gamma ray spectrum. This latter technique is obviously more attractive for meters in remote locations, and will be incorporated in future software releases. Finally, whenever practical a direct single-phase measurement can be performed on the water phase and the salinity can be derived thereof.

Multi Energy Gamma Meter

The Multi Energy Gamma Meter provides the volume fractions of oil, water and gas in the flow. Calculation of these fractions is based on the attenuation of gamma rays from two different gamma energy levels of a Barium 133 isotope, as explained earlier.

The system consists of the following main elements:

- Ba-133 source (10 milliCurie activity)
- A rugged NaI(Tl) scintillation detector with photomultiplier tube
- Cable Penetrators complete with special cables
- A High Voltage supply for the photomultiplier tube
- A pre-amplifier for signal conditioning
- A Multi Channel Analyzer for gamma spectroscopy

The Barium 133 isotope is encapsulated in a separate housing diametrically opposite the detector at the Venturi throat. The low intensity of the source in combination with multiple levels of protection has proven to completely prevent any radiation exposure outside the meter.

Venturi Meter
The bulk fluid flow is measured with a Venturi Meter immediately downstream of the Flow Mixer. Here the multiphase mixture can be treated as a single-phase fluid with equivalent mixture properties, and standard single-phase Venturi relations can be applied. The differential pressure transmitter and pressure transmitter are equipped with remote seal sensors of the pancake type, bolted to the sides of the Venturi section.

Subsea Package
Although most multiphase flow meters that have been installed to date have been for topside offshore service, their use on the sea floor is clearly of great importance. The Framo meter's subsea design is one of its greatest strengths. The first Framo Multiphase Flow Meter ever manufactured was a subsea prototype (Torkildsen, Olsen 1992 /4/), and although most experience with the Framo Multiphase Flow Meter has been achieved topside, the principle of the meter is identical for both subsea and topside designs. The subsea meters that were delivered in mid-1996 offer several advantages over the first generation design:

- Full metal to metal sealing
- Insert style reduces subsea handling weights
- Diverless running and retrieval, with or without the use of guidewires
- Subsea liquid sampling facilities included
- Design pressures up to 10,000 psi

Fig. 5 shows a cross section of the Framo Subsea Multiphase Flow Meter. The meter when in place is shown in **Fig. 5b** and during installation or retrieval in **Fig. 5a.**

The main components of the Framo Subsea Multiphase Flow Meter are described below.

Receiver Barrel
The subsea multiphase flow meter design utilizes a barrel style subsea configuration. An insert cartridge, which carries all active multiphase flow meter elements, is locked into the receiver barrel.

The receiver barrel is permanently installed on the subsea structure and includes no active elements. There are no requirements for straight pipe lengths upstream or downstream of the meter.

The receiver barrel serves the function as inlet and outlet housing and as a guide and support during installation of the insert cartridge. In addition, it forms the outer housing of the flow mixer. Standard flange connections at the receiver barrel are used for connection of the flow meter inlet and outlet to the subsea tree or manifold piping.

Insert Cartridge
The insert cartridge incorporates the following main elements:

- Cartridge body with metal-to-metal seals and mechanical clamp connector

- Flow Mixer internals
- Venturi Meter
- Gamma Source and Detector
- Pressure and Temperature Sensors
- Data Acquisition System
- Connectors for power / signal and flushing media

Data Acquisition System
All sensors of the subsea meter are connected to the Data Acquisition System at the upper section of the insert cartridge as shown in **Fig. 5(b)**. If required, the application software running in the processor can be changed or downloaded from the surface.

Supply voltage and communication can to a large extent be adjusted to meet any specific requirement. Typical supply voltage will be 24 VDC; typical power consumption is less than 20 W. Data to the surface is transmitted via an RS485 Modbus RTU link, which during metering will transfer data once every 60 seconds.

Control System Interface
The Framo Multiphase Flow Meter can be interfaced directly to a Control Pod in a Subsea Production Control System, with separate wires for power and data transmission. Operationally, this interface will present a minimum of interference with other Subsea Control System functions. Alternatively, the flow meter can receive power and transfer data through a dedicated single pair cable in a control umbilical.

MULTIPHASE FLOW METER PERFORMANCE

Table 1 shows the field locations and reference flow facilities where the Framo Multiphase Flow Meter has been tested. It should be emphasized that, in each of the cases shown, the meter was installed and calibrated by Framo personnel, then left for the user to operate and collect data without Framo in attendance.

To give the reader some idea of what can typically be achieved using a Framo Multiphase Flow Meter, results from the project Multiflow testing at NEL in 1996 are shown in **Figs. 6 and 7**. **Fig. 6** is a composite plot of the difference in watercut measurement, between the Framo meter and the NEL reference. The data shown represent 63 different measurements at gas volume fractions ranging from 0 up to 95%; the rms deviation is about 2%. **Fig. 7** plots the Framo measured oil flow rate versus the NEL reference; 171 points are shown, again at gas fractions ranging from 0 to 95%.

The data shown in **Fig. 8** are interesting because they demonstrate the stability and repeatability of the measurements as compared to those made with a test separator, on Gullfaks B in 1994. Two interesting points are worth noting. First, the oil production rate is quite constant during the testing periods, and returns to very nearly the same rate after a period of many hours between tests, as shown by the tests on Wells 1 and 5. Second, the variations in measured flow are smaller with the Framo meter than with the test separator.

FIELD EXPERIENCE

As shown in Tables 1 and 2, the Framo meter has been used in a variety of installations throughout the world. In the following, three typical, though very different, applications are considered in more detail with respect to operational considerations and experience.

BHP Liverpool Bay

The application is on three unmanned remotely operated wellhead platforms in the North Sea. This development has used the FRAMO Multiphase Flow Meter as its only means of well testing and allocation metering for the central combined process platform and two remote unmanned satellites. The field has a very high GOR, and the actual GVF are in the high end of the range originally designed for. The meters are designed for gas flow rates up to 80 MMscf/d with a maximum pressure loss of less than 1 bar. All three meters are installed on test manifolds, allowing individual wells to be tested locally at the wellhead platform, where the data are collected and transmitted to the central process facility over a serial link. The test headers on which the meters are installed are 8 and 10 inches, and the connections of the meters are made to match this.

Due to the phased development of the field, two of the meters have been in operation for more than two years and the third for about 6 months. Based on the feedback from the operator, the meters have been operating to his full satisfaction. Only one site visit has been made by Framo service personnel, this to verify the calibration and set up of one of the meters. No changes were made.

Petroleum Development Oman

This is a remotely-operated, solar-powered installation. The meter is located on a test manifold in a remote well cluster in the desert of Oman. The meter was originally installed as part of a test program for the operator to verify the meter performance at actual conditions. The installation was consequently rigged as a temporary system, with only local readout of the flow meter through a portable PC system. Power was derived from a small solar array, since the unit draws less than 20 watts. A schematic diagram of the operation is shown in **Fig. 9.**

The meter was operated in this mode for several months. As the meter has performed to the operator's satisfaction over the period (Mhos, Mar A and Al-Hindi, Ruqaiya, 1997 /10/), it is now being procured and the installation made permanent, including providing remote data collection through a radio link to the meter using standard Modbus RTU protocol. The use of Modbus protocol permits interface to all common control systems, including those used for subsea systems.

East Spar Development

The East Spar Development, offshore West Australia, was the first oil field in which subsea multiphase flow meters were used in commercial application. As of September 1997 the meters have been in operation subsea for twelve months. It is a two well subsea completion producing gas and gas condensate, and is located 62.5 km offshore. The wells are commingled into a single pipeline through a subsea manifold and are individually metered with dedicated multiphase flow meters. Communication with the

meters is via a field- installed buoy, where the flow computer and all the other field control systems are located. Communication of the processed meter data from the field buoy to the shore terminal control room is via a telemetry link. The real-time operational data from these subsea multiphase meters are also available anywhere in the World via satellite telemodems.

The meters are of the insert retrievable design described earlier. The operating conditions are:

- GVF: 87-95%
- WC: 0-70%
- Design Pressure: 200 bar
- Operating Pressure: 100 bar

Calibration data were obtained for both meters immediately following the installation subsea. This was done on a routine basis without any problems. The calibration values were then remotely downloaded to one of the meters, which since has been operating to the full satisfaction of the operator.

Remote downloading of calibration data to the second meter was hampered, and downloading required access to the flow computer located in the unmanned buoy, which for a long time was not accomplished. However, also the second meter has been in full operation since field start-up and stable reading have been recorded, although slighly biased for the reason mentioned. Since the calibration values are known, the data can be corrected manually topside based on the recorded raw data.

Performance Verification

It is important for the user to be able to verify the correct operation of his multiphase meter throughout its life. Since the Framo Multiphase Flow Meter is based purely on gamma ray attenuation physics and Venturi flow measurement, there is no need to "tune" the meter to any reference. If all sensors are correctly calibrated and accurate input parameters are used, the meter will maintain its accuracy through its lifetime.

At various points in time the user will likely want to verify its correct operation. Some ways of doing this are listed.

Factory Testing

Prior to delivery, each meter should be put through a complete test matrix of flow conditions representative of what is anticipated at the field installation site. This should be the first time the user sees the meter in correct operation, and should raise his confidence level.

Calibration Checks

Once the Framo Multiphase Flow Meter has been installed in the field, by simply isolating and letting the trapped fluids settle, static conditions can be attained. At this point, calibration checks on each of the four sensors can be performed; if each is within an acceptable tolerance, the meter verification is complete and the user should be confident in its correct operation. This is a significant advantage over meters that depend

on flow models and flowing calibrations. The details of these calibration checks are reported in greater detail elswhere (Hanssen, Torkildsen, 1995 /7/).

Sampling
With the built-in sampling capabilities of the Framo meter, as shown schematically in **Fig. 10**, the user can verify the correct operation of the meter or detect physical changes in water salinity, oil density, or the like.

Site-Specific Testing
In certain field operations, production trends from individual and commingled well streams can be used to check the meter's overall performance.

Service Company Proving
On an infrequent schedule, or whenever there is a question regarding the correct operation of the meter, production can be tested by a qualified service contractor to assess the performance of the meter

Operational Problems Experienced
Framo Multiphase Meters have been installed on more than 25 different locations to date, of which approximately 20 have been in actual operation. The first meters installed have been in operation for more that two years, and as a consequence the accumulated operational time for Framo Multiphase Meters is substantial, and increasing by more than 8000 hours each month.

As shown by Table 2 the breadth of experience gathered is quite extensive in terms of applications, flow rate, pressure, gas volume fraction, and watercut. Additional experience about to be gained through meters that are installed and will be commissioned in 1997 is highlighted by the shaded section.

During the operational life of the meters listed in Tables 1 and 2, only two significant problem areas have been experienced. On a meter that was installed on a North Sea platform, a mechanical problem leading to an oil leak and subsequent contamination of the gamma collimator was experienced. This problem was identified as an isolated mistake in the final assembly of the meter not detected by quality assurance procedures. Appropriate procedures have been put in place in the ISO 9001 certified QA program to avoid this kind of incident in the future.

Another problem area identified during the commercial introduction of the meter has been the gamma ray detector and certain of its associated nuclear electronics. Even though a rigorous QA screening process was in place, there have been cases of detector failures. Their incidence has been dramatically reduced by turning to detector vendors who specialize in the hostile environments of the oilfield. Improved performance from previously failure-prone nucleonics has been achieved by working with vendors to select high-temperature components, to perform chamber testing on completed assemblies, and so on. The 3-Phase Measurement partnership, described later in this article, should make this an area of strength, as two of the three partners specialize in instrumentation for difficult oilfield environments.

FUTURE TRENDS

The trend in multiphase metering which all users care most about in the *price trend.* At today's prices for the devices, often only high-volume, expensive production systems can justify their use. If this situation were to endure, multiphase metering would have only a minimal impact on the worldwide economics of production. Happily, this is not the case; in the coming years multiphase meters will come down in price and go up in usage, primarily due to the factors listed below.

Economies of Scale

Thus far no manufacturer of these meters has delivered enough quantity of product to bring their prices down substantially. However, as these manufacturers begin to see a strong market for their product, they will build to forecast rather than demand, they will achieve savings in both purchase and production of parts, and they will be able to pass these savings on to the user.

Cost Reduction Efforts

When it is clear that there is a solid market for multiphase meters, manufacturers will address every part of their manufacturing process to take cost out - and will do it over and over again. Some of these improvements will require re-design, some will necessitate new machines or tooling. However, when it is perceived that there will be a return on this investment by the manufacturers, they will surely make the changes, and the end user will be the beneficiary.

Alternate Less Expensive Technology

As with the manufacturing processes, manufacturers will invest in alternative designs - some of which may be radical - if they feel that these investments will pay off with increased meter sales and better margins. Thus, new technology and improved designs will produce even further reductions in prices.

The phenomena described here are certainly not unique to multiphase meters; on the contrary, they are typical of what happens in a competitive market where there is strong demand for products that are technology-laden. **Fig. 11** presents an interesting example of how the prices of non-volatile computer memories have come down during the past eight years as demand for this technology has gone up.

Another trend which will appear in coming years is that suppliers will offer a portfolio of multiphase meters rather than a "one size fits all" product. This will be a consequence of the natural market segmentation due to larger sales volumes and a richer variety of measurement methods. For example, certain land applications might accept a reduced-accuracy, low-cost unit, whereas deep subsea applications might demand the most accurate, reliable meters money can buy. Successful suppliers will recognize this diversity of requirements and offer the market a range of products.

A final trend worth mentioning is that of intelligent metering systems. Intelligent meters are those which are capable of providing more information than simply a measure of flow. Probably the most important ancillary information in most cases is the fitness of the

meter. Given the power of imbedded processors used in today's instruments, it is mandatory that meters be able to diagnose both their own health and the quality of their measurements. This data should be reported to the user just as is the information on flow.

3-Phase Measurements AS

Daniel Industries, Framo Engineering, and Schlumberger Limited announced recently their intent to cooperate in the area of multiphase flow measurement. The vehicle for this cooperation will be a jointly owned technology center, to be called 3-Phase Measurements AS, located in Bergen, Norway. It will be staffed by specialist personnel from each of the three companies, and will be tasked with the design and manufacture of multiphase meters for use both topside and on the sea floor.

3-Phase Measurements will initially offer the latest version of the Framo meter as its standard product for both topside and subsea applications, since it is a fully commercial and proven concept. As new multiphase developments are brought forward from the three partners, these will be refined and offered commercially by 3-Phase Measurements.

CONCLUSIONS

1. Multiphase meters have the potential to provide significant savings in both capital and operational expenditures, and to provide continuous or near-continuous monitoring of production performance.

2. There are significant technical differences between metering technologies. The user should beware of those which he cannot understand or the details of which the supplier can't adequately explain.

3. Flow regime effects and salinity are the two most important environmental effects on these meters. The Framo mixer removes uncertainties due to flow regime. Salinity changes can be dealt with by direct sampling, by new methods of gamma ray spectral analysis or by direct single-phase measurements.

4. The Framo Multiphase meter has extensive operational experience on land, topside offshore, and subsea. In fact, the two East Spar subsea meters are unique as the only multiphase meters ever installed on the sea floor for any significant period of time.

5. There are, at every stage of installation and operation, verification methods that can be applied to assess the health of the meter.

6. These meters will continue to become more robust, more performant, and less expensive as the technology and the market mature.

ACKNOWLEDGEMENTS

The authors wish to thank Broken Hill Proprietary, Ltd., Petroleum Development Oman, and the East Spar Alliance for permission to discuss details of their producing properties. They further gratefully acknowledge the permission of Royal Dutch Shell to use the data shown in Figures 3.

REFERENCES

/1/ Rafa K., Tomoda T., Ridley R. "Flow Loop and Field Testing of a Gamma Ray Compositional Meter". Energy-Sources Technology Conference and Exhibition, January 22-25, 1989, Houston Texas.

/2/ Martin W., Woiceshyn G. E., Torkildsen B. H. "A Proven Oil-Water-Gas Flow Meter for Subsea". The 23rd Annual Offshore Technology Conference, May 6-9, 1991, Houston, Texas.

/3/ Olsen A. B., Torkildsen B. H. "Subsea Multiphase Flowmeter System". Underwater Technology Conference, March 30 - April 1, 1992, Bergen, Norway.

/4/ Torkildsen B. H., Olsen A. B. "Framo Multiphase Flow Meter Prototype Test". 10th North Sea Flow Measurement Workshop, October 26-29, 1992, Scotland.

/5/ Olsen A. B., "Framo Subsea Multiphase Flow Meter System". Multiphase Meters and their Subsea Applications, April 13, 1993, London, UK.

/6/ Olsen A. B., Hanssen B. V., "Framo Multiphase Flow Meter - Field testing experience from Statoil Gullfaks A and B platforms and Texaco Humble test facilities." 12th North Sea Flow Measurement Workshop, October 24-27, 1994, Scotland.

/7/ Hanssen B.V., Torkildsen B.H., "Status of the Framo Subsea Multiphase Flow Meter", North Sea Flow Measurement Workshop, Lillehammer, October 1995.

/8/ Slijkerman W.F.J., Jamieson A.W., Priddy W.J., Økland O., Moestue H. "Oil companies needs in multiphase flow metering", North Sea Flow Measurement Workshop, Lillehammer, October 1995.

/9/ Hanssen B.V., Svaeren J.A. "Diverless subsea multiphase meter", Underwater Technology Conference, Bergen - March 1996.

/10/ Mohsen, Amr A. and Al-Hinai, Ruqaiya, "Experience with the Framo Multiphase Flowmeter in Petroleum Development Oman", 1997 Saudi Aramco Chapter SPE Technical Symposium, Dhahran, Saudi Arabia, 8-9 June 1997.

/11/ Torkildsen, Bernt H. and Hanssen, Birger V., "Practical considerations related to multiphase metering of a well stream", North Sea Flow Measurement Workshop, Scotland, October 1996.

Table 1. Test sites for the Framo Multiphase Flow Meter

User	Platform / Field	GVF at actual condition (%)	WC at actual condition (%)	Total flow rate (m^3/h)	Design pressure (bar)	Date
Statoil / JIP, Norway	Gullfaks B	20 – 50	0 - 90	250	96	1994
Statoil, Norway	Gullfaks A	40 – 60	0 - 80	120	250	1994
Texaco / JIP, USA	Humble, Texas	50 – 96	5 - 90	270	250	1994
Maersk Olie & Gas AS, Denmark	Dan F	89 - 92	0 - 40	200 - 750	20	1994
Statoil / Saga / Norsk Hydro, Norway	Porsgrunn Flow Loop Test	50 - 98	0 - 100	Up to 250	250	1995
Phillips Petroleum Co. Norway	2/4A, Ekofisk	83 - 98	0 - 76	1400	41	1995
Multiflow JIP, Scotland	National Engineering Laboratory, Glasgow	0 - 100	0 - 100	0 – 520	250	1996
Shell UK Exploration & Production	Gannet	75 - 86	0 - 90	60 – 200	25	1996
Petroleum Development Oman	Hazar	70 - 90	0 - 50	50 – 170	250	1996
Statoil / Saga / Norsk Hydro, Norway	Porsgrunn Flow Loop Test II	50 - 98	0 - 100	Up to 250	250	1996

Table 2. Operational conditions in which the Framo Multiphase Flow Meter has been commercially installed.

Meter Location	No. of Units	Design	GVF at actual Condition (%)	WC at actual Condition (%)	Total flow rate (m^3/h)	Installation
Offshore UK	1	Topside	90 - 99	0 - 90	200 - 5000	1994
Offshore UK	1	Topside	90 - 99	0 - 90	200 - 5000	1994
Offshore UK	1	Topside	85 - 99	0 - 90	200 - 5000	1994
North Sea	1	Topside	85 - 95	0 - 20	150 - 800	1995
North Sea	1	Topside	42 - 99	0 - 75	250 - 1370	1995
Gulf of Mexico	1	Topside	90 - 95	0 - 10	220 - 830	1996
Offshore Australia	2	Subsea	87 - 95	0 - 70	Up to 750	1996
North Sea	1	Subsea	Variable	Variable	---	1996
North Sea	6	Topside	85 - 95	0 - 63	Up to 1200	1996
North Sea	2+1	Subsea	41 - 99	0 - 90	Up to 1500	1997
North Sea	1	Topside	77 - 88	0 - 25	500 - 3000	1997
Mediterranean	1	Topside	30 - 50	0 - 10	10 - 200	1997
Mid East	1	Topside	27 - 97	0 - 84	20 - 1200	1997
North Sea	1	Subsea	60 - 80	0 - 92	100 - 550	1997
North Sea	1	Topside	47 – 87	0 – 86	Up to 3000	1997
North Sea	1	Topside	85 – 92	0 – 80	50 – 400	1997

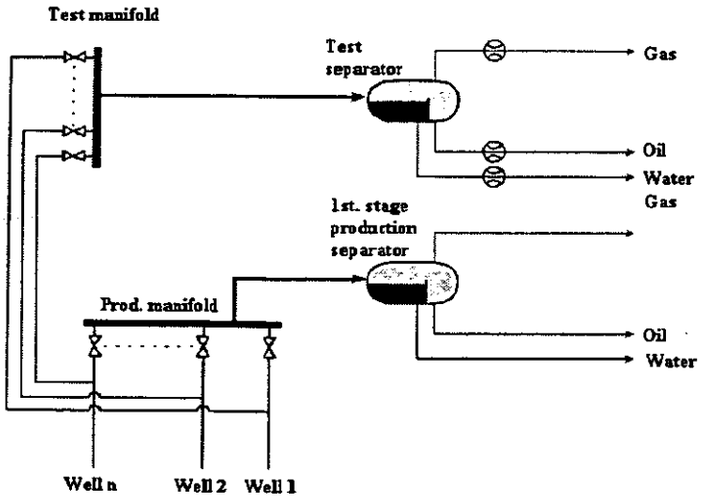

Fig. 1(a) Typical offshore arrangement of production and test manifolds and separators

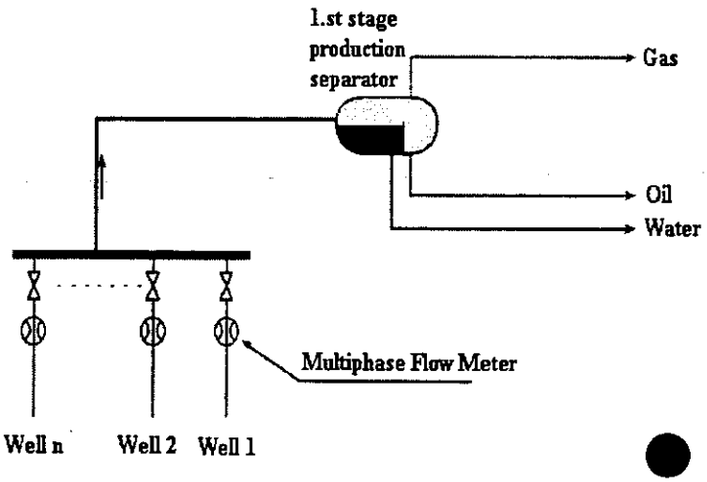

Fig. 1(b). Replacement of test manifold, test line, and test separato by use of a multiphase flow meter on each well stream.

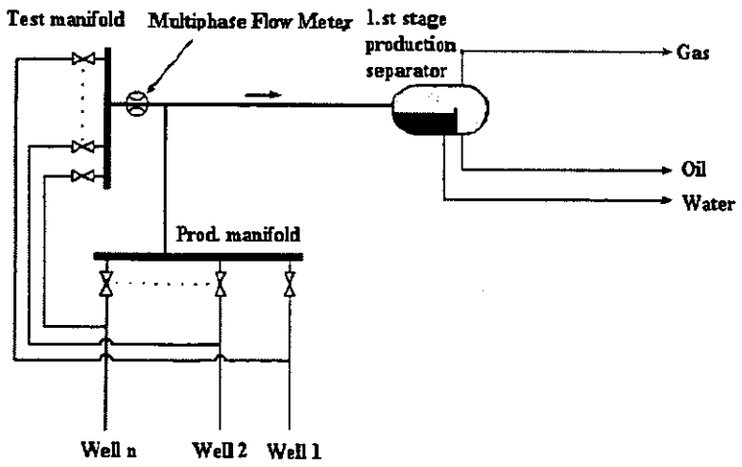

Fig. 1(c). Replacement of test line and test separator by use of one multiphase flow meter downstream of the test manifold.

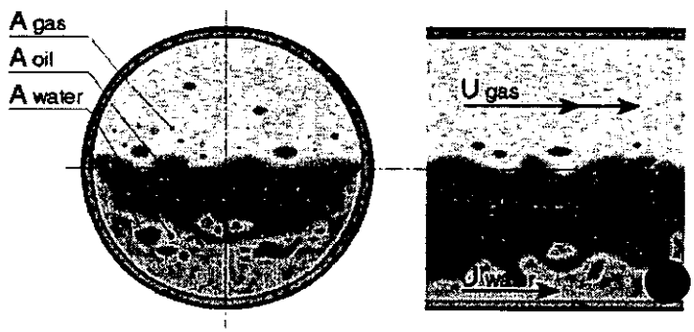

Ug : Gas velocity
Uw : Water velocity
Uo : Oil velocity
Ag : Area occupied by gas
Ao : Area occupied by oil
Aw : Area occupied by water

Fig. 2. Schematic showing three-phase flow through a pipe.

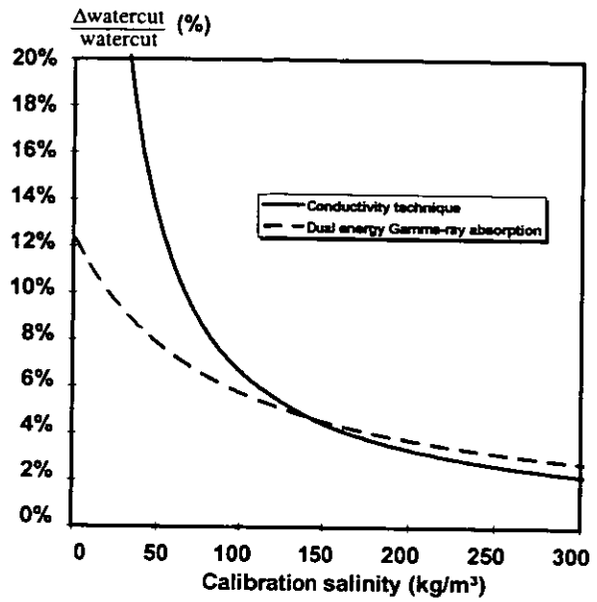

Fig. 3: The relative error in water cut, as a function of calibration salinity, due to a change in salinity of 10 kg/m^3.

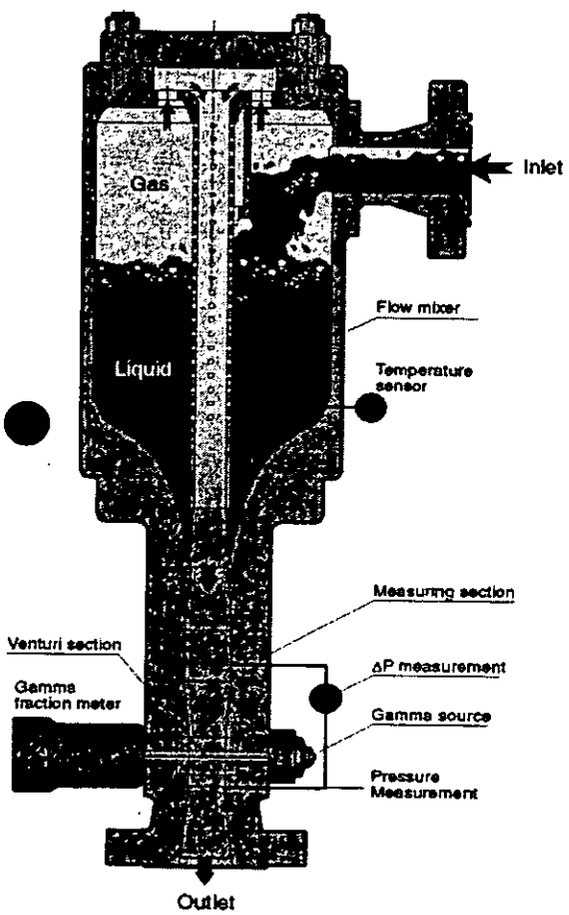

Fig. 4: Topside version of Framo Multiphase Flow Meter

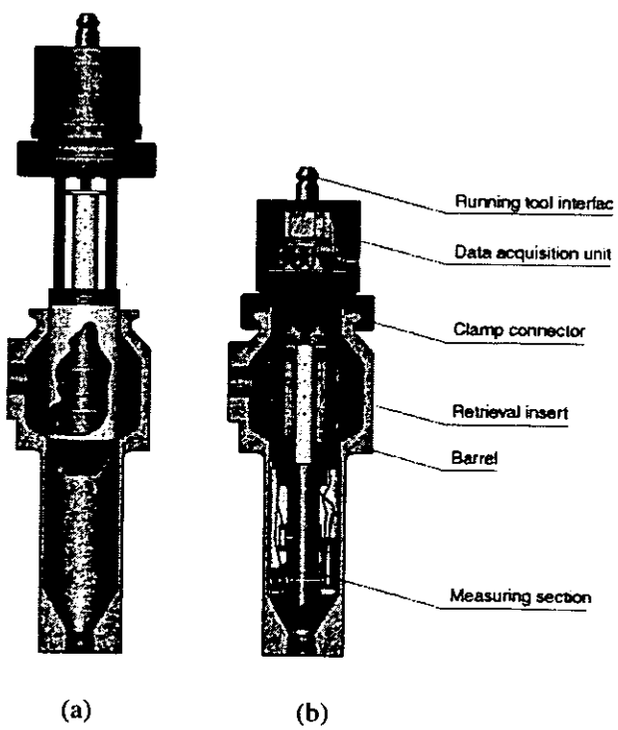

Fig. 5: Subsea version of Framo Multiphase Flow Meter. (a) During cartridge insertion. (b) With cartridge secured in receiver barrel.

Fig. 6: Absolute Framo meter watercut deviation from NEL reference (1996).

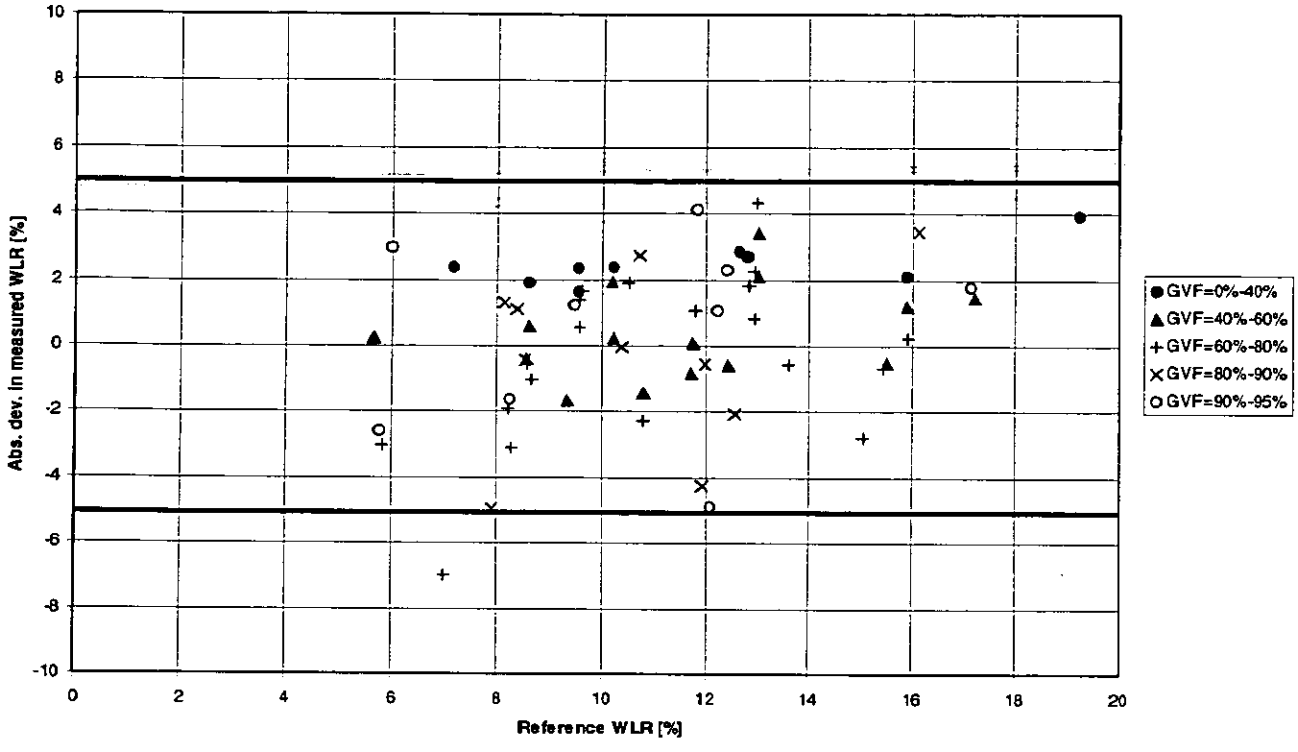

Fig. 7: Framo oil rate measurement versus NEL reference (1996) for gas volume fractions of 0 - 95%

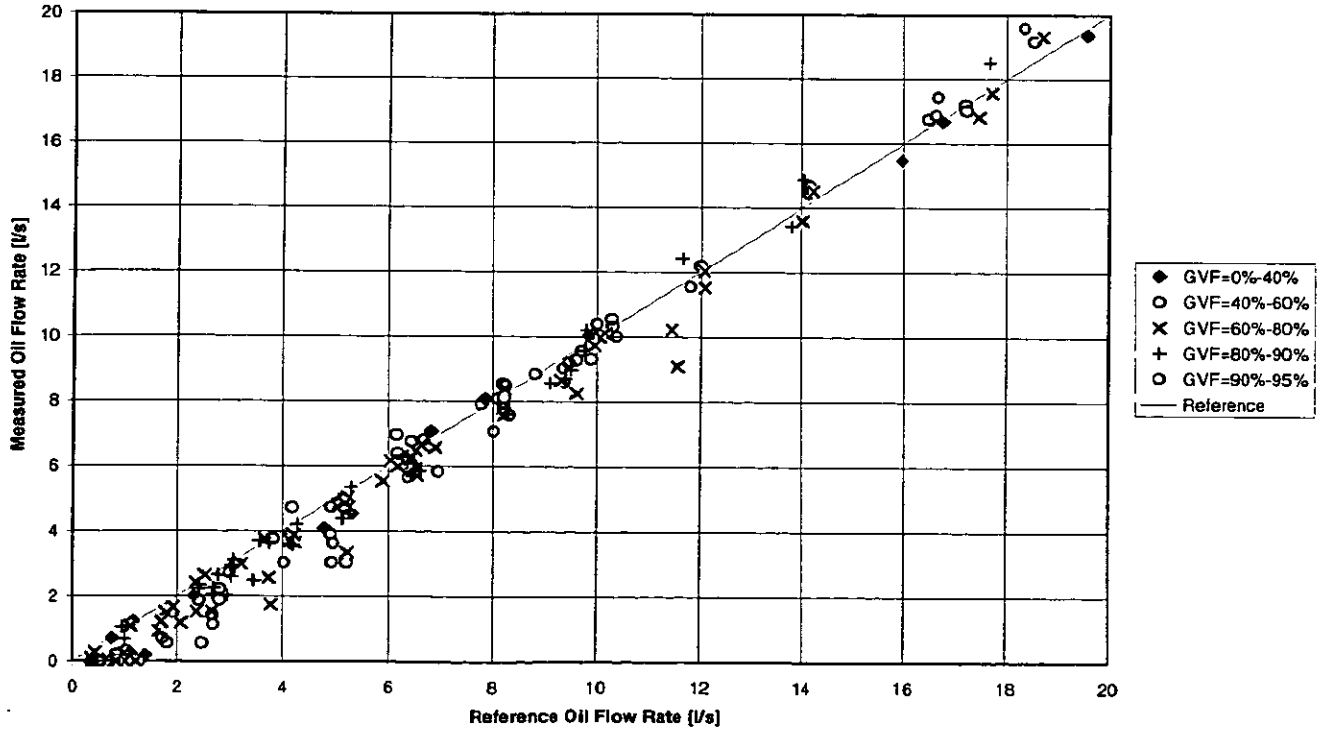

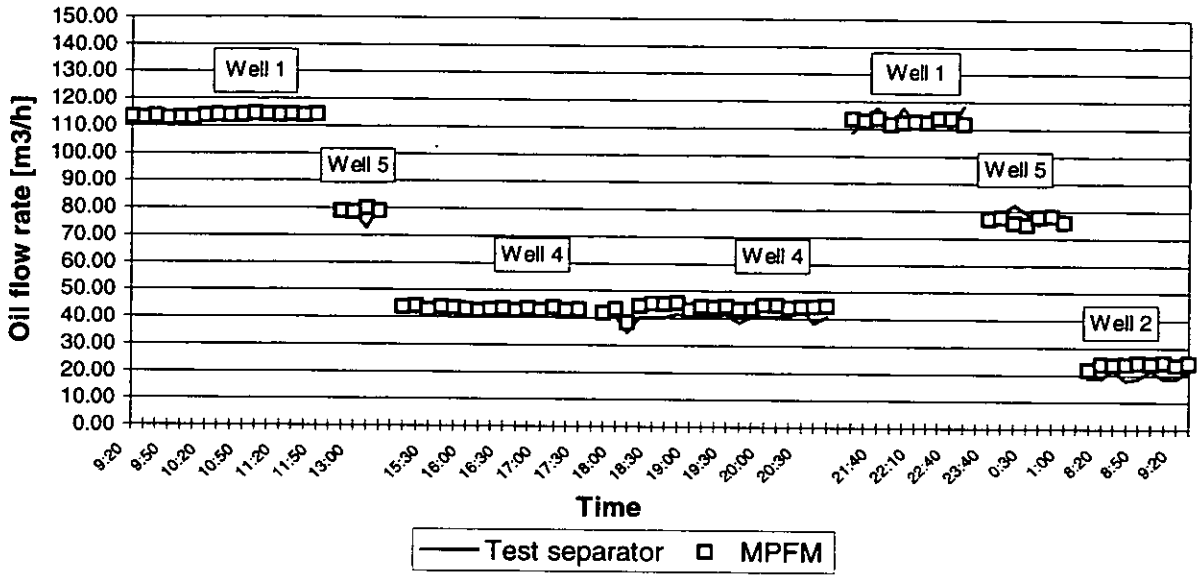

Fig. 8: Gullfaks B 24-hour well test results with Framo Multiphase Flow Meter and test separator.

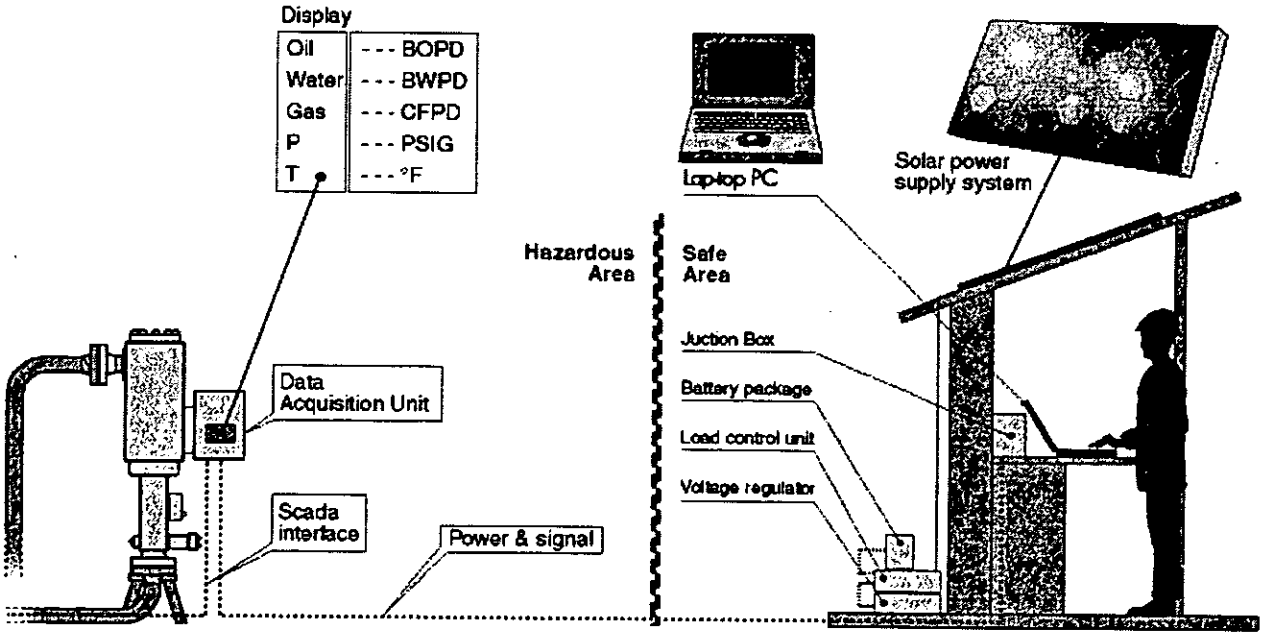

Fig. 9: Application of the Framo MPFM at a remote land location in Oman.

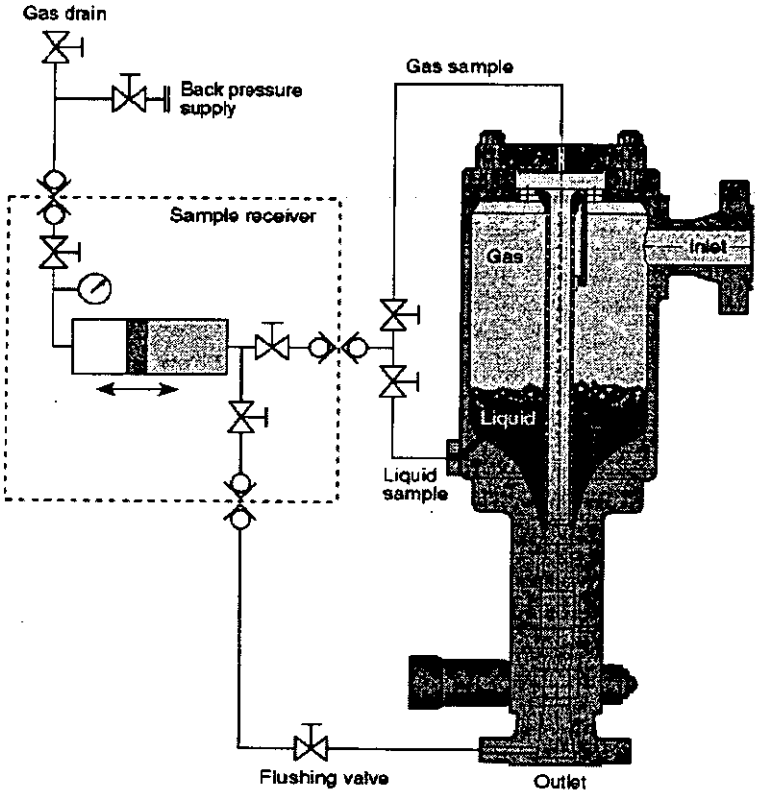

Fig. 10: Sampling capabilities with the Framo MPFM.

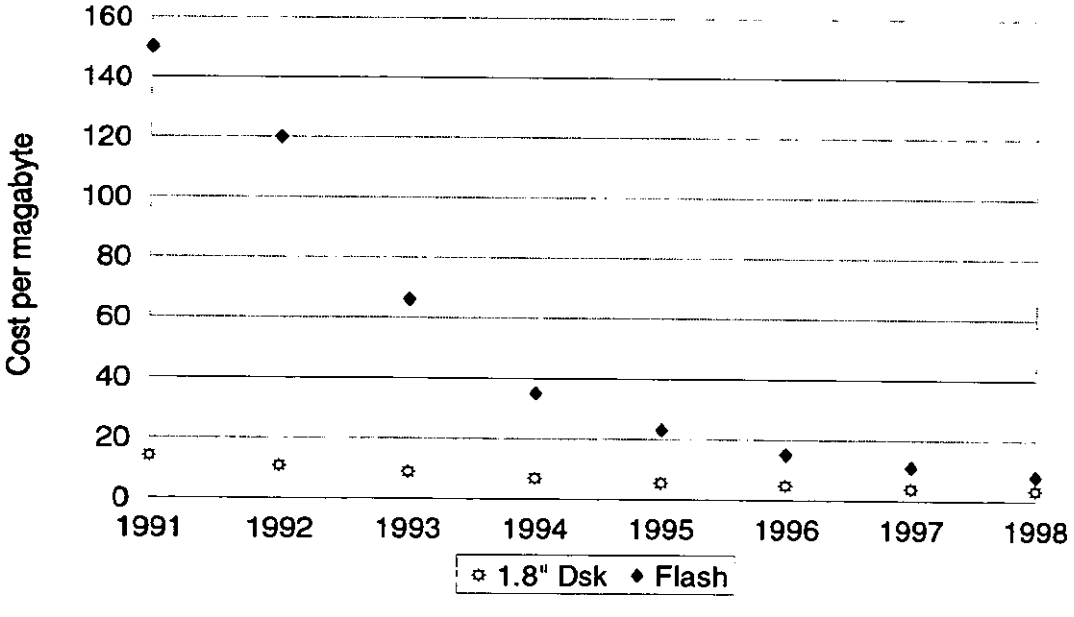

Fig. 11: Cost reduction of microdisk and flash memories, 1991-98.

NSFMW.97

North Sea FLOW Measurement Workshop

Paper ~~4~~: 1·4

ÅSGARD AND GULLFAKS SATELLITES FIELD DEVELOPMENTS

- Efficient Integretioan of Multiphase Meters -

Authors:
S. Klemp and H. Berentsen, Statoil, Norway
B. L. Pedersen, Multi-Fluid ASA, Norway

Organiser:
Norwegian Society of Chartered Engineers
Norwegian Society for Oil and Gas Measurement
Co-organiser:
National Engineering Laboratory, UK

ÅSGARD AND GULLFAKS SATELLITES FIELD DEVELOPMENTS

- Efficient Integration of Multiphase Meters -

North Sea Flow Measurement Workshop 1997

Authors: Sven Klemp, Statoil, Norway
Hans Berentsen, Statoil, Norway.
Bjørn L. Pedersen, Multi-Fluid ASA, Norway.

SUMMARY

Multiphase Meters are extensively being installed in two large field development projects on the Norwegian continental shelf: The Åsgard - and the Gullfaks Satellites Project.

The meters will be used for reservoir monitoring, allocation metering and well testing.

This paper presents the technical solutions, developed by Statoil as the operator and indicates the cost savings that are expected for installing the meters on the different applications.

The latest field test results are also presented.

INTRODUCTION

The large economical potential for applying multiphase meters has been the driving force behind the various development projects supported by the oil industry for the last 10-15 years. Today, several first generation meters are commercially available and the oil industry is now starting to use them in large numbers. The main areas of applications are for well testing or for production allocation metering.

The main issue the last couple of years has been to investigate the performance of various meters with respect to accuracy and operational reliability, and to find "the application envelope" with respect to flow rates, phase fractions and flow regimes relative to planned field developments. In Norway, the focus the last couple of years has furter been changed from testing of topside multiphase meters to developing and qualifying subsea multiphase meters, as well as integration of such meters with standard subsea production systems.

Added Value

The added value obtained from the use of multiphase meters is low investment cost, less maintenance cost, less production loss during well testing and better production maximation. The elimination of test line and subsea test manifolds will further reduce the investment cost in relation to subsea developments.

Using multiphase meters topside, new production/test separator for measuring and testing satellite fields can be avoided.

The maintenance cost of a multiphase meter is considerably lower than for a test separator. Using deduction testing with a test separator, some wells must be closed during the test period. This gives a loss in production capacity compared with continuous monitoring with multiphase meters.

Well production can be maximised by use of multiphase meters, since gas/water breakthrough can be detected at an early stage. This is essential when producing from reservoirs with thin oil layers.

CASE HISTORY

The Åsgard Field will use subsea multiphase meters, while the Gullfaks Satellites Project will use both subsea and topside meters as a part of their development concept. It is very difficult to accurately determine the general cost saving potential from applying multiphase meters. The cost reduction will depend on many different factors, such as size of the field, the distance to the processing platform, partner and government approved allocation solution, reduced investments at the processing facilities, increased production due to better reservoir management, test separator capacity etc.

ÅSGARD

The Åsgard field complex off mid Norway comprises a FPSO vessel -Åsgard A- for the oil production and a semisubmersible platform -Åsgard B- for the gas phase. The complete field will consist of more than 60 subsea-completed wells for both production and injection. The wells are clustered on a total of 15 templates with some 300 km of seabed pipelines that will interconnect the FPSO and the semisubmersible platform with the templates.

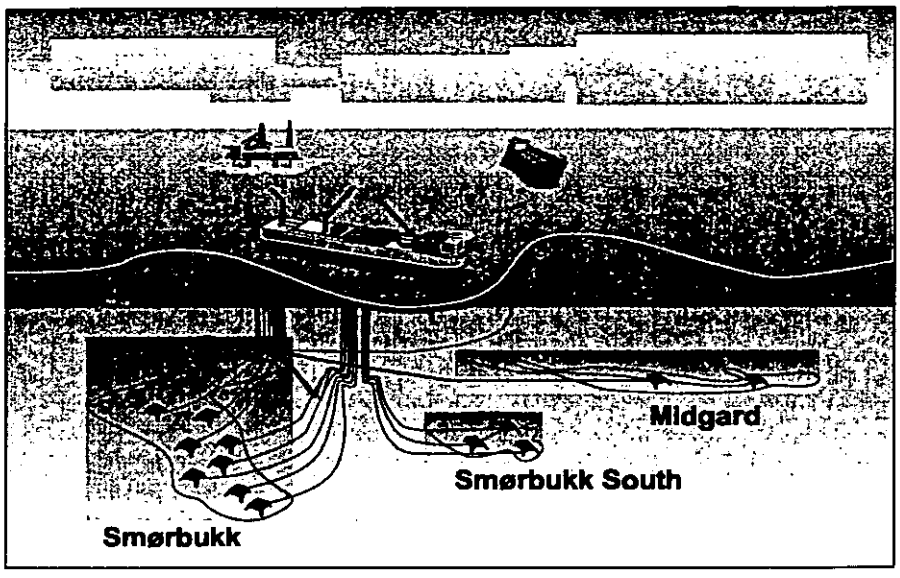

Two production flowlines will connect each template to the production units. Each template consists of four producing wells. Each of the wells can be routed to each of the two flowlines. Well testing without using multiphase meters must be done by testing one well through one flowline. This implies reduced production during the testing period due to increased pressure drop caused by three wells producing through the second flowline.

Using multiphase meters installed on each well has the following advantages:

- No production loss during well testing.
- Extended/increased production from low pressure wells due to increased availability of the test separator for production purposes.
- Immediate detection of water – or gas breakthrough.
- Improved recovery due to continuous well monitoring.

The Åsgard Project (PETEK) has calculated the added value (NPV) to be NOK 300 million by using subsea multiphase meters on each well. Based on this initiative, one subsea multiphase meter has been purchased for each production well at Smørbukk and Smørbukk South reservoirs amounting totally to 28 multiphase meters.

The start-up is scheduled for late 1998.

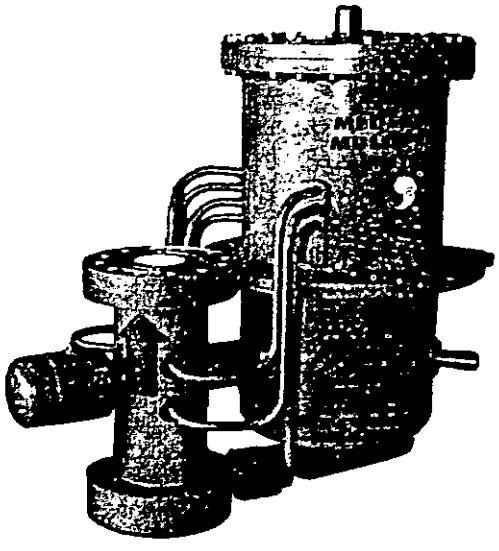

Subsea meter to be installed at the Åsgard and Gullfaks Satellite fields

THE GULLFAKS SATELLITES PROJECT

This project includes developing three different oilfields (-Gullfaks South - Rimfaks and –Gullveig-) by subsea completions tied back to an existing platform (-Gullfaks A-) for production purposes. The complete field development will consist of 8 subsea templates with a total number of 18 production wells.

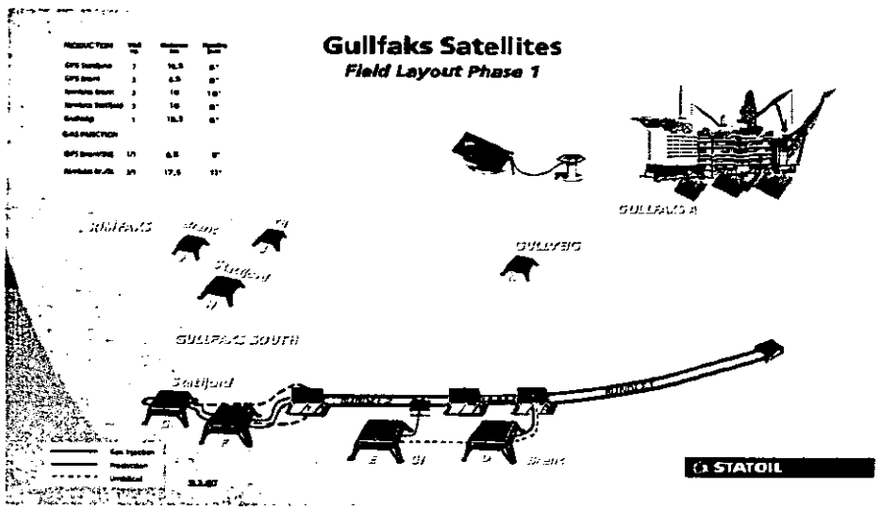

The current test separator on Gullfaks A does not have the capacity to also test the Gullfaks Satellites wells in addition to the platform's existing wells. The existing wells require the test separator 20 days per month for well maintenance and test purposes. The Satellites need the test separator for deduction testing and caused by the long stabilisation period, they need access to the test separator 18 days per month. To increase the well testing capacity on the platform, two differently sized multiphase meters are installed in series with the existing test separator. These will be used for testing Gullfaks As wells. By using two differently sized meters, one has achieved an increased operating envelope to cover both large and small producing wells.

For continuous reservoir monitoring purposes of the Gullfaks Satellites, 6 multiphase meters are installed, one on each riser from the satellites.

Multiphase meters eliminate the need for an extra test separator on Gullfaks A, which might cost some NOK 60 million. The cost of installation and integration of eight multiphase meters in the PCDA system is estimated at NOK 20 million. In this case, the added value (NPV) will be about NOK 40 million.

The installation of a multiphase meter instead of a test separator will most likely reduce the maintenance costs considerably each year, as an extra benefit.

The commissioning schedules for the meters on this projec are as follows:

- Gullfaks A: 2 topside meters in series with the test separator, start-up late 1997.
- Gullfaks Satellites: One topside meter on each riser, totally 6, start-up late 1998.
- Gullfaks Satellites: 2 subsea meters, start-up in1999.

In addition, Statoil considers installing subsea meters on all wells after start-up of the Gullfaks Satellites field.

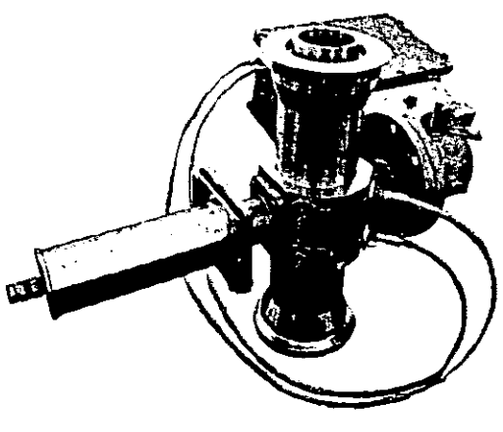

Multiphase meter installed tops on Gullfaks Sat.

TEST RESULTS

Some results from a long term test of an MFI MultiPhase Meter in 1997 are presented in the following. The results are from a topside version that has been continuously in operation since 1/12-1996. During the commissioning, the meter was calibrated against the test separator on Gullfaks B. Since then the meter has been regularly tested using the same test separator.

Fig.1 confirms that the multiphase meter can handle considerable flow rate variations. The meter maintains the accuracy compared with the test separator when well B-29 was choked down (3 April).

Fig 2A shows an unusually large difference between the test separator and the multiphase meter in some tests.

The gas-oil ratio (GOR) is normally very stable for this type of well and by multiplying the test separator's oil figures with a GOR of 85, a new gas curve is created. This curve comes up very close to the figures of the multiphase meter and indicates that the test separator on Gullfaks B sometimes has problems with the gas measurements (+/- 10%)

Fig 2B and C confirm good results and long term stability compared with the test separator's oil and water measurements (+/- 2-3% repeatability)

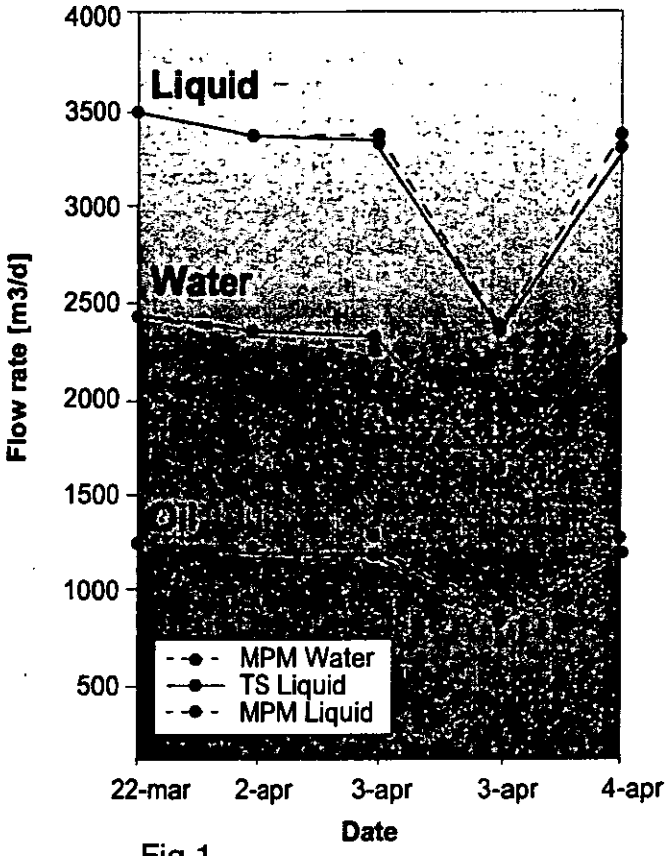

Fig.1

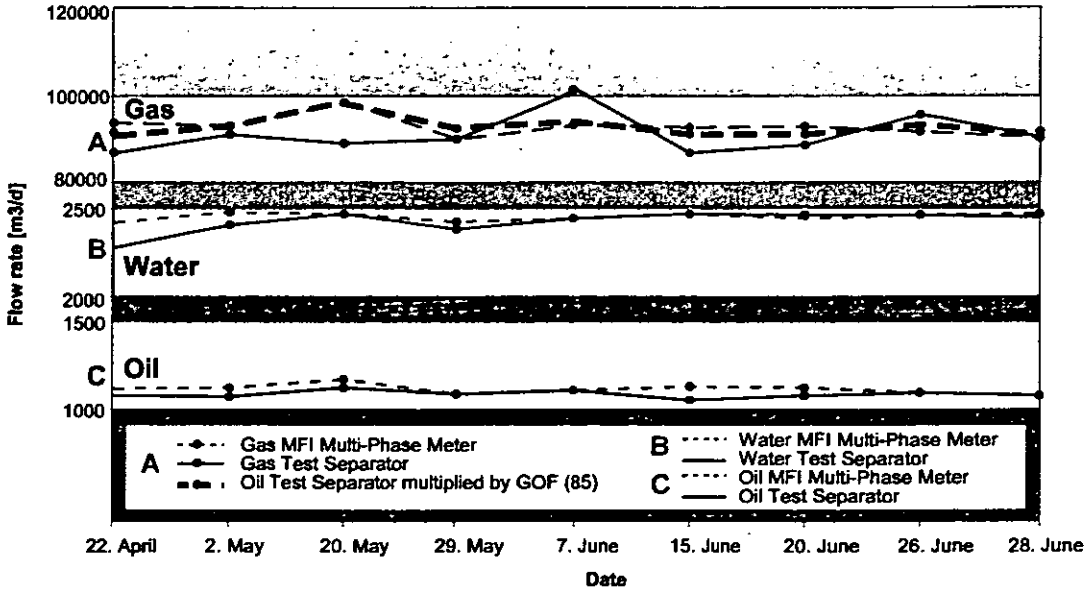

Fig.2 A-B-C

REFERENCES

- Tore Bratten & Bjørn Pedersen: `Multiphase Meters on the Gullfaks Satellite Project`. Multiphase Metering Conference 12th/13th March 1997, Aberdeen, Scotland.

- Harald B. Danielsen: 'Bakgrunn for valg av allokerings- og målingskonsept for Gullfaks Satellitter'. Norwegian Society for Oil and Gas Measurement's 'Temadag', Bergen, 21/3-1996.

- A. Mazzoni and Å. Bringsvor: 'MFI MultiPhase Meter verification at the AGIP Trecate Test Loop'. North Sea Flow Measurement Workshop 96', Peebles, Scotland.

- H.O. Hide, R. Wium: 'Subsea MultiPhase Meter'. Subsea 96' Conference, London December 96'.

- O. Økland, H. Berentsen, G. Flakstad, S.A. Kjølberg, H. Moestue: 'The Norwegian test programme for qualification of multiphase meters'. North Sea Flow Measurement Workshop 95'. Lillehammer, Norway.

- O. Økland, H. Berentsen, J. Bruun-Olsen: 'Multiphase Meters, Ready for Field Applications: Results from full scale qualification testing.' 27th Annual Offshore Technology Conference 95'. Houston, Texas.

- O. Økland, H. Berentsen: 'Using the MFI MultiPhase Meter for well testing at Gullfaks B'. North Sea Flow Measurement Workshop 94', Peebles, Scotland.

NSFMW.97

North Sea FLOW Measurement Workshop

Paper ~~5~~: 1·5

X-RAY VISUALISATION AND DISSOLVED GAS QUANTIFICATION: MULTIPHASE FLOW RESEARCH AND DEVELOPMENT AT NEL

Authors:
Andrew R.W. Hall and Anne E. Corlett, NEL, U.K.

Organiser:
Norwegian Society of Chartered Engineers
Norwegian Society for Oil and Gas Measurement
Co-organiser:
National Engineering Laboratory, UK

X-RAY VISUALISATION AND DISSOLVED GAS QUANTIFICATION: MULTIPHASE FLOW RESEARCH AND DEVELOPMENT AT NEL

Andrew R.W. Hall & Anne E. Corlett
National Engineering Laboratory, UK

SUMMARY

NEL is actively investigating new techniques for the measurement of multiphase flows. This paper describes two such investigations, an X-ray system to visualise three-phase flows and a manometric/volumetric system to quantify the dissolved gas content of oil/gas flows.

The X-ray system was used in both horizontal and vertical flows, covering slug, annular and bubble flow regimes. Also covered were stratified (horizontal only) and churn (vertical only) flows. The system was able to provide visualisation of features not visible in flows with low water cut (due to poor light transmission through oil) and therefore increased the understanding of three-phase flow behaviour.

Quantifying the amount of dissolved gas within a hydrocarbon oil is of importance to the oil industry due to the problems associated with the artificial decrease in density of a gas filled oil and the effects of gas breakout. The present study found that the gas uptake by the oil was highly dependent on the following factors; volumetric gas fraction, line pressure and liquid flowrate. The underlying water cut of the oil also appeared to have an effect.

X-RAY VISUALISATION OF THREE-PHASE FLOWS

INTRODUCTION

The X-ray visualisation system provides imaging of flow patterns through a section of pipe using the principle of simultaneous radiographic imaging in two orthogonal directions, using X-ray sensitive linear array detectors. The data from each linear array detector is read out at high speed to provide time-dependent information on different flow patterns.

The system can discriminate between all three phases (gas, water and oil). Dual energy X-ray data, combined with the use of a dopant (zinc sulphate) in the aqueous phase is needed to achieve adequate discrimination between the two liquid phases, which have similar X-ray attenuation characteristics. Facilities are also provided for imaging of any two of the three phases, using single-energy X-ray data. The key role of the system is to match one flow pattern against a previous one by visual comparison of the recorded data.

DATA ACQUISITION & PROCESSING

Computer System

The computer system consists of a desktop Pentium IBM-compatible PC, running Windows NT based software. The special-purpose software for the X-ray Visualisation system is accessed from a single icon within the Windows NT user-interface.

The block diagram in Figure 1 illustrates the key components of the computer system, and the interfaces with the overall system hardware.

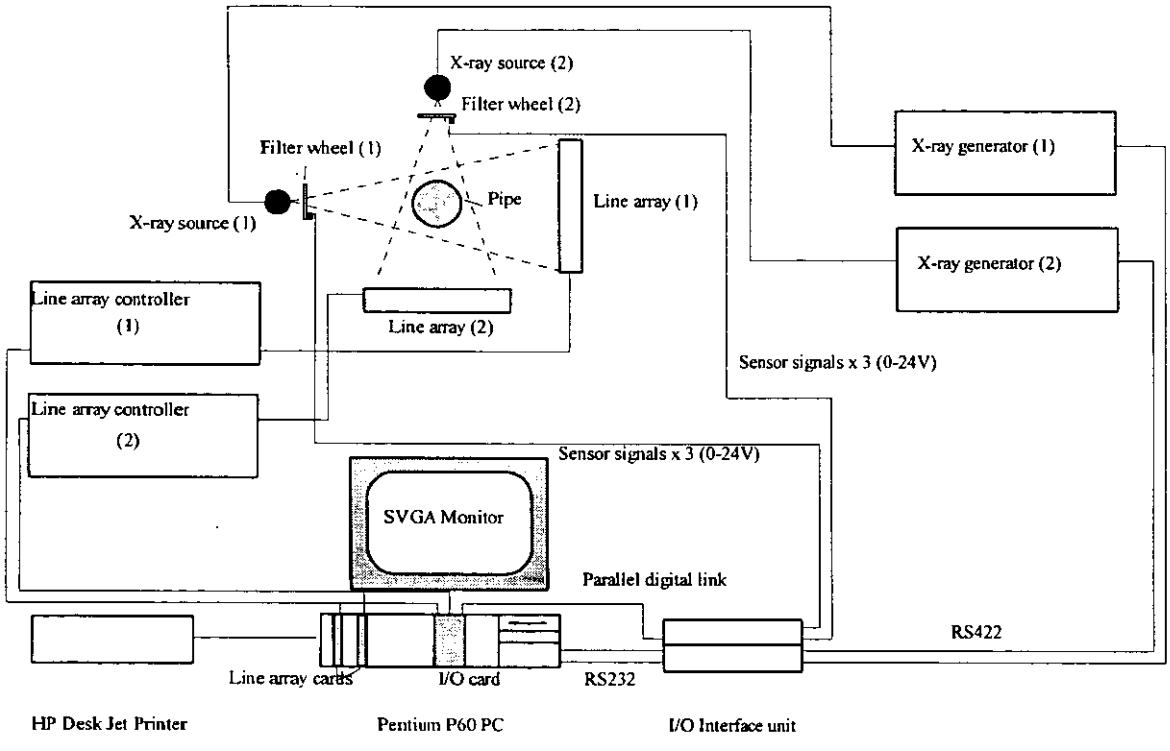

Figure 1: X-ray computer system block diagram

Data Acquisition

The system is provided with two orthogonal line array detectors each with a separate X-ray generator. Figure 2 shows the locations of the two line arrays in relation to the external shape of the X-ray enclosure. Also shown in Figure 2 are the directions in which the data from the two arrays are plotted on the screen. The ends of the arrays marked Top/Right appear on the top of the images for a horizontal pipe and on the right-hand side of the images for a vertical pipe. Similarly, the ends marked

Bottom/Left appear on the bottom of the images and the left-hand side of the images for horizontal and vertical pipes respectively.

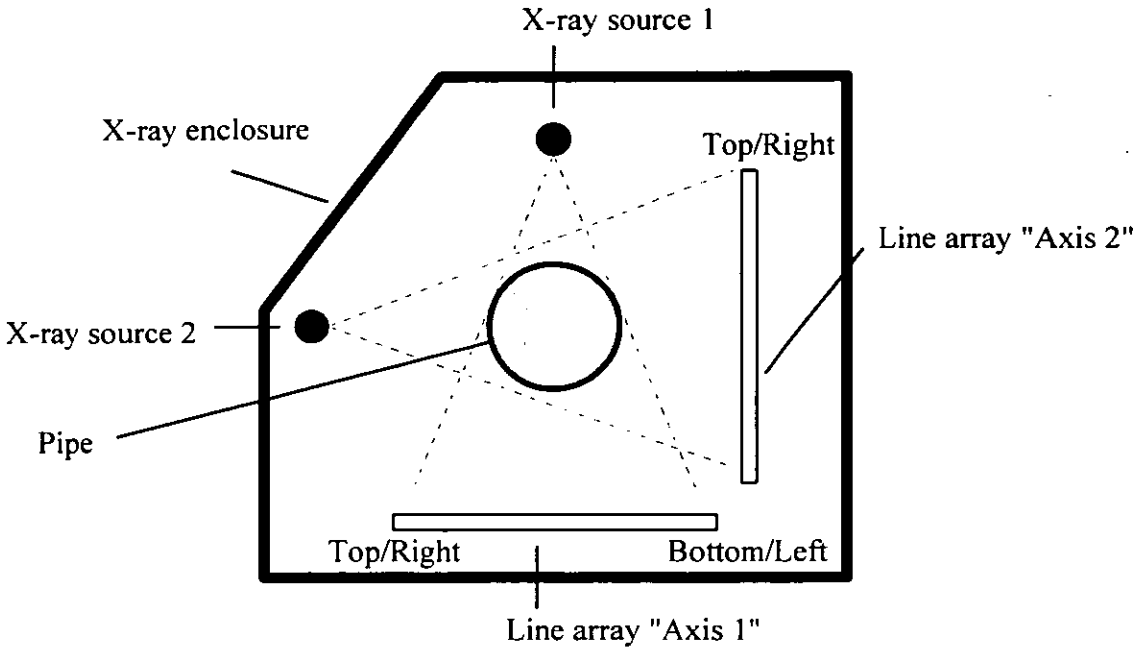

Figure 2: Arrangement of X-ray sources and detectors

In front of each X-ray generator is a rotating filter wheel, with three different sections (opaque lead, air and a sheet of copper). The rotation of the two wheels is synchronised, to prevent cross-talk between the two X-ray beams.

The copper and air sections of the rotating filter allow line array data to be collected at two different effective X-ray energies (hard and soft spectra, respectively) without the need to alter the X-ray supply voltage which could not be accomplished at the necessary speed. This allows three-phase (oil, gas and water) saturation information to be derived at high speed for both of the line arrays.

Data Processing

Time-dependent Radiographic Images

To obtain time-dependent radiographic (attenuation) images, the data from the line array is read out repeatedly, giving time-dependent information on the detected X-ray intensity at each pixel in the line array. This information is shown as a two-dimensional image in which one dimension of the image is the position across the line array, while the second dimension is time.

This allows a moving flow pattern to be visualised.

The data from the line array is presented in a number of different formats. The simplest shows the grey levels from the line array detector, which gives a radiographic image in which the image brightness is related to the intensity of the X-ray beam transmitted through the pipe.

Time-dependent Saturation Images

The line array data can also be processed to produce two- and three-phase saturation information, as follows. For the single-energy line array data, two-phase information (i.e. the relative proportions of two different components, e.g. oil and water, along the line joining each pixel in the line array to the X-ray source) can be calculated. For the dual-energy line array data, three-phase information (i.e. the relative proportions of oil, water and gas) can be obtained.

To calculate saturation (or phase) information, it is necessary to have first recorded calibration information from the line array. This is obtained first by measuring the gain and offset of each line array independently, followed by a calibration of the two X-ray sets and line arrays with the pipe full of gas, oil and then water, with a slow speed rotation of the filter wheel mechanism.

It should be noted that the derivation of saturation information is complicated by the range of energies present in the soft and hard X-ray spectra. For dual-energy X-rays which are monochromatic at each energy, an exact mathematical solution is possible. However, for the continuous spectra of X-ray energies from the X-ray sources, no exact formula can be derived. Instead, the software uses an approximate method, based on an empirical correction method for the effects of "beam hardening". ("Beam hardening" is an effect which occurs due to the energy-dependent attenuation of the continuous X-ray spectra by the pipe contents - the lower X-ray energies are attenuated more than the higher energies, so that the average X-ray energy transmitted through a material increases with material thickness.)

The empirical correction method for the effects of beam hardening requires the use of two numerical parameters, the values of which have been fitted to the particular characteristics of the system. Numerical simulations suggest that the inherent accuracy of this method is typically about ±5%, for the full three-phase calculations, in the absence of random noise on the data.

Thus, using the system the following three types of data can be displayed:

- Radiographic images (i.e. grey levels from line array detectors).
- Two-phase saturation information (relative proportions of phase 1 and phase 2).
- Full three-phase saturation information (relative proportions of oil, gas and water).

RESULTS

Horizontal flow

Figure 3 shows an example of imaging of a three-phase slug flow in a horizontal 4-inch pipe. The flowrates for this image were:

Water	0.279 m/s
Oil	0.196 m/s
Gas	2.26 m/s

The top figure (3a) shows the X-ray attenuation plot for the vertical and horizontal axes (axis 1 and axis 2 respectively). In this flow, separation of oil and water layers occurred between slugs and the oil can be seen clearly as a grey layer on top of the black layer representing the water. The thickness of the oil layer increases with time from the slug tail.

The lower figure (3b) shows the calculated saturation plots. The first two rows show the fraction of water, oil and gas as observed on the two axes, with white representing 100% and black 0% of a phase. The bottom row shows the effect of combining the two axes to give a cross-sectional image which is an average over the 2 minutes data recording period. This shows the water to be dominantly present at the base of the pipe, oil in the central layer and gas in the upper central region.

The software allows the averaging region to be focused in on any time interval to give the cross-sectional information resolved to more detail.

Vertical flow

Figure 4 shows an example of imaging of a three-phase slug flow in a vertical 4-inch pipe. The flowrates for this image were:

Water	0.728 m/s
Oil	0.258 m/s
Gas	1.96 m/s

Again the top figure (4a) shows the X-ray attenuation data and the bottom figure (4b) the saturation data. In this flow condition, the flow observed consisted of 'plugs' of liquid alternating with a long gas bubble / churning region. The liquid plugs correspond to the dark regions on the attenuation plot and the churn regions to the greyer areas.

The oil and water were well-mixed and this is shown on the saturation plots (this type of saturation plot is very typical of those observed in vertical flows). The right hand column in figure 4(b) shows the cross-sectional averages of water, oil and gas fractions, which indicate a very low average liquid fraction and a large gas core. (The

eccentric position of the gas core resulted from a slight misalignment of the X-ray instrument with the vertical test section).

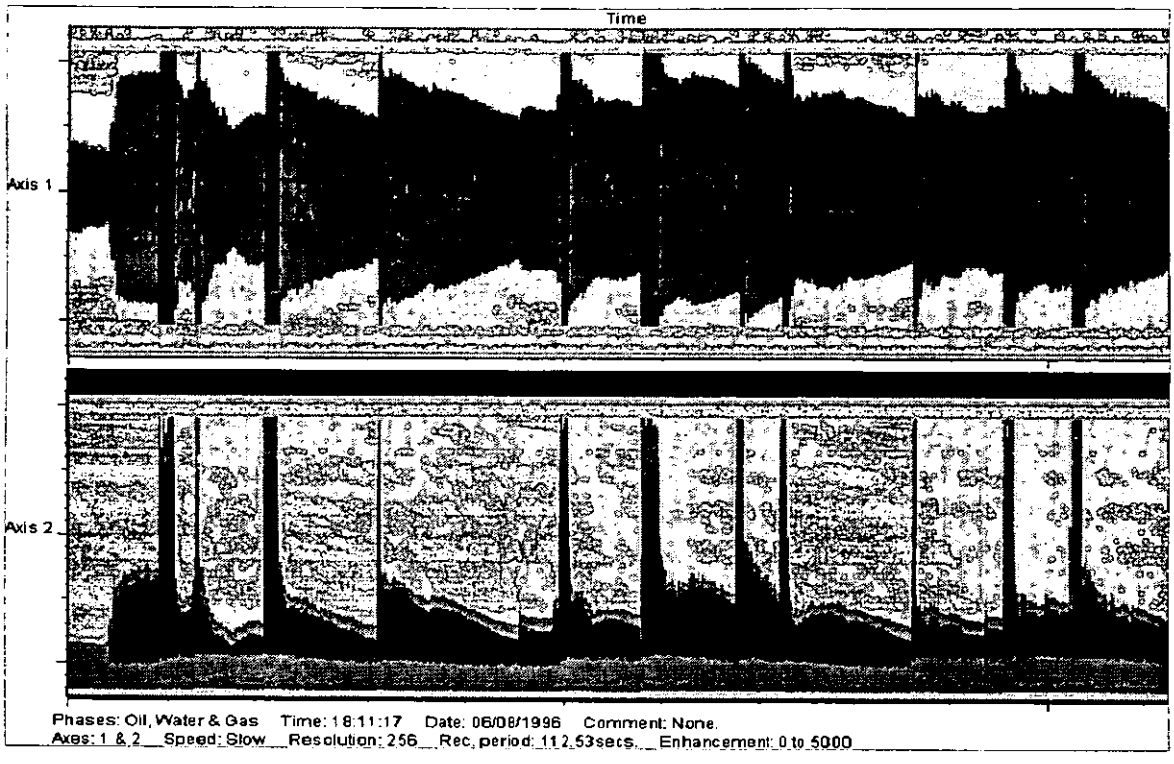

Figure 3(a): X-ray attenuation plot for horizontal 3-phase slug flow

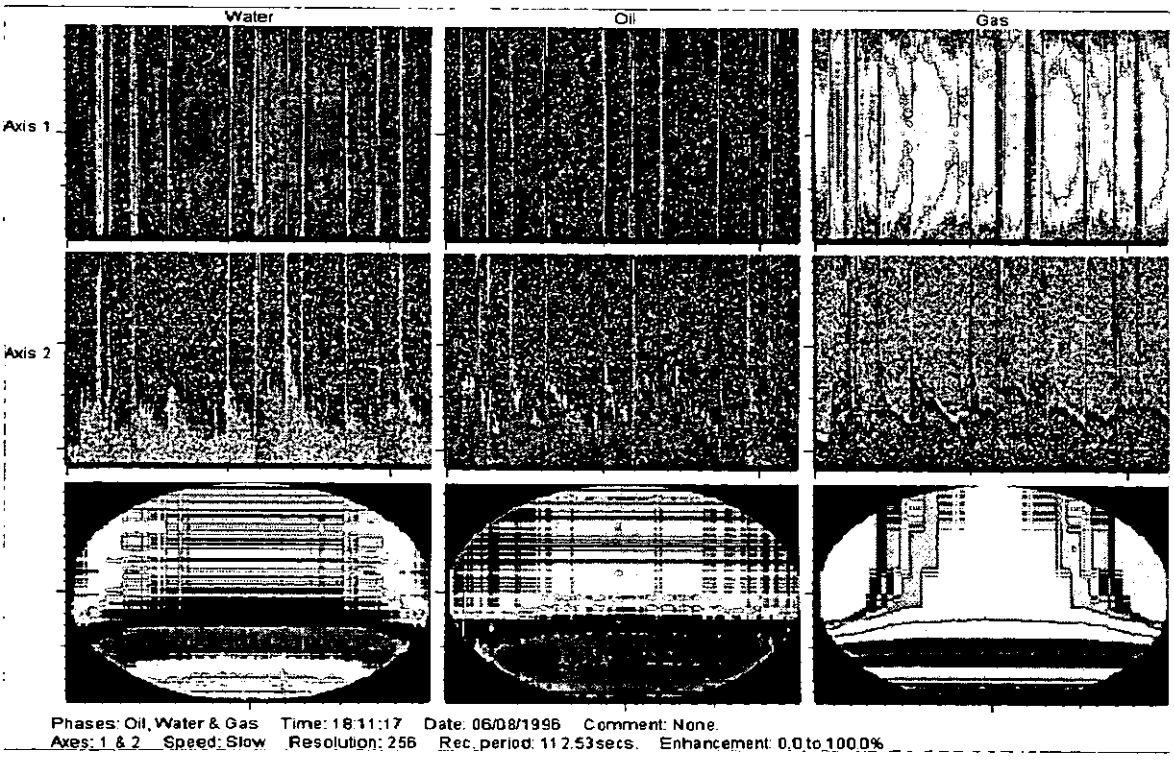

Figure 3(b): X-ray saturation plot for horizontal 3-phase slug flow

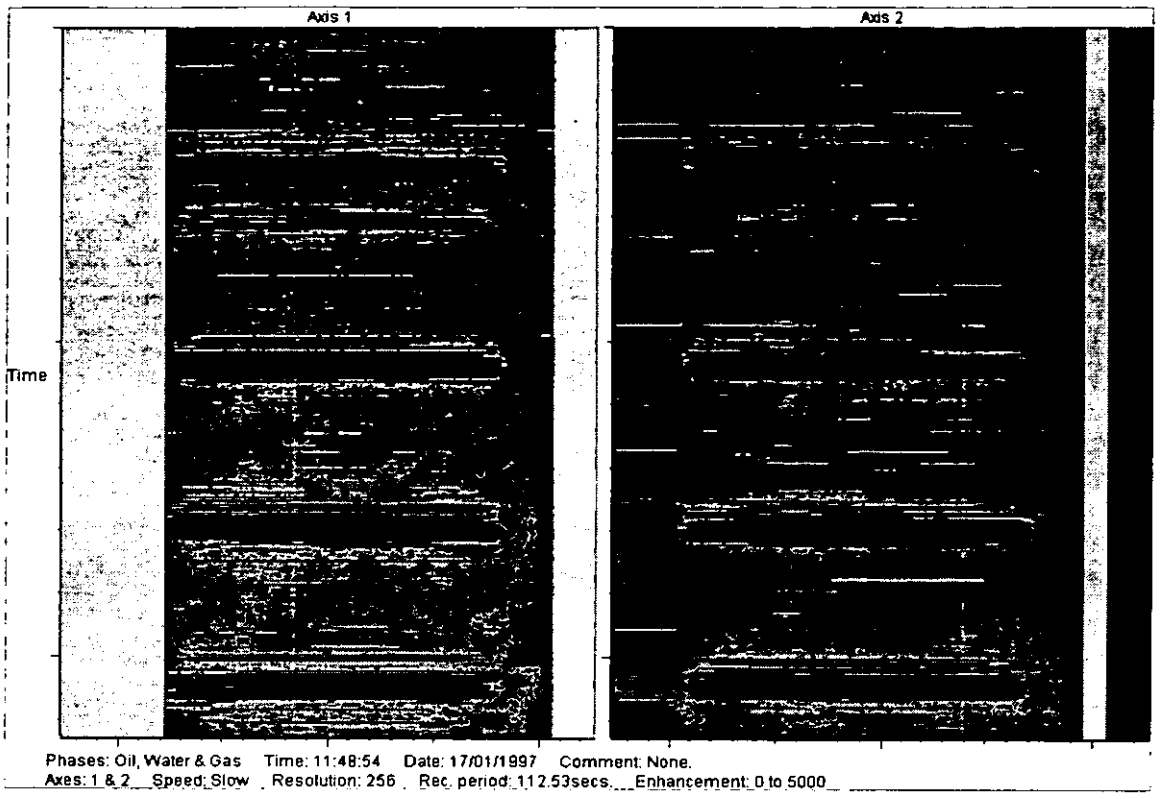

Figure 4(a): X-ray attenuation plot for vertical 3-phase slug flow

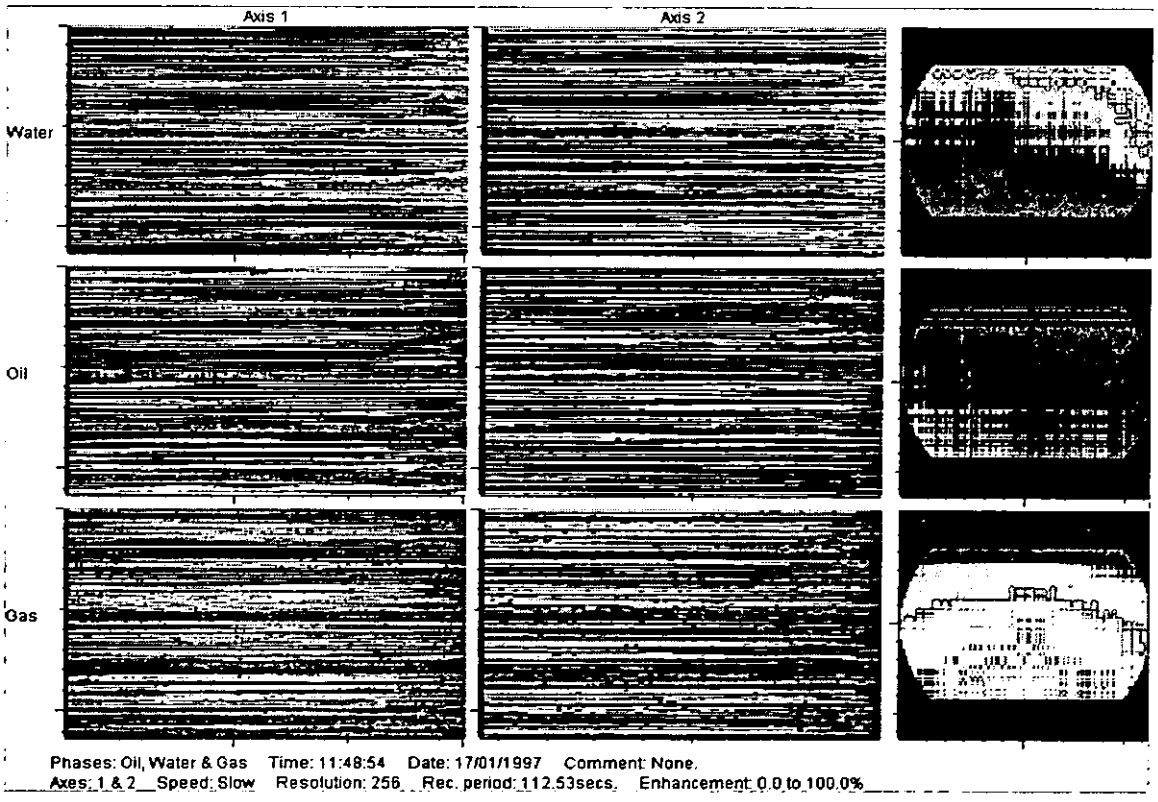

Figure 4(b): X-ray saturation plot for vertical 3-phase slug flow

DISSOLVED GAS QUANTIFICATION

INTRODUCTION

The principle of this study is that the solubility of a gas in a liquid is proportional to the absolute pressure. If a sample of liquid is subjected to a vacuum, the entrained gas is released and so can be measured. The method used to facilitate this measurement is a modification of that of Hayward [1], in which an oil sample was expanded and then compressed. The present method employs a dual expansion technique.

Experiments were performed at a constant pressure of 5 bar and with a mixture of crude oil and nitrogen. The gas volume fraction was changed to investigate the effect of this parameter on the gas absorption of the oil. The volume fractions at which the data points were taken were repeated using oil with a higher water content. Further data points were taken at lower pressures in order to analyse any effects due to a change in line pressure. Static experiments were performed also in which oil was poured directly into the sampler.

THEORY

The gas content of a liquid, α, is defined as

$$\alpha = \frac{100\, V_{gas}(T_{STP}, p_{STP})}{V_{liq}} \qquad (1)$$

where $V_{gas}(T_{STP}, p_{STP})$ is the volume of gas evolved at standard temperature and pressure, T_{STP} and p_{STP} are the absolute temperature and pressure corresponding to conditions of standard temperature and pressure, 273.15 K and 101325 Pa respectively and V_{liquid} is the volume of the liquid sample. If a dual expansion procedure is executed, using Henry's Law, the value of α can be calculated as follows,

$$\alpha = 100\frac{\left[(p_1 - p_2)/p_{STP}\right](T_{STP}/T)\left\{\left[V_1 + V_{prtr}(T/T_{prtr})\right]/V_{liq}\right\}(1 + p_{gas2}/p_{line})}{\left\{-n - \left[(p_{gas1} - np_{gas2})/p_{line}\right]\right\}} \qquad (2)$$

where

p_i: pressure after ith expansion
p_{line}: line pressure
p_{gasi}: $p_i - p_{vac}$
p_{vac}: pressure after manometric system has been evacuated
n: expansion ratio from first to second deaeration chambers
V_1: volume of first deaeration chamber and associated pipework
V_2: volume of second chamber and associated pipework
V_{prtr}: volume of pressure transducer

T: ambient temperature
T_{prtr}: temperature of pressure transducer

METHOD

Figure 5 shows the apparatus used to perform the present experiments. It consists of a sampling system to remove a known volume of liquid, free of gas bubbles, from the flowline and a manometer system to perform the dual expansion. In the figure, valves are labelled as 1 to 5 and A and B are the expansion cylinders. The apparatus was positioned in the multiphase loop at NEL, approximately 25 m downstream of the gas injection point.

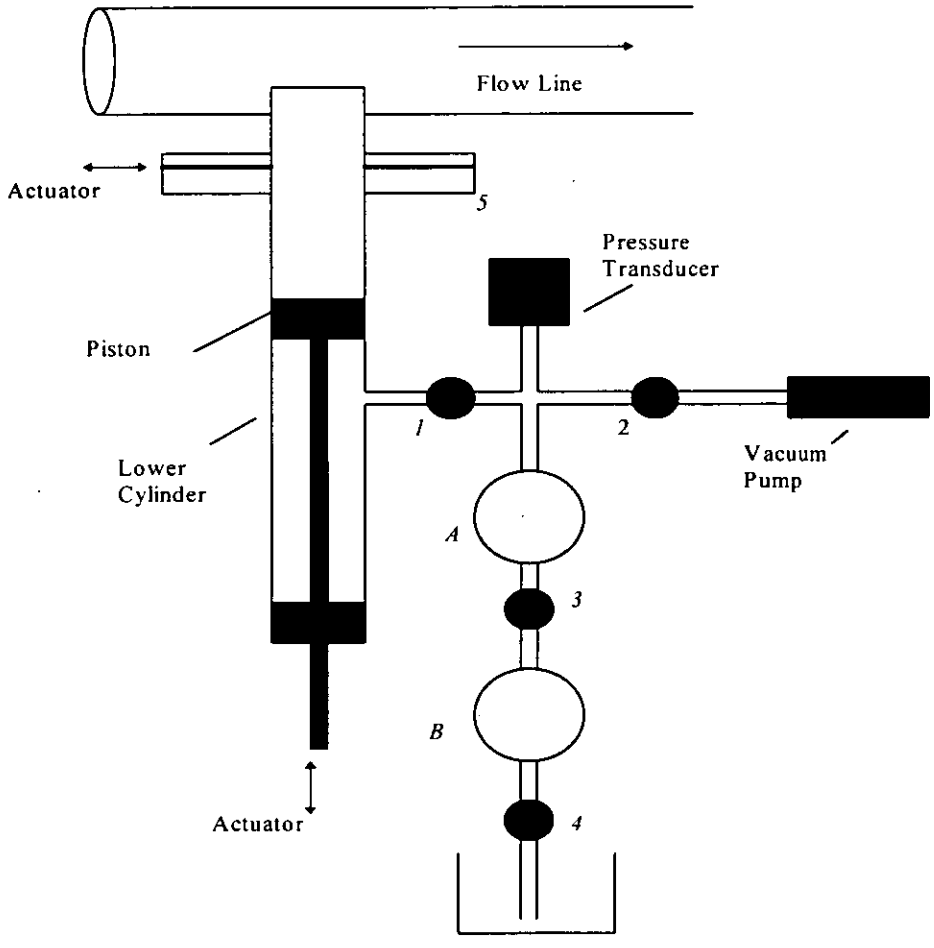

Figure 5: Schematic diagram of sampling and manometric systems

Prior to sampling, valve 1 is shut and the manometer evacuated. To take a sample, valve 5 is opened and the piston slowly lowered. It is essential that the sample is withdrawn slowly, in the order of 30 s, to ensure that bubbles are not drawn far below the neck of the tube. Valve 5 is then shut and valve 1 opened to allow expansion in to the first cylinder. Once the pressure is stable, valve 3 is opened and the liquid is

expanded in to the cylinder B. Three observations of pressure, that of the initial vacuum and after both expansions, together with the ambient air temperature reading are used to calculate the gas content α as described in the previous section.

Initial results indicated that the system design is such that a time of greater than ten hours is necessary for the first expansion. However, the majority of the gas appears to come out of solution within an hour of the second expansion. Hence the sample was left overnight for the first expansion process and an hour for the second.

RESULTS

Variation of α with Gas Volume Fraction

The gas content of the oil is highly dependent on the gas volume fraction (G.V.F) of the flow.

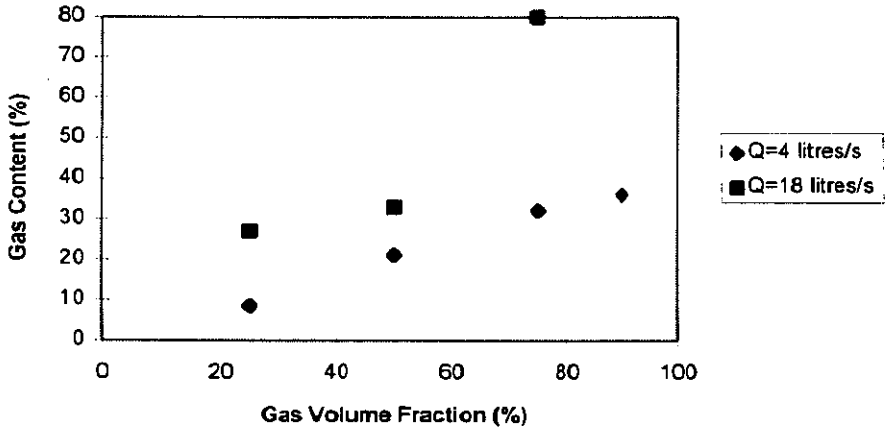

Figure 6: Variation of α with gas volume fraction at 3% water cut

Figure 6 shows that in an oil with a low water cut (3%), the value of α increases as the percentage of gas within the flow increases. This occurs at both the liquid flowrates investigated. It is also clear that for a given gas volume fraction (G.V.F), α increases if the liquid flowrate is increased from 4 litres/s to 18 litres/s.

If the water content of the oil is increased, although the general trend of increasing gas content with G.V.F is continued, the value of α at a particular gas volume is decreased. This can be seen in Figure 7 . For example, at a G.V.F value of 90%, α has a value of 19% as compared with 36% in Figure 6. The flowrates within this figure are 3-4 litres/s.

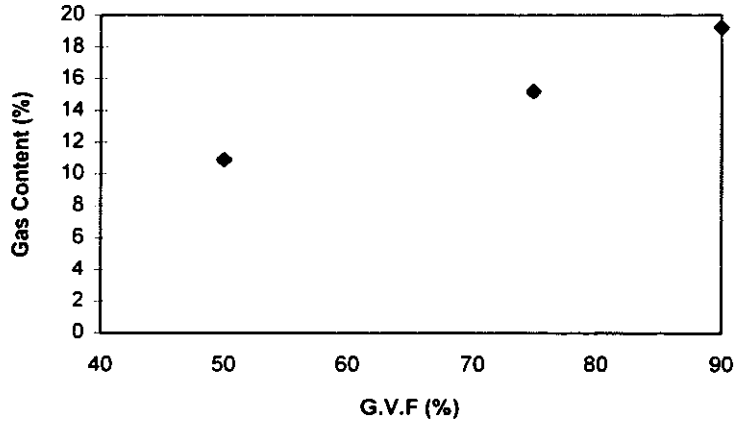

Figure 7: Variation of α with gas volume fraction at 12% water cut

Variation of Gas Content with Line Pressure

Three experiments which were performed at a line pressure lower than 5 bar. The results are shown in Table 1. The flowrates for this data were between 4 and 6 litres/s and the water cut was 3% for the points at 2 bar and 6% at 0.6 bar.

Table 1: Effect of line pressure on the gas content of the oil

P_{line} (bar)	G.V.F (%)	α (%)
0.6	95	9.0
2	90	13.4
2	75	4.3

Although the gas volume fraction for the point taken at 0.6 bar is slightly higher than that at 2 bar, there is a considerable difference in the value of α which is larger than the estimated uncertainty (approximately 6%). The value at 2 bar is lower than that found at 5 bar. When the gas volume fraction is decreased, the value of α decreases also, consistent with previous trends, but the value itself is lower than that at 5 bar. This indicates that line pressure significantly affects the gas absorption by the oil; the greater the line pressure, the higher the gas content of the oil.

Static Tests

Samples of crude oil were left in trays to become saturated with air. This technique was found by Hayward [2] to be the easiest method for air absorption. Two samples of oil were used in these tests, one had been left for several weeks (Oil I) and the other for two days (Oil II). The oils were then poured into the top of the sampling tube, the ball valve shut and the rest of the experimental procedure continued. The corresponding values of gas content for these two oils are as follows

Oil I: $\alpha = 3.5\ \%$
Oil II: $\alpha = 2.3\ \%$

The difference in the two values may be either the result of experimental error or that two days was insufficient for the oil to become fully saturated with air. These values do not correspond to those found by Hayward [2] for a variety of air saturated oils. He found that, on average, α had a value of 8 % at atmospheric pressure. A possible reason for this disparity is that the depth of the tray in the present experiments may have been too large for the bulk of the oil to become saturated with air. Thus the above values of α may correspond to oil with only surface saturation.

CONCLUSIONS

X-ray Visualisation

Imaging of three-phase flows using X-ray attenuations has been successfully demonstrated using this system. The flow structure can be resolved in some considerable detail, with the greatest success in horizontal flows.

Gas Quantification

A dual expansion volumetric/manometric system can be used to calculate the dissolved gas content of a hydrocarbon oil. The value of dissolved gas content, α, increases as the gas volume fraction increases. Results also indicate that α depends on the line pressure at which the tests are conducted and the background water content of the oil.

ACKNOWLEDGEMENTS

The work described in this paper was funded by the Flow Programme of the UK Department of Trade & Industry.

REFERENCES

1. HAYWARD, A.T.J., "Two new instruments for measuring the air content of oil", Journal of the Institute of Petroleum, 47(447), 99 - 106, 1961

2. HAYWARD, A.T.J., "The air-solubility of hydraulic oils", NEL Report 53, 1962

NSFMW.97

North Sea FLOW Measurement Workshop

Paper 6: 1 · 6

MEASUREMENT STRATEGIES FOR DOWNHOLE MULTIPHASE METERING

Authors:
Erling A. Hammer, Geir Anton Johansen, Jarle Tollefsen and Eirik Åbro
University of Bergen, Norway

Organiser:
Norwegian Society of Chartered Engineers
Norwegian Society for Oil and Gas Measurement
Co-organiser:
National Engineering Laboratory, UK

MEASUREMENT STRATEGIES FOR DOWNHOLE MULTIPHASE METERING

Erling A Hammer, Geir Anton Johansen, Jarle Tollefsen and Eirik Åbro
University of Bergen, Norway

SUMMARY

There will be an increasing demand for multiphase subsea and downhole meters in the future. Both at the sea bottom and downhole the flow regimes in the production pipes or in the manifolds at the templates, may differ from the ideal homogeneous mixture. Further, in line mixers should be avoided to reduce pressure drops and maintenance costs.

The next generation multiphase meters will therefore call for flow regime independent and non-intrusive sensor systems. Since all sensor principles used in multiphase flowmeters today are highly dependent on the distribution of the components in the mixture, and thus make the measurement range limited, multi-sensor principles may be the solution to obtain better accuracy for larger ranges of component fractions and applications. Both the capacitance-, conductance-, microwave- and gamma-principles can be used in multi-sensor arrangement to provide cross-sectional information about the component distribution. Hence, the meter can be used at all types of flow regimes and at any position without mixers or separators.

INTRODUCTION

Today's multiphase flow meters either require flow mixing or installation on pipe lines where the flow regimes are known [1]. Some measurement principles are less dependent on the flow regime than others. Helical capacitance electrodes for fraction measurements perform, as an example, better than parallel electrodes when the flow regime varies. Multi-sensor instruments dividing the flow cross section into several smaller measurement volumes, have to the authors knowledge not yet been used in production processes in the oil industry. These instruments have many properties in common with industrial tomographs which have been used in multiphase flow rigs for testing and research purposes.

The multi-sensor principle will, without any doubt, be taken into use in the oil process industry as the reliability of this technology and the demand of more accurate multiphase metering increases. A multi-electrode or a multi-beam instrument can be used to measure the distribution of the liquid and the gas phases at non homogeneous mixtures and thus make the three phase meters independent of the flow regime. This is of particular interest in down hole metering where mixers can not be used and there is a need for flow regime independent meters.

The multi-electrode and multi-beam principle can also be utilized for improving the accuracy of multiphase meters top side or sub sea and thus make it possible to implement three phase meters for allocation purposes. Multi-sensor systems using capacitance- and gamma-technology, are being developed at the University of Bergen. The performance of these methods will be presented and discussed with respect to issues like measurement accuracy, flow regime dependency, reliability and physical constraints concerning installation and use.

HELICAL SENSORS

The problem of flow-regime dependency can, to a certain degree, be overcome using helical sensors (see Figure 1). In order to study the performance of this sensor, a three dimensional mathematical capacitance model has been developed at University of Bergen [2]. The model is based on the "Finite Element Method" (FEM) and Poison's equation. Using this model it is

possible to simulate how the capacitance for different sensors varies with changes in flow parameters including water-fraction, void fraction, permittivity of the flow components, flow regime types and distributions and changes in sensor geometry and design. The model has been verified against measurements on different types of sensors and flow regimes, and the discrepancy between simulated and measured results was less than ±5%.

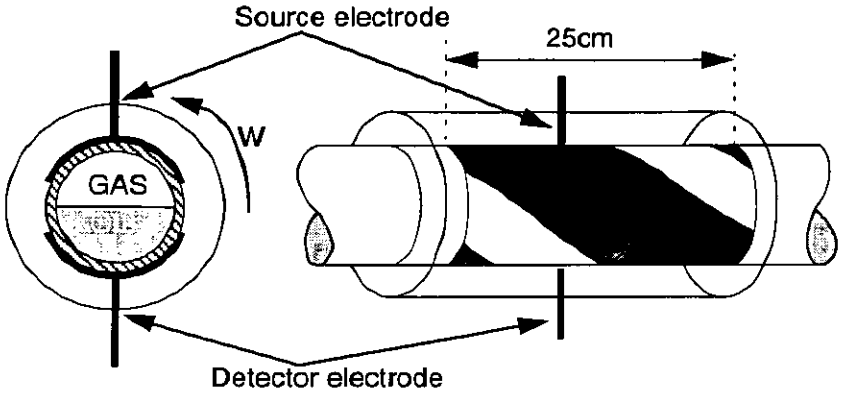

Figure 1. The 180° helical surface plate capacitance sensor configuration.

Figure 2 shows the measured and simulated capacitance characteristics for a surface plate capacitance sensor versus the angle of orientation (W) when the electrodes are straight, 90° helical, 180° helical and 360° helical. The regime consists of stratified air and glycerol at a volume fraction of 0.3.

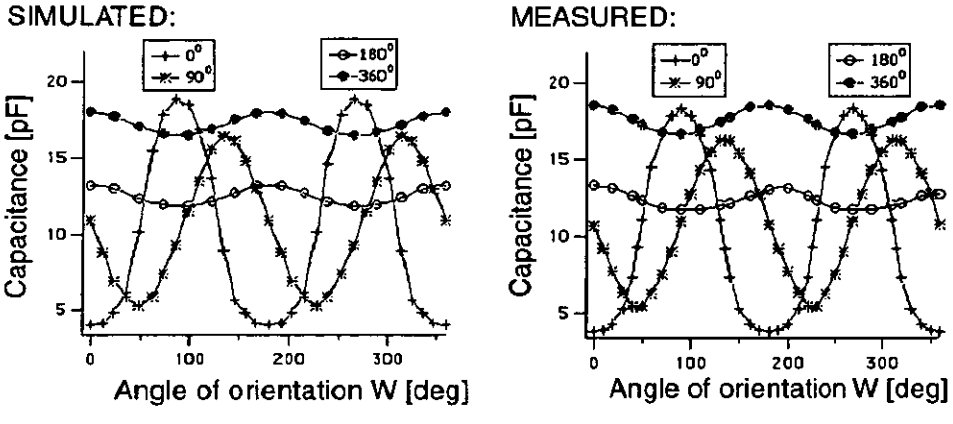

Figure 2. Measured and simulated capacitances versus the angle of orientation (W) of stratified flow for a surface plate capacitance sensor with straight electrodes (0°) and for 90°, 180° and 360° helical electrodes. The components are air and glycerol ($\varepsilon_r \approx 50$) and the glycerol volume fraction is 0.3.

Thus, by calculating the capacitance, using the 3D FEM-model, for a great number of flow regime distributions, at a fixed volume fraction, the flow regime dependency can be estimated. Figure 3 shows some of the flow regime types used in the simulations.

On basis of a large number of such randomly generated flow regimes, as those shown in Figure 3(a) to (d), the flow regime dependency has been estimated by studying the variation in the capacitance characteristics. Based on these simulations the average uncertainty in the measured oil fraction for bubble/churn/slug regimes is estimated to be about ±0.4% of full scale for the 180° helical surface plate capacitance sensor, and about ±4% for the classical surface plate capacitance sensor with straight electrodes.

Thus, the simulations indicate that using a 180° helical surface plate capacitance sensor instead of the classical sensor with straight electrodes, enables reduction of flow regime dependence by a factor of about 10 for gas and oil flows. It is, however, obvious that with annular flow the

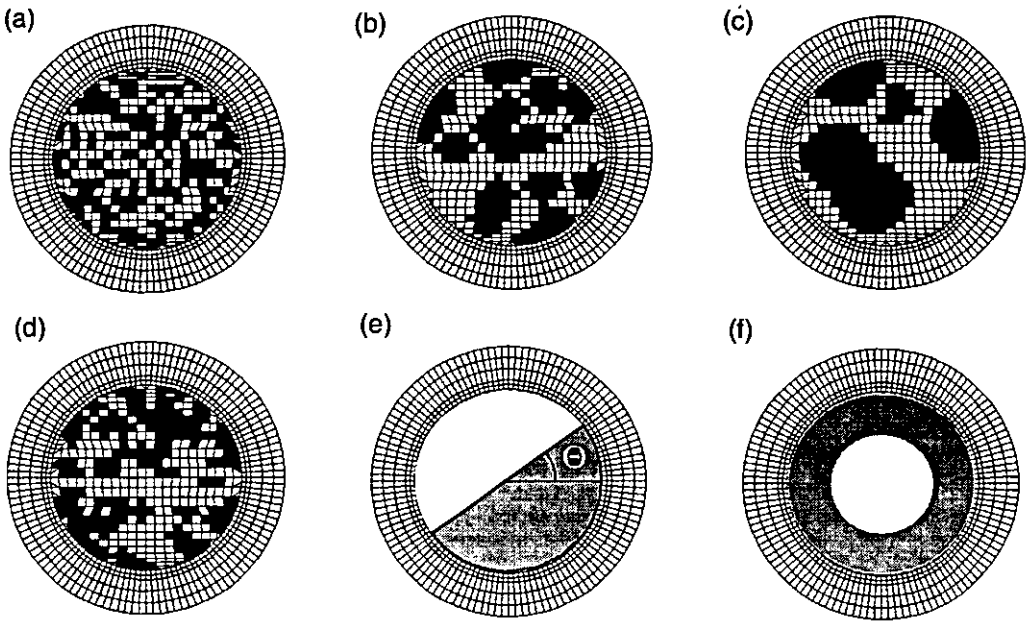

Figure 3. **a)** to **d)** Random generated bubble, churn and slug flow. **e)** Stratified flow where the angle, Θ, varies between 0^{o} and 90^{o}. **f)** Annular flow.

helical sensor and the straight electrode sensor will have the same measurement error. Finally, due to the short circuiting effect neither the helical sensor nor the straight plate sensor can be used at water continuous mixtures.

MULTI-ELECTRODE CAPACITANCE SENSORS

UMIST developed the first multi-electrode capacitance system for imaging of oil and gas in two phase flow [3]. This instrument was further developed by Schlumberger in Cambridge and used for research on two phase flow. A similar system was developed by University of Bergen/ Christian Michelsen Research AS [4]. A sketch of the basic principle of a multi-electrode capacitance system is given in Figure 4.

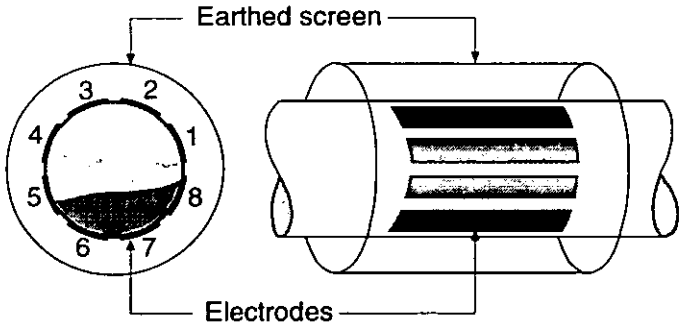

Figure 4. Basic principle of an eight-electrode capacitance sensor system for flow regime identification.

A capacitance image (tomogram) is generated by first measuring the independent capacitances between all the electrode-pair combinations. This is done by exciting the electrodes in sequence. The results of the measurements, which contain information about the dielectric constant distribution inside the pipe, are transferred by a data-acquisition system to a reconstruction unit. This converts, by reconstruction, measurement data to an image of the phase distribution across the pipe cross-section. Several capacitance multi-electrode systems using so-called modified back projection reconstruction algorithms, are in use at the multi-compo-

nent flow rigs at CMR, UiB and Norsk Hydro a.s. Research Centre. Reconstructed images from the multi-phase flow rig at Norsk Hydro are shown in Figure 5.

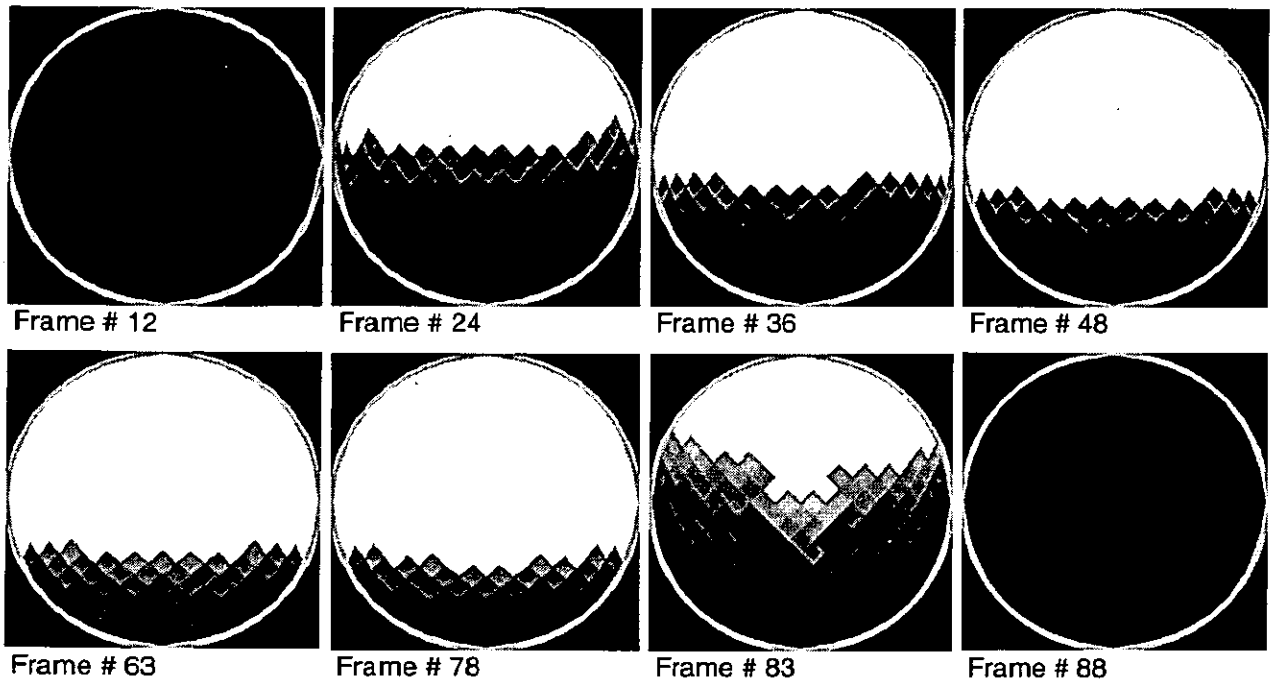

Figure 5. Oil/gas imaging with the eight-electrode capacitance tomograph and LBP-reconstruction at Norsk Hydro a.s. Research Centre [5]. The example shows the propagation of a gas bubble (slug) in horizontal flow. Note that only a few frames of the 2 seconds sequence are shown.

It is important to be aware of that the capacitance multi-electrode system can not be used directly for imaging of the component distribution in the pipe if the mixture is water continuous due to the short circuiting effect caused by the conductive water [6]. However, this effect can be utilized because it contains important information of the flow regime.

In water continuous oil/ water mixtures the electrical conductivity in the mixture will decrease with increasing oil concentration [2]. Resistance tomography based on electrodes in galvanic contact with the mixture can therefore be used to detect the distribution of the oil in the liquid. Resistance tomographs have been developed by UMIST and tested on water continuous liquids [7].

UMIST has also developed multi-electrode impedance system which are measuring both the capacitance and conductance between pairs of electrodes around the periphery of the pipe. These electrodes are uninsulated and in direct contact with the mixture. Uninsulated electrodes can be used as capacitance electrodes as well in oil continuous mixtures. Switching between capacitance and resistance measurements is well known from commercial multiphase meters (Fluenta AS).

The rotating field sensor

One example of use of the multiple capacitance electrode system is the rotating field sensor. In principle, this sensor will work as an helical sensor. Adjacent electrodes are connected together on both side of the pipe in such a way that the electrostatic field will be equal to an ordinary surface plate sensor. By adding one electrode at a time at one side and delete one electrode at the other side of each electrode "plates" the field will rotate and the mean value of one rotation is calculated: The result of this is shown in Figure 6

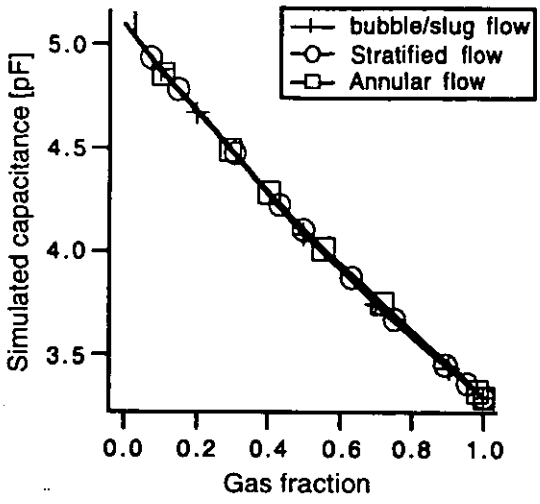

Figure 6. Measured capacitance as function of gas fraction in oil for a 16-electrode rotating field sensor. The mean capacitance is calculated using the finite element models for the electrostatic field distribution at the different regimes shown in figure 3.

The accuracy of this system is calculated to be ± 0.5% of the total range for all the different regimes shown in Figure 3, i.e. a performance comparable to that of the helical electrode sensor.

Rotating field is a simple way of utilizing the information available from multi-electrode sensors. By taking measurement between all possible combinations of the different electrode segments, like in imaging systems, a much more flow regime independent detection can be done.

MULTIPLE BEAM GAMMA-RAY DENSITOMETRY

Gamma-ray densitometry is a frequently applied method for measuring density or component fractions of multi-component flows. A gamma-ray densitometer typically uses a shielded and collimated nuclear isotope on one side of the pipe cross section and a radiation detector system operated in pulse counting mode on the other side (see figure 7). The read-out system consists of an amplifier and filter circuitry where the output pulse amplitude is proportional to the detected radiation energy. The average density, or more correct, the average linear attenuation coefficient of the flow is found by counting the number of transmitted photons in a certain energy window over a period (the integration time). In single energy densitometry this energy window normally covers only the full-energy peak of the desired emission line of the isotope, whereas in multiple energy densitometry several windows and counting circuits are used to cover the emission lines of interest.

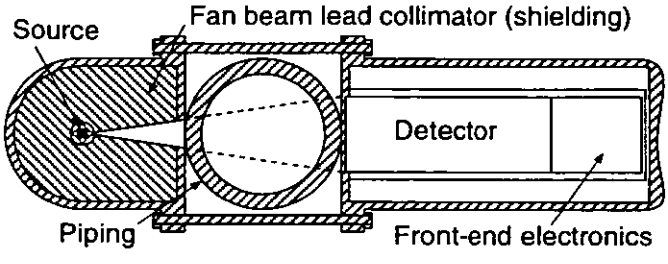

Figure 7. Schematic view of a typical clamp-on gamma-ray densitometer.

Measurements with this type of single beam gamma-ray densitometers are flow regime dependent since the flow cross-section normally is only partially covered by the measurement volume (see figure 7). To cope with this, compensations are made to reduce the measurement

error. These compensations are either based on measurements from other meters, models assuming the flow regime is known, or a combination of these.

The flow regime dependency can be reduced, and practically removed, by utilising a multiple beam system. The feasibility of such a system is demonstrated by a gamma-ray flow imaging tomograph developed by the University of Bergen (UoB) [4]. This instrument uses five radiation sources and 85 compact detectors in an arrangement schematically shown in figure 8. Experiments show that it is possible to do three-component flow regime identification and void fraction measurements at rates several of hundred frames per second with this system, provided the reconstruction unit has sufficient computing power [8].

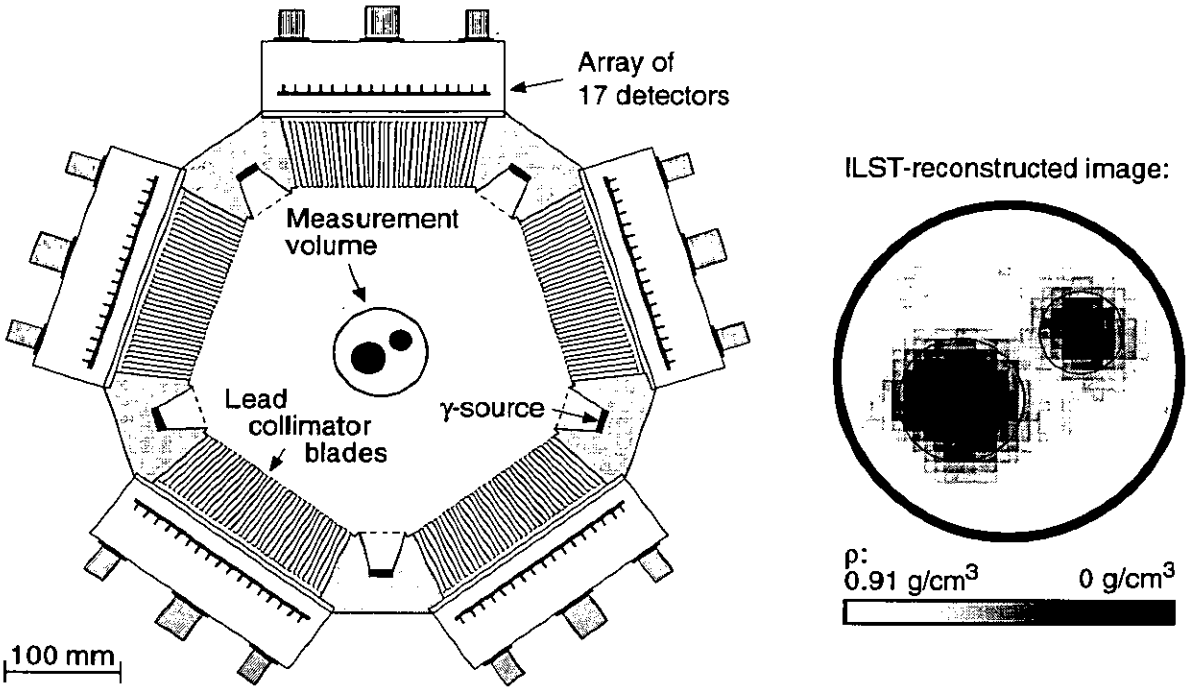

Figure 8. Cross sectional schematic view of the 85-channel UoB gamma-ray tomograph with a reconstructed image of a gas/liquid phantom (where the circles show the true surface position of the gas bubbles).

It should be emphasized that this tomograph is meant for research purposes only, and not as a part of a multiphase meter. It is, however, possible to reduce the number of radiation sources and detectors in comparison to the tomograph, and still be able to identify the flow regime and calculate the void fraction. A system using one source and three detectors embedded in the pipe wall is now being developed and characterized, see figure 9. In order to fully utilize the

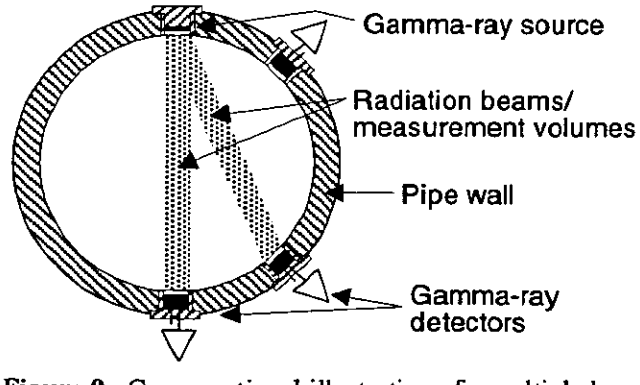

Figure 9. Cross sectional illustration of a multiple beam gamma-ray densitometer using one radiation source.

measurement principle this measures scattered radiation in addition to the transmitted radia-

tion. An experimentally verified simulation model (EGS4) of this densitometer has been developed and used for homogenous, stratified and annular flows. Results with this model show distinct differences in the spectral responses of the detectors for the different flow regimes. These data may therefore be used to identify the flow regime in addition to measuring the void fraction.

Neural networks have been used successfully in the interpretation of simulated data from this multiple beam densitometer. Both flow regime and void fraction were accurately determined for relatively simple flow regimes. One attractive feature of combining neural networks and system models, is that the model can be used to generate training data for the network at different conditions. This, which of course requires accurate (and verified) models, simplifies the use of neural networks which otherwise could be too complex to utilise.

Gamma-ray measurement which are frequently used in other down-hole applications, e.g. lithology and neutron density logging, is known to be a reliable and relatively inexpensive technique. There are several possibilities when it comes to the realization of a multi-beam gamma-ray densitometer: Concerning geometry, several measurement planes (sets of densitometers) may be required, eventually with different radiation energies to allow three component fraction measurements. The integration of source(s) and detectors in the pipe wall is necessary to achieve the desired compactness. This, in turn, calls for compact radiation detectors. One solution may be novel semiconductor detectors where the latest developments have led to substantial improvements in performance and reliability [9, 10]. Dense semiconductor detectors fulfils the efficiency requirement provided low energy sources such as 241-Am (60 keV) are used. This is feasible here since the high penetration capability of clamp-on meters using high energy sources like 137-Cs, is not required. Lower energy is also advantageous from a safety point of view, since the radiated dose from a low energy system is several orders of magnitude less, even with less shielding and higher intensity. The latter is desirable as it is the key to improve measurement accuracy [11].

MULTI-SENSOR SYSTEMS IN MULTIPHASE FLOW METERING

The multi-sensor principle can be used in two different ways to improve the multiphase flow metering:

- By detecting the flow regime in the measurement volume.
- As a multiphase flowmeter

The first method is based upon the fact that if the flow regime is known the measurement results from different sensors used in the multi-phase flowmeter can be corrected according to their flow regime dependency. The second method is much more elaborated and represents new possibilities in multiphase flow metering.

It is necessary to have two independent measurements of the mixture characteristic parameters to determine the fraction of each component in a three component mixture. The two measurements makes two independent equation and the third equation is simply the sum of all fraction in the measurement volume which is equal to one.

For fraction measurement in an oil/water/gas mixture common independent measurements are density and electric permittivity. The density is mainly sensitive to the gas fraction and the permittivity is mainly sensitive to the water fraction in the mixture. Density is usually measured by a one beam gamma-ray densitometer and the permittivity is measured either by two electrode capacitance sensors or by microwave sensors. If the permittivity measurement can be done by a capacitance or microwave multi-sensor system, the permittivity distribution in the

meter cross section, and hence the flow regime, will be known. Thus the gamma-ray measurement can be corrected for flow regime dependent error.

A multiple beam gamma-ray densitometer can be utilized in the same way to make the two-electrode permittivity detector flow regime independent. Some meters are using two energy gamma measurements. This principle is based upon the fact that the attenuation of gamma photons is dependent on the gamma source energy. Using two different gamma-ray energy sources two independent measurements can be done. A single energy gamma-ray densitometer with multiple beams together with a one-beam gamma densitometer using a different energy, can make the instrument flow regime independent and hence the in line mixer can be omitted.

Here, capacitance, resistance and the gamma-ray sensor principles have been discussed, but other sensor principles like microwave-, inductance- and to some extent ultrasound-techniques, can be applied in multi-sensor mode to make the system less flow regime dependent [12].

Down hole multiphase metering

The existing multiphase meters have already been taken into use sub sea, but only for process measurements. There is a demand for using the sub sea multiphase meters for allocation purposes but that can only be done if these meters obtain an increased accuracy. This accuracy will be dependent on the economical balance; i.e. the reduction of installation costs by using sub sea meters in stead of top side separation. It is likely to believe that if the multiphase meters can display an accuracy of ±5% of measured flow rate, these meters will be of great economical interest for the oil production companies.

The necessity of accuracy will be less if the multiphase meters are used only for process optimization or control purposes like in down hole metering. Nevertheless, since the production pipes in a well often are positioned inclined and horizontal the flow regime will be so different from homogeneous mixed regime that it will be necessary to use multiple sensors for multiphase metering. Modern drilling technology has also made it possible to drill lateral wells connected to a common production pipe (see Figure 10).

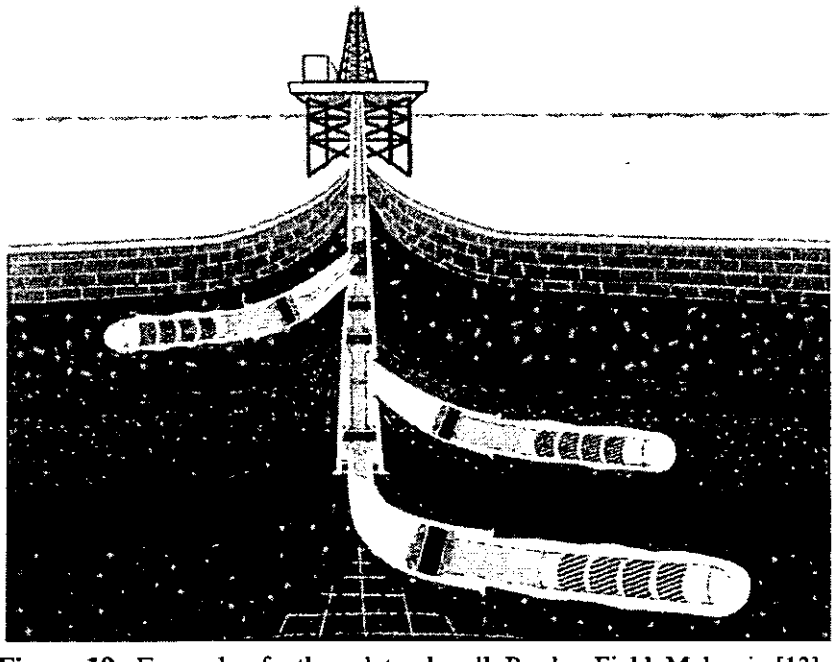

Figure 10. Example of a three-lateral well. Booker Field, Malaysia [13].

The lateral production pipes are either positioned inclined or even horizontal, and the flow regime in these pipes are unpredictable. It is vital for efficient production to measure the con-

tent of the flow in each production pipe. Thus the production can be optimized. (A lateral well that produces mainly water can be shut off; or by reposition the flowmeter, zones producing too much water can be plugged).

The only known technique that can be used for measuring the flow of the different components in the flow regimes, likely to occur in these type of wells, is actually the multi-electrode technique.

A down hole meter must be able to work at high pressure (up to 300 bar), and high temperature (up to 200 °C) and limited space. This, and the requirement of multiple read-out channels, make it necessary to apply micro electronics to obtain the desired compactness and reliability. The maximum temperature for conventional electronic circuits is presently 150°C. At higher temperatures the current leak will increase rapidly. Ongoing research on High Temperature Application Specified Integrated Circuits (HTASIC) [14] has shown that those special designed circuits can operate, and will have an acceptable long-term stability, at temperatures up to 220°C.

This indicates that multi-sensor, multiphase flowmeters can be designed to be used down hole. Capacitance- and resistance electrodes are the less space consuming detectors. An impedance multi-sensor system containing two independent measurements; capacitance and resistance. It might be possible, by using high-frequency detector circuits to develop multiphase flow regime independent meters with the desired accuracy for down hole metering. and a system based on this dual detection will probably give the demanded accuracy for a wide range of component ratios by utilizing the additional spatial information a proper multi-electrode system will give.

CONCLUSON

The latest developments in multi-sensor systems and high temperature micro electronics can be utilized to develop flow regime independent multiphase flowmeters which can be used down hole. Even helical capacitance or conductance electrodes used together with the multiple gamma ray densitometer, using one radiation source, may be utilized in a down hole meter with acceptable accuracy for down whole multiphase metering.

The research and development done so far, within this subject, indicates that the necessary reliability and accuracy can be obtained. The necessary technology is available but the question is: Will the cost of development pay off?

Literature

1. Thorn R, Johansen G A and Hammer E A *Recent Developments in Three-Phase Flow Measurement* Meas. Sci. Techn. **8** (1997) pp. 691-701
2. Tollefsen J *New capacitance sensor principles in flow measurements* Dr. Scient. thesis at University of Bergen (1995).
3. Yang W Q, Stott A L, Beck M S and Xie C G *Development of capacitance tomographic imaging systems for oil pipeline measurements* Rev. Sci. Instrum., **66**, No. 8 (1995) pp. 4326-4332.
4. Johansen G A, Frøystein T, Hjertaker B T and Olsen Ø *A dual sensor flow imaging tomographic system*, Meas. Sci. Technol., **7**, No. 3 (1996) pp. 297-307.
5. Johansen G A, Frøystein T, Hjertaker B T, Isaksen Ø, Olsen Ø, Strandos S K, Skoglund T O, Åbro E and Hammer E A: *The development of a dual-mode tomograph for three-component flow imaging.* The Chem. Eng. Journ. **56**, No. 2 (1995) pp. 175-182

6. Hammer E A, Tollefsen J and Cimpan E *The importance in calculating the permittivity and conductivity in two component mixtures for image reconstruction* Frontiers in Industrial Process Tomography II - Delft, 8. - 12. April, 1997

7. McKee S L, Abdullah M Z, Dickin F J, Mann R, Brinkel J, Ying P, Boxman A and McGrath G *Measurement of concentration profiles and mixing kinetics in stirred tanks using a resistance tomography technique* Mixing, **8**, IChemE Symposium Series No. 136, IChemE, Rugby (1994) 9-16.

8. Frøystein T *Gamma-ray tomography for multiphase pipe flow* (preliminary title) Dr. Scient. (PhD) thesis to be submitted to the University of Bergen.

9. Åbro E and Johansen G A: *Low noise gamma-ray and X-ray detectors based on CdTe-materials.* Nucl. Instr. Meth. **A377** (1996) pp. 470-474.

10. Johansen G A *Recent Developments in Detector Systems for Gamma-ray Tomography* Proc. Frontiers in Industrial Process Tomography II, Delft 8-12 April (1997) pp. 161-166.

11. Johansen G A and Åbro E *Advances In Nuclear Radiation Detectors For Fluid Flow Measurement* IEE C11 Colloquium Digest 96/**092**, 18 April (1996)

12. Hammer E A and Johansen G A *Process Tomography in the Oil Industry - State of the art and Future Possibilities* In press, Measurement+Control (1997)

13. Editorial *World's first isolated tri-lateral well in Booker field* Scandinavian oil-gas Magazine 1/2-1997

14. Førre G, Jakkestad J and Fallet T *HTASIC - et hett tema* Elektronikk **4**, 1994

North Sea FLOW Measurement Workshop

Paper ~~7~~: 2.1

REVISED DTI GUIDELINES FOR PETROLEUM MEASUREMENT

Authors:
D. Griffin, L.N. Philip,
DTI Oil & Gas Office, Aberdeen, UK

Organiser:
Norwegian Society of Chartered Engineers
Norwegian Society for Oil and Gas Measurement
Co-organiser:
National Engineering Laboratory, UK

NORTH SEA FLOW MEASUREMENT WORKSHOP 1997

Revised DTI Guidelines for Petroleum Measurement

D Griffin, L Philp, DTI Oil & Gas Office, Aberdeen

Introduction

The DTI's guidelines on petroleum measurement have been extensively revised and enlarged. The new guidelines cover a much wider scope of measurement situations than before. Included in the new issue is guidance on allocation measurement, well testing, multiphase flow measurement, new technology acceptance procedures and operating procedures for different types of measurement systems.

Significant changes have taken place in recent years both in the way the oil and gas industry conducts its business and in the fiscal regime operated by the UK government. New developments in flow measurement have progressed to such an extent that they have now been adopted by the industry or are close to being adopted as beneficial methods of the measurement of hydrocarbons in whatever form they present themselves for measurement.

The rapid pace of development has left the standards-making bodies behind and in some cases there is insufficient quality data to enable the standards makers to produce guidance of the generic type appropriate for national or international standards.

The case-by-case approach of the DTI in approving methods of measurement lends itself better to consideration of new technology where there may be no existing standards.

These, amongst other considerations, make it appropriate for the DTI to extend the scope of its guidance into these new areas.

The policy developments behind the changes in the new guidelines are not static and this new document has been produced in response to an evolutionary process which is still continuing but it is right to collate and make defining statements from time to time to put on record the current status of measurement requirements for the purpose of attaining DTI approval.

The main changes in the new approach are:-

1. Earlier contact and bringing together of Annex B and detailed engineering design appraisal into a continuous "one stop shop" procedure.

2. Early agreement on purpose and category of measurement with attendant benefits in reducing the amount of work involved in the option screening process.

3. Uncertainty objectives set for each category of measurement system.

4. Options to consider "health-checking" methods rather than elapsed time for periodic verification of system component performance.

In this paper I do not intend to go through the new document clause by clause (you will be pleased to hear) but try to give a flavour of the new guidelines and what we are trying to achieve. A full copy of the new guidelines is appended to the paper so you will all be able to conduct your own review.

In that context I intend that there will be a permanently open file in my office so that any comments, observations or suggestions for improvement can be sent to us at any time. I don't know when the next revision will be issued but the value of having a file of user comments is to help shorten the consultation process at each revision. A contact address is included in the new guidelines.

The Guidelines

In contrast to the previous guidelines [1-3], the new issue is a self-contained document dealing with all aspects of petroleum measurement (liquid, gas and multiphase) as well as operating procedures.

The document is split into 5 main parts:

1. General
2. Liquid Petroleum
3. Gaseous Petroleum
4. Muliphase Petroleum
5. Operating Procedures

Part One, General is a new addition to the previously issued guidance and outlines the area of application of the guidelines, briefly describes the underling regulatory framework, puts into context the purposes for which measurement is required, establishes broad categories of measurement systems, and indicates the documentation required for our review, the reference standard documents of most relevance and their value as underpinning guidance.

Part Two updates the existing liquid document and adds new sections dealing with allocation metering and the use of test separators for reservoir management. Included in this part is guidance for offshore loading fields not attracting field specific taxes.

Part Three broadly parallels the liquid part but is concerned with gaseous petroleum measurement.

Part Four briefly addresses the subject of multi-phase measurement. This is a short part not because there in little to say about multi-phase metering. On the contrary, much new information and data is being produced and digested but a consensus has not yet emerged on how best to write standards or even codes of practice. In the UK and elsewhere evaluation of the technology is proceeding apace. The case by case approach which we use in conventional metering systems is adopted with modifications when considering the use of new technology. I would like to add that the papers and discussions which are such a prominent feature of the NSFMW are the main source of data and information which inform the deliberations of the standards makers. Clearly views on the deployment and use of multi-phase meters are developing along with the maturing of the technology. Our guidance will likewise evolve.

Part Five covers operating procedures for the three process types, liquid, gas, and multi-phase.

As before the guidance contained in the document is intended as representing general minimum requirements for each "class" of metering considered.

The guidance is not intended to stifle innovation and alternative specifications will be considered provided that they can be shown not to result in any diminution of the reliability and accuracy of the measurement. Should a Licensee wish to incorporate novel elements in the design of either

- a proposed new metering station, or
- an existing metering station

the Department may require that the Licensee establish an evaluation programme. The Department may wish to be involved in its design and implementation and in the evaluation of the findings of any such programme.

One of the most important features of the new Guidelines is the introduction of the concept of "Measurement Category". Rather than apply a blanket requirement for "fiscal-quality" metering, The DTI Oil & Gas Office (OGO) now determines the measurement requirements for each field on a case-by-case basis. Among other things, OGO takes account of:

- the fiscal regime in which the field itself lies - does it attract Petroleum Revenue Tax (PRT) or Royalty?
-
- the evacuation route of the metered petroleum - does it form part of an allocation system with PRT/Royalty-paying petroleum?
-
- the petroleum production rate of the field
-
- the field economics

The time allocated to this presentation is quite short and in many ways the new guidance document speaks for itself, so I will conclude by commending the new guidance document as a first attempt tocover the more general aspects of petroleum measurement rather than the previously narrower perspective in the UK of full "fiscal" quality metering. I am happy to answer any questions you may have about the content of the document or the policy changes behind the new approach.

References

[1] DTI Metering Standards for Liquid Petroleum Measurement, Issue 4a, Aberdeen 1994

[2] DTI Metering Standards for Gaseous Petroleum Measurement, Issue 4a, Aberdeen 1994

[3] DTI Approved Metering Stations - Operating Procedures (Liquid Hydrocarbon Measurement), Issue 4a, Aberdeen 1994

Appendix 1

Insert
New guidelines June 5

Department of Trade and Industry

dti

Oil and Gas Office

GUIDANCE NOTES FOR

STANDARDS FOR PETROLEUM MEASUREMENT

Under the Petroleum (Production) Regulations

SEPTEMBER 1997

ISSUE 5

This page is intentionally left blank.

CONTENTS

PART THREE

Gaseous Petroleum

3.1 "Fiscal quality" measurement *(revision of existing document).*

3.2 Allocation, dry gas measurement.

3.3 Allocation, wet gas measurement.

3.4 Utility and fuel gas.

3.5 Flare or Vent Gas Measurement.

3.6 Test separator for reservoir management.

PART FOUR

Multiphase Petroleum

4.1 Allocation.

4.2 Well testing.

PART FIVE

Operating Procedures

5.1 Liquid measurement systems *(revision of existing document).*

5.2 Gaseous measurement systems.

5.3 Multiphase measurement systems.

APPENDICES

Appendix 1 Addresses and contacts.

Appendix 2. Measurement Model Clause.

Appendix 3. Reference Standards.

Appendix 4. Uncertainty Calculations.

PART ONE

General

1.1 Introduction

1.1.1 This document contains guidelines for Licensees and Operators in Great Britain, the territorial waters of the United Kingdom and on the United Kingdom Continental Shelf, for use in the design, construction and operation of metering systems for which the Secretary of State for Trade and Industry's approval is required under the model clause relating to the measurement of petroleum which is incorporated into licences issued under section 2 of the petroleum (Production) Act 1934 and which is reproduced in Appendix 2 (in these guidance notes referred to as "the measurement model clause").

1.1.2 The guidance on "fiscal quality" metering systems is a revision of documents already issued. However the Department recognises that there have been significant changes in recent years both in the fiscal regime and regulatory climate as well as in the way the industry conducts its business. In recognition of these changes this document contains guidance on other categories of measurement systems.

1.1.3 It is intended that the guidance contained in this document should be interpreted as representing general minimum requirements, and relaxation will only be considered in special circumstances. This guidance should not be viewed as prescriptive and alternative specifications to those given in this document will be considered provided that they can be shown to give a similar or greater level of fidelity, accuracy and reliability. It is not intended that adherence to this guidance inhibit innovation, but if a Licensee wishes to use new technology or to deploy existing technology in a novel setting then it will be necessary for the Licensee to provide full justification for his choice. In any case where new technology is proposed the Department may require that the Licensee establish an evaluation programme. The Department will wish to be involved in the design, implementation and evaluation of the findings of any such programme, and may call for independent experts to assist it in this.

1.1.4. In order to assist the Licensee in determining the purpose and selecting a measurement category he should contact the DTI Oil and Gas Office (OGO) at an early stage in the consideration of the development (pre Field Development Plan). Early consideration of measurement requirements will enable the Licensee to complete the screening of options an earlier stage and so minimise the effort in system evaluation. This procedure is intended to avoid the pitfall of the Licensee proceeding with a system design which is unacceptable to the OGO.

1.1.5. The OGO is committed to reviewing the way existing regulations are administered and in the spirit of deregulation will seek to lessen the regulatory burden on industry where appropriate. Taking this and CRINE into account there have been a number of relaxations both in levels of accuracy required from a metering system and in the recertification requirements. These new measures are particularly significant where a field pays neither Royalty nor Petroleum Revenue Tax (PRT) and does not impact on fields which do. The details of these relaxations are given in the relevant sections of this guidance.

1.1.6. Organisation charts for the DTI, Oil & Gas Division and Branch 3, Oil and Gas Office, Aberdeen together with contact addresses and telephone numbers are given in Appendix 1.

1.2 Regulatory Framework

1.2.1. The principle legislation which applies to the oil and gas production industry particularly in relation to petroleum measurement is as follows.

The Petroleum (Production) Act 1934.

The Act vests ownership of the petroleum which exists in its natural condition in strata in Great Britain and beneath the territorial waters of the United Kingdom in the Crown and gives the Secretary of State, on behalf of the Crown, the exclusive right to grant licences to search and bore for and get petroleum. The Act also authorises the Secretary of State to make regulations which, inter alia, prescribe the model clauses for incorporation into such licences.

The Continental Shelf Act 1964

The Act extends the powers conferred by the 1934 Act to the United Kingdom Continental Shelf.

The Petroleum Act 1987

Sections 17 and 18 and Schedules 1 and 2 to this Act amend the measurement model clauses which were incorporated into licences in force at the time it was enacted.

1.2.2. Petroleum measurement is implied by obligations in the licence in addition to those contained in the measurement model clause. This is discussed in paragraph 1.3.3 below.

1.2.3. Where petroleum is delivered to the UK via a pipeline which serves as a common transportation route for a number of fields then the "method of measurement" will include the measurement of petroleum at the terminal serving the relevant pipeline and the allocation procedures used to determine each contributing field's share of the petroleum used at or exported from the terminal.

1.2.4 In order to satisfy the Secretary of State that no unauthorised alterations to the approved method of measurement have been made, officers from the OGO may at their discretion inspect metering systems at any stage from construction through commissioning into production. Throughout the producing life of a field operators may expect that fields liable to pay Royalty or PRT or being co-produced or transported with such fields will routinely be inspected by officers of the OGO on an annual basis. Additional non-routine inspections may be required if circumstances warrant. Fields with no impact on Royalty or Petroleum Revenue Tax (PRT) are liable to be inspected on commissioning and thereafter at the discretion of the OGO on a less frequent basis than Royalty or PRT sensitive fields.

1.3 Purpose for which Measurement is Required

1.3.1 The first task in determining the suitability of a proposed measurement system or systems is to identify the purposes for which measurement is required;

a) where measurements are to account for petroleum won and saved from the licensed area;

b) for other purposes relevant to the licence.

1.3.2 Amongst the most usual purposes under (a) are;

i) To safeguard revenues from Royalty and PRT paying fields.

ii) To allocate terminal out-turns to contributing fields in shared transportation systems.

iii) To account for production of petroleum won and saved from stand alone fields not subject to Royalty or PRT.

iv) To account for petroleum in the form of crude oil, gas or LPG exported from terminals or other export facilities.

v) To allocate production into shared transportation systems from different fields commingled in shared process equipment.

vi) Fuel gas, utilities use and flare gas measurement.

1.3.3 And under (b);

i) To improve understanding of reservoir behaviour to enable effective reservoir management strategies to be implemented.

ii) To establish viability of reservoir as production prospect as for example with extended well tests (EWT).

iii) Flare gas measurement, fuel gas and utilities use.

iv) To account for gas or condensate re-injected into a reservoir for pressure maintenance or conservation.

v) To establish clearly whether a reservoir is no longer economically viable prior to initiating abandonment procedures.

1.4 Categories of Measurement Systems

1.4.1 In this section a number of categories of measurement systems are described along with indications of the accuracy levels to be expected in each of the categories. The list is not intended to be exhaustive or prescriptive but to indicate the broad area of operation of each category associated with a particular purpose. Within each category of measurement there will be scope to vary the detailed method of achieving the measurement objective. The categorisation of a system is agreed between the Licensee and the OGO at the early discussion stage.

"Fiscal quality" measurement

1.4.2 This quality of measurement by industry consensus is ±0.25% uncertainty for liquid (i.e. oil, LPG, condensate) and ±1.0% for gas. These are overall uncertainties and are derived from an appropriate statistical combination of the component uncertainties in the measurement system. The equipment used to achieve this level of performance will vary according to the particular circumstances of each development. The deployment of new technology in this area, while superficially attractive, carries with it in the early phases of its use, the additional problem of establishing confidence in the equipment and the suitability of the recertification procedures.

"Allocation" Metering.

1.4.3 This quality of measurement is usually taken to mean measurement by which a quantity of product which has been metered to a higher standard is attributed to different sources. The quality of measurement needed will depend on whether the contributing sources are in the same fiscal regime, have the same equity, or in

some way influence the measurement of production from fields sharing the same processing or transportation infrastructure. In some cases "fiscal quality" measurement may be the appropriate standard for field allocation. In the case of liquids from fields with differing fiscal status where "fiscal quality" metering is not technically or economically feasible then **continuous** measurement to an uncertainty of ±0.5% to 1.0% would be required and in the case of gaseous petroleum 2.0% to 3.0%, provided that the overall larger uncertainties do not mask significant systematic errors which would introduce bias in the production accounting.

"Allocation" measurement by intermittent methods; "Flow Sampling".

1.4.4 The use of a test separator to allocate field production to individual wells is a long-established method for the purpose of optimising well performance and managing reservoir operations. Industry tends to use the term "allocation by well test" when this method is used to allocate commingled production between contributing fields rather than wells in the same field. To permit the use of a test separator for field allocation it would normally be necessary to enhance the test separator metering capability both in terms of the instrumentation used and in the operating procedures. It is preferred to use the term "Allocation By Flow Sampling" to distinguish between the procedures used for "field allocation" and reservoir management. Target uncertainties for allocation by flow sampling should be of the order of ±5%.

The use of test separators for reservoir management.

1.4.5 This is a well-established method and the expected levels of uncertainty are 5% to 10%. If it is proposed to use the new technology of multiphase metering it would be expected to perform as well as or better than the traditional test separator method. There are at present six or seven leading contenders in the field of multiphase metering but as yet no single instrument can meter the full range of flow patterns and oil/gas/water mixes in every possible combination of concentrations from 0 to 100%. The manufacturers make claims for their instruments which are difficult to verify independently but various claims are made purporting to show equivalent performance to that of test separators. The technology is still at an early stage in its development and there are prospects for significant improvements. A significant problem with the new technology is that the rate of development is so rapid that the various standards bodies both national and international are unable to produce standards or codes of practice on a time scale that would permit early deployment. While the prospects appear good at present for the rapid improvement of this technology to the stage where it will achieve wider acceptance by the industry a watching brief will be kept on the developing situation with a view to issuing an updating addendum in about eighteen months.

Stand-alone Fields loading offshore. (Fields which do not share production or transportation facilities with other fields)

1.4.6 Provided satisfactory procedures can be developed for initial and periodic verification liquid ultrasonic meters may offer a satisfactory solution to the cost effective metering in these circumstances. The target uncertainty for this method would be 0.5% to 1.0%.

Fuel Gas and Utilities

1.4.7 For fuel gas and utilities use the measurement is usually categorised as normal process quality measurement. The measurement uncertainty expected for this class of measurement is 2.0% to 4.0%.

Summary

1.4.8 This approach introduces an element of prescription which has hitherto not been DTI policy. The aim has been to operate the "good oilfield practice" requirement in the regulations on a case by case basis. However by agreeing the purpose for which the measurement is required and assigning a measurement category and target uncertainty at the Annex B stage, the somewhat adversarial approach of earlier years should be eliminated. This will result in the Licensee being able to concentrate on a design that will meet the agreed objective rather than preparing economic and technical arguments to persuade the Department to agree a method which falls short of what is normally described as "full fiscal quality". Although the introduction of an element of prescription into the review process appears at first sight to run contrary to the spirit of deregulation, in practice it should result, through the change in administrative procedure, in a reduction of the regulatory burden on operators.

1.5 Reference Standard Documents

1.5.1 Reference standards commonly used in the oil and gas industry for petroleum measurement are listed in Appendix 3. The standards listed deal by their very nature with established methods and technology and offer no guidance as to best practice in the deployment of new and emerging technologies in the field of fluid flow measurement and allied topics. In relation to published standards in flow measurement it is not intended that Licensees should adhere slavishly to the detailed provisions of the standards but rather to use the standards to guide and inform their discussions with the OGO in arriving at a consensus view as to what constitutes "good oilfield practice" in the specific context of the proposed development.

1.5.2 If a Licensee proposes to deploy a new technology in his proposed method of measurement for which no recognised standards exist then it will be necessary for the Licensee to provide a detailed justification for his choice. This justification may involve the establishment of a programme of tests to evaluate the performance of the chosen equipment. The objectives, design, methodology and acceptance criteria of any evaluation programme should be agreed in advance with the OGO. The OGO should be given the opportunity to witness tests at its discretion. Such evaluation programmes may also be necessary where it is intended to deploy existing technology in a novel setting. The Licensee should consider the inclusion of independent experts in any evaluation programme.

1.6 Documentation Requirements

1.6.1. The Department of Trade and Industry Petroleum Operations Notice (PON) No. 6 contains details of the documentation needed for the OGO to conduct its review of the method of measurement. It is reprinted in Appendix 2.

1.6.2 The production reporting requirements are the subject of a separate operating notice, PON No. 7. This is also reprinted in Appendix 2.

PART TWO

Liquid Petroleum including Crude, LPG, Gas Condensate.

2.1 Fiscal Quality

Mode of Measurement

2.1.1 Hydrocarbon measurements for requirements under the measurement model clause should be either in volumetric or mass units. The choice of measurement should be discussed with the OGO. Volumes should be measured in cubic metres and mass in tonnes (in vacuo). Volume will normally be used for stand-alone field tanker loading operations and mass for multifield pipeline or offshore pipeline with an allocation requirement. The overall level of uncertainty required is ±0.25%.

2.1.2 Where the approved measurement is in volumes, these should be referred to standard reference conditions of 15°C temperature and 1.01325 bar pressure. The metering system should compute referred volumes by means of individual meter temperature compensation and totalisers. Pressure compensation will always be required whether continuously or by a fixed factor determined at each proving as appropriate. Alternative systems giving equivalent results can be considered.

2.1.3 Where the approved measurement is in mass units the established method is by measuring the volume and density. The density should if necessary be compensated to the volume meter inlet conditions and the mass computed as the product of this density and the measured volume, $V_{mi} \times \rho_{mi}$, where Vand ρ_{mi} are volume and density respectively, measured at meter inlet conditions of pressure and temperature. When mass is not $V_{mi} \times \rho_{mi}$ then any factors used in computing metered mass (Q_m) at some other set of conditions should cancel with respect to volume meter inlet conditions. This procedure is unnecessary if mass is measured directly by Coriolis meter.

Meters and Associated Pipework

2.1.4 The meter should generate the electrical signal directly from the movement of the meter internals without any intermediate gearing or mechanical parts. Electronic interpolation systems may be accepted. Although the meters traditionally used for this service are either turbine or positive displacement meters new types are available which if properly installed and operated can deliver similar levels of performance. The main new contender for this category of measurement is the Coriolis meter, but with ongoing developments in the field of petroleum measurement other technologies may be able to perform at the fiscal quality level.

2.1.5 A sufficient number of parallel meter streams should be provided to ensure that, at the nominal maximum design production rate, at least one stand-by meter is available, to maintain a high level of availability. Adequate valving should be provided such that individual meters may be removed from service without shutting down the entire metering system.

2.1.6 Metering stations should have a common inlet header and, if necessary, a common outlet header to ensure uniform measuring conditions at all metering streams, temperature and pressure transducers and density meters. However if product of differing physical properties is produced by separate production trains and is not fully commingled before metering then it may be necessary to have separate measurement of the differing fluids.

Secondary Measurements

2.1.7 Temperature and pressure measuring points should be representative of conditions at the meter inlet and situated as follows:-

(a) In volumetric measurement systems: as close as to the meter as possible without infringing the requirements of the API Measurement Manual.

(b) In mass measurement systems: an additional set of measurements may be required as close to the densitometers as possible.

2.1.8 Temperature measurements that affect the accuracy of the metering system should have an overall loop accuracy of at least 0.5°C, and the corresponding readout should have a resolution of at least 0.2°C. This is equivalent to an uncertainty of approximately 0.05% in CTL. Thermowells should be provided adjacent to the temperature transmitters to allow temperature checks by means of certified thermometers.

2.1.9 Pressure measurements that affect the accuracy of the metering system should have an overall loop accuracy of at least 0.5 bar and the corresponding readout should have a resolution of at least 0.1 bar.

2.1.10 Dual density meters should normally be used and should feature a density discrepancy alarm system. Single density meter systems, where they have been allowed should feature high and low set point alarms. Suitable sampling facilities shall be provided in close proximity to the density meter(s) in all cases. Provision should be made for solvent flushing on systems where wax deposition may be a problem. Densitometers should be installed as close to the volume flow meters as possible and be provided with thermowells and pressure indicators so that it may be demonstrated that there is no significant difference from the volume flow meters' inlet conditions. If this is not the case, temperature and pressure compensation must be applied. If the densitometers are in a recirculation loop then the inlet probe should be a correctly designed sample take-off probe and positioned to extract a flow of representative composition.

Prover Loops and Sphere Detectors

2.1.11 Preferably prover loops should be of the bi-directional type to eliminate possible directional bias. They should have a suitable lining. The flanged joints within the calibrated volume should have metal to metal contact and there should be continuity within the bore. Connections should be provided on the prover loop to facilitate recalibration with suitable calibration equipment which may be a dedicated water draw tank, portable calibration prover loop and transfer meter, or small volume type prover, where this is approved by the OGO for use in the particular application using the in-service liquid as the transfer medium, or other suitable liquid if approved by the OGO.

2.1.12 Provers should be constructed according to the following criteria:-

i. Number of meter pulses generated over swept volume to be 20,000 pulses. (This is equivalent to 10,000 pulses between detectors on bi-directional provers.)

ii. Resolution of detector/displacer system to be compatible with requirement (i).

iii. Displacer velocity not to exceed 3m/s to avoid slippage past the displacer but may be faster with piston type provers if seal integrity can be demonstrated.

Because the resolution of the detector/displacer system can only be gauged by the actual performance of the prover, the Department expects the manufacturer to demonstrate an acceptable repeatability during calibration of the prover, such that on 5 consecutive round trips the range of volumes does not exceed ±0.01% of the mean volume. Alternatively, a statistically equivalent repeatability criterion for small volume provers or meter pulse gating systems may be used.

2.1.13 For offshore use, or in remote locations, prover loops should be fitted with dual sphere detectors and switches at each end of the swept volume. At least two volumes should be calibrated so that failure of a detector or switch does not invalidate the prover calibration. The detector should be designed such that the contacting head of the detector protrudes far enough into the prover pipe to ensure switching takes place at all flow rates met with during calibration and normal operation. Detectors and switches should be adequately waterproofed against a corrosive marine environment.

2.1.14 In the case of mechanical switches, each sphere detector should have a dedicated micro-switch. The actuation of each detector unit should be set during manufacture so that should it be necessary to replace a detector unit during service there will be a minimal change in prover calibrated volume.

NOTE: Other designs of prover may be considered subject to their being in accord with good oilfield practice.

Recirculation Facilities

2.1.15 The Department does not normally permit the fitting of recirculation loops to metering systems except in production systems featuring rapid tanker-loading. Where recirculation systems are fitted around the metering system, full logging of recirculation and any other non-export flows through the meters must be maintained. Any such system must be properly operated and maintained.

2.1.16 Recirculation facilities intended for the use of pump testing etc. should be fitted upstream of the metering system.

Pulse Transmission (PD and Turbine Meters)

2.1.17 The metering signals (see also section 5.1) should be generated by a dual meter head pick-up system in accordance with either Level A or Level B of the IP 252/76 Code of Practice. This is to indicate if signals are "good" or to warn of incipient failure of meter or pulse transmission.

2.1.18 A pulse comparator should be installed which signals an alarm when a pre-set number of error pulses occurs on either of the transmission lines in accordance with the above code. The pre-set alarm level should be adjustable, and when an alarm occurs it should be recorded on a non-resettable comparator register. Where the pulse error alarm is determined by an error rate, the error threshold shall be less than 1 count in 10^6. Pulse discrepancies that occur during the low flow rates experienced during meter starting and stopping should be inhibited. This is to avoid the initiation of alarms for routine process situations thereby tending to induce a casual attitude to alarms in general.

2.1.19 The pulse transmission to the prover counter should be from one or both of the secured lines to the pulse comparator, and precautions should be taken to avoid any signal interference in the spur from the comparator line. This is to ensure that meter factors are determined with as good pulses as are used to totalise production.

Totalisers and Compensators

2.1.20 All totalising and compensating functions, other than data input conversions, should be by digital methods, to establish a high level of confidence in the accuracy of the system.

2.1.21 Each meter run should have an instrument computing uncorrected volumes at line conditions in which meter factors should be capable of being set to a resolution of at least 0.03% of value. In volumetric measuring systems, a liquid pressure correction may be included in the computation as this correction is usually small and of constant magnitude. Where a metering skid operates over a wide range of pressures as a routine then continuous correction for pressure effects may be appropriate.

2.1.22 Totalisers on individual meter run instruments, and on station summators, should have sufficient digits to prevent roll-over more frequently than every 2 months and normally have a resolution of 1 unit of volume or mass. Totalisers should be non-resettable and, where they are of the non-mechanical type, should be provided with battery driven back-up memories.

The procedures to be used for correcting flow during any period of mismeasurement should be made available.

2.1.23 For the volumetric mode of measurement, automatic temperature compensation is required. Temperature compensation should be carried out on each individual meter stream. The liquid thermal expansion coefficient should be fully adjustable over the range likely to be encountered in practice and have a resolution of at least 1%.

2.1.24 Corrections to meter throughput for water and sediment content should be applied retrospectively based on the analysis of the flow-proportional sample. However it is recognised that the new generation of water-in-oil meters is approaching levels of performance associated with traditional methods and is likely to become acceptable within the currency of this document. Any application to use new methods will be reviewed on a case by case basis according to the policy for adopting new technology.

Other Instrumentation

2.1.25 To provide a history of meter operation and flowing conditions and a record of meter malfunctions, each meter-run should be provided with a continuous chart recording of flow rate and metering temperature. Alternatively, electronic data recording will be accepted provided that the recording frequency is adequate and the system logs all metering alarms. Recording intervals no greater than 4 hours will normally be considered adequate.

2.1.26 In mass measurement systems, the density signals from the density meters should also be recorded continuously by a chart recorder or electronic data recorder at the same interval as in 2.1.25 above. A digital read-out is also required with a resolution of at least 4 significant figures.

2.1.27 Crude oil metering systems should be provided with automatic flow proportional sampling systems for the determination of average water content, average density and for analysis purposes. It is important to ensure that properly designed sample probes are used and positioned in such a way as to ensure representative sampling. Sample extraction rates should be "isokinetic" according to ISO 3171. These samples are required to account for dry oil quantities and allocated quantity determination. They may also be used for valuation purposes. In special circumstances when flows are specifically held constant (e.g. well testing) spot or time based sampling may be acceptable. The use of on-line water-in-oil monitors will be dealt with in accordance with the new technology procedures.

2.1.28 In crude oil systems where slugs of water may occur, in line water detection probes should be fitted to detect abnormal levels of water content. Continuous recordings of percentage water content and a high-level alarm system should be provided. Data from this source should not normally be used in determining dry oil quantities. This may only be used as a back-up in case of failure of agreed sampling and analysis procedures.

Security

2.1.29 In order to show if accidental or malicious interference with these critical components has occurred, all meter factor settings and reset buttons, where allowed, should be secured with a seal, lock or password to prevent unauthorised adjustment. Prover loop sphere detectors and associated micro-switches should also be secured by locks or seals.

2.1.30 Valves on re-circulation lines, provided for the purposes of off-line meter testing via re-circulation loops, must be provided with approved type locks.

Calibration Facilities

2.1.31 Adequate test facilities should be provided with metering systems to facilitate the checking and calibration of all computing and totalising systems. The calibration of test equipment shall be traceable to National Standards of measurement.

2.2 Allocation: Continuous Measurement

2.2.1 Where, but for technical or economic reasons, it is agreed that product streams which would otherwise be separately metered to fiscal quality standards may be accounted for by the class of measurement system referred to as "allocation" the target uncertainties are 0.5% to 1.0%. These levels may not always be attainable for technical reasons. The best levels of allocation metering sometimes approach "fiscal" standards.

2.2.2 In order to approach fiscal standards of allocation metering it will be necessary to have separate processing of the product streams which are to be commingled prior to metering to fiscal standards before entry into a common carrier pipeline system.

2.2.3 Allocation metering systems approaching fiscal standards will in most cases use traditional equipment in the design of the metering system. The main relaxation from full fiscal metering standards is likely to be the removal of in-situ proving requirements. The meters would be installed on the outlet of the last separator stage and each train would be nominally identical. The fiscally metered out-turn would then be prorated using the allocation meters.

2.2.4 This method has the advantage of reducing the effect of any systematic errors which may be present in the allocation metering system but are masked by the larger overall random uncertainties of the allocation meters.

2.2.5 In circumstances where it is not practicable to fully process the product streams then the next best option will be to place the allocation meters in the outlet pipework of the first stage separator. This option runs the risk of free gas being present in the product streams unless precautions are taken to ensure that the meters are installed in such a position where gas breakout is not likely to occur.

2.2.6 If the choice of allocation meter is not of the traditional variety but is for example a Coriolis or ultrasonic meter, particular care should be taken in matching the expected range of process conditions to the operational envelope of the selected meter type. These newer meters can be particularly sensitive to installation effects or process conditions particularly if there is a risk of free gas being present in the product stream.

2.3 Allocation: Intermittent Measurement

2.3.1 In circumstances where there is no practical alternative, allocation using intermittent or "flow sampling" techniques may be permissible. In most cases this will involve the use of a three phase test separator. These tests are usually conducted on a monthly basis.

2.3.2 In the case of a new development where it is proposed at the outset to use a single production installation to co-produce more than one field then maximum advantage should be taken to make use of the opportunities afforded by a new-build situation to configure the process equipment to maximise the accuracy that the use of a test separator can provide.

2.3.3 Positioning the test separator within reach of the export meter prover may be possible. If that is the case then the small additional investment in a few metres of pipe and some valves offers the possibility of in-situ proving of the test separator meter(s). This, taken in conjunction with the selection of high quality instrumentation and flow computers, will result in the contribution to the overall uncertainty in the measurements used for allocation of the commingled out-turn by the meters being as small as practicable. The main contribution to the uncertainty will then arise from causes basically outside the operator's control. These uncertainties stem principally from the variability of the process conditions in relation to flow rates, densities, water cut, incomplete separation, free gas in liquid streams, liquid carry over in gas streams, oil remaining in the water etc.

2.3.4 One of the new generation of water in oil meters should be installed in the oil leg of the separator to reduce the error in dry oil accounting when the oil stream has a significant water content.

2.3.5 If wells of significantly different physical properties and process conditions are to be allocated using flow sampling techniques then additional precautions will be necessary to ensure that each well is treated equitably in the allocation process. The pressure and temperature in the main production separators may be significantly different from those obtaining in the test separator during different well tests. This will result in a different test GOR from a production GOR. To compensate for this a process simulation should be run for each well on both the test separator and the main production separator. This will enable a correction or "shrinkage" factor to be determined. The use of such a factor should result in the sum of well head production being in closer agreement with the sum of the installation out-turn. Such adjustments have the merit of tending to reduce any systematic differences between wells of significantly different properties when using flow sampling for allocation purposes. This is particularly important if some of the wells are sub-sea completions tied back through long sub-sea flow lines.

2.3.6 In the circumstances where a new satellite field is to be co-produced using existing process equipment on a parent platform the scope for the operation of the test separator to the levels of accuracy achievable in the new-build circumstances described above is severely limited.

2.3.7 If an operator proposes to use an existing test separator to allocate production between different fields then it will be necessary to provide the OGO with full engineering details of the test separator and its instrumentation in order that an evaluation can be made of its likely performance as an allocation flow sampler. In general it is unlikely that pipework modifications would be called for but where there is scope to enhance the metrology by upgrading instruments and flow computers this would normally be required.

2.3.8 Although the provision of permanent in-situ proving facilities for the test separator meters is unlikely to be feasible, consideration should be given to the proving of the meters in-situ using a portable small volume prover. It is recognised that there may be space and access restrictions which would make this approach impractical.

2.3.9 The allocation of the commingled out-turn should be based on the principal of prorating the sums of the well-head production (corrected if necessary for differences between test and production process conditions) from each contributing field. This procedure has the effect of minimising the impact that any undetected systematic errors might have on the equitability of the allocation.

2.3.10 In very exceptional circumstances, where the migration of uncertainties caused by relative flow rates and differing uncertainties of metering methods does not introduce unacceptable bias in the allocation of production, the use of difference methods may be permitted.

2.4 Test Separator for Reservoir Management

2.4.1 Since the test separator may be called on to test wells exhibiting very wide differences in product quality, process conditions and flow rates it is unrealistic to expect universally high standards of metering. The conditions ranging from steady flowing dry oil to slugging flow of high water content oil with significant amounts of produced solids as well as temperature variations from sea bed conditions to 100°C imposes severe limitations on the results achievable. In view of this a wide range of uncertainties is associated with this type of measurement. Typical target uncertainties are 5% to 10%. It is acknowledged that some installations with very favourable operating conditions may improve significantly on these figures.

2.4.2 While a conventional test separator may be equipped with a turbine meter or meters in the oil leg, orifice plate in the gas leg and magnetic flow meter in the water leg there is scope for significant variations in test separator meter configurations. Operators might wish to consider whether Coriolis, vortex shedding, ultrasonic or other meter types offer advantages in the provision of test separator meters.

2.4.3 The majority of wells are tested by diverting the well to be tested from the main production separator to the test separator for direct exclusive testing of the well. There may be circumstances where testing by difference may be a viable or even preferred option. Where circumstances permit there may be advantages particularly with sub-sea satellites for testing by difference. For developments where it is not necessary to provide for round trip pigging the elimination of a sub-sea test line may benefit the field economics.

2.4.4 Special precautions may be necessary when testing satellite wells connected to a parent platform by long sub-sea lines that when switching from production to test that the same flowing tubing head pressure exists under both test and production configurations. Failure to test the well under normal operating conditioned will introduce additional errors to the test data.

2.5 Stand-alone Fields: Offshore Loading

2.5.1 The class of field where the relaxed measurement requirements of 0.5% to 1.0% overall uncertainty is considered appropriate includes those fields which pay no Royalty or PRT and load the product of a single field into shuttle tankers. Offshore loaders where more than one field is commingled prior to loading onto shuttle tankers are unlikely to be considered suitable for this approach to measurement.

2.5.2 While such techniques as on-board tank gauging may have developed to the stage where they are suitable for cargo measurements with the vessel alongside a jetty in a sheltered anchorage they are not suitable for cargo measurement in the dynamic conditions of a disturbed sea state such as occurs frequently in the waters surrounding the United Kingdom.

2.5.3 If operators of offshore loaders in this category having the more conventional type of metering installation wish to operate to the relaxed uncertainty of 0.5% to 1.0% a number of options will be open to them. They should however note that there may be an increased likelihood of "letters of protest" if the relaxed uncertainty results in Bills of Lading differing by more than 0.5% from the out-turn quantities.

2.5.4 New developments in liquid ultrasonic meters have brought the performance of this class of instrument into the target uncertainty range for stand-alone offshore loaders where there is no tax or Royalty due. However the advantages to be gained by adopting these measurement techniques will only be achieved by careful design of the installation and operating procedures. Their use will be considered on a case by case basis.

2.5.5 By utilising clamp-on or spool mounted liquid ultrasonic meters directly in the loading line to the shuttle tanker and eliminating an intervening conventional metering skid, a potential bottleneck may be eliminated. This means that loading rates are only limited by the available pumping power or the rate at which the vessel may receive cargo. The reduction of the time spent on station taking cargo improves the safety status of both the tanker and the production facility.

2.5.6 In order to optimise the performance of this type of meter it is essential that the pipe or spool to which the meter is attached should be of better dimensional accuracy than run-of-the-mill pipe. In order to achieve overall uncertainties in the range 0.5% to 1.0% with an instrument, which is essentially a velocity meter, the internal diameter and circularity of the pipe or spool should be determined to an uncertainty of 0.05%. This may be achieved ether by direct gauging of the pipe or by inferring the effective diameter by appropriate in-situ calibration methods. Manufacturers' recommendations for the necessary upstream straight lengths should be adhered to.

2.5.7 In order to provide the high level of availability and reliability required for cargo measurement purposes it will be necessary to install two meters in series so that in the event of failure in any component of the metering system loading may continue without interruption. This configuration provides a more cost-effective redundancy than having a parallel run with attendant valve, pipework and pressure drop costs.

2.5.8 The provision of a redundant series meter provides comparative data for instrument health monitoring and makes available a meter for the purposes of periodic verification by alternatively cycling the meters to an onshore calibration facility.

PART THREE

Gaseous Petroleum

3.1 Fiscal Quality Measurement

Mode of Measurement

3.1.1 All measurements should be made on single phase gas streams. Hydrocarbon measurements may be in either volumetric or mass units. The choice of measurement should however be discussed with the Department of Trade and Industry (OGO). Volumes should be measured in cubic metres and mass in tonnes.

3.1.2 Where volume is the approved measurement, it should be referred to the standard reference conditions of 15°C temperature and 1.01325 bar absolute pressure (dry).

3.1.3 Where gas is subject to custody transfer suitable sampling facilities shall be provided for the purpose of obtaining representative samples. This requirement may be influenced by the type of instrumentation incorporated in the measuring system.

3.1.4 The continuous measurement of gas density is preferred for custody transfer but the density of the gas being metered may, under certain circumstances, be computed from pressure and temperature measurements together with gas composition using a suitable equation of state and agreed computational techniques.

Design-Criteria

3.1.5 Where orifice meter systems are used, the design and operation should comply with ISO 5167-1 1991 but with the additional specifications given below:-

a) Maximum beta ratio 0.6

b) Maximum Reynolds number 3.3×10^7

c) Maximum differential pressure 0.5 bar is preferred. Higher differential pressures may be used where it is demonstrated that the conditions of e), f) and g) are met.

d) The metering assembly should be designed and constructed such that the minimum uncertainties specified in ISO 5167-1 1991 are achieved.

e) The total deformation including static and elastic deformation of the orifice plate at maximum differential pressure shall be less than 1%.

f) The uncertainty in flow caused by total deformation of the orifice plate shall be less than 0.1%.

g) The location of the differential pressure tappings with respect to the orifice plate shall remain within the tolerances given in ISO 5167-1 1991 over the operating range of differential pressures. Where plate carriers utilise resilient seals care must be taken to ensure that the load on the plate caused by the maximum differential pressure does not move the plate out of pressure tapping tolerance.

h) Special considerations may be applicable where pulsations are unavoidable but normally the uncertainty due to any such effects should be kept below 0.1%.

3.1.6 Where metering systems other than orifice plate metering are to be used, the systems together with their flow compensating devices, should be of the types agreed by the Department of Trade and Industry (OGO) (see paragraph 1.2) and should be calibrated over as much of the operating pressure, temperature and flow range as is reasonably practicable. Proposals for any extrapolation of such calibrations and correlations of the operating conditions should be presented.

3.1.7 Secondary instrumentation, line pressure and temperature, differential pressure, flowing density, density at base or reference conditions where appropriate and the flow computers should be specified and their positions in the system should be located such that representative measurement is ensured. In many applications the compositional analysis of the gas is required and it is necessary to provide for gas sampling or on-line analysis.

3.1.8 Sufficient meter runs should be provided to ensure that, at the maximum design field production rate or utility rate, at least one stand-by meter is available. Due consideration should be given to the provision of adequate valves so that individual meters may be removed from service without shutting down the entire metering system.

3.1.9 Consideration should be given during design to the provision of back-up instrumentation to cover the failure of normal instrumentation, and to the on-site calibration of primary and secondary metering equipment.

3.1.10 Metering stations should be designed to be free from any carry over into the metering section, and from any condensation or separation, that would have a significant effect on measurement uncertainties.

3.1.11 An indication of the overall design accuracy and measurement uncertainty of the metering system together with the sources of error should be given (paragraph 11.1 of ISO 5167-1 1991). The assessment of uncertainties in gas measurement should preferably be calculated in accordance with ISO 5168 1978 (the Appendix 4 contains guidance).

Computers and Compensators

3.1.12 A flow computer should be dedicated to each meter run. Alternatively if multiple meter runs are computed by one machine a hot operating standby must be provided to allow maintenance or replacement to be carried out without interruption.

3.1.13 All computer and compensating functions, other than data input conversions, should be made by digital methods. All calculation constants should be securely stored in the computer and should be easily available for inspection. Equipment should be designed so that constants can be adjusted, but only by authorised personnel. After initial agreement of stored constants subsequent changes in the computer should be made only with agreement of the Department. Where it is necessary to use manual inputs of data into the computer, e.g. base density, the use of this data should be automatically logged.

3.1.14 Totalisers on individual and station summators should have sufficient digits to prevent roll-over more frequently than every two months. Totalisers should normally have a resolution of 1 tonne or 1000 standard cubic metres, or decimal submultiples thereof. Totalisers and summators should be non-resettable and where they are of the non-mechanical type should be provided with battery driven back-up memories.

3.1.15 Where rotary positive displacement or turbine meters are used both compensated and uncompensated flow quantities should be recorded.

3.1.16 Compensation for influencing parameters, such as pressure and temperature, should be carried out in the flow computer by digital methods using approved algorithms.

3.1.17 If it is proposed to use new technology such as time of flight ultrasonic meters then details of the proposed equipment, layout and verification procedures should be discussed with the OGO at the earliest opportunity.

3.1.18 In a gas gathering system the operator responsible for the gathering should ensure that the basic metering data, flow formulae and computational techniques are compatible throughout all the fields connected to the gathering system.

3.1.19 The Petroleum Production Reporting System, agreed between the UKOOA and the Department of Trade and Industry (OGO), calls for the average calorific value (energy per unit volume) of custody transfer gas to be reported to the Department monthly. Provision for the determination of the calorific value of custody transfer gas should be made.

3.1.20 The Department of Trade and Industry (OGO) will require adequate notice (normally at least 14 days) of the factory inspection and calibration of primary and secondary equipment, including flow computers, in order that the Petroleum Measurement Inspectors may witness these tests at their discretion.

3.1.21 Adequate verification or, where appropriate, calibration equipment should be provided to enable the performance of meters, computers, totalisers, etc. to be assessed. Reference or transfer standards shall be certified by a laboratory with recognised traceability to National Standards (via for example, NAMAS).

The Calculation of Design Uncertainties in Flow Measurement using Orifice Plate Meters According to ISO 5167-1 1991; ISO 5168 1978.

3.1.22 The uncertainty in the measurement of a mass flow rate, q_m, should be calculated using the simplified formula given in ISO 5167-1 1991 paragraph 11.2.2 (see appendix 4). Over normal production flowrates the overall uncertainty should be better than ±1.0%.

3.2 Allocation: Dry Gas Measurement

3.2.1 For the purposes of this section the term "dry gas" is taken to mean gas which is at a temperature sufficiently above the dew point that condensation does not occur in the meter tubes upstream of the principal flow measuring element or within the downstream section of pipe between the principal element and the sample take-off point.

3.2.2 In circumstances where the fiscal status of production from different fields using common process or transportation infrastructure does not call for full fiscal quality metering it is normal to refer to the class of measurement system as "allocation" metering. Care should be taken to differentiate between the *process* of allocation where fiscal quality measurement may be required and the *class* of measurement frequently refereed to as "allocation metering" where relaxed standards of measurement may be appropriate.

3.2.3 Target uncertainties for dry gas allocation metering systems will be of the order of 2.0%. In order to achieve this level of uncertainty the basic design of the metering station will be similar to a fiscal quality metering station. The relaxed level of uncertainty is achieved through simplified procedures for the operation and periodic verification of the metering system.

3.2.4 If a multi-path ultrasonic meter is the preferred instrument in a particular application it may be possible depending on the circumstances to dispense with a redundant meter run. The multi-path nature of such instruments may be deemed to provide the required level of redundancy. In order for such a configuration to be accepted it would be necessary to demonstrate that the loss of accuracy suffered by the failure of one chord does not take the system outside the agreed uncertainty and that a spare set of transducers is available to enable full operational capability to be reinstated within a reasonable time.

3.2.5 If it is proposed to operate a single stream metering system the ability to change transmitters under pressure should be fully assessed. If for safety or operational reasons it is not possible to replace transmitters under pressure then suitable isolation valves upstream and downstream of the meter must be provided and the impact of such a configuration on the ability of the installation to meet daily nominations when it is necessary to work on the meter be recognised.

3.2.6 If the proposed allocation metering system is to be installed on a "not normally manned platform" then in order to ensure the required level of availability and to avoid unscheduled visits to the installation it may be necessary to include an appropriate level of redundancy in the instrumentation associated with the meter(s).

3.3 Allocation: Wet Gas Measurement

3.3.1 For the purpose of this section, wet gas is taken to mean gas which is in equilibrium with either water or gas condensate or both in the flowing gas stream. It is not intended to address the measurement of gas with a sufficient liquid content to be deemed two phase flow. The precise value of the liquid-to-gas ratio (LGR) defining wet gas or two phase boundary cannot be stated as it will depend on process variables such as gas velocity, water/condensate ratio, line temperature and pressure. As a guide LGRs greater than about 0.2% for stratified flow and 0.5% for annular mist flow are likely to require two phase flow measurement techniques.

3.3.2 The types of meter presently considered suitable for wet gas metering are; orifice plates with drain holes, Venturis, V-cone meters and ultrasonic meters.

3.3.3 Special precautions over and above those required for dry gas will be necessary in the design and operation of any meter to be used in wet gas.

3.3.4 Recent work with Venturis indicates that there may be acoustic problems and discharge coefficient instabilities at Reynolds numbers below the allowable value stated in ISO 5167-1. As this instrument is potentially very useful in wet gas application, work is ongoing to try to resolve the problem.

3.3.5 If an operator chooses to meter wet gas using a Venturi, the arrangement of pressure tappings quoted in ISO 5167-1 should not be used as this could result in liquid finding its way into the impulse lines of the pressure and differential pressure transmitters. Single pressure tapping on the top of the meter would normally suffice.

3.3.6 When any differential pressure device is used to measure wet gas, corrections should be applied to the discharge coefficient to take account of the liquid content. The methods of Murdock[1] and Chisholm[2] as modified by Jamieson and Dickenson[3] may be used to correct for the effect of liquid content.

3.3.7 As present work to correlate the difference between calculated pressure recovery and measured pressure recovery as a function of liquid content holds the promise of a direct on line measurement of liquid content. All new developments should provide a pressure tapping at the recovered pressure position in the downstream section of the metering tube. This small pre investment offers the prospect in the near future of measuring the LGR continuously on line at a negligible cost.

3.3.8 Operators of existing wet gas metering systems should consider whether the potential benefits of such a system warrant the retrofitting of a suitable pressure tapping.

3.3.9 If wet gas allocation meters are to be installed on not-normally-manned installations redundant instrumentation should be utilised to minimise the need for unscheduled visits to the installation while providing a high level of availability.

[1] J W Murdock, Two Phase Flow Measurements with Orifices. Journal of Basic Engineering 1962.

[2] D Chisholm, Two Phase Flow Through Sharp Edged Orifices. Research Note. Journal of Mechanical Engineering Science 1977.

[3] A W Jamieson and P F Dickenson, High Accuracy Wet Gas Metering. North Sea Flow Measurement Workshop 1993.

3.4 Utility and Fuel Gas Measurement

3.4.1 Where gas is used for utility purposes such as gas lift, oxygen stripping and power generation process quality measurement will generally be considered adequate. The level of measurement uncertainty considered appropriate for this class of measurement system is of the order of 3% to 4%. It will normally be considered sufficient for a single measurement point to be used to account for all utility consumption. However for operational reasons the platform operator may wish to have separate metering for each consumption unit on his installation. This will be acceptable to the OGO. Details of the selected measurement system should be included in the documentation sent to the OGO for review.

3.4.2 If the gas used on an installation does not originate from the field being produced by the parent platform other procedures may be required.

3.4.3 In circumstances where a satellite field is produced using the process equipment of a parent installation then a method of accounting for the amount of gas used in producing a satellite should be provided. In some cases this may involve the provision of dedicated measurement equipment. It may also be possible to account for individual field usage based on the relative proportions of service required. This may take into account such factors as throughput, pumping or gas compression requirements, water treatment or injection requirements and any other service which involves the use of gas in its provision.

3.4.4 If an installation is gas deficient and it is necessary to import gas from a pipeline system for power generation and utilities use then it will normally be necessary to have a "fiscal quality" metering system to account for gas imported as the pipeline will be transporting "fiscally" metered gas.

3.4.5 Gas transported between two installations via a dedicated pipeline for use on the importing platform for utilities purposes may, depending on the fiscal status of the exporting installation, make use of less-than-fiscal quality measurement.

3.5 Flare or Vent Gas Measurement

3.5.1 Flare or vent gas should be measured or otherwise accounted for.

3.5.2 In recent years significant advances have been made in the technologies of flare gas measurement and operators are encouraged wherever practical to measure the quantities of gas flared or vented from an installation. The uncertainties likely to be achievable in flare gas metering systems will be of the order of 5% to 10%.

3.5.3 The term "otherwise accounted for" means the process of accounting for gas flared or vented by difference between the estimated sum of individual well-head gas production and the other measured disposals whether by export, injection or use. It is expected that this method produces uncertainties of 10% to 20% but in some circumstances may be significantly higher. Difference methods of accounting for flare will only be acceptable in exceptional circumstances.

3.6 Test Separator for Reservoir Management

3.6.1 Traditional instrumentation may still be the favoured option for gas field test separator operations. However if wet gas allocation metering is also to be used on the installation then the use of the test separator to determine LGRs takes on an additional importance as well as the reservoir management function.

3.6.2 The use of new technology such as ultrasonic and Coriolis meters may offer significant advantages in terms of space and weight requirements while offering comparable levels of accuracy.

3.6.3 The use of a Coriolis meter in the liquid leg may in some circumstances provide a measure of the proportions of water and condensate in the liquid stream using the density measurement capability with a knowledge of the densities of the produced water and condensate.

PART FOUR

Multiphase Petroleum

4.1 Allocation

4.1.1 No standards exist as yet to assist engineers in designing multiphase metering systems. The difficulty is compounded by the fact that there is no accepted standard for quoting the performance and accuracy characteristics of multiphase meters. It is essential when considering a manufacturer's performance and accuracy statements to understand the implications of accuracy's quoted in different ways. There are three common ways in which multiphase meter accuracy's are presented:

i) % phase volume flow rate.
ii) % total multiphase flow rate.
iii) % gas and liquid flow rate plus absolute uncertainty of water cut in liquid phase.

Method i) is favoured by metrologists and clearly represents performance as stated. This method may not be the most practical for extreme cases of phase fractionation. Methods ii) and iii) while quoting relatively small numbers of the order of 5% to 10% for gas/liquid phase uncertainties and 2% or 3% for percentage water cut may nevertheless exhibit very large individual phase errors of 100% or more depending on the absolute value of the percentage water. A useful guide to multiphase metering is to be found in the Handbook of Multiphase Metering produced by the Norwegian Society for Oil and Gas Measurement in Stavanger, Norway.

4.1.2 Any operator contemplating the use of multiphase metering should make contact with the OGO at as early a stage as possible. The acceptability of such technology for production allocation will depend in large measure on the match between the instrument's operating characteristics and the process envelope and variability. It may in any case be necessary to mount an evaluation programme to assess the suitability of a meter for any particular set of process conditions.

4.1.3 The OGO should be involved in agreeing the design and conduct of any evaluation programme proposed for the purpose of qualifying and instrument for use in a production allocation system. The objectives and acceptability criteria should be agreed in advance with the OGO before the start of any testing. Inspectors from the OGO may, at their discretion, witness the testing of a meter under evaluation.

4.1.4 The first task when considering the use of a multiphase meter for allocation purposes is to decide the levels of uncertainty which are appropriate for each phase. This will depend on the value of the phase and the production rate. Clearly a highly accurate measurement on a phase comprising only a few per cent of the production is unlikely to be either cost effective or necessary. The accuracy with which the hydrocarbon flows can be determined will take precedence over the accuracy of water flows. However water fraction measurement may have a high significance depending on the absolute value of the water cut in any particular multiphase flow.

4.1.5 At present the "universal" multiphase meter covering all flow regimes and all possible phase proportions from 0% to 100% of oil, water and gas does not exist. Consideration should be given at the outset to the possible need to use different types of multiphase meters at the start of production than those that may be required at different stages in the life of the field. A detailed evaluation of the predicted production profiles in terms of the changes to GOR and water cut expected over the life of the field will give some indication of the possible changes in multiphase meters which should be planned.

4.1.6 As these instruments at present have large uncertainties there is a risk that significant systematic errors could be masked by the overall random uncertainties. When considering the use of these meters, good repeatability is an important consideration particularly where the opportunity exists for in-situ calibration. By considering other measurement points throughout the production and transportation system procedures can be devised to establish if any bias exists and steps taken to eliminate it as part of the initial verification. If such opportunities do not exist within the basic design of the production facilities then modifications should be considered to enable verification tests to be performed.

4.1.7 It is not practicable to suggest what verification provisions should be made in this document, as any such provision will of necessity be tailored to the particular type of instrument and the process environment in which it is installed.

4.2 Well Testing

4.2.1 There are a number of options for the use of multiphase meters for well testing. Potential benefits include the elimination of the need for test separators and for subsea satellite developments with long subsea test flowlines. These benefits will only be available if the individual fields' process characteristics are amenable to such treatment. Depending on pipework configuration and deployment strategy of multiphase meters another potential benefit is continuous well monitoring or failing that, frequent well monitoring at, say, daily intervals.

4.2.2 Topside use of multiphase meters may be either on their own or in conjunction with a test separator. A multiphase meter in each well flowline may provide a satisfactory level of well management information without the need for a test separator although such an arrangement makes the extraction of well samples more difficult. In some instances a test separator may be required for multiphase meter calibration and well sampling.

4.2.3 If it is proposed to dispense with a test separator and rely entirely on multiphase metering for well testing then care must be taken to ensure that the full range of process conditions presented by wells is within the performance envelope of the selected meter. If flow rates from the range of wells to be managed by the system is very wide then it may be necessary to install more than one meter to provide cover for the full range of flows and process conditions likely to be encountered. As one meter or type of meter may not cover the range of conditions which may arise throughout the life of the installation consideration should be given at the outset to the possible need to change either the size or type of instrument needed.

4.2.4 In the case of subsea satellite clusters the choice of individual well meters or a single meter on a test manifold should be considered. If the properties of the process fluid are such that round trip pigging is not required the saving of a subsea test line can be significant compared to the costs of subsea multiphase meters.

PART FIVE

Operating Procedures

5.1 Liquid Measurement Systems

5.1.1 The procedures cover the metering of liquid mass and volume with particular emphasis on crude oil measurement, and are based on the operational characteristics to be expected of a typical metering station equipped with turbine meters. Where other types of meter have been approved a variant of these procedures may be appropriate. The performance of individual metering stations will depend on the particular characteristics of both the metering system and flow system and the type of hydrocarbon being metered: therefore deviations from these procedures may be necessary in special cases, for example measurements on very viscous crude oils, or low lubricity fluids such as gas condensate.

5.1.2 Operators are required to submit their proposals for the operation and calibration of their metering systems to the DTI OGO Aberdeen address prior to the commencement of commissioning and operation (see section 3.1.20).

Prover Calibration

5.1.3 Prover loops shall be calibrated at the manufacturer's works by methods described in IP or ISO standards as part of their systems checks, and again after installation on site. One copy of the calibration certificate for each of these and all subsequent calibrations should be sent to the OGO. Such certificates should show the reference numbers of the sphere detectors used in the calibration, and the traceability to national standards of the calibration equipment.

5.1.4 While a metering station is in service, prover loops must be calibrated at a frequency of not less than once a year. Where this is not possible for operational or weather reasons, a two month period of grace will be allowed. Inspection of all critical valves and instrumentation along with the sphere, checking of sphere size, sphericity, etc. should take place prior to calibration. After calibration the sphere detectors and switches should be sealed.

5.1.5 Any maintenance work on the prover that could affect the swept volume, e.g. changes of sphere detectors and switches, should not be undertaken without prior notice to the OGO which will advise if a recalibration is required.

5.1.6 The OGO must be given at least 14 days notice of all prover loop calibrations so that arrangements for witnessing can be made.

Determination of Meter Characteristics

5.1.7 For new or modified meters which are to be operated over a wide flow range covering flow rates below 50% of maximum, characteristic curves of meter factor versus flow rate should be determined for each meter. These curves should cover a range of approximately 20% to 100% of maximum flow rate, subject to any system restriction on flow rate. From these curves the permissible flow rate variations at a given meter factor setting will be determined.

5.1.8 Meters that are to be operated normally only at above 50% maximum flow rate, except during starting and stopping, will not be subject to the above requirement provided it can be shown that a meter factor variation of not greater than 0.1% occurs over the working flow rate range.

Meter Proving in Service

5.1.9 The requirements governing the intervals between turbine meter proving are:-

5.1.10 For a newly commissioned metering station in a continuous production system (as distinct from tanker loading), meters shall be proved three times a week at approximately equal intervals between proving. Provided the meter factor scatter is acceptable to the OGO, this frequency may be reduced to twice a week at the end of the first month, and once a week at the end of the second month.

5.1.11 For the tanker loading systems, the frequency of proving will depend on the duration of the loading and the individual production system characteristics. The frequency of proving will therefore be subject to the approval of the OGO on an individual basis.

5.1.12 Meters must also be proved:-

(a) When the flow rate through the meter changes by a significant amount - this change in flow will depend on the gradient of the meter's flow characteristics in any particular installation (see Section 2.0) and would normally be such that a change in meter factor greater than 0.1% does not arise from the change in flow rate. If the change in flow rate is a scheduled long-term change then the meter(s) should be reproved at the first opportunity. If the flow rate change is unscheduled then the meters should be reproved if the estimated duration of the changed flow is 6 hours or more.

(b) When any significant change in a process variable such as temperature, pressure or density of the liquid hydrocarbon occurs for extended periods as for flow in (a) above that is likely to cause a change in meter factor of 0.1% or more. In typical North Sea production systems practical values of these limits are of the order of 5°C temperature, 10 bar pressure and 2% density.

(c) If scale or wax deposition occurs then a higher frequency of proving may be necessary until the deposition problem can be overcome.

5.1.13 Where meter types other than turbine meters are in use, the type and frequency of meter factor proving by the Licensee will be determined on an individual basis by the OGO after consultation with the Licensee. Account will be taken of the meter type, process fluid and operational load cycle. Where meters employing novel technology are to be used, extra evaluation periods and tests will usually be required before acceptance of a long-term operational schedule can be determined.

Meter Factors

5.1.14 Meter factors should be based on the average of at least five proof runs. All consecutive five proof runs must lie within ±0.05% of the mean value. Full details of the proof runs, together with flow rates, pressures and temperatures should be entered in the Record of Meter Provings. In particularly difficult situations where process stability sufficient for proving purposes cannot be achieved then a special proving regime may be agreed after consultation with the OGO. The purpose of a non-standard proving regime is to arrive at a good average meter factor which represents the meter's performance under unstable operating conditions. In seeking to determine a meter factor under unstable process conditions it is acknowledged that a significant proportion of the variability in meter factors is not due to the meter's intrinsic repeatability but to the variations in process conditions during the meter proving.

5.1.15 On metering installations where the meter factor is set manually, the change in factor should be done in such a way as to prevent loss in the measured flow. Also, the new factor setting should be checked by a second person who should sign to this effect in the Record of Meter Provings.

General Procedures

5.1.16 Metering stations should be operated and maintained in accordance with the manufacturers' recommendations: particular attention should be paid to flow stabilisation prior to meter proving, checking of block and bleed valves for leaks.

5.1.17 The temperature-compensated totals associated with the individual meters are to be used as the basis of the approved measurements at each metering station, except where the approved measurement is in mass units.

5.1.18 The operator should check the accuracy of the individual meter temperature compensation daily to detect the occurrence of possible errors. Correspondingly, in a mass measurement system a daily check of the mass computation should be done by comparing the totalised mass with that calculated from the individual metered volumes and density meter readings.

Documentation to be kept at the Meter Station

5.1.19 The operator must maintain a log book for the prover detailing all calibrations, sphere detector serial numbers and any maintenance work done on the prover loop and its associated equipment.

5.1.20 A log must be kept for each meter showing details of:-

i) type and identifying particulars including location and product measured;
ii) totaliser reading(s) on commencement of metering;
iii) all mechanical or electrical repairs or adjustments made to the meter or its read-out equipment;
iv) metering errors due to equipment malfunction, incorrect operation etc., including date, time and totaliser readings both at the time or recognition of an error condition and when remedial action is completed;
v) alarms, together with reasons;
vi) any breakdown of meter or withdrawal from normal service, including time and totaliser readings;
vii) replacement of security seals when broken.

5.1.21 The operator must also keep a Meter Proving Record for each meter giving the full details of each proof run. This record may be kept in either hard copy or approved electronic form and should include a running plot, or similar control chart, so that any undue change or fluctuation in meter factors may be easily detected.

5.1.22 A manual log or automatic recording should also be kept, at intervals of not more than 4 hours, of the following parameters;-

i) all meter totaliser readings;
ii) meter flow rates (also relevant meter factors), pressure and temperature, and (if measured continuously) density;
iii) any change in meter pulse comparator register readings.

One of these sets of readings should be recorded at 24.00 hours, or at the agreed time for taking daily closing figures if different.

Other parameters such as liquid density and percentage BS & W content should be recorded at agreed intervals, if not already included in the automatic log.

5.1.23 Records of parameters such as meter flow rate, liquid temperature and density should be kept at the metering station for at least 4 months.

5.1.24 All above records should be available at all reasonable times for inspection by the OGO.

Direct Reporting to the DTI Oil and Gas Office (OGO)

5.1.25 Operators should notify the OGO prior to any major maintenance or re-calibration work on the metering and proving system. The OGO should also be notified, preferably by telephone or fax, when any abnormal situation or error occurs which could require significant adjustments to the totalised meter throughputs.

5.1.26 If a flow or density meter should require removal for maintenance work or replacement, a fax should be sent to the OGO by notification detailing the serial numbers of the meters concerned and the reasons for the action taken.

5.1.27 When corrections to meter totalised figures are required due to known metering errors, a formal report should be submitted to the OGO detailing the times of the occurrence, totaliser readings at start and finish, required corrections to these readings, and reasons for the errors occurring.

5.2 Gaseous Measurement Systems

5.2.1 These procedures cover the metering of petroleum in the gaseous phase. They will also be appropriate for gas at high pressure when it is sometimes referred to as a "dense phase fluid". By far the largest number of gas metering stations serving the UK and UKCS gas production industry use orifice plate meters. These procedures primarily address this type of metering station. Many of the provisions will be applicable to metering stations employing other measurement technologies with variations as appropriate.

5.2.2 Pre-commissioning. Operators are required to submit their proposals for the operation and periodic verification of their metering systems to the OGO prior to the commencement of commissioning and operation. These will include proposed calibration intervals for the ancillary instrumentation.

5.2.3 The operator should prepare a schedule of pre-commissioning tests which are designed to demonstrate the operability of salient aspects of the metrology. In particular there shall be an examination of the interior of the meter tubes and of the orifice plates to ensure that they conform to the relevant provisions of the standard.

5.2.4 If there is a risk that debris including dust, mill scale or other foreign matter may be present in the process upstream of the meters then consideration must be given to the use of "start-up" plates to avoid damage to the primary elements for long-term metering service. Instruments which may be susceptible to damage or malfunction if exposed to foreign matter should be isolated from the process for the first 24 to 48 hours after start-up. Instruments most likely to be affected are densitometers and gas chromatographs. During this period the flow computers should preferably use a default gas composition to calculate the gas density at operating conditions or use a keypad value of gas density representative of the operating conditions. The computer should be returned to "live input" density as soon as the clean-up is complete.

5.2.5 For metering stations at onshore terminals differential pressure transmitters should be calibrated at high static pressure representative of the normal operating pressure for the instrument.

5.2.6 At offshore metering stations high static calibrations should be performed at a suitable calibration facility and subsequently "footprinted" at atmospheric pressure for use in periodic verifications offshore. With new developments in differential pressure measurement and calibration there may be scope for new offshore differential pressure verification procedures.

5.2.7 Detailed procedures for the verification of ancillary instrumentation such as pressure, temperature, gas chromatography, density and relative density where appropriate should be prepared for review by the OGO.

5.2.8 Sampling systems for product characterisation may use conventional methods or where appropriate on-line gas chromatographs.

5.2.9 Calibrations should be carried out using test equipment which is dedicated to the metering systems and is traceable to National Standards (via for example, NAMAS).

5.2.10 The recalibration frequency for each component in the system should be included in the procedures document. It is expected that initially the calibration frequency for most components will be monthly. As a history of the stability of the instrumentation is built up it may be appropriate to increase the intervals between recalibrations. As this would constitute a change in the "method of measurement" prior consent must be sought by the operator before any relaxation of calibration procedures can be granted. In order to support such an application it will be necessary to show that the instruments remain within tolerance on a number of successive recalibrations and are returned to service in the "as found" condition.

5.2.11 The Department may consider a recalibration schedule based on "health checking" procedures in circumstances where signal data analysis systems are in place to monitor the condition of the instrumentation and indicate when an instrument is moving out of its specification. A full justification should be supplied if an operator wishes to adopt such procedures. This should include an analysis of the impact such procedures would have on the overall uncertainty of the metering system.

5.2.12 When calculating the overall uncertainty of metering installations operators should use realistic "field" values for the uncertainties of the ancillary instrumentation rather than the manufacturers' claimed values. The uncertainties claimed by manufacturers for their equipment is usually the best the equipment is able to deliver under ideal laboratory conditions.

5.2.13 In the case of differential pressure transmitters it is important to use realistic field values as the choice of uncertainty value has an impact on the setting of the change over point for systems with high and low range transmitters.

5.2.14 The tolerances used when recalibrating ancillary instrumentation should be set at a level which, while not being so tight as to make their achievement under field conditions extremely difficult, should not be so lax as to risk compromising the overall target uncertainty for the class of measurement in question.

5.2.15 When density is calculated from a compositional analysis and process conditions of pressure and temperature using an approved equation of state, the accuracy of the ancillary instrumentation has an additional significance. Typical sensitivities of calculated density to process variables are;

Variable	**Change**	**% Change in Density**
Pressure	1%	1.0
Temperature	1°C	0.7
Molecular Wt	1%	1.6

5.2.16 When carrying out an examination of an orifice plate in the field it is not necessary to conduct a full gauging examination to ISO 5167-1 tolerances. The main points to look for in a field inspection of an orifice plate are, plate flatness, cleanliness, freedom from damage to the plate surfaces and particularly damage or rounding of the sharp edge.

5.2.17 It may from time to time be necessary to examine the condition of the meter tubes in pressure differential metering systems, (orifice plate or Venturi) to ensure that corrosion, erosion or contamination has not occurred to an extent likely to affect the accuracy of the meter. These examinations may be considered necessary if periodic plate examinations show persistent contamination. Particular attention should be paid to the section extending 2 pipe-diameters upstream of the orifice plate and to the condition of the penetration of the pressure tappings through the meter tube wall. If flow conditioners are used these should also be examined.

5.2.18 Where other meters are used such as turbine meters or multi-path ultrasonic meters singly or in combination and appropriate operating procedure and procedures for periodic verification should be discussed at the design stage with the OGO.

5.3 Multiphase Measurement Systems

5.3.1 As operating experience in the field with multiphase meters is at present extremely limited, it is not proposed to give detailed guidance on operating procedures for this class of instrument.

5.3.2 Operators should discuss the details of their proposed operating procedures at an early stage with the OGO. All opportunities for periodic verification should be investigated. This is likely to involve plans to make use of scheduled shut downs of contributing production streams to establish continued satisfactory operation of the meter. Contingency plans should also be in place to make opportunistic use of unscheduled shut downs to provide supporting evidence of meter performance.

5.3.3 As the technology is developing rapidly, operators should keep a watching brief on developments which may refine their instrumentation capability through increasingly sophisticated signal-processing techniques. As our understanding of multiphase metering advances there is significant scope to use advanced signal processing techniques to get more and better information from the existing multiphase metering hardware.

APPENDICES

Appendix 1

Addresses and Contacts

The Department of State with responsibility for the oil and gas industry is The Department of Trade and Industry (DTI). Within the DTI the day-to-day responsibility for carrying out the Government's policies rests with the Oil and Gas Division. The full address is:-

Department of Trade and Industry
Oil and Gas Division
1 Victoria Street
London SW1H 0ET

The administration of the Division's responsibilities for petroleum measurement are handled by the Branch 3, OGO. This office is located in Aberdeen and handles all petroleum measurement issues for the UK and Continental Shelf as a whole.

The address is:-

Department of Trade and Industry
Oil and Gas Office
Atholl House
86 - 88 Guild Street
Aberdeen
AB11 6AR

Enquiries telephone	01224 254064
Fax (thermal)	01224 254089
Fax (plain)	01224 590210

Oil & Gas Directorate structure (as from 1/8/97)
(OG3 shown in detail)

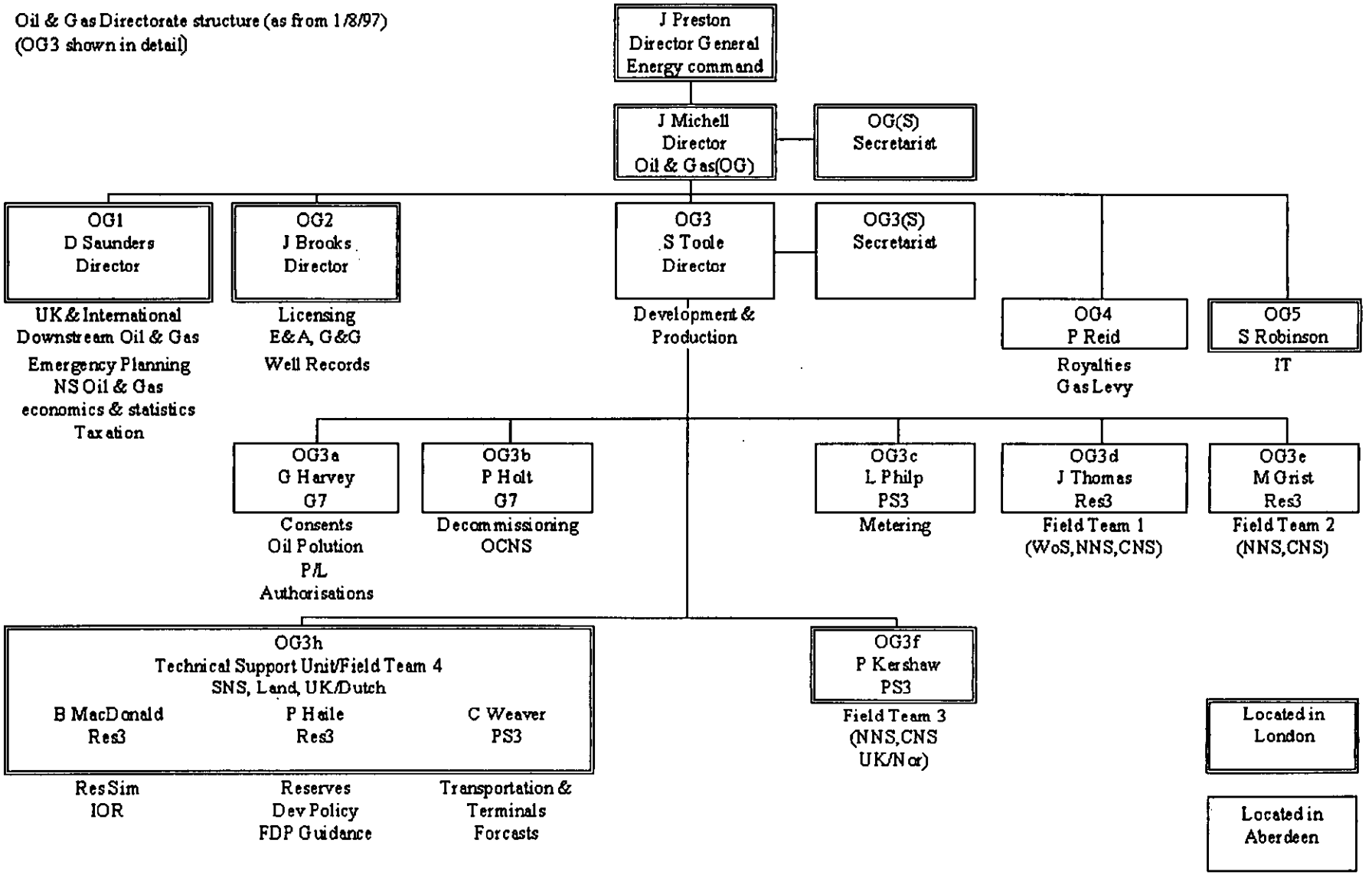

Appendix 2

The Measurement Model Clause.

(As printed in The Petroleum (Production) (Seaward Areas) Regulations 1988 and subsequent regulations.)

(1) The Licensee shall measure or weigh by a method or methods customarily used in good oilfield practice and from time to time approved by the Minister all petroleum won and saved from the licensed area.

(2)* If and to the extent that the Minister so directs, the duty imposed by paragraph (1) of this clause shall be discharged separately in relation to petroleum won and saved -

(a) from each part of the licensed area which is an oil field for the purposes of the Oil Taxation Act 1975,

(b) from each part of the licensed area which forms part of such an oilfield extending beyond the licensed area, and

(c) from each well producing petroleum from a part of the licensed area which is not within such an oilfield.

(3)* If and to the extent that the Minister so directs, the preceding provisions of this clause shall apply as if the duty to measure or weigh petroleum included a duty to ascertain its quality or composition or both; and where a direction under this paragraph is in force, the following provisions of this clause shall have effect as if references to measuring or weighing included references to ascertaining quality or composition.

(4) The Licensee shall not make any alteration in the method or methods of measuring or weighing used by him or any appliances used for that purpose without the consent in writing of the Minister and the Minister may in any case require that no alteration shall be made save in the presence of a person authorised by the Minister.

(5) The Minister may from time to time direct that any weighing or measuring appliance shall be tested or examined in such a manner, upon such occasions or at such intervals and by such persons as may be specified by the Minister's direction and the Licensee shall pay to any such person or to the Minister such fees and expenses for test or examination as the minister may specify.

(6) If any measuring or weighing appliance shall upon any such test or examination as is mentioned in the last forgoing paragraph be found to be false or unjust the same shall if the Minister so determines after considering any representation in writing made by the Licensee be deemed to have existed in that condition during the period since the last occasion upon which the same was tested or examined pursuant to the last foregoing paragraph.

* Paragraphs (2) and (3) are not incorporated into licences which contain the model clauses in Schedule 6 to the Petroleum (Production)(Landward Areas) Regulations 1991.

The DTI Petroleum Operations Notice Number 6 is reprinted below for convenience.

DTI - PETROLEUM OPERATIONS NOTICE

No. 6

MEASUREMENT OF PETROLEUM

1. Production licences for both landward and seaward areas incorporate a Model Clause which requires the Licensee to measure by methods customarily used in good oil field practice and from time to time approved by the Minister all petroleum won and saved from the licensed area. It is, therefore, necessary for the Licensee to submit his metering proposals to Petroleum Measurement Inspectors for approval, and it is advisable to do this at the early design stage of the metering station. Petroleum Measurement Inspectors should be contacted for all metering proposals for oil and gas at the address given below in section 5.

2. The Licensee will be required to submit following information:

   (a) A complete specification of the metering station with dimensioned drawings and relevant descriptive literature. Sufficient information should be included to enable a check on the design of the metering station to be made.

   (b) A description of the proposed operating procedure including routine calibrations and checking of equipment for maintenance of accuracy.

   (c) Specimen calculations indicating how reported quantities of oil or gas production are obtained giving correction factors proposed for converting meter and instrument readings to standard conditions.

3. It should be noted that:

   (a) Petroleum Measurement Inspectors must be advised in sufficient time to witness factory tests such as prover loop calibration, systems check, flow tests, etc.

   (b) Before start up and commissioning of a metering station an inspection by a Petroleum Measurement Inspector may be carried out. The operator will be expected to provide the Inspector with all relevant data and information, and to carry out such tests as the Inspector may reasonably require. Reasonable notice should be given to the Petroleum Measurement Inspector as to when an operator will be ready for a pre-start up inspection.

   (c) No alterations to a metering system may be carried out without the previous consent of a Petroleum Measurement Inspector.

4. The method of reporting petroleum production and the details required is the subject of a separate Notice PON No. 7.

Any enquiries regarding this Notice should be addressed to:

The Head of Metering.

Department of Trade and Industry
Oil and Gas Office
Atholl House
86-88 Guild Street
ABERDEEN
AB11 6AR

Telephone 01224 254064
Facsimile 01224 254089

The DTI Petroleum Operations Notice Number 7 is reprinted below for convenience.

DTI - PETROLEUM OPERATIONS NOTICE

No. 7

REPORTING OF PETROLEUM PRODUCTION

1. The Department of Trade and Industry requires Licensees to make monthly returns of petroleum production in accordance with the requirements of the Minister under the above model clauses concerning "Keeping of Accounts" and "Returns". These returns, known as the Petroleum Production Reporting System, must be in computer compatible format as specified by the Oil and Gas Division in the Petroleum Production Reporting System, Data Reporting Format (DRF).

2. The PPRS DRF, which is also known as the Blue Book, specifies the detailed format of the required returns. Copies of the DRF and guidance on creating returns are available from Russell Hornzee, Oil and Gas Data Manager, at the address given at the bottom of this Notice.

3. Operators who are due to commence production must ensure that they can make returns in accordance with the standards specified in the PPRS DRF and must ensure that the proposed format of a return is made prior to the commencement of production in order that the Department may approve the format.

4. This notice does not apply to the reporting procedure for landward fields in production prior to 1 January 1978.

Any enquiries regarding this Notice should be addressed to:

The Data Management Team.

Department of Trade and Industry
Oil and Gas Division
1 Victoria Street
London SW1H 0ET

Telephone 0171 215 5128
Fax 0171 215-5237

Appendix 3

Reference Standard Documents

3.1 Institute of Petroleum,
61 New Cavendish Street,
London W1M 8AR,
United Kingdom.

Petroleum Measurement Manual
Part VI Sampling.
Part VII Density.
Part X Meter Proving.
Part XIII Fidelity and Security of Measurement Data Systems.
Part XV Metering System. Section 1 A Guide to Liquid Metering Systems 1987.

IP 200 (API 2540; ASTM D1250) Petroleum Measurement Tables 1980.
Vol. VII Table 54A Generalised Crude Oil, Correction of Volume to 15°C Against Density at 15°C.
Vol. IX Table 54C Volume Correction Factors for Individual and Special Applications, Volume correction to 15°C Against Thermal Expansion Coefficients at 15°C.
Vol. X Background, Development and Computer Documentation.
Petroleum Measurement Paper No. 2.
Guidelines for Users of the Petroleum Measurement Tables (API Std 2540; (IP200); ANSI/ASTM D 1250) - September 1984.

3.2 American Petroleum Institute
1220 L Street, Northwest,
Washington D.C. 20005,
U.S.A.

Manual of Petroleum Measurement Standards.
Chapter 4 Proving Systems.
Chapter 5 Liquid Metering.
Chapter 6 Metering Assemblies.
Chapter 8 Sampling.
Chapter 9 Density Determination.
Chapter 10 Sediment and Water.
Chapter 11.2.1 Compressibility Factors for Hydrocarbons, 600 to 1074 Kg/m^3.
Chapter 11.2.1M Compressibility Factors for Hydrocarbons 350 to 637 Kg/m^3.
Chapter 12 Calculation of Petroleum Quantities.

3.3 ISO (International Organisation for Standardisation)
Case Postale 56
CH-1211 Geneva 20
Switzerland

ISO 2714	Liquid Hydrocarbons - Volumetric measurement by displacement meter systems other than dispensing pumps.
ISO 2715	Liquid Hydrocarbons - Volumetric measurement by turbine meter systems.
ISO 3170	Petroleum Liquids - Manual sampling.
ISO 3171	Petroleum liquids - Automatic pipeline sampling.
ISO 3675	Crude petroleum and liquid petroleum products - Laboratory determination of density or relative density -- Hydrometer method.
ISO 3735	Crude petroleum and fuel oils - Determination of sediment -- Extraction method.
ISO 4124	Liquid hydrocarbons --Dynamic measurement --Statistical control of volumetric metering systems.
ISO 6551	Petroleum liquids and gases - Fidelity and security of dynamic measurement - cabled transmission of electric and/or electronic pulsed data.
ISO 7278	Liquid hydrocarbons -- Dynamic measurement -- Proving systems for volumetric meters.
ISO 5167-1	Measurement of fluid flow by means of pressure differential devices.
ISO 6796	Natural gas -- Calculation of calorific values, density, relative density and Wobbe index from composition.

A number of relevant international standards are at the Draft International Standard (DIS) stage. When these documents are adopted as full ISO standards they should be included in the list of standards to which reference would routinely be may in arriving at the design of a metering system.

3.4 British Standards Institute
389 Chiswick High Road,
London W4 4AL,
United Kingdom

Many British Standards are now uniform with international standards and where this is the case are issued by the British Standards Institute as dual numbered standards. BS 1042 is one such standard. However only part one of the British standard is uniform with the ISO equivalent, ISO 5167-1. The other parts of the British standard give guidance on the use of orifice plates with drain holes and the effect on discharge coefficients of non-ideal installation. The additional parts of the British standard are a useful source of practical guidance.

BS 1904	Industrial Platinum Resistance Elements.

Appendix 4

Gas Uncertainty Calculations

4.1 The percentage uncertainty E_x of a variable x can be substituted for the relative uncertainty $\frac{\delta x}{x}$ throughout this equation (equation 2).

4.2 The uncertainties used should be those with a confidence level of 95%. At this confidence level uncertainty can be assumed to be equal to twice the standard deviation of measurements. If no information is available for the uncertainty of any particular variable an estimate should be made of the highest and lowest probable true values. The uncertainty should then be taken as half the difference between these values.

4.3 The uncertainty in C should be taken from ISO 5167-1 paragraph 8.3.3.

4.4 The uncertainty in the expansion factor ε should be taken from paragraph 8.3.3.2 of ISO 5167-1.

4.5 The uncertainties in D and d should be taken as those given in ISO 5167-1 paragraph 11.2.2.3.

4.6 The uncertainty in the differential pressure, $E_{\Delta p}$, should include the uncertainties in signal conditioners or converters and any other transmission component. These uncertainties should be combined with the transducer uncertainty on a root-sum-square basis. This procedure also applies to the derivation of the uncertainty in the measurement of the operating density, $E_{\rho 1}$.

4.7 The uncertainty of the computer should be included by means of an additional term, $(E_{cm})^2$ under the square root sign in equation 2, (equation 3).

4.8 Where volume flow q_v is being computed, the uncertainty in the measured value of density at base conditions $E_{\rho b}$, should be derived, giving consideration to the principles of paragraph 31.

4.9 The term $(E_{\rho b})^2$ should be included under the square root sign in equation 3. (equation 4).

4.10 If the operating density is calculated from measurements of pressure, temperature compressibility factor, and molecular weight then the term $\frac{1}{4}(E_{\rho 1})^2$ should be deleted from equations 2, 3 and 4, and the following terms substituted (see equation 5), respectively,

$$\frac{1}{4}(E_{P1})^2 + \frac{1}{4}(E_{T1})^2 + \frac{1}{4}(E_Z)^2 + \frac{1}{4}(E_M)^2$$

where E_{P1} is the percentage uncertainty in the measured operating pressure etc.

4.11 The uncertainty of a meter tube should be calculated at the design flow rate and one third of this flow rate.

4.12 In the statement of uncertainty of flow rate it is not necessary to distinguish between random and systematic components.

4.13 Where the gas flow is shared equally amongst a number of meters of identical design arranged in parallel the uncertainties in the factors C, the discharge coefficient and epsilon should not be considered to be randomly distributed between the meters. The following procedure for calculating the uncertainty in the total flow, E_Q, should be performed. Considering a single meter, the sum of the first two terms under the square root sign in equations 2 to 5 should be called $(E_X)^2$.

The uncertainty in the total flow, E_Q, is then given by;

$$E_Q = \left[(E_X)^2 + \left(\frac{E_Y}{\sqrt{N}} \right)^2 \right]^{1/2}$$

Where N is the number of meters in parallel, and $(E_Y)^2$ is the sum of the remaining terms in equations 2 to 5.

Equations modified for ISO 5167-1:1991 uncertainty equation (Section 11.2.2).

EQUATION 1

$$\frac{\delta q_m}{q_m} = \left[\left(\frac{\delta C}{C}\right)^2 + \left(\frac{\delta \varepsilon}{\varepsilon}\right)^2 + \left(\frac{2\beta^4}{1-\beta^4}\right)^2 \left(\frac{\delta D}{D}\right)^2 + \left(\frac{2}{1-\beta^4}\right)^2 \left(\frac{\delta d}{d}\right)^2 + \frac{1}{4}\left(\frac{\delta \Delta P}{\Delta P}\right)^2 + \frac{1}{4}\left(\frac{\delta \rho_1}{\rho_1}\right)^2 \right]^{1/2}$$

EQUATION 2

$$Eq_m = \left[(E_C)^2 + (E\varepsilon)^2 + 4\left(\frac{2\beta^4}{1-\beta^4}\right)^2 (E_D)^2 + \left(\frac{2}{1-\beta^4}\right)^2 (E_d)^2 + \frac{1}{4}(E_{\Delta P})^2 + \frac{1}{4}(E\rho_1)^2 \right]^{1/2}$$

EQUATION 3

$$Eq_m = \left[(E_C)^2 + (E\varepsilon)^2 + \left(\frac{2\beta^4}{1-\beta^4}\right)^2 (E_D)^2 + \left(\frac{2}{1-\beta^4}\right)^2 (E_d)^2 + \frac{1}{4}(E_{\Delta P})^2 + \frac{1}{4}(E\rho_1)^2 + (E_{cm})^2 \right]^{1/2}$$

EQUATION 4

$$Eq_v = \left[(E_C)^2 + (E\varepsilon)^2 + \left(\frac{2\beta^4}{1-\beta^4}\right)^2 (E_D)^2 + \left(\frac{2}{1-\beta^4}\right)^2 (E_d)^2 + \frac{1}{4}(E_{\Delta P})^2 + \frac{1}{4}(E\rho_1)^2 + (E_{cm})^2 + (E\rho_b)^2 \right]^{1/2}$$

EQUATION 5

$$Eq_v = \left[(E_C)^2 + (E\varepsilon)^2 + \left(\frac{2\beta^4}{1-\beta^4}\right)^2 (E_D)^2 + \left(\frac{2}{1-\beta^4}\right)^2 (E_d)^2 + \frac{1}{4}(E_{\Delta P})^2 + (E_{cm})^2 + (E\rho_b)^2 + \ldots \right.$$
$$\left. \frac{1}{4}(E_{P1})^2 + \frac{1}{4}(E_{T1})^2 + \frac{1}{4}(E_Z)^2 + \frac{1}{4}(E_M)^2 \right]^{1/2}$$

EQUATION 6

$$E_Q = \left[(E_X)^2 + \left(\frac{E_Y}{\sqrt{N}}\right)^2 \right]^{1/2}$$

NSFMW.97

North Sea FLOW Measurement Workshop

Paper 8: 2.2

THE NORWEGIAN REGULATIONS RELATING TO FISCALS MEASUREMENTS OF OIL AND GAS - 1997 UPDATE

Authors:
Olav Selvikvåg, Norwegian Petroleum Directorate, Norway

Organiser:
Norwegian Society of Chartered Engineers
Norwegian Society for Oil and Gas Measurement
Co-organiser:
National Engineering Laboratory, UK

Regulations relating to fiscal measurement of oil and gas. Stipulated by the Norwegian Petroleum Directorate 3.7.1991 pursuant to Act. No. 11 of 22 March 1985 relating to petroleum activities, section 15, fourth paragraph, cf. regulations supplementing the Act relating to petroleum activities stipulated by Royal Decree of 14 June 1985, Section 15, 19 and 47. Cf. letter of delegation 28 June 1985. Last amended 20 January 1997.

In the "Regulation relating to fiscal measurement of oil and gas etc.", (unofficial translation) stipulated by the Norwegian Petroleum Directorate 3 July 1991, the following changes are made:

Section 3 Definitions:

New definition for Calibration factor will be:

Calibration factor:
Relationship between the measured value coming from a flow meter and the measured value from a reference measurement system.

Definition of Metering tube is applicable both for oil and gas.

Metering tubes (oil gas):
Straight pipe section where a flow meter is installed.

New definition of flow meter will be:

Flow meter:
Equipment located in or clamped to a pipe and its signal transformer, to provide a primary signal proportional to the amount of flow through the pipe.

Section 23. Design of the metering system (oil/gas)

The second part of the section will be:

When metering gas, the mechanical part of the metering system shall consist of gas metering tubes and orifice plates designed in accordance with recognised standards, or of one or more metering tubes equipped with multipath ultrasonic meters.

(replacing existing second part)

Section 24. Operation range of the metering system (oil/gas)

The last three parts are new (comes in addition to the last part in force). These parts will be:

When using ultrasonic flow meters, the maximum flow velocity shall not exceed 80% of the maximum rate specified by the vendor.

When using ultrasonic flow meters on sales gas metering stations, the metering station shall consist of at least two parallel tubes, each allowing for 100% capacity.

When using ultrasonic flow meters on allocation metering stations, one metering tube could be adequate, provided the requirements as given in section 28 are taken care of. It is the availability of the flow meter which determines whether a solution with one single metering tube can be allowed.

Section 25. Requirements for the isolation valves (oil/gas)

In the third sentence the word "testing" has been replaced with "verification".

Section 28. Requirements for the orifice plate (gas)

The title of this section is changed to:

Requirements for the flow meter (gas).

The section is divided into two points marked with a) and b).

a) Requirements for the orifice plate:
The diameter ratio shall not exceed 0.60, if the applied standard gives a flow coefficient with less accuracy for higher diameter ratios. (previous text is kept).

b) Requirements for the ultrasonic flow meter:
The ultrasonic flow meter shall have the number of sound paths which have been proven to be necessary to provide a representative velocity measurement for the cross section during the relevant flow conditions.

All geometric dimentions of the ultrasonic flow meter which affect the measurement result shall be measured using traceable equipment, at known temperatures. The material constants shall be available for corrections.

The meter shall be designed and installed so that any accumulation of impurities in the form of liquid and solid particles in the proximity of the transducers is avoided.
The meter shall either by its own design or by necessary piping arrangement always be available for necessary maintenance.

The meter shall be designed so that measurements of acceptable quality can be achieved when one transducer pair is out of service.

The ultrasonic flow meter shall be individually calibrated at a traceable laboratory at process conditions (velocity of flow, pressure and temperature) as similar to the operational conditions as possible. The influence of variations in pressure and temperature shall be determined. The zero point correction and the calibration factor shall be determined. The meter shall be individually identified, and a certificate shall be issued.

The ultrasonic flow meter shall be tested in the upper and lower part of the range, and at three points distributed between the minimum and the maximum values. Five repeats shall be made for each point. When the zero point correction and calibration factor correction are done the deviation from the reference shall be less than +/-0,5%. The requirement applies to velocities above 5% of maximum range. The calibration factor which derives from the calibration shall always be used.

Section 29. Requirements for metering tube (gas)

In addition to the last part, concerning requirements for orifice metering, four new parts have been added:

When using ultrasonic flow meters the minimum upstream length shall be 10 D. The minimum downstream length shall be 3 D. It shall further be verified that the ultrasonic meter is not influenced by the lay out of the piping upstream or downstream in such a way that overall uncertainty requirements laid down in section 16 are exceeded. If it is necessary, flow straighteners of recognised standard can be installed.

The ultrasonic flow meter must not be installed in the immediate vicinity of pressure reduction systems (valves etc.), which may affect the ultrasonic signals. An evaluation shall be carried out which shows that surrounding equipment (both upstream and downstream), will not affect the ultrasonic signals.

When doing ultrasonic measurement, quality requirements for the inner quality of the metering tubes shall be determined.

The ultrasonic flow meter with associated metering tube shall be insulated upstream and downstream in order to reduce temperature gradients.

Section 30. Requirements for the flow profile (gas)

In front of the text it has been added:

Requirements for the orifice measurement.

Section 31. Location of sensors (oil/gas)

After the text in force, a new part has been added:

The ultrasonic flow measurement requires that temperature, pressure and if applicable density measurement are to be carried out according to the same guidelines as applicable to conventional orifice measurement.

Section 33. General requirements for the instrument loops (oil/gas)

After the text in force, a new part has been added:

A certificate indicating the critical parameters related to electronic and transducers shall be issued. When a test cell is used, the pressure and temperature shall be as similar to the operational conditions as possible.

Section 37. Differential pressure loop (gas)

New heading to this section will be:

Instrument loop for primary signal (gas).

In the beginning of this section, a new sentence has been introduced:

In respect of orifice plates, the differential pressure is the primary signal.

In addition to the text in force, two new paragraphs have been added, which are:

With regard to ultrasonic flow meters, the signals between the acoustic transducers are the primary signals. Critical parameters related to electronic and transducers shall be determined. It shall be possible to verify the quality of the electric signal which represents the acoustic pulse by automatic monitoring procedures in the instrument or by connecting external test equipment.

The transducers shall be identified by serial number or similar, location in the meterhouse etc. A dedicated certificate stating critical parameters shall be attached.

Section 43. General requirements for the computer part (oil/gas)

The ninth paragraph has been changed to:

The computer part shall be designed so that during calibration the amounts shall be registrated separately and independently of measured amounts.

Section 49. General (oil/gas)

In addition to the last paragraph in force, a new paragraph has been added, which is:

Ultrasonic flow meters for gas shall be individually tested at a traceable laboratory according to the requirements in section 28. Turbine meters for hydrocarbons in liquid phase shall be in a test facility to verify that the requirements laid down in section 27, can be achieved.

Section 62. Operating requirements for the turbine meters (oil)

New heading to this section will be:

Operating requirements for flow meters (oil/gas).

The section is divided into two points indicated by letters.

a) the existing text in section 62.

b) new text which will be:

After being pressurised before being put into operation, the ultrasonic flow meters shall be checked to verify velocity of sound and zero point for each individual sound path. Deviation limits for the various parameters shall be determined prior to or as soon as possible after the meters are put into service.

Section 65. Inspection of the metering tubes (gas)

Addition of a first sentence in this section:

Requirements for the orifice measurement:
(the text onward as before)

Section 66. Inspection of the orifice plates (gas)

New heading which will be:

Inspection of flow meters (gas)

In addition to the last paragraph in force a new paragraph is added. The text of this paragraph is the following:

During the operational phase, the parameters relevant to verify the condition of the meter shall be checked. Zero point check of the transducers by using an external test cell shall be done when necessary. If the acoustic signals from the transducers are weakened or if an alarm mode so indicates, the necessary verifications and corrections shall be done.

Guidelines to the regulations relating to fiscal measurement of oil and gas. Issued by the Norwegian Petroleum Directorate 3 July 1991. The following changes are made:

To section 23:

Gas Metering

The third paragraph is changed to:

Ultrasonic flow measurement may be used when metering gas for fiscal purposes.

To section 24

New paragraph:

If, on an allocation metering station a concept based on only one gas metering tube is selected, two meters in series should be used, or alternatively a spare meter for installation in the metering tube should be available if necessary.

To section 28:

New paragraph no six.

The number of sound paths which are required for ultrasonic flow measurement should be evaluated from the geometry of the sound paths and their coverage over the cross section.

New paragraph no seven:

When regulations require that the ultrasonic flow meter shall always be available for necessary maintenance, this means that combined oil/gas processing facilities may use one metering tube if the flow meter may be made available for maintenance by injecting gas. On gas processing facilities or riser platforms with higher availability requirements an extra metering tube should be installed. Meters equipped with transducers that can be replaced during operations, may contribute to increase availability.

New paragraph no eight:

For ultrasonic flow meters, the relevant parameters to be logged and documented during calibration should be:
- Gain factor
- Velocity of sound and velocity of flow for each sound path

New paragraph no nine:

The material constants in question will be the thermal expansion coefficient and Youngs modulus.

New paragraph no ten:

The most important part of a flow test is to determine that the transducers can handle the specified gas velocity. Accordingly, for large meters this will require a need to perform tests at lower pressure than the operational pressure, to increase the gas velocity.

To section 29.

Two new paragraphs which comes in addition to the previous four:

Paragraph no five:

The requirements determined for the inner quality of ultrasonic metering tubes, should be developed from similar requirements for the orifice plate measurement. Somewhat lesser requirements may however be acceptable on account of the fact that the ultrasonic flow meter is not as sensitive to the parameter flow profile as the orifice plate measurement.

Paragraph no six:

Reducer in the metering tube may be used to straighten the flow profile.

To section 30.

First sentence is changed to:

Recognised standard for orifice plate measurement will be: ISO 5167-1 or research results which are mutually accepted.

New paragraph no two:

Both for orifice plate measurement and ultrasonic flow measurement, flow straighteners of recognised type may be used to improve the flow conditions through the meter.

To section 31.

New paragraph in addition to the existing last paragraph:

During ultrasonic measurement of gas, the common pressure recovery method of density measurement can not be used. Gas will have to be vented to a vent/flare system or be recovered.

To section 33.

New paragraph no three:

Instrument loops based on pulse/frequency or digital communication may be used from the field to the control room. When using digital communication it is essential that the number of instruments on one communication line do not exceed the line capacity with regard to response/reading capacity.

New paragraph no four:

When using digital communication, calibration may normally be simplified compared to the regulatory requirements for analogue/digital communication. A rational calibration program should be developed to meet the requirements of the regulations and the capabilities of the equipment.

New paragraph no five:

Duplication of equipment on the instruments part for meters on transmitters will present a good basis for extending calibration and certification intervals for measuring and instrument equipment.

To section 41:

Three new paragraphs which comes in addition to the previous seven paragraphs.

New paragraph no eight:

When measuring dry gas, the use on one line gas chromatograph may be an alternative to provide composition and density data. Relevant standards to be followed may be ASTM 1945 (1991) and NORSOK standard I-SR-106, On line gas chromatograph. If such a system is selected, special attention should be paid to that the sample tubing into the chromstograph are properly designed, so that any liquid contamination is prevented. To achieve this the pressure should be reduced stepwise. Temperature sensors should be installed on critical locations and necessary heat supply to the sample line should be available.

New paragraph no nine:

On sales gas metering stations two chromatographs should be installed for mutual monitoring.

New paragraph no ten:

On allocation metering stations the parameter water in oil may be determined by using on line measurement equipment of recognised standard.

To section 43:

New paragraph no nine:

When doing ultrasonic flow measurement it should be possible to verify time measurement and pulse detection.

To section 46:

New paragraph:

The ultrasonic flow meter should either by direct read out or by internal check functions monitoring the velocity of flow and the velocity of sound for each ultrasonic path. Automatic alarms should be generated when deviation from present limits are detected.

To section 47:

New paragraph in addition to the existing paragraphs:

Litra d) of the section does not apply to ultrasonic flow measurement.

To section 62:

New second paragraph:

Ultrasonic flow meters should, as soon as possible after installation, be tested using a chosen flow rate. The vendor should inform about parameters of importance to monitor. It would be reasonable that parameters mentioned in the guidelines to section 46, are used for further follow up.

New third paragraph:

Zero point checks as mentioned in the regulations are done to determine basis figures for various parameters. These may then be used for further monitoring of the flow meter. Due to the relatively high uncertainties involved in this test, this is just meant to be a rough check of the flow meter.

To section 66:

New paragraphs are:

Ultrasonic flow meters should be recalibrated at a traceable laboratory when needed. A simple check to verify the various transducers would be to check the zero point in a test cell.

Trending of various critical parameters should be done.

Alarm list which defines critical alarms and describes the handling of them should be developed.

It should be defined how critical alarms are to be monitored by self diagnosis in the computer.

When using ultrasonic flow meters, the supervisory computer should calculate VOS (velocity of sound) based on P,T and gas composition to monitor the VOS calculated by the ultrasonic flow meters.

In addition also some corrections in the Guidelines for the Regulations have been performed. These have mainly been simplifications.

NSFMW.97

North Sea FLOW Measurement Workshop

Paper 9: 2.3

FLOW METERING CONCEPTS, AN ENGINEERING CONTRACTORS EXPERIENCE

Authors:
Lars Brunborg and Dag Daler, Kværner Oil & Gas as, Norway

Organiser:
Norwegian Society of Chartered Engineers
Norwegian Society for Oil and Gas Measurement
Co-organiser:
National Engineering Laboratory, UK

FLOW METERING CONCEPTS, AN ENGINEERING CONTRACTORS EXPERIENCE

by
Lars Brunborg
Kværner Oil & Gas as, Norway

and
Dag Daler
Kværner Oil & Gas as , Norway

FLOW METERING CONCEPTS, AN ENGINEERING CONTRACTORS EXPERIENCE

Lars Brunborg and Dag Daler, Kværner Oil & Gas as, Norway

SUMMARY

We will give a brief discussion of an engineering company's experience regarding fiscal measurement systems. This will be seen in relationship to the use of NORSOK standards, versus functional and detailed specifications, and simplified and cost efficient concepts.

The constrains on the design is also commented on, and the influence of these constraints on layout, maintainability and operability.

Further a brief review of the computer concepts available, including integration with DCS

Finally we will review the relationships between Supplier - Engineering Contractor - Operator, seen in relationship to integrated teams, frame agreements, etc.

INTRODUCTION

Kværner Engineering, now an integral part of Kværner Oil & Gas as, has an extensive experience in the design and construction of oil production facilities and platforms, including fiscal metering systems, from the early 1970'ies and up to today. The company has been involved, over the years, in the changes from EP contracts with detailed specifications and detailed inquiries through to EPCI contracts with functional specifications and frame agreements, based on NORSOK.

NORSOK STANDARD VERSUS FUNCTIONAL SPEC

Detailed specifications.

Establishing specifications has always been one of the problems at the start of a new project.
As the specifications included a great deal of details, they are normally a time consuming activity. It is also often difficult to copy information from earlier projects due to the inherent differences between the oil companies, and various requirements within their operational groups.
Detailed specifications are also placing hard constraints on the suppliers who quite often had to follow a new standard on every project. This practice has also often resulted in budget growth and planning difficulties for the supplier resulting in delayed deliveries and/or uncompleted deliveries with a number of punch items to be rectified at site.

On the other, hand it made life easier for the engineering companies and the commissioning teams, because specified requirements were available during punch out of the equipment. This furthers the standardisation of equipment and solutions for the users,

but not for the suppliers, and thus leads to a higher price level. (One would normally expect the suppliers to deliver at lower prices if they can use their own standard specifications.)

Functional specifications.

Functional specifications were the first step towards cutting expenses. As they do not contain as much detailed information they are less time-consuming to write and the engineering effort decreases. As the level of details goes down, the problems around acceptance of the delivered items increase. The engineering and commissioning teams' doe not have the same number of "detailed data" to use when checking the equipment. This will inevitably lead to controversy with the supplier, as several items will depend on the preferred solutions by one or the other of the individuals involved.

NORSOK

NORSOK is the last step in this trend, where the industry wants to standardise and cut expenses. It furthers standardisation on a "higher" level, outside the oil companies. It also makes it easier for the suppliers to get their own standard specifications accepted, as long as they conform to what is laid down in the NORSOK standards. The supplier standard therefore becomes acceptable to a large number of end users.
One can say that NORSOK bridges the gap between the detailed and the functional specifications. Quite a few of the details from the detailed specifications are agreed between several end users and laid down in NORSOK. The engineering companies can then use their time to get the best functionality for the system. At the same time there is an agreed set of details to use during checking of the equipment, and approval of the delivery.

NEW CONCEPTS

Ultrasonic meters.

What sort of new concepts are we looking for today? The ultrasonic fiscal gas meter is finally on the way into the marked, but we are still waiting for the full impact of the ultrasonic fiscal liquid meter. The technical aspects behind these meters will be dealt with in details in other presentations, and is not a topic of this presentation. We are looking forward to further developments around these meters.

Prover concepts

The standard bi-directional prover has been used in all projects KoG AS has been involved in since Oseberg A. The compact prover installed on this skid has later been removed.
A compact prover was discussed on the EKOII project but was rejected due to size restraint. A vertical compact prover was too high.

As the prover is a heavy and large part of an oilskid, the suppliers should do their utmost to revert with more compact designs. Possibly looking into solutions where the prover becomes redundant. - One such solution would be a liquid ultrasonic meter where a spare, calibrated meter, was available on the platform ready to be installed.

Oil companies unwillingness to try, due to NPD reluctance

New measuring principles are not apearing every day, and when something as the ultrasonic flowmeter appears, there is always a great interest in the industry for these new "components". Everyone would like to test it, but in the end there is a great reluctance to tray out something where the field experience is limited, or none existing.

Well proven technology is a good thing, but more willing to try new techniques are missing.

We are looking for the oil companies to start discussions with NPD at an early stage, to clear the way for new ideas.

More openness for new concepts

The metering industry as a total, but especially the oil companies, should be more open for trying new concepts. With this we do not only mean new components as the ultrasonic meter, but also new ways of utilising these and the existing measuring concepts. We feel that it should be possibly to introduce new "concepts" if discussions are started, for example with NPD, at an early stage, and the oil company has done its homework properly.
An example of this, are the discussions started by one of Statoil 's metering experts, with NPD, regarding the Sleipner T gas measurement. This was an allocation metering station in a 20" line, based on a senior orifice fitting, the fiscal measurement being done on the SLA platform. He presented a case where he showed that the total uncertainty over a long period was unneglible if a 1x100% meter run with a bypass was used instead of 2x100 %. This was based on the assumption that the flow during the short time the bypass was open was taken as the average of the flow the last minute before the bypass was opened. The bypass was only used during inspections of the orifice. This concept has later also been used for fuel gas measurements.

CONSTRAINTS ON DESIGN

Size, weight (available envelope very small - standards for "guesstimate" during preengineering)

One of the major problems during the preengineering phase of a development project is to estimate the size and the weight of the equipment to be installed. This also includes the metering system(s), as these are of a significant size. This was originally done as pure guess work by layout engineers, based on the size and weight of the system from an earlier project, with approximately the same flow as the one being "sized. This could also

be based on very preliminary input from the suppliers. More common was to take the available space and us it. In the end, this normally resulted in a small envelope. Further, a small envelope results in a "crowded" design (i.e. narrow accesses ways, bad accessibility to components, etc.), from the supplier.

We feel the suppliers should involve themselves in this area and help to develop these thoughts into sizing guidelines for preengineering.

To reach as optimum an envelope as possible, it should, in our opinion, be possible to start with an existing skid and "resize" this to new dimensions. If we try to analyse this situation, we should be possible to single out some important factors that govern the change of size, as for instance:

- The number of the metering runs. This will determine the width of the skid if this was the only item being changed. It could then be argued that the width of a meter run is a factor of the diameter plus access, which would be of the order of 1m assuming access only from one side
- The meter run dimension. This would influence both the width and the length of the skid, the latter due to the influence on the straight length (number of D's)
- Flow. This will decide the number and size of the meter runs.

From these reflections it should be possible to resize a skid, after the flow per meter run has been established.

This should be a fairly straight forward exercise for a gas skid, where the length is easily increased in proportion to the size. The width can easily be treated similar. Similarly increasing the headers proportional to the meter runs.

For a oil/condensate skid this becomes more complicated as the prover must be taken into consideration. One could assume that the prover size should be extrapolated as for the meter runs, and the prover located below or on the outside of the skid. Similar assumptions should be made for a compact prover.

If one assumes a certain weight split between the baseframe, meter runs, and the prover, it should also be possible to scale the weight.

Following this line of thought will not give an exact weight, and size envelope, but it should improve the "estimate". It should also enable the suppliers to produce better and more user friendly skid layouts during the detailed engineering phase.

Skid layout (stairs, ladders, functionality, serviceability, etc.)

The problem with skid layout, as discussed above, resulted very often in a "crowded" design, and has been a challenge to the suppliers, even if this has improved over the years. This has mainly been a problem with oil metering skids, as the gas metering layout is less complicated and more a function of the constraints given by international standards.

In our experience there is certain problems that are more common than others, by listing them we hope not to meet these items as often in the future as we have in the past:

- Good access between meter runs
- Avoid pipes/instruments, etc. intruding into the access area.
- Make sure all items to be read or accessed can be read/reached from the access way on the skid, not from the outside.
- Make sure that lager pieces of equipment, for example valves can be removed for maintenance.
- Do not forget the instrument enclosures in the design (if applicable)
- Make sure stairs and ladders are according to regulations and standards.
- Make sure the heights of doors to GC houses, etc. are according to regulations and standards

COMPUTER CONCEPTS

Main computer (single, dual, PCS node)

A hot standby dual main computer system was the standard some years back, as this system fulfilled the Norwegian regulations. When the regulation was modernised, an opening was given for using only 1 main computer system. This has led to 3 trends, regarding main computer systems:

1. Dual main computer system
   This has been the traditional system over the years and is still used by oil companies, but it is also the most complicated one, both hardware and software wise. This is mainly due to the hot-standby layout with hardware connection for switching between the computers. It is also the most expensive since two complete computer systems are involved

2. Single
   This has been used by some oil companies since it is a simpler and cheaper system. Its main drawbacks are the availability, as there is no permanent back-up, and the main computer system will be down, during breakdown, until spare parts have been brought from the platform spare stores.

3. use of platform control system (PCS) node
   It has been common in the last years for the main metering computer system to communicate with the platform control and monitoring systems via a datalink or network connection. Since the state of the art for hardware platforms for metering main computer system often, is the same as for the platform control and monitoring systems, a natural step is then to combine the metering supervisory computer system with a PCS node. As this in reality is a "single" system, it has the same drawback. It's main advantages is the hardware functionality and that the operation of the metering system, for the operator, is similar to the rest of the system

Traditionally, in solution 1 and 2 above the main metering computer has been the full responsibility of the metering computer system supplier. In solution 3, on the other hand, two different concepts emerges:

1. The Metering system supplier purchases, or are free issued, a PCS node, and uses this as the hardware for the supervisory computer system, with full responsibility as in 1 and 2 above.

2. The metering system supplier supplies a functional description covering the supervisory metering computer system functionality, including the communication with the flowcomputers. The DCS supplier must then use this to program the DCS node. This solution has, so far, been used on the Åsgard A platform, and will be used on Åsgard B.

Flowcomputer (dedicated units versus standard computers)

Two trends has been seen the last years regarding the subject of flowcomputers.

Most suppliers use dedicated units, with 1 flowcomputer for each metering run. The alternative has been to program the flowcomputer functions standard computer system.

What are the pros and cons for these two alternatives:

- Dedicated units
  Normally cheaper, 1 per metering run
  Easily programmable from front of unit (or PC)
  Application software in PROMs, can easily be updated.
  Easily replaceable with new unit from spares.
  Requires less space in cabinet

- Standard computer
  More expensive, this must be compensated by programming two flowcomputers for two different metering stations into the unit.
  Replaced with cards from stock.
  More elaborate programming tools (and equipment) needed.

Taken these items into consideration our opinion is that the dedicated flowcomputer is the more cost effective and flexible solution in the long run.

SUPPLIERS

Number of available suppliers.

The bidders list for metering systems are established very early in the projects, in the pre-engineering or basic engineering phases. To get a good competitive situation it is important to have a sufficient number of bidders. For most instrument packages this has

been in the order of 4 to 5. The use of too many bidders creates to much work during the evaluation stage, and to many suppliers have to put down a substantial number of hours without getting anything back. Experience has shown that 3 is an optimum number, one get a good competitive situation, and the amount of work involved in the evaluation is acceptable.

This is ideal for the metering situation in the Norwegian sector, as there is only 3 suppliers normally capable of delivering complete metering skids/systems.

Taking the number off project over the years into account, our experience is that this is in line with the work available. We are thus certain that we will have at least 3 competitors fighting for every project in the years to come.

Frame agreements - long term agreements between suppliers and oil companies.

Then on to frame agreements, which binds an end user or a contractor to a supplier for a period over several years. A positive side of this is that the contact between supplier and end user is very close. This can result in early involvement by the supplier giving optimum designs, as the design is done in close co-operation, and not in a bid situation.

We have seen that the competitiveness of the suppliers changes all the time with respect to prices, delivery times, etc.. During one period one supplier delivers the best bid, whiles in other periods' one of the others have most success.

This might lead to the unfortunate situation that one supplier wins several frame agreements during the same period, whilst the rest are short of work. A dangerous outcome of such a situation is that the number of suppliers decreases, with the result this would have on the competitive situation in the marked.

NSFMW.97

North Sea FLOW Measurement Workshop

Paper ~~10~~: 2.4

SOFTWARE TESTABILITY, TESTING AN VERIFICATION IN FISCAL OIL AND GAS FLOWMETERING

BASED ON VOLUME, DENSITY, TEMPERATURE AND PRESSURE MEASUREMENTS

Authors:
Kanaga Saba Pathy Mylvaganam, Bergen College, Norway

Organiser:
Norwegian Society of Chartered Engineers
Norwegian Society for Oil and Gas Measurement
Co-organiser:
National Engineering Laboratory, UK

SOFTWARE TESTABILITY, TESTING AND VERIFICATION

IN FISCAL OIL AND GAS FLOWMETERING

BASED ON

VOLUME, DENSITY , TEMPERATURE, AND PRESSURE MEASUREMENTS

Kanaga Saba Pathy Mylvaganam
Høgskolen i Bergen (Bergen College)
Postbox 6030
N- 5020 Bergen
(Visiting Address: Nygårdsgate 112, N-5008 Bergen)
NORWAY
Tel: + 47 55 58 76 09
Fax: + 47 55 58 77 90
email: Saba.Mylvaganam@lhg.hib.no

NORTH SEA FLOW MEASUREMENT WORKSHOP 1997

27 - 30 October 1997

Kristiansand

NORWAY

SOFTWARE TESTABILITY, TESTING AND VERIFICATION IN FISCAL OIL AND GAS FLOWMETERING BASED ON VOLUME, DENSITY, TEMPERATURE, AND PRESSURE MEASUREMENTS *

Kanaga Saba Pathy Mylvaganam
Høgskolen i Bergen (Bergen College),Norway

Keywords: Fiscal Flowmetering, testing and verification, oil & gas measurement, flow computer.

ABSTRACT

Many of the companies in the oil and gas industries have different program modules for including volume, density and temperature measurements to evaluate the amount of oil/gas in the context of fiscal measurements. These measurements are very often done not at the same location in the pipe lines, but in different locations of the oil and gas transportation lines. These modules have to be put together and run on a main frame computer to get at the desired result, viz. the mass flow. The Norwegian Petroleum Directorate states in its "Regulations relating to fiscal measurement of oil and gas etc.": "The computer part shall be tested for each metering tube to verify that the different functions are operational. Each independent program routine, shall be verified to be in accordance with, or better than, the accuracy stated in §47 (e) ". This is an outcome of testability paradigm very much in discussion in many standards and regulations not only in the oil and gas industry.

Due to the need for a compact programme to handle such measurements along with the standards ISO 6976, ISO 5167 and stipulations covered in AGA No.8, Norsk Hydro in Bergen along with the Høgskolen i Bergen (Bergen College) developed programs to verify the results obtained from fiscal flowmeters. How this testability paradigm is incorporated in ultrasonic flowmeters is also discussed in this paper.

This paper presents the background (both physical and software) for the program development with some relevant details from the program, which in a modified form is currently used by the Norsk Hydro in fiscal oil and gas flowmetering. The experience of the end user is also presented. This paper is an outcome of a work performed for Norsk Hydro.

The demonstration of the programs discussed here is an integral part of the workshop presentation.

* This paper is based on a collaboration with Norsk Hydro as. Thanks are due **Mr. Trond Folkestad of Norsk Hydro as, Sandsliveien 90, N-5020 Bergen , Tel: +47 55 99 57 90, Fax: +47 55 99 66 05, email: Trond.Folkestad@nho.hydro.com** for valuable information from practical experience in using the programs developed for software testability under discussion.

BACKGROUND

The amount of oil or gas sold/bought is basically dependent on four different measurands: volume flow rate, density, temperature, and pressure. Due to reasons of space unavailability at the same spot for the necessary measuring devices, all these measurands are monitored in slightly different locations of the pipeline transporting oil or gas, necessitating calculation among different conditions of state as well as calculations to standard conditions. Both measurements and calculations must be performed to a very high degree of accuracy, as it involves huge amount of monetary transactions.

All the oil & gas companies use computer programs to verify the calculations in the metering stations. These computer programs are not very user-friendly nor efficient to use. Hence the need for testing and verification of existing programs. The practising engineer needs more user-friendly computer programs to enable efficient verifications.

The procedures are described in various documents including some ISO papers and guidelines published by local oil/gas companies, [1], [2], [3].

The Norwegian Petroleum Directorate stipulates [4], various procedures as to how the calculation of the volume flow of gas and oil should be performed in order to insure that accurate measurements are behind the calculation of sales value, royalty and tax on the measured quantity of produced oil and gas. In fact the measured quantity used for sale or calculation of royalty and tax is called fiscal quantity.

The following paragraphs in the set of regulations [4], are specially relevant to this paper:

§47 The computer routines for fiscal measurement calculations shall fulfil the requirements detailed in the applied standards. The computer routines shall further include the following:
(e) Algorithm and unintentional rounding off errors for computations of fiscal quantities in the computer part shall be less than ±0.001 %.

The computer part shall be tested for each metering tube to verify that the different functions are operational. Each independent program routine, shall be verified to be in accordance with, or better than, the accuracy stated in §47 (e). The integration accuracy shall be checked over at least three values, maximum, and minimum hydrocarbon flow and one value at mid range.
§72 Checking of the computer part (oil/gas): An independent review of the calculation accuracy of the computer part shall be performed at least on an annual basis (c.f. §47 (e), 57)

Earlier, the verifications of the flow computer calculations were carried out with the help of many small modules within the larger program. This procedure took considerable amount of time and the person doing the checking had to have a good insight in the program before doing the calculation.

The Norwegian Petroleum Directorate stipulates that the calculation accuracy of the computer shall be reviewed independently at least on an annual basis, implying, for example usage of an independent PC based program.

This paper touches on the topics of testing, testability and verification of programs in general and describes the main parts of the PC- programs developed for fiscal metering of both oil and gas. Part of the work for these programs are described in [5], [6] and [7].

MEASURANDS

The measurement system for the gas transport normally consists of,

1. an orifice plate to measure the volume flow
2. differential pressure transmitter to measure the differential pressure between the input and output sides of the orifice plate mentioned in 1
3. PT-100 resistance based temperature sensor to measure the temperature of the gas in the pipe.
4. a pressure gauge to measure the pressure in front of the orifice plate
5. a densitometer to measure the density of gas

as shown in **Figure 1**.

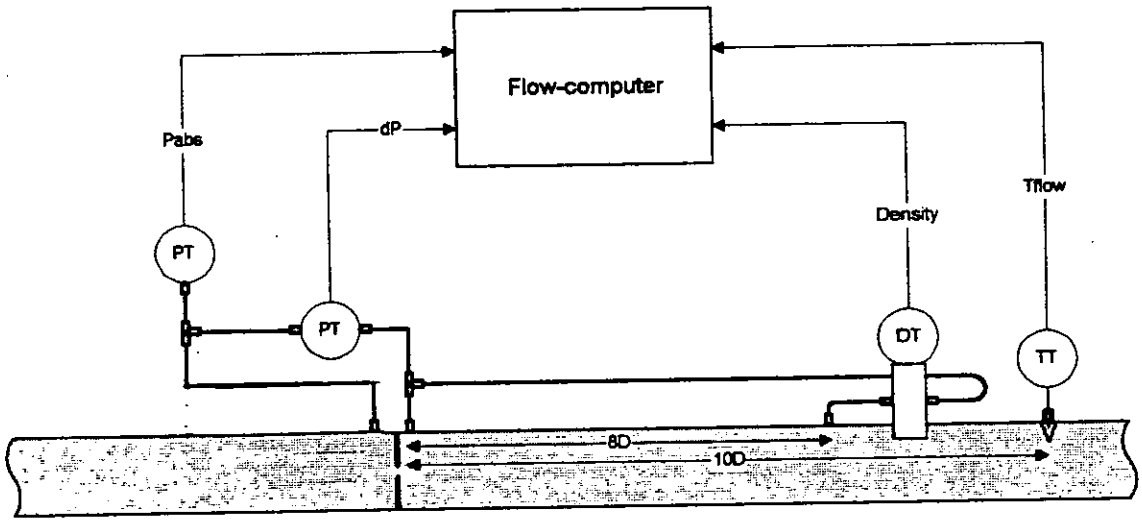

Figure 1 The schematic representation of a gas metering station. DT : Density transmitter; TT: Temperature transmitter; PT: Pressure Transmitter; Pabs: Absolute pressure; dP: Pressure difference. 10D and 8D represent the length in number of diameters of the pipe.

Similarly, the measurement system for the oil transport generally consists of

1. a turbine meter to measure the volume flow
2. PT-100 resistance based temperature sensor to measure the temperature of the oil in the pipe.
3. a pressure gauge to measure the pressure
4. a densitometer to measure the density of oil (only applicable for pipeline transport)
5. the meter prover designed so that five consecutive trials leads to values within a band of 0.020% of the average volume

Figure 2 shows the measurement loop used for oil.

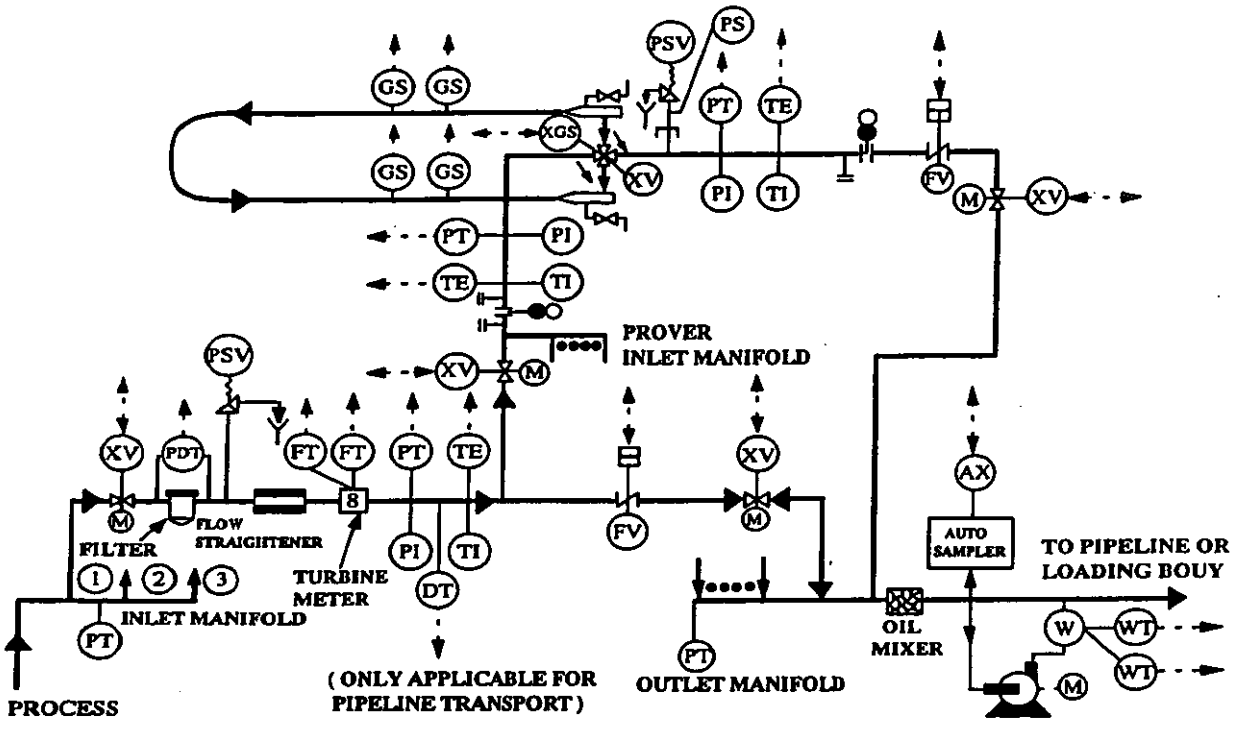

Figure 2 The schematic representation of an oil metering station, reproduced from [4].

The volume flow can also be determined using the contrapropagating transit time ultrasonic flowmeter, which in its multi-path form has been formally accepted as a fiscal meter for gas flowmetering by the Petroleum Directorate.

SOFTWARE TESTABILITY, TESTING AND VERIFICATION

European System and Software Initiative (ESSI) is an active action within the European Union paralleling the stipulations of the Norwegian Petroleum Directorate and has Software Best Practice as the target. Software Best Practice is aiming in all industrial sectors to improve their efficiency, provide better quality and better value for money. In the sense of Software Best practice, we could visualise a series of steps given in **Figure 3**.

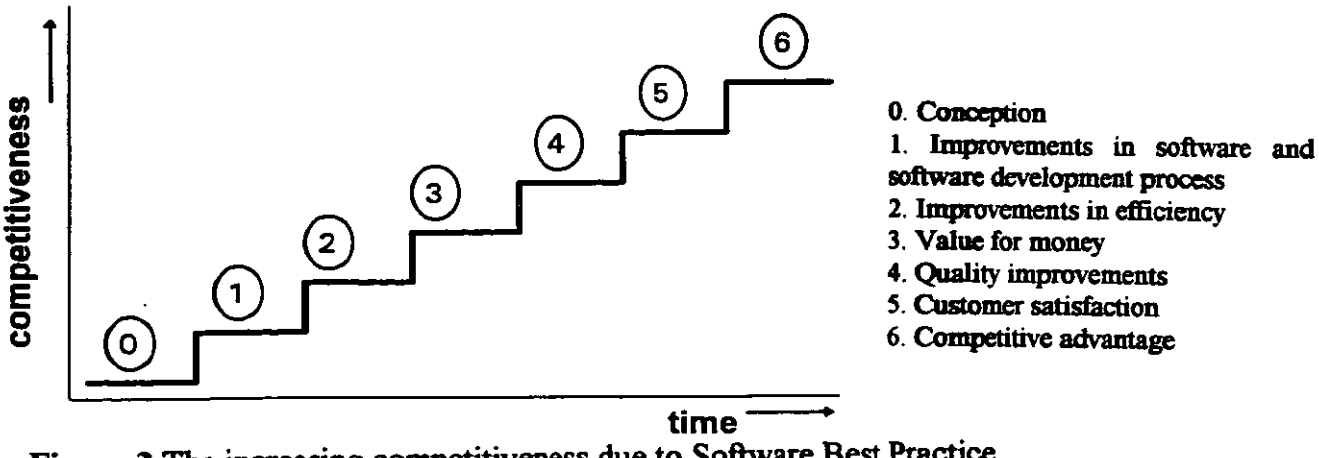

Figure 3 The increasing competitiveness due to Software Best Practice

Testability is used to confirm that each sub-unit performs its required function, that the sub-units are interconnected in the correct manner, that they interact correctly, and that the whole program executes its intended function. In the hardware branch, especially in the production of ICs , electronic devices are selected, where possible, with Built-In Self-Test (BIST) to perform test pattern generation and response analysis. This is the primary test mechanism used during wafer probe testing of ICs and should provide a high degree of fault coverage (>95%). This could be seen as the extension of the traditional test points selected already in the design stage of a circuit to test whether the circuit is functioning as intended without showing signs of faulty operation.

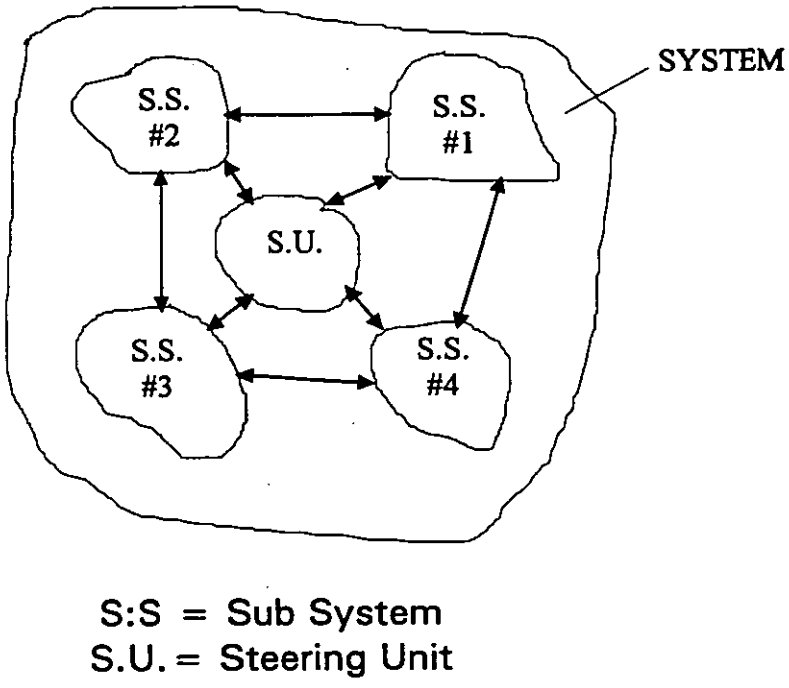

Figure 4 The interaction within a program with the subsets of modules (called sub-units in figure) with the steering unit.

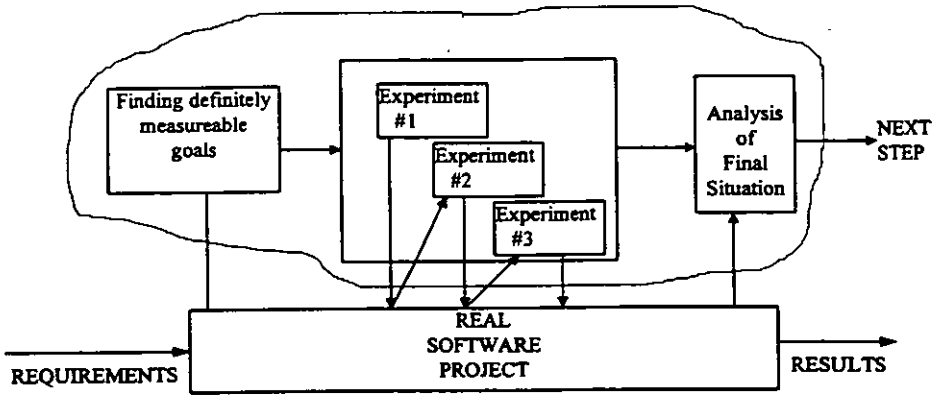

Figure 5 Process Improvement Experiments as part of testing, testability and verification. The tests done in the context of the present paper can be looked upon as a venture to improve the process based on testing and verification.

There are a plethora of discussions and definitions of testability and testing in the context of software development, [8],[9],[10], and [11]. The present forum is not the right place or the present author is not the right person to delve into these nuances in the software engineering. However, it is interesting to look into some of the definitions in use.

Testability

" (1)The degree to which a system or component facilitates the establishment of test criteria and the performance of tests to determine whether those criteria have been met, and (2) the degree to which a requirement is stated in terms that permit establishment of test criteria and performance of tests to determine whether those criteria have been met." [11]

Testing

Dynamic software testing is the process of executing the software repeatedly until a confidence is gained that either (1) the software is correct and has no more defects, which is commonly referred to as probable correctness, or (2) the software has a high enough level of acceptability. Testing can alternatively be subdivided into two main classes: white-box and black-box. White-box testing bases its selection of test cases on the code itself; black-box testing bases its selection on some description of the legal input domain, [11].

Verification

IEEE Software Dictionary [10] defines software verification to be the
"process of evaluating a system or component to determine whether the products of a given development phase satisfy the conditions imposed at the start of that phase."

This tallies very well with the concept of Process Improvement Experiments discussed in the circles of ESSI.

Software verification can be seen as the process that assesses the degree of "acceptability" of the software, where acceptability is judged according to the specification. In the present context, the specifications as given by Norwegian Petroleum Directorate and Norsk Hydro.

Finally, we quote from [11]:,

"Software testability, software testing, and formal verification are three pieces in a puzzle: the puzzle is whether the software that we have, has a high enough true reliability. Every system has a true (or fixed) reliability which is generally unknown; hence we try to estimate that value through reliability modelling. If we are lucky enough to have a piece of software that (1) has undergone enormous amounts of successful testing, (2) has undergone formal verification, and (3) has high testability, then we have three pieces that fit together to suggest that the puzzle is solved—high reliability is achieved.

Software testability, software testing, and formal verification are three pieces of the reliability puzzle, which developers must complete to get a picture of the software's true reliability. Each of the three puzzle pieces offers a unique bit of information about software quality. The goal is to combine all three. Testability analysis is related to but distinct from both software testing and formal verification, which makes it a good complement to the other two pieces. Like

software testing, testability analysis requires empirical work to create estimates. Unlike testing, however, testability analysis does not require an oracle a program that performs the same functions as the software being developed. Thus, testing can reveal faults, while testability cannot, but testability can suggest places where faults can hide from testing, which testing cannot do. Testability complements formal verification by providing empirical evidence of behavior, which formal verification cannot do."

That the software system should undergo enormous amounts of successful testing and verification is the motivation behind the stipulations from the Norwegian Petroleum Directorate.

ALGORITHMS USED

Introduction

Due to the variables (measurands as well as constants related to the gas composition, pipe dimensions etc.) involved in the equations for volume and mass flow, some of the necessary routines in a dedicated PC-program will involve

- extracting and storing values of measurands
- extracting and storing variables associated with gas/oil
- extracting and storing constants associated with the pipe line
- extracting and storing the constants associated with the orifice meter[1] or turbine meter
- extracting and storing the constants associated with the density meter

It is not the aim of this paper to go into the details of the physics behind all these calculations. However, it is essential to note that the state variables at the orifice meter or turbine meter will not be the same as those at the density meter, or those at the locations of pressure and temperature transmitters. In the estimation of fiscal quantities, the unit used in transactions is the standard cubic meter, written [m^3 (15 °C, 1.01325 bar)]. This means all the measurements should be reduced to standard temperature and pressure conditions. Hereby, the stipulations of Institute of Petroleum, American Gas Association and Norwegian Petroleum Directorate should be taken into account. For purposes of verification, the mass flow will also be calculated although the sales quantity is the standard volume.

Fiscal Gas Metering

The volume flow on the downstream-end of the orifice plate is given by ,

$$q_{vu} = A_2 \sqrt{\frac{2(p_1 - p_2)}{\rho(1-m^2)}} \quad \text{with} \quad m = \frac{A_2}{A_1} \leq 1 \tag{1}$$

where

A_1 = pipe diameter

A_2 = orifice diameter

ρ = density of gas

[1] in future, possibly the multi-path ultrasonic transit- time flowmeter

The corrections for vena contracta positioning and compressibility are taken care of by the factors α and ε in the following form:

$$q_v = \alpha\varepsilon q_{vu} \tag{2}$$

In equations (1) and (2), the parameters involved all vary according to the changes in state variables. The volume flow changes with temperature, the orifice diameter changes with pressure and temperature and so on. The calculation of these parameters under changing state variables is clearly specified by international organisations. The essence of the program is the handling of these parameters and the necessary recursive routines to arrive at the required quantities such as volume flow, mass flow, energy flowrate etc.

Energy flowrate is also required to be calculated by the and Norwegian Petroleum Directorate. Energy flowrate Q_e is given by

$$Q_e = Q_{vr} CV \tag{3}$$

where Q_{vr} = Volume flowrate and CV = calorific value as defined in ISO 6976.

For the program meant for the fiscal metering of gas, from Figure 1, we can see that we need information on the measurands, gas composition, calibration data, densitometer calibrations and means of converting the results to standard conditions.

Fiscal Oil Metering

Figure 2 illustrates that there are four major components in the case of oil metering station: oil flow based on the number of pulses form the turbine meter, prover readings, the temperature and pressure. There are a number of equations for all these calculations. The important ones are:

$$V_L = \frac{MR}{Mkf} C_{tsm} C_{psm} \tag{4}$$

V_L = volume at line conditions, MR = number of pulses in the measurement period , Mkf = meter k-factor for the turbine meter, C_{tsm} and C_{psm} are correction factors, [12].

The mass is calculated, with the subscripts S and L referring to "standard" and "line" conditions, from the volume flow and density V_L, ρ_L and $V_S \rho_S$

$$M = V_L \rho_L = V_S \rho_S \tag{4}$$

The series of coupling equations of different line parameters, state variables etc. are given in [12]. When an on-line densitometer is used for measuring the density at line conditions of a flowing liquid, the density at standard conditions has to be calculated.

PROGRAM STRUCTURE

Gas

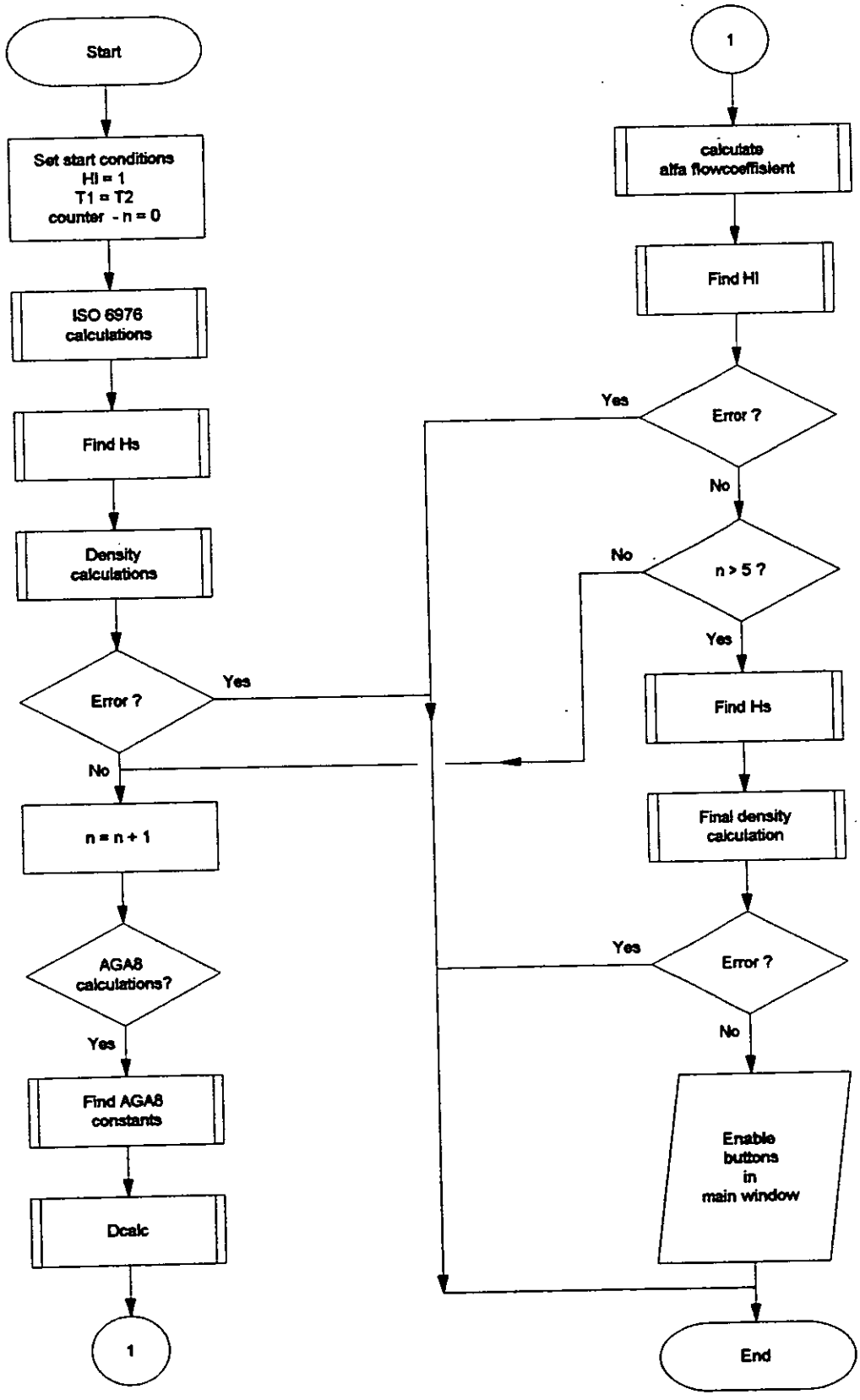

Figure 6 Main program flowchart, [5]. More details during demonstration of program.

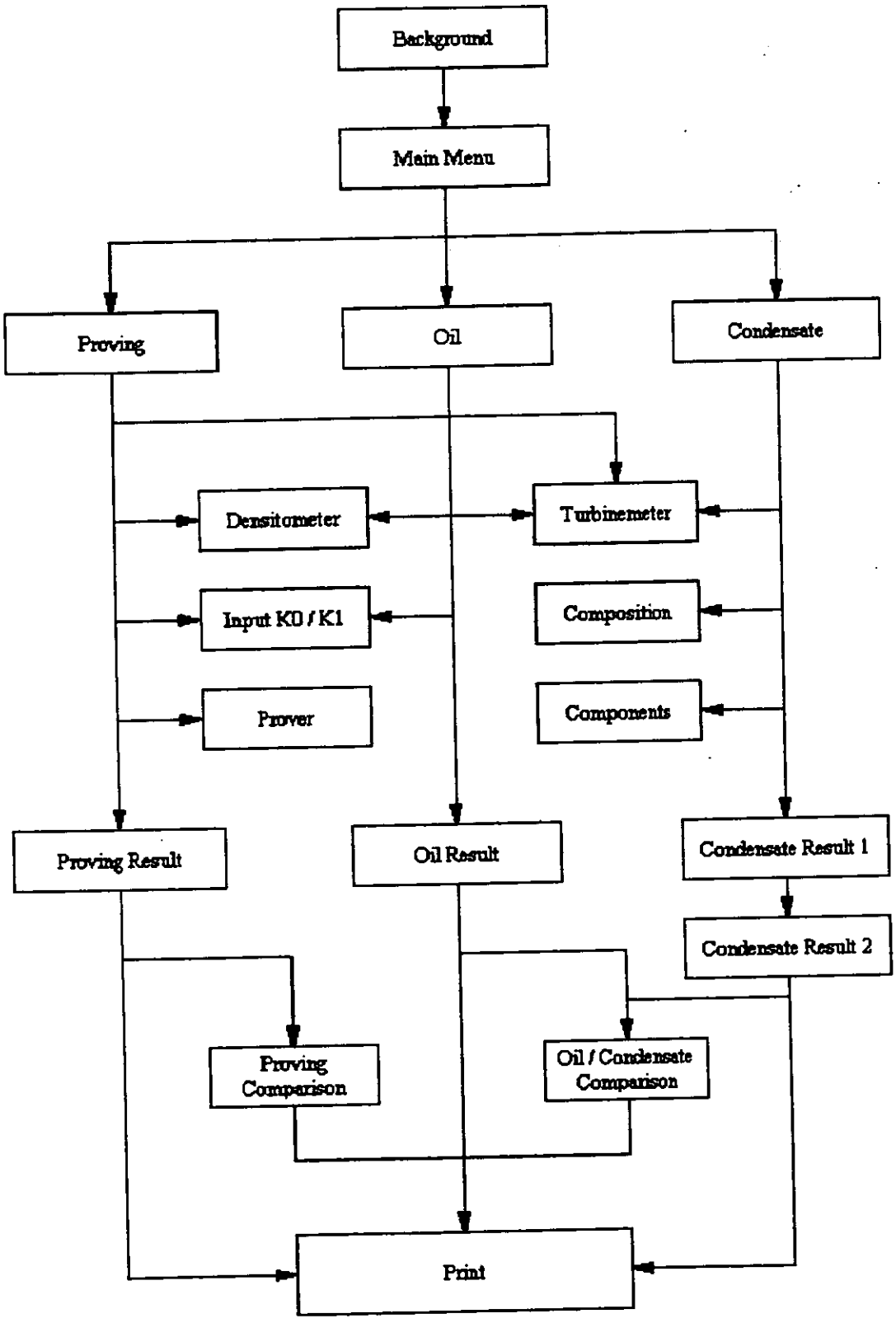

Figure 7 Structure of the program for fiscal oil metering calculations, [6]. More details during demonstration of program.

USER EXPERIENCE

The program discussed in this paper is used by Norsk Hydro to perform the stipulated verifications of the values delivered by the flow computer. Both programs are currently being used by Norsk Hydro for verification on all Norsk Hydro platforms and in new projects. User interface is assessed to be very user friendly compared to earlier verification tools.

As far as the testing is concerned, with the existing flowmeters, the situation is the same as it was, before the verification programs were incorporated into the fiscal metering routines. The verification of the flow computer results is done much faster due to the GUI aspects of the VISUAL Basics programs developed for oil and gas. In fact, the programs are used in fiscal, fuel[2] and flare[3] applications.

Figure 8 and Figure 9 show one of the many GUIs for verifying the flowcomputer estimates of oil and gas flow. Figure 8 is for oil measurement and has the options of selecting the type of calcualtion, viz. IP 2000, computer's full accuracy or the house internal standard at Norsk Hydro.

Figure 9 is the starting window for gas calculations and has the options shown on the different buttons shown there.

See Figure 10 to see the advantage of terminal vs. GUI based verification.

Norsk Hydro is very satisfied with the results and the co-operation with the students and staff of Bergen College.

---

[2] fuel used to run the gas turbines used in the electricity generation on platforms, which again has to be accounted for by the platform operator to the authorities

[3] gas flared is in effect gas lost and in addition gives rise to an increase in CO_2, which are factors needed by the authorities for fiscal and regulatory purposes.

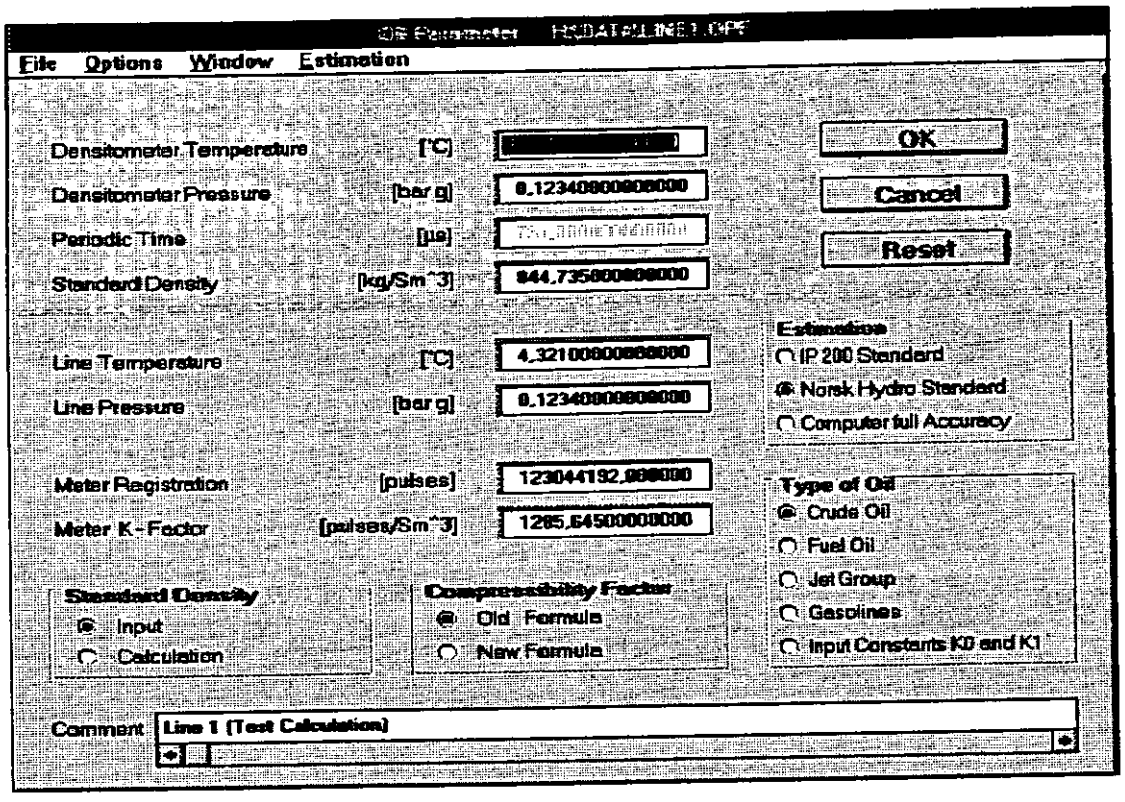

Figure 8 GUI interface from the verification program developed for oil, [6]. More details during demonstration of program.

In the case of oil, IP 2000, computer's full accuracy or the house internal standard at Norsk Hydro can be used in the calculations. In addition, the program can handle different types of oil as shown in the menu under "Type of oil".

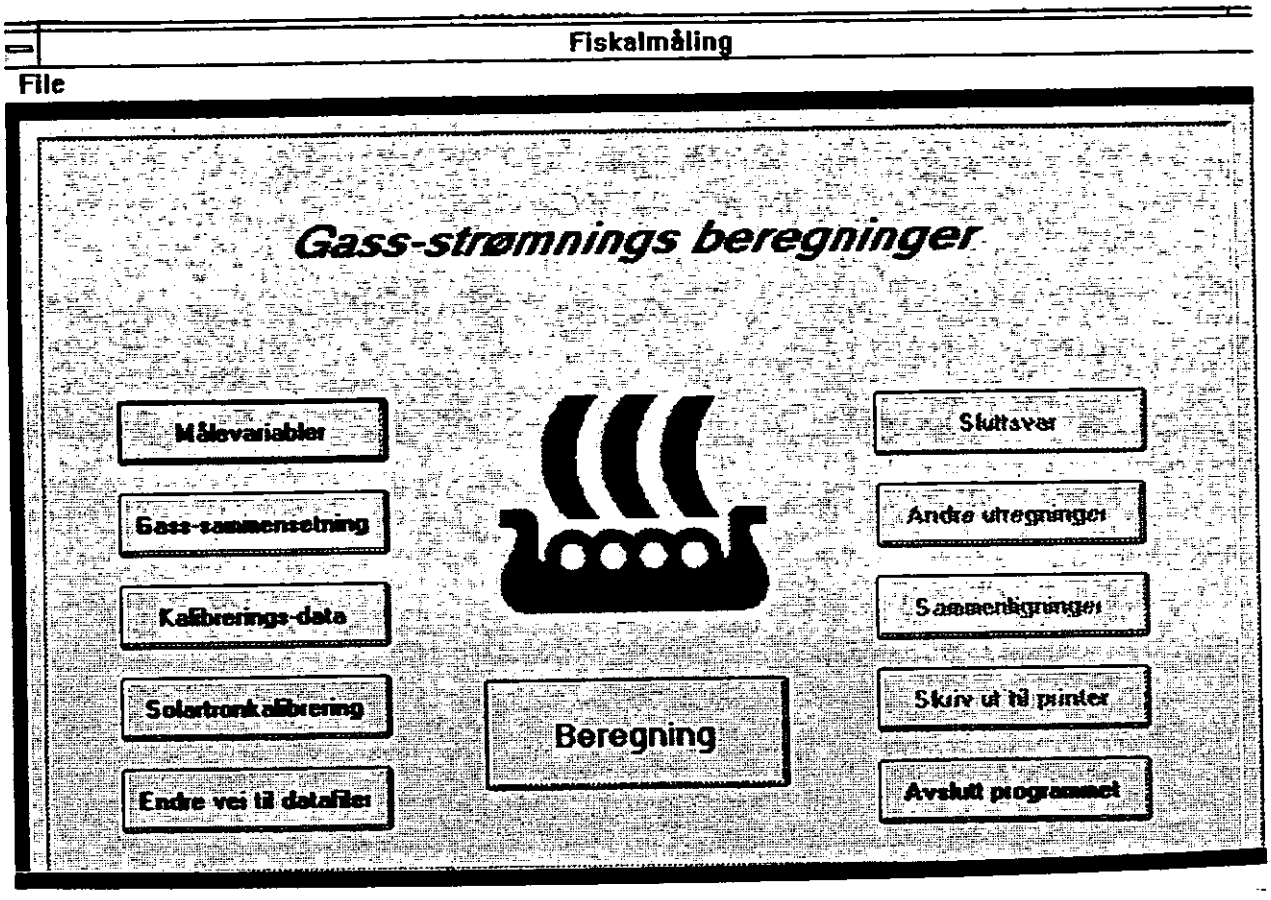

Figure 9 GUI interface from the verification program developed for gas, [5]. Opening window for the program with different options given in Norwegian. The equivalent English formulations are: Målevariabler = Measurands; Gass sammensetning = Gas composition; Kalibrerings-data = Calibration data; Solartronkalibrering = Calibration of the Solartron density meter. Beregning = Calculation; Avslutt programmet = Exit. More details during demonstration of program.

A typical print out given by the programs is given in APPENDIX.

Figure 10 shows the contrast between terminal based operator interaction and GUI based operator interaction. Once the values for parameters are assigned, these parameters can be retrieved selecting the right window and modified if necessary without much work interactively.

Terminal inputs (DOS era)

c: \ give line_temp (° C) ? 14.238

c: \ give line_dens (kg/ Sm^3)? 844.730

c: \ give line _ pres (bar g) ? 0.1234

etc. etc.

(Once you make the mistake, you are back in "square number 1"! Do the same things again, give the answers for questions generated by the program!!)

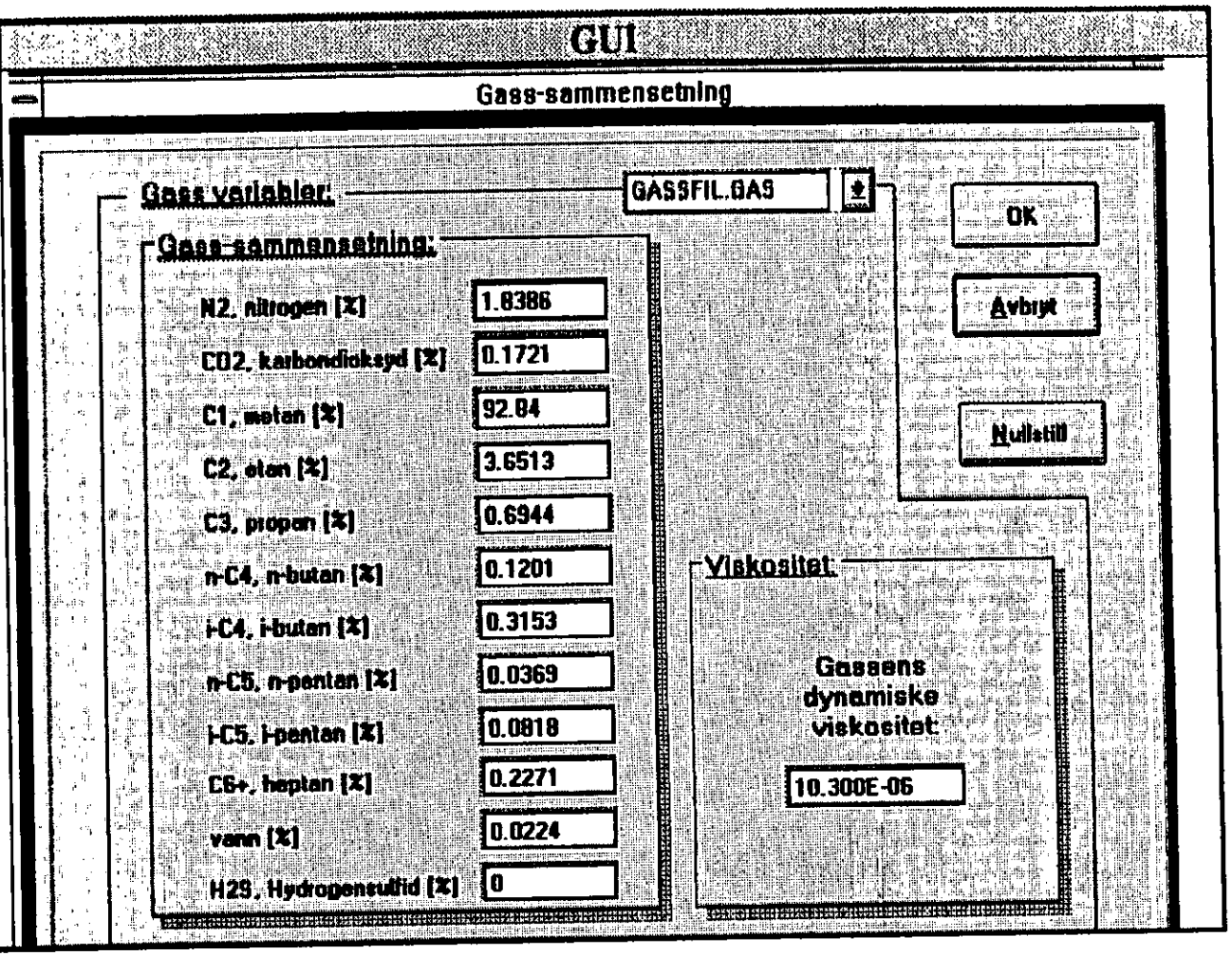

Figure 10 Terminal inputs from the purely DOS- era to GUI input in tersting and verification.

Comments on accuracy

All the modern PCs use 80 bits in the FPU. The accuracy strived for in the verification calculations are ± 0.001 % (10 ppm). Table 1 shows the accuracy of flowcomputer calculations and the accuracy in the verification routines. The results used for fiscal calculations should be independent of the type of flow computer used.

Table 1 Verification accuracy vs. Flow Computer accuracy

	Significant Digits	CPU Operation
Current Flow Computer	7 digits (example1.103759)	8 bits
Verification	15 digits (example1.10375859321368)	32 bits

It is essential at this stage to look at the plethora of data from earlier studies, mostly based on empirical findings, which have been collected from 8-bits FORTRAN calculations. We are using these empirical results such as the one shown in Figure 11 to achieve the 10 ppm accuracy in the verification programs. We can easily see a numerical anomaly in the process. The stipulations as such leads to a series of routines which will help us to achieve good repeatability and high reliability. The measurement problem remains the same.

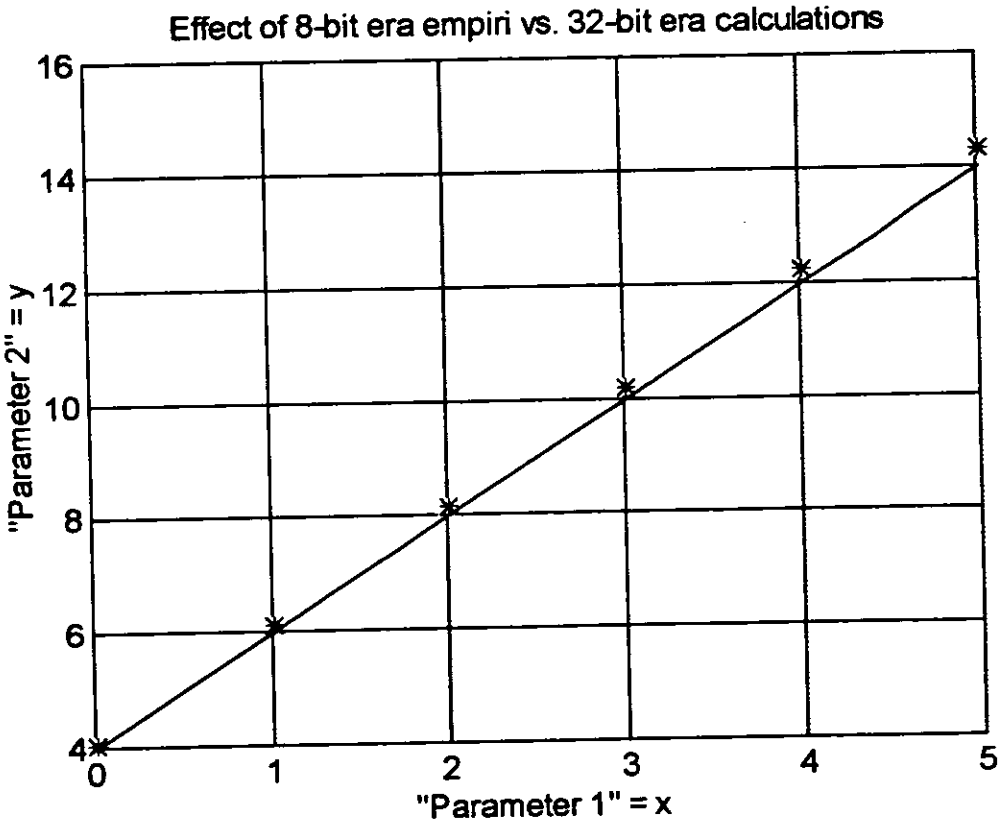

Figure 11 Effect (*exaggerated*) of 8-bit era empiri vs. 32-bit era calculations. The only difference is the variations in the coefficients in the equation $y = a\,x + b$. The continuos line show the line for a set of values for a and b. The values marked '*' are for another set of values given with differing mantissa.

FUTURE TREND

Software in flow computer today is dedicated for measurement purposes. It would be advantageous if the testing facility is in-built in the program used in the flow computer. The testing facilities have to be included already in the design stage in such a way that the program is easily testable. Earlier, they used debugging instead of interface. New flow computers have 15 digits operation with 32 bits CPU / double. Hence, the demand on testing and strategy used for testing will need to be changed.

The strategy used in the production of IC s shown in Figure 12 can be used also in software design. For known series of inputs, the sub-units (modules) in the program should deliver a series of outputs, which are to be obtained with high expectancy. A deviation from the expected values, would indicate faulty operation. One could visualise such test points as "handles" (similar to test points in hardware circuits). Joint Test Action Group (JTAG) bus is defined by IEEE [13] for on-module testing. JTAG is a serial bus containing four signal lines: Test Clock (TCK), Test Mode Select (TMS), Test Data Input (TDI), and Test Data Output (TDO) as illustrated in Figure 12. The system description shown in Figure 4 can be used to adapt this strategy of testing from the hardware industry, at the input and out "ports" of the sub-units shown. The challenge for the measurement and software engineers would be to find the pairs of relevant sets (TDI, TDO) for these sub-units.

In looking at the short term developments, discussions with people in various software engineering branches in industrial applications indicate that the user might continue using the flow computers, but performing tests and verifications using programming tools such as MATHCAD, MATLAB or MATHEMATICA, tools which enables tracing the TDI and TDO according to the system schematic shown in Figure 4 easily.

Long term developments will be based on the philosophy of Built-In Self-Test (BIST) used in the IC design discussed above, incorporated into the system already in the design stage, thus facilitating the solving of the puzzle mentioned earlier: software testability, software testing, and formal verification, which will lead to more reliable engineering in general.

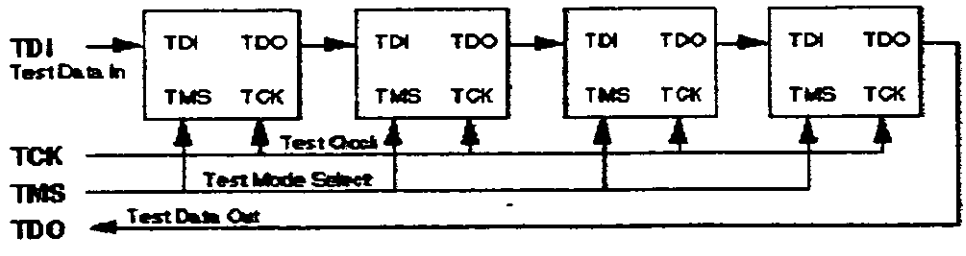

Figure 12 Bus serial connection of components with Built-In Self-Test (BIST) to perform test pattern generation and response analysis. From [13]. TDI and TDO in our system described in Figure 2 might be at any input and output port to and from the sub-units shown there.

NOTE ON ULTRASONIC GAS FLOWMETERS

There is a definite statement in the directives of the Norwegian Petroleum Directorate allowing the use of ultrasonic gas flowmeters for fiscal purposes. It is a well known fact that ultrasonic gas flowmeters are used in flare gas metering. It is planned to install the first ultrasonic gas flowmeter for fiscal measurements already in 1998.

Some of the modern ultrasonic gas flowmeters incorporate the testing and verification facilities in the flow computer itself. As an example of BIST in the ultrasonic gas flowmeter applications is the equation coupling the speed of sound in the medium c to the up-stream and down-stream transit times t_{12} and t_{21}. For a given well, the components of gases will be known and hence also the sound velocity. In the case of a multi-path ultrasonic gas flowmeter, the sound speeds calculated using the transit times for each path should be the same, allowing for variations due to some slight temperature changes in the flowing medium. From experience, one could define an acceptable upper and lower limit for the calculated speed of sound. When the estimated speed of sound is outside this band, the BIST will indicate faulty operation. Thus for the case under discussion, we can say that [TDI, TDO] = [[t_{12} t_{21}] , c]. In case , no BIST is available, this set could be used as one of the means in controlling the flow computer calculations.

One could envisage a series of such measures which will help to have BISTs in the software used in the metering process.

Thus, the future flow computers may make programs such as the ones described in this paper redundant! However, the testability, testing and verification paradigm will be dominating the software sector in the sense described in Figure 3, in our discussions above.

ACKNOWLEDGEMENT

The author acknowledges his organisation for the help, facilities and permission in working on and publishing this paper. Preliminary works for the programs discussed have been done by a number of students of Bergen college. Discussions with Mr. Trond Folkestad of Norsk Hydro have given good insight into the practical applications of the verification software discussed in this paper. Dr. C. Thiruarooran of Berkeley Technology Laboratories of the British Nuclear plc, Berkeley in the UK has given the author valuable information on testability, testing and verification in software engineering both in theory and practice.

REFERENCES

1. International Organization for Standardisation, 1983, "ISO 6976 - Natural gas - Calculation of calorific value, density and relative density."

2. International Organisation for Standardisation, 1980, "ISO 5167 - Measurement of fluid flow by means of orifice plates, nozzles and venturi tubes inserted in circular cross-section conduits running full"

3. Norsk Hydro, 1991, "Håndbok for målesystemer for fiskal kvantumsmåling av olje, kondensat og gass."

4. Oljedirektoratet (Norwegian Petroleum Directorate), 1997, "Forskrift for fiskal kvantumsmåling av olje og gass i petroleums-virksomheten" ("Regulations relating to fiscal measurement of oil and gas etc.").

5. Solheim, J.-A., Sætre, L. J.: "Fiskalt kvantumsmålingsprogram for gass."), 1993, Engineering Degree Thesis, Bergen Ingeniør Høgskole (Bergen College of Engineering).

6. Michael, D. , Heinze, T., 1995: "Fiscal Oil Calculations: Visual Basic Program for Verification of Flow Computer Calculations", Høgskolen i Bergen, Project Report Submitted on Completion of in-plant training, Collaboration between Norsk Hydro, Høgskolen i Bergen (Bergen College), Western Norway UETP and Hochschule für Technik und Wirtschaft.

7. Mylvaganam, S., Sætre, L.J., Solheim, J. A., 1993: "Compact Visual Basic Program for PC-based Verification of Fiscal Gas Flowmetering Calculations, incorporating Volume, Density, Temperature and Pressure Measurements", SEARCC Conference 95, Colombo, Sri Lanka.

8. Wing, J. M., "Formal Testability Analysis", 1990, Encyclopaedia of Software Engineering, Marchiniak, J.J., (Editor), Wiley.

9. Voas, J., Morrel, L., Miller, K., March 1991: "Predicting Where Faults can Hide from Testing", IEEE Software, 8(2), 41-47.

10. IEEE, 1990, "IEEE Standard Glossary of Software Engineering Terminology"

11. Voas, J., Miller, K., May 1995: "Software Testability: The New Verification", IEEE Software, 12(3), 17 - 28.

12. Norsk Hydro, 1993: "Håndbok for fiskal kvantumsmåling av olje, kondensat og gass"

13. IEEE Standard: Test Access Port and Boundary-Scan Architecture, IEEE 1149.1-1990, 21 May 1990.

APPENDIX A: Typical Print-out generated with the program in discussion for the platform managers. **GAS**

Solartron Densitetsmåler: Solartron Densitometer
Gass Sammensetning : Gas composition
Rør og blendeplate data: Pipe and orifice meter data
Målte verdier: Measured values
Beregninger: Calculations

The data of different densitometers can be retrieved from files to the GUI. Downstream and upstream measurements are taken into account in measurements as well as calculations.

Hydro
U&P Drift
Bergen

FISKAL GASSBEREGNING

Ver. 4;0

ISO-5167(1980), ISO-6976 OG SOLARTRON DENSITETSBEREGNING. FLANGETAP.

Linje Nr : 1	Brenngass, CO4	Dato :	23.03.95
Tag Nr : FE-45-0201	Feil blendediameter fra 11.09.94 til 17.01.95	Tid :	16:53:54

Konstanter

SOLARTRON DENSITETSMÅLER		
K0	-82,860110	kg/m³
K1	-2,228380E-02	kg/m³/µs
K2	4,534184E-04	kg/m³/µs²
K3	1344,0	kg/m³
K4	197,8	kg/m³
K18	-7,620E-06	/°C
K19	1,550E-03	kg/m³/°C
Kal.temp.	15,000	°C
Kal.Gassk.	0,00282	
Molvekt Luft	28,9641	g/mol
PTZ-korreksjon fra dens.-densitet til linjedensitet		

GASS-SAMMENSETNING		
Nitrogen	0,750	mol%
CO2	1,110	mol%
Metan	82,340	mol%
Etan	8,480	mol%
Propan	4,800	mol%
n-Butan	1,060	mol%
i-Butan	0,450	mol%
n-Pentan	0,280	mol%
i-Pentan	0,260	mol%
C6+(=C7)	0,420	mol%
Vann	0,000	mol%
H2S	0,000	mol%
SUM	99,950	mol%

RØR OG BLENDEPLATE DATA		
Blendeplatediameter	56,123	mm
Blende Kal.temperatur	12,345	°C
Indre Rørdiameter	102,900	mm
Rør Kal.temperatur	20,00	°C

TEMPERATUR UTVIDELSESKOEFFISIENTER		
Blendeplate	1,07650E-05	/°C
Rør	1,60920E-05	/°C

Variabler

GASSENS EGENSKAPER		
Dynamisk Viskositet	1,190E-05	Pa-s
Brennverdi Inferior ISO-6976	40,613945	MJ/m³
Isentropisk Eksponent Std.	1,37176976	
Isentropisk Eksponent Linje	1,36446144	
Spesifikk Varmekapasitet Std.	1,37615648	
Spesifikk Varmekap. Linje	1,48085792	

MÅLTE VERDIER		
Trykk Oppstrøms Blendeplate	38,25000	bar g
Trykk Oppstrøms Blendeplate	39,26325	bar a
Differansetrykk Blendeplate	164,000	mbar
Temperatur v/10D Nedstrøms	53,40000	°C
Temperatur v/Densitetsmåler	53,40000	°C
Periodetid Densitetsmåler	650,00000	µs

Beregninger

Korrigert Blendeplatediam.	56,148 mm
Korrigert Indre Rørdiameter	102,9557 mm
Diameterforholdet, beta	0,54536023
Utstrømningskoeffisient, C	0,60428855
Hastighetskoeffisient, E	1,04739742
Strømningskoeffisient, alfa	0,63293027
Ekspansjonsfaktor, epsilon	0,99865012
Reynoldstall, ReD	2,8731522E+06
Z Standard ISO-6976	0,99665473
Z Standard BWR	0,99681522
Z Densitetsmåler BWR	0,91888316
Z Linje BWR	0,91877452

Temp. Oppstrøms Blendep.	53,64935 °C
Trykk v/10D Nedstrøms	39,15121 bar a
Trykk v/Densitetsmåler	39,09925 bar a
Densitet Std. ISO-6976	0,86028632 kg/Sm³
Densitet Densitetsmåler	94,80393324 kg/m³
Densitet Linje	95,14019412 kg/m³
Kritisk Temperatur	-57,019522 °C
Kritisk Trykk	46,051126 bar a
Molvekt ISO-6976	20,272860 g/mol
Massestrøm	9952,872184 kg/t
Volumstrøm Linje	104,6126958 m³/t
Volumstrøm Standard	11569,256718 Sm³/t
Energistrøm Inferior	469,8731607 MJ/t
Hastighet	3,4905275 m/s

TOTALER	Beregnet	Målt	Avvik	Strømningstid
Masse	9952,872184 kg	9952,000000 kg	-0,0087631%	3600,000 s
Volum Linje	104,6126958 m³	104,0000000 m³	-0,5856801%	
Volum Standard	11569,256718 Sm³	0,000000 Sm³	-100,0000000%	
Energi Inferior	469,8731607 MJ	0,0000000 MJ	-100,0000000%	

Oljedirektoratets minstekrav til regnenøyaktighet er 0,001%

APPENDIX B: Typical Print-out generated with the program in discussion for the platform managers.

OIL

The data of different densitometers can be retrieved from files to the GUI.

Hydro
U&P Drift
Bergen

FISCAL OIL CALCULATION

ESTIMATION : NORSK HYDRO IP200	COMPRESS. FACTOR : OLD FORMULA	TYPE OF OIL : CRUDE OIL

Line Nr : 1 Tag Nr :	Line 1 Test Print-Out!	Date : 26.06.95 Time : 13:46:36

Constants

DENSITOMETER		
K0	-1.2290 E+03	kg/m³
K1	-4.5515 E-01	kg/m³/µs
K2	3.9942 E-03	kg/m³/µs²
K18	-3.2079 E-05	/°C
K19	-1.4253 E-02	/°C
K20a	-1.3469 E-05	/bar g
K20b	-1.2207 E-07	/bar g²
K21a	-1.8708 E-02	/bar g
K21b	-1.6955 E-04	/bar g²
Cal.Temp.	20.0	°C
Cal.Press.	0.0	bar g

TURBINE METER	
Y-Coefficient	0.00003861 /bar
EH-Coefficient	0.00000846 /°C
ER-Coefficient	0.00000846 /°C

Variables

DENSITOMETER		
Densitometer Temperature	4.3210	°C
Densitometer Pressure	0.1230	bar g
Periodic Time	781.00	µs

TURBINE METER		
Line Temperature	4.3210	°C
Line Pressure	0.1234	bar g
Meter Registration	123044192.0000	pulses
Meter K-Factor	1285.6450	p./Sm³

TYPE OF OIL : CRUDE OIL	
K0	613.9723
K1	0.0

Calculation

Standard Density	844.7350000	kg/Sm³	Line Density	852.4968197	kg/m³
Compress. Factor Fd	0.0000683		Compress. Factor Fl	0.0000683	
Help Factor Alpha 15	0.0008604		Correction Factor Ctlm	1.0091800	
Correction Factor Ctld	1.0091800		Correction Factor Cplm	1.0000084	
Correction Factor Cpld	1.0000084		Correction Factor Ctsm	0.9997290	
			Correction Factor Cpsm	1.0000048	

	Calculation		Measurement		Deviation
Stand. Density	844.7350000	kg/Sm³	844.7350000	kg/Sm³	0.0000000 %
Gross Volume	95680.7143930	m³	95680.7488918	m³	0.0000361 %
Stand. Volume	96559.8734817	Sm³	96559.9106650	Sm³	0.0000385 %
Mass	81567.5047256	Tonnes	81567.5522923	Tonnes	0.0000583 %

Norwegian Petroleum Directorate specifies a minimum accuracy of 0.001%

Calculated by :	Sign :	Date : 26.06.95
Checked & Authorized by :	Sign :	Date : 26.06.95

APPENDIX C: Typical Print-out generated with the program in discussion for the platform managers.

CONDENSATE

Hydro
U&P Drift
Bergen

FISCAL CONDENSATE CALCULATION

CONDENSATE DENSITY CALCULATION IS BASED UPON THE USE OF THE COSTALD EQUATION

Line Nr : 1 Tag Nr : 30-UY-651	Oseberg A Test Print-Out!	Date : 26.06.95 Time : 13:17:02

Constants

COMPOSITION OF CONDENSATE	
Methane	16.5527800 mol%
Ethane	5.6764200 mol%
Propane	3.3262660 mol%
i - Butane	2.9790970 mol%
n - Butane	1.5895970 mol%
i - Pentane	2.1453070 mol%
n - Pentane	1.2627170 mol%
Frac - 01	2.9843780 mol%
Frac - 02	4.7615500 mol%
Frac - 03	9.2429810 mol%
Frac - 04	10.3320800 mol%
Frac - 05	11.3299100 mol%
Frac - 06	11.8058200 mol%
Frac - 07	7.5094790 mol%
Frac - 08	6.6016230 mol%
Sum	98.1000050 mol%

TURBINE METER	
Y-Coefficient	0.00007861 /bar
EH-Coefficient	0.00000679 /°C
ER-Coefficient	0.00005678 /°C

Variables

TURBINE METER	
Line Temperature	-12.13145 °C
Line Pressure	39.8769 bar g
Meter Registration	40020002.0000 pulses
Meter K-Factor	424.5000 p./Sm³

Calculation

STANDARD CONDITIONS	
Reduce Temperature	0.5713514
Coefficient Vr0	0.3783342
Coefficient Vrs	0.2285533
Volume at Vapour Pressure	0.1235540
Reduce Density	722.7615893 kg/m³
Coefficient F	-4.4575210
Coefficient Pr0	-1.7498690
Coefficient Pr1	-1.9901723
Reduce Pressure	0.0049081
Vapour Pressure	0.1687905 bar a
Coefficient B1	16.6698041
Coefficient D1	1.0015665
Standard Density	722.8700215 kg/m³

OPERATING CONDITIONS	
Reduce Temperature	0.5175544
Coefficient Vr0	0.3658068
Coefficient Vrs	0.2362538
Volume at Vapour Pressure	0.1191867
Reduce Density	749.2456923 kg/m³
Coefficient F	-6.8679340
Coefficient Pr0	-2.1824873
Coefficient Pr1	-2.6356821
Reduce Pressure	0.0011937
Vapour Pressure	0.0410533 bar a
Coefficient B1	19.8785266
Coefficient D1	1.0629146
Operating Density	753.6522589 kg/m³

RESULTS INDEPENDENT OF STAND./LINE CONDITIONS	
Acentric Factor (Meth. A)	0.2809899
Molecular Weight	89.3001013
Critical Pressure (Meth. A)	34.3902528 bar a
Spherical Volume	0.3489861
Critical Temp. (Meth. A)	504.3306500 K
Coefficient E	142.0754465

CORRECTION FACTORS	
Correction Factor Ctsm	0.9980917
Correction Factor Cpsm	1.0031347

	Calculation	Measurement	Deviation
Stand. Density	722.8700215 kg/Sm³	722.8700000 kg/Sm³	-0.0000030 %
Gross Volume	94390.6796873 m³	94390.0000000 m³	-0.0007201 %
Stand. Volume	98410.1523715 Sm³	98410.0000000 Sm³	-0.0001548 %
Mass	71137748.9624447 Tonnes	71137.7970000 Tonnes	0.0000675 %

Norwegian Petroleum Directorate specifies a minimum accuracy of 0.001%

Calculated by : -	Sign :	Date : 26.06.95
Checked & Authorized by :	Sign :	Date : 26.06.95

APPENDIX D: Typical Print-out generated with the program in discussion for the platform managers.

PROVER

The data of different densitometers can be retrieved from files to the GUI.

Hydro
U&P Drift
Bergen

FISCAL PROVING CALCULATION

ESTIMATION : NORSK HYDRO IP200	COMPRESS. FACTOR : OLD FORMULA	TYPE OF OIL : CRUDE OIL
Line Nr : 1 Tag Nr :	Line 1 Test Print-Out!	Date : 26.06.95 Time : 13:15:15

Constants

DENSITOMETER

Input of a given Standard Density!

TURBINE METER

Y-Coefficient	0.00003861 /bar
EH-Coefficient	0.00000846 /°C
ER-Coefficient	0.00000846 /°C

PROVER

Diameter of the Prover Pipe	736.60 mm
Wall Thickness of the Prover Pipe	12.70 mm
Modulus of Elasticity of Prover Steel	2060000.0 /bar
Coefficient of Cubical Expansion	0.0000335 /°C
Base Volume of the Prover	5.0096300 Sm³

Variables

DENSITOMETER

Densitometer Temperature	14.2380 °C
Densitometer Pressure	4.9510 bar g
Standard Density	846.0000 kg/Sm³

TURBINE METER

Line Temperature	14.2380 °C
Line Pressure	4.9510 bar g
Meter Registration	9999.0930 pulses

TYPE OF OIL : CRUDE OIL

K0	613.9723
K1	0.0

PROVER

Prover Temperature	15.9170 °C
Prover Pressure	5.1240 bar g

Calculation

Standard Density

Standard Density was given!

Line Density	846.8467952 kg/m³
Compressibility Factor Fl	0.0000722
Correction Factor Ctlm	1.0006430
Correction Factor Cplm	1.0003577
Correction Factor Ctsm	0.9999807
Correction Factor Cpsm	1.0001912

Meter K-Factor	1998.7619620 p./Sm³
Compressibility Factor Fp	0.0000730
Correction Factor Ctlp	0.9992280
Correction Factor Cplp	1.0003740
Correction Factor Ctsp	1.0000307
Correction Factor Cpsp	1.0001443

	Calculation	Measurement	Deviation
Meter K-Factor	1998.7619620 pulses/Sm³	1998.7620000 pulses/Sm³	0.0000019 %

Norwegian Petroleum Directorate specifies a minimum accuracy of 0.001%

Calculated by :	Sign :	Date : 26.06.95
Checked & Authorized by :	Sign :	Date : 26.06.95

NSFMW.97

North Sea FLOW Measurement Workshop

Paper 11: 2.5

RECENT DEVELOPMENTS IN THE UNCERTAINTY ANALYSIS OF FLOW MEASUREMENT PROCESSES

Authors:
Jos G. M. van der Grinten, Nmi Certin B.V. The Netherlands

Organiser:
Norwegian Society of Chartered Engineers
Norwegian Society for Oil and Gas Measurement
Co-organiser:
National Engineering Laboratory, UK

RECENT DEVELOPMENTS IN THE UNCERTAINTY ANALYSIS OF FLOW MEASUREMENT PROCESSES

Jos G.M. van der Grinten

NMi Certin B.V., The Netherlands

SUMMARY

For the evaluation of uncertainties in flow measurement two different documents are used at present. These are the "Guide to the expression of uncertainty in measurement" [1] and ISO 5168 [2]. The Guide represents the present state of the art of uncertainty analysis. ISO 5168 is much older, is still under revision [3] and is familiar to most people in the flow community. Although the working methods for evaluating measurement uncertainties are basically the same, the two documents are based on significantly different views on measurement uncertainty [7]. So the dilemma for the experimentalist is whether to use the Guide with which he may not be familiar, or to use ISO/DIS 5168 [3] which is subject to change.

This paper discusses the developments in uncertainty analysis in past decades, the agreements and differences between the Guide and ISO 5168, and will illustrate by an example how simple uncertainty analysis can be if all unnecessary terminology can be avoided.

From the present analysis the following conclusions are drawn. Currently, the Guide is the only accepted document that is neither expired nor under revision. Uncertainty is a measure for the amount of missing information. If corrections are not applied, information is discarded and the resulting 2s-uncertainty is twice the absolute value of the deviation.

1. RECENT DEVELOPMENTS

In the past decades the view on measurement uncertainty has changed significantly which has lead to a new document on uncertainty analysis [1] shortly referred to as the Guide. Despite the fact that this document has been circulated extensively for comments, the Guide has obtained little publicity in the flow community. Instead, ISO 5168 [2,3] is the document which is more familiar to people working in the field of flow measurement. The original ISO 5168 (1978) [2] is currently being revised. The latest draft of this revised standard dates from 1989 [3]. However, the latter document and later revisions of ISO 5168 were never accepted by ISO, because these documents on uncertainty analysis were not in line with the Guide. This year a new call was made to the national standardization organisations for volunteers to write a new ISO 5168. This means that several years will be required before a new ISO 5168 will be published.

So the dilemma for the flow experimentalist whether to use the Guide [1] with which he may not be familiar, or to use ISO/DIS 5168 [3] which was rejected, is now solved. The

Guide is the only available document on measurement uncertainties. Moreover, before a new version of ISO 5168 will be accepted in the future, it must be in line with the Guide.

Since the new philosophy on evaluation of measurement uncertainty is described in the Guide, quite some reading is required before one can make an uncertainty analysis. A more readable document on measurement uncertainty is WECC Doc. 19 [8]. This document published in 1990, is based on the same principles [9] as the Guide. However, this document is also currently under revision [10] to bring it in full agreement with the Guide. Fortunately, in the field of flow measurement a few examples [4,5,7] exist at present in which the uncertainty analysis is performed according to the Guide.

In the remainder of this paper the following items will be discussed:
1. The new view on measurement uncertainty.
2. Additional uncertainties due to not correcting for known deviations.
3. Terminology and procedures to be used in uncertainty analysis.
4. A practical example of uncertainty analysis of a flow measurement process.

2. INFORMATION AND UNCERTAINTY

Missing information

The most important new view in uncertainty analysis is that uncertainty is a measure for the amount of missing information. By taking measurements we make observations of the object or system from which we want information. The more measurements we take, the more information we retrieve. Since the measurement object may be subject to change and since there is a minimum interval for taking measurements, this inherently implies that it is not possible to collect the complete information available for any system. For that reason it is useful to introduce a quantity that expresses the amount of missing information: *uncertainty*.

The definition of uncertainty used in the Guide [1] and the VIM [6] is *a parameter, associated with the result of a measurement, that characterizes the dispersion of values that could reasonably be attributed to the measurand.* In fact, this definition is the reality that we miss information when taking measurements. For that reason, in stead of a single value, a range of values can be attributed to the measurand. If we do not take measurements there is no information at all and consequently a high degree of uncertainty is experienced. If measurements are taken this uncertainty is reduced. This will be illustrated by a very simple example.

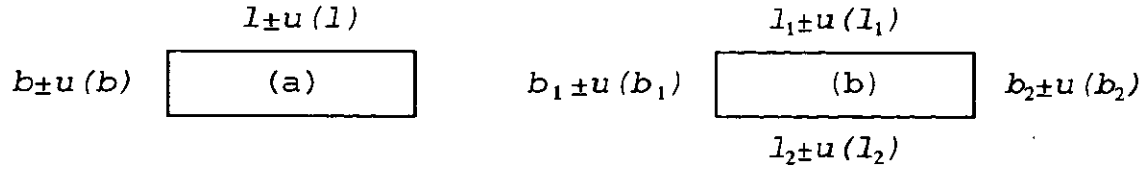

Fig. 1: Circumference of a rectangle measured by 2 independent measurements (a) and by 4 independent measurements (b).

Consider a rectangle of which we want to determine the circumference. In order to do so, a minimum of two independent measurements is required to determine length (l) and width (b) of the rectangle. In addition the opposite length and width can be measured, so there are four independent measurements. The two methods are schematically displayed in figures 1a and 1b, respectively. All dimensions are measured only once using one single instrument. The uncertainties are also indicated in figure 1. The uncertainty of l and b are denoted by $u(l)$ and $u(b)$ respectively. The circumferences are
The uncertainties in the circumferences are obtained by taking the root sum square of the

$$O_a = 2(l+b) \quad , \quad O_b = l_1+b_1+l_2+b_2 \tag{1}$$

uncertainties of the measured lengths and widths.

$$u(O_a) = 2\sqrt{u^2(l)+u^2(b)} \quad , \quad u(O_b) = \sqrt{u^2(l_1)+u^2(b_1)+u^2(l_2)+u^2(b_2)} \tag{2}$$

Since all dimensions are measured using one instrument, we will assume all uncertainties in l, b, l_1, b_1, l_2, b_2, to be equal to $u(l)$. Using this substitution the following result is obtained

$$u(O_a) = 2\sqrt{2}\,u(l) \quad , \quad u(O_b) = 2\,u(l) \tag{3}$$

The result is that the uncertainty of the circumference in the second case is smaller than in the first situation. The reason is that four independent measurements contain more information than two independent measurements, since one assumption, i.e. $l_1=l_2$ and $b_1=b_2$, has been abandoned.

The relationship between information and uncertainty is not unique to metrology. In other fields, e.g. statistical physics and thermodynamics (Mach [11]), a relationship between uncertainty (standard deviation) and amount of missing information (entropy) exists.

Uncertainty due to not applying corrections

One of the basic assumptions in the Guide is that known deviations are corrected for. However, in many measurement corrections are not applied, e.g. weighing measurements in shops, domestic gas meters at home, and fuel dispensers. Since many measurements in field applications are not corrected for deviations, it is rather unfortunate that this is not discussed in the Guide. From the previous discussion it is understood that if corrections are not applied, information is discarded. So, this results in an additional uncertainty.
The formal derivation of the relationship between uncertainty and the deviation not corrected for, is given in the appendix to this paper. The result is given here.

If a known deviation is not corrected for, this results in an extra uncertainty equal to twice the absolute value of the deviation.

The factor 2 is the consequence of the fact that uncertainties are represented as the equivalent of double standard deviations.

3. TERMINOLOGY TO BE USED IN UNCERTAINTY ANALYSIS

The difference in terminology used in the Guide [1] and ISO 5168 [2,3] is the result of the difference in philosophy between the two documents. An extensive comparison of these documents is made by Van der Grinten [7]. A brief summary will be given here.
For ISO 5168 the concept of true value plays an important role. The *true value* is an ideal value which is assumed to exist and which would be obtained if all imperfections of the measurement process could be eliminated. The *error* is the difference between the measured and true values of the quantity measured. Please, note that by this definition the true value cannot be measured which implies that the error is unknowable.
Instead of the true value the Guide uses the *reference value*, i.e. the value which is obtained by using a calibrated instrument. The *deviation* is the difference between the value measured and a reference value. Please, note that the latter two definitions are more practical than the definitions used by ISO 5168.
In practice, most people use the word true value in the sense of reference value and the word error in the sense of measured deviation.
In the view of the Guide *uncertainty* is a measure for the information missing in the measured value. In fact the uncertainty analysis as presented in the Guide is based on the notion of maximizing the amount of missing information. On the other hand ISO 5168 aims at maximization of the known information. These starting points are implied by the definitions used for uncertainty. According to the Guide the uncertainty interval is the range of values which could be attributed to the measurand. According to ISO 5168 the uncertainty interval is the range of values in which the true value of the measurand lies.
So the terminology needed for the uncertainty analysis of practical measurements, consists of four concepts: measured value, reference value, deviation and uncertainty (in the sense of missing information).

The evaluation of uncertainties has to be performed in two ways. Type A evaluation of uncertainties is the method by which the available information is reduced by statistical means. Here averaging or regression methods lead to a calculable standard deviation. The result of data reduction is that information is thrown away. As a result uncertainty is returned. Type B evaluation of uncertainties involves the application of all other means. Here a thorough knowledge of the measurement process and often the theoretical skill of the experimentalist is required to estimate equivalent standard deviations. In fact this is the result of the question "What mount of information is missing?".

Throughout this paper all uncertainties are represented as equivalents of double standard deviations, a method preferred by the Guide.

4. PROCEDURES FOR EVALUATING UNCERTAINTIES

The Guide evaluates uncertainties using the following procedure which is very much equal to ISO 5168. Differences in the procedures followed by the Guide and ISO 5168 are discussed by Van der Grinten [7]. The procedure contains the following steps:

1. Express mathematically the relationship between the measurand and the input quantities. This relationship should contain all quantities, including corrections and correc-

tion factors, that can contribute significantly to the uncertainty of the result of measurement.

2. Determine estimated values of all input quantities, either based on statistical analysis or by other means.
3. Evaluate the uncertainty estimate of all input estimates, both by statistical means (type A) and by other means (type B). Document all uncertainty sources for each input estimate.
4. Evaluate the covariances associated with any input quantities that are correlated. This step can be avoided by complete substitution of all variables in the mathematical model.
5. Calculate the result of measurement from the functional relationship, using the estimates of all input quantities.
6. Calculate all sensitivity coefficients i.e. the partial derivatives of the measurand with respect to each of the input quantities. Combine all uncertainties. The easiest way is to put everything in a table as shown in the example later in this paper.

The procedure for computing propagation of uncertainties is briefly reviewed here.
Assume, the dependency of a quantity measured y of m variables x_i (i=1..m) is described with a function f:

$$y = f(x_1, x_2, \ldots, x_m) \tag{4}$$

The absolute uncertainty in each of the quantities x_i is $u(x_i)$. If all quantities x_i are mutually independent the uncertainty in the quantity y is described by

$$u^2(y) = u_0^2(y) + \sum_{i=1}^{m} c_i^2 \, u^2(x_i) \tag{5}$$

where c_i is the sensitivity factor [1,2,3,7,8,10], the partial derivative of f with respect to x_i

$$c_i = \frac{\partial f}{\partial x_i} \tag{6}$$

The uncertainty $u_0(y)$ is the result from repeated observations of the measurand.
For convenience later on, the quantity $u_i(y)$ is defined which is the uncertainty contribution in y due to the individual quantity x_i.

$$u_i(y) = c_i \, u(x_i) \tag{7}$$

Of course the uncertainty $u(y)$ is the root sum square of the uncertainty contributions $u_i(y)$.

5. MATHEMATICAL MODEL OF THE MEASUREMENT PROCESS

In order to demonstrate the use of uncertainties in a practical application an example will be discussed: application of a turbine gas meter for custody transfer purposes. In order to convert the line volume into a normal volume V_n (1013,25 mbar and 0°C) a flow computer is used with temperature and pressure input. The set-up is schematically displayed in figure 2. Calibration curves of the instruments are programmed into the flow computer. This means that corrections are made for known deviations. For calculation of the real gas factor the S-GERG algorithm is used.

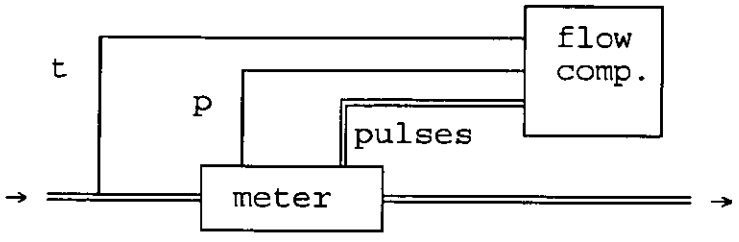

Fig. 2: Schematic set-up of a custody transfer metering system for high-pressure natural gas.

In the procedure of uncertainty evaluation, a mathematical model is set up. Since metering flow is a continuous process, split up in many small time intervals, all process conditions are stationary. Also it is assumed that the piping and the meter casing are completely rigid and dimensions do not vary with the changes in temperature and pressure. So, conversion from actual volume increment to an increment in normal volume is based on conservation of mass in each time interval:

$$\rho_1 \, \Delta V_1 = \rho_2 \, \Delta V_2 \tag{8}$$

in which ρ is the density and ΔV is the volume increment. The indices 1 and 2 refer to actual conditions and normal conditions, respectively.
Densities are obtained using the state equation of a real gas:

$$P_i = Z_i \rho_i R_a T_i \qquad (i = 1, 2) \tag{9}$$

P is the absolute pressure, T the absolute temperature, R_a the specific gas constant for air and Z_i the real gas constant or super compressibility, depending on P, T and the gas composition.

The quantity determined during calibration of the instruments, is the relative deviation of the turbine gas meter e_m. This quantity is defined as the relative difference of the quantity indicated by the instrument and the quantity at the instrument:

$$e_m = \frac{\Delta V_m}{\Delta V_1} - 1 \tag{10}$$

where the volume increment ΔV is obtained from the number of pulses ΔN collected in

the time interval and the impulse factor of the meter I:

$$\Delta V_m = \frac{\Delta N_m}{I_m} \tag{11}$$

All temperatures are measured in °C, so

$$T_1 = T_0 + t_1 \quad , \qquad T_2 = T_0 \tag{12}$$

Another assumption is that pressure and temperature readings are corrected for know deviations. This means that t_1, P_1 and P_2 can replaced by t_m, P_m and P_n, respectively. Substitution of equations (10)-(12) into the mass balance equation (8) leads to:

$$\Delta V_n = \frac{P_m}{P_n} \frac{Z_n}{Z_m} \frac{T_0}{T_0 + t_m} \frac{\Delta N_m}{I_m} \frac{1}{1 + e_m} \tag{13}$$

The total converted volume is the sum of all increments.

6. UNCERTAINTY EVALUATION

All instruments are calibrated in a standards laboratory. Calibration certificates issued by this laboratory state for all instruments measured deviations and the associated 2s-uncertainty, i.e. the uncertainty represented as the equivalent of a double standard deviation. The uncertainty statement of the calibration laboratory refers to calibration conditions. If an instrument is used in the field additional uncertainty sources may be present, e.g. due to varying environmental conditions.

The calibration uncertainty of the flowmeter is 0,27%. During initial verification of the flow computer it is observed that deviations of V_n are smaller than 0,15%. This means that there are known deviations not corrected for, that lead to an additional uncertainty of 0,30%. The uncertainty of the S-GERG algorithm is 0,10% [12].
Due to the temperature and pressure dependency of the real gas factor Z, covariances are introduced. These covariances are neglected for the following reason. In the ideal gas law there are linear contributions of P and T. In the real gas law Z is a correction to the ideal gas law. Values of Z vary between 0,7 and 1,0. The direct influence of temperature and pressure uncertainties via P and T in the real gas law will be much higher than the additional influence via Z.

In order to evaluate the uncertainty of the calibration result the uncertainty sources mentioned in the Guide [1] are listed below. The letters used to indicate the uncertainty source, will be used later in this section to make reference to. In the Guide the following uncertainty sources are distinguished:

a. incomplete definition of the measurand;
b. imperfect realization of the definition of the measurand;
c. nonrepresentative sampling - the sample measured may not represent the defined measurand;

d. effects of environmental conditions inadequately known or measured imperfectly
e. personal bias in reading analogue instruments;
f. finite instrument resolution or discrimination threshold;
g. inexact values of measurement standards and reference materials;
h. inexact values of constants and other parameters obtained from external sources and used in the data-reduction algorithm;
i. approximation and assumptions incorporated in the measurement method and procedure;
j. variations in repeated observations of the measurand under apparently identical conditions.

The following uncertainty sources are present during the metering process described:
1 (d) additional uncertainties due environmental conditions differing from calibration conditions;
2 (g) uncertainty resulting from instrument calibration as stated on the certificate;
3 (j) fluctuation of pressures and temperatures in a single time interval;
4 (b) temperature gradients in the cross section of the pipe where the temperature is measured;
5 (f) pulses can be missed, however, this problem is avoided by using double pulse lines;
6 (i) uncertainty of the S-GERG algorithm;
7 uncertainty due to not applying corrections (in which the linear interpolation between the programmed calibration points is included).

For this high pressure gas flow metering process the uncertainty estimates are listed by variable in Table I. For each variable the measured value, sensitivity coefficient, applied uncertainty sources, and estimated uncertainties are listed. The uncertainty sources are indicated by numbers and letters which correspond to the uncertainty sources mentioned above. From this uncertainty analysis two dominant uncertainty sources appear, i.e. the deviation of the flow meter and the uncertainty due to not applying corrections.

7. CONCLUSIONS

From the previous discussion the following conclusions can be drawn.
- Currently, The Guide is the only available document to be referenced to for uncertainty analysis. Other documents must be in line with the Guide and are either under revision or not accepted as a standard. So, the experimentalist who want to make an uncertainty analysis of his measurement process, can better start using the Guide today than wait for other documents to be published.
- Uncertainty is a measure for the amount of missing information. This is the fundamental aspect in which the Guide differs from ISO 5168.
- One of the basic assumptions in the Guide is that known deviations are corrected for. If corrections are not applied, information is discarded. This results in an additional uncertainty equal to twice the absolute value of the deviation. The factor 2 is the consequence of the uncertainty representation chosen: the equivalent of double standard deviations.

Table I: Uncertainty estimates based on the Guide. For each variable the value, the sensitivity coefficient, the uncertainty of the input estimate and the uncertainty contribution to the deviation of the meter are listed.

variable x_i	value $[x_i]$	sensitivity coefficient c_i	c_i $[x_i]^{-1}$	source	$u(x_i)$ $[x_i]$	$u_i(\Delta V_m)$ [m³]	$u_i(\Delta V)/\Delta V$ [-]
P_m (bar)	36,25	$\Delta V_n / P_m$	2,8	1 (d) 2 (g) 3 (j)	0,0181 0,0181 0,0036	$7{,}2 \cdot 10^{-2}$	0,07%
P_n (bar)	1,01325			-			
Z_n	0,9997	$\Delta V_n / Z_n$	$1{,}0 \cdot 10^{+2}$	6 (i)	0,000999	$1{,}0 \cdot 10^{-1}$	0,10%
Z_m	0,9752	$-\Delta V_n / Z_m$	$-1{,}0 \cdot 10^{+2}$	6 (i)	0,000975	$1{,}0 \cdot 10^{-1}$	0,10%
T_0 (°C)	273,15			-			
t_m (°C)	15,35	$-\Delta V_n / (T_0+t_m)$	$-3{,}5 \cdot 10^{-1}$	1 (d) 2 (g) 3 (j) 4 (b)	0,05 0,05 0,05 0,02	$3{,}1 \cdot 10^{-2}$	0,03%
ΔN_m	19384,63	$\Delta V_n / \Delta N_m$	$-2{,}8 \cdot 10^{-2}$		0	0	0,00%
I_m (m^{-3})	6646,16			-			
e_m	+0,25%	$-\Delta V_n / (1+e_m)$	$-1{,}0 \cdot 10^{+2}$	2 (g)	0,0027	$2{,}7 \cdot 10^{-1}$	0,27%
ΔV_n (m^3)				7	0,303	$3{,}0 \cdot 10^{-1}$	0,30%
ΔV_n (m^3)	101,02					**$4{,}4 \cdot 10^{-1}$**	**0,43%**

- The terminology needed for uncertainty analysis consists of four concepts: measured value, reference value, deviation and uncertainty (in the sense of missing information).
- In the example of the high pressure gas metering system two dominant uncertainty sources appear, i.e. the deviation of the flow meter and the uncertainty due to not applying corrections.

ACKNOWLEDGEMENT

The author wishes to thank his colleague Charles M.E.E. Peters, member of ISO/TAG4/WG3, for his theoretical support and the stimulating discussions.

NOTATION

c	sensitivity coefficient $\partial f/\partial x_i$	
e	relative deviation	[-]
f	functional relationship between x_i and y	
g	distribution function representing our knowledge of x (appendix)	
I	impulse factor of a gas meter	[m^{-3}]
N	number of pulses counted	[-]
P	absolute pressure	[bar]
R_a	specific gas constant	[$Jkg^{-1}K^{-1}$]
T	absolute temperature	[K]
t	celsius temperature	[°C]
u	absolute uncertainty	
u_s	standard uncertainty, i.e. uncertainty represented as the equivalent of a single standard deviation	
V	volume	[m^3]
x	measured quantity	
x_i	input quantity	
y	measurand	
y	uncorrected measurement result (appendix)	
Z	real gas factor or (super)compressibility factor	[-]
z	expectation value, corrected measurement result (appendix)	

Greek

Δx	increment of quantity x	
ρ	mass density of the fluid	[kg/m^3]

Subscripts

1	at line conditions
2	at reference conditions
i	rank number of the input quantity
m	indicated at the metering site
n	at normal conditions, 1,01325 bar and 0°C

REFERENCES

1 BIPM/IEC/IFCC/ISO/IUPAC/IUPAP/OIML (1993): Guide to the expression of uncertainty in measurement, first edition, ISO 1993.

2 ISO 5168 (1978): Measurement of fluid flow - Estimation of uncertainty of a flow rate measurement, International Organization for Standardization, 1978.

3 ISO/DIS 5168 (1989): Measurement of fluid flow - Estimation of uncertainty of a flow rate measurement, International Organization for Standardization, revision of ISO 5168 (1978).

4 Grinten, J.G.M. van der (1993): The primary standard for gas flow measurement in the Netherlands, *in:* Proceedings of the 6th international conference on flow measurement, FLOMEKO '93, edited by S.D. Park and F.C. Kinghorn, pp 42-50.

5 Grinten, J.G.M. van der and Charles Peters (1994): Trend analysis, general model and application to high pressure gas flow standards, *in:* Proceedings of the IMEKO XIII conference, September 1994, Turin, Italy, pp 1161-1164a.

6 BIPM/IEC/IFCC/ISO/IUPAC/IUPAP/OIML (1993): International vocabulary of basic and general terms in metrology, second edition, ISO 1993.

7 Grinten, J.G.M. van der (1994): A comparison of the methods for uncertainty analysis based on ISO 5168 and the Guide prepared by ISO/TAG4/WG3, *in:* proceedings of the Flomeko '94, Flow measurement in the mid 90's, June 1994, NEL, East Kilbride, Scotland.

8 WECC Doc. 19 (1990): Guidelines for the expression of the uncertainty of measurement in calibrations, Western European Calibration Cooperation.

9 Kaarls, R. (1981): Procès-verbaux du Comité International des Poids et Mesures, 49, pp. A1-A12.

10 EAL-R3 (1997): Guidelines for the expression of the uncertainty of measurement in calibrations, Revision of WECC Doc. 19 - 1990, at present under consideration.

11 Mach E. (1919): Die Prizipien der Wärmelehre, Minerva GMBH, Leipzig, p 296.

12 Jaeschke, M., S. Audibert, P. van Caneghem, A.E. Humphreys, R. Janssen, Q. Pellei, J.A. Schouten, J.P.J. Michels and C.A. ten Seldam High accuracy compressibility factor for natural gasses and similar mixtures by use of a truncated virial equation, GERG technical monograph TM2 (1988).

CONTACT POINT

Jos G.M. van der Grinten
NMi Certin B.V., P.O. Box 394, 3300 AJ DORDRECHT, The Netherlands
Phone: +31 78 63 32 332, Fax: +31 78 63 32 309, E-mail: JvanderGrinten@NMi.nl

APPENDIX: UNCERTAINTIES DUE TO NOT APPLYING CORRECTIONS FOR KNOWN DEVIATIONS

In this appendix the additional uncertainty will be computed which is due to not correcting for known deviations.

The definition of the expectation value z is:

$$z = \int x\, g(x)\, dx \tag{A1}$$

Analogous to the statistical definition of standard deviation, the standard uncertainty in z, $u_s(z)$, is defined by:

$$u_s^2(z) = \int (z-x)^2\, g(x)\, dx \tag{A2}$$

in which $g(x)$ is the distribution function that represents our knowledge of x.

Assume that instead of z the uncorrected measurement result y is taken. Like in formula (A2) the standard uncertainty in y, $u_s(y)$, will be defined by.

$$u_s^2(y) = \int (y-x)^2\, g(x)\, dx \tag{A3}$$

Expanding formulas (A2) and (A3) results in

$$u_s^2(y) = \int (y^2-2yx+x^2)\, g(x)\, dx \tag{A4}$$

$$u_s^2(z) = \int (z^2-2zx+x^2)\, g(x)\, dx \tag{A5}$$

The difference between the squared standard uncertainties is:

$$u_s^2(y) - u^2(z) = \int (y^2-2yx-z^2+2zx)\, g(x)\, dx \tag{A6}$$

Substituting formula (A1) results in

$$u_s^2(y) - u_s^2(z) = y^2-2yz-z^2+2z^2 \tag{A7}$$

so that

$$u_s^2(y) = u_s^2(z) + (z-y)^2 \tag{A8}$$

In other words, not applying corrections for known deviations results in an extra standard uncertainty which equals the absolute value of the deviation. If the uncertainties are represented as the equivalent of double standard deviations, equation (A8) becomes

$$u^2(y) = u^2(z) + 2(z-y)^2 \tag{A9}$$

in which the factor 2 is the result from the uncertainty representation chosen. This uncertainty contribution is added to the other uncertainty contributions by means of root sum square summation.
Note that this result is generally valid, since no specification of the knowledge distribution function $g(x)$ is required.

NSFMW.97

North Sea FLOW Measurement Workshop

Paper ~~12~~: 2.6

A PRACTICAL EXAMPLE OF UNCERTAINTY CALCULATIONS FOR A METERING STATION - CONVENTIONAL AND NEW METHODS

Authors:
Ø. Midttveit and J. Nilsson, Christian Michelsen Research AS, Norway

Organiser:
Norwegian Society of Chartered Engineers
Norwegian Society for Oil and Gas Measurement
Co-organiser:
National Engineering Laboratory, UK

North Sea Flow Measurement Workshop
Kristiansand, Norway, 27.-30. October 1997

A PRACTICAL EXAMPLE OF UNCERTAINTY CALCULATION FOR A METERING STATION - CONVENTIONAL AND NEW METHODS

by
Øyvind Midttveit, Christian Michelsen Research AS (CMR)
Jannicke Nilsson, Christian Michelsen Research AS (CMR)

SUMMARY

The principles and results of a "conventional" uncertainty analysis provided by a major supplier of metering systems, are briefly presented. Temperature, pressure, density and gross observed volume are considered. The basis of the results are real data and instrument specifications of a metering package delivery to a field development in the North Sea. Thereafter, the *Guide* procedure which is referred to as the "new" method, has been applied for calculating the uncertainty of the same quantities based on the same vendor specified instrument uncertainties and process condition at the oil export station. The results indicate that different uncertainty estimates are achieved by a conventional approach and an alternative one rested on the principles of the ISO *Guide*. The main reason for the difference is that the conventional method does not take the sensitivity coefficients of the different variables sufficiently into account, in addition to some inconsistent calculations of the relative uncertainty of some of the input quantities.

1. INTRODUCTION

A conventional fiscal oil metering station normally consists of metering runs of two or several turbine meters equipped with temperature, pressure, density and water liquid ratio measurements. The system is also equipped with a permanent installed prover or a compact prover in addition to sampling analysis equipment. The fiscal measurement of oil and gas in the North Sea must be in accordance with the regulations of the Norwegian Petroleum Directorate (NPD). An uncertainty analysis of the metering system is also required in accordance with "recognised standards" [1]. In practise different methods for evaluation of measurement uncertainties have been used. The various methods have some kind of root-sum-square calculation as the basis, but the evaluation and combination of the individual uncertainty contributions from the basic measurements differ. As a consequence different results for the estimated uncertainty of the quantity of interest, e.g. density or the standard oil volume, may be achieved.

In 1993 the International Organisation for Standardization (ISO) issued, on behalf of several national organisations, the first draft version of the "Guide to the expression of uncertainty in measurement". The document is commonly referred to as the *Guide*. A corrected and reprinted version was published in 1995 [2]. The overall objective of the *Guide* has been to establish an internationally accepted method for estimating measurement uncertainty, and to provide guidelines for the calculation procedure and the reporting of the results. In addition, the *Guide* has introduced some new terms and suppressed some traditional terminology to standardise the concepts so that "everyone speaks the same language" and agrees on how uncertainty should be

quantified. For instance conventional terms like errors, accuracy, tolerance, precision, linearity and repeatability should be avoided and replaced by, or defined in terms of, standard or expanded uncertainties.

It should be noted that at present the *Guide* is an ISO recommendation and not a standard. However, the standard published this year by the European cooperation for Accreditation of Laboratories (EAL), [3], is in conformity with the *Guide*.

This paper briefly presents the principles and results from a "conventional" uncertainty analysis provided by a major supplier of metering systems for the oil and gas industry. Some quantities related to a typical oil metering station such as temperature, pressure, density and gross observed volume are presented. The results are based on real data and instrument specifications of a metering package delivery to a field development in the North Sea. Thereafter, the *Guide* procedure which is referred to as the "new" method, has been applied for calculating the uncertainty of the same quantities based on the same vendor specified instrument uncertainties and process condition at the oil export station. Finally, the results of this case study using the two methods are compared.

2. DEFINITIONS OF TERMS

In metrology and metering technology applications certain terms are frequently used in relation to expressing the quality of a measurement. In this section some important of these are briefly reviewed according to definitions given by ISO [4], [5] and NFOGM [6]. Furthermore, in the definitions of the terms the description in Appendix D of ref. [7] have been adopted since these are more in accordance with the *Guide*.

In the following the terms have been classified into two groups. Terms of most relevance in conjunction with calculating uncertainties using the *Guide* procedure are presented first, followed by other and more "conventional" terms. All terms, however, have been defined with the terminology of the *Guide* as basis.

2.1 Important "new" terms specific to the *Guide*

Measurand:
Particular quantity subject to measurement.

Result of a measurement:
Value attributed to a measurand, obtained by measurement. It is an estimated value of the measurand.

Standard uncertainty:
Uncertainty of the result of a measurement expressed as a standard deviation.

Type A evaluation (of uncertainty):
Method of evaluation of uncertainty by the statistical analysis of series of observations.

Type B evaluation (of uncertainty):
Method of evaluation of uncertainty by means other than the statistical analysis of series of observations, i.e. by engineering/scientific judgement.

Correction:
Value added algebraically to the uncorrected result of a measurement to compensate for systematic error. The result of a measurement after correction for systematic error is referred to as corrected result.

Correction factor:
Numerical factor by which the uncorrected result of a measurement is multiplied to compensate for systematic error.

Comments:
The uncertainty of a correction applied to a measurement result to compensate for a systematic effect, is a measure of the uncertainty of the result due to incomplete knowledge of the required value of the correction. The correction must be included in the functional relationship and the calculation of the combined standard uncertainty must include the associated standard uncertainty of the applied correction[1].

2.2 Other (conventional) terms

Influence quantity:
Quantity that is not the measurand, but that affects the result of the measurement.

Accuracy of measurement:
The closeness of the agreement between the result of a measurement and the value of the measurand.

Comments:
1. The value of the measurand may refer to an accepted reference value[2].
2. "Accuracy" is a qualitative concept, and it should not be used quantitatively. The expression of this concept by numbers should be associated with (standard) uncertainty[3].

Uncertainty of measurement:
Parameter, associated with the result of a measurement, that characterises the dispersion of the values that could reasonably be attributed to the measurand[4].

Repeatability:
A quantitative expression of the closeness of the agreement between the results of successive measurements of the same measurand carried out under the same conditions of measurement, i.e. by the same measurement procedure, by the same observer, with the same measuring instrument, at the same location at appropriately short intervals of time.

---

1 Cf. Section 3.2.1.

2 In some documents it also points to the "true value" or "conventional true value". However, according to the *Guide* this definition should be avoided since the word "true" is viewed as redundant; a unique "true" value is only an idealised concept [2], and "a true value of a measurand" is simply the value of the measurand.

3 E.g. the accuracy of the velocity measurement is high; the standard uncertainty is as low as 0.002 m/s.

4 A definition based on more traditional concepts of uncertainty may be given as follows: A measure attached to the result of a measurement which states the range of values within which the value of the measurand is estimated to lie.

Reproducibility:
A quantitative expression of the closeness of the agreement between the results of measurements of the same measurand, where the individual measurements are carried out under different specified conditions, e.g. by different methods, with different measuring instruments, by different observers, at different locations, after intervals of time that are appropriately long compared with the duration of a single measurement, or under different customary conditions of use of the instruments employed.

Error of measurement:
The result of a measurement minus the value of the measurand. In general, the error is unknown because the value of the measurand is unknown. Therefore, the uncertainty of the result of the measurement should be evaluated and used in specifications and documentation of e.g. test results.

Random error:
The result of a measurement minus the mean that would result from an infinite number of measurements of the same measurand carried out under repeatability conditions.

Comment:
Because only a finite number of measurements can be made, it is possible to determine only an estimate of the random error. Since it generally arises from stochastic variations of influence quantities, the effect of such variations are referred to as random effects in the *Guide*.

Systematic error[5]:
The mean that would result from an infinite number of measurements of the same measurand carried out under repeatability conditions minus the value of the measurand.

Comment:
As pointed out in the *Guide* and also mentioned above, error is an idealised concept which cannot be known exactly. In practise, therefore the recognised effect from which the systematic error arises, can be quantified and it is generally referred to as a systematic effect.

Some additional used terms in metering applications have also been included here for the sake of completeness:

Range:
The interval between the minimum and maximum values of the quantity to be measured, for which the instrument has been constructed, adjusted or set.

Span:
The algebraic difference between the upper and lower values specified as limiting the range of operation of a measuring instrument, i.e. it corresponds to the maximum variation in the measured quantity of interest[6].

5 The systematic error of the indication of a measuring instrument is also referred to as bias.

6 E.g. a flow metering system which covers the range 50-200 m^3/h, has a span of 150 m^3/h.

3. METHODS FOR UNCERTAINTY CALCULATIONS

3.1 Conventional approach

For a fiscal metering station using turbine meters as the prime element, there is no dedicated standard for the uncertainty calculations. However, the method adopted and referred to as the conventional approach here, is based upon the calculation of the uncertainty of (individual) parameters and combining them using the root-sum-square (RSS) method. The uncertainties of these parameters are all quantified in relative percentage terms (in some cases a quantity is first calculated as a "worst case figure" and the relative deviation to the nominal value is identified as the associated uncertainty). The uncertainty of each parameter is denoted by "E_{xi}" where "x_i" refers to the parameter whose uncertainty contributes to the total measurement uncertainty. Using the RSS method the resulting uncertainty in the different quantities are calculated [8].

The total relative uncertainty, E_y, is determined as:

$$E_y = \sqrt{(E_{x_1})^2 + (E_{x_2})^2 + (E_{x_3})^2 + \cdots + (E_{x_n})^2} \qquad (1)$$

The different uncertainty parameters are weighted equally with sensitivity coefficient[7] of 1.

3.2 The *Guide* procedure

The starting point of the *Guide* in assessing measurement uncertainty is that all measurements are estimates of the quantities of interest. An estimate may be defined as a prediction that is equally likely to be above or below the actual result [9]. In many cases a measurement process can be represented by a mathematical model which the *Guide* refers to as the functional relationship [2][8]. For instance, often a quantity is determined as a result of several individual measurements which combined through a mathematical expression define the resulting measurand. Theoretically the uncertainty of the output quantity may then originate from one of the following sources:

a) Measurement uncertainties of (some of) the input variables.
b) Uncertainties due to incorrect assumptions about a model's input parameters (e.g. their estimates, or probability distributions).
c) Uncertainty of the (empirical) mathematical model itself because it is an abstraction of reality which may not include all the factors that affect the measurement.

The *Guide* procedure includes establishment of the equations for mathematically combining the standard uncertainties based on the functional relationship between the measurand and the input quantities. This means that the sensitivity of the quantity in question with respect to the different input measurements can be taken into account through calculated sensitivity coefficients. Furthermore, the *Guide* puts definite requirements to the documentation and reporting of the uncertainties. The objective has been to establish a universal method where the (standard) uncertainties are transferable so that the result of an uncertainty analysis can be used directly in a subsequent uncertainty evaluation. Ideally this make measurements taken at different times and at different places comparable [12].

---

7 Sensitivity coefficients are defined by Eqs. (5) and (10), respectively.

8 Other important documents dealing with estimating measurement uncertainties based on, or in harmony with the Guide, can be found in references [3], [7] and [10], see also discussion in [11].

3.2.1 Procedure for evaluation of uncertainties

The *Guide* procedure for evaluating and expressing the uncertainty of the result of a measurement can be summarised as follows [2]:

1. Derive mathematically the *functional relationship* between the measurand Y and the input quantities X_i upon which Y depends: $Y = f(X_1, X_2, \ldots, X_N)$. The function f should include all corrections for systematic effects. The modelling of the measurement by the function f is further used (in step 5) to calculate the output *estimate*[9], y, of the measurand, Y, using the *estimates* $x_1, x_2, \ldots x_N$ for the values of the N input quantities $X_1, X_2, \ldots X_N$:

$$y = f(x_1, x_2, \ldots, x_N) \tag{2}$$

2. Determine the estimated value, x_i, of input quantity X_i, either on the basis of the statistical analysis of series of observations, or by other means.

3. Evaluate the *standard uncertainty* $u(x_i)$ of each input estimate x_i, either based on statistical analysis of observations (Type A evaluation of standard uncertainty), or obtained by other means (Type B evaluation of standard uncertainty).

4. Evaluate the *covariances* associated with input estimates that are correlated:

$$u(x_i, x_j) = u(x_i)\, u(x_j)\, r(x_i, x_j) \tag{3}$$

   where $r(x_i,x_j)$ is the correlation coefficient between x_i and x_j.

5. Use the functional relationship, Eq. (2), to calculate the result of the measurement y based on the estimates x_i obtained in step 2.

6. Determine the *combined standard uncertainty* $u_c(y)$ of the measurement result y from the standard uncertainties and covariances associated with the input estimates. The combined standard uncertainty $u_c(y)$ is the positive square root of the combined variance $u_c^2(y)$, which is given by[10]:

$$u_c^2(y) = \sum_{i=1}^{N} \left(\frac{\partial f}{\partial x_i} \right)^2 u^2(x_i) + 2 \sum_{i=1}^{N-1} \sum_{j=i+1}^{N} \frac{\partial f}{\partial x_i} \frac{\partial f}{\partial x_j} u(x_i, x_j) \tag{4}$$

   The partial derivatives are referred to as sensitivity coefficients, c_i:

$$c_{y\_x_i} \equiv \frac{\partial f}{\partial x_i} \tag{5}$$

7. The *expanded uncertainty* $U(y)$ of the output estimate y can be evaluated by multiplying the combined standard uncertainty $u_c(y)$ by a coverage factor, k, on the basis of the level of

---

9 This "estimate" is also generally referred to as "the result of the measurement".

10 Eq. (4) is frequently referred to as the law of propagation of uncertainty.

confidence required for the interval $y \pm U(y)$. Assuming a normal[11] distribution of y, and a level of confidence of close to 95%, k equals 2, the value of k used in this work[12].

$$U(y) = k \cdot u_c(y) \tag{6}$$

8. Report the result of the measurement y together with its combined standard uncertainty $u_c(y)$ or expanded uncertainty $U(y)$. This includes documentation of the value of each input estimate, x_i, the individual uncertainties which contribute to the resulting uncertainty and the evaluation method used to obtain the reported uncertainties of the output estimate as summarised in steps 1 to 7.

Of practical reasons it is useful to define a symbol for the *relative* (*standard, combined standard, or expanded*) *uncertainty* of an input/output estimate. The following definitions are used[13]:

The *relative standard uncertainty* of an input estimate, x_i:

$$\delta x_i \equiv \frac{u(x_i)}{|x_i|}, |x_i| \neq 0 \tag{7}$$

The *relative combined standard uncertainty* of an output estimate, y:

$$\delta y \equiv \frac{u_c(y)}{|y|}, |y| \neq 0 \tag{8}$$

The *relative expanded uncertainty* of an output estimate, y:

$$\delta y_U \equiv \frac{U(y)}{|y|} = k \cdot \delta y, |y| \neq 0 \tag{9}$$

Finally, the *relative sensitivity coefficient*, s_i, is defined as:

$$s_{y\_x_i} \equiv \frac{\partial f}{\partial x_i} \cdot \left| \frac{x_i}{y} \right| \tag{10}$$

As distinct from the sensitivity coefficient, c_i, the relative sensitivity coefficient, s_i, is dimensionless. It is a useful quantity. The relative sensitivity coefficient and the relative standard uncertainty can be used for assessing the uncertainty contribution of each individual input variable under investigation.

---

11 If x is a normal variable with mean μ and standard deviation σ, $x \sim N(\mu, \sigma)$, then the probability distribution of the normal variable is given by the expression [13]: $p(x) = \frac{1}{\sqrt{2\pi}\sigma} e^{-\left(\frac{1}{2}\right)\left(\frac{x-\mu}{\sigma}\right)^2}$.

12 Note that a coverage factor of $k = 2$ produces an interval corresponding to a level of confidence of 95.45% while that of $k = 1.96$ corresponds to a level of confidence of 95%. Since the calculation of intervals having specified levels of confidence is at best only approximate, the *Guide* justifiably emphasises that for most cases it does not make sense to try to distinguish between e.g. intervals having levels of confidence of say 94, 95 or 96%, cf. Annex G of the *Guide* [2]. In practice, it is therefore recommended to use $k = 2$ which is assumed to produce an interval having a level of confidence of approximately 95%.

13 It should be noted that the present version of the *Guide* [2] does not assign distinct symbols for the defined relative uncertainties. The terminology used here has been introduced by the authors.

3.3 NPD regulations

The estimated uncertainties should be reported as stated by the regulations of the NPD for fiscal metering of oil and gas (§16 in [1]). According to these regulations an uncertainty analysis should be carried out at a 95% confidence level. This means that the probability is 95% for the real measurement being confined within the specified interval, and according to the *Guide* this corresponds to a coverage factor of $k = k_{95} = 2$.

4. CALCULATION EXAMPLE - OIL METERING STATION

In the following, results of a "conventional" uncertainty calculation carried out by a major supplier of metering systems, are summarised in Section 4.2. These data are part of a metering station delivery to a field development in the North Sea. The vendor's uncertainty data of pressure, temperature, density and gross observed volume are briefly presented. In Section 4.3, the uncertainty of the same quantities are calculated based on the same vendor specified instrument uncertainties and process condition at the oil export station. These calculations have been carried out using the procedure of the *Guide*.

4.1 Oil metering station and process condition

The calculations that follow are based on vendor specified uncertainties of an oil metering station consisting of the equipment listed in Table 1 and the process condition in Table 2.

Table 1 Equipment of the oil metering station used as basis for the presented uncertainty evaluations.

Item	Type
Turbine meter	Turbine Meter 8" 300lb
Densitometer	ITT Barton 668
Pressure Transmitter	Rosemount Model 3051CG
Temperature Transmitter	Rosemount 3044CA, temperature element 13669
Flow computer	Liquid Turbine Flow Computer

Table 2 The process condition of which the presented uncertainty evaluations have been carried out.

Quantity	Condition
Service	Hydrocarbon liquid
Operating pressure	20.2 barg
Design pressure	32 barg
Operating temperature	65.4 °C ± 10 °C
Ambient temperature	-10/23 °C
Operating density	776 kg/m^3
Normal flow rate	1867 Sm^3/h

The turbine meter is a flow sensing device with a rotor that senses the velocity of flowing liquid in a closed conduit. The flowing liquid causes the rotor to move with a tangential velocity that is proportional to volumetric flow rate. A volume prover is used for calibration of the meter. Density is normally measured by densitometers mounted in the meter run or in connection with the inlet or outlet manifold. Pressure and temperature are measured close to the turbine meter, at the inlet and outlet of the volume prover and at the density measuring device.

4.2 Results from "conventional" calculation

The uncertainty in pressure, temperature, density and gross observed volume are determined as outlined in Section 3.1 [8]. The uncertainty analysis calculated by this vendor is reported to be within a confidence level of 95%, where the confidence level of 95% is equivalent to 2σ (i.e. two standard deviations). The supplier identified the following parameters as the main source contributors to the overall uncertainty in a turbine based metering system:

a) Turbine meter calibration
b) Turbine meter linearity
c) Turbine meter repeatability
d) Stream density measurement error
e) Stream and prover loop temperature and pressure measurement errors
f) Flow computer calculation error and pulse interpolation

In addition the following instrument uncertainties were included:

g) Uncertainty in pressure measurement as a result of primary measurement ("*ptx*"), calibration ("*pcal*"), stability ("*pstab*") and ambient temperature effects ("*paT*").
h) Uncertainty in temperature measurement as a result of primary temperature measurement ("*ttx*"), calibration ("*tcal*"), stability ("*tstab*") and ambient temperature effects ("*taT*").
i) Uncertainty in density measurement calculated on the basis of the data sheet of the densitometer uncertainty specification.
j) Pulse interpolation.

For this metering station the vendor has obtained the following results [8][14] :

Uncertainty of pressure measurement

$E_{pressure} = \sqrt{(E_{ptx})^2 + (E_{pcal})^2 + (E_{pstab})^2 + (E_{paT})^2} = 0.44\%$. At the operating pressure of 20.2 barg, the uncertainty in the pressure measurement equals 0.09 bar, which is within the NPD regulation of 0.2 bar.

Uncertainty of temperature measurement

$E_{temperature} = \sqrt{(E_{ttx})^2 + (E_{taT})^2 + (E_{tcal})^2 + (E_{tstab})^2} = 0.29\%$ .With an operating temperature of 65°C, the uncertainty in the temperature measurement equals 0.19 °C, which is within the NPD regulation of 0.30 °C.

Uncertainty of density measurement

$E_{density} = \sqrt{(E_{pd})^2 + (E_{temperature})^2 + (E_{freq})^2} = 0.41\%$. The result is outside the NPD requirement of 0.30% of measured value. In fact the uncertainty of the raw density measurement is calculated to $E_{pd} = 0.29\%$, thereafter this figure is RSS-combined with the temperature uncertainty to estimate the uncertainty of the temperature corrected density (the contribution from the uncertainty of the frequency reading by the flow computer, E_{freq}, is negligible). This procedure increases the uncertainty to 0.41%. However, it can be shown that the sensitivity coefficient with respect to temperature in this case is very low so the uncertainty of 0.41% is likely to be a conservative estimate.

[14] The calculations as such have not been quality checked by the authors.

Uncertainty in gross observed volume, E_{gov}

Turbine meter linearity, $E_{lin} = 0.15\%$,
Turbine meter repeatability, $E_{rep} = 0.02\%$,
Meter factor, $E_{MKF} = 0.044\%$
Correction factor, $E_{Clsm} = 0.0007\%$
Correction factor, $E_{Cpsm} = 0.0135\%$
Calculation, $E_{cal} = 0.001\%$
Flow computer clock, $E_{clock} = 0.0001\%$

$$E_{gov} = \sqrt{(E_{lin})^2 + (E_{rep})^2 + (E_{MKF})^2 + (E_{Clsm})^2 + (E_{Cpsm})^2 + (E_{calc})^2 + (E_{clock})^2} = 0.1582\%$$

4.3 Results from "new" method; i.e. according to the ISO *Guide*

To calculate the uncertainty in pressure, temperature, density and the gross observed volume, the functional relationship of each quantity and the different associated input variables must first be established. Some of these primary measurements may again be related to other parameters. Such relations must be included as part of the functional relationship. In addition, basis documentation and certificates of equipment from the supplier which give details of the primary measurement uncertainties have been evaluated based on engineering judgement (i.e. Type B evaluation of uncertainties), and the (relative) expanded uncertainties have been calculated using the *Guide* procedure presented in Section 3.2. The detailed calculations have been separately reported [14], and only the main results are summarised here for simplicity. However, the detailed calculations of the relative expanded uncertainty of the density measurement have been included as an example and given as an attachment to this paper. The principles of the *Guide* have been used for uncertainty calculations in several projects at CMR [15], [16].

Uncertainty of pressure measurement

By using the procedure of the *Guide*, the expanded uncertainty of the pressure measurement has been estimated to: $U(P) = P \cdot \delta P_U = k_{95} \cdot P \cdot \delta P = 0.19$ barg. The expanded uncertainty of 0.19 barg ($k = 2$) is closely within the NPD requirements of 0.2 barg [1]. Note that the estimated uncertainty is higher than that given by the conventional method.

Uncertainty of temperature measurement

By using the procedure of the *Guide*, the combined standard uncertainty of T at 65.4 °C, $u_c(T)_{T=65.4}$, has been estimated to 0.13 °C. The corresponding expanded uncertainty of the temperature measurement is: $U(T)_{T=65.4} = k_{95} \cdot u_c(T)_{T=65.4} = 0.26\,°C$.

The expanded uncertainty of T as a function of the actual value, i.e. the measured temperature, throughout the temperature range 55-75 °C, is shown in Figure 1.

It is observed that the expanded uncertainty increases marginally with temperature (less than 8 millidegrees for temperatures between 55 and 75 °C). From a practical point of view the expanded uncertainty can be regarded as constant throughout this temperature range with a numerical value of 0.26 °C. The expanded uncertainty of 0.26 °C ($k = 2$) is within the NPD requirements of 0.30 °C [1]. However, note that the estimated uncertainty is higher than that reported using the conventional method.

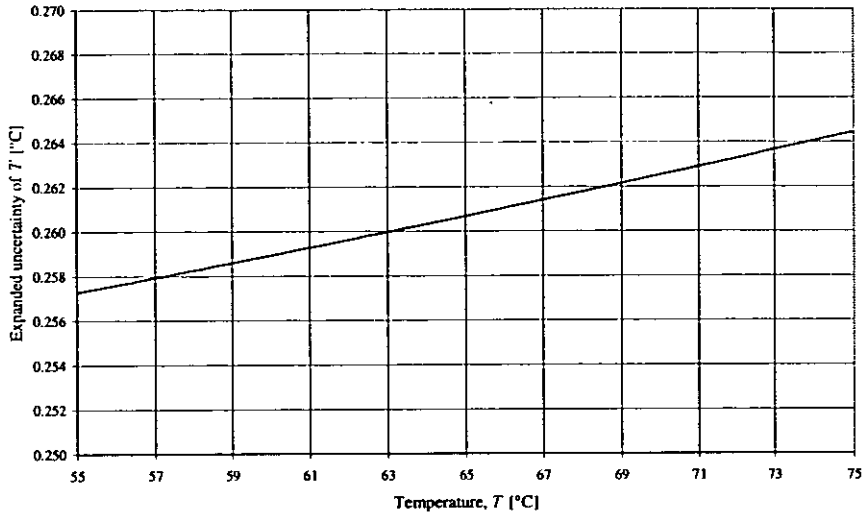

Figure 1 Expanded uncertainty of the temperature measurement as a function of actual value in the measurement range 55-75 °C. The level of confidence is 95%, $k = 2$. The span of the temperature transmitter is 100 °C.

Uncertainty of density measurement[15]

By using the procedure of the *Guide*, the expanded uncertainty of the measured density has been estimated to: $U(\rho) = k_{95} \cdot u_c(\rho) = 2 \cdot 0.843$ kg/m^3 = 1.686 kg/m^3 where $u_c(\rho)$ is the combined standard uncertainty of ρ.

The relative expanded uncertainty of ρ ($k = 2$) is: $\delta\rho_U = \dfrac{U(\rho)}{\rho} = 0.22\%$.

Note that the estimated uncertainty in this case is lower than that given by the conventional method. The uncertainty is within the NPD requirement of a relative uncertainty lower than 0.30% in the density measurement.

Uncertainty of liquid volume flow rate (Gross Observed Volume Flow rate)

The principle for calculating the uncertainty of the gross observed volume[16] in accordance with the *Guide* is presented in this section. The functional relationship of the gross observed volume, V_l, may be expressed as:

$$V_l = \frac{MR \cdot C_{tsm} \cdot C_{psm}}{MKF} + V_{calc} \qquad (11)$$

where the value of the variable V_{calc} is zero, but to which associated uncertainty is assigned as a result of finite resolution of the calculation procedure in the flow computer. MR is the number of interpolated pulses from the turbine meter during the measurement period. MKF is the meter factor of the turbine meter whose unit is (pulses/m^3). Since a metering station is considered here, the MKF is determined using a pipe prover rather than by an external calibration. C_{tsm} and C_{psm} are correction factors. The relative expanded uncertainty of V_l is calculated based on the associated

15 The details of the uncertainty calculation of the density are included as an attachment at the end of the paper.

16 Gross observed volume is the volume measured by the turbine meter at process or line conditions. Corrections for changes in liquid volume as a result of influence of temperature and pressure, must further be taken into account to convert V_l to the volume, V_s, at standard conditions of temperature 15 °C and reference pressure of 1.01325 bar a [1]. This procedure which is not dealt with further here, includes the correction factors C_{tlm} and C_{plm}, respectively.

uncertainties of the input quantities in Eq. (11) which were first evaluated giving the following relative standard uncertainties:

$\delta V_{calc} = 0.0005\%$

$\delta MR = 0.0085\%$

$C_{tsm} = 1.001974$ and its standard and relative standard uncertainty are estimated to:
$u_c(C_{tsm}) = 5 \cdot 10^{-6}$ and $\delta C_{tsm} = 0.0005\%$, respectively.

$C_{psm} = 1.000191$ and its standard and relative standard uncertainty are estimated to:
$u_c(C_{psm}) = 2 \cdot 10^{-6}$ and $\delta C_{psm} = 0.0002\%$, repectively.

The functional relationship for the meter factor, MKF, may be given by:

$$MKF = MKF_p + MKF_{lin} + MKF_{rep} \tag{12}$$

where the values of the variables MKF_{lin} and MKF_{rep} both equal zero, but to which uncertainties are assigned associated with the linearity and repeatability of the meter factor. Using a pipe prover the meter factor (at standard conditions), MKF_p, is calculated according to the following expression:

$$MKF_p = \frac{MR_p \cdot C_{tsm} \cdot C_{psm} \cdot C_{tlm} \cdot C_{plm}}{BV \cdot C_{tsp} \cdot C_{psp} \cdot C_{tlp} \cdot C_{plp}} \tag{13}$$

where MR_p is the number of pulses from the turbine meter throughout the measurement (or "proving") period, BV is the base volume of the prover and C_{ijk} are correction factors.

The uncertainty of the calculated metering factor should be estimated according to the *Guide* based on the standard uncertainties of MR_p, BV and the 8 eight correction factors C_{ijk} using Eq. (4). The calculation includes six partial derivatives of the expressions[17] for the correction factors C_{ijk} in addition to those of C_{tsm} and C_{psm}. These calculations have not been carried out here. Instead, in this limited study, the uncertainty of MKF_p is assumed to be satisfactorily estimated by the conventional uncertainty calculation method [8], but the "new" uncertainty estimates of C_{tsm} and C_{psm} calculated in this work are accounted for. The uncertainty of the six remaining correction factors have not been evaluated, i.e. the quoted vendor uncertainties have been adopted. The uncertainty in the estimate of MKF using a pipe prover is then found as $\delta MKF_p = 0.0155\%$. Uncertainties due to linearity and repeatability are given directly by data sheets from vendors as $\delta MKF_{lin} = 0.075\%$ and $\delta MKF_{rep} = 0.01\%$, respectively.

Based on the relative standard uncertainties of the different quantities of which V_l depends, the relative combined standard uncertainty of the gross observed volume is estimated to:
$\delta V_l = 0.0777\%$, and the relative expanded uncertainty of V_l ($k = 2$) is: $\delta V_{l\_U} = k \cdot \delta V_l = 0.1554\,\%$.

The result shows that in this case with the individual uncertainties of the primary quantities (T, P, EH[18], ER, R, AT, t), the uncertainty in gross observed volume is mainly caused by the uncertainty in the meter factor MKF. Furthermore, if the uncertainty in the estimate of MKF as a result of the proving, δMKF_{p_U}, had been evaluated stringently according to the *Guide* giving an estimate larger than 0.031%, the relative expanded uncertainty of the gross observed volume would be

17 The expressions for the correction factors can be found in reference [17] and [18].

18 EH is the coefficient of the linear expansion of the meter housing, ER is the coefficient of the linear expansion of the meter rotor, R is the inner radius of the meter housing, AT is the area of the rotor in the plane of the flow and t is the wall thickness of the housing [14].

larger than the estimate reported here. The estimated relative expanded uncertainty in this work of 0.155% holds true as long as the relative expanded uncertainty in the meter factor as a result of proving, is lower than 0.031%. If this uncertainty limit of the meter proving is exceeded due to e.g. high uncertainties in pressure or temperature, a thorough evaluation of Eq. (13) should be carried out based on the individual standard uncertainty contributions of *MR*, base volume of the prover, *BV*, and the different correction factors. Such an evaluation based on the procedure of the *Guide* should be addressed in future as a coming step in further standardising measurement uncertainty evaluation of metering stations. This should also include the conversion to standard conditions, the calculation of mass rates and inclusion of water cut measurement uncertainty facilitating the evaluation of the uncertainty in the gross standard volume and the net oil observed volume.

5. DISCUSSION

The preceding calculations summarised in Table 3 below, show that different results are obtained using a conventional uncertainty calculation method compared to the results following the *Guide* procedure. The main reason for the differences is that the conventional RSS method does not sufficiently take the sensitivity of the measurand with respect to the different input variables into account. Also, when studying the details of the calculations, the method for determining the individual relative uncertainties of the input variables has, in some cases, been found to be some subtle. This may make the method "vendor or application dependent" leading to lower uncertainties than that obtained by the *Guide* method for some quantities and vice versa for others as shown by the results presented here.

By taking the uncertainty of the density measurement as an example, it is shown that the uncertainty estimate of the conventional approach is too conservative since the uncertainty of the temperature correction is given too high sensitivity by the RSS combination. In this case the uncertainty associated with the temperature correction is in fact negligible with a very low sensitivity coefficient compared to the raw density measurement itself as shown in Table 4. It should be noted that conventional method gives an uncertainty estimate of the density of 0.29% if the uncertainty contribution from the temperature correction is neglected.

Finally, it should be pointed out that in addition to giving recommendations for the uncertainty calculations, the *Guide* also puts clear requirements to the documentation of the results. This means that more effort may have to be put into the measurement uncertainty evaluation than experienced previously.

Table 3 Summarised quantitative comparison of the results of the conventional uncertainty calculation with those obtained by the method of the ISO *Guide* for a fiscal oil metering station. The process condition is characterised by a temperature of 65.4 °C, pressure of 20.2 barg and a density of 776 kg/m^3.

	Conventional method	**The *Guide***		
Quantity	Uncertainty	Expanded uncertainty (k=2)	Unit	NPD requirement
Pressure, P	0.09	0.19	[bar]	0.20
Temperature, T	0.19	0.26	[°C]	0.30
	Relative uncertainty	Relative expanded uncertainty (k=2)		
Density, ρ	0.41	0.22	[%]	0.30
Gov, V_l	0.1582	0.1554	[%]	-

6. CONCLUSIONS

This case study using an oil metering station as basis for the calculations, indicates that different uncertainty estimates are achieved by a conventional approach and an alternative one rested on the principles of the ISO *Guide*. It should be noted that this study does not include the evaluation of any systematic effects which may occur in practise and which have to be corrected by re-calibration. The main reason for the differences is that the conventional RSS method does not sufficiently take the sensitivity of the measurand with respect to the different input variables into account. Furthermore, it has been found that the individual relative uncertainties of the input variables, in some cases, have been determined by some inconsistent methods. This may make the method vendor or application dependent leading to lower uncertainties than that obtained by the *Guide* method for some quantities and larger for others.

Even though the *Guide* is frequently considered as a difficult document it may represent a more sound approach for measurement uncertainty calculation in particular with respect to the documentation of the results.

With respect to the uncertainty calculation of the gross observed volume, MKF_p is the most complicated variable to evaluate. A thorough evaluation of Eq. (13) should be carried out based on the individual standard uncertainty contributions of MR, base volume of the prover, BV, and the different correction factors[17]. The contribution from the uncertainty in any of these fundamental parameters on the resulting uncertainty in gross and net observed volume could then be evaluated for different process conditions and prover characteristics. Such an evaluation based on the procedure of the *Guide* should be addressed in future as a coming step in further standardising measurement uncertainty evaluation of metering stations.

7. ACKNOWLEDGEMENT

Kjell-Eivind Frøysa at CMR is acknowledged for useful comments to this work.

8. REFERENCES

[1] Norwegian Petroleum Directorate (1997): *Regulations relating to fiscal measurement of oil and gas in petroleum activities.* ISBN 82-7257-522-1.

[2] ISO (International Organisation for Standardization) (1995): *Guide to the expression of uncertainty in measurement.* On behalf of BIPM, IEC, IFCC, ISO, IUPAC, IUPAP, OIML. ISBN 92-67-10188-9.

[3] EAL-R2 (European Cooperation for Accreditation of Laboratories) (1997): *Expression of the uncertainty of measurement in calibration.* Edition 1. April 1997.

[4] ISO (International Organisation for Standardization) (1993): *International vocabulary of basic and general terms in metrology (VIM).* Second edition.

[5] ISO (International Organisation for Standardization) (1993): *Statistics - vocabulary and symbols - Part 1: Probability and statistical terms.* ISO 3534-1.

[6] Dykesteen E (-ed), Amdal J, Danielsen H, Fløtlo D, Grendstad J, Hide H O, Moestue, H and Torkildsen, B H on behalf of The Norwegian Society for Oil and Gas Measurement (NFOGM) (1995): *Handbook of multiphase metering.* Report No. 1, September 1995.

[7] Taylor B N, and Kuyatt C E, on behalf of NIST (National Institute of Standards and Technology, USA) (1994): *Guidelines for evaluating and expressing the uncertainty of NIST measurement results.* Technical Note 1297 1994 Edition.

[8] "A major vendor of metering stations" (1996): *Uncertainty calculations of oil export station.* Confidential.

[9] Kitchenham B and Linkman S (1997): *Estimates, uncertainty and risk.* IEEE Software, Vol. 14, Iss 3, pp 69-74.

[10] NIS 3003 (1995): *The expression of uncertainty and confidence in measurement for calibrations.* Edition 8 May 1995, NAMAS Executive, National Physics Laboratory, England.

[11] Orford G R (1996): *Why so many uncertainty documents?* Proc. of IEE Half-Day Colloquium on Uncertainties Made Easy, London, October 10, 1996, The Institute of Electrical Engineers.

[12] Horwitz W and Albert R (1997): *The concept of uncertainty as applied to chemical measurements.* Analyst, Vol. 122 (615-617) June 1997.

[13] Wonnacott T H and Wonnacott R J (1977): *Introductory statistics.* Third Edition. ISBN 0-471-02528-3.

[14] Midttveit Ø and Nilsson J (1997): *A practical example of uncertainty calculation for a metering station - conventional and new methods.* Ref. no CMR-97-F10024. Confidential.

[15] Lunde P, Frøysa K E and Vestrheim M (1997): *Garuso-Version 1.0. Uncertainty model for multipath ultrasonic transit time gas flow meters.* Ref. no CMR-97-A10014.

[16] Midttveit Ø, Nilsson J, Villanger Ø and Johannessen A A (1997): *Cost effective allocation. Functional specification of the AMC-program-Version 1.0.* Ref. no CMR-97-F10004. Confidential.

[17] API Manual of Petroleum Measurement Standards (1980): Chapter 11 Physical Properties Data, Section 1 Volume correction factors.

[18] API Manual of Petroleum Measurement Standards (1987): Chapter 12 Calculation of Petroleum Quantities, Section 2 Calculation of Liquid Petroleum Quantities Measured by Turbine or Displacement Meters.

[19] ITT Corporation. Barton (1991): Model 668 Integral Drive Liquid Densitometer. Product Bulletin 668-2.

[20] ITT Barton Instruments (1995): Certified calibration report of model 668.0001A.

[21] Flow computer Operator Guide.

CALCULATION OF THE UNCERTAINTY OF THE DENSITY MEASUREMENT

The expanded uncertainty of the liquid density measured by a Barton Model 668 densitometer [19], [20] which is temperature corrected by the flow computer [21], can be determined according to the *Guide* as follows:

The functional relationship may be expressed as:

$$\rho = A_0 + A_1 \cdot t + A_2 \cdot t^2 - A_B \cdot (T - 20) + A_{B1} \cdot t^2 \cdot (T - 20) + A_{B2W} \cdot t^2 \cdot (T^2 - 20^2) + \rho_{meter} \quad (14)$$

where t is the time period for one pulse (the reciprocal of frequency), T is the temperature and the variable ρ_{meter} can be expressed by:

$$\rho_{meter} = \rho_{dt} + \rho_{cal} + \rho_{res\_temp} + \rho_{res\_press} + \rho_{rep} + \rho_{model} \tag{15}$$

where the estimated values of the parameters ρ_{dt} , ρ_{cal}, ρ_{res_temp}, ρ_{res_press}, ρ_{rep} and ρ_{model} all equal zero. These six variables have associated uncertainties and affect the resulting uncertainty of the density measurement. However, the uncertainties are about the nominal parameter values of zero. Hence, the statistical expectation of the variable ρ_{meter} is zero; i.e. $\rho_{meter} = 0$.

The raw density which is not temperature corrected, can then be expressed as:

$$\rho_{rd} = A_0 + A_1 \cdot t + A_2 \cdot t^2 + \rho_{meter} \tag{16}$$

where the standard uncertainty of the raw density measurement is mathematically represented by the virtual variable ρ_{meter}; i.e. $u(\rho_{rd}) = u(\rho_{meter})$.

Calibration constants of the densitometer [20]:
$A_0 =$ -434.43 kg/m^3
$A_1 =$ -206.93 (kg/m^3)/ms
$A_2 =$ 7122.46 (kg/m^3)/ms^2

Coefficients for temperature compensation of the raw density measurement:
$A_B =$ 0.00 (kg/m^3)/°C
$A_{BIC} = -4.2 \cdot 10^{-2}$ (kg/m^3)/(°C· ms^2)
$A_{BIW} = 8.7 \cdot 10^{-2}$ (kg/m^3)/(°C· ms^2)
$A_{BI} = A_{BIW} + A_{BIC} = 4.5 \cdot 10^{-2}$ (kg/m^3)/(°C· ms^2)
$A_{B2W} = -6.4 \cdot 10^{-4}$ (kg/m^3)/((°C)^2· ms^2)
The operating density at the metering station is: $\rho = 776$ kg/m^3 which corresponds to a time period and frequency of:
$t = 0.427$ ms
$f = 2.342$ kHz
$\rho_{rd} = 775.84$ kg/m^3
$\rho = 775.76$ kg/m$^3 \approx 776$ kg/m^3

Assumed variations in temperature about the operating condition for calculation of uncertainty in density due to these residual temperature effects: $T_{res} = 41$ °C = 5 °F.

Assumed variations in pressure about the operating condition for calculation of uncertainty in density due to these residual pressure effects: $P_{res} = 10$ bar = 145 psi.

The level of confidence of the uncertainties is not specified in the data sheets from the suppliers. In the uncertainty estimation that follows it is assumed that the level of confidence is approximately 95%, i.e. $k = k_{95} = 2$ except for some of the uncertainty contributions which are reported as "precisions" and stated as a "$\pm a$ maximum" value. In the lack of further documentation of these figures, it is assumed that the "$\pm a$ maximum" values represent endpoints of the interval $-a$ to $+a$ of a uniform or rectangular probability distribution of the quantity "x_i" in question. Under these assumptions, the standard uncertainty is [2]:

$$u(x_i) = \frac{a}{\sqrt{3}} \tag{17}$$

Then the different specified uncertainties can be converted into standard uncertainties:

Uncertainty of the primary densitometer (linearity):
± 1.2 kg/m^3 maximum, i.e. $u(\rho_{dt}) = (1.2$ kg/m$^3)/\sqrt{3} = 0.693$ kg/m^3

Uncertainty due to the calibration reference standard:
$U(\rho_{cal}) = 0.3$ kg/m^3 ($k_{95} = 2$), i.e. $u(\rho_{cal}) = (0.3$ kg/m$^3)/k_{95} = 0.150$ kg/m^3

Uncertainty due to residual temperature effects:

±6 kg/m^3 per 100 °F maximum, i.e.:

$$u(\rho_{res\_temp}) = \frac{6}{\sqrt{3}} \cdot \frac{T_{res}(^\circ\mathrm{F})}{100} \tag{18}$$

With T_{res} = 5°F, $u(\rho_{res\_temp})$ = 0.173 kg/m^3.

Uncertainty due to residual pressure effects:

±0.2 kg/m^3 per 100 psi maximum, i.e.:

$$u(\rho_{res\_press}) = \frac{0.2}{\sqrt{3}} \cdot \frac{P_{res}(\mathrm{psi})}{100} \tag{19}$$

With P_{res} = 145 psi, $u(\rho_{res\_temp})$ = 0.167 kg/m^3.

Uncertainty due to repeatability:

±0.3 kg/m^3 maximum, i.e. $u(\rho_{rep})$ = (0.3 kg/m^3)/$\sqrt{3}$ = 0.173 kg/m^3

Uncertainty associated with density model calibration (curve fit)[19]:

±0.6 kg/m^3 maximum, i.e. $u(\rho_{model})$ = (0.6 kg/m^3)/$\sqrt{3}$ = 0.346 kg/m^3

By assuming that the different variables are independent, the combined standard uncertainty of ρ_{meter} can be calculated.

The combined standard uncertainty of the raw density measurement:

$$u_c(\rho_{meter}) = \sqrt{u(\rho_{dt})^2 + u(\rho_{cal})^2 + u(\rho_{res\_temp})^2 + u(\rho_{res\_press})^2 + u(\rho_{rep})^2 + u(\rho_{model})^2} = \sqrt{(0.693)^2 + (0.150)^2 + (0.173)^2 + (0.167)^2 + (0.173)^2 + (0.346)^2} = 0.843 \tag{20}$$

The corresponding expanded uncertainty of the raw density measurement is:

$$U(\rho_{meter}) = k_{95} \cdot u_c(\rho_{meter}) = 2 \cdot 0.843 = 1.686\,;\ \text{i.e. } 1.686\ \text{kg/m}^3 \tag{21}$$

The relative expanded uncertainty of ρ_{rd} (k = 2) is:

$$\delta\rho_{rd\_U} = \frac{U(\rho_{meter})}{\rho_{rd}} = 0.0022\ ;\ \text{i.e. } 0.22\ \% \tag{22}$$

Overall uncertainty of the density measurement:

The combined standard uncertainty of the measured density, ρ, can be derived on the basis of Eq. (14):

$$u_c(\rho) = \sqrt{\left(\frac{\partial\rho}{\partial t} \cdot u(t)\right)^2 + \left(\frac{\partial\rho}{\partial T} \cdot u_c(T)\right)^2 + \left(\frac{\partial\rho}{\partial\rho_{meter}} \cdot u_c(\rho_{meter})\right)^2} \tag{23}$$

where

$$\frac{\partial\rho}{\partial t} = A_1 + 2t \cdot [A_2 + A_{B1} \cdot (T - 20) + A_{B2W} \cdot (T^2 - 20^2)], \tag{24}$$

[19] Note, the curve fit calibration results in an overall model calibration uncertainty included here which incorporates the uncertainty of the individual calibration coefficients A_0, A_1 and A_2. These calibration coefficients are therefore assumed to be fixed constants which do not have any associated uncertainties.

$$t = \frac{1}{f} \Rightarrow u(t) = \sqrt{\left(\frac{\partial t}{\partial f}\right)^2 \cdot u^2(f)} = \frac{1}{f^2} \cdot u(f) = \frac{1}{f^2} \cdot f \cdot \delta f = \frac{\delta f}{f} \tag{25}$$

where the relative uncertainty of the flow computer frequency input is [21]:
$\delta f_U = 0.0013\%$ ($k_{95} = 2$), i.e. $\delta f = 1.3 \cdot 10^{-5} / k_{95}$,

$$\frac{\partial \rho}{\partial T} = -A_B + t^2 \cdot (A_{B1} + 2 \cdot A_{B2W} \cdot T), \tag{26}$$

$$\frac{\partial \rho}{\partial \rho_{meter}} = 1 \tag{27}$$

and $u_c(T)$ and $u_c(\rho_{meter})$ have been estimated previously, cf. Section 4.3 and Eq. (20), respectively.

An uncertainty budget for the uncertainty of the measured density is given in Table 4.

Table 4 Orderly summary of the uncertainty estimation of the density measurement at the actual process condition of ρ = 776 kg/m^3 and T = 65.4 °C. The sensitivity coefficients are: $\partial\rho/\partial t$, $\partial\rho/\partial T$, $\partial\rho/\partial\rho_{meter}$.

Measurand: density		Value of measurand at process condition:			ρ = 776 kg/m^3
		Standard uncertainty			**Expanded** uncertainty
Parameter, x_i	Estimate	$u(x_i)$	Sensitivity coefficient,	$u_i^2(\rho)$	(k=2)
			c_i		[kg/m^3]
Time period, t	0.427 ms	0.00000278	5875.28000000	0.00026591	
Temperature, T	65.4 °C	0.13000000	-0.00706000	0.00000084	
Density, ρ_{meter}	0 kg/m^3	0.84300000	1	0.71064900	
			$u^2(\rho)$	0.71092	$U(\rho)$
	Combined standard uncertainty:		$u(\rho)$	0.8432	1.686

Hence, it is observed that the uncertainty in the temperature measurement and the resolution of the frequency measurement by the flow computer do not significantly contribute to the resulting uncertainty of the density measurement. The uncertainty of the density measurement originates from the raw density measurement.

The estimated expanded uncertainty of the measured density is:

$$U(\rho) = k_{95} \cdot u_c(\rho) = 2 \cdot 0.843 = 1.686 \text{; i.e. } 1.686 \text{ kg/m}^3 \tag{28}$$

The relative expanded uncertainty of the density measurement:

The relative expanded uncertainty of ρ (k = 2) is:

$$\delta\rho_U = \frac{U(\rho)}{\rho} = 0.0022 \text{ ; i.e. } 0.22\ \% \tag{29}$$

NSFMW.97

North Sea FLOW Measurement Workshop

Paper ~~13~~: 2.7

EUROPEAN CALIBRATION INTER-COMPARISON ON FLOW METERS - HOW ACCURATE CAN ONE EXPECT TO MEASURE FLOW RATES

Authors:
Peter Lau, Swedish National Testing and Research Institute, Sweden

Organiser:
Norwegian Society of Chartered Engineers
Norwegian Society for Oil and Gas Measurement
Co-organiser:
National Engineering Laboratory, UK

EUROPEAN CALIBRATION INTER-COMPARISON ON FLOW METERS - HOW ACCURATE CAN ONE EXPECT TO MEASURE FLOW RATES

Peter Lau
Swedish National Testing and Research Institute, Sweden

ABSTRACT

Results of a calibration inter-comparison are reported that were performed on a flow meter transfer standard between nine primary flow laboratories in Western Europe. The purpose is to ensure that the equipment and methods used do not suffer from systematic errors. This inter-comparisons was performed on kerosene as a typical representative for light oil products. Traceable calibrations are a prerequisite for international trade and inter-comparisons form the base for the reliability in the calibration job performed at the laboratories. The outcome sets a limit for the reliability in flow measurement itself, which also is important to meter users.

The transfer standard consisted of a turbine being sensitive to changes in flow profiles and a displacement (screw) meter being not. A crucial quality for any exercise of that kind is the stability of the meter package in time. For both meters it was found to be within 0,004 %, which is an order of magnitude less than the measurement uncertainties (0.03 to 0,3 %) claimed by the participating laboratories. The inter-comparison revealed reproducibility figures of 0.16 and 0.17 % compared to 0,07 and 0,09 % within the co-ordinating laboratory. A few laboratories faced problems with non-ideal flow profiles in their test site, that could be overcome with a flow straightener in front of the turbine. The remaining differences in the reported calibration results were predominantly caused by differences in the calibration liquids used even though these were within small limits in both viscosity and temperature.

INTRODUCTION

Assume a situation where a tank boat is loading petrol from a storage tank at a refinery. If only one meter determines the volume of the shipment and the payment is based on it probably everyone would be happy. Suspicious people tend to question the correctness of a measurement. A captain on a boat for instance may have independent information on the received load as the changed displacement can be red off from the water level.

A real problem arises if both the deliverer and the receiver of a shipment use their own instrument. Due to various reasons these will seldom exhibit the same figures. As a natural consequence the question is asked which of the two is right and which one is wrong. This is not only a metrological question because immediately after the discovery of a difference in display the involved parties will discuss on which meter the shipment should be paid. The parties then will realise that meters, like every other instrument have errors, which means that non of the two results may be correct. Then probably both parts look up the specification of their respective instrument. There is a certain chance that the difference could be explained by the uncertainty statements given there. On the other hand with the experience from many meter test there is a high probability that the specifications are far to optimistic and definitely do not take into consideration all the facts that disturb a meter. It would be a good idea to involve a metrological institution to solve the discrepancy.

Calibration as a Means of Solving a Measurement Problem

A calibration laboratory would offer a specification telling how wrong a certain instrument will measure, at least under calibration conditions, and how the indication can be corrected. The service hopefully also contains a statement of uncertainty telling that even after a correction there will still be a certain range of values around the stated one that likewise could be appointed to the calibration result. Does this figure limit the accuracy with which the parties can expect to determine the amount of received petrol in a tank boat? If we assume that both parties engage the same calibration laboratory and it does a good job then the uncertainty figure stated in the certificate must be regarded as a lower limit in that sense that a flow or volume measurement at a production site never can give a value with a smaller uncertainty interval.

An important argument for this postulation is that meters most often do not measure flow or volume directly. Instead they sense the speed of the passing medium. If the measuring principle is sensitive to other disturbing effects, which normally is the case or the measuring spot is not really representative for the whole meter area then deviations from more or less ideal calibration situations are likely to arise. It is certainly not incidental that so many different principles have been used to measure flow, which can be regarded as there is no outstanding technique incorporating all demands a user might have.

Calibration Inter-comparison and Measurement Uncertainty

If the two parties in our example are situated in different countries it would be natural that both could show up a calibration certificate each from different institutions, let's say one from Sweden and one from the Netherlands. What to do if the corresponding meter factors and the belonging uncertainties still does not explain the observed differences in the metering of the ship load. One explanation could of course be that one of the meters is heavily disturbed. But how sure can a customer be that he receives the same calibration result from our laboratory than from an other one. Usually a customer is not willing to pay two times for an answer to that question. But in that also lies the question of how accurate he can expect to measure liquid volumes and flow rates. As argued above his measurement uncertainty can never be smaller than the one he receives from the calibration laboratory. But how good is the agreement in the calibration performance between different laboratories? Thinking of the complexity of flow calibration some consecutive questions are the following. How do national flow laboratories agree concerning their stated calibration uncertainty for a meter? How consistent would the outcome of a calibration inter-comparison be with respect to these uncertainties? Are different methods of calibration gravimetric or volumetric ones equivalent? Are there systematic differences due to installation facilities or references used?

EU-PROJECT

The interest in these questions made the European Community to finance the investigation described below (BCR-project 3476/1/0/203/92/9-BCR-S(30)). Problems of systematic differences between laboratories, the comparison between different methods, the skill of the personnel, traceability and quality assurance are not new ones within the metrological society. Concerning flow measurements a crucial problem has been and still is to find good and re-

peatable meters with a high stability over the time of the comparison, which is necessary to draw essential conclusions.

A proposal for an inter-comparison with a suitable transfer standard and certain test procedures for evaluation were send to all national flow calibration laboratories in Western Europe. A total of nine laboratories responded positively for this special work. They are listed below. The limitations for others were either the lack of a test rig within the specified flow range or kerosene, which was the liquid agreed upon. It is frequently used for testing purposes in the laboratories and is a good representative for a lot of different light oil products in the petrochemical industry. A viscosity of approximately 2 cSt and a temperature close to 20 °C were other parameters asked for.

Table 1. The participating laboratories

	Calibration institutions:	Laboratory code:
SP	Swedish National Testing and Research Institute	**Lab 3** cal I
		Lab 10 cal II
		Lab 11 cal III
NWML	National Weights an Measures Laboratory	**Lab 6**
EAM	Eidgenössisches Amt für Messwesen	**Lab 9** cal I
		Lab 12 cal II
IGM	Inspection Generale de la Metrologie	**Lab 8**
PTB	Physikalisch-Technische Bundesanstalt	**Lab 5**
NEL	NEL Flow Centre	**Lab 4**
NMi	Nederlands Meetinstituut	**Lab 7**
Force	Force Institutterne Dantest	**Lab 1**
BEV	Bundesamt für Eich- und Vermessungswesen	**Lab 2**

The Meter Package

The following demands were put upon a suitable flow meter transfer standard. It should consist of two meters with different physical measurement principles. On should be sensitive and one insensitive to flow profile disturbances. Both should be very stable in short and long time terms. Further both should be linear and insensitive to liquid properties and test methods. Using a turbine meter and a screw meter in series and performing two measurement series, one with and one without a flow straightener in front of it, the expectation was to detect installation induced effects. This is because the turbine meter is sensitive to swirl or asymmetric flow profiles whereas the screw meter is not.

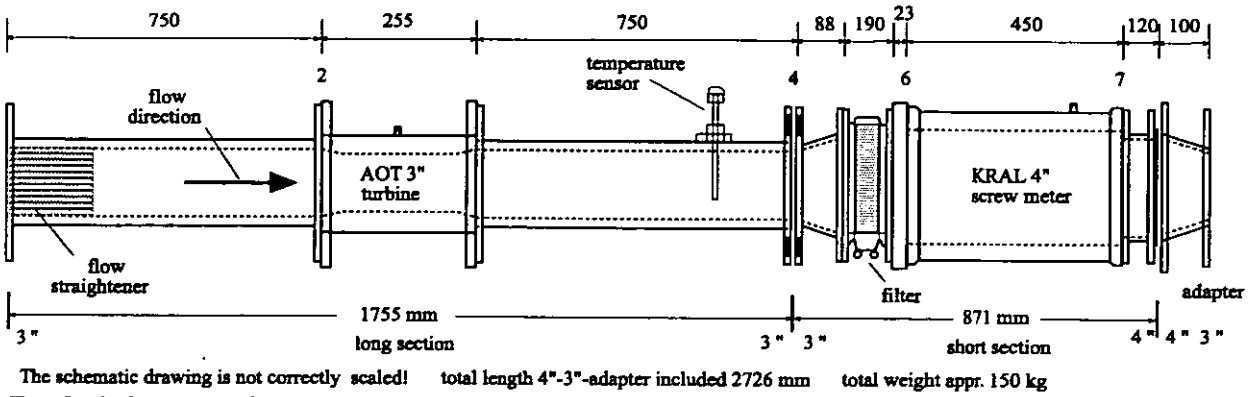

Fig.1: Schematic drawing of the transfer standard.

The Measurement Task

The primary idea of the inter-comparison was that each laboratory should perform the calibration as a routine task. For the sake of the comparison, however, certain aspects had to be in common. Thus the measurement task, as described in detail in the guide-lines, consisted of two separate, but simultaneous calibrations of both meters in a package arrangement at five obligatory flow rates. In the first one (configuration A) a flow straightener was placed in a specified position 10 D in front of the turbine. This configuration was thought to produce a well-defined and repeatable flow characteristic, thus equalising possible installation effects. The second calibration was a repetition without the flow straightener in place. In this configuration (B) the influence of non-ideal flow properties like swirl, asymmetric flow profiles etc. would be observed as a turbine is sensitive to these disturbances.

For the sake of comparability five obligatory flow rates, numbered 1 to 5, each with 10 single repetitions, were pre-defined and run in the order 3(1), 4, 5, 1, 2, 3(2). Any other additional flow rates were to be run after this series. No recommendations as to the calibration method, start-up procedure or any other part of the calibration were given.

The inter-comparison started and ended at SP as the co-ordinator. SP also performed a calibration at an intermediate state. Although this increased the costs it was accepted to secure the outcome if any technical failure should happen to the equipment. To characterise the meters special tests were run both before and after the inter-comparison measurements. The total project was actively run during 20 month and ended in 1995 with a meeting where the results were presented and discussed.

CHARACTERISTICS OF THE TRANSFER-STANDARD

Flow meter inter-comparisons often suffer from instabilities. The figures 2 and 3 are typical calibration results for the two meters in question, i.e. the meter factor as a function of the flow rate. Six curves, three with and three without a flow straightener, represent the SP-result at the start, in the middle and at the end of the intercomparison (corresponding to Lab3, Lab10 and Lab11 in the diagram). A stability judgement should be based on almost identical measurements, which is the case in these curves, where a long hose was used to connect the meter package with a Brooks piston prover as reference.

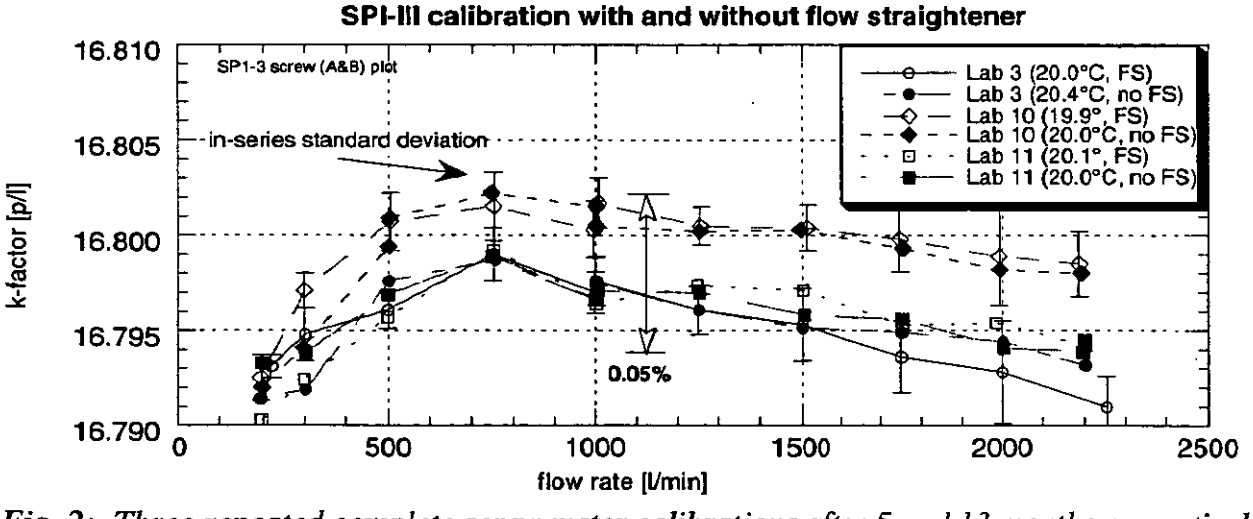

Fig. 2: Three repeated complete screw meter calibrations after 5 and 13 months respectively

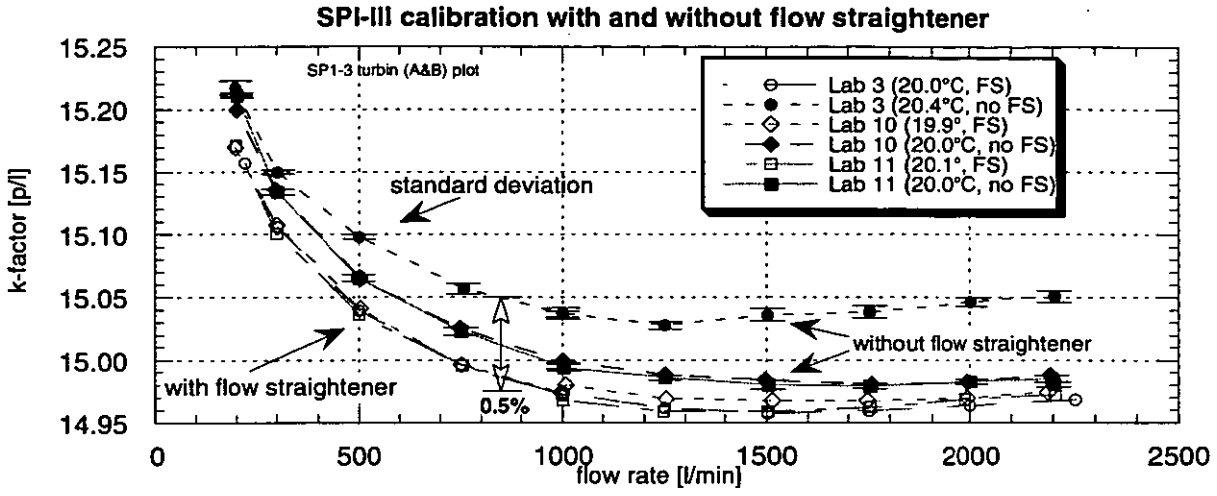

Fig. 3: Three complete turbine meter calibrations - open symbols with, dark symbols without flow straightener in place.

As expected the screw meter does not exhibit systematic differences between respective series with (white symbols) and without the flow straightener (black symbols). But so does the turbine. The existence of the straightener influences the flow profile, an effect that was found in all laboratories. The difference was largest in the first calibration in spite of the straightness over roughly 4 m of the hose upstream of the turbine.

A look on just those curves measured at identical situations i.e. with the flow straightener in front (white symbols) shows a much better agreement. Among these the intermediate result SPII or Lab 10 tends to have a generally higher meter factors, an observation which is better exposed when compared with measurements taken earlier and later. A very truly explanation is the fine and temporary layer of rust that was found on the inside pipe wall coming from a preceding calibration site with ordinary steel pipes. During the immediately following tests this difference had already disappeared.

Representative k-factor

A valuable concept to compare curves on a quantitative basis especially during the intercomparison was to extract a representative k-factor. Flowmeters are usually delivered with one k-factor rather than with a list of k-factors for different flow rates.

The question is, however, how to construct this k-factor in a representative way. If the flow rate dependence were strictly linear, a mean value over the measured k-factor values would be acceptable. If the meter is not linear, and that is especially true for the turbine, this is insufficient. Concerning the turbine in question, the volume passing through the meter during a given time interval would be overestimated at low flow rates and underestimated at high flow rates. The best suggestion was to construct a mean value by weighting each k-factor k_j with the corresponding flow rate q_j according to the following definition:

$$k_{rep} = \frac{\frac{1}{m}\sum_{j=1}^{m} q_j \cdot k_j(q_j)}{\frac{1}{m}\sum_{j=1}^{m} q_j}$$

where m is the number of tested flow rates

Applied on the curves in figures 2 and 3 the results are listed in the following table.

Table 2: Stability of meter-factors over 13 month.

	k(S) [p/l]		Δk(S) [%]	k(T) [p/l]		Δk(T) [%]
SP I	16.7952	I ⇨ II	0.027	14.9779	I ⇨ II	0.039
SP II	16.7998	II ⇨ III	-0.023	14.9837	II ⇨ III	-0.035
SP III	16.7959	I ⇨ III	**0.004**	14.9784	I ⇨ III	**0.003**

With this classification the differences Δk(S) and Δk(T) between two results for both the screw meter and turbine results are all below 0.04 %. This is less than the estimated uncertainty in the measurement being of the order of 0.08 % for the turbine and 0.06 % for the screw meter. The two situations I and III are most alike concerning the preconditions for the meters and the difference over 13 month and thus the stability over the inter-comparison period is even an order of magnitude better, which makes it worthwhile to look into details of the results from the different laboratories.

Repeatability and Reproducibility

Besides stability an other important precondition for an international comparison is a good reproducibility of the meters that make up the transfer standard. In order to assess eventual differences between laboratories with respect to test equipment, test volume or calibration technique, it is essential to know the response of the meters to variations in calibration parameters as temperature, liquid viscosity or pressure.

A simple method to determine the reproducibility is to plot the corresponding calibration curves into a common figure and to depict the minimum, maximum and average differences between these. This is done in the following figures 4 and 5, where the simultaneous calibration of both meters in the package in two liquids Exsol D80 and D40 at different temperatures are shown.

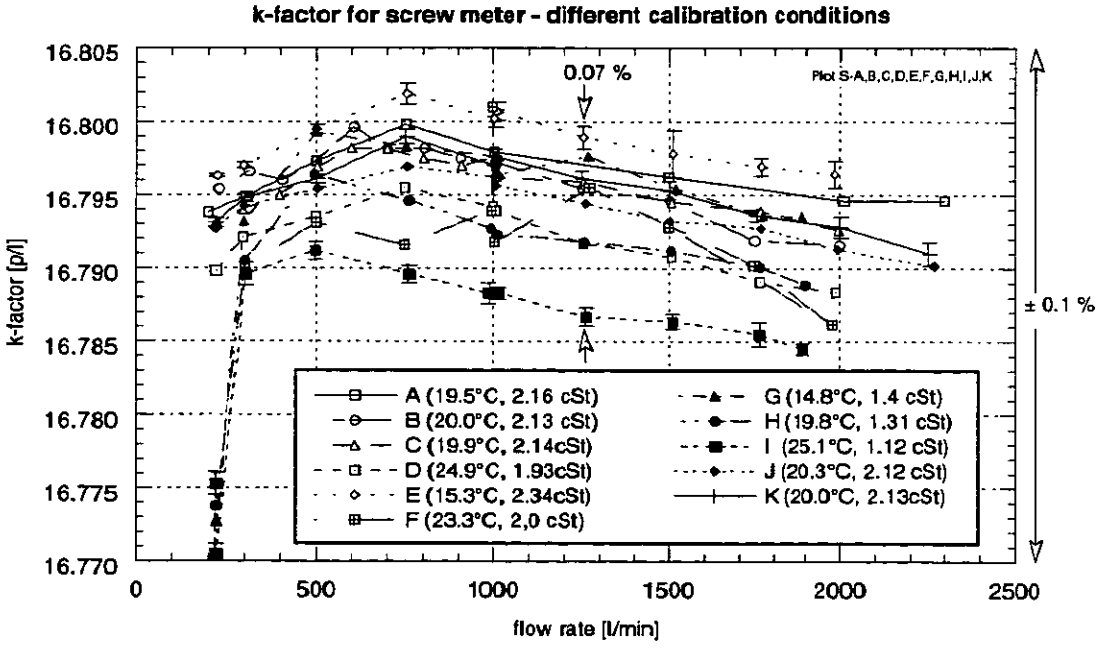

Fig. 4: Result of pre-tests at SP to reveal repeatability and reproducibility of the screw meter

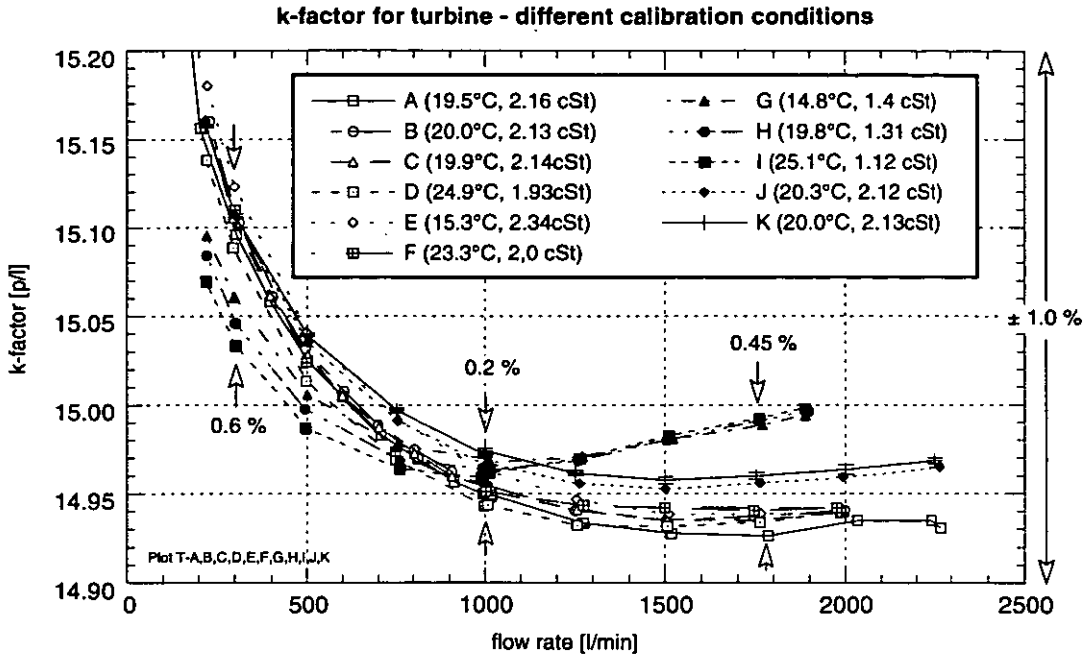

Fig. 5: Result from pre-tests on the turbine meter performance in two liquids and different temperatures involving variations in viscosity.

The figures 4 and 5 demonstrate two things. In the case of the screw meter the k-factor over the range of viscosities and temperatures is within 0.07 %. In the case of the turbine it is very obvious that both temperature and especially viscosity changes have a large influence on the meter behaviour. Thus corrections for both had to be worked out.

Compared to these effects all other factors like test method (gravimetric, volumetric, standing or flying start-stop), density changes of the liquid, size of test volume or testing time, type of reference and its installation etc., seem to be of second order. On the basis of the representative k-factors from the different curves the following numbers were calculated.

Table 3. Reproducibility of intercomparison and reproducibility within pilot laboratory (σ=2).

no flow straightener	reproducibility inter-comparison	reproducibility co-ordinating laboratory	repeatability co-ordinating laboratory	units
screw meter	0.16	0.07	0.01	[%]
turbine	0.17	0.09	0.03	[%]

Although the statistical treatment takes care of different sample sizes it can be mentioned that the tabulated values for both the inter-comparison and the co-ordinating laboratory are based on 12 calibration series each. The information is given on a 95 % confidence level, stating that any two results (representative k-factors) between the participating laboratories are within 0.027 and 0.025 p/l for the screw meter and the turbine respectively, corresponding roughly to 0.16 % in both cases. Removing the flow straightener results in a comparable reproducibility for the screw meter, whereas it increases by a factor of 4 to 5 for the turbine.

These values, which actually exceed the estimated uncertainty intervals by the participants, are of course a measure *per se*. However, related to the reproducibility within the co-ordinating laboratory they seem very satisfactory being only twice as large. The tests in the co-ordinating laboratory covered a temperature interval of 15 - 25 °C, a viscosity range of 1.3 - 2.4 cSt, 2

methods, 2 test facilities, different installations of the meters in one of them, 6 volume references and 2 operators. Thus the comparison of reproducibility figures should be valid.

RESULTS FROM THE INTER-COMPARISON

At the participating laboratories four basically different measuring methods were used. The majority utilised a volumetric technique. Some laboratories used two volume references, a smaller one for the lower flow rates. At one laboratory a reference meter was used that in turn was calibrated via two volume standards and one used a gravimetric technique. The result before any corrections were undertaken is shown in figure 6 and 7 below.

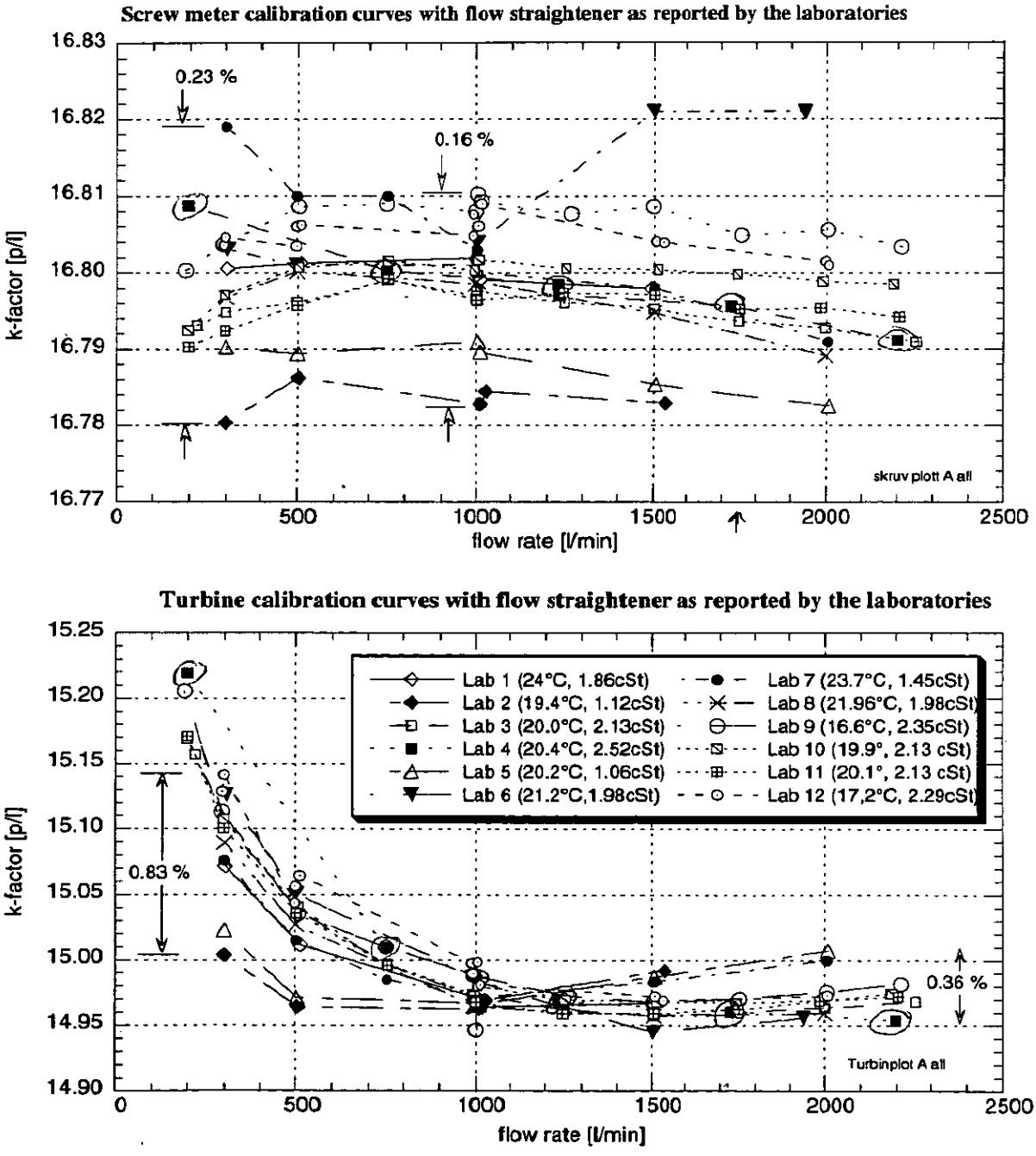

Fig. 6, 7: The calibration curves from the inter-comparison when the flow straightener was inserted. Each point represents the mean of 10 repeated measurements

Compared with the corresponding tests at SP (figure 4 and 5) the spread between the resulting curves is even larger, which is mainly due to a larger range in liquid viscosity, which was in the range 1.05 to 2.54 cSt. This does not seem very much, but was found to have a significant effect on the results of the turbine meter and also influenced the screw meter.

It was considered necessary to work out a correction for both the temperature and viscosity deviations. Different techniques were tried. Finally for the temperature just the expansion of the pipe wall with temperature was calculated. And for the viscosity a correction was suggested that is based on a forward translation from a k-factor as a function of the flow rate to a dependence of the Reynolds number *Re*. Using the reference viscosity instead of the actual one implied a movement to a different Reynolds number and belonging k-factor. The following diagram contains the Reynolds number dependency.

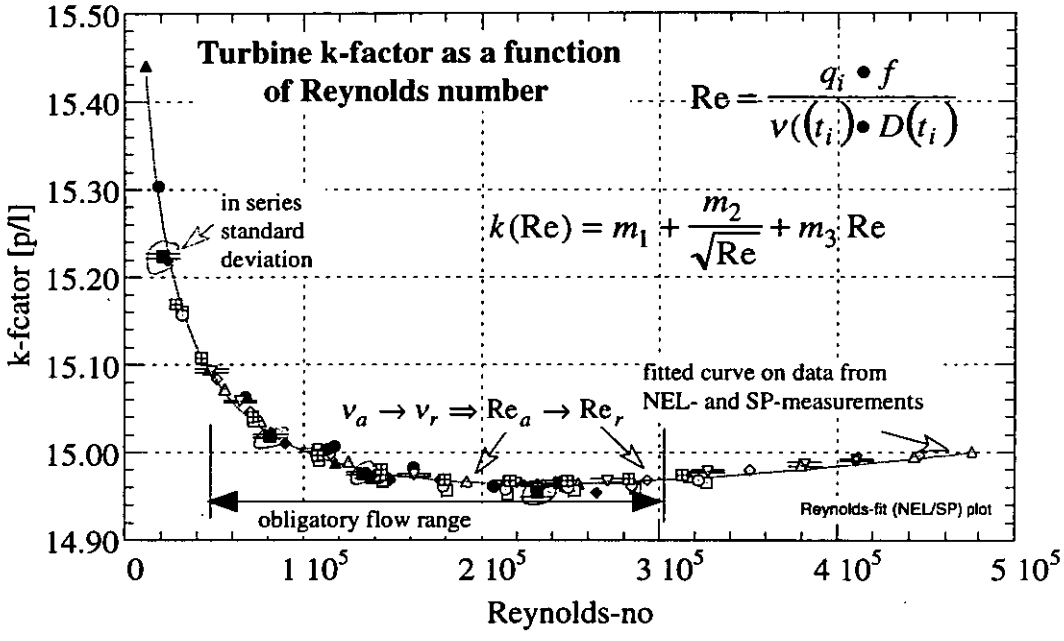

Fig. 8: The Reynolds number Re dependency as a translation help from one viscosity to an other. The experimental data is based on measurements at NEL and SP.

In order to extend the range of temperatures and viscosities several tests were repeated at NEL. The results from both laboratories fit well together.

The main task and most interesting question from the beginning was to reveal possible installation effects due to flow profile disturbances. Although the detailed curves from the measurements without a flow straightener are not shown here it should be mentioned that the spread for the screw meter, as expected, only increased very little from 0,11 to 0,14 % at mid flow rates. Concerning the turbine results, however, the curves diverged especially at higher flow rates from 0,36 to over 1 %. Although the available straight pipe length upstream of the meter package was between roughly one and seven meters at least 4 test sites faced problems with the flow profile. The following Youden plot summarises the problem. It is constructed by plotting a representative k-factor for the two simultaneously measured meter curves against each other. Figure 9 shows the original turbine and the screw meter factor on the x- and y-axis respectively, i.e. before any corrections were performed.

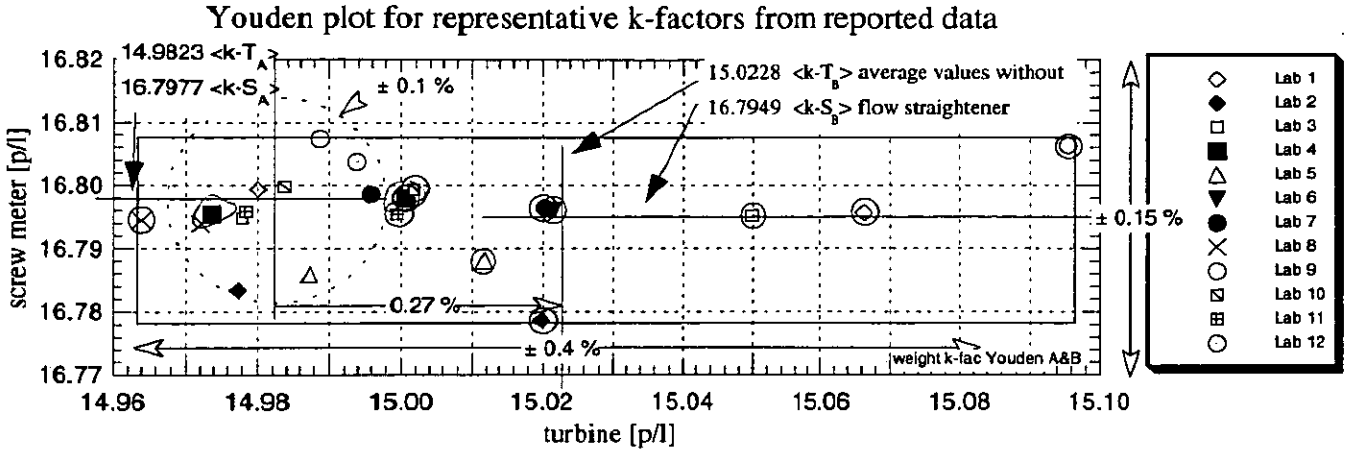

Fig. 9: Values of the representative k-factors with and without (encircled) a flow straightener to minimise flow profile disturbance. Definition of global values as the respective average from all laboratories.

One can distinguish between two groups of results. The encircled ones represent the configuration without the flow straightener. They are wide spread with more than ± 0,4 % on the x-axis. The same symbols without the circle give the corresponding result with the flow straightener in place. One can observe that, in contrast to the turbine, the results and the range of spread for the screw meter, i.e. with respect to the y-axis, is almost the same.

Inter-comparison Result and Measurement Uncertainty

The two pairs of crossing lines define two global mean values for respective meter and test configuration. They present as an overall outcome from the inter-comparison the most probable meter factor result. The large shift of 0,27 % between the two situations with and without the flow straightener in place is mainly due to the large overestimation in some test rigs. As an other effect the physical existence of the straightener has a strong influence on the turbine creating its own flow profile.

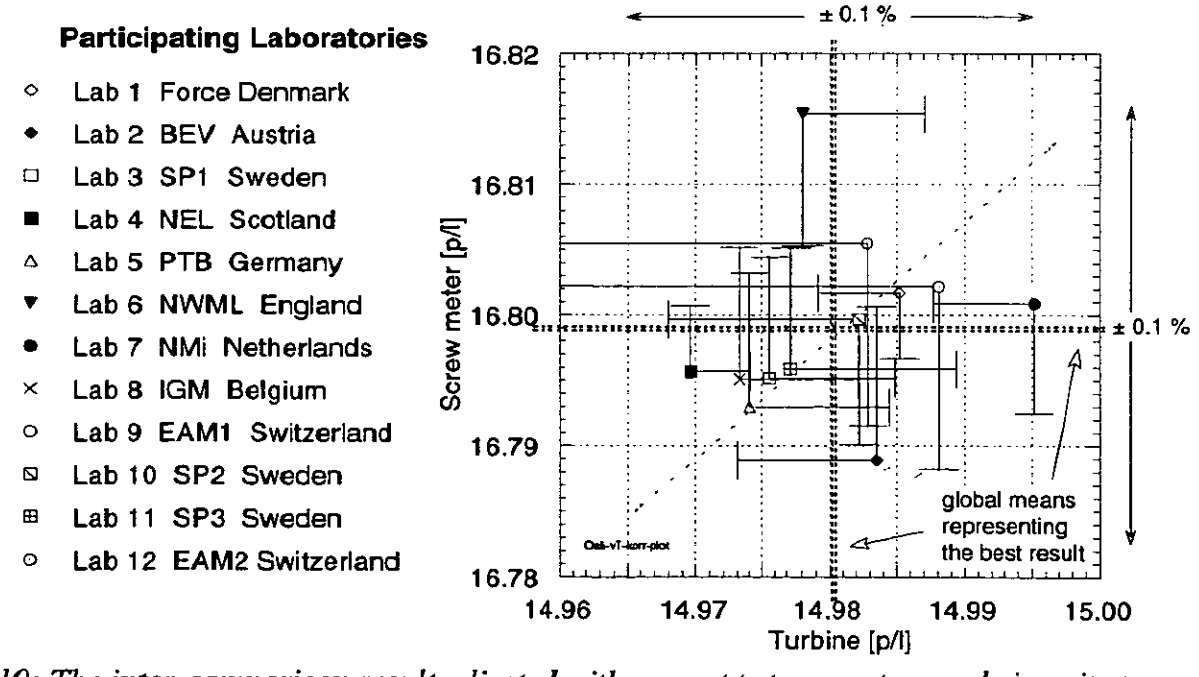

Fig. 10: The inter-comparison result adjusted with respect to temperature and viscosity together with the corresponding uncertainty judgements.

Figure 10 presents the most essential part of the inter-comparison. Here installation effects are effectively blocked of by the flow straightener and corrections both for temperature and viscosity deviations are applied for both meters. Thus the diagram represents a couple of results from very stable meters all taken at idealised measurement conditions but at different test sites. The results are further completed with the uncertainty estimations delivered by each laboratory, which range from ±0,03 to ±0,3 % with an average at about 0,06 %. The uncertainty bars given above cover in most cases the global mean values but do not necessary overlap with each other, which means that some estimations are too optimistic. From figure 10 one could state an uncertainty of the global mean itself of roughly ±0,08 % for the turbine and somewhat better for the screw meter.

A further observation from figure 10 is that the majority of results seem to fall into the vicinity of a correlation line. This might be interpreted as systematic differences in the volume references used at the participating laboratories.

Considering the situation that a number of national flow laboratories working at optimal calibration conditions with repeated measurements with a stable meter of good repeatability can agree to a common meter factor with an uncertainty of lets say ±0,06 to ±0,08 % means that the individual calibration uncertainties hardly can be much better. If a laboratory deviates from the well selected conditions and allows for a small change in temperature (±3 °C) and viscosity (±1cSt) then the new k-factor and the belonging uncertainty figure in that calibration certificate may still apply on the same level but it will not cover the earlier conditions without increasing the uncertainty to ±0,1 % or more. The same is true if the meter after calibration is run in somewhat different conditions, which is generally the case. Thus the owner of the meter cannot expect to be able to measure with the same low uncertainty as long as the calibration is not performed in the actual installation and at actual conditions. The whole discussion, however, still would demand that the flow profile conditions must be under full control. Otherwise as seen in figure 9 uncertainties of ±0,4 % are not unrealistic and the problem tends to increase for higher flow rates.

CONCLUSIONS FOR A USER OF FLOW METERS

A user of turbine meters and this is probably even true for other types of meters should first of all prepare for a good installation if accurate flow or volume measurements are of interest. Preferably a flow straightener should be used not only in the measurement installation. It is recommendable to send the meter with preceding and following pipe work including a straightener and keep everything unchanged in one package. A third recommendation, as a result of this work, would be to inform the calibration laboratory about the measurement conditions for the particular meter in terms of temperature and viscosity range and if ever possible to simulate those conditions during the calibration as close as possible. One also should consider to perform transformations between different liquid properties. Finally and this is most easily to accomplish a linearising equipment should be used. The uncertainty numbers given above concern just one k-factor chosen as a representative value for a whole curve. It is preferable to work with varying k-factors or different corrections along a meter curve in order to keep a god uncertainty even at low and high flow rates.

NSFMW.97

North Sea FLOW Measurement Workshop

Paper ~~14~~: 3.1

EXPERIENCES WITH ULTRASONIC METERS AT THE GASUNIE EXPORT STATIONS

Authors:
Gert Sloet and Gerrit de Nobel, N.V. Nederlandse Gasunie Groningen, The Netherlands

Organiser:
Norwegian Society of Chartered Engineers
Norwegian Society for Oil and Gas Measurement
Co-organiser:
National Engineering Laboratory, UK

EXPERIENCES WITH ULTRASONIC METERS AT THE GASUNIE EXPORT STATIONS

Gert Sloet / Gerrit de Nobel
N.V. Nederlandse Gasunie, Groningen, The Netherlands

SUMMARY

Gasunie has equipped a number of its export metering stations with ultrasonic gas flow meters. These ultrasonic flow meters are used as backup meters for the primary meters, which are turbine meters. On-line comparison results with these ultrasonic flow meters and the turbine meters are assessed. Given the results it is concluded that this new type of meter gives good results in the areas of availability and spread of results.

INTRODUCTION

Background

In 1996, Gasunie sold 47.9 billion m^3 natural gas on its home market and 45.9 billion m^3 natural gas was exported to other European countries. The exported gas is measured at 13 so-called export stations at the borders. The major amount of gas is transferred via 6 large export stations. Since their renovation in the early nineties [1],[2], these major stations have been equipped with a double flow metering system in which the primary measurement is done by means of turbine meters and a backup measurement is done with either ultrasonic meters or turbine meters. Depending on the capacity of the station the metering section consists of 3 up to 7 parallel meter runs. With the primary and backup flow measurement a continuous on-line comparison has been implemented. On an hourly basis the flow at line conditions and the flow converted to base conditions are registered and compared. This result of the comparison may generate automatically alarms.

Layout of an export station

In the station the incoming gas is cleaned by means of scrubbers. After the scrubbers the gas comes via an underground header and a double bend out of plane in the actual metering section. An overview of the metering section of an export station is given in Figure 1.

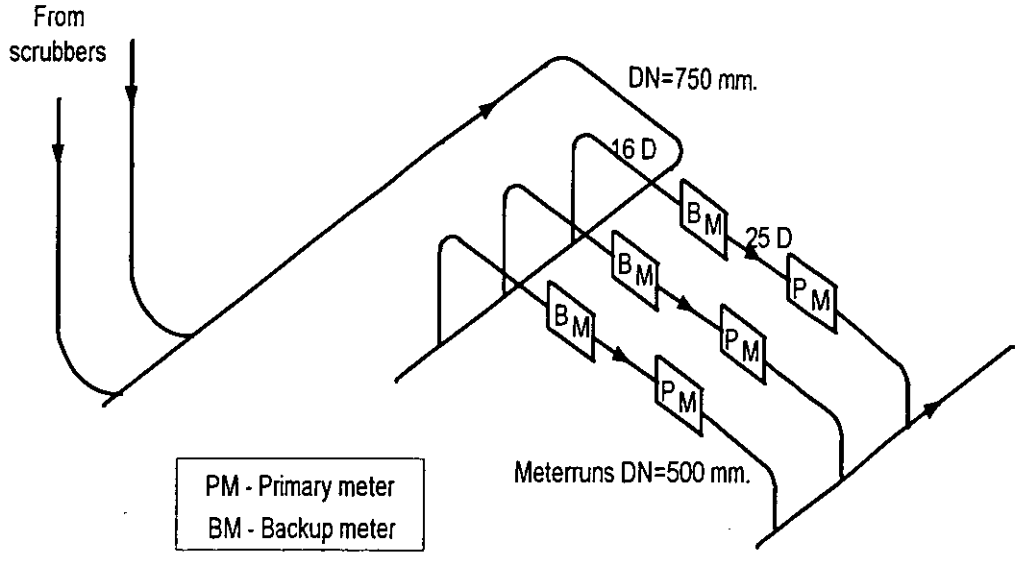

Figure 1 - Layout of the metering section of an export station

Issue

With the ultrasonic meters that were available at the time of the renovation of the export stations a number of problems were encountered. A relatively large scatter was discovered in the comparison results of the meter runs equipped with the ultrasonic meters. For a typical example refer to Figure 2.

Another problem was that the number of failures of the ultrasonic meter was too high, leading to an unacceptably low availability of the meter. Also the zero drift of the meter, which had to be corrected manually, was too high. These problems led to a research programme in which a new type of ultrasonic meter, with advanced electronics and software, was selected and tested to find out whether it could meet the requirements.

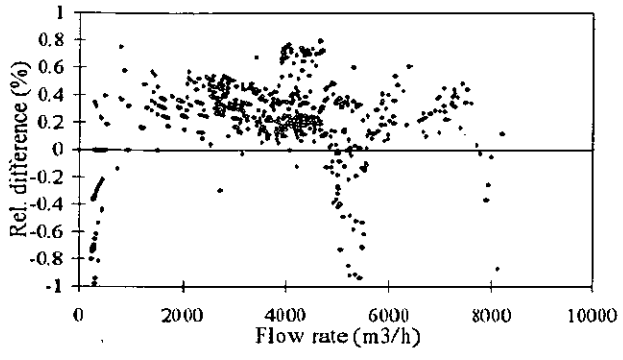

Figure 2 - Initial comparison results with an US meter of the original type

*In all graphs the relative difference between the primary and backup meter, expressed as $(V_p-V_b)/(V_b+V_p)$ * 200%, where V_p is the reading of the primary meter and V_b the reading of the backup meter totalized over an hour, is plotted against V_p. Each graph covers a period of one month.*

RESEARCH PROGRAMME

Set up of the programme

To test if the new meter could meet the requirements a two stage programme was started. In the first stage the meter was tested in Gasunie's flow laboratory and subsequently for a longer period of time field tests were carried out with meters built in on export stations.

Laboratory investigations

The 20" ultrasonic flow meter, with Q_{max}=10000 m^3/h was tested in Gasunie's Westerbork test facility. Although these test will not be discussed in this paper an overview of the major results is presented in Table 1.

Table 1 - Results from the laboratory programme

Repeatability	< 0.2 %
Linearity	< 0.5 %
Influence of swirling flow	0.2 %
Influence of exchanging transducers	<0.2 %
Range	5 - 120 % Q_{max}

The flow range is limited at the lower end to 5 % due to the fact that in the range of 2-5 % Q_{max} the dispersion in the results is too high. This is illustrated in Figure 3.

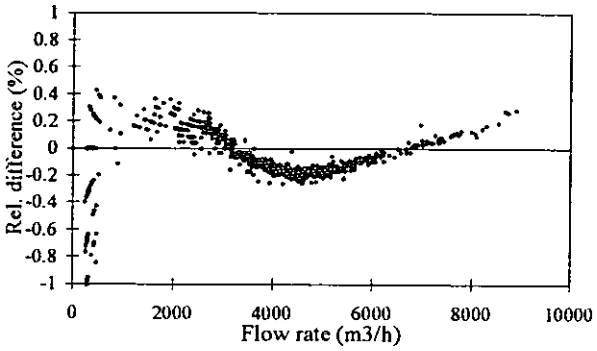

Figure 3 - Spread at low flow rate of the new type ultrasonic meter

Note:
The increasing difference at higher flow rates between turbine meter and ultrasonic meter is caused by the increasing pressure difference between the ultrasonic meter and the turbine meter. The graphs show actual flow rates.

Field test

For the field test an endurance test in the period 1994 -1995 was done. For this purpose three 20" ultrasonic meters were installed at three different export stations. During the field test swirl was detected in the meter runs of the export stations [3]. From experiments and theoretical studies [4] it is known that this type of flow disturbance is very persistent. To eliminate this swirl Laws flow conditioners [5] were installed in the pipe sections upstream of the ultrasonic meter. During the test, beside some minor problems with cabling and printed circuit boards, the meters functioned quite well. The availability in this period was > 99.9 %. No maintenance was done and the transducers were not cleaned nor exchanged. In the next section some details of the comparison results with the three meters will be discussed:

Meter 1

In the period April 1994 up to April 1995 this meter gave a typical pattern in the on-line comparison, an example of which is given in Figure 4. This was reason to re-calibrate both the turbine and the ultrasonic meter. It was discovered that the ultrasonic meter showed a difference of +0.2% and the turbine meter even of +0.4 % at low flows. The combination of these differences explains the behaviour if the comparison results. After the calibration the meter was built into another meter run on the export station. The on-line comparison now gave the result from Figure 5.

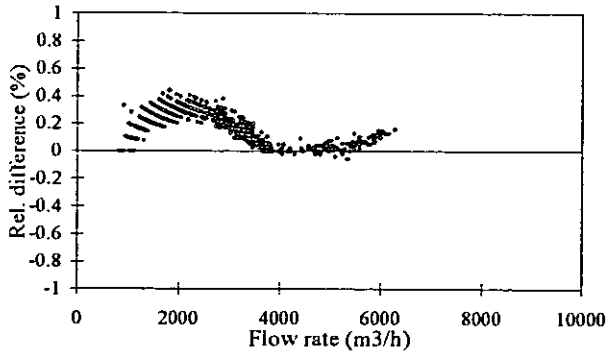

Figure 4 - Initial pattern for meter 1

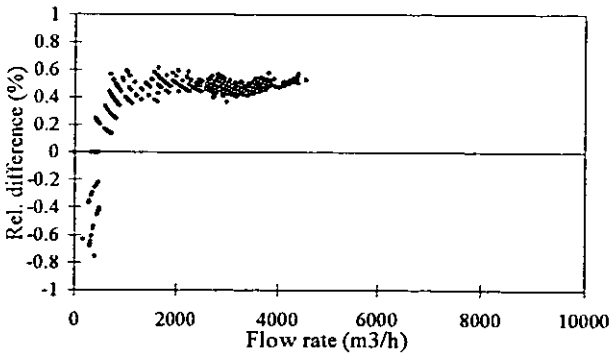

Figure 5 - Meter 1 after re-calibration

Note: For low flow rates the discretization steps caused by the meters electronics are visible

The pattern looks normal but there is a difference of 0.5 % between the primary and backup measurement. When the ultrasonic meter was built out and inspected blisters in the flow coating inside the meter were discovered. After removal of the coating and applying new coating another calibration was done. As can be observed from Figure 6 the difference between both meters is brought back to an acceptable level.

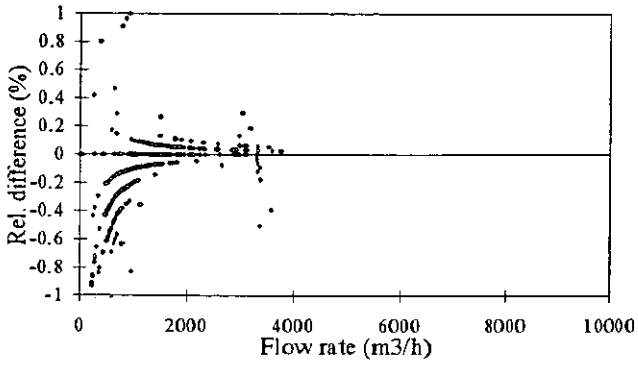

Figure 6 - Meter 1 with renewed coating

The drift of the meter in the period March 1994 - May 1995 based on the calibration results is +0.4 %, a substantial part of which can be attributed to the blisters in the coating. The spread of the on-line comparison data at $0.4*Q_{max}$ is about 0.2%.

Meter 2

This meter gave from the start a bias between the primary and backup measurement of +0.5%. as illustrated in Figure 7. The reason for this bias lies in the software that was not optimally tuned for the actual flow in the meter run. After the test period the software settings were adapted and this lead to much better results, as can be seen in Figure 8.
The spread at $0.4*Q_{max}$ in the on-line comparison is about 0.2 %.

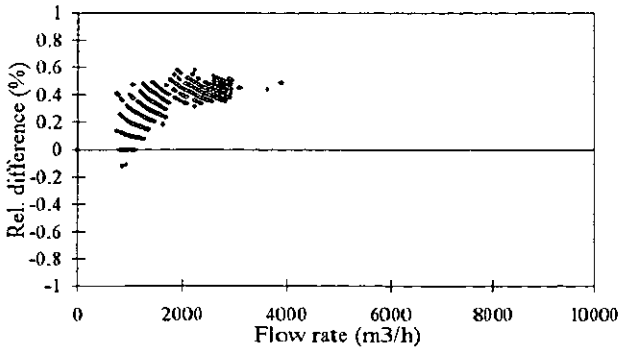

Figure 7 - Meter 2 before software tuning

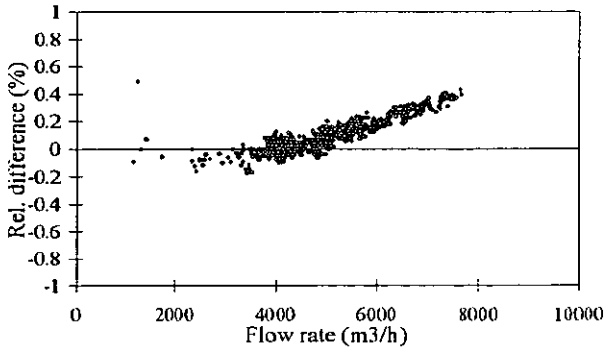

Figure 8 - Meter 2 after software tuning

Meter 3

The pattern in Figure 9 which was observed in the first period in the on-line comparison was again due to the turbine meter. After replacement of the turbine meter a behaviour as plotted in

Figure 10 was found. In the period March 1995- September 1995 a spread in the on-line comparison at $0.4*Q_{max}$ of 0.1 % was found.

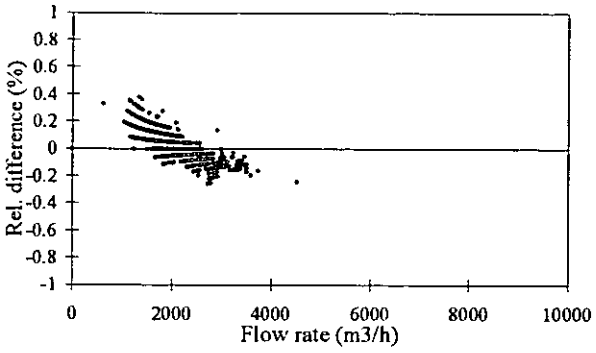

Figure 9 - Initial results of meter 3

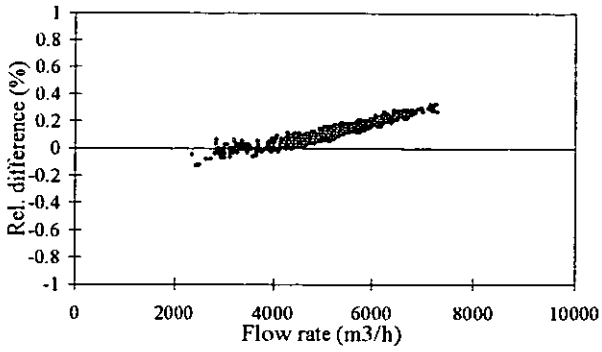

Figure 10 - Meter 3 after turbine meter replacement

Intermediate period

In the period after the end of field test the meters have been kept in operation. In Table 2 the figures for the spread of the results based on the on-line comparison are given.

Table 2 - Summary of the results in the period after the field test

METER	PERIOD	SPREAD AT $0.4*Q_{MAX}$	Refer to
1	January 1996 - October 1996	0.2%	Figure 11
2	September 1995 - October 1996	0.2%	Figure 12
3	September 1995 - September 1996	0.1%	Figure 13

The figures 11, 12 and 13 give an impression of the results of the comparison of the meters in this period.

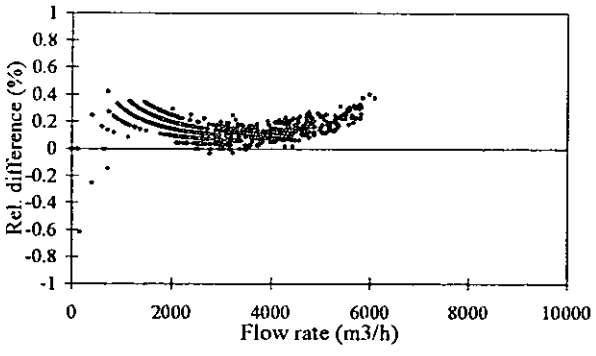

Figure 11 - Results of meter 1

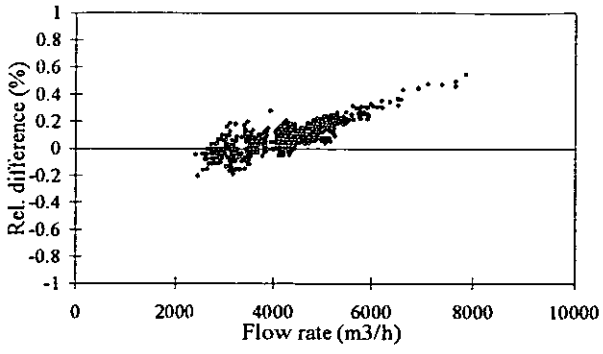

Figure 12 - Results of meter 2

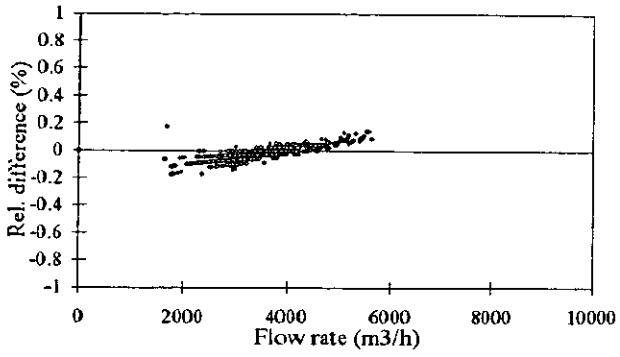

Figure 13 - Results of meter 3

FINAL SITUATION

Based on the results of the field test it was decided to select the tested ultrasonic meter as backup meter for the Gasunie export stations which were to be equipped with ultrasonic meters. The meters used in the field test were upgraded so that they are functionally equal to the new meters and installed in an export station. New meters were bought for the other meter runs and are to be installed now. No results are available yet from this period.

CONCLUSION

Based on the experiences with the three meters that were used in the field test the following conclusions may be drawn:

- The new type ultrasonic flow meter gives better results in the areas of availability and spread then ultrasonic flow meters of the previous generation.
- The number of defects is reduced to 1 -2 per year.
- The difference between the results of the turbine meter and the ultrasonic meter is about 0.2% in the range 0.2 -1.0 Q_{max}. For lower flows this number increases.
- Installation of a Laws flow conditioner lead to more stable results. The effect of flow conditioners on ultrasonic flow meters has to be further investigated.
- The ultrasonic meters serve excellent to monitor the quality of the turbine meter.
- Tests have demonstrated that components can be exchanged without significant influence on the meter performance.

---

1 Van der Kam, P.M.A. and Dam,A.M. "Large turbine meters for custody transfer measurements: the renovation of the Gasunie export stations". Flow Measurement and Instrumentation, Volume 4 Number 2 1993.

2 Van der Kam, P.M.A., Dam,A.M. and Van Dellen,K. "Gasunie selects turbine meters for renovated export metering stations", Oil & Gas Journal, December issue, 1990.

3 De Jong, S and Van der Kam, P.M.A. "Effects of header configurations on flow metering", 1995 International Gas Research Conference

4 Steenbergen, W., Voskamp, J., Krishna Prasad, K. "The decay of swirl in turbulent pipe flows" 7th Int. Conference on Flow measurement. FLOMEKO, Glasgow 1994.

5 Laws, E.M., "Flow conditioning - a new development ." Flow measurement and instrumentation 1990 Vol. 1

NSFMW.97

North Sea FLOW Measurement Workshop

Paper ~~15~~: 3.2

ON -LINE QUALITY CONTROL OF ULTRASONIC GAS FLOW METERS

Authors:
R. Sakariassen, Statoil/K-Lab, Norway

Organiser:
Norwegian Society of Chartered Engineers
Norwegian Society for Oil and Gas Measurement
Co-organiser:
National Engineering Laboratory, UK

On-line quality control of ultrasonic gas flow meters

by

Reidar Sakariassen

Statoil/K-Lab

ABSTRACT

An ultrasonic gas flow meter (USM) offers a great deal of information about the performance of the meter and the conditions in the gas flow. Some of the information is used by the computer of the meter itself to perform self diagnostics while other part of the available information is not yet fully utilised.

This paper will give principles and show examples of how information of the measured flow velocities, the measured velocities of sound and density could be utilised to perform an on-line quality control. Performing such quality control may in the end result in maintenance based on condition monitoring rather than the resource consuming concept of preventive maintenance. Even for single run meter stations with limited number of parallel measurements to compare this principle seems to be possible.

Our experience is built on the follow-up of a total number of 12 USM with diameter from 12" to 30" in operation offshore together with a number laboratory tests.
Examples of data collected, presentation of data and interpretation of the results will be presented and the paper will conclude with a proposed procedure for on-line quality control of the USM.

INTRODUCTION

Since 1997 the ultrasonic gas flow meters have been introduced into the Norwegian Regulation relating to fiscal measurement of oil and gas etc. (ref. 1). Among others it requires that "during the operational phase "the parameters relevant to verify the condition of the meter shall be checked". In the guidelines to the Regulations it is said that "the ultrasonic flowmeter should..monitor the velocity of flow and the velocity of sound for each ultrasonic path" and that it would be reasonable that those parameters "are used for further follow up".
In a recently developed American Draft Standard (ref. 2) it is said that the "the manufacturer should provide the following and other diagnostic measurements". Among the measurements listed are:

- average axial flow velocity through the meter
- flow velocity for each acoustic path (or equivalent for evaluation of the flowing velocity profile)
- speed of sound along each acoustic path
- average speed of sound.
- percentage of accepted acoustic pulses for each acoustic path

Those requirements have always been part of Statoil's specifications for ultrasonic gas flow meters. The utilisation of those parameters and the meters' own internal diagnostic tools has turned out to be of great value in verifying the performance of the meters. To know how the information should be treated and why it provides such good information, a good understanding of the meter's operating principle is necessary.

DESIGN OF ULTRASONIC METERING SYSTEMS

Figure 1 shows how most our ultrasonic gas flow metering systems are designed. The ultrasonic meter meters the actual or gross volume flow rate. To convert to mass flow rate, density is required. The densitometer is installed in a pocket in the main pipe wall. Flow through the densitometer loop is forced by the differential pressure across a doublesided pitot probe protruding into the pipe. (The probe inside the pipe is not shown on the sketch).

Figure 2 shows typical what type of information the metering systems reports.
In addition to the parameters listed above, this meter also reports standard deviation (Std.dev.) of the individual flow velocities. This number expresses how stable the velocity or velocity measurement has been during the measurement cycle.

The calculated values for density and velocity of sound is in this case based on a gas composition, pressure and temperature. It is most usual to see the figure for calculated density, for instance based on the method described in AGA report no. 8 (ref. 3). A calculated value for velocity of sound is more unusual. Different methods exist for this calculation. The best method seems to be based on AGA report no. 8 version 1994. This item will be treated later in the paper. It should be mentioned that a relation exists between velocity of sound and density although it is complicated.

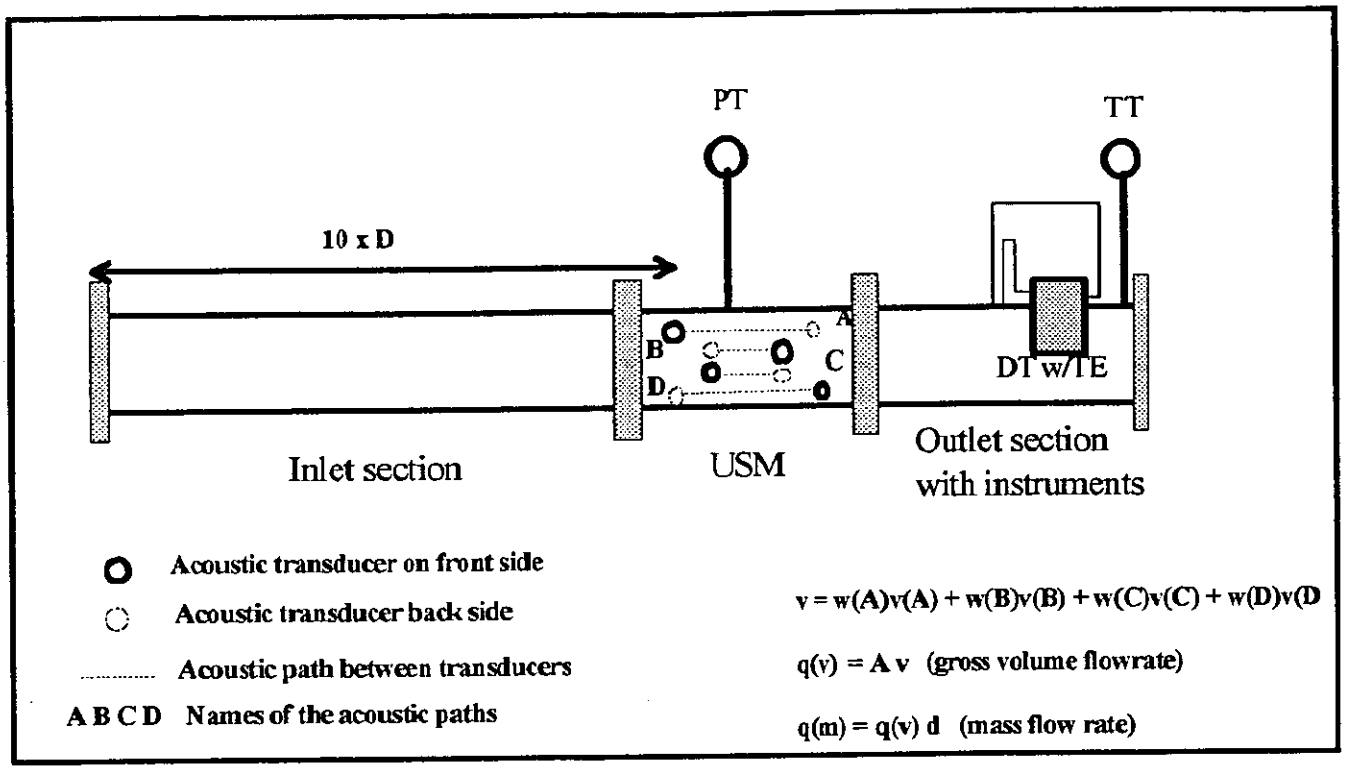

Figure 1 Typical layout for a meter run with a four paths ultrasonic meter. Included in the sketch is also the secondary instrumentation: pressure transmitter (PT), temperature transmitter (TT) and densitometer with internal temperature element (DT and TE respectively).

Transducer no.	Measurements % used
0	100
1	100
2	100
3	100
4	100
5	100
6	99
7	100
8	100
9	100
10	100
11	100

Pressure:	125.44 barg
Temperature:	12.36 degC
Density measured:	124.76 kg/m^3
Density calculated	124.37 kg/m^3

	FLOW VELOCITIES (m/s)		SOUND VELOCITIES (m/s)	
Path. no.	Measured	Std. dev.	Measured	Calculated
Tot,	**7.7839**	0.0139	**416,63**	**417,11**
0 - 11	7.1178	0.0188	416,58	
1 - 10	7.3468	0.0201	416,55	
2 - 9	8.1592	0.0117	417,05	
3 - 8	8.1736	0.0150	416,73	
4 - 7	8.0758	0.0116	416,49	
5 - 6	7.2234	0.0211	416,36	

Figure 2 Typical information from a system like fig. 1

BASIC TECHNICAL BACKGROUND

To understand how an on-line quality control could be performed, it is essential to understand the function of the ultrasonic meter and how physical parameters are related to each other.

Working principle of the ultrasonic meter

The fundamental principle is that the propagation velocity for sound (which is a pressure wave) in a fluid will be the sum of the velocity of sound and the fluid velocity long the path of the pressure wave. In an ultrasonic meter (ref. figure 1) the transit time is measured for a sound pulse travelling between two transducer mounted in meter section of the pipe. The transit time is measured both with the pulse travelling with and against the fluid flow direction.
The average fluid flow axial velocity along the acoustic path, v, can is calculated by the ultrasonic meter by equation (1):

$$v = \frac{L^2}{2 \cdot X} \cdot \frac{(t_2 - t_1)}{t_2 \cdot t_1} \qquad (1)$$

where

L	is the length of the acoustic path between the transducers in a pair
X	is the axial distance between a pair of transducers
t_1 and t_2	is the transit time in downstream and upstream direction respectively between the transducer fronts

To a good approximation the velocity of sound, c, is also determined by equation (2)

$$c = \frac{L^2 \cdot (t_1 + t_2)}{2 \cdot t_1 \cdot t_2} \qquad (2)$$

Transit time measurement

The principle of measuring the transit time for an acoustic pulse is shown in figure 3. The acoustic pulse is detected by the receiving transducer. The pulse consists of a number of pressure pulsations or periods. The pulsation frequency is normally between 100 kHz and 200 kHz for gas meters.

The timer for transit time measurement is triggered at the exact right period in the pulse.

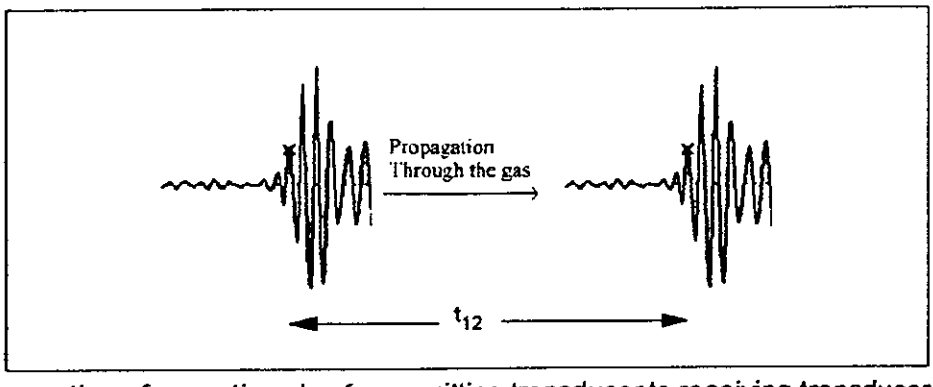

Figure 3 Propagation of acoustic pulse from emitting transducer to receiving transducer

t_1 and t_2 are determined from measured times between electronically transmission of the acoustic signal till electronically detecting received signal. Delay times in the transducers and electronics and delays caused by detection method must be taken into account.

$$t_1 = t_1' - \Delta t_1 \tag{3}$$

$$t_2 = t_2' - \Delta t_2 \tag{4}$$

where

t_1 and t_2	is the transit times as detected by the electronics
Δt_1 and Δt_2	is delay times

Internal diagnosis system

Most meters have a built in check and diagnosis system. This system checks for example for stability in transit time measurement, stability in the acoustic pulse, signal to noise ratio. During a measurement cycle the transit time is normally measured several times and then an average value is calculated. The number for "measurement used" tells how many (percentage) of the pulses are used to form the average value have passed the internal quality check.

If the number of pulses used to form the average transit times is higher than 10, normally 40 % of pulses should be accepted to make a reliable measurement.

Most meter also provide the reason why the quality of the pulse is rejected. Figure 4 shows an example of a pulse rejected because of low signal to noise ratio (SNR).
This example also shows how vital it is that the timer for transit time measurement is triggered at the exact right period in the pulse.

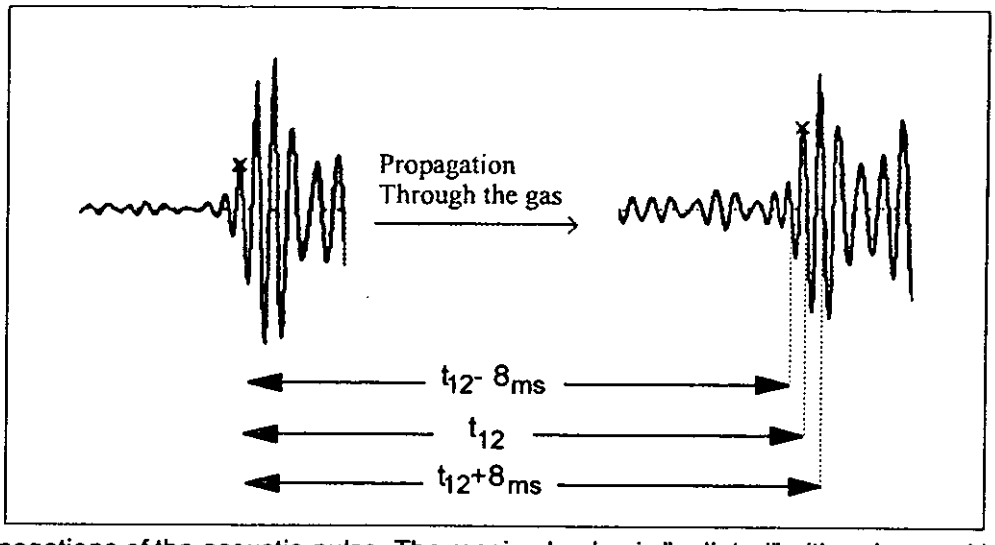

Figure 4 Propagations of the acoustic pulse. The received pulse is "polluted" with noise, making it impossible or difficult to determine exact arrival time of the pulse.

Effect of possible malfunctions of the meter

For an ultrasonic meter with all dimension correctly measured and flow calibrated, the main source of malfunctions is the transit time measurement.

Missing correct period in the received pulse

As indicated in figure 4, the error in transit time measurement will be approximate 8 μs if the timer is triggered one period away from the correct pulse. The effect of such a miss could be calculated by equation (1) and (2).
Table 1 gives examples of what effect it has on meters of different dimension.

Error in delay time

Error in the delay times defined in equation (3) and (4) affects in principle the end result in the same way as a miss of the correct pulse described in the previous section. However, the effect is much smaller. The delay times are normally in the order of 10 μs - 30 μs. The error in delay times caused either from the calibration of the transducer or by drift is normally maximum 1 μs. The effect is therefor normally less than 1/10 of the effect of missing the correct period in the pulse.

Table 1 Effect of error in transit times. Path notation refers to figure 1.

Dim. (inch)	Path	L (m)	X (m)	Parameter	t_1 and t_2 correct	t_1 error chord A and D 8 μs*	t_1 error chord B and C 8 μs*	t_1 and t_2 error all chords 8 μs*
6	A,D	0.205	0.0838	VOS (m/s)	400	396,9	400	393,85
				v (m/s)	9	1,34	9	8,72
	B,C	0.230	0.133	VOS (m/s)	400	400	397,24	394,51
				v (m/s)	10	10	5,11	9,72
	Total			VOS (m/s)	400	398,45	398,62	394,18
				v (m/s)	9,72	7,61	6,19	9,44
12	A,D	0.762	0.165	VOS (m/s)	400	399,16	400	398,33
				v (m/s)	9	5,1	9	8,92
	B,C	0.794	0.267	VOS (m/s)	400	400	399,2	398,39
				v (m/s)	10	10	7,58	9,92
	Total			VOS (m/s)	400	399,58	399,6	398,36
				v (m/s)	9,72	8,65	7,97	9,64
20	A,D	0.950	0.275	VOS (m/s)	400	399,33	400	398,66
				v (m/s)	9	6,65	9	8,94
	B,C	1.03	0.445	VOS (m/s)	400	400	399,38	398,76
				v (m/s)	10	10	8,53	9,94
	Total			VOS (m/s)	400	399,67	399,69	398,71
				v (m/s)	9,72	9,07	8,66	9,66

* 8 μs reflects a frequency of the ultrasonic signal of 125 kHz.

Relations between physical properties

As shown in figure 1 and figure 2 our metering systems determines velocity of sound and density as well as pressure and temperature. Both velocity of sound and density varies with variations in pressure and temperature. In addition, both velocity and density depends on gas composition.

For a given gas composition, the velocity of sound and density varies with pressure as shown in figure 5 and figure 6.

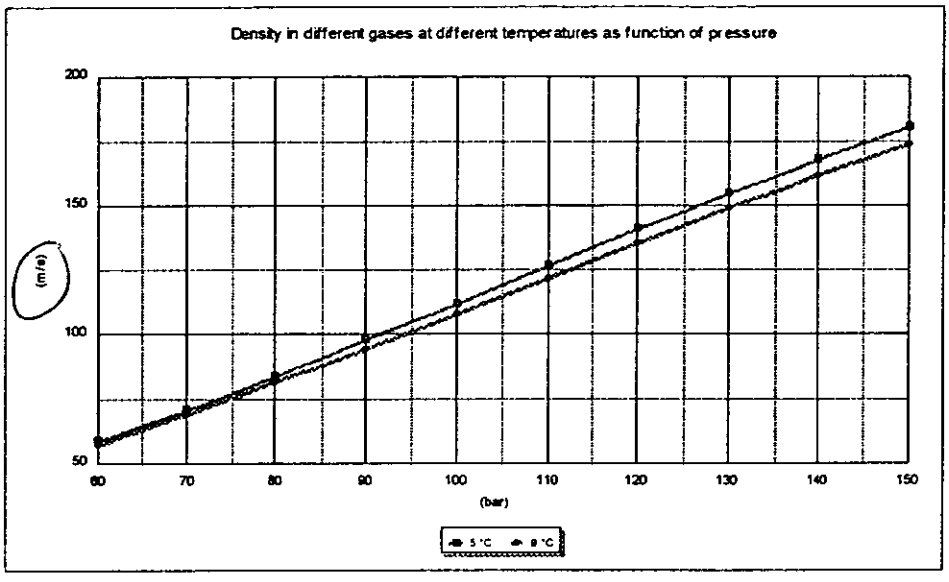

Figure 5 Density as a function of pressure at different temperature.
Gas composition in mole % ; C1 84.6, C2 11.4, C3 1.35, iC4 0.1, nC4 0.2, iC5 0.02, nC5 0.02, C6+ 0.03, N_2 1.3, CO_2 1

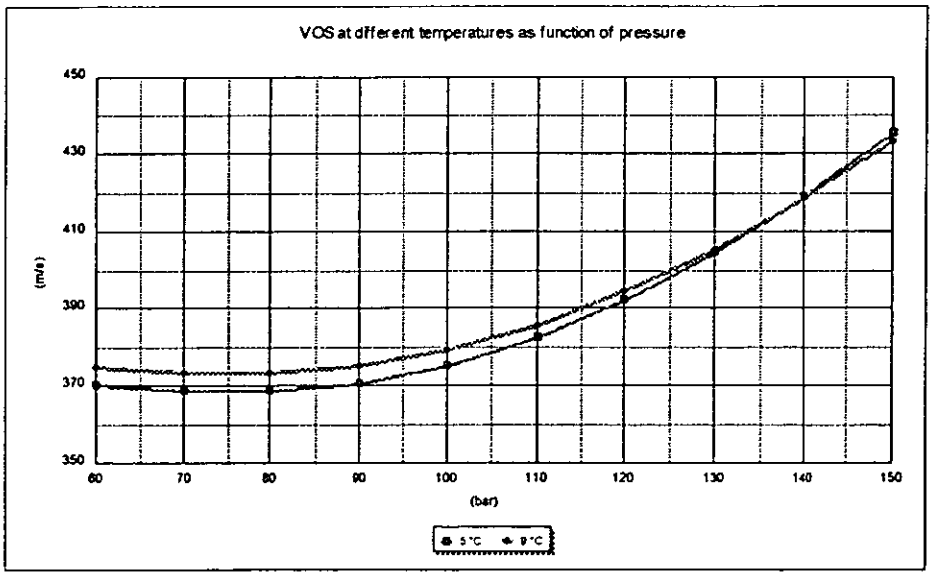

Figure 6 Velocity of sound as a function of pressure at different temperature. Gas composition as in figure 5

The relation between density and velocity of sound is described in the thermodynamic relation (5)

$$c = \sqrt{\gamma\left(\frac{\delta p}{\delta \rho}\right)_T} \tag{5}$$

where

γ is heat capacity ratio

Both ρ and $(\delta p/\delta \rho)$ can be calculated from a density model, for example AGA Report No. 8. It should be mentioned that to derive an expression for $(\delta p/\delta \rho)$ is a complex task.

Figure 7 shows an example of how density and velocity of sound is related to each other.

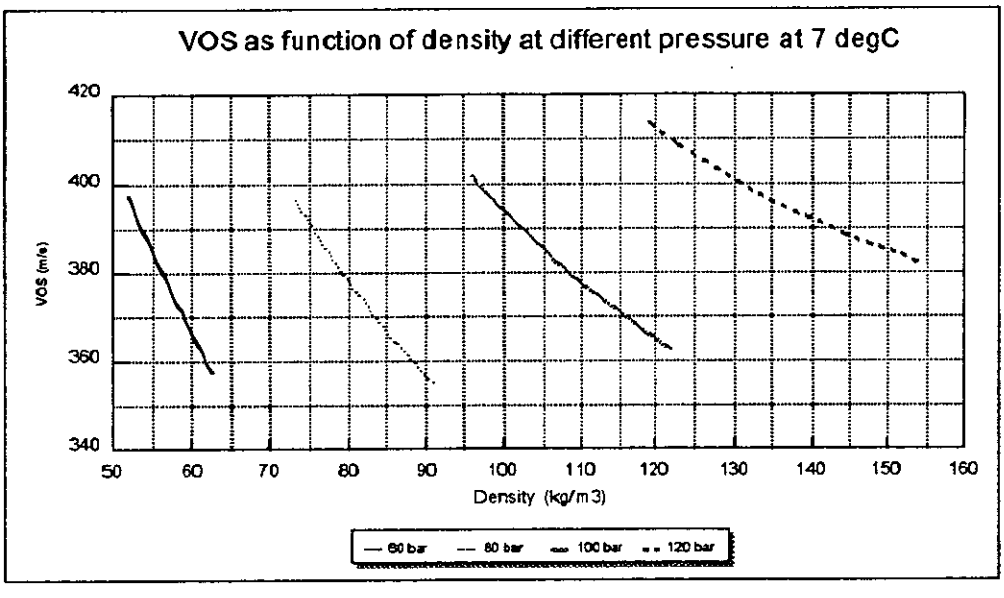

Figure 7 Velocity of sound as a function of density at different pressure. The variation in density and VOS for a given pressure and temperature is caused by variation in gas composition.

This relation can be utilised as a cross check between two independent measured values. From the measured density at a given pressure and temperature, velocity of sound can be calculated. This calculated velocity of sound can then be checked against measured velocity of sound for discrepancy. Vice versa can density be calculated from velocity of sound and checked against measured density for discrepancy. Action can be taken in case of discrepancies.

It should be mentioned a nice and simple relation is disturbed by variation in CO_2 and N_2 concentrations.

RECORDINGS OF DATA

Flow velocities

The reported flow velocities (ref. fig 2) can be recorded chronologically. The best way to get an overview is to set the readings in diagram.
From a flow meter in service such a diagram is shown in figure 8.

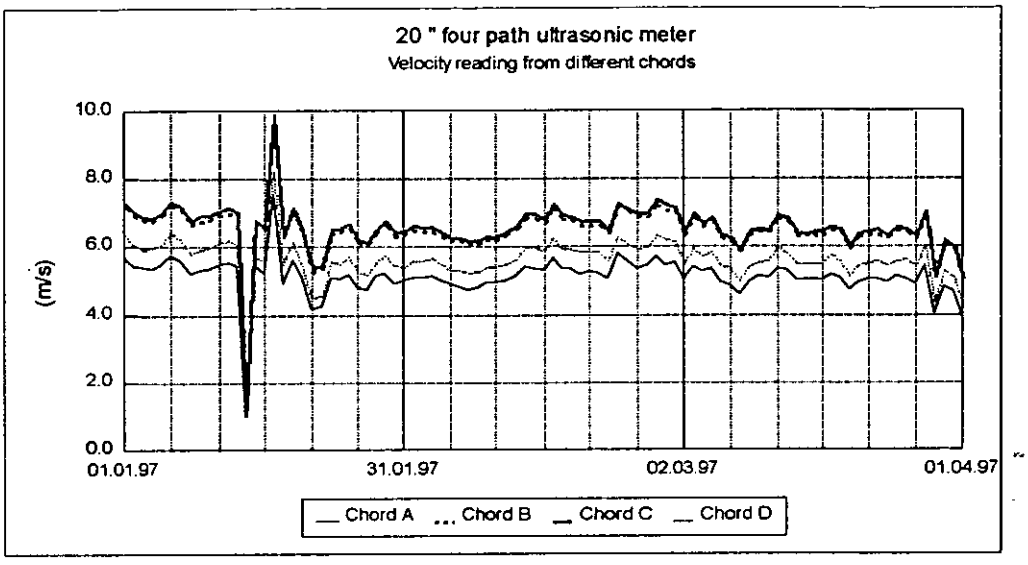

Figure 8 Recordings of flow velocity readings from all chords

A still better way of showing any effects on the individual measurement of velocity is to calculate the relative velocity for each chord. This means that the velocity for each acoustic path is divided by the average flow velocity. The data in fig. 8 then became as in figure 9.

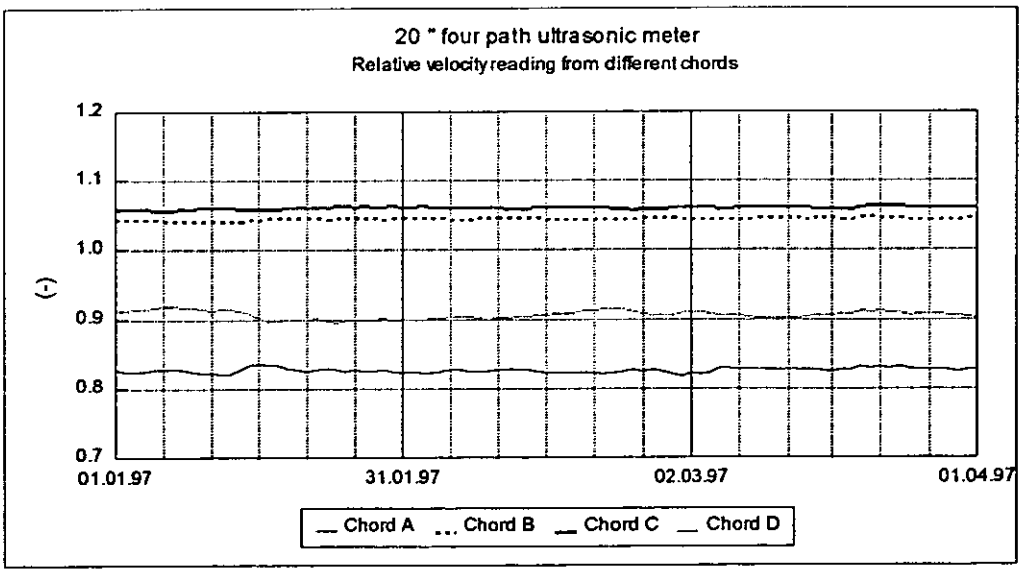

Figure 9 Recordings of velocities relative to average flow velocity for all chords The database is the same as in figure 8

Still another way of setting up the data is to set up the relative velocities as a function of flow velocities. The data set in figure 8 and figure 9 will then look like in figure 10:

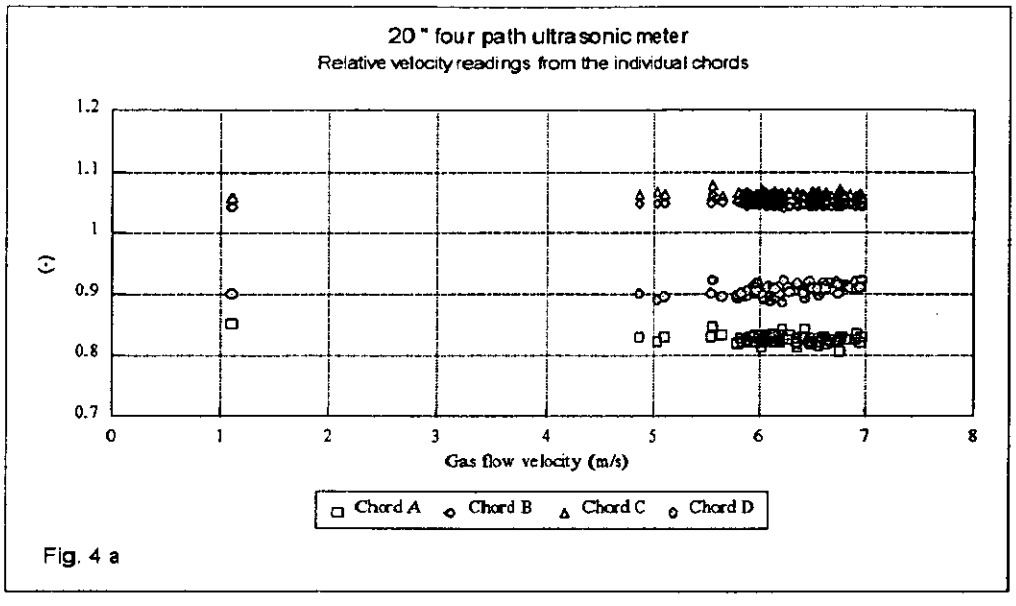

Figure 10 Relative velocity as a function of average flow velocity. The database is the same as in figure 9

Figure 8 to 10 indicate a stable meter function. Any miss in period triggering for any chord would result in large jumps in velocity and relative velocity for that chord. A miss in period triggering on all chords would have resulted in smaller jumps in relative velocity, but much in the velocity of sound checks.

The set up like in figure 10 can reveal even small errors in velocity. This is illustrated in figure 11 where the effect of a change in delay time (caused by calibration error or drift) of 1 μs in chord D is shown in a data set up like in figure 10.

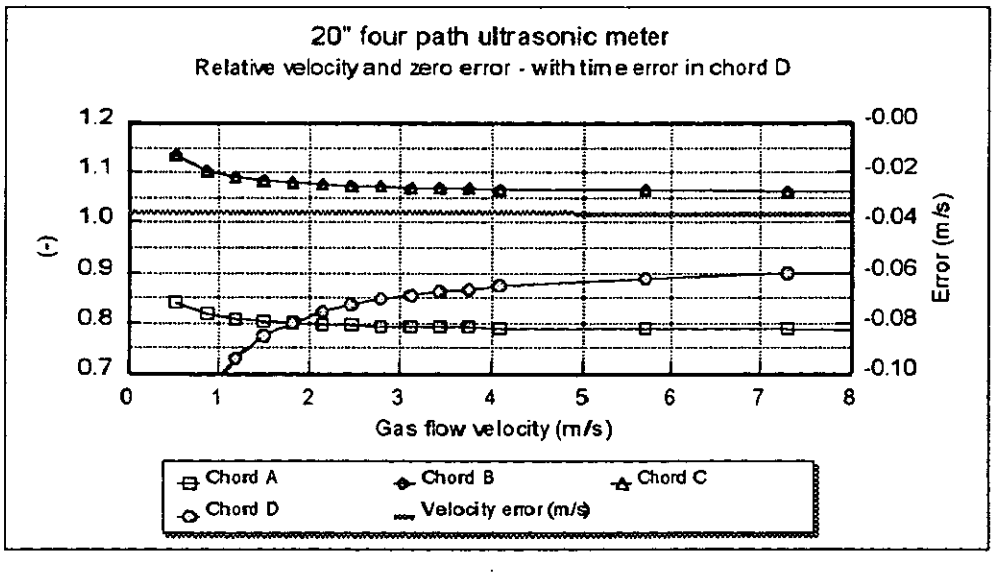

Figure 11 Calculated effect of an error in transit time for chord D of 1 μs in a 20" 4 path USM. The effect is a zero effect in average velocity of - 0.036 m/s

Velocity of sound data

The information about velocity of sound (ref. figure 2) can be treated in different ways.
One way is to intercompare the velocity of sound measured by the individual acoustic paths. This check in combination with the check of the velocity measurement can reveal whether there is an error in transit time in one direction or the other (t_1 or t_2), in both (t_1 and t_2) or not.

From the meter referred to in figure 8, 9 and 10, a chronological presentation of the difference between the individual measured velocity of sound and the average value is shown in figure 12.

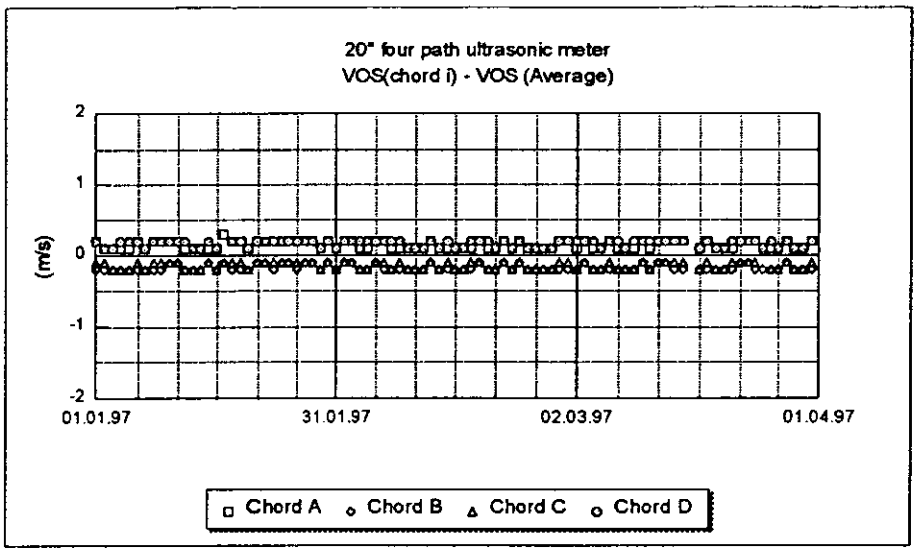

Figure 12 Velocity of sound measurement from the individual chords

Another way of checking the velocity of sound measurement is to compare the measured value with that calculated from measured density. Such a comparison is shown in figure 12 and 13.

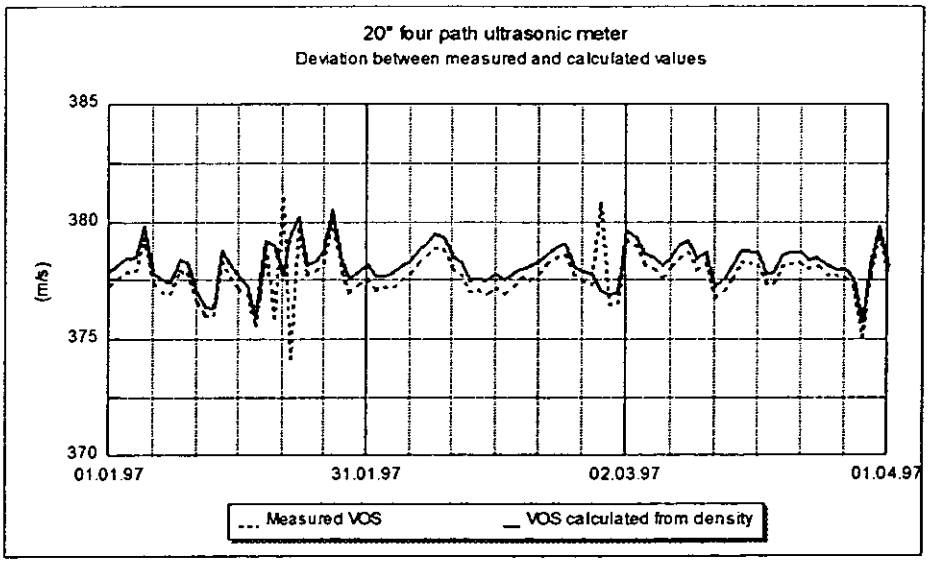

Figure 13 Comparison of measured VOS and VOS calculated from density, pressure and temperature. The database is as for figure 12. The occasional discrepancies is due to not simultaneously measured parameters. There is a delay in the densitometer loop.

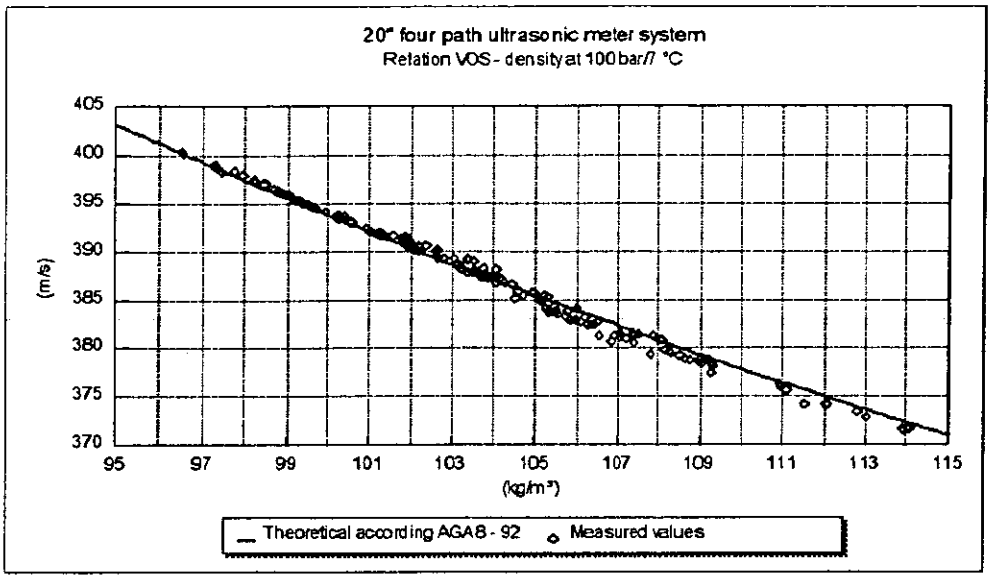

Figure 14 Measured velocity of sound reduced to 100 bar and 7°C. Each point of measured values is data from a period with varying gas composition. Ref. figure 7.

The sensitivity in velocity of sound calculation to change in density can be seen from figure 7. In most cases, change of 1% in density results in a change in VOS of 1 - 2 m/s.

Statoil is supporting further development of methods to calculate density from VOS and vice versa.

Investigation of flowing condition

The information from a multipath ultrasonic meter with chordial acoustic path can also to a certain degree be used to check the quality of the flowpattern inside the pipe.
In this paper only one example will be given.
At K-Lab a six inch FMU 700 from KOS was tested downstream a double bend out of plane with and without flowconditioner. Figure 15 shows the installation.

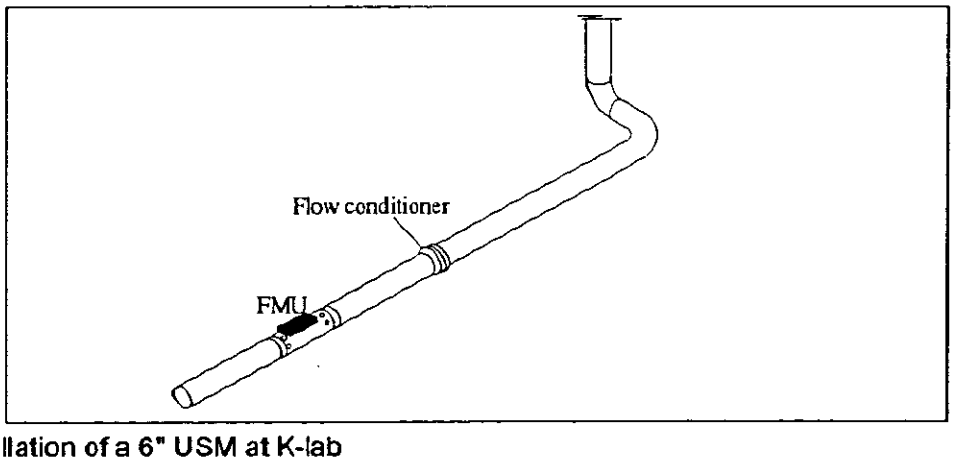

Figure 15 Installation of a 6" USM at K-lab

The FMU 700 has a path configuration that reveals very clear swirl condition. Figure 14 shows the velocity profiles as indicated by the meter in the two cases.

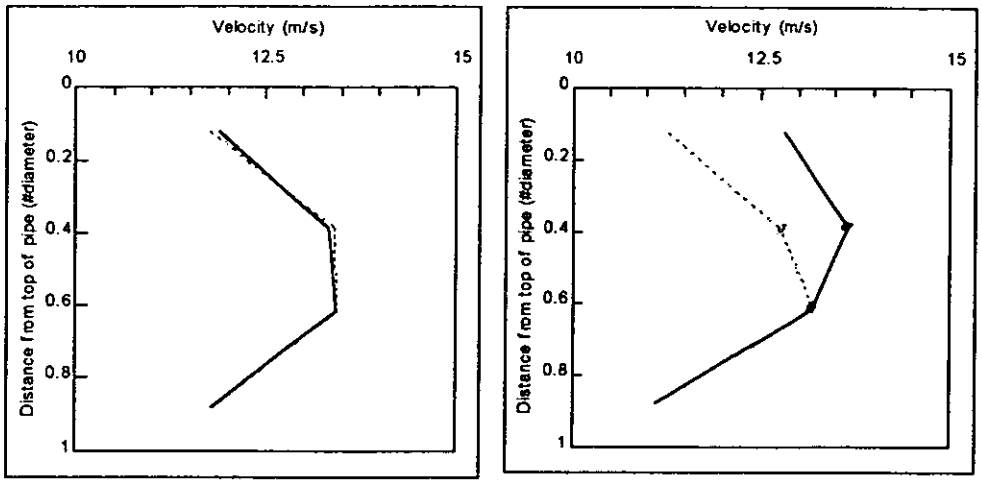

a b

Figure 16 Results from velocity readings installed as shown in figure 15. a) is with flow conditioner and b) is without the flow conditioner. There are two acoustic paths at the two top chords at different angles relative to the pipe axes. Deviation between dotted line and full line indicates swirl. The effect of flow conditioner is clearly indicated.

CONCLUSION

It is demonstrated that information provided by an ultrasonic meter enables the operator to check and verify stability of the meter.

In a system providing information about density, pressure and temperature it is possible to cross check. Discrepancies could indicate problem with any of the measured values and action should be taken.

It is also demonstrated the multipath ultrasonic meters can provide valuable information about flow pattern inside the pipe.

List of references

1. NPD, Regulations relating to fiscal measurement of oil and gas etc. 1997.

2. A.G.A. Report No. 9, Measurement of Gas by Ultrasonic Meters, 1997.

3. A.G.A. Report No. 8, Compressibility Factors of Natural Gas and Other Related Hydrocarbon Gases, 1992.

NSFMW.97

North Sea FLOW Measurement Workshop

Paper 16: 3.3

GAS WELL FLOWLINE MEASUREMENT BY ULTRASONIC FLOW METER

Authors:
J. B. Agricola,
Nederlandse Aardolie Maatschappij B.V. The Netherlands

Organiser:
Norwegian Society of Chartered Engineers
Norwegian Society for Oil and Gas Measurement
Co-organiser:
National Engineering Laboratory, UK

GAS WELL FLOWLINE MEASUREMENT BY ULTRASONIC FLOW METER

J.B. Agricola

NEDERLANDSE AARDOLIE MAATSCHAPPIJ B.V., The Netherlands

NAM

SUMMARY

In Underground Gas Storage plants the gas in the well flowlines flows bidirectional: from the well in production mode; to the well in injection mode.
Ultrasonic flow meters (UFM), bidirectional from origin, were therefore considered for this application.
However, no UFM had ever been designed for use in well gas flowlines.

This article emphasizes the design of an UFM for use in well gas flowlines and the starting problems that occurred during tests aimed at proving the reliability of the UFM. Some preliminary measurement results are given.

The prototype UFM has been installed and tested at NAM's Munnekezijl location and performs well.

A comprehensive report of field test results will be issued by NAM, Assen, The Netherlands, and Shell Exploration and Production Technology (EPT-OM), Rijswijk, The Netherlands.
Conclusions will be drawn and recommendations given.

1. INTRODUCTION

For the NAM Norg Underground Gas Storage (Norg-UGS) plant, fully operational by the end of 1997, flow meters had to be selected for measurement and control of bidirectional flow in the well flowlines (injection and production mode).

Conventional metering systems like orifices and venturis, normally in use in well flowlines, have the following drawbacks when used in bidirectional flow:
- no practical experience with the performance, reliability and uncertainty of orifices and venturis in bi-directional flow;
- necessity to use two sets of differential pressure (dP) transmitters to be switched with flow direction;
- doubts on the short- and longterm reliability and accuracy of the dP transmitters exposed to reverse dP's and
- limited rangeability.

In view of the above it was preferred to use UFMs, since this type of flow meters have the following advantages over orifices and venturis:
- in principle bidirectional flow measurement devices;
- high rangeability and
- no pressure drop.

However no UFM had ever been designed for and tested in well gas flowlines.
No experience in terms of mechanical design and performance of such a meter in this application was available.
It was therefore decided to design and test such a meter.

2. ULTRASONE MEASUREMENT PRINCIPLE

Ultrasonic gas flowrate measurement is based on the time difference (time-of-flight) between acoustic pulses transmitted from and received by one or more sets of sensors. Single or multiple reflection against the pipe wall can be applied.
Both sensors transmit pulses at the same time and the time difference between receipt of these pulses is measured.

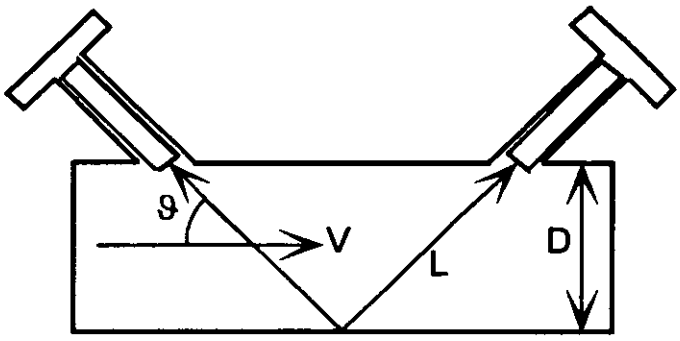

Drawing 1 Principle of operation

Gas flow velocity V_a, from which the flowrate can be established, is under ideal circumstances directly related to the time of flight and can be calculated from:

$$V_a = \frac{L}{2\cos\varphi} \times \left(\frac{1}{t_d} - \frac{1}{t_u}\right)$$

Measured down- and upstream times of flight t_d and t_u have the following relation to path length L, sensor angle φ, gas flow velocity V_a and the speed of sound in the gas C:

$$t_d = \frac{L}{C + V_a \cos\varphi} \quad \text{and} \quad t_u = \frac{L}{C - V_a \cos\varphi}$$

From above formulas it can be proven that ultrasonic flow measurement is basically independent of gas composition, pressure and temperature and that the impact of the speed of sound C is eliminated.

Flowrate Q at operational conditions is calculated from:
$Q = V \times A$ in which A is the cross sectional area of the pipe and $V = K \times V_a$.

K is a factor to correct for gas flow velocity profile and is established mathematically from the number of paths available, single or multiple pipe wall reflections, Reynolds nr., etc.
K-factor correction is based mainly on empirical data gathered during numerous tests at various test facilities all over the world.

Accurate positioning of the sensors is of extreme importance.
Angle and distance between the sensors form the basis for correct functioning of the meter and for achievable overall measurement accuracy.
The acoustical path length needs to be known as accurate as possible.

3. DESIGN AND INSTALLATION OF THE UFM

3.1 Basis of Design

The one pair sensor Psonic-1 UFM, drawing 1, from Instromet Ultrasonics, Dordrecht, The Netherlands, (IU, formerly Stork-Servex), was chosen as the basis of design.

For application in high pressure and high temperature gas well flowlines the meter had to be re-engineered with respect to:

- spoolpiece;
- flanges;
- sensor legs;
- sensor mounting assemblies;
- sensors and
- sensor cable glands.

3.2 Test Location

As test location for the UFM the 8 inch 2500# flowline of well 001 of NAM location Munnekezijl (MKZ) was selected for the following reasons:

- gas pressure and temperature of about 240 Bar and 100 °C respectively at a flowrate of about 3×10^6 $m^3(n)/d$;
- the well produces some sand;
- a venturi, installed for flow control, could serve as a reference.

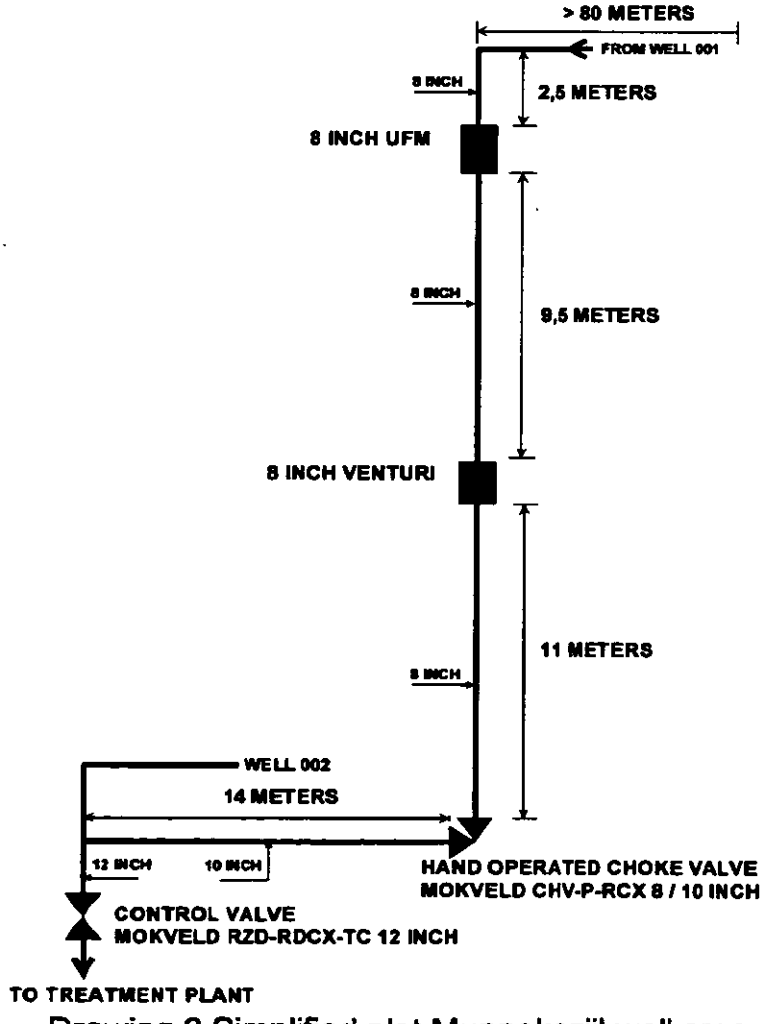

Drawing 2 Simplified plot Munnekezijl well area

MKZ gas was, at the time of the test, producing from two wells.
Produced gas is processed and brought on sales quality specifications in the Grijpskerk Depletion Facility (GDF), a silicagel drying plant.

3.3 Installation Requirements

Little knowledge and experience are available with manufacturers of UFM's on installation requirements for these meters in gas flowlines.

Necessary straight lengths, up- and downstream distance from potential sources of acoustical noise (chokes, thermowells, RTJ flanges, the venturi) are hardly known. Permitted (acoustical) noise levels and noise spectra are not defined.

Mechanical requirements of equipment for use at high pressures and high temperatures (type of flanges, gaskets, inspection, certification, etc.) are subjects the manufacturers of UFM's are not familiar with.

From discussions with the manufacturer, from publications and from company standards installation rules were defined.

3.4 Meter Sensors, Electronics, Meterbody and Sensor Legs

IU was responsible for the design of the sensors, (Ex) electronics, flowcalculations, data collection and data transmission.

Engineering of the meter was done by Tebodin, Hengelo, The Netherlands.

Veenstra, Coevorden, The Netherlands, manufactured the meter spoolpiece, ring type joint (RTJ) flanges, sensor legs and sensor leg flanges.

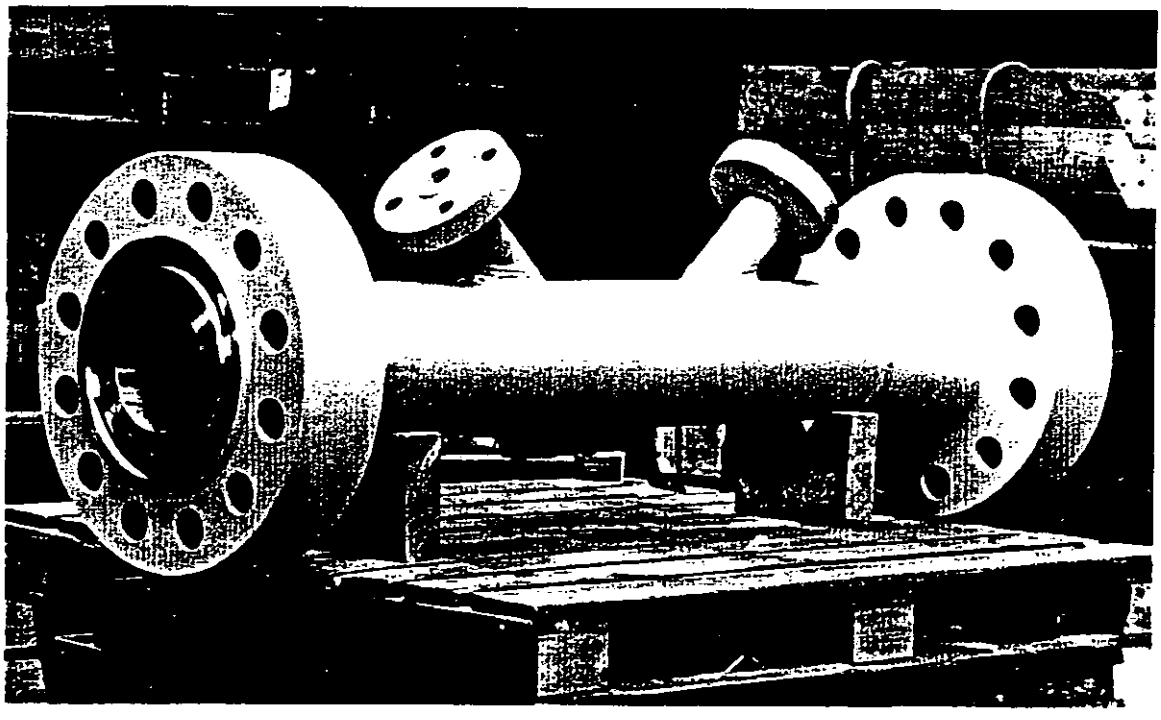

Photo 1 Manufacturing the UFM at Veenstra, Coevorden, The Netherlands

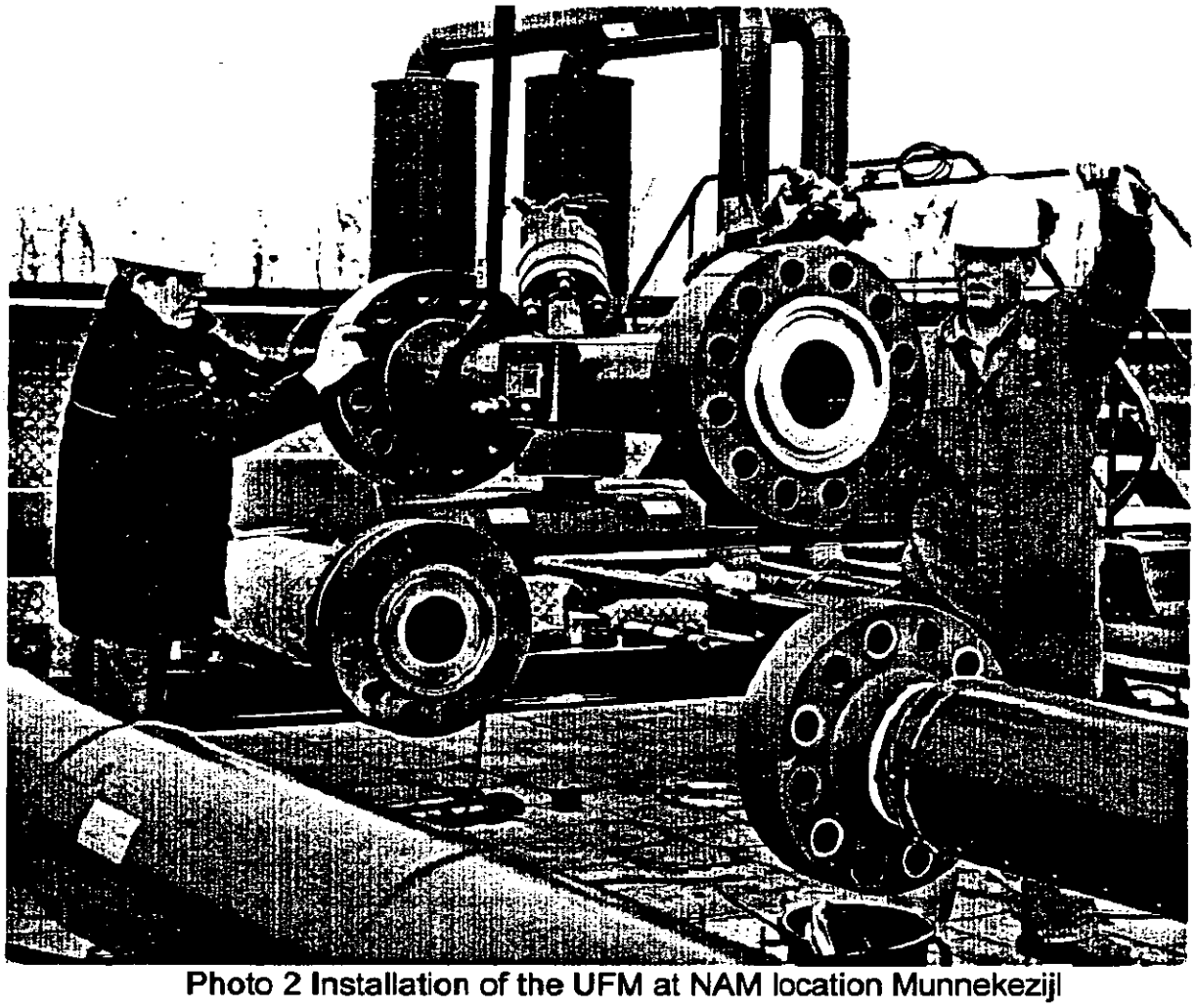

Photo 2 Installation of the UFM at NAM location Munnekezijl

Both IU and Veenstra were responsible for ensuring correct positioning in all planes of the sensor legs, in which the sensors are to be inserted, on the meter body.

All components were built together by Veenstra after which the meter was pressure tested for certification. Correct functioning of the sensors and electronics was executed by IU while the meter was pressurised at Veenstra's premises.

4. EXPERIENCED PROBLEMS

4.1 Sensors

The UFM was installed at the MKZ location in March 1995, see photo 2, and brought into operation by the end of that month.

Within 24 hours after becoming operational the performance of the meter fell down from 100 % to almost 0 %.
With performance is meant the percentage accepted sensor pulses for further processing in the meter electronics.

Checks on the electronics and observation of transmitted and received sensor pulses demonstrated that the sensors were not functioning properly.

After removing the sensors from the meter it turned out that the surface of the moulded synthetic sensor material of both sensors had gone spongy.

This resulted in a dramatically low transition of electrical into acoustical pulses and vice versa.

Investigations from IU and Shell Exploration and Production Technology, (SIEP EPT-IP, formerly KSEPL, Chemical Research), Rijswijk, The Netherlands, who were consulted for advise, made clear that the synthetic sensor material was sensitive to water in gas especially at the high MKZ operational gas temperature.
EPT-IP advised IU on new synthetic materials and moulding procedures.
A number of new sensors were produced, tested and installed in the meter.
Measurement results after this change were satisfactory, initially.

After a few weeks of operation however, new problems arose.
Slowly but surely the meter performance was decreasing again.

From investigations using X-ray techniques hairline cracks were discovered in the sensor material.
These cracks were caused by cohesive forces between the various types of synthetic material the sensor was made of.
Cohesive forces were found to result from depressurisation of the flow line.
Although depressurisation of a flowline is a controlled action the occurrence of inter-material forces in the UFM sensors could not be precluded.

Specialists on synthetic materials from the Dutch research organisation TNO, Delft, were approached for advise on possible solutions.
The problem was solved by using synthetic material and moulding techniques, commonly in use in spacecraft and satellite industry, neutralising internal forces due to depressurisation.

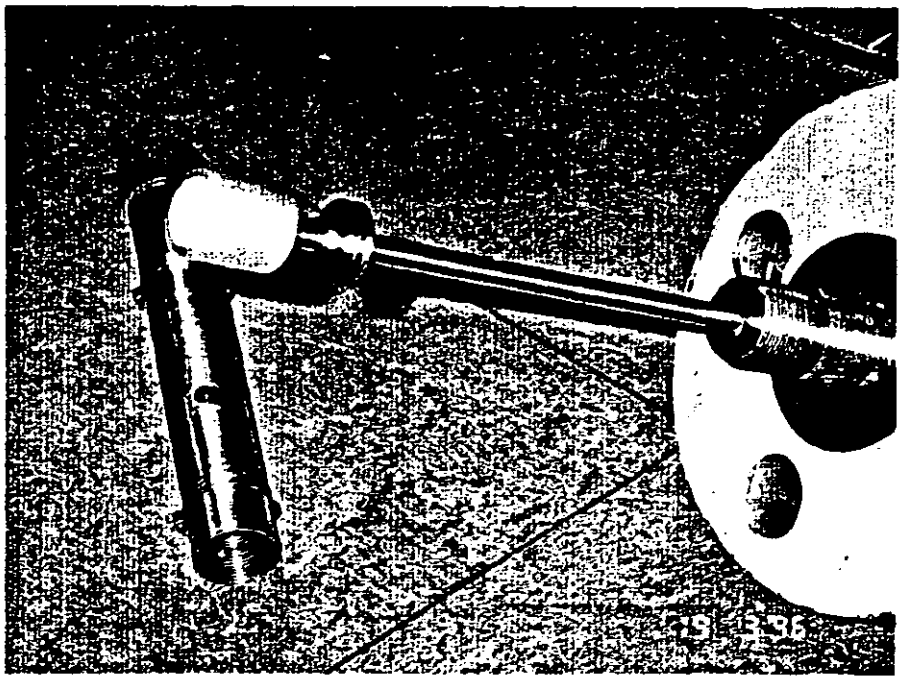

Photo 3 Final version of UFM sensors

The manufacturing and testing of prototype sensors turned out to be an extremely difficult task that, after a number of disappointments, led to a final version.

By the end of May 1996 sensors manufactured according to final laboratory test results were mounted in the UFM.
The meter has been performing without any problem since then.

Before these new sensors were installed an acoustical noise pattern survey was executed to measure noise levels and noise spectrum.
For this purpose a microphone was installed in one of the sensor legs of the UFM.
Data was collected under no-flow (flowline pressurised) and under operational flowing conditions.

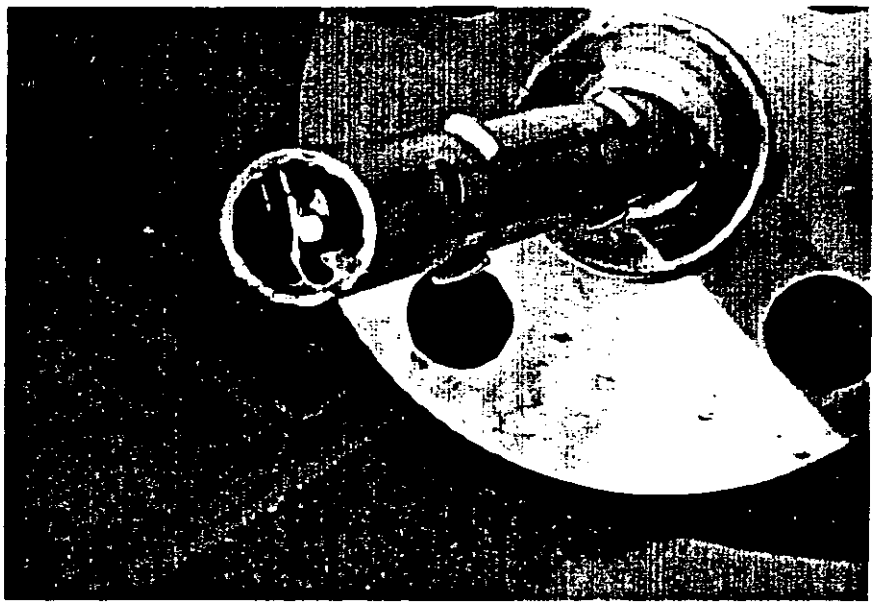

Photo 4 Microphone mounted in sensor assembly

From this data the signal-to-noise ratio could be established.
Noise spectrum measurements are of extreme importance in optimising UFM transmitter frequencies, for establishing required pulse energy and for defining acoustic noise filtering techniques.

4.2 Noise

At August 15th, 1996, Operations had to balance the flow production between wells 001 and 002 for which the hand operated angle choke valve in the flowline of well 001 was adjusted from 70 % open to about 50 % open.
Results on UFM meter performance were dramatic, see graph 1.

This graph shows a fall in UFM performance from 100 % to 10 % while the UFM measured flowrate increases and suffered from instability.
From sensor pulse measurements it became clear that the signal-to-noise ratio had reached such a level that discrimination between noise and sensor pulses was hardly possible.

The flowing gas in the flowline was clearly audible and was undoubtedly caused by the angle choke valve but also by the impulse lines from the venturi.

Personal from Operations were not allowed to readjust the choke valve and, after discussions with IU, it was decided to raise the transmission output to the sensors as high as the electronics allowed for.

UFM meter performance recovered thereafter to an average of 90 % and the metered flowrate became more stable and more in line with the venturi flowrate again.

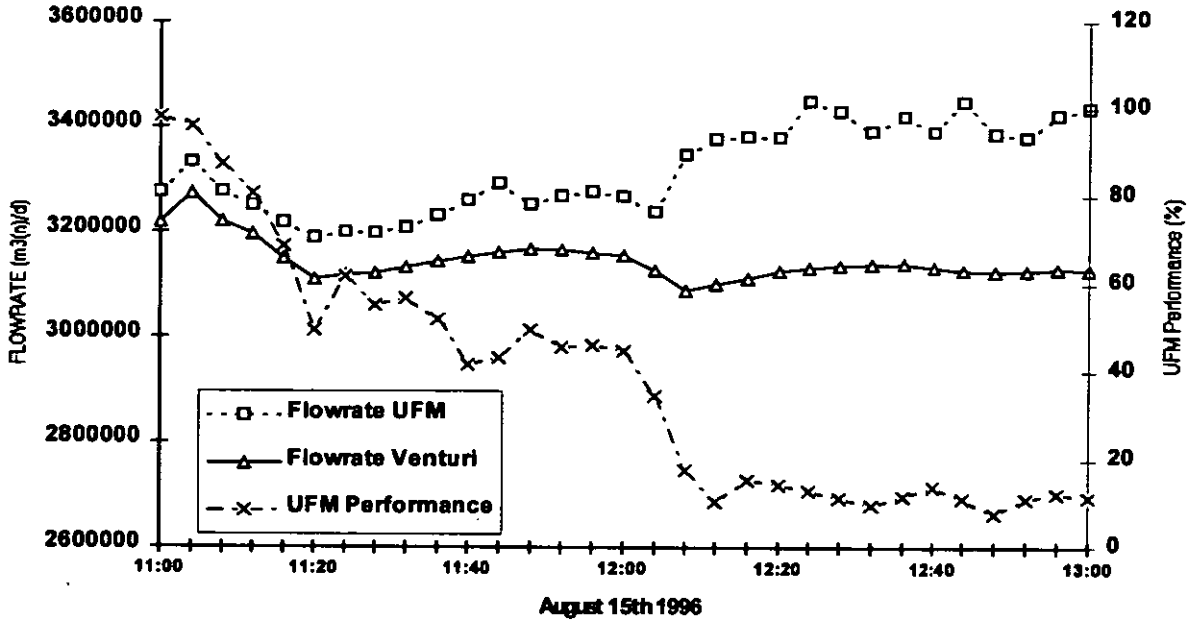

Graph 1 Influence of noise on UFM performance and measured flowrate

Although outside the scope of the test, a discussion was held with IU on observed rise of UFM measured flowrate during the period of low meter performance.
No clear explanation could be given as this phenomenon never occurred before.
A possible reason may be sought in received pulse detection philosophy and related electronic circuitry.

4.3 Other (minor) Problems

4.3.1 Power Supply

Power (24 V DC) for the meter was made available from the MKZ no-break set. For unknown reasons the fuse in the UFM-electronics blowed up randomly.
All possible causes were investigated (lightning, power dips from the mains, earth loops, shortage, etc.) but the real cause has never been found.
Power feed was finally established from a stabilised 220 V/24 V separate source and there haven't been any problems since.

4.3.2 Communication

Communication with the data logger for data collection and data readout was sometimes not possible due to a modem fault.
It was found by experiment that the modem fault occurred every time communication with the data logger was ended when using modem break signals.
By ending data transfer on data logger software level this fault never occurred anymore.

5 SET-UP OF FIELD INSTRUMENTATION

The venturi downstream of the UFM, engineered and designed fully in compliance with ISO 5167, served as a reference to the UFM.
Electronic instrumentation (P-, T- and dP-transmitters) was checked and calibrated regularly.

Venturi flowrate calculations, fully compensated for pressure and temperature to arrive at m3(n)/d [1]), are executed in a flowcomputer, make Digi Table, type DIC438, using AGA NX-19 for calculation of the compression factor.

The UFM flowrate (m3(n)/d) calculations are, according to IU, similar to these of the venturi.

To establish any possible differences from calculation routines between the venturi and the UFM a 2nd DIC438 flow computer was installed, see drawing 2.
This 2nd DIC438 received a frequency signal (F) from the UFM.
F is directly linear with UFM measured speed of the gas.

Compression factor calculation routines of this 2nd flowcomputer are exactly the same as these of the venturi flowcomputer.
Thermal expansion of the stainless steel UFM body is corrected for in the 2nd DIC438.

The calculated UFM flowrate from this 2nd flowcomputer, called UFM-dic, differed only slightly (0,5 % at the maximum) from the directly UFM measured flowrate.

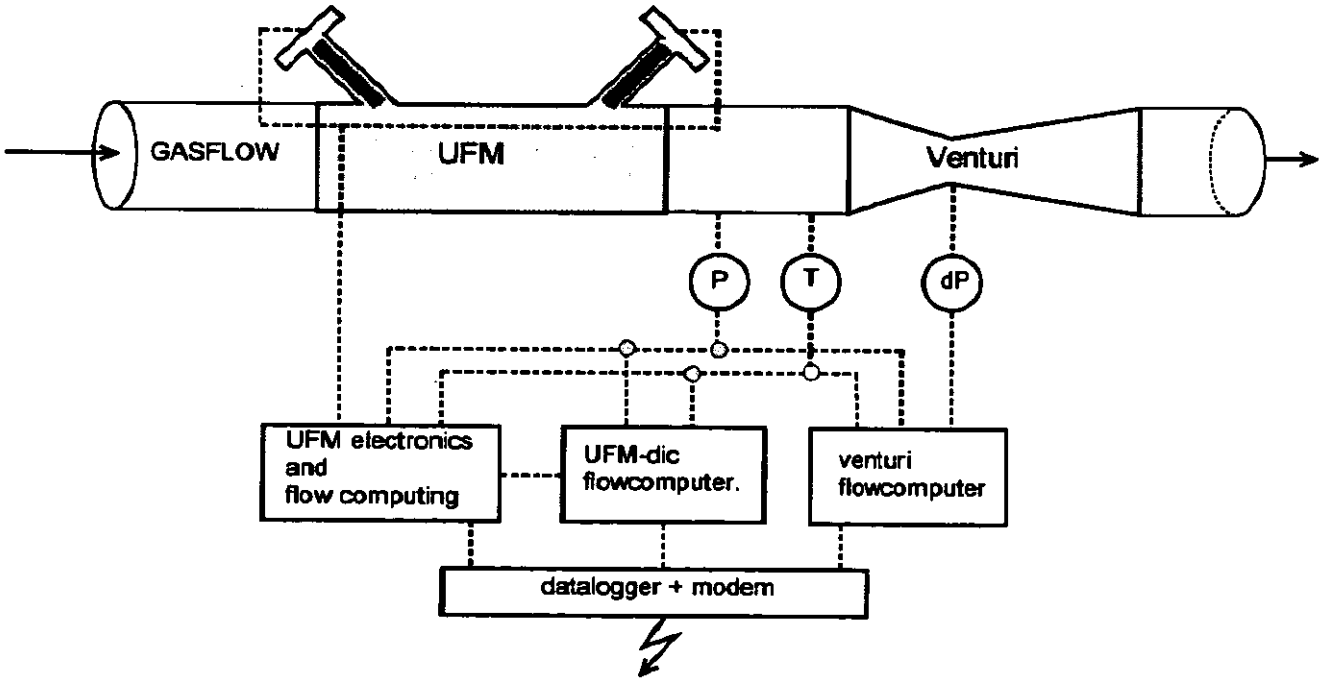

Drawing 2 Set-up of field instrumentation

[1]) m3(n) = m3 at normal conditions i.e. at a temperature of 273.15 K and a pressure of 101.325 kPa

6. MEASUREMENT RESULTS

6.1 Preliminary results

Although results from the field test will be reported and discussed extensively in the NAM/Shell report, some preliminary results are given here.

Graphs 2 and 3 show UFM and venturi measured flowrates, UFM-dic calculated flowrate and mutual percentage differences at the same conditions.

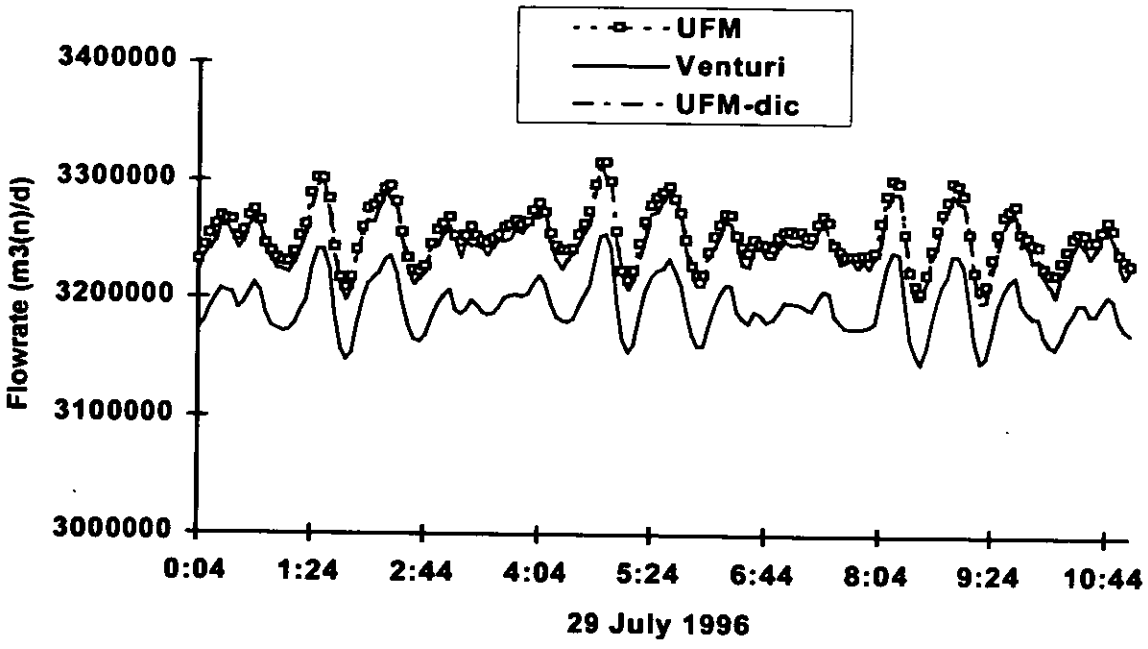

Graph 2 Flowrate comparison

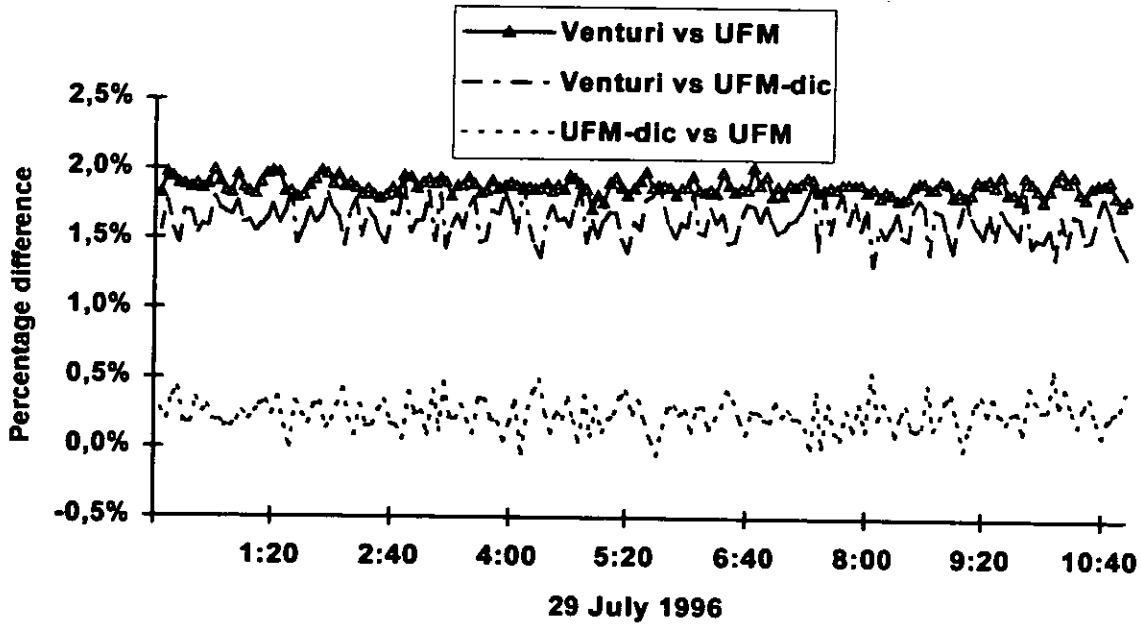

Graph 3 Percentage difference between flowrates

UFM measured flowrate is systematically positive compared to the venturi measured flowrate and to the UFM-dic calculated flowrate.

These differences can be quantified in detail only by executing a calibration run of each meter at a test facility.
The UFM was calibrated at the end of the test period, see paragraph 6.2.
Unfortunately the venturi could not be made available for such a calibration.

6.2 Rangeability

One of the main advantages of an UFM is its high rangeability.
An example of a typical venturi rangeability problem is given in graph 4.

A production raise to nearly 5×10^6 $m^3(n)/d$ causes saturation of the dP-high transmitter of the venturi resulting in a too low measured venturi flowrate.

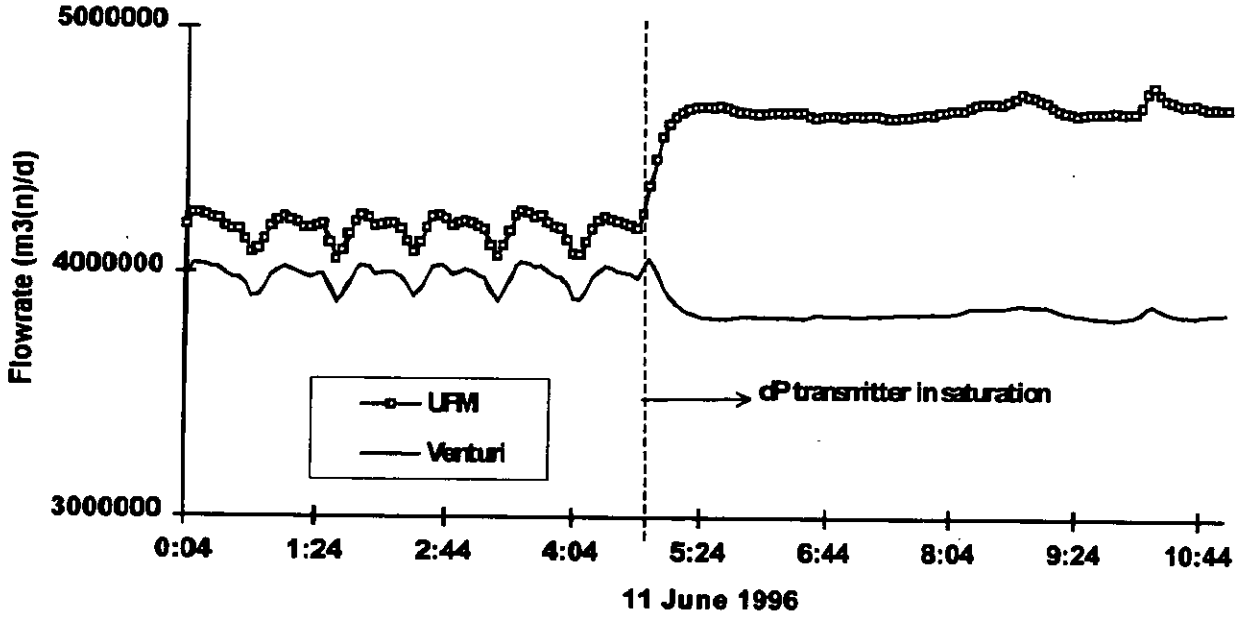

Graph 4 Example of limited venturi rangeability

6.3 Calibration

The UFM was calibrated at the end of the field test at the Ruhrgas (Pigsar) high pressure gas calibration facility in Dorsten, Germany.
Results are given in graph 5.

The calibration curve shows an UFM overreading of 2 to 3.5 % in the operational flowrate range as encountered during the test at MKZ.

Although this overreading is in line with observed difference between the venturi and UFM flowrates during the test, no strict comparison can be made as, for operational reasons, no calibration curve of the venturi could be made.

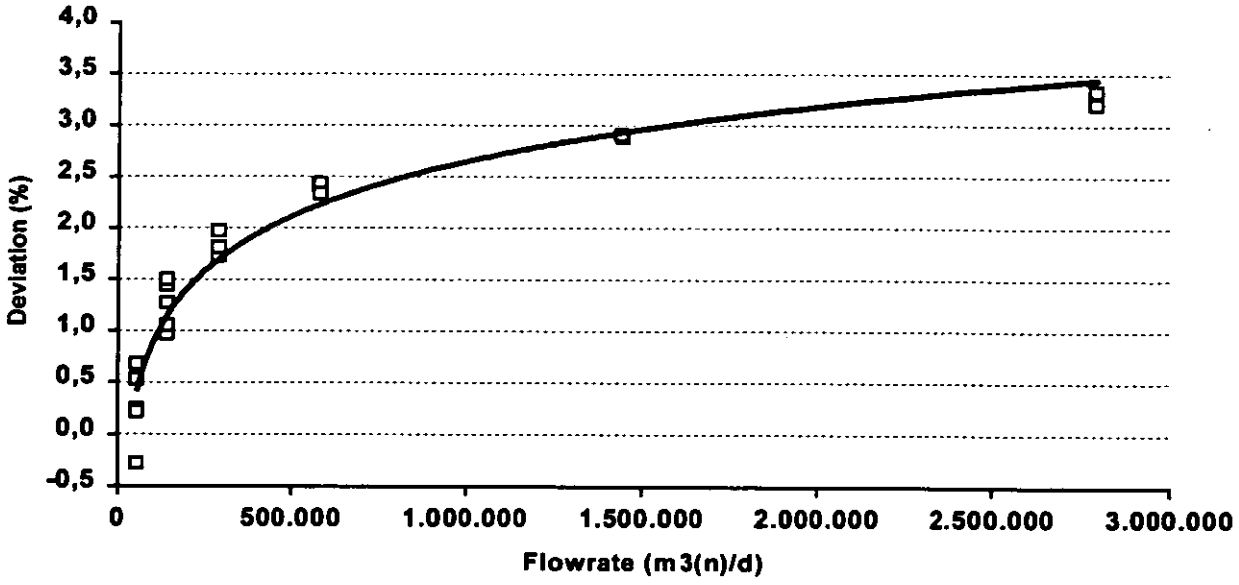

Graph 4 UFM Calibration results

The fact that the gas composition, operational temperature and pressure at the calibration facility (dry gas) are different compared to these parameters at MKZ introduces an extra, unknown, uncertainty.

Some data is available from a recent calibration of a venturi, in type and sizing comparable to the MKZ venturi, at the high pressure gas calibration facility of the Nederlands Meetinstituut (NMi), Bergum, The Netherlands.

From that calibration it may be concluded that the flowrate, measured with a standard venturi and using the ISO discharge coefficient of 0.995, is too low by 0.2 to 1.3 % over the flow range as encountered at MKZ.
This may imply that the difference between the UFM and venturi flowrates is smaller than the observed 2 % in practice.

7. COSTS

Cost price of an UFM may be split into the price of the sensors and related electronics and the body.
The price of a set of sensors and related electronics is more or less fixed.
The price of the body however depends on pressure class of the flowline, on material to be used (carbon, stainless or duplex steel) for the flowline and on (RTJ) flanges.
Body price may therefore be twice or more than that of sensors and electronics.

Overall costs of an UFM can be reduced significantly by not using flanges.
Price of such a meter is then comparable with that of a venturi of similar material.
The Norg-UGS UFM's do not have flanges.

8. THE USE OF FLOWLINE UFM'S IN THE FUTURE

Flowline measurements are necessary for flow control, for reservoir engineering and for product- and sales-allocations.

These applications, especially product- and sales-allocations, require reliable meters with reproducibilities and rangeabilities as high as reasonably possible.
Uncertainties are to be known.

Flowline UFM's are likely to meet with these demands.

Apart from the NAM Norg-UGS, flowline UFM's will be installed at the new NAM offshore production location L9, coming on stream early 1998.
Discussions to install these meters in the well flowlines of the Dutch Slochteren field are ongoing.

9. FURTHER INVESTIGATIONS

One of the goals of the NAM test was to proof the reliability of the UFM.
The test showed that the required reliability can be met.

However, further investigations are necessary and need to be undertaken the soonest.

Specifically the influence of (valve) noise, the wetness of gas and of sand particles on UFM measurement accuracy should be investigated, quantified and compensated for.

An on-line calibration or validation procedure need to be developed as dismantling of a flowline meter is normally not possible for operational reasons, apart from high costs and cumbersome logistics.

A complete different approach with respect to transmission frequency, filtering techniques and transmitted pulse characterisation may result from these investigations. Mathematical components within the currently used K-factor formula may need to be revised or may have to become dynamic.

Funds, facilities and manpower of gas exploration and production companies need to be made available for these investigations.

10. ACKNOWLEDGEMENTS

Designing the UFM and bringing the instrument "to life" was made possible through contributions from many people.
It was a result of close co-operation between manufacturers, research institutes and NAM, the end user.

I would specifically thank Mr. Ghis Boerwinkel of NAM.
He did most of the work to get and keep all the instrumentation operational.

NSFMW.97

North Sea FLOW Measurement Workshop

Paper ~~17~~: 3·4

TESTING OF NOISE SUPPRESSION SYSTEM FOR MULTIPATH ULTRASONIC GAS FLOW METERS

Authors:
Bård Dybwad Kristensen and Cecilie Lofsei, Kongsberg Offshore AS, Norway
Kjell-Eivind Frøysa, Christian Michelsen Research AS, Norway

Organiser:
Norwegian Society of Chartered Engineers
Norwegian Society for Oil and Gas Measurement
Co-organiser:
National Engineering Laboratory, UK

Kristensen, Lofseik & Frøysa, "Testing of noise suppression system for multipath ultrasonic gas flow meters ".
North Sea Flow Measurement Workshop, Kristiansand, Norway, October 27th-30th, 1997.

TESTING OF NOISE SUPPRESSION SYSTEM FOR MULTIPATH ULTRASONIC GAS FLOW METERS

Bård Dybwad Kristensen,* Kongsberg Offshore AS, Kongsberg, Norway.
Cecilie Lofseik, Kongsberg Offshore AS, Kongsberg, Norway.
Kjell-Eivind Frøysa, Christian Michelsen Research AS, Bergen, Norway.

SUMMARY

The use of ultrasonic meters for custody transfer metering is gaining acceptance within the oil companies as well as by the authorities. There is an ongoing effort to improve these meters to make them a competitive alternative to orifice plates and gas turbine meters. Operational experience has shown that ultrasonic meters are sensitive to noise generated by flow control valves. KOS has, in cooperation with CMR, developed an ultrasonic noise suppression system.

In the summer of 1997 KOS tested a 12" FMU-700 multipath ultrasonic gas flow meter at Statoil's K-Lab in Norway. The tests quantified the performance of the ultrasonic noise suppression method developed by KOS and CMR. The ultrasonic noise was generated by a 6" control valve with silencer trim manufactured by Mokveld. This valve is known to radiate noise in the ultrasonic frequency range [1]. The meter was tested for velocities from 0.5 m/s to 9 m/s giving a wide range of noise levels at the meter and signal to noise ratios from approximately 126 (42 dB) to 0.7 (-3 dB). The results show that the FMU-700 is capable of measuring accurately even in cases where there is more noise than signal.

ABBREVATION AND SYMBOL LIST

CMR	Christian Michelsen Research AS
FMU	Flow Metering Unit
KOS	Kongsberg Offshore AS
NFR	Norges Forskningsråd (Norwegian Research Council)
SNR	Signal to Noise Ratio (for the transducer receiving most noise)
USM	Ultrasonic Meter
P	Hydrostatic pressure at the USM [bar]
ΔP	Hydrostatic differential pressure (pressure drop) across the valve [bar]
v	Average axial flow velocity at line conditions [m/s]
D	Inner pipe diameter [m]

* Presenting author.

1. INTRODUCTION

Most ultrasonic meters are based upon an accurate measurement of the transit time of an ultrasonic signal traversing the gas flow in the pipe. When a USM is situated close to other sources of ultrasonic sound, this sound will interfere with the original signal and make the latter hard to detect. It is known that some flow control valves generate noise in the ultrasonic frequency range. To save space it may be desirable to place such valves in the vicinity of the metering device. This will, however, move the source of ultrasonic noise close to the USM. To avoid a conflict between the space requirements and the functionality of the USM, an ultrasonic noise suppression method has been developed. The noise immunity project has been a cooperation between KOS, CMR, NFR and Statoil. This paper is a follow-up of the paper presented by CMR at the NSFMW in 1996 [1]. The test results presented here are based on the test matrix used for the paper presented last year [1]. The meter used in this year's tests is the same as the one used in 1996. The electronics and software have been changed to implement the noise suppression method and to comply with the KOS product line for fiscal metering.

2. TEST PREPARATIONS

With basis in the tests performed in 1996, a theoretical method for suppressing noise in the received ultrasonic signal was developed by KOS and CMR. The object of the tests was to quantify the performance of this method for signal processing with the meter operating in a noisy environment. The problem with noise suppression basically consists in recognizing the arrival of the transmitted signal in cases where the transducers receive a lot of noise. This is done by a correlation and averaging technique.

Prior to the noise suppression tests at K-Lab, the meter was zero calibrated at KOS. The 6 transducer pairs were zero calibrated by mounting them in a pressure- and temperature-controlled zero calibration chamber. Nitrogen was used as the calibration gas. The distances between the transducers in the spool piece were measured to an accuracy of one tenth of a millimetre.

3. TESTING AT K-LAB

The tests were performed at Statoil's K-Lab gas research facility between the 23rd of June and the 10th of July 1997.

3.1 Test installation

The 12" USM was installed in the gas test loop at K-Lab in series with a 6" Mokveld control valve with silencer trim. Thus the gas flow velocity through the valve was

approximately four times higher than the gas flow velocity through the USM due to the difference in cross-sectional area.

It is known that some flow control valves will produce noise in the ultrasonic frequency range. Different types of valves will probably produce noise of different frequency and intensity. This has, however, not been investigated in this project.

It is seen that the level of ultrasonic noise received by the ultrasonic meter is depending on the distance between the valve and the meter, the differential pressure across the valve, the static pressure in the pipe and the gas flow velocity in the pipe. Whether the valve is placed up- or downstream of the meter is also influencing the noise level. The noise experienced by the individual transducers will vary with the length, angle and lateral position of the path, and whether the receiving transducer is facing the source of the noise or facing away from it [1]. The SNR values in the following are values for the transducer receiving most ultrasonic noise.

K-Lab offers a maximum flow velocity of 9 m/s for 12" pipes. The meter has therefore not been tested at higher velocities. The outdoor temperature at K-Lab in the test period was 20-25°C, and the typical composition of the test gas was: 82.8% methane, 14.2% ethane, 0.9% propane, 0.04% iso-butane, 0.05% normal-butane, 0.01% iso-pentane, 1.1% nitrogen and 0.9% carbon dioxide. The composition is given in molar-%.

The gas temperature and pressure were measured both upstream and downstream of the valve. The gas temperature at the USM was in the range 35-38.5°C. The valve was installed respectively 10D (≈3.4 m) downstream, 5D (≈2.1 m) downstream and 5D upstream of the ultrasonic meter, see Figure 1. The downstream installations correspond to the test installations that were used last year. In addition, the upstream installation (which this year was 5D from the USM instead of last year's 10D) was chosen in order to create sufficient levels of noise at the USM to investigate the limits of the noise suppression method.

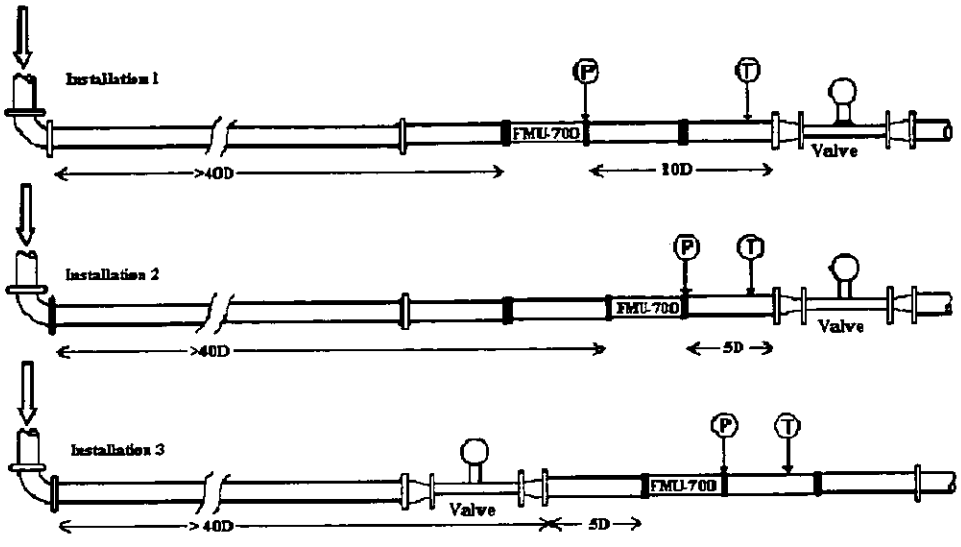

Figure 1: The three test installations at K-Lab. Installation 1; valve placed 10D downstream, installation 2; valve placed 5D downstream and installation 3; valve placed 5D upstream of the USM. The differential pressure across the valve is the calculated difference between the pressure measured up- and downstream of the valve. D is in this case the inner diameter of a 12" pipe, i.e. D=0.26 m.

The gas flow velocity, the static pressure in the pipe, the differential pressure across the valve and the position of the valve have been varied to investigate the behaviour of the ultrasonic meter at various levels of noise. See Table 1 for the complete test matrix.

3.2 Test matrix

Table 1: Test matrix for the USM valve noise testing at K-Lab 1997.

Test parameters according to plan				Actual parameters at K-Lab		
Valve position relative to meter, see Figure 1	**P**	**v**	**ΔP/P**	**P**	**v†**	**ΔP/P**
10D DOWN	20 bar	0.5 m/s	≈ 0%	22.27 bar	0.49 m/s	0.2%
			10%	22.63 bar	0.45 m/s	8.6%
			20%	22.83 bar	0.41 m/s	17.4%
		3 m/s	≈ 0%	22.42 bar	3.10 m/s	0.8%
			10%	22.65 bar	2.83 m/s	9.0%
			20%	22.98 bar	2.43 m/s	17.4%
		9 m/s	≈ 0%	22.44 bar	8.74 m/s	5.5%
			10%	22.54 bar	8.39 m/s	9.3%
			20%	23.16 bar	7.40 m/s	17.1%
	100 bar	0.5 m/s	≈ 0%	100.35 bar	0.46 m/s	0.1%
			10%	103.04 bar	0.41 m/s	10.4%
			20%	103.77 bar	0.38 m/s	16.8%
		3 m/s	≈ 0%	100.44 bar	2.92 m/s	0.8%
			10%	102.98 bar	2.64 m/s	10.2%
			20%	104.81 bar	2.36 m/s	20.1%
		9 m/s	≈ 0%	101.80 bar	8.20 m/s	5.9%
			10%	102.36 bar	7.84 m/s	9.9%
			20%	105.27 bar	6.89 m/s	19.0%
5D DOWN	100 bar	0.5 m/s	≈ 0%	100.42 bar	0.46 m/s	0.1%
			10%	103.00 bar	0.41 m/s	10.2%
			20%	102.96 bar	0.38 m/s	16.5%
		3 m/s	≈ 0%	100.88 bar	2.92 m/s	0.8%
			10%	101.85 bar	2.63 m/s	9.9%
			20%	103.50 bar	2.43 m/s	16.9%
		9 m/s	≈ 0%	101.42 bar	8.19 m/s	5.9%
			10%	101.78 bar	7.84 m/s	9.9%
			20%	103.50 bar	5.99 m/s	19.0%
5D UP	100 bar	0.5 m/s	≈ 0%	101.95 bar	0.46 m/s	0.2%
			3%	87.81 bar	0.47 m/s	3.5%
		3 m/s	≈ 0%	101.07 bar	2.93 m/s	0.4%
			10%	92.77 bar	2.91 m/s	10.8%
			15%	90.02 bar	2.91 m/s	16.1%
		9 m/s	≈ 0%	96.93 bar	8.54 m/s	4.6%
			10%	91.90 bar	8.50 m/s	10.8%

† The average axial gas flow velocity given in the table was calculated from the reference volume flow rates, and is the flow velocity through the USM. The flow velocity through the valve is approximately 4 times higher.

3.3 Reference measurement system

K-Lab uses sonic nozzles as the main reference flow meter. An 8" Instromet turbine meter was used as reference when the flow through the nozzles was subsonic. Subsonic flow through the sonic nozzle bank occurred when the control valve consumed too much of the total pressure drop in the loop. The total uncertainty in the reference volume flow rate at K-Lab is ±0.35%. In the setups with 20 bar pipe pressure and 0.5 m/s flow velocity, and when the valve is placed upstream of the USM, the uncertainty in the reference volume flow rate is increased to ±0.5%. At these conditions, temperature gradients in the gas will become significant, making it difficult to obtain representative values for the gas temperature[3]. This will influence the density calculation and the calculated volume flow rate will be less accurate.

3.4 Problem description

Figure 2 and Figure 3 visualize the effect of ultrasonic noise generated by valves on the signals transmitted and received by the USM for determining the transit times.

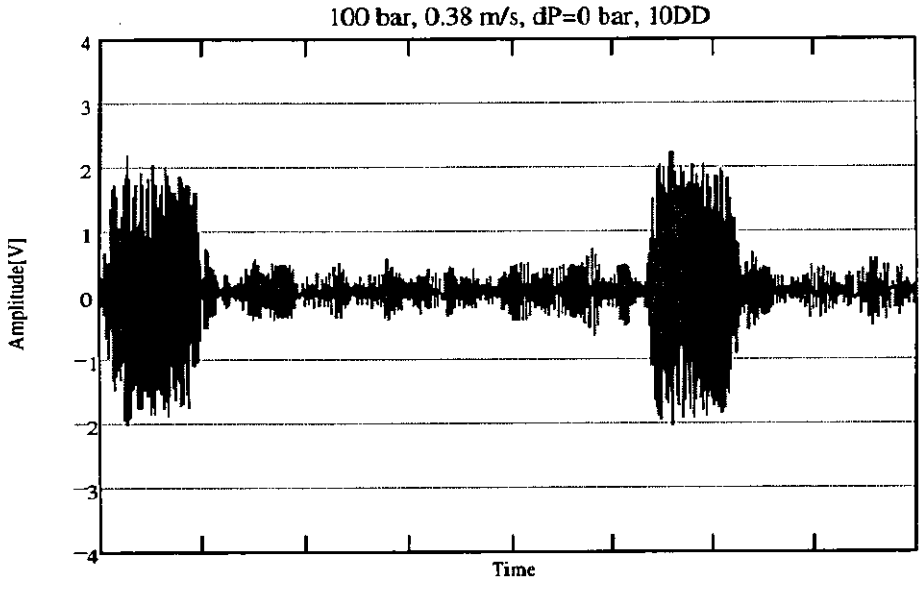

Figure 2:The signal used to measure transit times superimposed on ultrasonic noise generated by the valve, as received by the transducer. The valve is placed 10D downstream of the USM. The flow velocity is 0.38 m/s, the pressure is approx. 100 bar and the valve is open, i.e. the differential pressure across the valve is close to zero. The SNR is in this case 126 (42 dB).

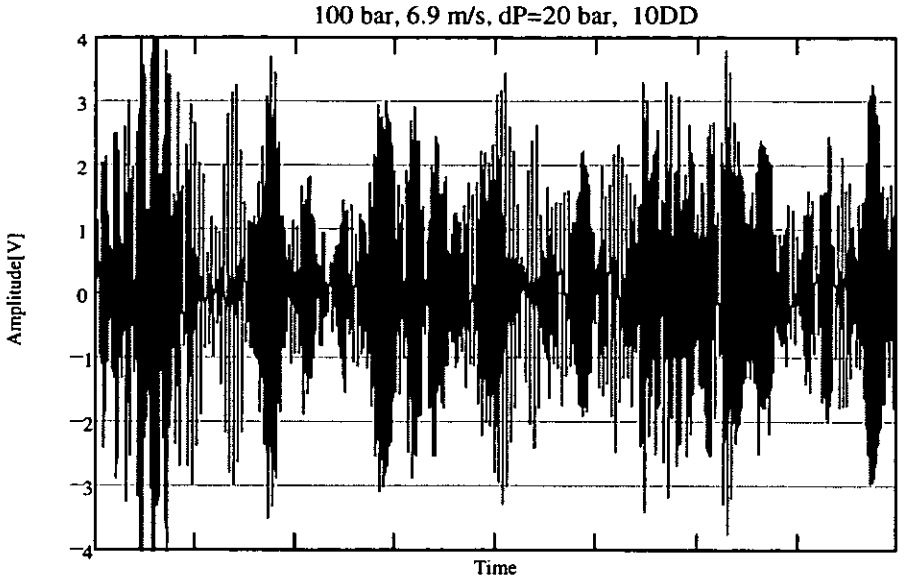

Figure 3: The signal used to measure transit times superimposed on ultrasonic noise generated by the valve, as received by the transducer. The valve is placed 10D downstream of the USM. The flow velocity is 6.9 m/s, the pressure is approx. 100 bar and the differential pressure across the valve is 18 bar. The SNR is in this case 1.25 (2 dB).

Figure 2 shows a setup with low gas flow velocity and open valve, a virtually noiseless operating environment. The signal is in this case easily detected. In Figure 3 the valve has been tightened and the gas flow velocity has been increased, the result of this being that the valve radiates much more noise. The SNR is in this case 1.25 (2 dB), and the signal is literally drowned in noise and impossible to detect visually.

The correlation and averaging method used by the USM is capable of removing the influence of the noise and detect the signal correctly in situations similar to this.

4. TEST RESULTS AND DISCUSSION

The evaluation of the test results is done by recording the deviation in percent between the USM and the reference meters. The repeatability, as defined by [2], is calculated and the SNR is estimated. Information from [1] put together with information extracted from sampling data recorded at K-Lab in the test period are used to find the SNR in the following. All values for the SNR should therefore be taken as estimates only.

The parameter that best indicates the meter's insensitivity to ultrasonic valve noise, is the repeatability. If the meter is able to measure constant over a period of time, this implies that the random signal disturbances introduced by valve noise are well suppressed. The repeatability should not exceed 0.2% [4].

Figure 4 shows the results when the valve is placed 10D downstream of the USM, see Figure 1, installation 1. The pressure at the USM is approximately 20 bar. Each curve represents a different pressure drop across the valve. Each point on the curve is a calculated average of measurements taken over a period of approximately ½ hour. The repeatability is indicated at each point. The SNR varied from 126 (42 dB) to 1.25 (2 dB), decreasing with the differential pressure across the valve and the flow velocity.

The figure shows that

– the deviation is within ±0.5% for all points.
– the repeatability is of the order of 0.2% for $v \leq 0.5$ m/s.
– the repeatability is of the order of 0.04% for $v > 0.5$ m/s.

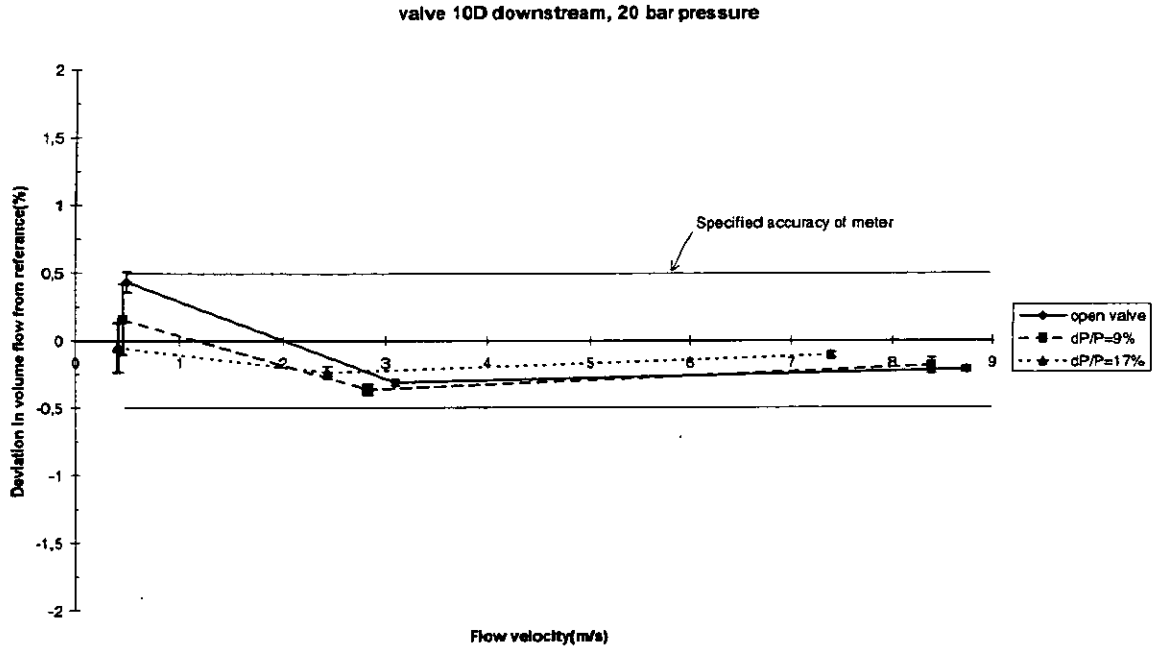

Figure 4: The deviation from the reference. The different curves represent various differential pressure across the valve. The repeatability for each point is indicated by error bars. For installation conditions, see figure legends.

As can be seen from Figure 4 the repeatability is very good for all points, indicating that the noise generated from the valve represents no source of error when the valve is placed 10D downstream of the USM. At the low flow, low pressure setups, the repeatability is poorer. This is due to the fact that the flow in the test loop at K-Lab is fluctuating somewhat on short term basis under these circumstances[3]. The SNR for the setups with this installation may be as low as 1.25 (2 dB). This constitutes no difficulties for the noise suppressing algorithm implemented in the USM.

Figure 5 shows the results from the same installation as Figure 4. The pressure at the USM is increased to approximately 100 bar. The SNR varied from 126 (42 dB) to 1.25 (2 dB), as above. This is due to the fact that the SNR is pressure dependent mostly through the ratio between the differential pressure across the valve and the pressure in the pipe.

The figure shows that

– the deviation is within ±0.5% for all points.

– the repeatability is of the order of 0.1% for $v \leq 0.5$ m/s.

– the repeatability is of the order of 0.03% for $v > 0.5$ m/s.

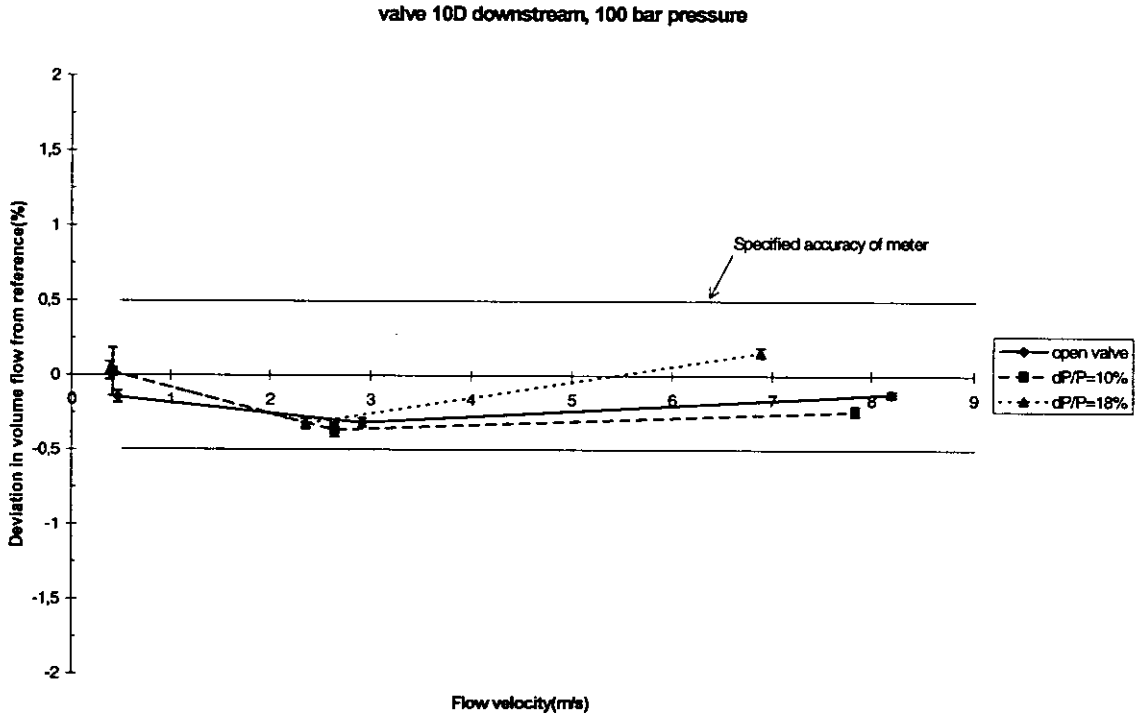

Figure 5: The deviation from the reference. The different curves represent various differential pressure across the valve. The repeatability for each point is indicated by error bars. For installation conditions, see figure legends.

As can be seen in Figure 5 the repeatability is very good for all points, indicating that the noise generated from the valve represents no source of error when the valve is placed 10D downstream of the USM. The SNR for these setups can be as low as 1.25 (2 dB). This constitutes no difficulties for the noise suppressing algorithm implemented in the USM.

Figure 6 shows the results when the valve is placed 5D downstream of the USM, see Figure 1, installation 2. The pressure at the USM is approximately 100 bar. The SNR varied from 126 (42 dB) to 1 (0 dB) at this installation.

The figure shows that

– the deviation is within ±0.5% for all points but one.

– the repeatability is of the order of 0.3% for the point with highest differential pressure and highest velocity.

– the repeatability is of the order of 0.05% for all other points.

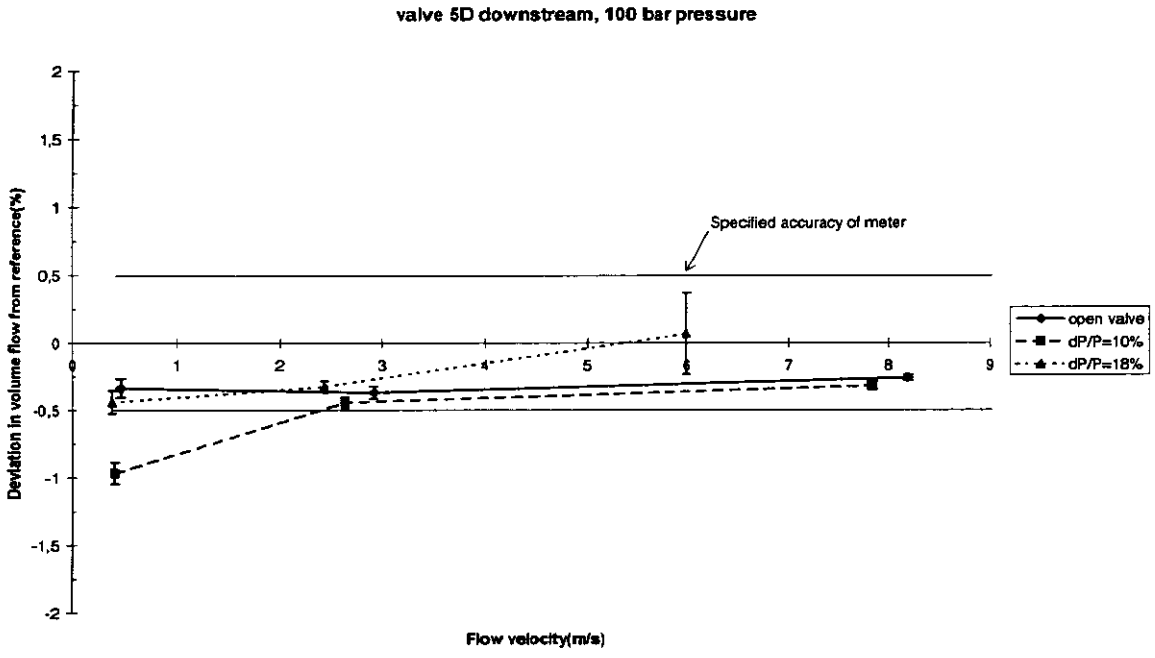

Figure 6: The deviation from the reference. The different curves represent various differential pressure across the valve. The repeatability for each point is indicated by error bars. For installation conditions, see figure legends..

When the valve is moved closer to the USM, it is seen, by inspection of the repeatability in Figure 6, that the meter still performs well with respect to noise immunity. At the highest flow velocity combined with the highest differential pressure across the valve, however, the repeatability is increased to 0.3%. Even though the meter measures the volume flow rate well within the specified 0.5% from the reference, this indicates that the noise generated by the valve is beginning to deteriorate the repeatability of the meter.

To fully test the noise suppressing algorithm, the USM was also tested with the valve placed upstream. At this installation the SNR will decrease significantly compared to all other installations in the test. In addition to generating noise, the valve is setting up strong secondary motion (swirl) in the gas, making it difficult to measure the volume flow rate accurately. Installations like this are not recommended due to both flow profile disturbances and generation of ultrasonic noise.

Figure 7 shows the results from the installation where the valve is placed 5D upstream of the USM, see Figure 1, installation 3. The pressure at the USM is approximately 100 bar. The SNR for the worst cases in this installation is as low as 0.7 (-3 dB). At this installation the volume flow rate measured deviated more from the reference than what is seen at the other installations. Setups described in the test matrix, where valve noise and secondary flow have made the meter unable to measure correctly, are not included in the figure.

The figure shows that

– the deviation is within ±0.5% for all points included.
– the repeatability is of the order of 0.25% for the point with highest velocity.
– the repeatability is of the order of 0.1% for all other points.

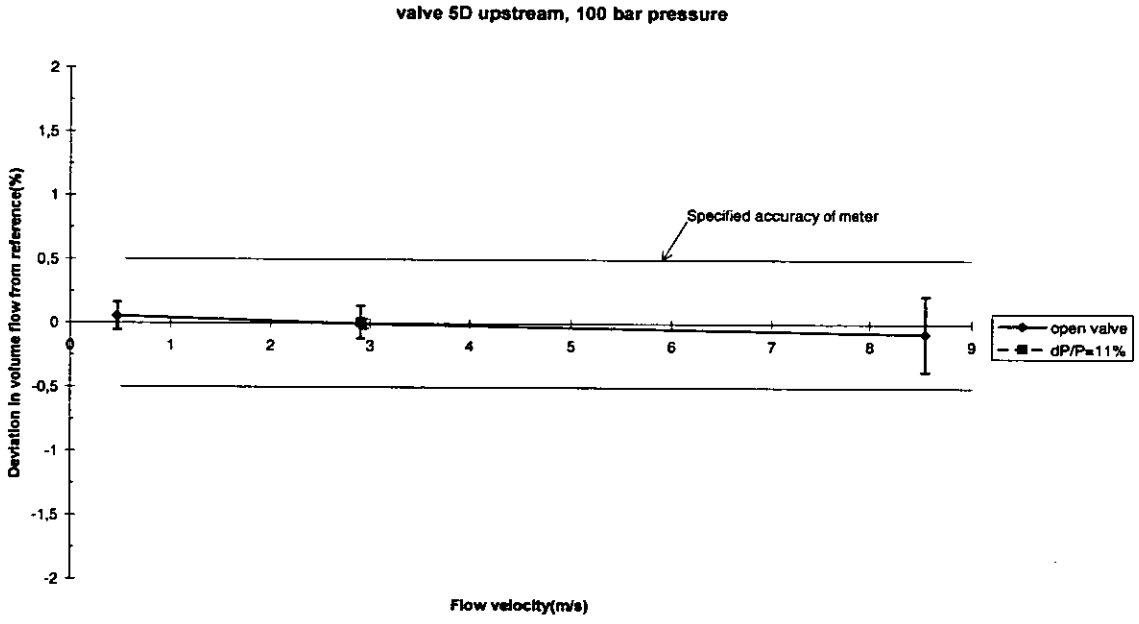

Figure 7: The deviation from the reference. The different curves represent various differential pressure across the valve. The repeatability for each point is indicated by error bars. For installation conditions, see figure legends.

As can be seen in Figure 7, the repeatability is getting worse as the differential pressure across the valve and the flow velocity increases. If the flow velocity is kept constant and the differential pressure is increased, the value of the repeatability will increase. If the differential pressure is kept constant and the flow velocity increased, the same phenomenon is observed. The algorithm is clearly stretched to its limit in this case. The SNR limit for the algorithm seems to be about 0.9 (-1 dB).

It is important to notice that the gas flow velocity through the 6" valve is 4 times higher than the gas flow velocity through the USM. This is due to the reduced cross section in the valve. The gas flow velocity through a 12" valve will be significantly lower, compared to a 6" valve, at the same gas volume flow. A 12" valve will therefore probably generate less ultrasonic noise at the same volume flow. This may make it possible to increase the volume flow through the USM further, before the SNR limit of the meter is reached.

Table 2 sums up the results from the tests at K-Lab, and shows at which setups the USM measures satisfactorily.

Table 2: Schematic result matrix for the USM valve noise testing at K-Lab 1997.

Valve position relative to meter, see Figure 1	P	v	ΔP/P	Deviation	Repeatability
10D DOWN	20 bar	All setups		OK	OK
	100 bar	All setups		OK	OK
5D DOWN	100 bar	0.5 m/s	10%	> 0.5%	OK
		9 m/s	20%	OK	> 0.2%
		All other setups		OK	OK
5D UP	100 bar	0.5 m/s	≈ 0%	OK	OK
			3%	> 0.5%	>0.2%
		3 m/s	≈ 0%	OK	OK
			10%	OK	OK
			15%	> 0.5%	OK
		9 m/s	≈ 0%	OK	> 0.2%
			10%	> 0.5%	> 0.2%

5. CONCLUSION

Based on the foregoing discussion it is concluded that the new noise suppressing algorithm implemented in the FMU-700 ultrasonic meter is able to separate the signal from the noise for SNR as low as 0.9 (-1 dB). This gives accurate measurements of the signal transit times and thus accurate calculations of volume flow even when ultrasonic noise generators such as flow control valves are present in the vicinity of the meter.

Other valves will most likely have other characteristics with respect to noise level and frequency content of the noise. The results obtained in this test is therefore not directly applicable to other valves.

ACKNOWLEDGEMENTS

A special thank to Reidar Sakariassen and the technical staff at K-Lab for the help and advice they have provided during the test period and in the preparation of this paper.

REFERENCES

[1] FRØYSA K.-E., LUNDE P., SAKARIASSEN R., GRENDSTAD J. & NORHEIM R. "Operation of multipath ultrasonic gas flow meters in noisy environments". Proceedings North Sea Flow Measurement Workshop, Peebles, Scotland, October 28th to 31st, 1996.

[2] LYGRE A., LUNDE P. & FRØYSA K.-E. "Present status and future research on multipath ultrasonic gas flow meters". GERG Technical Monograph TM8, Groupe Européen de Recherchers Gazières, Groningen, The Netherlands, 1995.

[3] SAKARIASSEN, R., Private communications, August 1997.

[4] AGA Report No. 9, draft 5. "Measurement of gas by ultrasonic meters". Transmission Measurement Committee, 1997.

NSFMW.97

North Sea FLOW Measurement Workshop

Paper ~~18~~: 3.5

DRY CALIBRATION OF ULTRASONIC GAS FLOW METERS

Authors:
G. de Boer, Instromet Ultrasonics B.V., The Netherlands
J. Lansing, Instomet Ultrasonic Technologies Inc, USA

Organiser:
Norwegian Society of Chartered Engineers
Norwegian Society for Oil and Gas Measurement
Co-organiser:
National Engineering Laboratory, UK

DRY CALIBRATION OF ULTRASONIC GAS FLOW METERS

G. de Boer - Instromet Ultrasonics B.V. - The Netherlands
J. Lansing - Instromet Ultrasonic Technologies Inc. - Texas, U.S.A.

ABSTRACT

At present in most European countries it is customary that turbine meters, or the newer ultrasonic gas flow meters, when used in fiscal metering or custody transfer metering applications, are calibrated in a test facility by comparison to standards or reference devices.

For reason of practical and operational drawbacks, costs involved and availability of only a limited number of calibration facilities, another way of meter verification is advantageous. For orifice metering the practice of dry calibration is well established; that is, meter verification is based upon examination of the geometry and installation of the orifice plate and a function check of the read out devices. Although for turbine meters a flow (wet) calibration may be a necessity, it will be shown that ultrasonic gas flow meters can be dry calibrated in the same way as orifice meters.

As a basis for the acceptance of a dry calibration procedure for ultrasonic gas flow meters, a sensitivity analysis of the relevant variables with respect to the meter's accuracy is presented. Further test results are presented that demonstrate the feasibility of the concept of dry calibration applied to ultrasonic gas flow meters.

INTRODUCTION

Ultrasonic gas flow meters, especially multi path ultrasonic flow meters, become more and more accepted for custody transfer applications. For these applications a calibration or verification of the metering device is often a legal requirement, or a requirement based on the contract between the buying and the selling partner. Ideally such a calibration or verification is performed by comparison of the meter with a standard or reference. Traceability of the standards used to national or international standards is a prerequisite.

Unfortunately, facilities where large gas flows are available, can be controlled and can be measured precisely with standard meters are very rare and also expensive to operate. For the operator it is quite a burden when a meter has to be taken out of the line and sent to a calibration facility for a calibration or verification. Costs for the calibration itself are already high and in addition to this the operators have to face the cost for taking the meter out of the line, transportation and having the production facility shut down. Another restriction, especially for calibrating large size meters, is that test facilities may be limited to flow large flow rates only a short time (some months) a year.

The advantage of a meter being calibrated at a calibration facility is that the owner will get a certificate with a precise statement about the accuracy of the meter and second, it allows to adjust the meter in order to minimize any measuring error or bias relative to the standards used.

However, considering costs and operational drawbacks, the idea of a calibration or verification that does not require a meter has to be sent to a calibration facility is an attractive idea. Similar practices are well established for orifice meters: meter verification is based upon examination of the geometry and installation of the orifice plate and a function check of the read out device. This practice has gained world wide acceptance.

Principle of an ultrasonic flow meter

The principle of an ultrasonic flow meters is illustrated in figure 1.

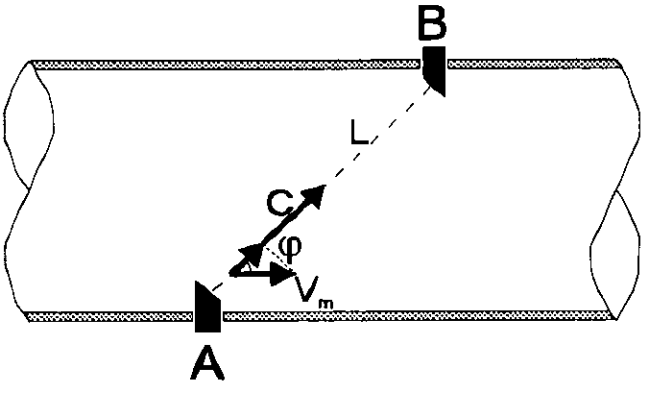

Figure 1: principle of an ultrasonic flow meter

Two transducers capable of emitting and receiving ultrasonic sound pulses are installed in the flow line in such a way that the ultrasonic sound pulses emitted from one transducer can be received by the other transducer, thus creating an acoustic path. The transducers in turn emit and receive pulses. The ultrasonic sound pulses travel, with respect to the gas, at the speed of sound. The velocity of a sound pulse along the acoustic path traveling downstream is increased with the projection of the gas velocity onto the acoustic path. The velocity of the sound pulse traveling upstream along the acoustic path is decreased with a projection of the gas velocity onto the acoustic path. This results in travel times for the upstream and downstream direction as:

$$t_{down} = \frac{L}{C + V_m \cos\varphi} \qquad (1)$$

$$t_{up} = \frac{L}{C - V_m \cos\varphi} \qquad (2)$$

where

L	:	length of the acoustic path
C	:	speed of sound in the medium (gas)
V_m	:	velocity of the moving medium (gas)
φ	:	angle between acoustic path and a vector representing the direction in which the medium moves

Using (1) and (2) the following expression for the measured gas velocity can be derived:

$$V_m = \frac{L}{2\cos\varphi}\left(\frac{1}{t_{down}} - \frac{1}{t_{up}}\right) \qquad (3)$$

Important to notice is that the speed of sound in the gas is eliminated in this expression. This means that the measurement of the gas velocity is independent of the gas properties such as pressure, temperature and gas composition.

Flow measurement with single path meters

To measure the gas volume flow the gas velocity must be multiplied with the cross section of the pipe. When the gas velocity is equal over the whole cross section, i.e. has a uniform flow profile, the flow calculated in this way would be the exact value. As this is not the case by law of nature we need to correct with a factor K which is related to the shape of the flow profile.

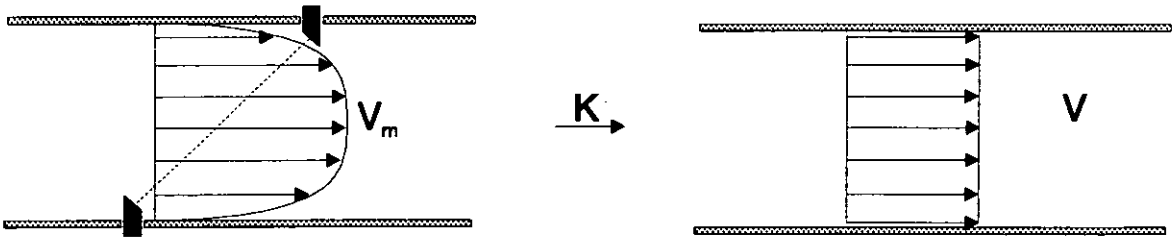

$$V = V_m \cdot K \cdot$$

Figure 2: Flow profile correction factor

V_m represents the average gas velocity as perceived by the ultrasonic flow meter. This is the linear weighted gas velocity averaged along the acoustic path.

This results in the following expression for the gas flow:

$$Q = \frac{L}{2\cos\varphi} \cdot A \cdot K \cdot \left(\frac{1}{t_{down}} - \frac{1}{t_{up}} \right) \qquad (4)$$

where

A : cross section of the pipe
K : flow profile correction factor

From studies, literature and our own research, Instromet established a relationship between the Reynolds number and the flow profile correction factor (also referred to as Reynolds factor) K, which is shown in figure 3.

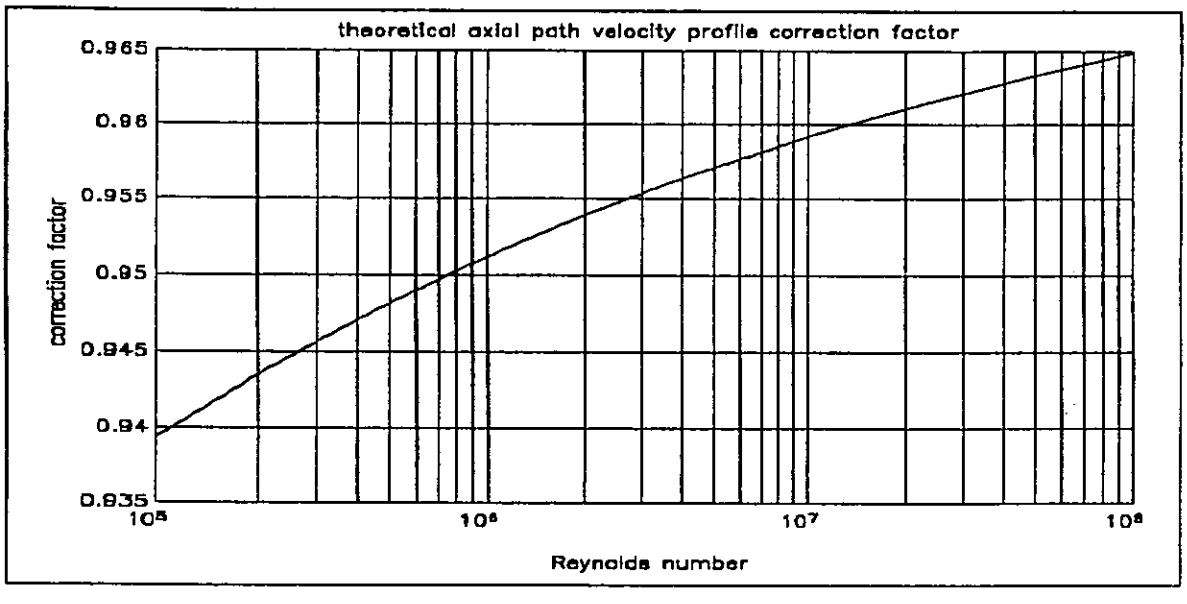

Figure 3: Graph of profile correction vs. Re

This is applicable to a single path meter with an acoustic path through the center of a circular pipe. Dependent on practical circumstances, the flow profile may show some variation resulting in an uncertainty in the flow profile correction factor K. This uncertainty can be estimated based on the residual errors as observed in numerous tests, as shown in figure 4. From this graph it appears that a realistic estimate for the uncertainty in the Reynolds correction factor for a single path meter would be approximately 1 %.

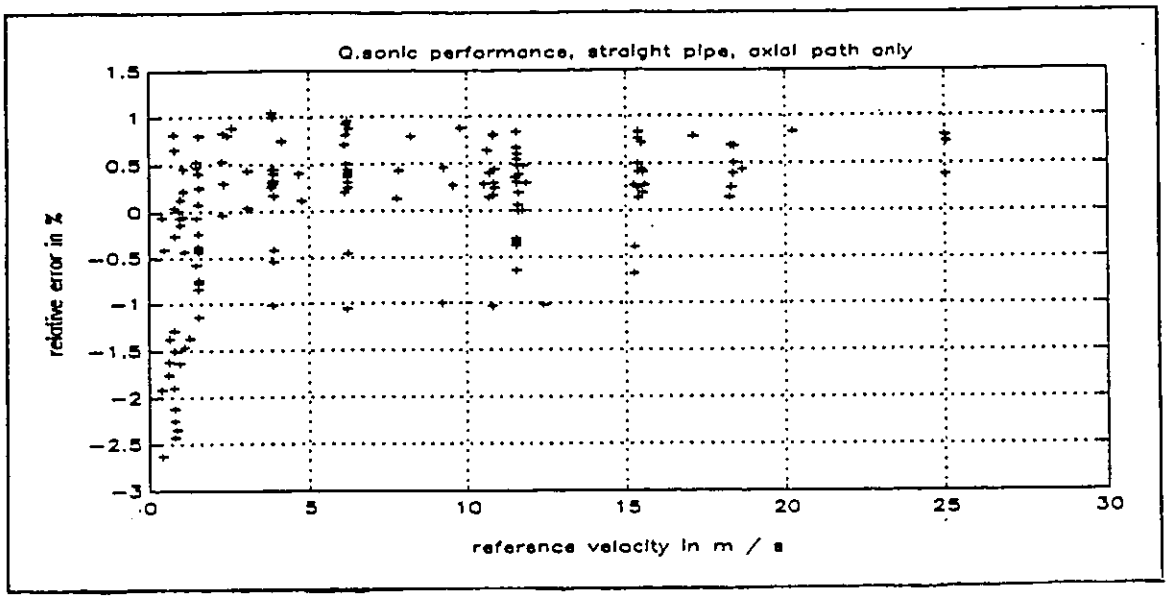

Figure 4: Graph of profile correction error of single path us meter

Flow measurement with multi path meters

Custody transfer applications typically require the use of multi path meters. The reason is the uncertainty of the profile correction factor for a single path meter is not acceptable for custody transfer applications. Multi path ultrasonic flow meters, by implementation of integration techniques, allow to use the data of multiple acoustic paths to improve the accuracy of the flow profile correction. Formally this can be represented with the following expression.

$$Q = \left\{ \frac{L}{2\cos\varphi} \cdot A \cdot K \cdot \left(\frac{1}{t_{down}} - \frac{1}{t_{up}} \right) \right\} \cdot F \qquad (5)$$

This expression is identical to that of a single path meter except that the part between brackets $\{\ \}$ represents the integration using all acoustic paths.

This expression also includes a multiplier, (F) which represents a correction factor. This correction factor typically has a default value of approximately 1 but can be adjusted based on a flow calibration of the meter in order to minimize the meter error.

DRY CALIBRATION

A dry calibration of a flow meter is not a calibration in the proper sense of the word, since it is not a check of the result - the measured gas volume / flow - based upon comparison with a standard or reference device and if necessary followed by an adjustment. The word "verification" would be more appropriate .
Similar to orifice practice a (dry) calibration of an ultrasonic gas flow meter is based on:

a) verification of geometry
b) measuring differential pressure or travel time differences
c) using tables, equations or mathematical expressions to relate a gas flow to the measured variable.

Ad a) The relevant geometry parameters can be measured for an ultrasonic gas flow meter just as accurate as for an orifice meter. Further, for an ultrasonic gas flow meter, the impact of geometry uncertainty can be assessed and analyzed completely, using fairly simple mathematics, as will become apparent in the following section.

Ad b) It should be appreciated that, using state of the art electronics and good quality quartz oscillators, time measurements can be performed with excellent accuracy and stability, equal or superior to differential pressure transmitters. As an example that demonstrates the basic stability of Instromet's ultrasonic gas flow meters figure 5 is included. This figure shows two error curves:

- one as found initially when the meter was new
- one approximately 2 years later and after the meter having been in service.

Due to the requirements of the application this meter was only calibrated over the low and of its range. It shows very good reproducibility; some more variation (normally random) at the very low flow end is normal and acceptable.

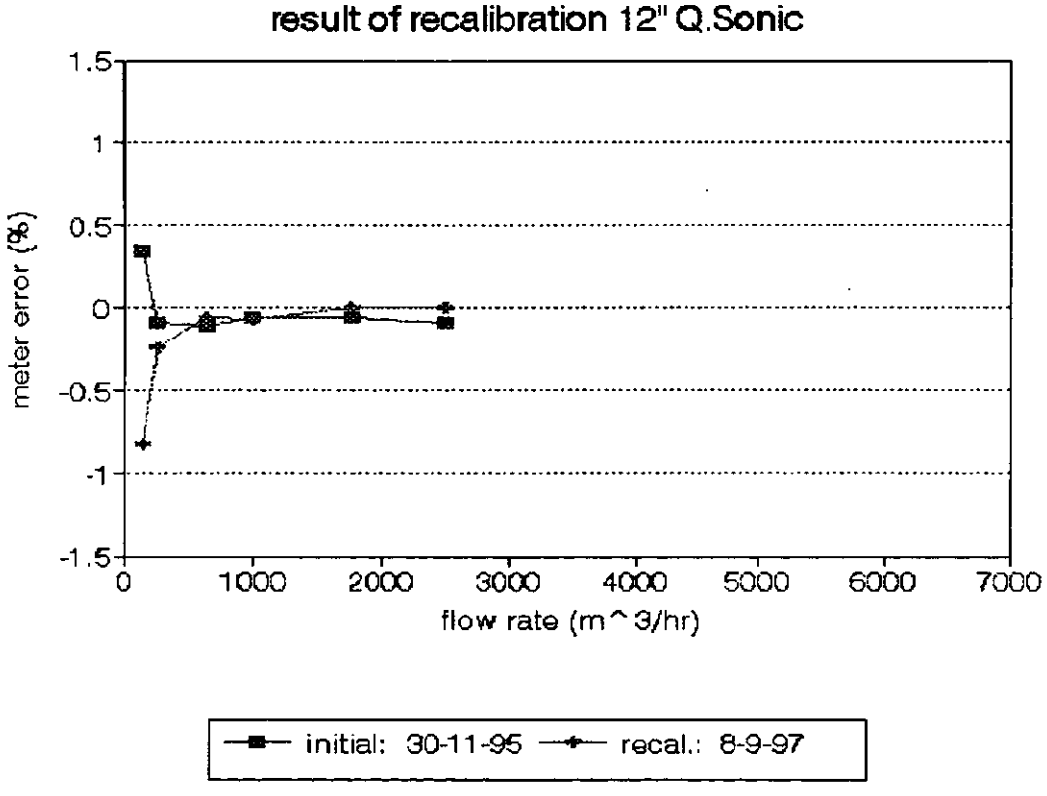

Figure 5: two error curves

Ad c) Discharge coefficients for orifices and profile correction factors for ultrasonic gas flow meters are based on research. For the ultrasonic meters manufactured by Instromet a fast growing database of empirical data is available. Some statistical results will be presented in the following sections.

UNCERTAINTY OF DRY CALIBRATION

As a general basis for the concept of dry calibration we will investigate the uncertainty in the measured gas flow (volume or flow rate). Using equation (5) we can calculate the impact of the uncertainty of each individual parameter or measured value with respect to the uncertainty of the measured gas flow. In this section we will examine the contribution of these individual parameters and measured values.

The parameter F is a correction factor used only when, - based on a flow calibration-, the reading of the meter is adjusted. In case of a dry calibration this parameter is set to its default value, based upon experience with numerous flow calibrations. In case of a dry calibration this parameter is a constant, therefore it is not associated with uncertainty. This may appear to be a contradiction, since based on a flow calibration this variable may have assigned a value that is different from the default value. However, in case of a flow calibration, this parameter corrects (compensates) the error due to all other parameters and variables. The data presented in this paper is based upon the results of numerous flow calibrations of ultrasonic meters. As a result of these flow calibrations the default value of the correction factor F is adjusted. Since the variation in the correction factors as found reflect the uncertainty due to the geometry and dimension parameters resulting from the manufacturing procedures as currently used as well as the other sources of uncertainty, the frequency distribution of this adjustment factor is a good tool to verify the overall uncertainty for meters manufactured without flow calibration.

Uncertainty of profile correction factor

The Reynolds (profile) correction factor for a single path meter is estimated, based on the graph as presented in figure 4, to have an uncertainty of ± 1.0%. Based upon Instromet's research and test results with Instromet's multi path meters and the path configuration as implemented, we estimate the uncertainty of the Reynolds (profile) correction factor to be approximately 0,3% for a 5 path meter and approximately 0,4% for a 3 path meter.

Uncertainty due to meter body geometry and dimensional variations

As far as the geometry and dimension of the meter body is concerned the relevant parameters that have an impact with respect to the accuracy of an ultrasonic flow meter are (as can be seen from equation 5) :

L	:	acoustic path length
φ	:	angle of acoustic path
A	:	cross section of the pipe

The acoustic path parameters are related to the position of the front side of the ultrasonic transducers, the surface that emits and receives the ultrasound pulses. This position is determined by means of the nozzles (parts marked (C) in figure 6) where the transducers are installed, in particular the center point (figure 6 (3)) of the face of the nozzle, that is used as a reference point.

In order to assess the uncertainty of the acoustic path parameters we need to take a closer look at the manufacturing process. For simplicity we will look at a single reflection path and use the dimensions of a 16" size meter body as an example.

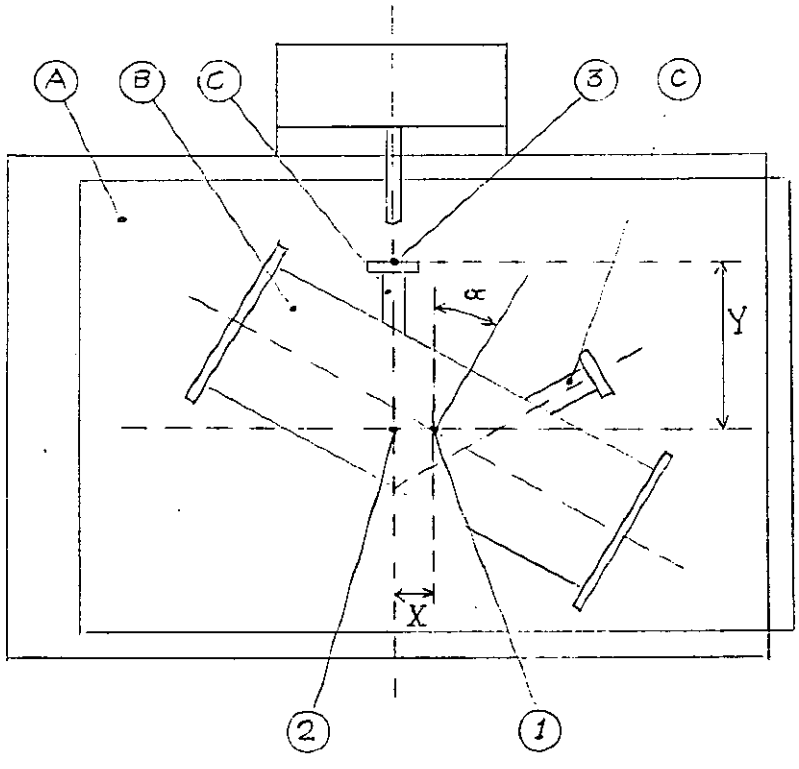

Figure 6: set up for meter body machining

Figure 6 shows a meter body (B) as installed on the support of numerical controlled machining equipment (A). Initially the meter body is positioned so that the center of the body (1) is aligned with the reference point (2) of the machining equipment, having coordinates (0,0).

In order to manufacture the meter body, in particular to machine nozzle C to the dimensions as required, the meter body is rotated over an angle α and the reference point of the front of the nozzle (3) is defined and machined using coordinates X and Y. X

represents a translation of the support and Y represents the distance of the nozzle face with respect to the reference point (0,0) of the machining equipment.

These machining parameters are calculated before the machining operation starts and checked during the manufacturing process of each meter body. The result is reported in a certificate provided by the machine shop. Certification of the accuracy of this data and traciblity with respect to national standards, by an independent body, is an option. Based on the machining parameters as reported, the actual path lengths and angles are calculated.

Data applicable to a 16" Q.Sonic used as an example are as follows:

Nominal bore is	406,4 mm
For a single reflection path applies:	
Nominal path angle is	60 degrees
Nominal path length is	469,27 mm

The reference point of the nozzles for the transducers is defined as:

angle	:	60 degrees
X	:	101.60 mm
Y	:	293.29 mm

We estimate that the value of these parameters as realized and reported are subject to an uncertainty as:

angle	:	± 0.05 degree
X	:	± 0,1 mm
Y	:	± 0,1 mm

For the uncertainty of the inner diameter we assume a practical value of ± 0,2 mm, although, depending on manufacturing technology this can be improved when necessary.

The contribution of each parameter's uncertainty can be calculated according to equation (5) as:

path length L	:	± 0,06 %
1/cos φ (path angle)	:	± 0,15 %
cross sectional area A	:	± 0,1 %

When all these factors add up to a worst case situation, the uncertainty due to the meter body geometry and dimensions would be ± 0,3 %. However, since each of these contributions are due to independent sources of error, the total error calculated according to the root mean square rule as 0,2% is more appropriate.

Uncertainty due to time measurement

The uncertainty due to the measurement of the travel times can be assessed by distinguishing (similar to DP transmitter practice) between the zero reading and gain errors.
The zero error is related to the resolution of the travel time measurements and small offsets in the travel time measurement. This could introduce a travel time difference being measured even when the gas flow velocity is zero. From equation (4) it can be derived that the following expression is applicable:

$$\delta V = \frac{C^2 \cdot \delta t \cdot \tan(\varphi)}{4D} \qquad (6)$$

where

D	:	meter body inner diameter
C	:	speed of sound in the gas
φ	:	acoustic path angle
δt	:	error in differential time measurement
δV	:	error in measured gas flow

The uncertainty in the travel time measurement is at maximum 10 ns. In this example (16" meter body) and using:

C	=	400 m/s
D	=	0,4 m
φ	=	60 degrees

the resulting uncertainty is calculated to be 1,6 mm/sec (gas velocity!)

Using the gas velocity range that can be handled with our ultrasonic flow meters (maximum gas velocity 30 m/s) this can be converted to a relative value (percentage). The next figure (7) presents a graph showing the absolute error (gas velocity error in m/s) and the relative error (in %) as a function of the gas flow. In order to be also applicable to smaller meter sizes the value for the absolute gas velocity error in this figure has been taken as 5 mm/s.

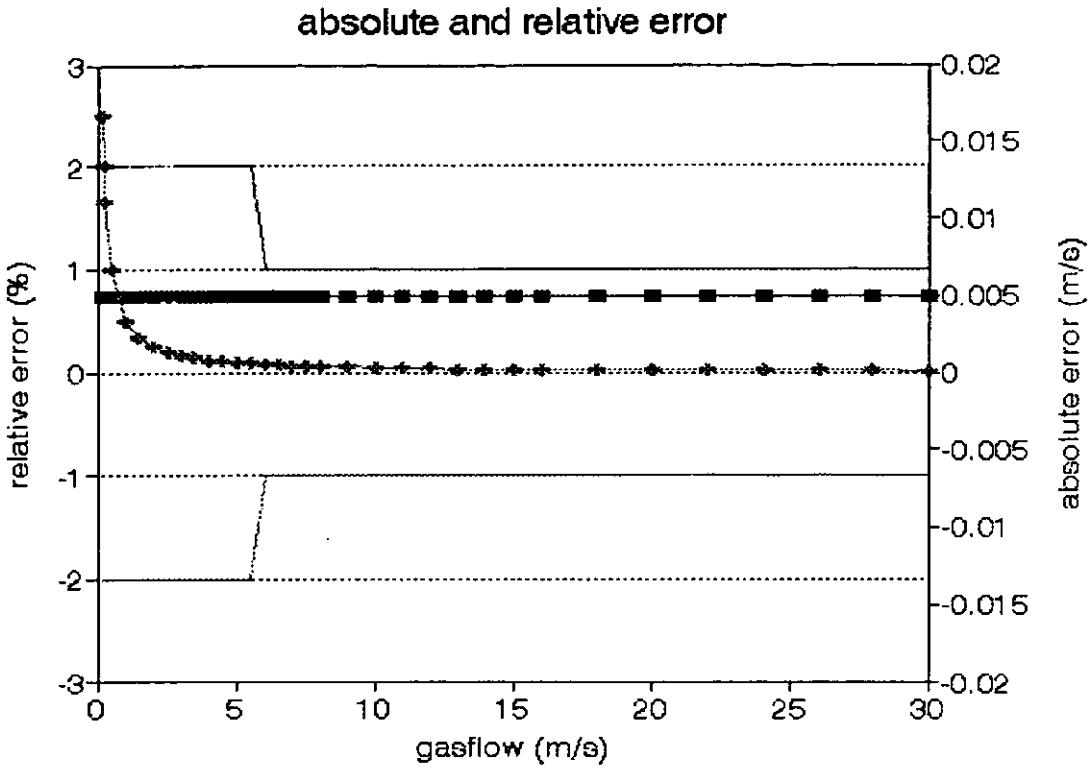

Figure 7: absolute and relative error due to travel time uncertainty / offset

This graph shows clearly that the uncertainty of the travel time measurement is the dominant factor at low flow rates. This imposes a limitation on the low side of the operating range but has no significant effect in the normal operating range.

The travel time measurement is related to a clock signal. When this clock is fast or slow it would have a proportional impact with respect to the measured gas flow. However since this clock is a high stability quartz clock (accuracy ± 50 ppm or 0.005 %) this can be ignored.

Total meter uncertainty

In the previous sections it has been shown that the significant sources that contribute to the total measurement uncertainty of an ultrasonic flow meter are:

Flow profile correction factor K	± 0,3 %
Meter body geometry (rms)	± 0,2 %.

Worst case the combination of both sources of uncertainty would result in a total uncertainty of 0,5 %. Since these are independent sources of uncertainty it is justified to estimate the total uncertainty using the square root rule to calculate total uncertainty as

$$\sqrt{0{,}3^2 + 0{,}2^2} = 0{,}36\%$$

This number is of the same order of magnitude as the uncertainty of the best flow calibration facilities (0,25 - 0,3 %).

Flow calibration results

From many calibrations we calculated the frequency distribution of the magnitude of the adjustment that appeared to be necessary in order to center the meter error around the zero line. This frequency distribution is presented in figures 8 up to and including 11. These graphs confirm the calculated uncertainty to be approximately 0,5 %. Figure 8 presents the frequency distribution of the adjustments for all sizes of meters.

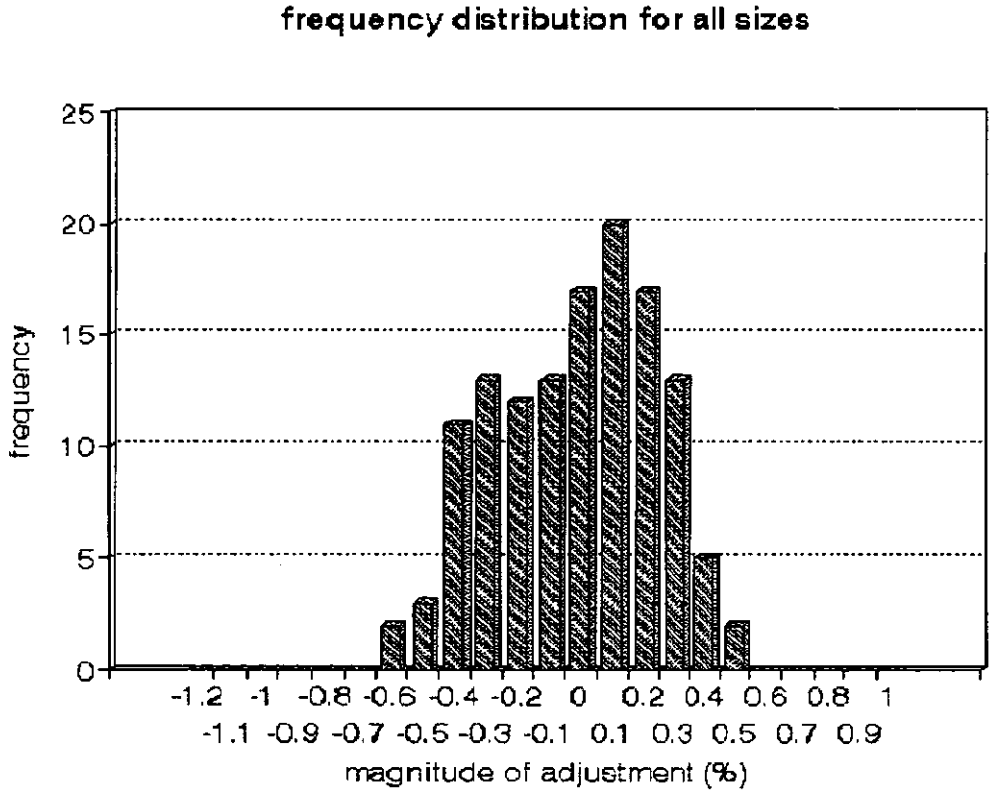

Figure 8: frequency distribution of meter adjustment for various sizes

Figure 9 presents the frequency distribution of the adjustments for meters of 12" nominal size.

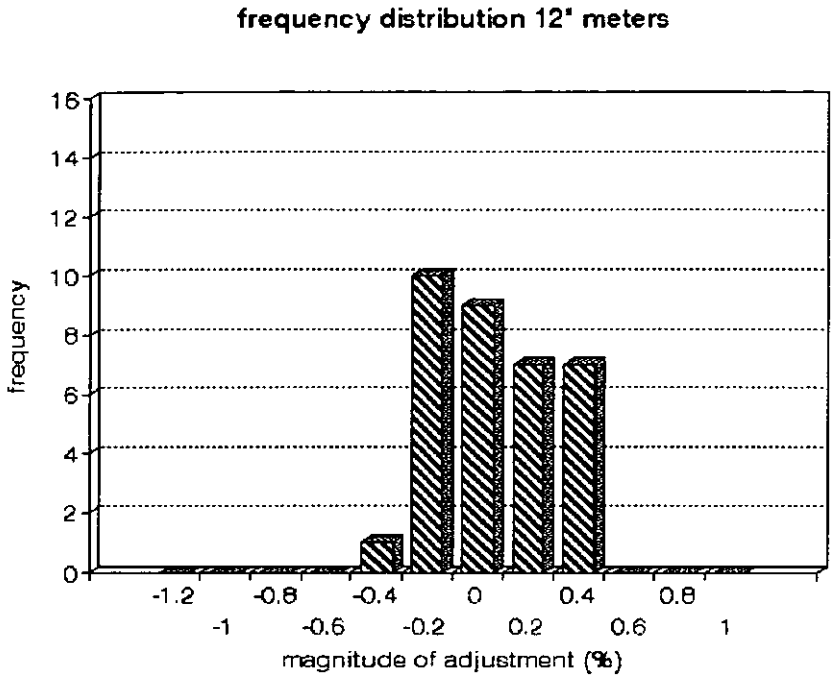

Figure 9: frequency distribution of meter adjustments for 12" meter

Figure 10 presents the frequency distribution of the adjustments for meters of 16" nominal size.

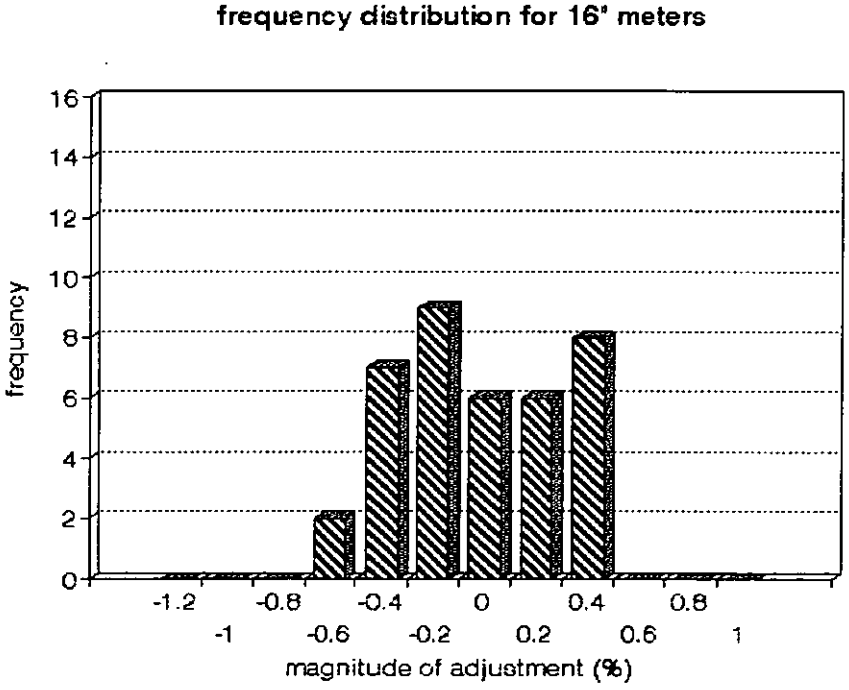

Figure 10: frequency distribution of meter adjustments for 16" meters

Figure 11 presents the frequency distribution of the adjustments for meters of 20" and 24" nominal size.

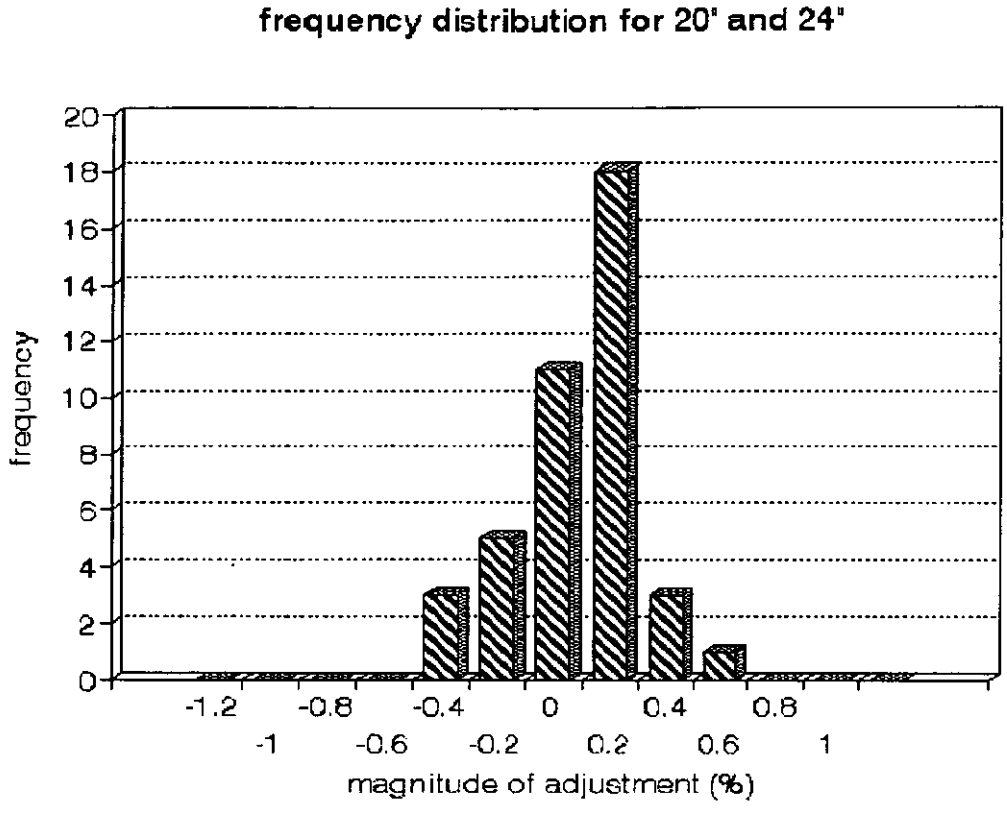

Figure 11: frequency distribution of meter adjustments for 20" and 24" meters

The preceding graphs (figures 9, 10 and 11) show that the frequency distribution of the adjustments is consistent for various nominal sizes. This confirms that the concept of dry calibration, using the calculation methods as implemented in the nominal sizes that have been tested, may be extrapolated to larger sizes as well.

The fact that mainly the geometry and dimensional parameters are determining the accuracy and uncertainty of our ultrasonic meters is further illustrated by the graphs in figures 12 and 13. Both graphs apply to a series of identical meters that have been manufactured in one batch.

Figure 12 shows the calibration result of 6 16" 5 path ultrasonic meters (Q.Sonic) before any adjustments have been made. The meter bodies (spoolpieces) are manufactured as one batch. The electronics and transducers are taken at random from our production and assembled with the spoolpieces.

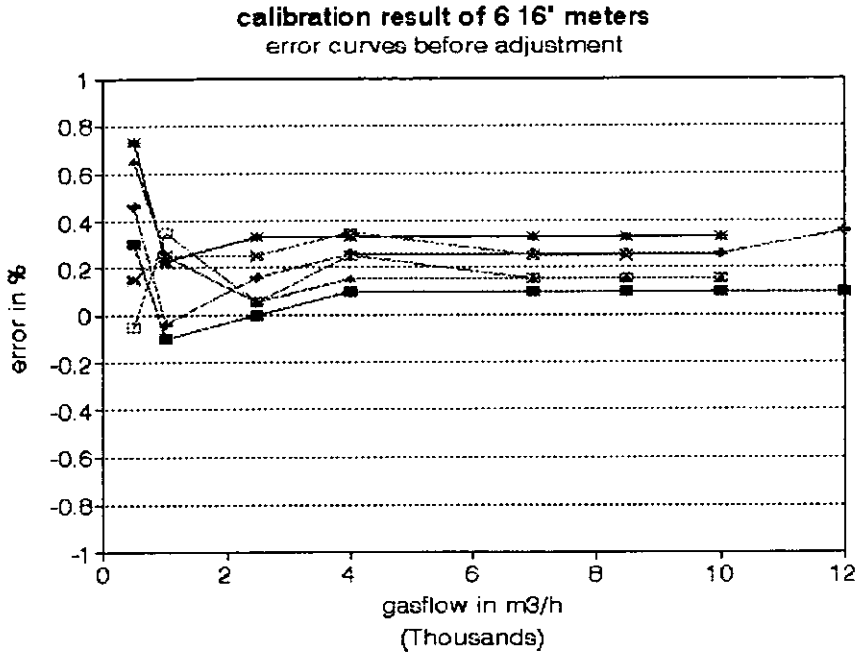

Figure 12: error curves of 6 16" meters (before adjustment)

Figure 13 shows the magnitude of the adjustment of a series of 20" meters.

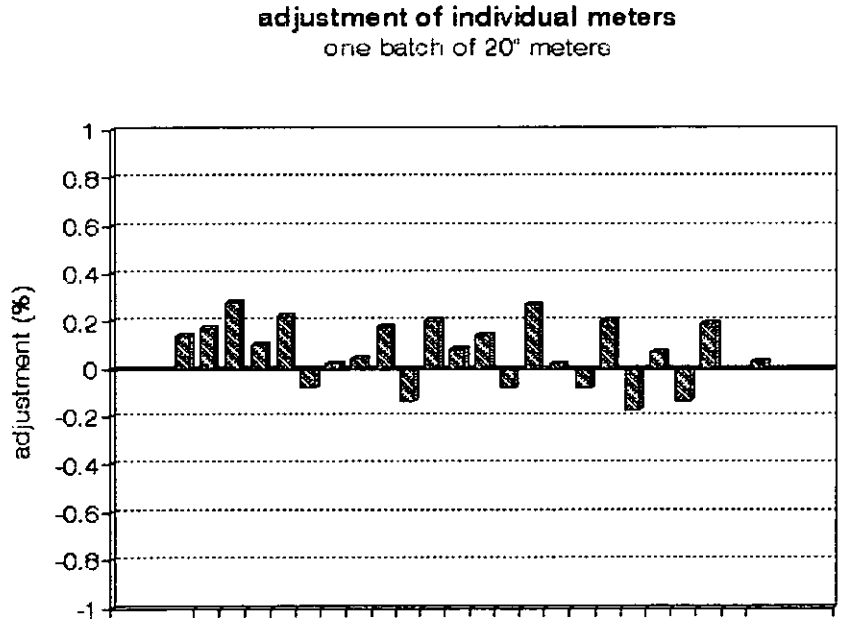

Figure 13: meter adjustment for a batch of identical meters

Both figures (12 and 13) demonstrate that the spread in the average error of individual meters due to manufacturing tolerances is in line with the rms value of ± 0,2 % as calculated before.

DRY CALIBRATION PROCEDURE

In order to implement the concept of dry calibration for our ultrasonic flow meters, Instromet has developed an extensive dry calibration procedure. In this section we will discuss some of the essentials of this procedure.

In the preceding sections it has been shown that geometry and dimension of the meter body and the Reynolds (profile correction) factor are the relevant sources of uncertainty.

The meter body geometry and dimensions reflect in the acoustic path geometry and are calculated using the data reported in the protocol provided by the machine shop where the spoolpiece is manufactured.

When the electronics and ultrasonic transducers are installed on the meter body to complete the ultrasonic gas flow meter, a function test is performed. This test verifies that the meter performs well with respect to all its functions, such as emitting, receiving and detecting ultrasonic sound pulses and the accuracy of the travel time measurement by means of a check of the frequency of the quartz clock.

Further this function test includes a zero flow test and a check based on the measured sound velocity in the gas. In order to perform these tests the ultrasonic gas flow meter is fitted with blind flanges and pressurized with compressed air or nitrogen.

Zero check

Since the meter is fitted with blind flanges, there cannot be any gas flow, and the gas velocity observed on all the acoustic paths should be zero. This test can also be performed with an ultrasonic gas flow meter installed in a practical application, provided that the meter can be isolated. However utmost care should be taken to avoid misleading results since it is our experience that isolation valve are not always perfect and small leakages create minimal but measurable gas flows. Also thermal driven convection currents may easily appear and be perceived as a gas flow.

Speed of sound check

The speed of sound check can be performed as either a function check or a verification. When the meter is to be flow calibrated a function check is sufficient and the check can be performed with compressed air as medium.
For the purpose of verification (dry calibration) the meter needs to be checked with a gas of a known composition, nitrogen is a practical choice. Further accurate temperature and pressure measuring devices must be installed in order to enable a precise calculation of the expected speed of sound at the pressure and temperature at hand. Sufficient time should be allowed in order to reach a state of thermal equilibrum.

The observed speed of sound compared to the expected value will reveal any error in the acoustic path length or the travel time measurement, whereas the latter is highly unlikely since the frequency of the quartz clock has been checked before this test.

The speed of sound of individual acoustic paths may show some variation, but the averaged value is very close to the expected value. Typically the observed value and the expected value agree as close as 0,1 %. This test may be performed in practical applications as well, but it is most critical to know the exact gas composition at the time of the test. Also accurate temperature and pressure measurements are a prerequisite.

CONCLUSION

As presented the concept of dry calibration can be applied to our ultrasonic gas flow meters in very much the same way as with calibrations of orifice meters. Based on the uncertainty analysis in this paper and supported by the results of flow calibrations the uncertainty is of the same order of magnitude of that of the best test facilities. We consider it justified to claim that the concept of dry calibration applied to our ultrasonic gas flow meters is feasible in order to assure the accuracy of the meter as specified. Based on the test results available the concept of dry calibration may as well be extrapolated to larger sized meters.

NSFMW.97

North Sea FLOW Measurement Workshop

Paper ~~19~~: 3.6

PERFORMANCE TESTING OF ULTRASONIC FLOW METERS

Authors:
Terrence A. Grimley, Southwest Research Institute, USA

Organiser:
Norwegian Society of Chartered Engineers
Norwegian Society for Oil and Gas Measurement
Co-organiser:
National Engineering Laboratory, UK

Performance Testing of Ultrasonic Flow Meters

Terrence A. Grimley
Southwest Research Institute
San Antonio, Texas, U.S.A.

ABSTRACT

This paper presents a portion of the ultrasonic flow meter research results from work sponsored by the Gas Research Institute (GRI) and the U.S. Department of Energy, conducted at the Metering Research Facility (MRF). Single and multipath 8-inch diameter ultrasonic flow meters were evaluated in baseline flow conditions, and in other piping installations with and without flow conditioners. In addition, tests were conducted to assess the effect on measurement accuracy of configurations with a thermowell upstream of the meter.

The results reported in this paper are intended to aid in the definition of installation requirements for single-path and multipath ultrasonic flow meters. The meters were installed in various piping configurations with single- or double-elbow combinations upstream of the meter, and in configurations with a thermowell upstream of the meter. Tests were performed both with and without a flow conditioner installed upstream of the test meters.

Baseline tests were conducted to define a reference condition to which the other piping configurations could be compared. The results for the baseline tests suggest that the velocity profile was not fully developed 59 pipe diameters downstream of a single, long-radius 90° elbow, and that the test meters were sensitive to the subsequent profile development.

The test results for the 8-inch diameter multipath flow meters indicate that, depending on the meter type and location relative to a flow disturbance, flow conditioners can improve the measurement accuracy. However, combinations also exist where the inclusion of a flow conditioner in the piping configuration would result in increased measurement errors.

The results for the single-path meters show potential for achieving flow measurement accuracies better than 0.5% in well-ordered flow fields. The results for single-elbow and two-out-of-plane-elbow configurations demonstrate shifts in flow measurement errors of 1 to 4% relative to the baseline tests. The results also indicate the level of improvement achievable when a flow conditioner was included in the piping configuration.

INTRODUCTION

Ultrasonic flow meters derive the volumetric flow rate of gas from time-of-flight measurements of ultrasonic energy pulses transmitted through the flow stream. Because the accuracy of the flow rate determination is a function of the meter design and calculation method, the upstream piping requirements for an ultrasonic flow meter may differ from those of more traditional measurement devices. For instance, orifice meters require symmetric, non-swirling flow to measure flow rate to within the accuracy of the established discharge coefficient equations. American Gas Association (A.G.A.) Report No. 3[1] recommends that a minimum

length of straight pipe be placed upstream of an orifice meter in order to establish proper flow characteristics, so that accurate flow measurements can be obtained. The sensitivity of the orifice meter to flow disturbances increases as the orifice size (i.e., beta ratio, β) increases (Morrow[2]) because there is less flow blockage and, therefore, less reshaping of the velocity profile caused by the presence of the plate. Turbine meters also reshape the flow profile by forcing the flow through an annulus. Even with their ability to reshape the inlet flow profile, turbine meters are sensitive to asymmetry in the velocity profile (Dijsterlbergen and Bergervoet[3]). Furthermore, A.G.A. Report No. 7[4] requires the use of a flow conditioner with a turbine meter to eliminate flow swirl at the meter inlet. Since an ultrasonic meter has essentially no flow blockage that can affect the inlet flow, the meter does not change the flow profile. Therefore, a meter of this type must rely on robust calculation methods to accurately determine the flow rate, based on the portion of the flow sampled by the meter.

In the design of multipath ultrasonic flow meters, manufacturers have attempted to optimize the meters so as to reduce their sensitivity to flow disturbances. If the meters can correctly compensate for all flow disturbances, then the need for flow conditioners is eliminated. However, the use of flow conditioners in combination with ultrasonic flow meters remains of interest, since there is little published documentation on how flow conditioners affect the performance of multipath ultrasonic flow meters. The potential benefits of flow conditioners have been mostly inferred from experience with other meter types. There is also interest in using flow conditioners in combination with less-expensive, single-path ultrasonic meters as a cost-effective alternative to multipath flow meters. Again, there are limited test data available to confirm the performance of single-path meters when used with flow conditioners.

The results presented in this paper are from a test plan designed to experimentally determine the performance of 8-inch diameter single-path and multipath ultrasonic flow meters when installed in various piping configurations and when used in combination with a flow conditioner. The meter tests described here were run with single- and double-elbow piping combinations upstream of the test meters. Tests were performed both with and without a flow conditioner installed upstream of the test meters.

TEST METHODS

Tests for this program were conducted in the GRI MRF High Pressure Loop (HPL) located at Southwest Research Institute. The meters were installed in the Test Section of the HPL and tested with transmission-grade natural gas. Data were collected simultaneously from the ultrasonic meters and from the HPL critical flow nozzle bank, which served as the flow reference. The five binary-weighted sonic nozzles were calibrated in-situ, at different line pressures, against the HPL weigh tank system (Park et al.[5]). An on-line gas chromatograph and equations of state from A.G.A. Report No. 8[6] were used to determine gas properties for all calculations. The static pressure, relative to a reference pressure in the HPL system, was measured two pipe diameters downstream of each meter. The gas temperature was measured three pipe diameters downstream of each meter using a 3.2-mm diameter probe. The temperature and pressure measurements were used in combination with the measured gas composition and the volumetric flow rate reported by the ultrasonic meter to calculate the mass flow rate at the ultrasonic meter. The test meter mass flow rate was compared against the rate determined by the critical flow nozzles to establish the flow measurement error.

The volumetric flow rate reported by each ultrasonic meter was acquired using different methods, depending on the meter options available from the manufacturer. The internal calibration mode of meters M3 and M4 was used to instruct the meter to totalize gas volume and time during the period when a specific register in the meter electronics was toggled. The average flow rate was then calculated from the totalized values. For meters M1 and M2, reported values of actual flow rate (which were provided at a rate of one per second) were averaged to determine the average volumetric flow rate. Individual path status, velocity, and speed of sound data were also recorded.

A typical test sequence consisted of recirculating gas through the flow loop for a period of time to allow the gas temperature and pressure to stabilize. Steady flow was established by selecting and choking different sonic nozzle combinations. A test point consisted of the average values of flow rate and other variables, computed over a period of 90 seconds. Test points were typically repeated six times back-to-back to calculate average values and standard deviations. Data were also collected simultaneously from two 12-inch turbine meters. The turbine meter data were used to verify the consistency of the experiments, including the long-term reproducibility.

Instromet Ultrasonic Technologies, Inc., and Daniel Instruments, Inc., each provided two flow meters for testing, at no cost to this program. All four of the test meters were commercially available in the United States as of the date of this paper. ***None of the meters had previously been flow calibrated prior to being tested as part of this program.*** Table 1 summarizes the meter configurations for the two multipath meters and two single-path meters. The meters were fabricated such that all had identical flange-to-flange dimensions (800.1 mm in length) and inside diameters (within 0.127 mm) to simplify the interchange of the meters at the different installation locations. The manufacturers provided the meter setup parameters based on their particular procedures for mechanical, electrical, and other measurements. At the time of the tests, the profile correction parameters used for meter M2 were under review by the manufacturer. Parameters specific to the operating pressure and temperature (i.e., fluid properties used internally by the meter electronics) were adjusted for each test condition, as required.

Table 1 – Test meter geometry.

Meter No.	No. of Paths	Acoustic Path Arrangement
M1	3	Two mid-radius double-reflecting, one centerline single-reflecting
M2	1	Centerline, single-reflecting, 60° incident angle, -30° from vertical
M3	4	Parallel, non-reflecting, horizontal
M4	1	Centerline, single-reflecting, 60° incident angle, +45° from vertical

BASELINE TEST CONFIGURATIONS

To determine the flow measurement error associated with a particular flow meter piping arrangement, it is necessary to have baseline meter performance data to compare against. Baseline performance is determined by testing a flow meter and its secondary instrumentation

under established test conditions. The test is then repeated using the same meter and instrumentation, and the piping installation of interest. The measurement error caused by the piping installation is then determined by comparing the results for the piping configuration of interest to those for the baseline test.

Figure 1 displays the piping arrangement for the baseline tests used in this investigation. All piping spools were fabricated with 8-inch diameter, schedule-40, carbon steel pipe (having a nominal 202.7-mm inside diameter) with all internal welds ground smooth. The test meters were installed at 40D, 59D, 78D, and 97D [nominal pipe diameters, where D = 203.2 mm (8 inches)] downstream of a single, long-radius, 90° elbow. The piping immediately upstream of the elbow consisted of a 12"x16"x10" Sprenkle flow conditioner followed by a 10"x8" concentric reducer, and then 43D of straight 8-inch diameter pipe.

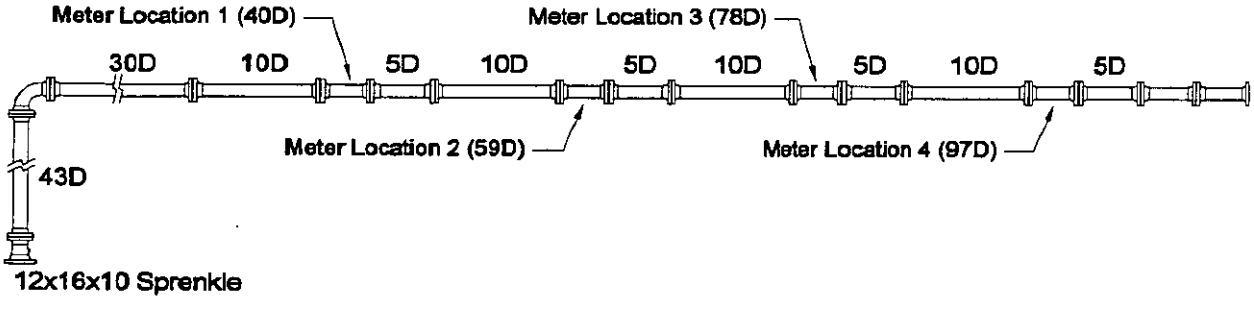

Figure 1 – Baseline meter installation.

Initial baseline testing was performed with the meters at the locations indicated in Table 2. The complete test plan calls for each meter to eventually be tested at all four locations. When the meters were moved from one axial location to another, the upstream and downstream spools (10D and 5D long, respectively) remained bolted to the meters so that there was no change in flange alignment immediately upstream or downstream of each meter. The pressure and temperature transducers associated with each meter also remained with the meter during changes in the baseline meter arrangement, to help minimize measurement bias errors. Roughly two months after this initial testing, all meters were tested at the 97D position as part of a separate test sequence.

Table 2 – Baseline test location by meter designation.

Meter	40D	59D	78D	97D
M1		X		X
M2	X		X	
M3		X		X
M4	X		X	

BASELINE TEST RESULTS

Figures 2 and 3 show the performance of the two multipath meters (M1 and M3, respectively) in the baseline configuration. The meter data are displayed as percent error, relative to the MRF HPL critical flow nozzles, as a function of the average velocity through the meter. The points shown represent the average of six repeats at each flow rate, and the error bars indicate the 95% confidence limits, based on six repeats (i.e., 2.6 times the standard deviation).

Figure 2 indicates that, at velocities above 3 m/sec, all the data for meter M1 fall within a 0.4% band, independent of velocity. The upward swing in the error curve below about 3 m/sec appears to be an artifact of the correction algorithm that does not fully account for velocity profile differences at the low flow rates. Examination of the flow calibration curves also reveals about a 0.2% difference between the flow measurement error when the meter was installed at 97D and when the meter was installed at 59D. The magnitude of the error is greater (i.e., more negative) at the 97D location than at the 59D location. A similar difference in measurement error exists between the 2.8 MPa and 6.2 MPa test cases. Subsequent testing, just prior to the start of the two-elbow-out-of-plane tests, with the meter installed at 97D, showed a difference of approximately 0.3% relative to the initial testing. It is not clear if this behavior is due to slight differences in the 97D installation, or to long-term variability in the meter performance. Other MRF HPL reference meters showed no shift for the same test dates.

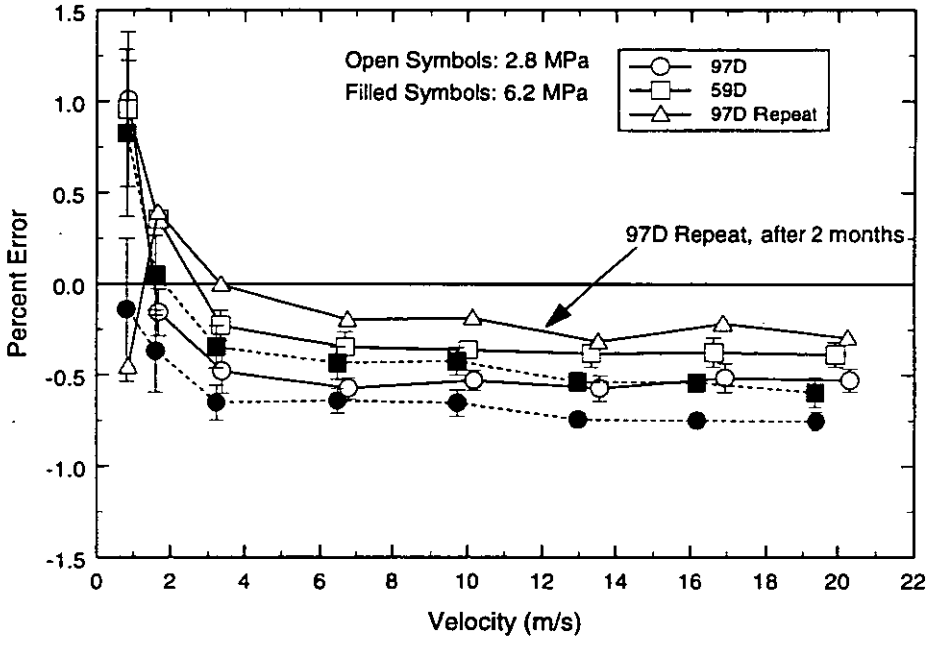

Figure 2 – Baseline results for multipath meter M1.

Figure 3 indicates that the measurement error for meter M3 was dependent on the meter velocity. The nonlinear characteristics of the measurement error for this meter were different from those observed for 12-inch diameter meters of similar design that were previously tested at the MRF (Grimley[7]) and elsewhere (van Bloemendaal and van der Kam[8]). Except for the data collected at 2.8 MPa with the meter installed at 59D, the error values for average gas flow velocities above 3 m/sec all fall within a 0.3% wide band that slopes downward as the velocity

increases. Individual path status information for the 59D, 2.8 MPa data set shows that the signal processor rejected some of the measurements on the outer paths because the measured transit times had failed an internal consistency check. This is likely the cause of the deviation from the other data sets. The data, including the problematic set, remain within a 0.5% wide band for velocities above 3 m/sec. The data also show flow measurement differences of about 0.2% as the pressure increases from 2.8 to 6.2 MPa. The 6.2 MPa results show a measurement difference of about 0.1% between the results when the meter was at 59D and the results when the meter was at 97D. The repeat 97D data collected for meter M3 indicate that, for velocities above 6 m/sec, there is essentially no change in the meter performance. Below 6 m/sec, the data fall within the increased error range of the previous runs.

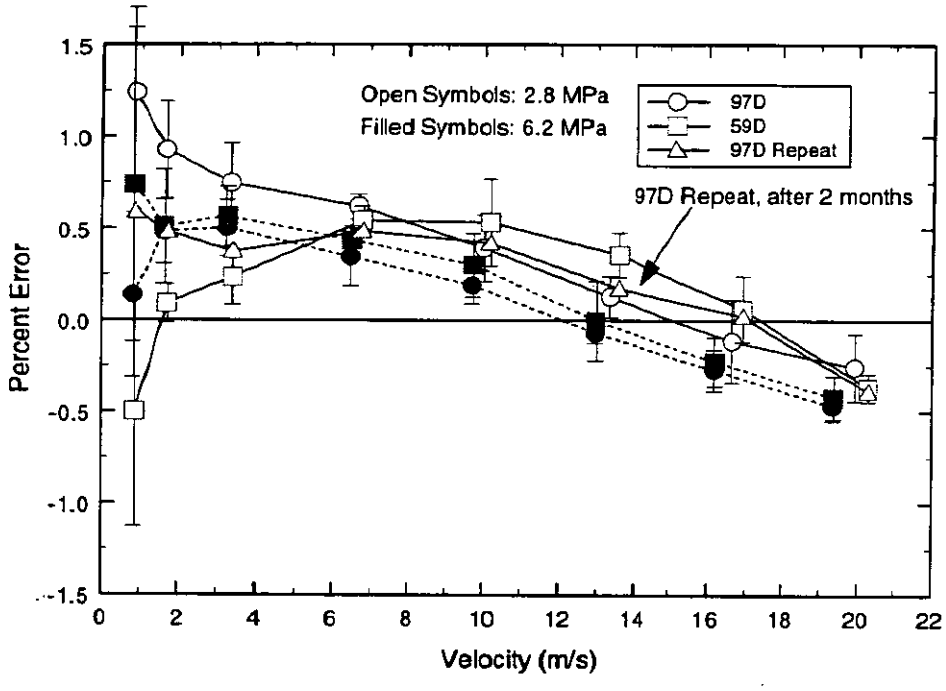

Figure 3 – Baseline results for multipath meter M3.

A potential explanation for the axial dependence of the meter is that the velocity profile was continuing to develop past the 59D location. Insight into the profile shape can be gained by comparing ratios of the individual path velocities. The ratio of the path velocities nearest the axial centerline of the pipe, to the average of the outer path velocities, increases with axial location for both meters. The smaller ratios for the data recorded at the 59D location suggest a flatter velocity profile than that at the 97D location. Velocity profile measurements are currently in progress to aid in the comprehension of these results.

Figures 4 and 5 contain the baseline information for single-path meters M2 and M4, respectively, at two operating pressures and two axial distances downstream of a single 90° elbow. Figure 4 indicates that the single-path meter M2 had an offset of about −1.2% when installed at the 78D position, and about −1.8% when installed at the 40D position. The test results for this meter suggest that, within the data scatter, the flow measurement error is independent of pressure, but dependent on the axial location. The subsequent 97D tests conducted with this meter appear to be consistent with the trend shown in the original data with an error of about –0.5%.

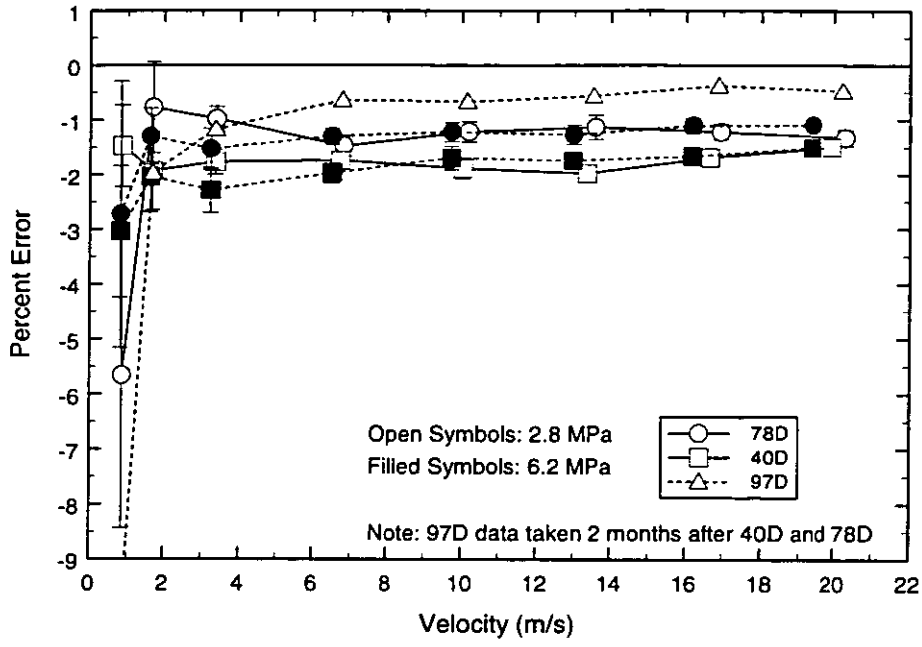

Figure 4 – Baseline results for single-path meter M2.

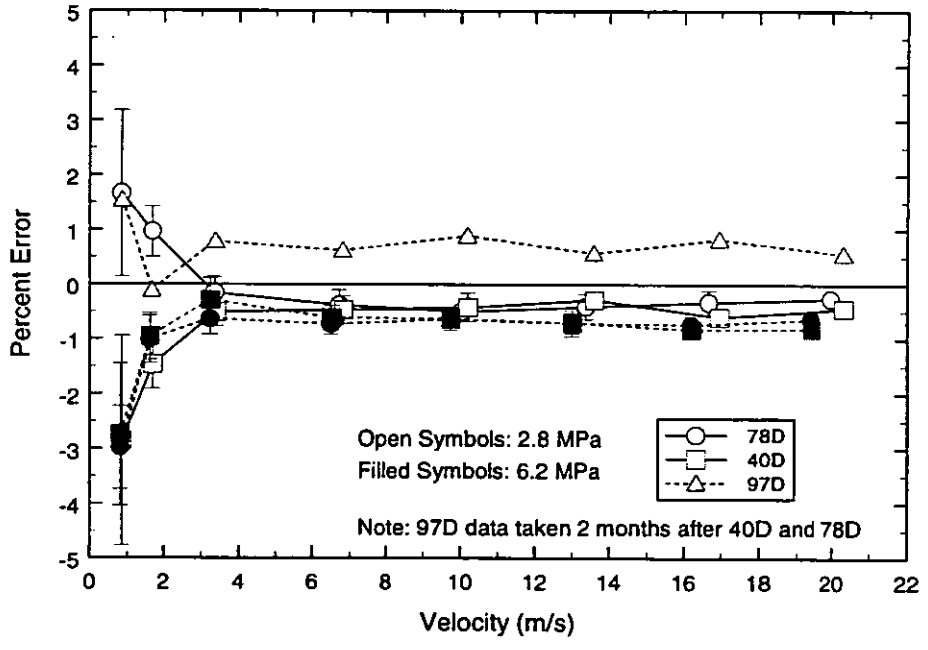

Figure 5 – Baseline results for single-path meter M4.

The results for meter M4 contained in Figure 5 indicate a mean offset of about –0.5%, which appears to be more dependent on line pressure than on the axial distance between the 90° elbow and the meter. The 2.8 MPa, 78D data appear to be inconsistent with the other results at velocities below 3 m/sec where there was a deviation of more than 2% between the two groups. The subsequent 97D data taken with this meter suggest that the meter baseline had shifted, since the earlier data set showed no significant dependence on axial position. Further testing of this meter in the baseline configuration will be conducted to verify this apparent change.

In general, the single-path meters exhibit more scatter in their data than do the multipath meters. The increased data scatter in the single path meters is likely related to the fact that these meters do not have the benefit of multiple ultrasonic paths over which to average the gas flow velocity.

INSTALLATION EFFECTS TEST CONFIGURATIONS

Figures 6 and 7 show plan views of the test configurations used for the installation effects flow tests. For the configuration shown in Figure 6, the single-path meters were tested in two different orientations at locations 1 and 2 (i.e., 10D and 19D, respectively, downstream of the single 90° long-radius elbow). The multipath meters were tested downstream of the two-in-plane-elbow configuration, at locations 3 and 4 (i.e., 10D and 19D downstream of the second elbow). For this configuration, tests were performed with a bare tube, and with two different flow conditioners (19-tube bundle, and GFC™) installed upstream of locations 3 and 4. The flow conditioners were installed such that the outlet was fixed at 5D from the elbow, and therefore, 5D upstream of the first meter (consistent with the minimum installation requirements for turbine meters as described in A.G.A. Report No. 7). The manufacturer of the GFC™ does not recommend this installation for their conditioner, but rather an installation with at least 6.5D between the elbow and the flow conditioner outlet. For convenience, the two-in-plane-elbow configuration for the multipath meter tests was set up with all the piping in the horizontal plane. Since this configuration was meant to represent an installation where the elbows provide a vertical offset, the meters were rotated 90° about their axial centerline to keep the correct orientation of the measurement paths relative to the flow disturbance.

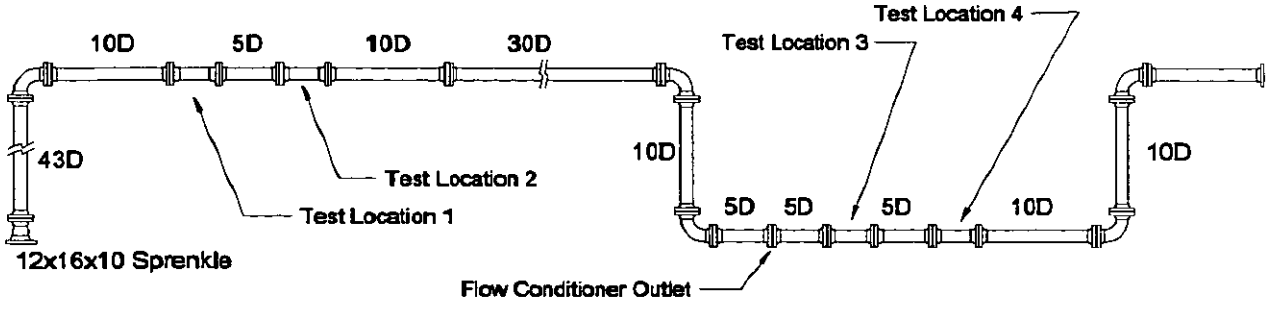

Figure 6 – Single-elbow and two-in-plane-elbow configuration.

Figure 7 displays a plan view of the piping arrangement used for the two-out-of-plane elbow configuration. This test setup also contains four test locations at different axial locations downstream of the disturbance. Three flow conditioners (19-tube bundle, GFC™, and VORTAB™) and a bare meter tube configuration were utilized for these tests. The 19-tube bundle and GFC™ were installed at the 5D location in the same manner as described for the two-in-plane-elbow configuration. The manufacturer's recommendation for the VORTAB™ flow conditioner was followed for this configuration, so the flow conditioner inlet was installed at the outlet flange of the second elbow (at the 0D) position). The meters were all installed in their "normal" orientation relative to vertical. Although data were recorded with each meter in each of the axial positions with the flow conditioners, only a portion of that data will be presented here.

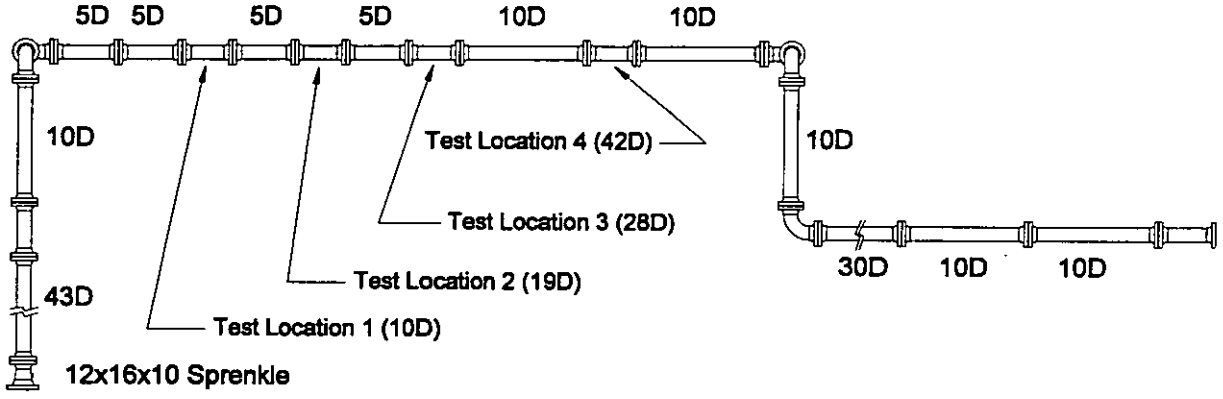

Figure 7 – Two-out-of-plane-elbow configuration.

INSTALLATION EFFECTS TEST RESULTS

The results given in this section are presented in the same error units as those for the baseline data (relative to the sonic nozzle reference flow rate). For reference purposes, the baseline curves (97D for meters M1 and M3, and 78D for meters M2 and M4) are also included on the plots. The results are presented relative to the sonic nozzles because, for some of the meters, there is some ambiguity regarding the location of the baseline curve. This allows comparisons within data sets, for each of the piping configurations, without influencing the results by the choice of the baseline.

Figure 8 displays the results for multipath meter M1 tested 10D and 19D downstream of the two in-plane elbow configuration. The test data indicate that the bare tube arrangement produced a flow measurement error that is independent of the axial location, and within about 0.5% of the baseline, with relative errors being on the order of 0.3% to 0.5%. Lower relative error values occur at higher gas velocities. The absolute error for the bare tube data is less than about 0.25% for velocities above 3 m/sec. There is no significant difference between the results for each of the two flow conditioners when the meter was at 10D with both curves tending towards the baseline at high velocities and deviating by as much as 0.5% at 3 m/sec. However, the results for the 19D position indicate that with the GFC™, the meter error had returned to the baseline value, while the 19-tube results were nearly the same as the bare meter results.

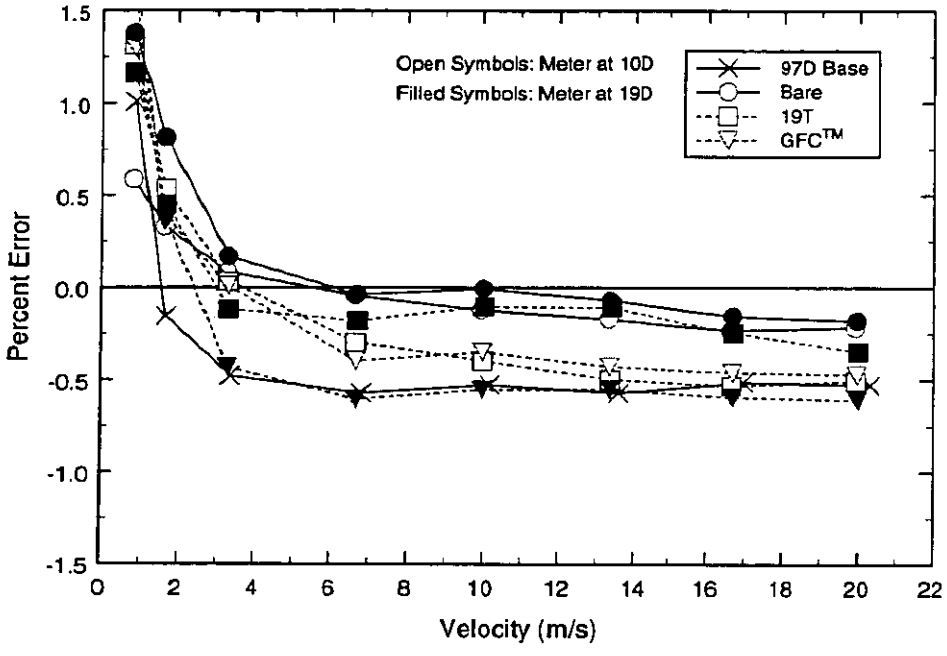

Figure 8 – Multipath meter M1 performance downstream of two in-plane elbows separated by 10D.

The results for multipath meter M1 at various locations downstream of two out-of-plane elbows are shown in Figure 9. These data show that with the meter installed at the 10D position, the results are essentially the same as the baseline results. With the meter further downstream (19D, 28D, and 42D) of the disturbance, the data cluster together in a 0.25% wide band with an absolute error of roughly 0.1%, which is about 0.6% from the baseline. The calculation method used by this meter may account for the large separation in the results at 10D versus the other axial positions. The calculations can be considered to be "active," since different equations can switch in and out of the resulting calculation, depending on the individual path information. The active calculation method may lead to a non-continuous meter response to the continuous changes in the flow properties, which occur downstream of a disturbance. However, a repeat of these tests is suggested to verify their consistency.

Figure 10 indicates that the data with flow conditioners was bounded by the bare tube results at 10D and 19D. The data were all within a 0.7% wide band. A check of the stability number reported by meter M1 indicated that each of the flow conditioners had removed the swirl (as far as the calculation algorithm was concerned) as compared to the cases without the flow conditioners where the meter indicated the presence of a symmetric swirl pattern. The results with the flow conditioners were similar to those for the two-in-plane elbow configuration in that the 19D results with the GFC™ were within about 0.1% of the baseline, as were the VORTAB™ results for the 10D configuration. The results for the 19-tube bundle were offset by 0.25% to 0.4% from the baseline for the 10D and 19D configurations, respectively.

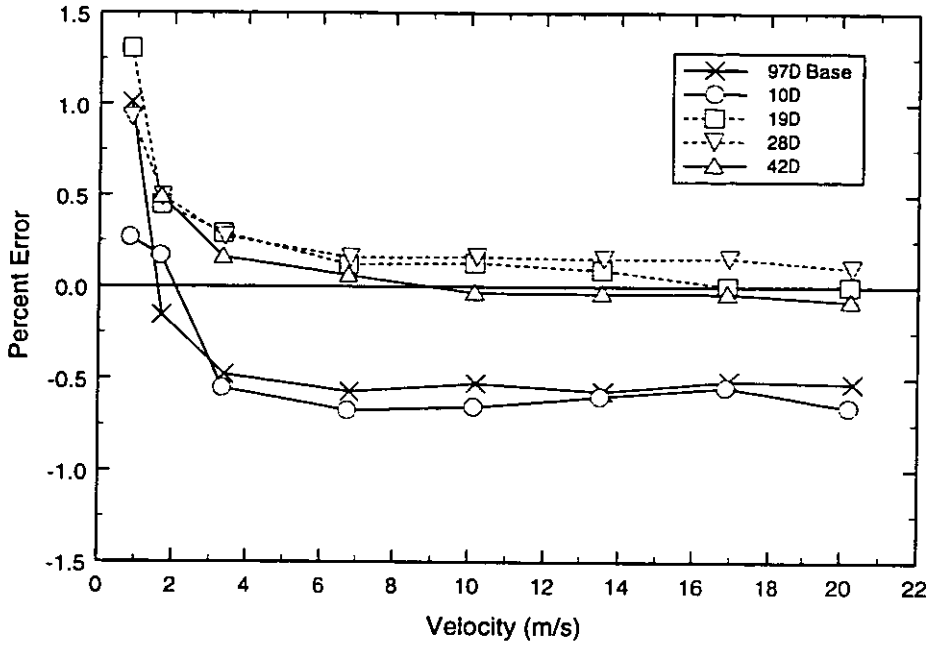

Figure 9 – Multipath meter M1 performance downstream of two out-of-plane elbows.

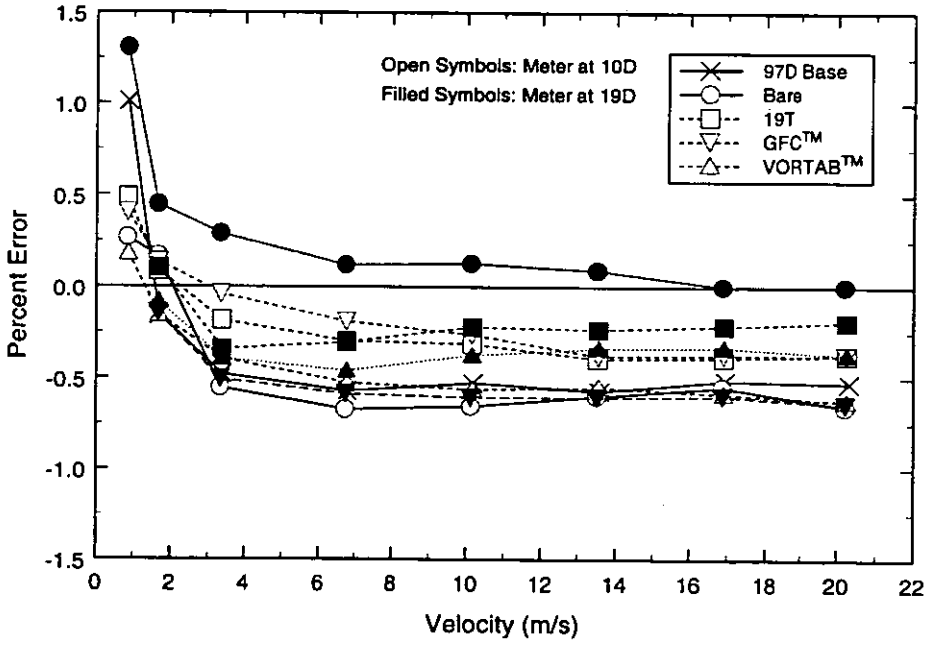

Figure 10 – Multipath meter M1 performance downstream of two out-of-plane elbows.

Figure 11 presents the results for multipath meter M3 when located 10D and 19D downstream of the two in-plane elbow configuration. The figure indicates that with the bare tube, the meter showed less than 0.25% error relative to the baseline, for velocities higher than 6 m/sec. This result is independent of the axial position of the meter. At 10D, the 19-tube bundle and the GFC™ results surround the results of the bare tube, with relative differences of –0.3% and 0.2%, respectively. At velocities lower that about 6 m/sec, there is a departure from the baseline data. Except for the highest test velocities, the data for the 19-tube bundle and the GFC™ are nearly identical for the 19D position. For gas velocities above 14 m/sec, the GFC™ produced measurement errors that are closer to the baseline than the 19-tube bundle.

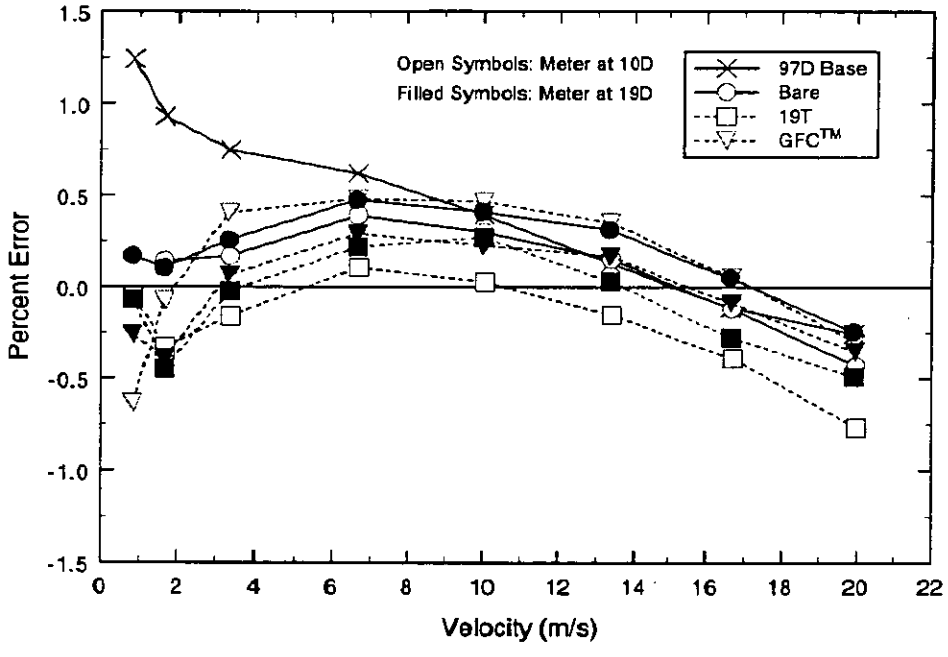

Figure 11 – Multipath meter M3 performance downstream of two in-plane elbows separated by 10D.

Test results for multipath meter M3 in the two-out-of-plane elbow configuration are shown in Figures 12 and 13. The bare meter results of Figure 12 display a mean shift of about 0.4% relative to the baseline data, for velocities above 6 m/sec. The data for the different axial positions are clustered together with a spread of about 0.3%, suggesting that the meter performance for this case is independent of the axial position.

Figure 13 indicates the effect of various flow conditioners on the performance of multipath meter M3 when installed downstream of two out-of-plane elbows. The results with the flow conditioners fall primarily between the 97D baseline data and the bare meter results at 10D and 19D. With the meter installed at 10D, the 19-tube bundle and GFC™ follow the bare meter performance curves. The VORTAB™ conditioner shifted the results close to the baseline curve for the 10D and 19D cases, as did the GFC™ for the 19D position at velocities above 14 m/sec. The 19-tube bundle is also within 0.25% of the baseline for the 19D position.

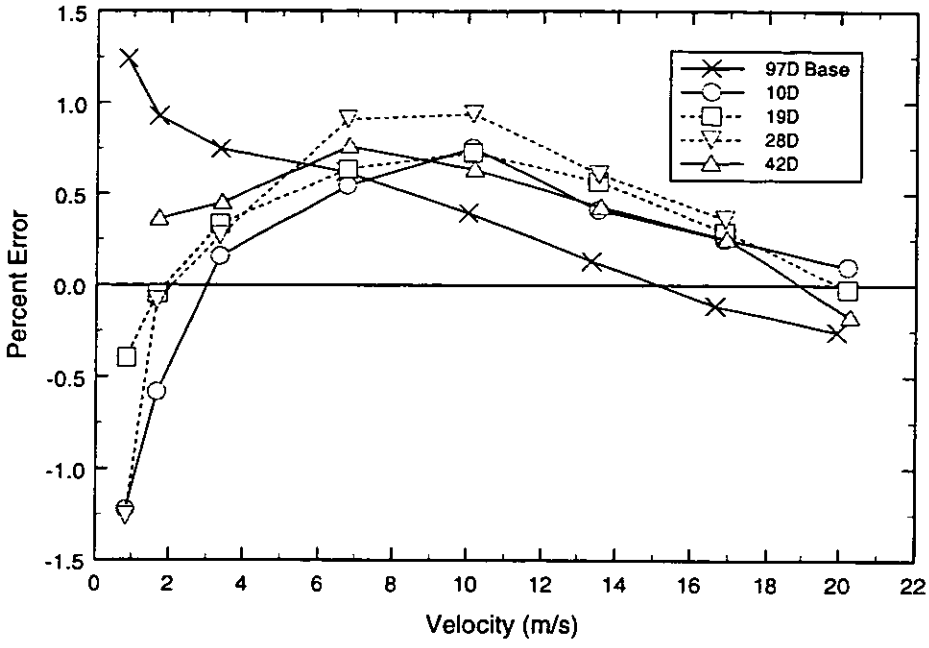

Figure 12 – Multipath meter M3 performance downstream of two out-of-plane elbows.

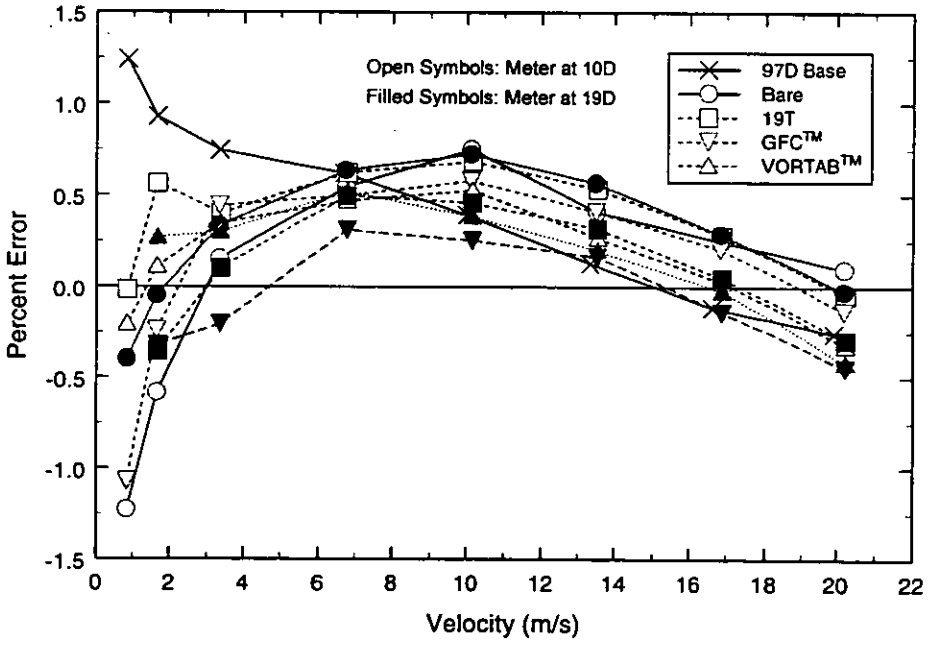

Figure 13 – Multipath meter M3 performance downstream of two out-of-plane elbows.

The results shown in Figures 8 through 13 indicate that, depending on the meter type and location, there are potential benefits to using flow conditioners with multipath ultrasonic flow meters. For some of the above cases, the measurement error shifts relative to the baseline result in absolute measurement errors that are actually closer to zero error than the baseline results. It is not clear if this result is fortuitous, or the result of the meter development having occurred with less than ideal velocity profile conditions.

Figure 14 displays the results of tests performed with single-path meter M2 at locations 10D and 19D downstream of a single 90°, long-radius elbow. The results indicated a measurement error shift of about 2% to 2.2% relative to the 78D baseline error. When the meter was rotated 90° about its axial centerline, there was an additional 1.3% shift in error beyond the results at 0° (i.e. "normal") orientation. Table 1 indicates that the single ultrasonic path of this meter was located 30° from vertical when the meter was installed in its "normal" orientation. Since the major component of the flow asymmetry in this test configuration was in the vertical plane, rotation of the meter 90° caused the path orientation relative to the flow disturbance to change, and therefore, the resulting meter performance to shift.

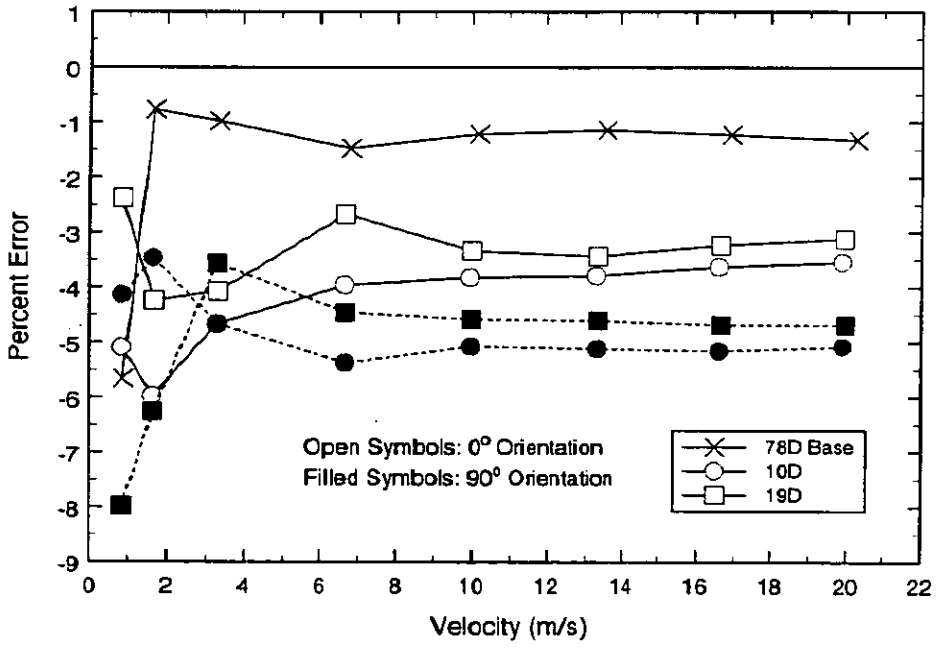

Figure 14 – Single-path meter M2 performance downstream of single elbow.

Figure 15 indicates that when the single-path meter M2 was installed downstream of two out-of-plane elbows, the error increased by 2% relative to the baseline, which is roughly the same amount as was the case for a single elbow (in the 0° orientation). As the axial distance from the disturbance increased, there was little change in the results until the meter was installed at the 42D position where the shift relative to the baseline data was approximately 1%.

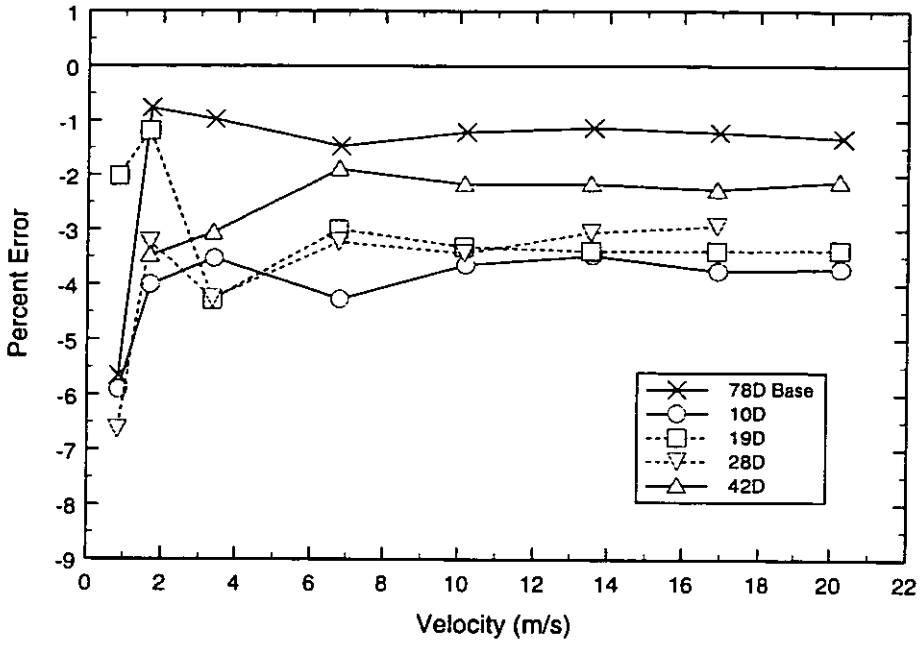

Figure 15 – Single-path meter M2 performance downstream of two out-of-plane elbows.

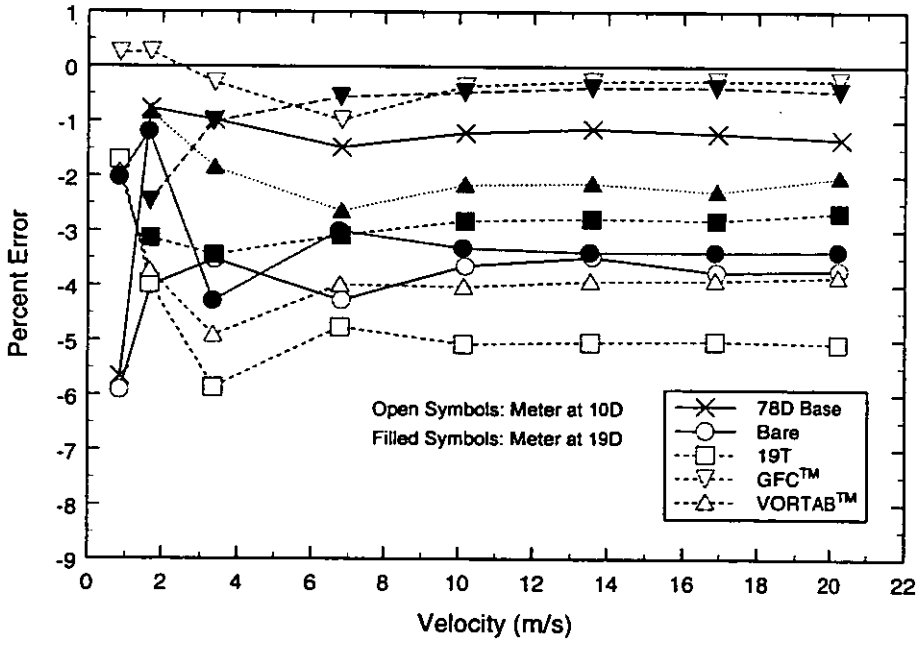

Figure 16 – Single-path meter M2 performance downstream of two out-of-plane elbows.

The results of single-path meter M2 tested with various flow conditioners are shown in Figure 16 for the two-out-of-plane elbow configuration. These results indicate a significant difference in the behavior of the meter with the different flow conditioners. The 19-tube bundle increased the measurement error by 1.5% over that for the bare meter performance when the meter was installed at the 10D position. With the meter at 19D, the 19-tube bundle had decreased the magnitude of the error relative to the 19D bare meter results by about 1%, but still had a negative shift of 1.5% relative to the 78D baseline. The VORTAB™ results are similar to those for the 19-tube bundle, but have less of an error increase at 10D than that for the 19-tube bundle. With the meter at the 19D position, the VORTAB™ results shift by 1% relative to the 78D baseline. Results with the GFC™ indicate a positive shift of 1% relative to the 78D baseline data and are essentially the same as when the meter was installed at 10D and 19D.

Figure 17 presents the results for single-path meter M4 for the single 90° elbow test configuration. With the exception of the 90° orientation tests with the meter installed 19D downstream of the elbow, the results indicate a measurement error shift of about 1.5% to 2% relative to the baseline. This meter showed little dependence on orientation, as should be expected since the measurement path was oriented 45° from vertical. For this meter, the path orientation relative to the disturbance remained the same even when the meter body was rotated about the axial centerline of the meter.

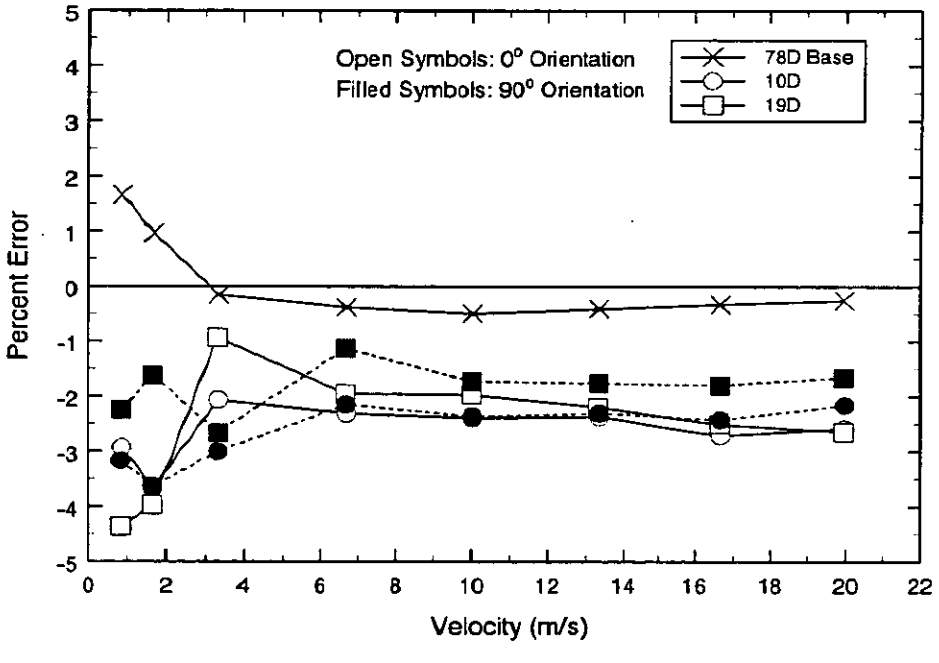

Figure 17 – Single-path meter M4 performance downstream of single elbow.

Figure 18 suggests a systematic dependence of the meter performance on axial position for single-path meter M4 when installed downstream of two out-of-plane elbows. The error magnitude decreased as the meter was moved away from the flow disturbance and the velocity profile had a chance to develop. The maximum absolute error was about –3% at the 10D position and was less than 0.25% at the 42D position.

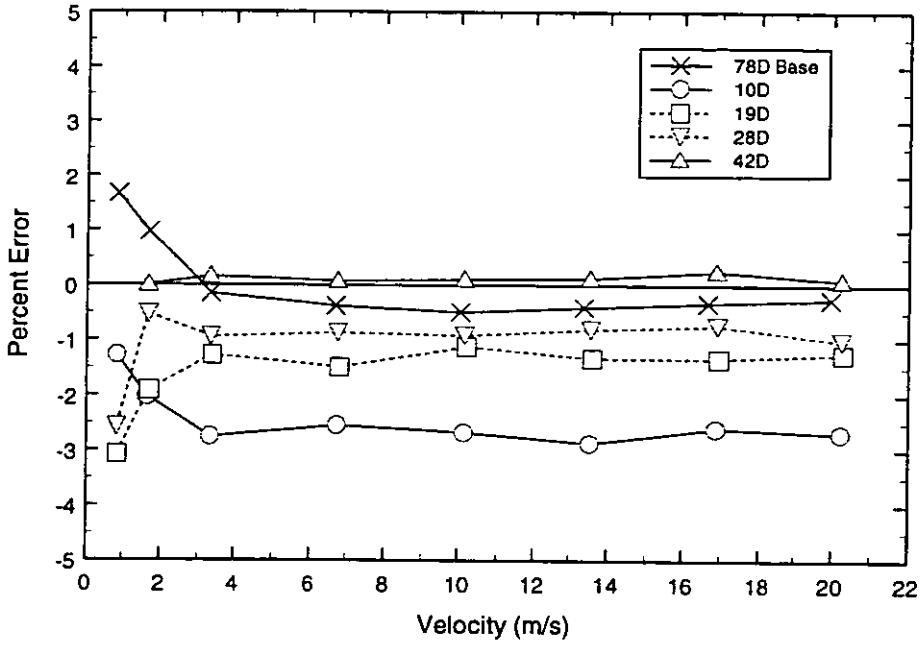

Figure 18 – Single-path meter M4 performance downstream of two out-of-plane elbows.

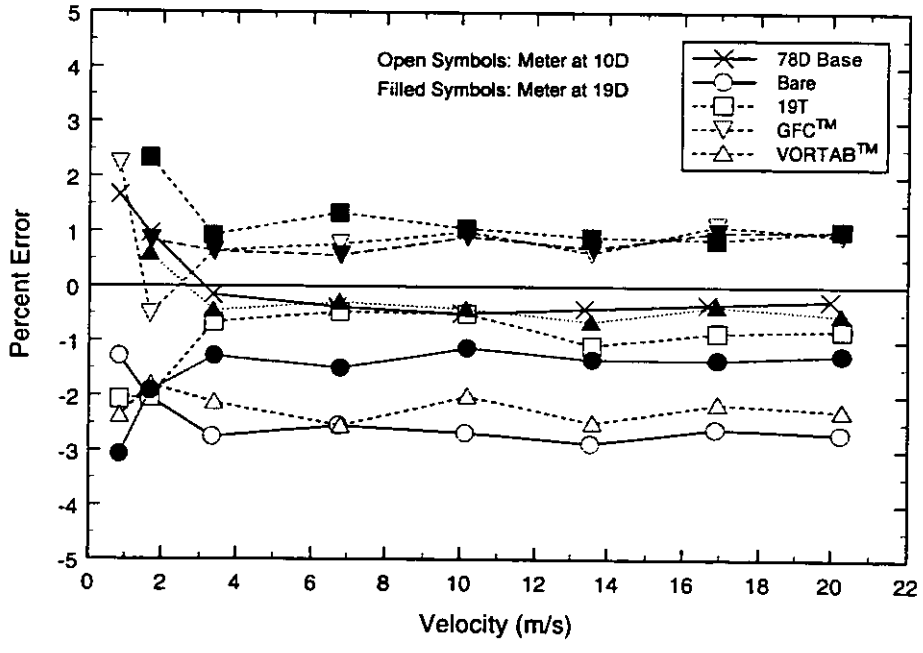

Figure 19 – Single-path meter M4 performance downstream of two out-of-plane elbows

Figure 19 indicates the performance of single-path meter M4 with various flow conditions for the two-out-of-plane elbow configuration. As was the case for single-path meter M2, the GFC™ produced results that were the same for meter installation positions of 10D and 19D. The 19-tube bundle results with the meter installed at 19D matched those for the GFC™ while with the meter at 10D, the 19-tube bundle followed the VORTAB™ results with the meter at 19D. Results for the VORTAB™ with the meter installed at 10D are consistent with those of meter M2 and follow the 10D bare meter data.

In considering the results from the two single-path meters, it is important to acknowledge that the path orientation relative to the disturbance is different for these two meters. Since the types of flow disturbances tested here create flow asymmetries, the results for the two meters should not be expected to be identical. The results of the two meters indicate similar trends and demonstrate the viability of a single-path ultrasonic flow meter with a flow conditioner.

THERMOWELL INFLUENCE TEST RESULTS

Thermowells are typically installed within a few diameters downstream of the meter to provide a representative measurement of the gas temperature at the meter. In bi-directional applications, one flow direction will necessarily have a thermowell protruding into the gas stream upstream of the flow meter. Since the presence of the thermowell will disturb the flow, there is a possibility of introducing additional error into the meter's volumetric measurement. The tests here do not consider the error introduced by an incorrect temperature determination at the meter.

To assess the effect on the meter performance of this protrusion, a special piping spool was constructed with nine thermowell access locations at three axial locations (1D, 3D, and 5D) from the end of the spool, and three angular positions (0°, 45°, and 90°). Thermowells were simulated by using 12.7-mm diameter rods that could be inserted or retracted from the flow at the various test locations, without depressurizing the pipe section. A gauge block was used to set the insertion level at either 1/2D (101.3 mm) or 1/3D (67.6 mm). These two insertion depths represent flow blockages of 4% and 2.7% for the 1/2D and 1/3D levels, respectively. The special piping spool was installed upstream of the test meter with the test meter at the 97D location, as previously shown in Figure 1. For each test flow rate, baseline data (without a probe in the flow) were collected before and after the series of 18 tests with the simulated thermowells inserted into the flow. For each position, six repeat data sets were collected and referenced to the baseline data.

Figure 20 indicates the relationship between the thermowell location and the ultrasonic paths for each of the test meters. The thermowell influence results for meters M1, M3, and M4 are presented in Tables 3, 4, and 5, respectively. These tables indicate the meter error relative to the baseline meter error, for each of the thermowell test positions. The data obtained for single-path meter M2 are not presented because the meter was not operating properly during the thermowell tests.

The tabulated results indicate the thermowell influence is larger at lower velocities than at higher velocities. This effect can be explained by increased turbulence that occurs at high velocities, which reduces the size of the wake produced by the flow around the thermowell. At lower velocities, the wake persists downstream and results in metering error.

The largest errors indicated for the multipath meters occur for the low velocity condition with the thermowell at the 1D position. Errors as large as 0.8% are indicated, with multipath meter M1 showing a negative shift, and multipath meter M3 showing a positive shift. As expected, as the distance between the thermowell and the meter increases, the shift in measurement error decreases. It appears that the 3D location was a sufficient distance away for meters M1 and M3, as long as the 45° thermowell position was avoided for meter M3.

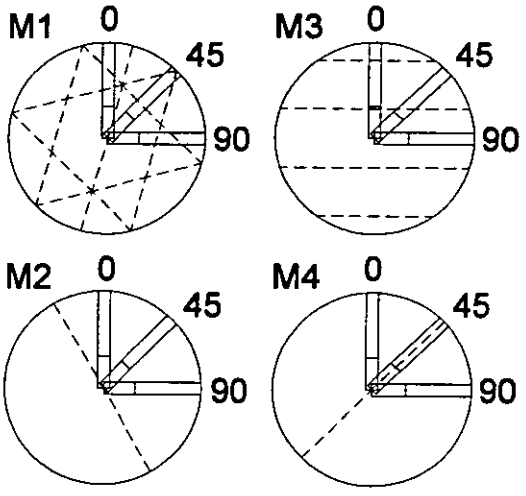

Figure 20 – Meter path orientation relative to thermowell test locations.

Table 3 – Multipath meter M1 relative error for various upstream thermowell positions.

Position		1D		3D		5D	
Vel.	Ang.	1/2	1/3	1/2	1/3	1/2	1/3
3.4	0	-0.76	-0.17	-0.39	-0.06	-0.02	0.20
	45	-0.69	-0.43	-0.13	-0.21	-0.14	-0.02
	90	-0.23	-0.51	-0.22	-0.28	-0.17	-0.26
10	0	0.03	-0.01	-0.12	-0.05	-0.02	0.19
	45	0.10	-0.36	0.08	-0.04	0.37	-0.09
	90	0.28	-0.08	0.00	-0.13	-0.02	-0.09
20	0	0.03	0.13	-0.11	-0.04	-0.15	0.23
	45	0.11	-0.48	0.03	-0.21	0.13	0.00
	90	0.09	-0.37	-0.11	-0.20	-0.06	-0.28

The single-path meter M4 showed larger relative errors than did the multipath meters for the thermowell tests. The largest relative errors occurred with meter M4 when the thermowell was directly aligned with the measurement path. Relative errors as large as –1.6% are indicated in Table 5 for the 1D position, with the probe at 45° and an insertion length of 1/2D. When the insertion length was reduced to 1/3D, the relative error was reduced by nearly 1%. The results

for single-path meter M4 suggest that thermowells at the positions away from the measurement path (i.e., the 0° and 90° positions) did not influence the flow measurement error.

Table 4 – Multipath meter M3 relative error or various upstream thermowell positions.

Position		1D		3D		5D	
Vel.	Ang.	1/2	1/3	1/2	1/3	1/2	1/3
3.4	0	-0.01	0.14	-0.07	-0.05	-0.01	0.02
	45	0.78	0.66	0.66	0.51	0.58	0.42
	90	-0.23	-0.09	-0.11	-0.09	-0.14	-0.07
10	0	-0.19	-0.06	-0.01	-0.03	-0.02	0.10
	45	-0.11	-0.04	0.02	0.11	0.08	0.09
	90	-0.06	-0.13	0.01	-0.10	0.01	0.04
20	0	-0.25	0.02	-0.15	0.07	-0.21	0.00
	45	0.05	0.41	0.21	0.33	0.07	0.14
	90	-0.14	-0.11	-0.03	-0.03	0.10	0.04

Table 5 – Single-path meter M4 relative error for various upstream thermowell positions.

Position		1D		3D		5D	
Vel	Ang.	1/2	1/3	1/2	1/3	1/2	1/3
3.4	0	0.14	0.36	0.01	0.04	-0.06	-0.18
	45	-1.59	-0.68	-0.76	0.16	-0.08	0.68
	90	-0.06	0.33	-0.04	0.07	0.10	0.00
10	0	0.14	0.20	-0.04	0.09	-0.13	-0.04
	45	-1.31	-0.35	-0.35	0.26	-0.52	-0.03
	90	-0.05	0.17	0.03	0.09	0.02	-0.04
20	0	0.03	0.26	0.11	0.08	0.31	0.00
	45	-1.38	-0.59	-0.61	0.42	-0.58	0.35
	90	-0.39	0.16	0.23	0.04	-0.46	0.18

CONCLUSIONS

The results for the baseline tests suggest that the velocity profile was not fully developed 59 pipe diameters downstream of a single, long-radius 90° elbow, and that the test meters were sensitive to the subsequent profile development. The baseline results indicate that the accuracy of the 8-inch meters tested can be improved by flow calibration.

The test results for the 8-inch diameter multipath flow meters indicate that, depending on the meter type and location relative to a flow disturbance, there are potential benefits to using flow conditioners to improve measurement accuracy. However, the influence of the flow conditioner is dependent on both the flow conditioner type and the multipath meter type. For certain combinations, the presence of a flow conditioner creates more flow measurement error than would be present without the flow conditioner.

The results for the single-path meters show potential for achieving flow measurement accuracies better than 0.5% in well-ordered flow fields. The level of sensitivity to a simple disturbance was demonstrated by installing test meters 10D and 19D downstream of a single 90° elbow and at various distances for two out-of-plane elbows. In these tests, the flow measurement error ranges from about 1% to 4%, relative to the results for the baseline test configuration.

The effect of using flow conditioners with single-path meters was demonstrated for the two out-of-plane elbow configuration. The results show that accuracy levels close to that of multipath meters could be achieved in meter runs less than 20 pipe diameters long.

The effect on flow metering accuracy of an upstream thermowell has been quantified for single-path and multipath meters. The data suggest that a thermowell located 3D upstream of the meter will result in little additional error in most cases. The error induced by an upstream thermowell aligned with the measurement path of a single path meter persists for more than three pipe diameters.

The apparent shifts in baseline performance of some of the meters need to be investigated further since the long-term stability of the meters is essential to their use in the gas industry.

When drawing conclusions from these results, it is important to note that these results are based on the performance of a single instance of the particular meter designs. Variations in the manufacture and installation of these meters may result in different values for meter bias in the various piping configurations. Therefore, the results should not be generalized in terms of the *absolute* meter performance, but should be considered as indicating the *relative* change in performance for different piping configurations.

REFERENCES

1. *Concentric, Square-Edge Orifice Meters*, A.G.A. Transmission Measurement Committee Report No. 3 (3rd Edition), American Gas Association, Arlington, Virginia, October, 1990.
2. Morrow, T. B., "Orifice Meter Installation Effects: Research Update for A' = 29 D Meter Tubes," A.G.A. Operating Section Operations Conference, Nashville, Tennessee, May 1997.
3. Dijstelbergen, H. H. and J. T. M. Bergervoet, "Optimal Straightening Vanes for Turbine Meters," Third International Symposium on Fluid Flow Measurement, San Antonio, Texas, April 1995.
4. *Measurement of Gas by Turbine Meters*, A.G.A. Transmission Measurement Committee Report No. 7, American Gas Association, Arlington, Virginia, 1996.
5. Park, J. T., K. A. Behring, II, and T. A. Grimley, "Uncertainty Estimates for the Gravimetric Primary Flow Standards of the MRF," Third International Symposium on Fluid Flow Measurement, San Antonio, Texas, April 1995.
6. *Compressibility of Natural Gas and Other Related Hydrocarbon Gases*, A.G.A. Transmission Measurement Committee Report No. 8, American Gas Association, Arlington, Virginia, 1985.
7. Grimley, T. A., "Metering Research Facility Program: Performance Tests of 12-inch Multipath Ultrasonic Flow Meters," GRI Topical Report No. GRI-96/0291, Gas Research Institute, Chicago, Illinois, August 1996.
8. van Bloemendaal, K. and P. M. A. van der Kam, "Installation Effects on Multipath Ultrasonic Flow Meters: The 'ULTRAFLOW' Project," Third International Symposium on Fluid Flow Measurement, San Antonio, Texas, April 1995.

NSFMW.97

North Sea FLOW Measurement Workshop

Paper ~~20:~~ 3.7

DIAGNOSTIC OF INDUSTRIAL GAS FLOWS BY ULTRTRASONIC TOMOGRAPHY

Authors:
Jacques Demolis, Pierre Gajan and Alain Strzelecki, O.N.E.R.A., France

Organiser:
Norwegian Society of Chartered Engineers
Norwegian Society for Oil and Gas Measurement
Co-organiser:
National Engineering Laboratory, UK

Diagnostic of Industrial Gas Flows by Ultrasonic Tomography

Jacques DEMOLIS, Pierre GAJAN, Alain STRZELECKI

O.N.E.R.A., France

ABSTRACT

To minimise the influence of transversal flows or asymmetry of the axial profile, more and more manufacturers have resorted to ultrasonic multipath flowmeters.

Since a few years, some authors have shown that it is possible to get more information on the flow conditions using multipath systems. With numerous differences in transit times given by multiple transducers pairs, one can reconstruct the three components of the velocity field. This technique, called « Ultrasonic Tomography », has only been developed in laboratory environment. This present work has been carried out in order to apply tomography to the diagnostic of *in situ* industrial gas flows.

First of all, we have reached this goal for transversal components. For this, we had to design an operational device with 8 transducers in a reduced distance that means, to minimise ultrasonic transmission across the wall and to resolve mechanical restrictions due to the number of transducers. Then, as all the flight distances between transducers pairs are smaller than in classical flowmeters, we had to increase the accuracy in the determination of the transit times. Finally, it was necessary to perfect existing reconstruction algorithms to make them more robust and faster for the run-time.

INTRODUCTION

A flowmeter, independently of its technology, must be used in reference conditions of calibration to be accurate, that is to say, in fully developed flow. In some industrial networks, it is very difficult to find these conditions, particularly downstream of a delivery station. In this case, some errors in the flow rate measurement will appear.

The studies conducted at ONERA have shown that singularities, for example pressure

reducers, generate strong perturbations which propagate along the pipe until the flowmeter. And Strzelecki *et al.* [1] have shown that this kind of flow implicates supplementary errors. As it is very difficult to predict the kind of flow at the place of the meter regarding the installation geometry, it seems interesting to develop a diagnostic tool which would be able to give the maximum of information concerning it. As such a device has to be installed on an industrial set-up, it has to work in real conditions. Therefore, we tried to find a method which is non-invasive, which needs no artificial seeding, as few calibrations as possible, which is easily transportable on the study place and, consequently, robust while being reliable.

During the last decade, due to their efficiency, ultrasonic flowmeters have been widely used for gas applications. Furthermore, recent papers have shown that, combining information delivered by multiple transducers, it is possible to reconstruct the three components velocity profile through a test section. For these reasons, we have decided to apply this technique, called ultrasonic tomography, to diagnostic industrial flows. To verify the reliability of the developed device, swirling flows had been measured and compared to a hot wire characterisation. A last test shows that it is possible to reconstruct the Dean vortices downstream from a 90°-bend.

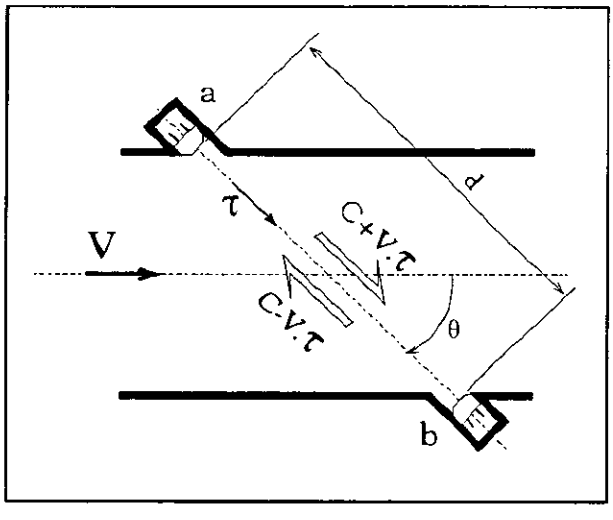

Figure 1. Ultrasonic flowmeter principle.

ULTRASONIC FLOWMETER PRINCIPLE

Ultrasonic flowmeters measure the mean velocity of a flow from the modification of the sound velocity in it. If the wave propagates in the flow direction, the sound velocity increases ;otherwise, it decreases. Of course, this phenomena appears if the direction of propagation of the wave is not perpendicular to the flow direction. For this reason, in ultrasonic flowmeters, the couple of ultrasonic transducers is inclined at an angle θ to the pipe axes as it is shown in figure 1.

The time of flight of the wave from the upstream transducer *a* to the downstream one *b*, is given by the following equation :

$$t_{ab} = \int_a^b \frac{ds}{C + V \cdot \tau} \qquad (1)$$

and in the other direction :

$$t_{ba} = \int_a^b \frac{ds}{C - V \cdot \tau} \qquad (2)$$

In many cases, the flow velocity can be considered much more inferior than the sound speed, then these two expressions become :

$$t_{ab} = \frac{1}{C}\int_a^b \left(1 - \frac{V \cdot \tau}{C}\right) ds \qquad \text{and} \qquad t_{ba} = \frac{1}{C}\int_a^b \left(1 + \frac{V \cdot \tau}{C}\right) ds \qquad (3) \text{ and } (4)$$

Now, subtracting (4) from (3) and noting d the distance between the two transducers, it is possible to get the mean velocity V_m of the flow :

$$\Delta t = t_{ab} - t_{ba} = \frac{-2}{C^2}\int_a^b V \cdot \tau \, ds = \frac{-2d\, V_m \cos\theta}{C^2} \qquad (5)$$

ULTRASONIC TOMOGRAPHY PRINCIPLE

The principle of the tomography is to use many transit time Δt obtained on numerous ultrasonic lines to determine the velocity profile through a pipe section. Ultrasonic lines are materialised by a couple of source/receiver transducers. To get the three velocity components, Johnson *et al.* [2] proposed the transducers distribution of the figure 2.

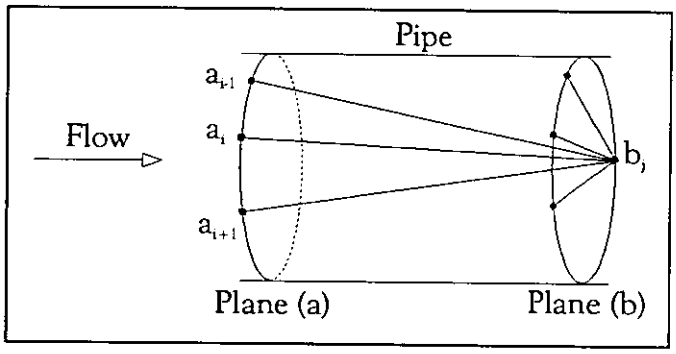

Figure 2. Transducers distribution on a pipe.

Assuming that flow conditions do not change between planes (a) and (b), the set of pairs (a_i,a_j) allows the reconstruction of transversal components of the flow, while the pairs (a_i,b_j) are used for the axial component.

The time of flight difference between the transducer a_i and the transducer b_j, is expressed by an expression similar to equation (5). One has only to put a_i in place of a, b_j in place of b. The unit vector tangent τ to ultrasonic ray has to be expressed in the cartesian coordinate system (x,y,z), with z-axis in direction of pipe axis, by the following expression :

$$\tau = (\mathbf{x}\cos\theta + \mathbf{y}\sin\theta)\sin\gamma + \mathbf{z}\cos\gamma \qquad (6)$$

Where γ is the angle between z and τ and, if $\boldsymbol{r}$ is the projection of τ on the plane (xOy), θ is the angle between $\boldsymbol{x}$ and $\boldsymbol{r}$.
So, we obtain the new expression :

$$\Delta t = T_0(a_i, b_j) = \frac{-2}{C^2}\int_{a_i}^{b_j} \left[\left(V_x \cos\theta + V_y \sin\theta\right)\sin\gamma + V_z \cos\gamma\right] ds \qquad (7)$$

In the same way, an expression can be obtained for a time of flight difference measured uniquely in the plane (*a*):

$$T_1(a_i,a_j)=\frac{-2}{C^2}\int_{a_i}^{a_j}\left(V_x\cos\theta+V_y\sin\theta\right)dr \qquad (8)$$

If a_j is the projection of b_j along the cylindrical axis onto the plane (*a*), Johnson *et al.* [2] now define the fictitious time:

$$T_2(a_i,b_j)=T_0(a_i,b_j)-T_1(a_i,a_j)=\frac{-2\cot an\gamma}{C^2}\int_{a_i}^{b_j}V_z\,ds \qquad (9)$$

which allows to reconstruct the component V_z independently of the transversal components of the flow.

TIME OF FLIGHT EVALUATION

For tomography to be effective, it is necessary to increase the number of ultrasonic paths (see figure 2) in order to cover the maximum of the test section. Moreover, because of the difference of acoustic impedance between the gas and the pipe metal which highly attenuate the acoustic wave, transducers are installed directly in contact with the fluid. Figure 3 represents the plane (*a*) of figure 2 with 12 transducers around the section. Lines materialise theoretic ultrasonic rays defined by one receiver and seven sources. Each of these couples defines one difference of transit time $T_1(a_i,a_j)$ given by relation (8).

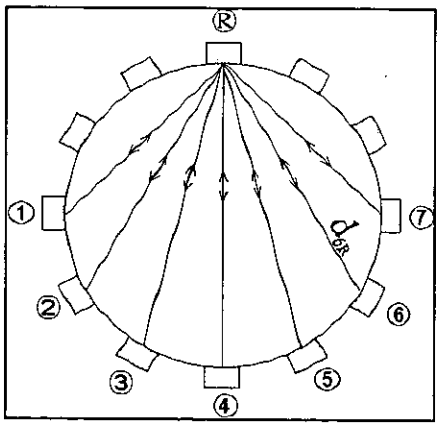

Figure 3. Transducers distribution for a perpendicular section.

From this figure, two remarks can be done. The first one concerns the angle directivity of sources, especially ① and ⑦. In this configuration, the directivity is at least 90° while in ultrasonic flowmeters, this angle is much smaller, that is to say a better signal-to-noise ratio and so, better quality of the reception signal. The second is about the length of ultrasonic rays. In a flowmeter, it is generally $\sqrt{2}D$ and it could be easily increased multiplying the number of reflections on the inner wall. Here, the minimal length is $D/\sqrt{2}$ and the maximal is D. Consequently, to obtain the same relative accuracy as for classical flowmeter in the determination of the time of flight measurement, the absolute accuracy have to be increased in the tomographic system.

To solve these problems, we have first chosen transducers which are able to emit a useful

signal with an attenuation of less than 6 dB at an angle of 120°. They are of frequency 40 kHz and diameter 16 mm.

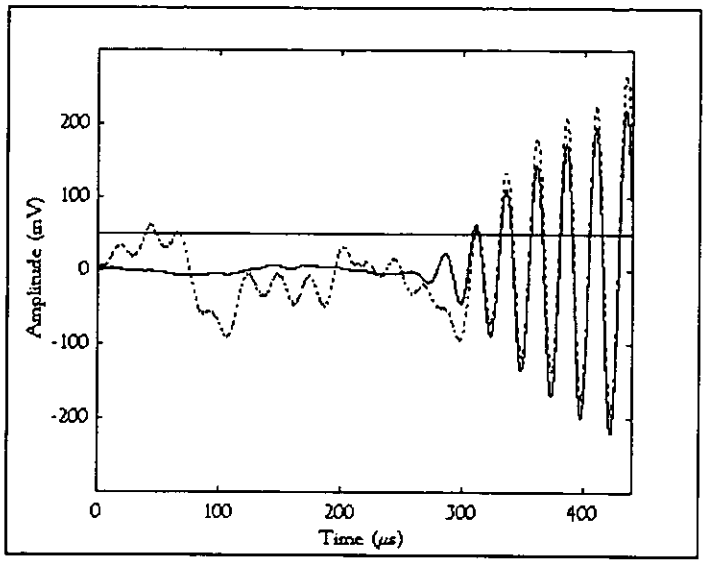

Figure 4. Comparison between raw signal and averaged signal.

Then, like Frøysa *et al.* [3], to reduce the noise which perturb the reception signal, an average is operated on a certain number of signals. For that, they are recorded with an analogic-numeric converter and, then, numerically averaged by a computer. Figure 4 shows the result of an average of 50 traces for the couple ®-① of figure 3. The raw signal without treatment is represented with solid line (—), and the averaged signal with the dotted line (- - -).

In fact, in the same time, this average can solve the problem of measurement accuracy of one transit time on a short distance. The method used for such averaged signals is said to be a « zero crossing » method. It is the measure of a first zero crossing point after the detection of a minimal amplitude threshold. On figure 4, this threshold is materialised by the horizontal line at 50 mV. The exact time of propagation from source to receiver is obtained by the subtraction of the number of periods preceding this zero crossing (in the case of figure 4, two periods are omitted, i.e. 50 μs).

From this operating procedure, the developed method gets a fairly good accuracy because, for 20 measures of transit time, the mean of the rms is about 2.5 ns whatever the separation length of transducers.

MEASUREMENT TOOL

At the first stage of this study, only one section of the pipe is considered to reconstruct the secondary flow. Figure 5 shows this measurement tool. It is made of stainless steel, its internal diameter is D=100 mm and its length is 3D. Althoug there are only 8 transducers, the device can rotate around the conduit axis so, rather than limiting the distribution to one transducer at every 30°, experiences have been conducted considering one transducer every 10° (which is equivalent to a pipe with 36 transducers).

Electronic instrumentation includes : a signal generator, a scanner to select the source transducer, a preamplifier-filter and an ADC installed in a PC which manage the signal acquisition and the reconstruction of the velocity profile.

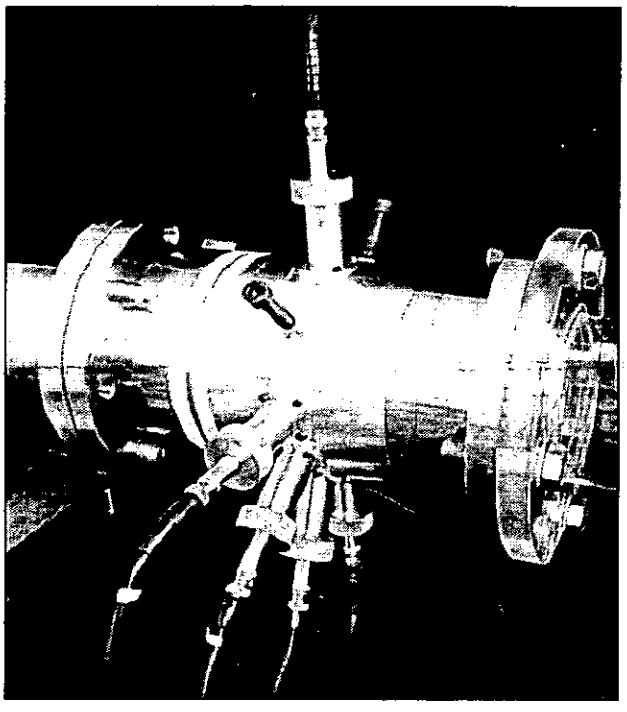

Figure 5. Measurement tool for transversal components.

ALGORITHM OF RECONSTRUCTION

When we get all necessary transit time differences, these data have to be processed to reconstruct the initial speed profile.

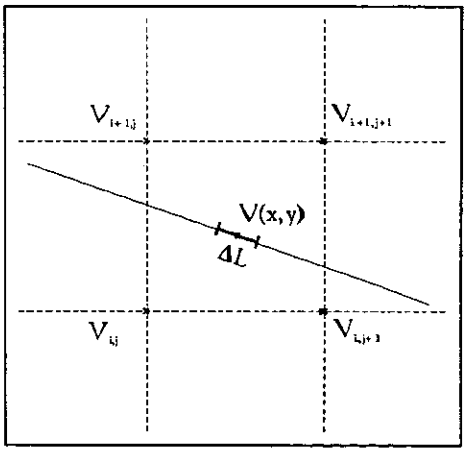

Figure 6. Bilinear interpolation on a cartesian mesh.

The reconstruction algorithm used here is a combination of the approach of Johnson *et al.* [2] and Herman's [4]. In fact, the integral in equation (8) is written in terms of an approximate sum by subdividing the segment $[a_i a_j]$ into elements of approximately constant length ΔL. The velocity is considered constant on each element and equal to its value at the middle point $V(x,y)$. But, the reconstruction can only be done for a finite number of points which are the nodes of a square grid of discretisation of the test section. In this way, the velocity V of any point (x,y) placed in a mesh defined by the four speeds $[V_1, V_2, V_3, V_4]$ is expressed by the bilinear interpolation described in figure 6 and given by the following relation :

$$\begin{cases} V(x,y) = \varepsilon_{i,j} V_{i,j} + \varepsilon_{i,j+1} V_{i,j+1} + \varepsilon_{i+1,j} V_{i+1,j} + \varepsilon_{i+1,j+1} V_{i+1,j+1} \\ \varepsilon_{i,j} + \varepsilon_{i,j+1} + \varepsilon_{i+1,j} + \varepsilon_{i+1,j+1} = 1 \end{cases} \quad (10)$$

So, considering all the ultrasonic beams, equation (8) can become a set of linear equations (Démolis [5]) as :

$$A_{xy} V_{xy} = T_{xy} \quad (11)$$

where A_{xy} is a matrix built from the mathematical decomposition of integral lines (8) of every transducers couples, T_{xy} a column vector containing all transit time differences measured, and V_{xy} the column vector corresponding to the solution, that is to say, the velocity on each point of the mesh.

If there are N nodes into the pipe, V_{xy} gets $2N$ coefficients with the N first ones for the V_x component and the next N ones for V_y component.

Because of the flow turbulence, the rms of the time measurement, which is 2.5 ns without flow, may reach 90 ns behind a bend. In these conditions to solve the system (10), one has to use an iterative algorithm to minimise the inaccuracy on time of flight measurement. That is why a quasi-solution algorithm, called « conjugate gradient method », is used here.

To test the algorithm, computer simulations have been realised on a theoretical vortex. The radial profile is strictly nil and the tangential profile is 1 $m.s^{-1}$ amplitude sinusoid. Figure 7 shows the quality of the reconstruction made with 126 equations on a 10×10 mesh for sinusoidal profile. With a solid line (—), theoretical velocities and, with plus (+ signs), reconstructed ones.

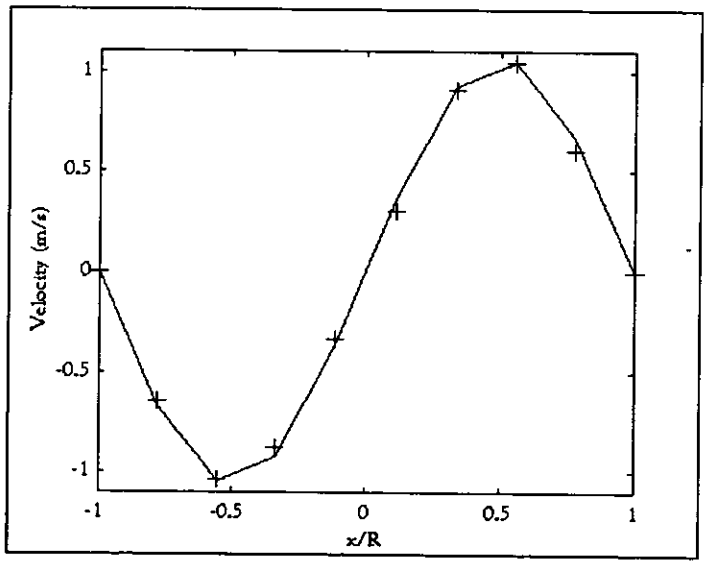

Figure 7. Comparison between a theoretical profile (—) and a reconstructed profile (+).

EXPERIMENTAL SET-UP

The ultrasonic tomography device of figure 5 has been tested on the testing bench described in figure 8.First of all, we used swirling flows which are generated by a swirl generator and for which intensity is defined by the adimensional swirl number S and the swirl angle α_s :

$$S = \frac{\int_0^R V_{axial}\left(\rho V_{tangential} r\right) r\,dr}{R\int_0^R V_{axial}\left(\rho V_{axial}\right) r\,dr} \qquad (12)$$

$$\alpha_s = \arctan\left(\tfrac{3}{2}S\right) \qquad (13)$$

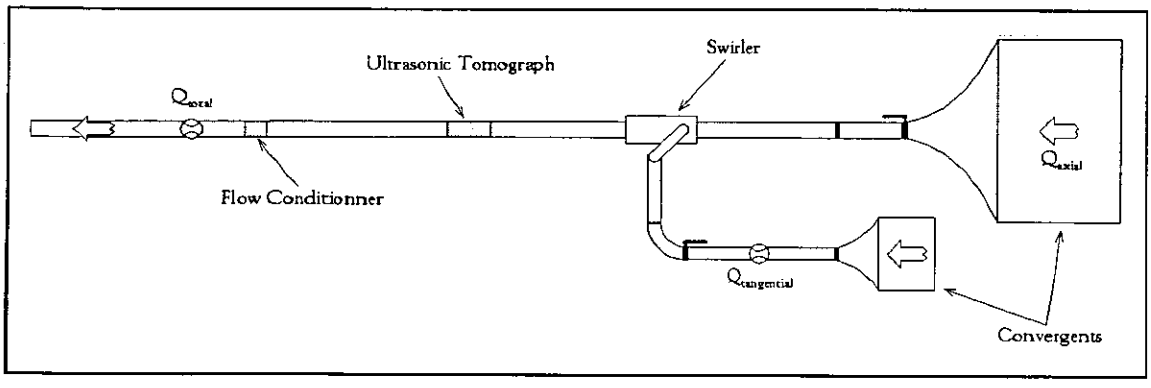

Figure 8. Testing bench.

Figure 9 compares the tangential profile obtained from the tomographic reconstruction, in dotted line (- - -), with the one measured by a hot wire probe, in solid line (—). The volumic flowrate is Q_{total}=200 m^3h^{-1} and the swirl number S = 0.46 (α_s=34.5°). The turbulence is about 8% near the wall and can reach 20% on the pipe axis.

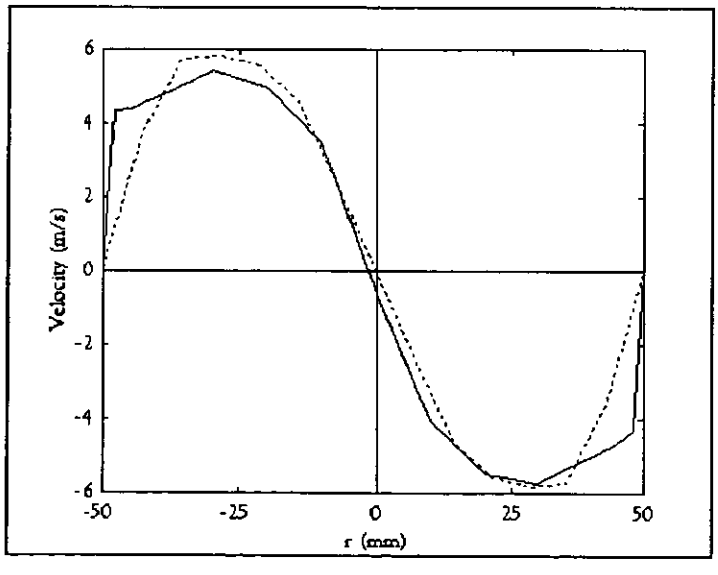

Figure 9. Comparison between an ultrasonic reconstruction (- - -) and a hot wire profile (—) for S = 0.46.

The reconstructed profile can be decomposed in three parts. The first one, which is near the wall, because of the lack of meshes, is not so well reconstructed. The result will certainly be better if the discretisation of the section is thinner. The second part is around the maximum of the velocity profile. For r<0, the difference between the reconstructed profile and the hot wire one is about 9%. But it is not the case for r>0 where they are quite similar. Indeed, the dissymetry which appears on the hot wire profile is due to a blockage effect of the probe. As the ultrasonic tomography is a non-invasive technique, the dissymetry is not visible on the

reconstructed profile. The last part of these profiles is at the pipe centre where the tomographic profile confirms the flow symmetry.

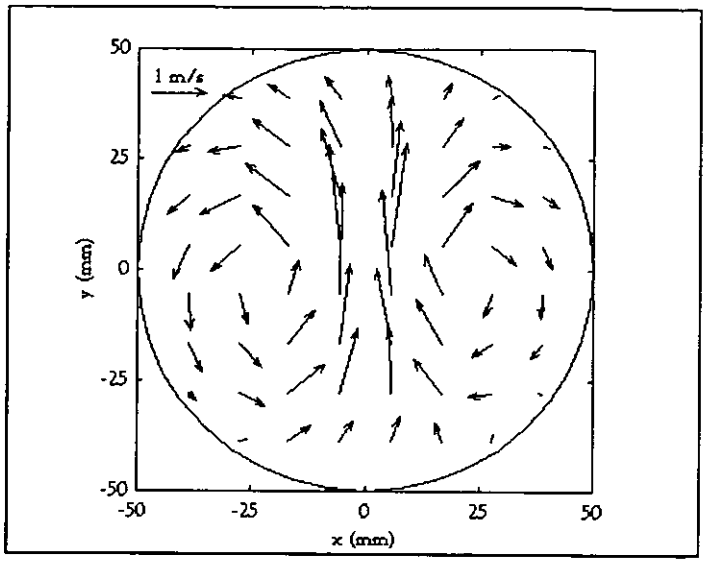

Figure 10. Reconstruction of Dean vortices behind a 90° bend.

The great difference between these two techniques is that hot wire anemometry can only give the velocity profile along a diameter whereas the ultrasonic tomography device gives it over the all section.

To illustrate this advantage and to show possibilities of such a device, an other example was conducted. The measurement section is put 2D downstream from a 90°-bend for which the ratio {curvature radius of the bend}/{pipe radius} is equal to 2. On figure 10, ultrasonic tomography has allowed to reconstruct Dean vortices which are characteristic of such a flow. They are symmetric to the symmetry plane of the bend. The curvature centre of the bend is at the bottom of the figure.

CONCLUSION

A device using the ultrasonic tomography has been realised to reconstruct the secondary flow profile in a pipe. This diagnostic tool is compact and does not need sophisticated instrumentation. No speed calibration is needed, neither is artificial seeding (which is not the case for LDA). It does not disturb the flow because the measurement is non-invasive (as opposed to hot wire probe).

If the principle is near the one of ultrasonic flowmeters, we have had to improve the time of flight measurement for low level signal and difficult transducers positions. And we have had to develop a robust algorithm to reconstruct the flow profile.

Measurements made with success in flows encountered in industrial set-up (swirl, flow downstream from bends), the simplicity of the tool (compactness, transportability, adaptability to a pipe of fixed diameter), its mechanic robustness, and little electronic material, are many advantages for this tool to be developed to an industrial device.

REFERENCES

[1]. Strzelecki A., Gajan P., Malard L., Donat D., Bosch M. : « Investigation of the influence of a pressure reducer placed upstream of a turbine meter », *3rd International Symposium of Fluid Flow Measurement*, San Antonio, Texas, U.S.A., 20-22 Mars 1995.

[2]. Johnson S. A., Greenleaf J. F., Tanaka M., Flandro G. : « Reconstructing three-dimensional temperature and fluid velocity vector fields from acoustic transmission measurments », *ISA Transactions*, Vol. 16, No. 3, pp 3-15, 1977.

[3]. Frøysa K. E., Lunde P., Sakariassen R., Grendstad J., Norheim R. : « Operation of multipath ultrasonic gas flow meters in noisy environments », *North Sea Flow Measurment Workshop*, Scotland, 28-31 Octobre 1996.

[4]. Herman T. G. : « Image reconstruction from projections, The fundamentals of computerized tomography », *Academic Press, Inc. (London)*, 1980.

[5]. Démolis J. : « Reconstruction du profil de vitesse d'un écoulement d'air en conduite par tomographie ultrasonore », *Thèse de l'Ecole Nationale Supérieure de l'Aéronautique et de l'Espace*, 1997.

NSFMW.97

North Sea FLOW Measurement Workshop

Paper ~~21~~: 14.8

LIQUID CORRECTION OF VENTURI METER READINGS IN WET GAS FLOW

Authors:
Rick de Leeuw, Shell International Exploration & Production, The Netherlands

Organiser:
Norwegian Society of Chartered Engineers
Norwegian Society for Oil and Gas Measurement
Co-organiser:
National Engineering Laboratory, UK

LIQUID CORRECTION OF VENTURI METER READINGS IN WET GAS FLOW

Rick de Leeuw

Shell International Exploration & Production, The Hague, The Netherlands

SUMMARY

Venturi flow meters can be used to measure the actual gas flow rate in wet gas streams, provided the liquid content is known. An empirical correlation is presented which accurately predicts the effect of the liquid phase on venturi meter readings in wet gas horizontal flow. The correlation is based on a comprehensive experimental data set which was collected in a full scale multiphase flow test facility. The test envelope covers the majority of the wet gas operating conditions encountered in the field. Deviations between the new correlation and the experimental base are better than 2%. The new correlation differs fundamentally from the well known orifice plate correlations of Murdock and Chisholm in that the observed dependence on the gas Froude number is accounted for and the pressure dependence is verified from 15 bar to effectively dense phase conditions. Test results of the overall pressure loss across the venturi meter are also presented. The liquid content of the gas stream can be measured using the tracer dilution method. Field experience with the tracer method over the last couple of years have demonstrated that the flow rates of water and condensate can be determined within the target uncertainty of 10%. At present the tracer method is available to the industry via two licensed contractors.

1. INTRODUCTION

The development costs of gas/condensate fields can be reduced significantly if test separators are replaced by venturi flow meters in each well flow line, and the wetness of the flow is measured periodically, typically 1 to 2 times a year, using a (non-radioactive) tracer method[1,2], see figure 1. The production from different fields can then simply be commingled prior to transporting and processing by shared facilities.

The tracer method involves injection of suitable tracers into the flow line followed by sampling of the liquids. Measurement of the tracer dilution ratio allow the determination of the water and condensate flow rates. Combining these liquid flow rates with the venturi meter readings and the correlation predicting the effect of the entrained liquids on the readings, enable the condensate gas ratio and water to gas ratio to be determined. Using the established CGR and WGR, the raw venturi

readings can be interpreted continuously in terms of gas, water and condensate flow rates, until such time that the liquid to gas ratio has substantially changed.

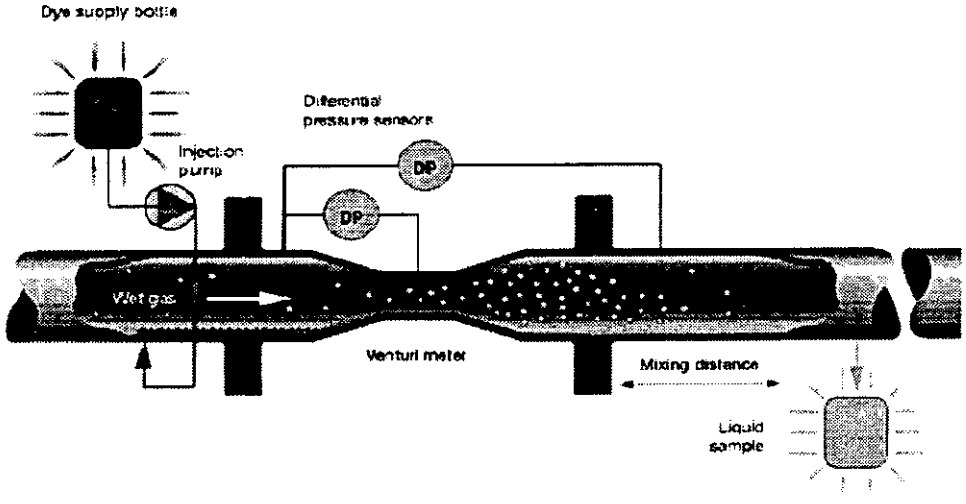

Figure 1. Wet Gas Metering Technique

To date various investigators have proposed expressions to describe the effect of entrained liquid on venturi or orifice meter readings[3]. However, as empirical correlations should only be used within their corresponding experimental range, the applicability of these expressions is limited as they have mainly been established from experiments at low to moderate pressures and flow rates as compared to field conditions. Furthermore, the most well known relationships of Murdock[4] and Chisholm[5] apply to orifice plates only.

Previous experiments at Coevorden[6,7], a field location in The Netherlands, have shown that the overreading of an orifice meter measuring natural gas at pressures around 90 bar and liquid fractions up to 4% by volume closely followed the coinciding predictions by Murdock and Chisholm. However, their apparent similarity at around 90 bar is a coincidence as extrapolation shows that for all other pressures each correlation gives a different predicted overreading. In addition the venturi meter showed a higher overreading than the orifice meter.

The experimental test range covered at Coevorden, however, was still relatively limited. Although natural gas at high pressure could be tested, variations in pressure were limited. The corresponding flow conditions were all located in a small part of the flow map: stratified wavy flow with almost no entrainment. Therefore, a comprehensive experimental data set on the performance of a venturi flow meter in

wet gas flow was called for. Such a data set was gathered at the SINTEF Multiphase Flow Laboratory in Trondheim, Norway[8]. The test envelope at this facility covered the majority of the wet gas flow conditions to be encountered in the field. The resulting data set allowed a better correlation to be developed, which is presented in this paper.

2. THE TEST SET-UP

The wet gas venturi tests were conducted at the SINTEF Multiphase Flow Laboratory, located near Trondheim, Norway. The line pressure of this large scale facility could be varied between approximately 15 and 95 bar. The entire system was insulated and heat traced to keep the temperature constant at around 30 °C. The flow loop was equipped with a horizontal, as well as a vertical riser section. The overall length of the loop was about 1 km. Single phase volumetric flow rates could be varied between 26 and 11,000 m^3/d for the liquid and between 1,200 and 35,000 m^3/d actual for the gas. All tests were performed with diesel oil as the liquid and nitrogen as the gas phase. The 4 inch test venturi had an inner pipe diameter of 97.18 mm and a throat diameter of 39 mm, resulting in a beta ratio of 0.401. As the nominal pipe diameter of the test loop was 8 inch, 70 D of 4 inch pipe was installed upstream of the venturi meter and 20 D downstream. This formed a 4 inch test section which had been located in the horizontal section of the test loop, approximately 850 meters from the beginning of the loop and 70 meters upstream from the inlet of the riser.

The venturi meter was equipped with 4 differential pressure transmitters. Two for measuring the differential pressure over the throat of the venturi, for the flow rate calculation, and two for measuring the overall pressure loss across the meter. Pressure and temperature transmitters were also provided, as well as a single energy gamma densitometer. The densitometer was used to monitor the liquid level in the pipe in order to get an indication when a new flow condition had reached the venturi section. As the total upstream length consisted of approximately 850 meters of 8 inch pipe this could take more than half an hour, depending on the actual flow velocities.

After a flow condition at the venturi section had stabilised two measurements were taken, separated by approximately 5 minutes. An individual measurement consisted of 2 minutes of data logging at a sample rate of 2 samples per second. After the logging period the averages and the standard deviations were calculated and stored.

3. TEST ENVELOPE

The test envelope was chosen to cover the majority of the wet gas operating conditions which can be encountered in the field. This is important as empirical relationships can not be applied outside their corresponding experimental range.

The tests were performed at four different line pressures of 90, 45, 30 and 15 bar, with liquid fractions up to respectively 10%, 8%, 6% and 4%. The wetness of the gas, in LGR terms, varied between 0 and 1000 m^3/million nm^3 at 90 bar, 1500 m^3/million nm^3 at 45 bar, 1800 m^3/million nm^3 at 30 bar, and 2500 m^3/million nm^3 at 15 bar. In Lockhart-Martinelli terms these values correspond to 0 and 0.3 for all conditions. Gas velocities, expressed in terms of the densiometric Froude number, were selected in the range between 1.5 and 4.8. A detailed overview of the test conditions can be found in table 1. In total, about 100 different flow conditions were covered.

Table 1. Summary of the flow conditions at the venturi meter.

Pressure	Gas velocity	Gas Froude number	Liquid velocity	Liquid Froude number	Lockhart-Martinelli parameter	LGR	GVF
[bar]	[m/s]		[m/s]			[$m^3/10^6$ nm^3]	[%]
90	12	4.8	0 - 1.2	0 - 1.31	0 - 0.3	0 - 1000	100 - 90
	8	3.2	0 - 0.9	0 - 0.97	0 - 0.3	0 - 1000	100 - 90
	4	1.6	0 - 0.4	0 - 0.44	0 - 0.3	0 - 1000	100 - 90
45	11.4	3.2	0 - 0.8	0 - 0.85	0 - 0.3	0 - 1500	100 - 92
	5.8	1.6	0 - 0.4	0 - 0.42	0 - 0.3	0 - 1500	100 - 92
30	14.5	3.2	0 - 0.8	0 - 0.83	0 - 0.3	0 - 1800	100 - 94
	7.3	1.6	0 - 0.4	0 - 0.41	0 - 0.3	0 - 1800	100 - 94
15	17	2.5	0 - 0.7	0 - 0.71	0 - 0.3	0 - 2500	100 - 96
	10	1.5	0 - 0.4	0 - 0.41	0 - 0.3	0 - 2500	100 - 96

The lowest test pressure of 15 bar corresponds to a gas density of approximately 17 kg/m^3. Nitrogen was used as the test gas. This means that the developed correlation should not be used for gas densities much below 17 kg/m^3. The maximum test

pressure was 90 bar, corresponding to a gas density of approximately 100 kg/m^3. However, the new correlation is also valid for pressures above 90 bar as the overreading reaches a well defined theoretical limit for conditions at which the gas density equals the liquid density.

The range of the Lockhart-Martinelli parameter from 0 to 0.3 corresponds to different ranges for the gas volume fraction and the liquid to gas ratio depending on the actual pressure. As can be seen from table 1. In fact, the minimum GVF, or the maximum LGR, increases at lower pressures. Basically, parameters like LGR or GVF are not particularly suitable to compare specific flow conditions at different pressures. The relationship between the GVF and the Lockhart-Martinelli parameter (X) can be expressed as:

$$GVF = \frac{Q_g}{Q_g + Q_l} = \frac{1}{1 + X\sqrt{\frac{\rho_g}{\rho_l}}} \qquad (1)$$

The relationship between the LGR and X as:

$$LGR = \frac{Q_l}{Q_{g,nc}} = X \cdot \frac{\rho_{g,nc}}{\sqrt{\rho_g \cdot \rho_l}} \cdot 1{,}000{,}000 \qquad (2)$$

Where 'nc' stand for normal conditions i.e. 0 °C and 101325 Pa. The LGR is commonly expressed in m^3 of liquid per million m^3 of gas at normal conditions. Often standard conditions are used of 15°C and 101325 Pa.

Wet gas flow conditions are best expressed in terms of their gas and liquid densiometric Froude numbers, equations 3 and 4 respectively. These give a more consistent relationship between flow parameters and flow regimes, i.e. corresponding flow regimes are obtained by corresponding Froude numbers.

$$Fr_g = \frac{v_{sg}}{\sqrt{gD}} \cdot \sqrt{\frac{\rho_g}{(\rho_l - \rho_g)}} \qquad (3)$$

$$Fr_l = \frac{v_{sl}}{\sqrt{gD}} \cdot \sqrt{\frac{\rho_l}{(\rho_l - \rho_g)}} \qquad (4)$$

The ratio of liquid Froude number to gas Froude number is equal to the Lockhart-Martinelli parameter. This parameter has proven itself to be a successful correlation parameter in the area of multiphase flow.

$$X = \frac{Q_l}{Q_g} \cdot \sqrt{\frac{\rho_l}{\rho_g}} \qquad \left(= \frac{Fr_l}{Fr_g}\right) \qquad (5)$$

The experimental test envelope as drawn in a Froude number map is illustrated in figure 2. The borders between the various flow regimes, as well as the previous Coevorden test envelope, and a typical gas/condensate field production profile are also indicated. As can be seen, the current experimental envelope covers a large range of conditions in the stratified and annular dispersed flow regimes, close up to the border with the intermittent slug flow regime.

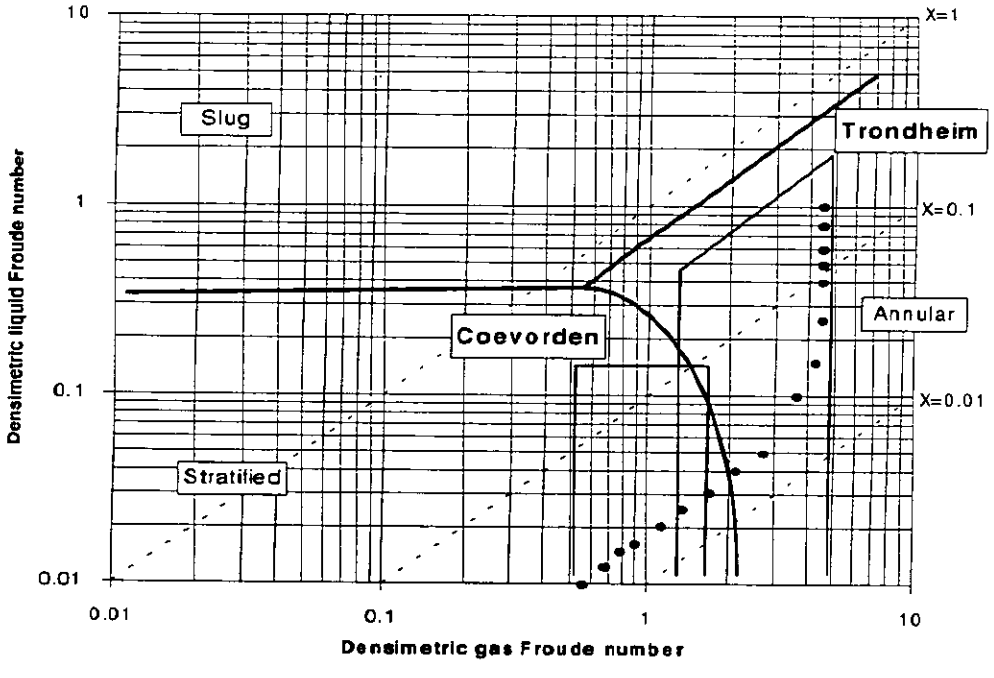

Figure 2. Flow map showing the Trondheim test envelope (various pressures), compared to Coevorden (90 bar only), and a typical production profile.

4. TEST RESULTS AND PRESENTATION OF THE NEW CORRELATION

4.1. Venturi flow rate overreading

The presence of liquid in the gas stream causes the differential pressure over the venturi meter to increase with respect to the case when only the gas is flowing. This larger differential pressure results in a larger calculated gas flow rate, hence the

venturi meter is said to "over-read". In the following the term overreading will refer to the ratio $Q_{tp}/Q_g = (\Delta P_{wet}/\Delta P_{dry})^{1/2}$.

Some typical test results are shown in figure 3. In this figure the venturi meter overreading is plotted against the liquid fraction expressed in terms of the Lockhart-Martinelli parameter. The dependence of the overreading on the actual line pressure, or better on the gas density, can clearly be seen. The lower the pressure the higher the overreading. At 15 bar and a Lockhart-Martinelli parameter of around 0.3 a venturi meter overreading of almost 1.8 is reached.

Figure 3 also shows the theoretical limit line. This line represents the condition for which the density of the gas phase equals that of the liquid. Consequently, the overreading can never go below this line. Therefore, overreading curves for pressures above 90 bar have to lie between the 90 bar and the theoretical curve. The theoretical line has been taken into account during the development of the correlation.

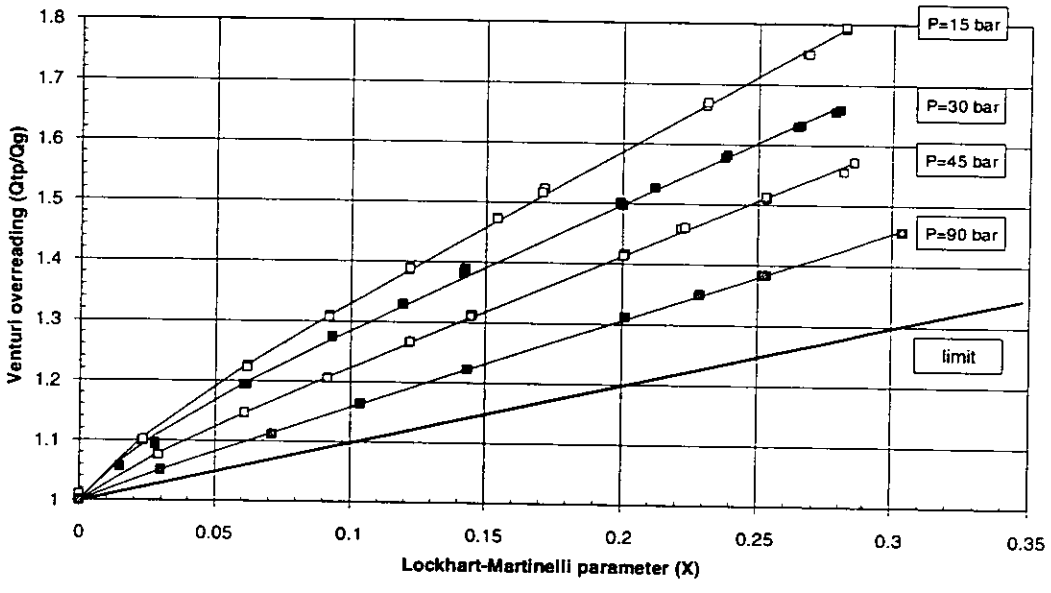

Figure 3. Trondheim test results showing venturi overreading against liquid fraction, expressed as the Lockhart-Martinelli parameter. Frg = 3.2

The test results furthermore show that the venturi meter overreading is dependent on the actual gas velocity, or gas Froude number. This is illustrated in figure 4, where the overreading is plotted for a single line pressure, but for two different gas velocities, i.e. 12 m/s and 6 m/s, corresponding to gas Froude numbers of approximately 3.2 and 1.6, respectively. Without showing the similar graphs for all

other pressures, it can be said that the lower the pressure the larger the spread. This dependence of the venturi meter overreading on the gas Froude number has not been reported in any earlier publication. Hence, all previous reported correlations are limited in their validity as none of them take this dependence into account.

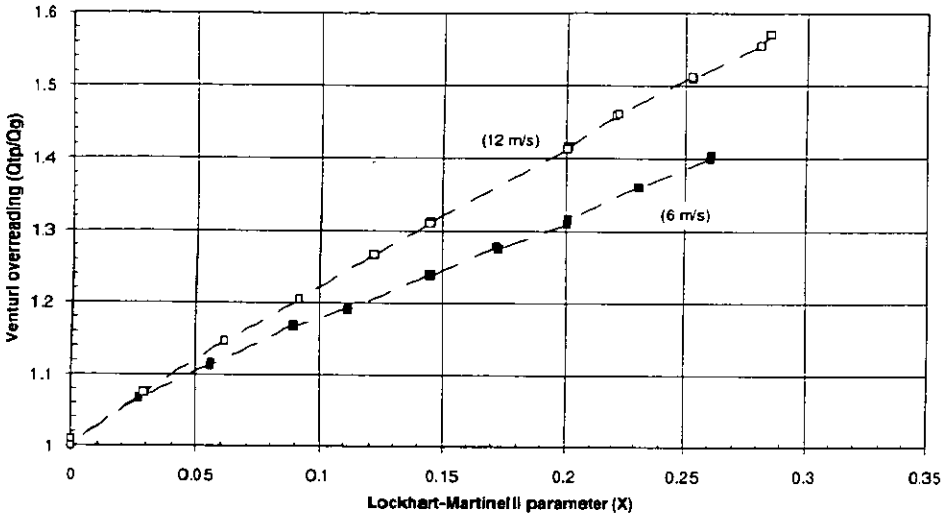

Figure 4. Typical test results showing the venturi meter overreading at 45 bar and two different gas velocities.

In particular, the experimental data shows that the well known relationships of Murdock and Chisholm do not predict the correct venturi overreading. The reason being, apart from the fact that they were originally developed for orifice plates, is that the Murdock equation neither takes the pressure nor the gas Froude number dependence into account, while the Chisholm equation does not include the gas Froude number dependence.

4.2. Venturi overreading correlation

Based on the experimental data a new correlation for use with venturi meters has been developed. The final relationship is given by equation 8. A more detailed derivation can be found in Appendix A.

$$\frac{Q_{tp}}{Q_{go}} = \sqrt{1 + CX + X^2} \qquad \text{where:} \quad C = \left(\frac{\rho_l}{\rho_g}\right)^n + \left(\frac{\rho_g}{\rho_l}\right)^n$$

$$\left.\begin{array}{lll} \text{and} \quad n = 0.606\left(1 - e^{-0.746 \cdot Fr_g}\right) & \text{for} & Fr_g \geq 1.5 \\ n = 0.41 & \text{for} & 0.5 \leq Fr_g < 1.5 \end{array}\right\} \qquad (8)$$

Above relationship is valid for gas densities above 17 kg/m³ (up to the liquid density), gas Froude numbers above 0.5, and Lockhart-Martinelli parameters up to 0.3.

A measure of how well the new venturi correlation describes the experimental data is shown in figure 5. This figure shows the absolute difference between the correlation and the actual test points. It can be seen that the difference stays within approximately ±2%. The standard deviation of the difference is only 1%. Furthermore, the individual differences have a zero mean and are normally distributed.

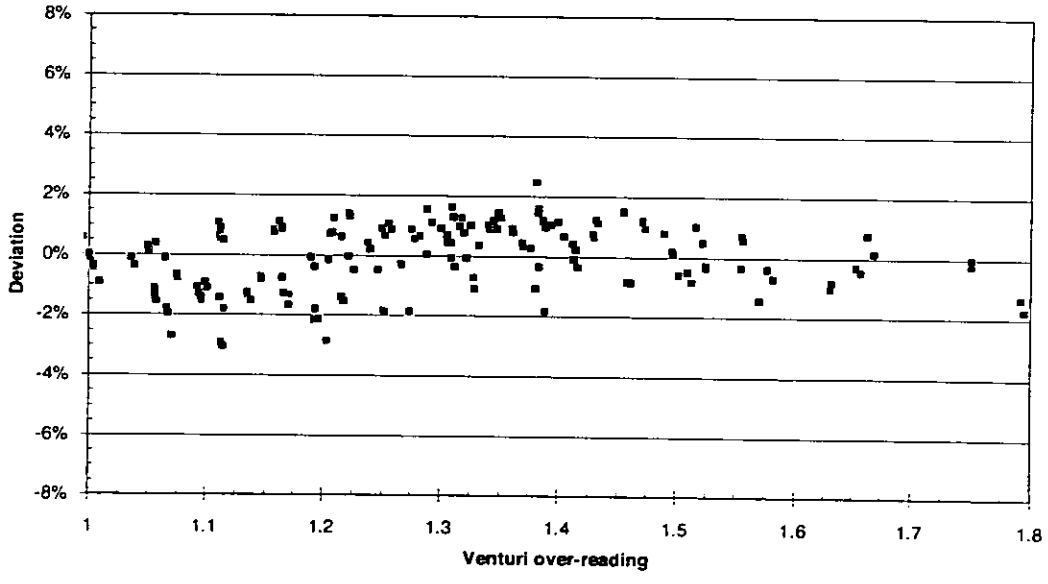

Figure 5. Plot of the difference between the developed correlation and the experimental data expressed in percentage overreading. The results are plotted as a function of the actual overreading.

To illustrate the difference between the new venturi correlation and the Murdock and Chisholm expressions, a plot has been made, see figure 6, for a typical condition for which the gas density is 80 kg/m^3 and the liquid density 700 kg/m^3. As mentioned earlier, the Murdock and Chisholm relationships do not differ too much at this condition. In contrast the new correlation predicts a different overreading for different gas Froude numbers, which leads to significant differences.

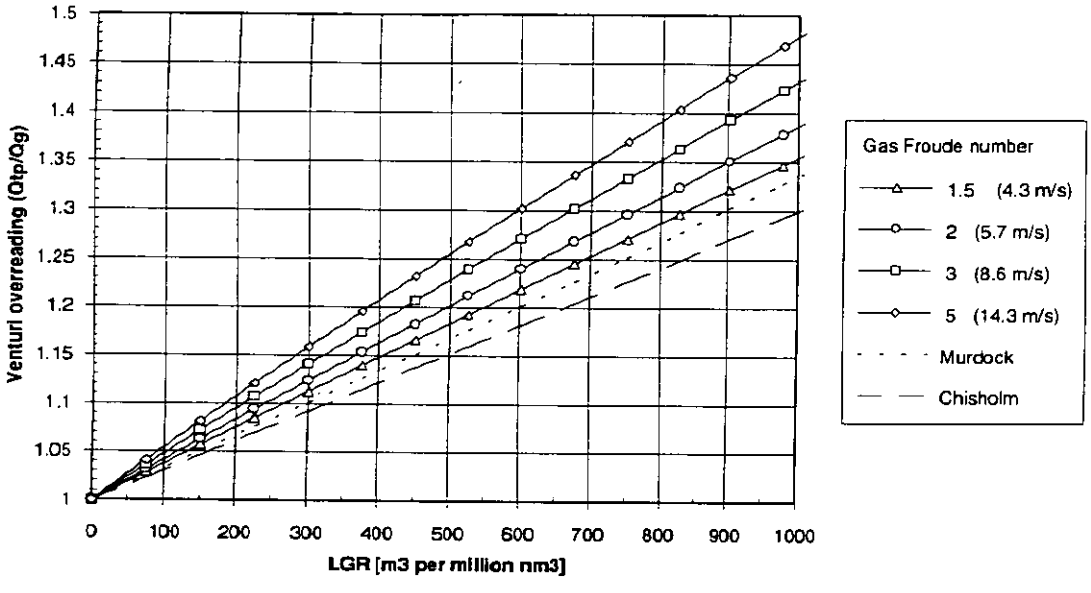

Figure 6. Illustrative comparison between the new venturi correlation and the Murdock and Chisholm orifice relationships, for the case ρ_l=700 kg/m^3 and ρ_g=80 kg/m^3.

4.3. Venturi pressure loss ratio

The pressure loss across a venturi meter is larger in two-phase flow than in single phase flow. Part of the energy which is transferred from the gas to the liquid phase when flowing through the inlet and throat sections, is not recovered in the diffuser section.

Some typical 90 bar test results are shown in figure 7, in which the venturi pressure loss ratio is plotted against the Lockhart-Martinelli parameter. The pressure loss ratio is defined as the ratio between the overall pressure drop across the meter divided by the differential pressure over the throat. The results show that the pressure loss ratio

depends on the actual liquid content. Similar to the venturi meter overreading, the pressure loss ratio also depends on the actual gas velocity or gas Froude number.

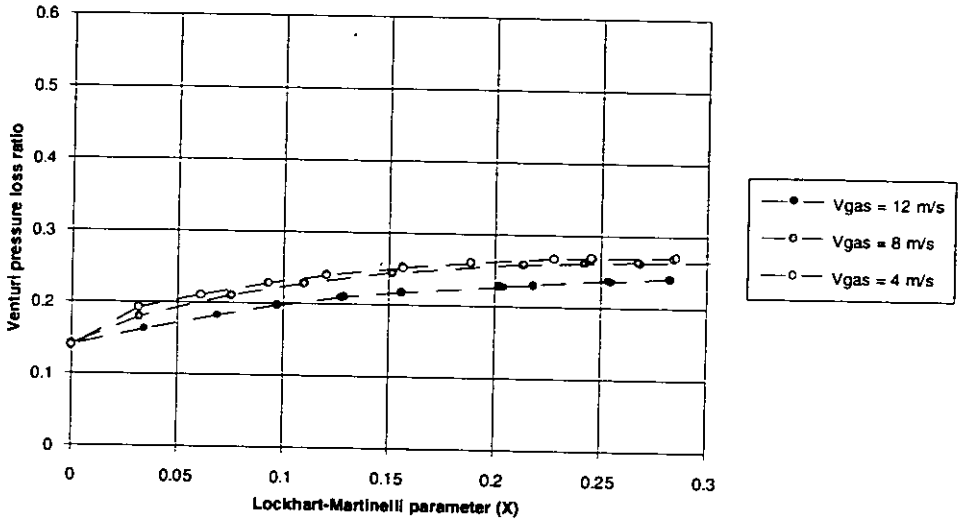

Figure 7. Test results at 90 bar showing the venturi pressure loss ratio against the Lockhart-Martinelli parameter for various gas velocities.

The potential for the pressure loss measurement is to use it as a means to determine the liquid content of the flow, from which the overreading factor can be determined accordingly. In essence this would form a simple two-phase flow meter. To date, however, no acceptable correlation formula has yet been found which would relate the pressure loss ratio to the actual liquid content and the overreading. Additional experiments might be required.

Although the exact behaviour is not yet known, the pressure loss ratio can still be used to monitor changes in the liquid content. This can be an important feature when using the tracer dilution technique for measuring the liquid content. Only when the pressure loss ratio has indicated a significant change in the liquid content, tracer measurements have to be organised.

The sensitivity of the pressure loss ratio to the actual liquid content is not constant, but varies depending on the actual wetness and line pressure. The sensitivity, which is equal to the slope of the curves, is adequate in the lower wetness range, but decreases with increasing wetness. The change in sensitivity with pressure can be seen in figure 8 where the pressure loss ratio measurements at 45 bar are shown. In this case the pressure loss ratio becomes virtually independent of the liquid content for Lockhart-Martinelli parameters larger than approximately 0.15.

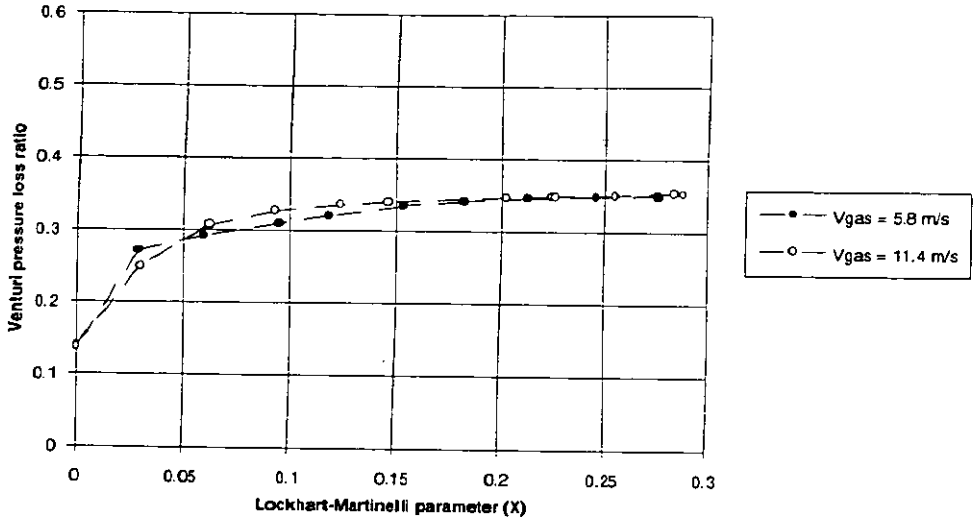

Figure 8. Test results at 45 bar showing the venturi pressure loss ratio against the Lockhart-Martinelli parameter.

5. TRACER METHOD STATUS

To determine the liquid content of the gas stream a method based on the tracer dilution technique has been developed, which was the subject of an earlier paper[4] presented at the North Sea Flow Measurement workshop in 1994. A schematic of the technique is included in figure 1. A suitably chosen tracer is injected into the flowing stream at a precisely metered rate. Downstream of the injection point, where the tracer has mixed thoroughly with the fluid, a liquid sample is taken. From the tracer dilution ratio and the injection rate the liquid flow rate can be determined.

Using different tracers the water and condensate flow rates can be measured at regular intervals. As the wetness is expected to change only gradually with time once or twice a year is expected to be sufficient. More regular measurements, however, could be required during the beginning of the field to establish the wetness behaviour over time.

Over the last number of years various field trials with the tracer method have been done to prove the technique under actual conditions. An overview of the test results is given in figure 9, which shows the deviation between the tracer and the reference measurements. It can be seen that the deviations are well within the target range of 10%. Taking into account that the plotted deviation is in fact the combined

uncertainty of the tracer method and the reference measurements, the uncertainty of the tracer method itself is even better.

After the field trials the tracer technology was licensed to SGS Redwood at Ellesmere Port, UK, and Petrotech a.s. at Haugesund, Norway, making the tracer method commercially available to the industry.

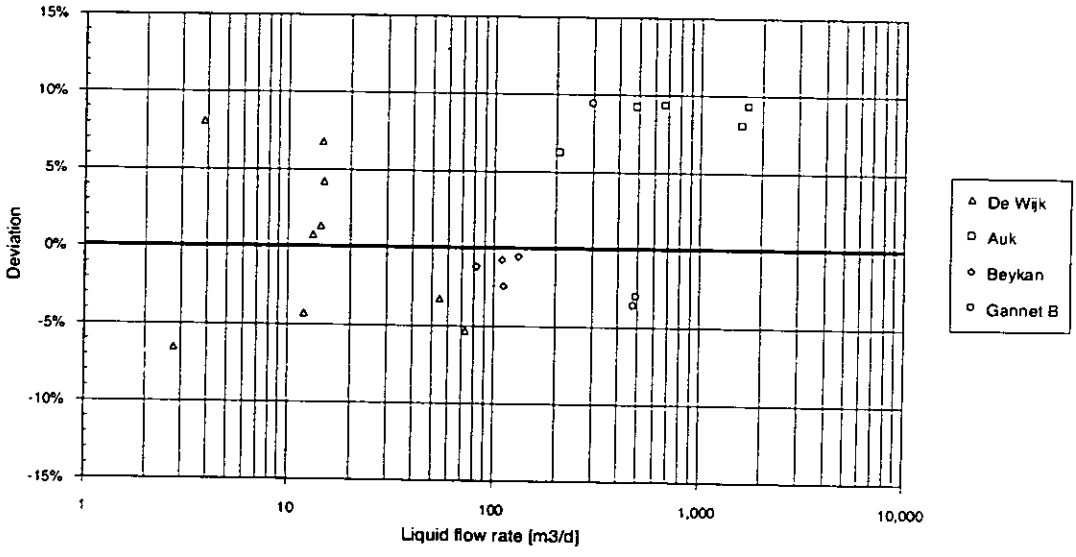

Figure 9. Overview of the various field tests, showing the deviation between the tracer method and reference measurements.

6. CONCLUSION

An empirical correlation to determine the overreading effect of the liquid phase on venturi meter readings in wet gas horizontal flow has been derived, which is in part similar to the Chisholm equation for orifice plates. The correlation is based on an extensive experimental data set, gathered at the SINTEF Multiphase Flow Laboratory in Trondheim, Norway, covering a wide range of wet gas flow conditions. The developed correlation describes the experimental data set better than ±2% absolute with a standard deviation of 1%, using only two free parameters. The theoretical overreading limit occurring at the (high) pressure for which the gas density equals the liquid density is exactly predicted. The relationships originally developed by

Murdock and Chisholm for orifice plates do not predict the venturi overreading correctly.

The experiments at SINTEF were done using a 4 inch venturi meter with a beta ratio of 0.4. Test fluids used were nitrogen and diesel oil. As the new relationship is empirical, different venturi dimensions and fluid properties should in principle be studied for their effect. However, these effects are expected to be minimal. Experiments by earlier investigators[9] with orifice plates showed no significant effect of the beta ratio. Moreover, the effect of different dimensions is basically accounted for as dimensionless Froude numbers are used. The data from the previous Coevorden tests, beta ratio 0.4, nominal line size 3 inch, and natural gas and water as test fluids, overlap with the SINTEF data for similar flow conditions.

The liquid content of the gas stream can be determined by means of the tracer dilution technique. Field trials at a number of different locations have demonstrated that the water and condensate flow rate can be measured within the target uncertainty of 10%. Using the new correlation this means that the gas flow rate can be corrected to within approximately 2% to 4%, depending on the actual liquid content. At present, the tracer method is commercially available through two licensed service companies, Petrotech a.s. in Norway and SGS Redwood in the UK. Continuous monitoring of variations in the liquid content can be done by measuring the venturi pressure loss ratio.

7. LIST OF SYMBOLS AND UNITS

β	venturi beta ratio (= d/D)	[-]
C	variable defined in eq. 4	[-]
D	internal pipe diameter	[m]
Fr_g	densiometric gas Froude number	[-]
Fr_l	densiometric liquid Froude number	[-]
g	gravitational constant	[m/s^2]
LGR	Liquid to Gas Ratio	[$m^3/10^6$ nm^3]
n	variable defined in eq. 5	[-]
P	pressure	[Pa]

Q_l	liquid flow rate	[m^3/s]
Q_g	gas flow rate	[m^3/s]
Q_{tp}	gas flow rate calculated using the two-phase pressure drop	[m^3/s]
ρ_l , ρ_g	liquid, gas density	[kg/m^3]
v_{sl} , v_{sg}	liquid, gas superficial velocity	[m/s]
X	Lockhart-Martinelli parameter	[-]

8. REFERENCES

[1] De Leeuw, H., "Venturi meter performance in wet gas flow," Proceedings Multiphase '97 conference, Cannes, Jun. 1997.

[2] De Leeuw, H., "Wet gas flow measurement using a combination of venturi meter and a tracer technique," North Sea Flow Measurement Workshop, Peebles, Scotland, Oct. 1994.

[3] Lin, Z.H., "Two-phase flow measurements with orifices," Encyclopedia of Fluid Mechanics, vol. 3, Gulf Publishing Company, Houston, Texas, 1986, pp. 841-862.

[4] Murdock, J.W., "Two phase flow measurement with orifices," Journal of Basic Engineering, December 1962.

[5] Chisholm, D., "Two phase flow through sharp-edged orifices," Research note, Journal of Mechanical Engineering Science, 1977.

[6] Nederveen, N., Washington, G.V., Batstra, F.H., "Wet gas flow measurement," SPE 19077, June 7-9 1989.

[7] Washington, G., "Measuring the flow of wet gas," North Sea Flow Measurement Workshop, Haugesund, Norway, Oct.1991.

[8] De Leeuw, H., "High pressure wet gas experiments at SINTEF Norway," Internal report, July 1994.

[9] Mattar, L., Aziz, K., Gregory, G., "Orifice metering of two phase flow," SPE paper 7411, Oct. 1978.

APPENDIX A DERIVATION OF THE VENTURI CORRELATION

The experimental data presented in this paper shows that the well known relationships of Murdock and Chisholm do not predict the correct venturi overreading. The reason being, apart from the fact that they were developed for orifice plates, is that the Murdock equation neither takes the pressure nor the gas Froude number dependence into account, while the Chisholm equation does not include the gas Froude number dependence. This can be seen clearly if the Murdock and Chisholm relationships are written in terms of the Lockhart-Martinelli parameter (X).

Murdock's relationship:

$$\frac{Q_{tp}}{Q_g} = 1 + 1.26X \qquad \text{(A-1)}$$

Chisholm's relationship:

$$\frac{Q_{tp}}{Q_g} = \sqrt{1 + CX + X^2} \qquad \text{where } C = \left(\frac{\rho_l}{\rho_g}\right)^{0.25} + \left(\frac{\rho_g}{\rho_l}\right)^{0.25} \quad \text{(for } X<1\text{)} \qquad \text{(A-2)}$$

It shows that the overreading predicted by the Murdock equation only depends on the Lockhart-Martinelli parameter. The effect of pressure and gas Froude number on the overreading, as illustrated in the figures 3 and 4, can therefore not be predicted. The Chisholm equation does take the line pressure into account via the C parameter which contains the gas density, but the explicit gas Froude number dependence shown in figure 4 is not predicted.

The general shape of the Chisholm curve, however, closely resembles those of the experimental curves. In particular the observed small curvature at low liquid fractions is well predicted. In fact, the experimental data for a single gas Froude number and line pressure can be described very well by the Chisholm equation by tuning the C factor.

Furthermore, it was found that a general form of Chisholm's relationship for parameter C,

$$C = \left(\frac{\rho_l}{\rho_g}\right)^n + \left(\frac{\rho_g}{\rho_l}\right)^n \qquad \text{(A-3)}$$

could be used to describe the pressure effect for a specific gas Froude number by selecting the right magnitude for parameter *n*. This is illustrated in figure A1. A fixed value for *n* thus describes the overreading curves for a single gas Froude number but for the whole pressure range.

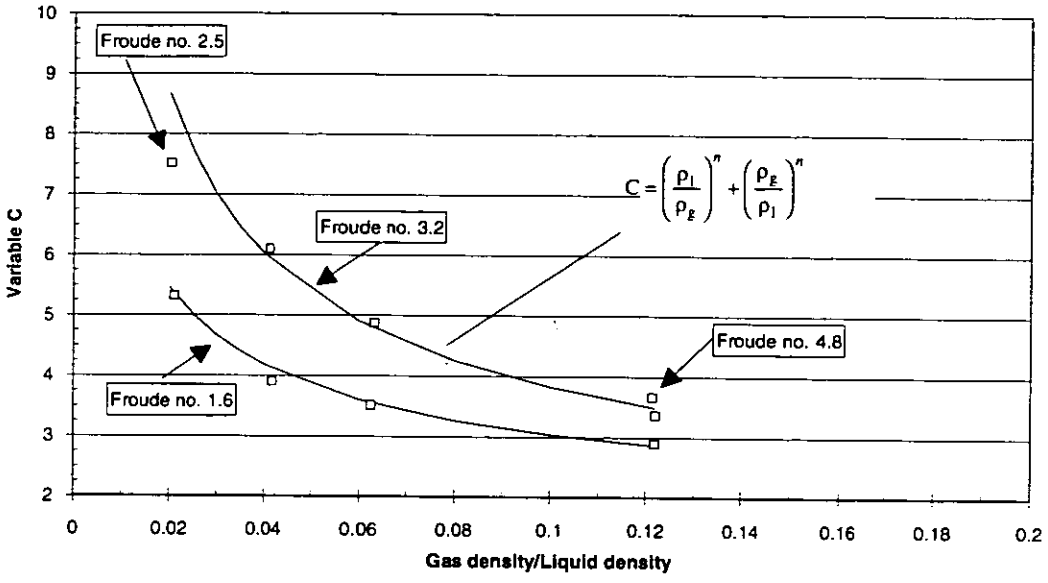

Figure A1. Resulting C values for the complete data set as a function of the density ratio and gas Froude number.

The theoretical limit condition is included automatically. When the gas density equals the liquid density C is equal to 2, independently of n. With C equal to 2, equation A-2 and A-3 exactly describe the theoretical line which holds for dense phase conditions, i.e. very high pressures.

All the resulting values for n, which are obtained by fitting equation A-3 to the data, are shown in figure A2. These values were fitted with the following empirical relationship:

$$n = 0.606\left(1 - e^{-0.746 \cdot Fr_g}\right) \qquad \text{for} \quad Fr_g \geq 1.5 \qquad \text{(A-4)}$$

The complete SINTEF data set has now been described by using only two free parameters, i.e. 0.606 and 0.746.

The value of n for gas Froude numbers between 0.5 and 1.5 is derived from the previous Coevorden data set and was found to be 0.41. As indicated in figure A2, the Coevorden test envelope partly overlaps with the SINTEF one, but extends further down to lower gas Froude numbers.

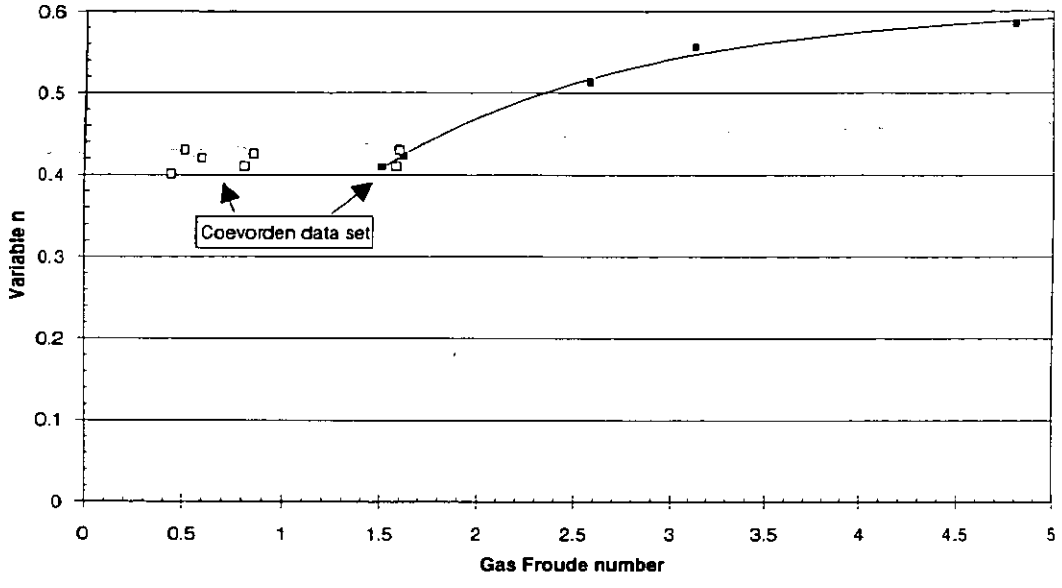

Figure A2. Resulting n values for both the Trondheim and Coevorden data.

The overlapping conditions are well predicted by the new correlation. However, the Coevorden results for Froude numbers below 1.5 show that the value of n does not decrease any further and stays constant at about 0.41. This effect is attributed to the fact that the Coevorden flow conditions were all in the stratified flow regime with a constant, but almost zero entrainment. At higher Froude numbers n increases as the entrainment increases.

The final relationship to calculate the venturi meter overreading is given by formula A-5. The relationship is valid for gas densities above 17 kg/m^3 (up to the liquid density), gas Froude numbers above 0.5, and Lockhart-Martinelli parameters up to 0.3.

$$\frac{Q_{tp}}{Q_{go}} = \sqrt{1 + CX + X^2} \qquad \text{where:} \quad C = \left(\frac{\rho_l}{\rho_g}\right)^n + \left(\frac{\rho_g}{\rho_l}\right)^n$$

$$\left.\begin{array}{lll} \text{and} \quad n = 0.606\left(1 - e^{-0.746 \cdot Fr_g}\right) & \text{for} & Fr_g \geq 1.5 \\ n = 0.41 & \text{for} & 0.5 \leq Fr_g < 1.5 \end{array}\right\} \qquad \text{(A-5)}$$

NSFMW.97

North Sea FLOW Measurement Workshop

Paper 22: 4.2

WET GAS TESTING WITH THE V-CONE FLOWMETER

Authors:
Stephen A. Ifft, McCrometer Inc., USA

Organiser:
Norwegian Society of Chartered Engineers
Norwegian Society for Oil and Gas Measurement
Co-organiser:
National Engineering Laboratory, UK

WET GAS TESTING WITH THE V-CONE FLOWMETER

Stephen A. Ifft
McCrometer Inc., USA

SUMMARY

This paper discusses a series of tests conducted at the Southwest Research Institute for McCrometer Inc. Southwest Research in San Antonio, Texas has developed a wet gas testing loop using nitrogen gas and water. McCrometer contracted with Southwest Research to conduct a series of tests to evaluate the performance of the V-Cone flowmeter in wet gas applications. The geometry of the V-Cone provides a clean measurement of wet gas without liquid build up before or after the meter section.

Three V-Cone flowmeters were tested with a beta ratio range from 0.45 to 0.67. The test loop controlled the water loading from 0 to 5% by mass. Each meter was tested at six flowrates under two different pressures.

In addition to the performance testing, Southwest also installed a McCrometer supplied "clear" V-Cone made with acrylic pipe. This clear meter, under low pressure, allowed a visualization of the flow of wet gas through the meter. Still photography and video cameras were used to capture several combinations of gas flow and water loading.

Results show, as expected, that the V-Cone held no water either upstream or downstream of the cone section. Performance tests indicate a slight and consistent positive shift in flow coefficient under increasing water loadings. Smaller beta ratios showed less deviation from baseline conditions than larger beta ratios.

INTRODUCTION

For this paper, wet gas flow will be defined as the flow of a gas with the addition of liquid between 0 and 5% fraction by mass. Many field applications could fall into this category of flow, particularly in the oil and gas production industry. Wet, natural gas applications include flow after a separator or slug catcher or gas production without a separator.

Orifice plates have historically been used to measure the vast majority of natural gas flow in the world. The extended knowledge of the orifice plate is based on dry gas calibrations. With the introduction of liquid into a gas flow line, the calculations and parameters that the orifice calculations are based on become less accurate. Murdoch[1], Ting[2], and others have researched the effect of wet gas on orifice plate measurement. While the data for these

research efforts have not always agreed, the conclusions point in the same direction...that wet gas can effect meter accuracy and more work should be done to quantify the effect.

An observed effect of wet gas on an orifice plate meter is the holding of liquid before or after the plate. As the velocity increases, the amount of liquid held before the plate is minimal. The low pressure, recirculating region after the plate, however, can hold a significant amount of liquid, as shown in figure 1.

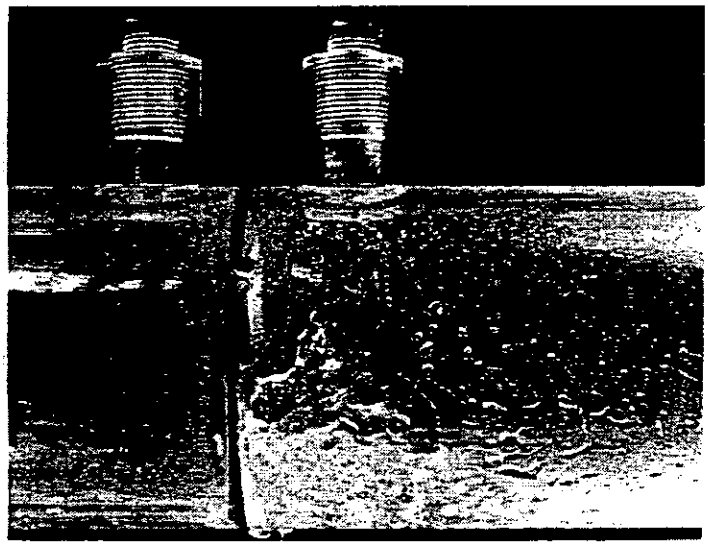

Figure 1. Photograph of an orifice plate in clear meter tube with wet gas. Flow is from left to right. Fluid is nitrogen with water injected upstream (Photograph courtesy of Southwest Research Institute)

The V-Cone differential pressure meter was introduced in 1986 as an alternative metering technology. Previous studies have shown the V-Cone insensitive to many installation conditions found in industrial field applications[3,4,5,6,7]. These papers considered the effects of flow disturbances upstream and downstream of the meter. The design of the V-Cone improves the performance of the meter in less than ideal conditions. The V-Cone is designed with a centrally located cone as a restriction. This is unlike other traditional differential pressure devices where the restriction comes from the pipe wall. The V-Cone leaves an annular opening around the cone. In wet gas, any free running liquid along the pipe wall would simply pass through, without touching the cone.

The V-Cone, therefore, should be well suited for wet gas applications. Prior to this testing, no research had been formally completed to analyze the effect of wet gas on the accuracy of a V-Cone meter.

TESTING

Facility

Southwest Research describes their flow loop with the following:

The experiments were conducted on a recirculating flow loop at Southwest Research Institute. The flow loop consists of a roots type compressor with a variable speed motor,

compressor suction and discharge bottles to eliminate compressor pulsations, and a heat exchanger and chiller to control the gas temperature. The flow loop can flow at up to 550 ACFM at pressures up to 120 psia.

The wet gas flow meter performance tests were conducted using nitrogen as the gas phase and water as the liquid phase.

Figure 2 shows how the V-Cone meter was installed in the test facility and the location of the instrumentation. The V-Cone meter was installed in a 4-inch diameter horizontal pipe section that was located downstream of a sonic nozzle bank. The sonic nozzles were used as the reference gas flow meters for the tests. No flow conditioner was installed directly upstream of the V-Cone flow meter. A scrubber removed the liquid from the gas stream downstream of the V-Cone meter. A pump recirculated the liquid from the scrubber back to the liquid injection port.

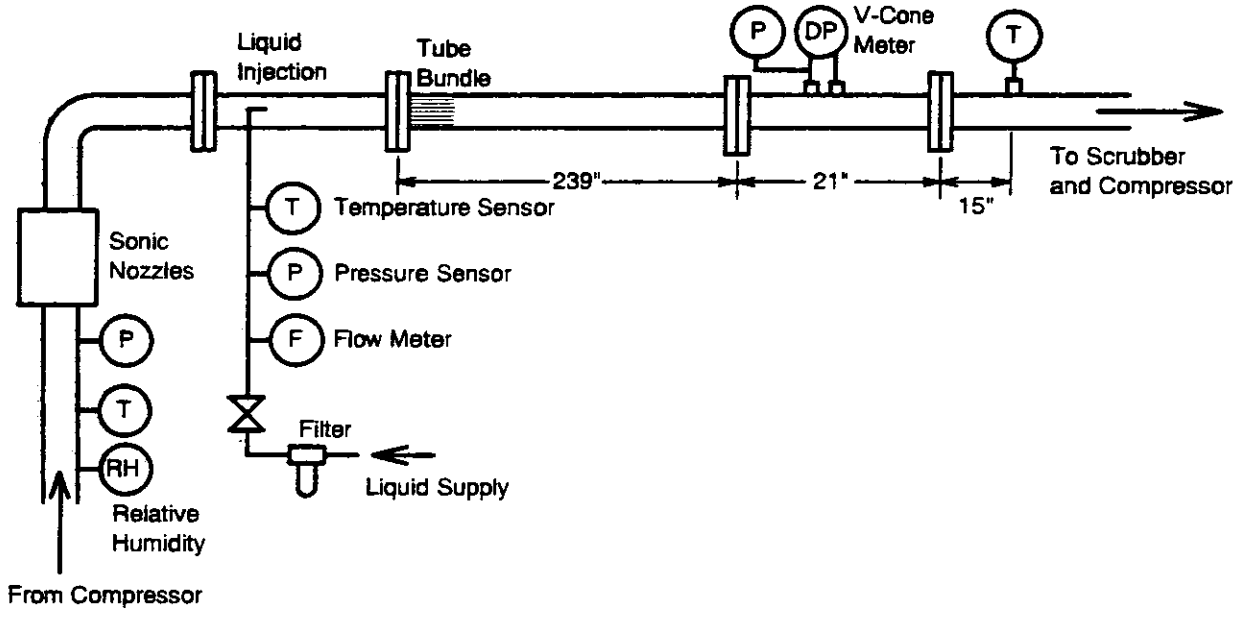

Figure 2. Schematic diagram of the V-Cone meter installation in the test facility. *The liquid was injected between the sonic nozzles and the V-Cone meter. This allowed the gas flow rate to be accurately metered, without the liquid present in the gas.*

Liquid was injected upstream of the V-Cone meter and allowed to mix with the gas for 59 pipe diameters before it entered the flow meter. This mixing length allowed the two-phase flow to be established in its natural flow regime, independent of the water injection method. The flow regimes for the tests were stratified-wavy and annular-mist.

Liquid was injected through a 3/8-inch outside diameter tube that was inserted straight into the pipe. The tube had seven 1/8-inch diameter holes drilled in the downstream side of the tube for water injection into the flow stream. Just downstream of the water injection tube, a 19-tube tube bundle was installed to eliminate any flow disturbance caused by the injection tube (this tube bundle was located 59 pipe diameters upstream of the flow meter).

Test Procedure

The following procedure was outlined and followed:

- The gas flow rate was selected by opening the valves to the desired sonic nozzles.
- The compressor was turned on and the flow loop allowed to come to thermal equilibrium (~65°F). The liquid pump was also turned on to circulate liquid through the test section.
- The flow loop was briefly turned off and the "zero" reading taken on the differential pressure sensors. This was to check for any sensor drift.
- The compressor and liquid pump were turned back on and the desired gas flow rate established. The pressure drop across the sonic nozzles was set so that the flow was choked in the sonic nozzles.
- With a constant gas flow rate, seven different nominal liquid loadings were tested. The liquid rates were varied in the following order: 0%, 5%, 3%, 0.5%, 4%, 1%, 2%, 0% liquid mass fraction. For each liquid rate, three separate readings were recorded. Each separate data "reading" consisted of an average of 31 samplings of the sensors over a period of 2.5 minutes.

The tests were conducted to determine the effect of liquid on the V-Cone meter measurement accuracy. The sonic nozzles held the gas flow rate constant as the liquid flow rate was varied. Using this approach, the exact value of the gas flow rate was not important--the flow rate just had to be constant. The sonic nozzles provided the constant flow rate so that small changes in the V-Cone metering accuracy (caused by liquid loading) could be measured.

Three meters were tested with beta ratios of 0.45, 0.59, and 0.67. The beta ratio of the V-Cone equates to the same open area in the meter as an orifice of similar beta ratio. SwRI tested at two different pressures, with three flowrates at each pressure. The liquid loading was varied between 0 to 5% by mass in seven increments.

The V-Cone meter discharge coefficient, C_d, was computed for each test using the gas flow rate measured with the sonic nozzle ($\dot{m}_{nozzle}$), and the measurements of the V-Cone upstream static pressure, differential pressure (ΔP), and the downstream gas temperature. The gas density (ρ) was calculated using the AGA-8 equation of state. The following equation was used to calculate the V-Cone meter flow coefficient:

$$C_d = \frac{\dot{m}_{nozzle}\sqrt{1-\beta^4}}{A_o Y\sqrt{2\rho\Delta P}}$$

In the above equation, Y is the expansion factor and β is the beta ratio. For the V-Cone meter, the beta ratio equation is:

$$\beta = \sqrt{1 - \frac{d^2}{D^2}}$$

where D is the pipe diameter, and d is the cone diameter.

TEST RESULTS

A visual recording of wet gas flow through a V-Cone was taken using both video and still photography. A clear section of 4" pipe held specially made V-Cone components. The stainless steel cone was a non-working model and used only for photography.

The V-Cone held no water along the pipe walls, as expected. A slight amount of water held to the downstream, low pressure face of the cone.

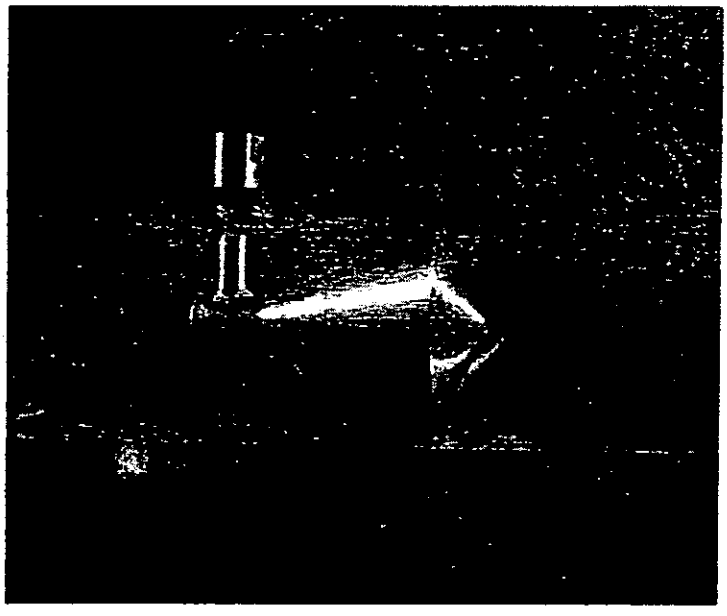

Figure 3. Photograph of V-Cone in clear meter tube with wet gas flow. Flow is from left to right. Fluid is nitrogen with water injected upstream

The following graphs display the test results as the error in gas reading vs. liquid mass fraction, both in percentages. The baseline point for each V-Cone was calculated as the average of all readings taken with no water flowing through the meter. The error in gas reading was calculated as:

$$Error(\%) = \frac{Q_{ind} - Q_{sn}}{Q_{sn}} \times 100$$

where Q_{ind} is the indicated flow from the V-Cone using an averaged baseline discharge coefficient, and Q_{sn} is the flow measured from the sonic nozzle bank.

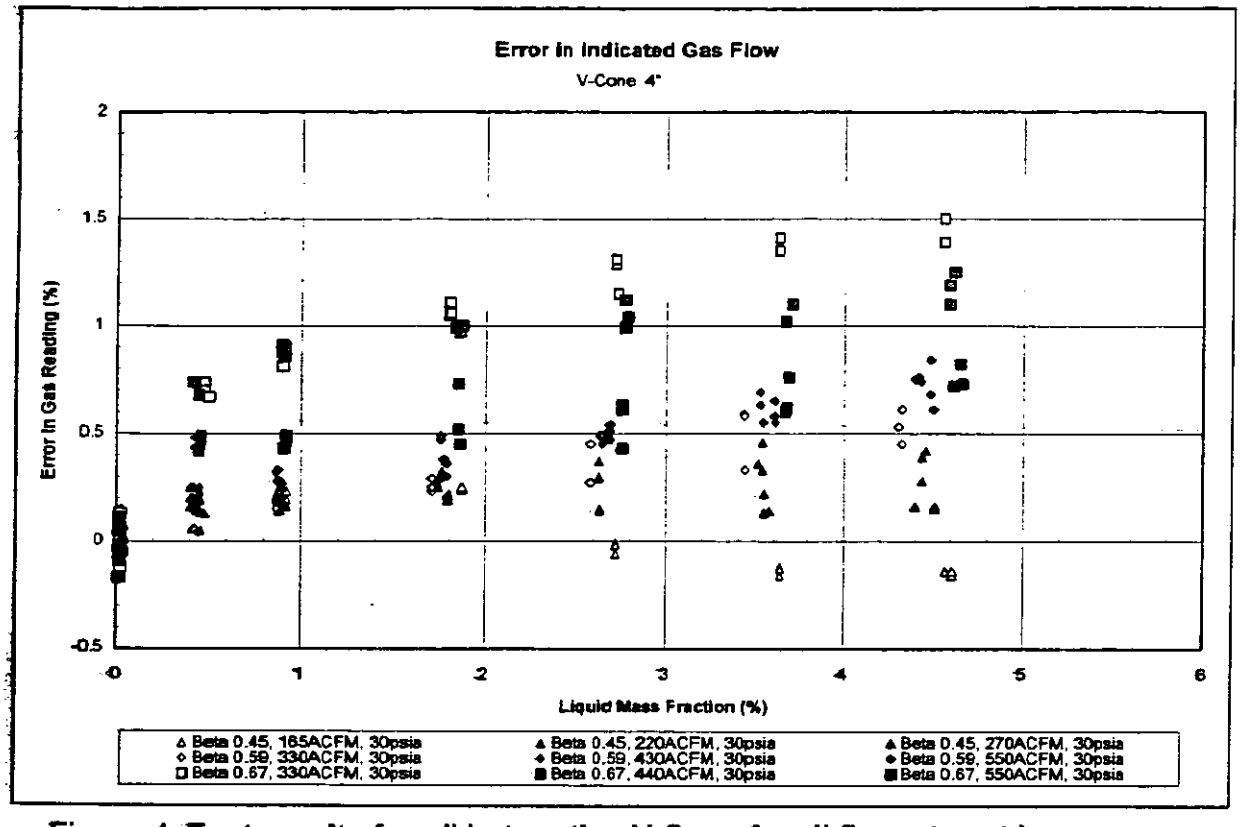

Figure 4. Test results for all beta ratios V-Cone for all flowrates at low pressure.

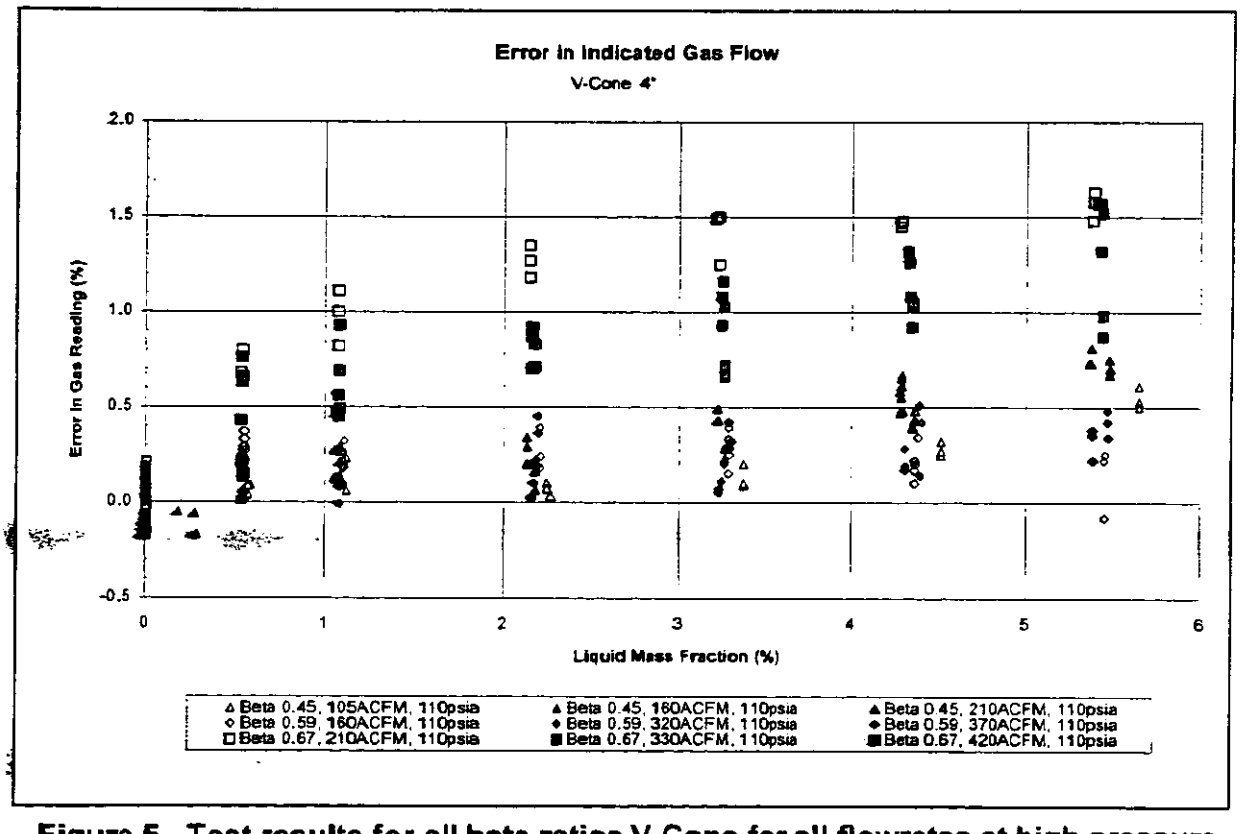

Figure 5. Test results for all beta ratios V-Cone for all flowrates at high pressure.

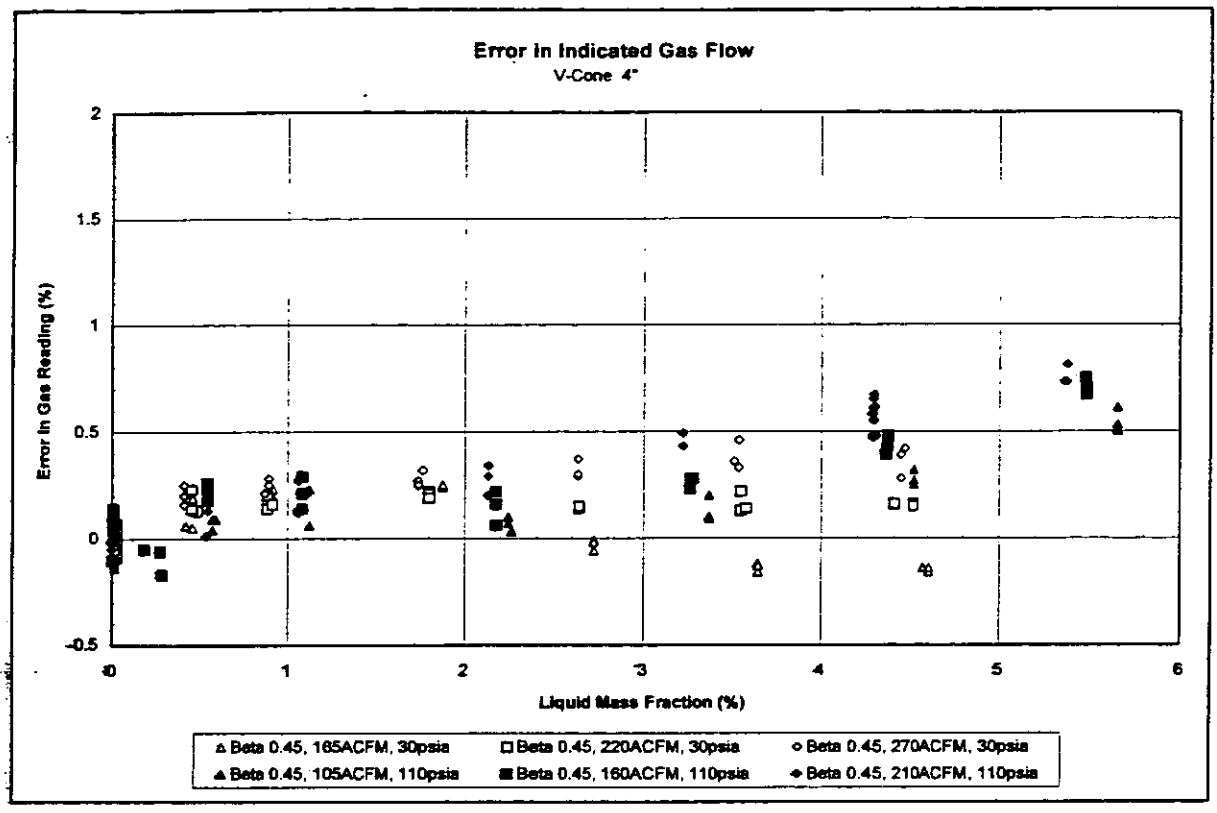

Figure 6. Test results for beta 0.45 V-Cone for all flowrates and pressures.

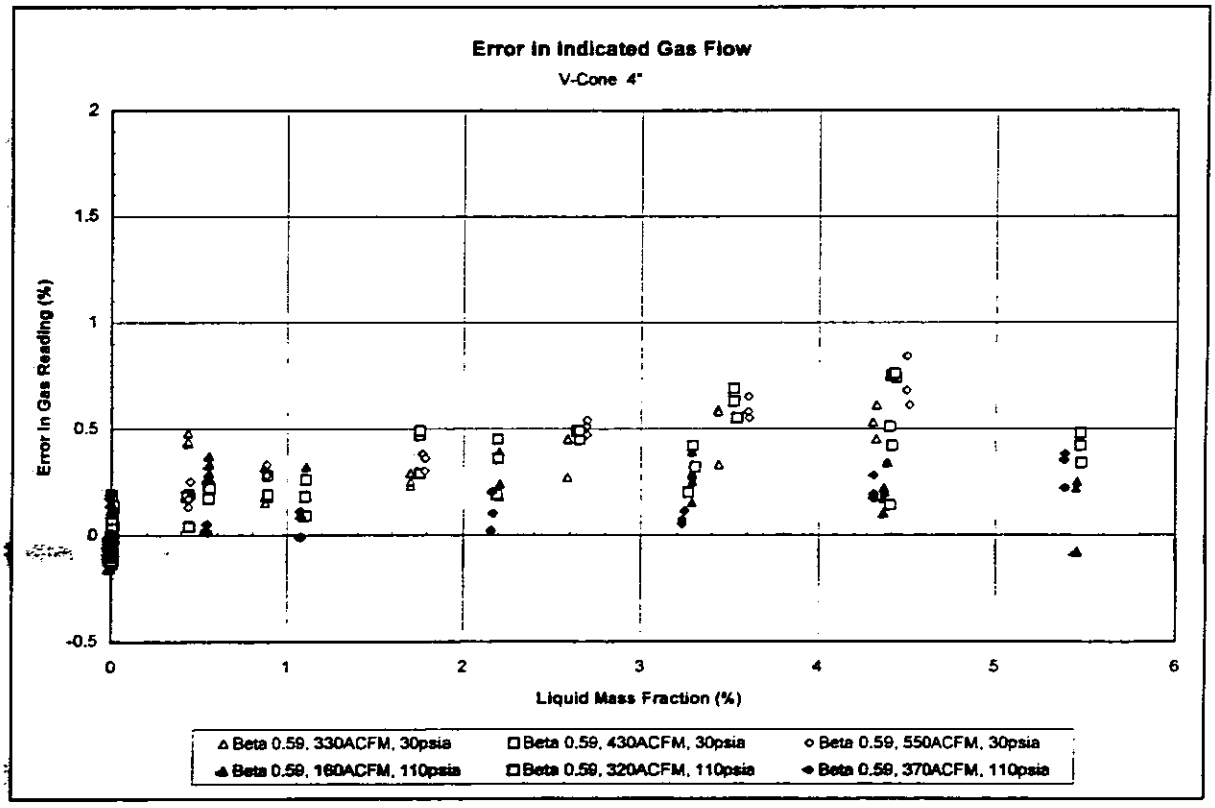

Figure 7. Test results for beta 0.59 V-Cone for all flowrates and pressures.

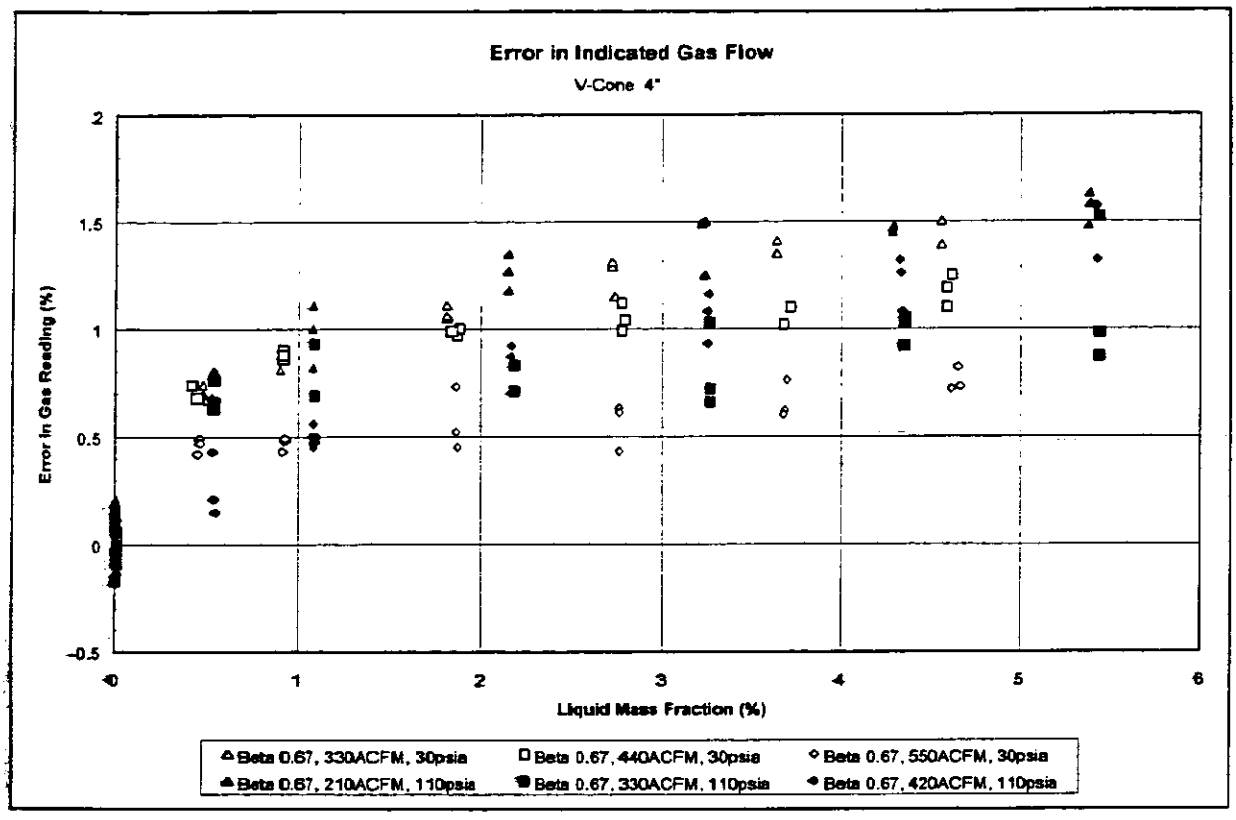

Figure 8. Test results for beta 0.67 V-Cone for all flowrates and pressures.

CONCLUSIONS

Visual recording of the V-Cone meter in low pressure wet gas flow reveals that very little liquid is held before or after the meter section.

Performance tests show the V-Cone discharge coefficient will decrease with increased water loadings. The amount of this decrease depends on the beta ratio of the meter and the line pressure. The decrease in discharge coefficient will cause a positive error in the gas reading calculation. Thus the meter will overpredict the gas flow in the pipe.

The errors in indicated gas flow were nearly always positive. For the two smaller beta ratios, the errors reached a maximum of 1.0%. At the lower pressure, the beta 0.45 error stayed within –0.25% to 0.5%. For the higher pressure, the beta 0.59 performed best with errors between 0 and 0.5%. The largest errors of 1.5% were measured with the beta 0.67 meter at both pressures.

The V-Cone appears capable of measuring wet gas flow to a system accuracy of better than ±1.0% of rate. Beta ratios smaller than 0.59 would be recommended. The consistent positive errors are conducive to easy correction factors in the presence of wet gas.

REFERENCES

1. Murdock, J. W., "Two-Phase Flow Measurement with Sharp-Edged Orifices," J. Basic Engineering, Vol. 84, No. 4, pp. 419-433, 1962.

2. Ting, V. C. and G. P. Corpron, "Effect of Liquid Entrainment on the Accuracy of Orifice Meters for Gas Flow Measurement," presented at the 1995 International Gas Research Conference, November 1995, Cannes, France.

3. Ifft, S. A. and E. D. Mikkelsen, "Pipe Elbow Effects on the V-Cone Flowmeter," North Sea Flow Measurement Workshop, October 1992, Peebles, Scotland.

4. Dahlstrøm, M. J., "V-Cone Meter: Gas Measurement for the Real World," North Sea Flow Measurement Workshop, October 1994, Peebles, Scotland.

5. Ifft, S. A., "Installation Effects on the V-Cone Flowmeter," 3rd International Symposium on Fluid Flow Measurement, March 1995, San Antonio, Texas, USA.

6. Shen, J. S., J. Bosio, and S. Larsen, "Performance Study of a V-Cone Meter in Swirling Flow," North Sea Flow Measurement Workshop, October 1995, Lillehammer, Norway.

7. Ifft, S. A., "Partially Closed Valve Effects on the V-Cone Flowmeter," 8th International Conference on Flow Measurement, October 1996, Beijing, China.

NSFMW.97

North Sea FLOW Measurement Workshop

Paper ~~23~~: 4·3

EUROPEAN INTERCOMPARISON OF THE CALIBRATION OF GAS DENSITY METER AND AN INTRODUCTION TO A GUIDELINE TO THE DETERMINATION OF GAS DENSITY

Authors:
Marianne Tambo and Tove Søgaard, The FORCE Institute, Denmark

Organiser:
Norwegian Society of Chartered Engineers
Norwegian Society for Oil and Gas Measurement
Co-organiser:
National Engineering Laboratory, UK

EUROPEAN INTERCOMPARISON OF THE CALIBRATION OF GAS DENSITY METERS AND AN INTRODUCTION TO A GUIDELINE TO THE DETERMINATION OF GAS DENSITY

AUTHORS: Marianne Tambo and Tove Søgaard, The FORCE Institute, Denmark

SUMMARY

For more than 10 years Nordic countries have been producing, selling and/or buying natural gas. One of the major issues has been how to determine the amount of gas. Several of the methods involve the determination of gas density. Two laboratories in the Nordic countries perform calibration of vibrating element gas density meters and an intercomparison was performed as part of a NORDTEST* project between these two laboratories and three European calibration laboratories. The intercomparison was performed in 1996 at the laboratories listed in table 1. The calibration gas was nitrogen. The main conclusion of the intercomparison was that all the laboratories were well within an uncertainty of ± 0,1 % for the calibration of gas density meters with nitrogen, if the same source of nitrogen data was applied.

Table 1: Laboratories participating in the intercomparison

Country	Company
Denmark	The FORCE Institute
Germany	Ruhrgas AG
The Netherlands	NMI
Norway	FIMAS
United Kingdom	Solartron Instruments Ltd.

As another part of the NORDTEST project the applied methods for the determination of gas density on an industrial level in the Nordic countries were gathered and on the basis of this information a guideline for the determination of gas density was set up.

The determination of gas density in the Nordic countries is mainly performed in the natural gas industry and the two methods most commonly applied are 1) the application of a gas density meter with a vibrating element as sensor and 2) the application of the real gas equation. The guideline describes instrumentation, installation, maintenance for these two methods with an emphasis on the methods for the calculation of the uncertainty of the density determination.

* NORDTEST was founded in 1973 by the Nordic Council of Ministers to promote viable industrial development, the competetiveness of industry and to remove technical barriers to trade. NORDTEST finances joint research in testing technology and the development of test methods. NORDTEST also funds participation in European and other international standardization work. Each year NORDTEST funds around 200 projects in over 40 institutes and companies with up to 8 million FIM (~ 1 million £).

INTRODUCTION AND BACKGROUND

For over 10 years 4 out of 5 Nordic countries have been producing, selling and/or buying natural gas. One of the major issues has been how to determine the amount of gas. Several of the methods involve the determination of gas density. In the period 1995-1997 a NORDTEST project has been performed with the aim to gather existing applied methods for the determination of gas density in the Nordic countries and on the basis of this information to set up a guideline for the determination of gas density. At the same time an intercomparison on the calibration of vibrating element gas density meters with nitrogen has been carried out.

The project has resulted in three reports:

1) The determination of gas density - part 1 [1]
   State of the art in the Nordic countries

2) The determination of gas density - part 2 [2]
   Intercomparison: Calibration of gas density meters with nitrogen.

3) The determination of gas density - part 3 [3]
   A guideline to the determination of gas density

THE INTERCOMPARISON

The intercomparison was performed with 5 laboratories, see table 2, and on the subject calibration of vibrating element gas density meters. The calibration gas was nitrogen. The full address of the laboratories can be found in annex 1. All laboratories have a long history in calibrating gas density meters for the natural gas industry.

The intercomparison was performed with three Solartron 7812 vibrating element gas density meters as transfer standards. The meters were calibrated with pure nitrogen, 99,998 % or better, at 20 °C in the pressure range 1 MPa to 20 MPa.

Table 2: Laboratories participating in the intercomparison

Country	Company
Denmark	The FORCE Institute
Germany	Ruhrgas AG
The Netherlands	NMI
Norway	FIMAS
United Kingdom	Solartron Instruments Ltd.

The transfer standards of the intercomparison

A vibrating element gas density meter consists of a measuring unit and an amplifier unit.

The vibrating element is situated in the measuring unit and is activated at its natural frequency by the amplifier unit. The output signal is a frequency or a periodic time in the range 200 - 900 μseconds. Any change in the natural frequency will represent a density change in the gas that surrounds the vibrating element. As the output of the meter is periodic time the density meter must be calibrated before it can be applied in the industry to determine gas density.

The calibration of a gas density meter normally consists of a pure gas calibration at several points along the meters measuring range at one specific temperature. Following the pure gas calibration the density meters sensitivity to temperature and gas changes are determined. For some types of meters it is also necessary to determine the pressure sensitivity.

The pure gas calibration was the subject of the intercomparison. Information about the determination of the sensitivity of gas density meters to temperature, pressure and gas changes can be found in references [4],[5],[6],[7],[8].

Pure gases normally applied in the calibration of gas density meters are nitrogen, argon and methane. One of the reasons for choosing these gases is the number of aknowledged data on these gases, which have an uncertainty around ± 0,1 % - 0,2 % [9],[10],[11],[12],[13],[14],[15],[16]. The stated uncertainty today of the laboratories participating in this intercomparison is ± 0,10 - 0,15 %, so the above mentioned data sources are one of the main contributors to the uncertainty of the calibration of gas density meters.

The density meter, after calibration, is then furnished with calibration constants which are constants of regression curves that are approximations to the meters function. As an example the density of a Solartron 7812 gas density meter can be approximated with following regression curve:

$$\rho = A\tau^2 + B\tau + C \qquad 1)$$

ρ:density of gas in kg/m^3

τ: periodic time in μseconds

A,B,C : calibration constants

The systematic error, when applying the calibration constants, see equation 1), is always set to be negligible compared to the uncertainty of the density measured in each measurement point of the calibration. This means that it is possible for one meter to have several sets of calibration constants to cover the whole measurement range of the meter.

Type of measurements of the intercomparison

Each laboratory was to perform a check of each meter upon receival of the meters and before shipping the meters to the next laboratory. The check consists of noting the signal of the meters at a vacuum below 1 mbar. The behaviour of the meters could with these checks be held under close surveillance throughout the intercomparison.

Each laboratory was then to perform a nitrogen calibration following their normal calibration procedures for all three meters. The calibrations were to be performed at 20 °C and at minimum 8 measurement points in the range 12 kg/m^3 to 220 kg/m^3.

It was optional whether the laboratories wished to calibrate with increasing pressure or with decreasing pressure or with both as the hysteresis of the gas density meter is known to be very small.

The results were to be sent to the pilot laboratory (the FORCE Institute).

The pilot laboratory was to perform the first and the last series of calibrations.

Data treatment

The data from all the laboratories were treated by the pilot laboratory. Full data treatment can be found in [2].

Several acknowledged data sources for the density of nitrogen exist. In table 3 the density, as predicted from 4 sources at 20 °C, can be seen. The prediction of density differs up to 0,18 %. Wagner & Span[11] was chosen as it was the most recent data source and had a stated uncertainty of ±0,02 % for the density range up to 12 MPa and ± 0,05 % over 12 MPa.

Table 3 Nitrogen density as predicted from different sources, 20 °C

Pressure MPa	L'Air Liquide[12] kg/m^3	IUPAC[10] kg/m^3	NIST[9] kg/m^3	Wagner & Span [11], kg/m^3
1	11,5320	11,5184	11,5191	11,5185
5	57,9056	57,8182	57,8185	57,8139
10	115,0640	114,8535	114,8538	114,8397
20	219,0181	218,6067	218,6054	218,5805
Stated uncert.	±0,1% - 0,2%	±0,1%-0,2%	±0,1%	±0,02%(≤12 MPa) ±0,05%(>12MPa)

The density predicted from each laboratory should be compared to the "true density". As it is not possible to achieve the "true density" it was chosen to compare each of the laboratories density with the density obtained as a mean of all the laboratories values for density. This could of course only be done because the mean deviation between all the measurements was less than 0,03 % and thereby comparable to the repeatability and the stability of the meter.

The results were divided into calibrations where increasing gas pressure(increasing density) was applied and where decreasing gas pressure(density) was applied. Therefore following laboratories are compared:

Increasing pressure: Laboratories: FIMAS, FORCE, NMI and SOLARTRON.

Decreasing pressure: Laboratories: FIMAS, FORCE, NMI and RUHRGAS.

As the results for all three meters showed the same tendencies, here will only be shown the results for one meter. Please refer to the report [2] for full data.

Increasing pressure

The result of the comparison with increasing pressure can be seen for meter No. 120930 in figure 1. The data basis for figure 1 can be seen in table 4. The results showed for all three meters, that all the laboratories have an absolute deviation less than 0,035 % from the mean value above 22 kg/m^3. Three of the laboratories deviate less than 0,035 % from the mean value in the range below 22 kg/m^3.

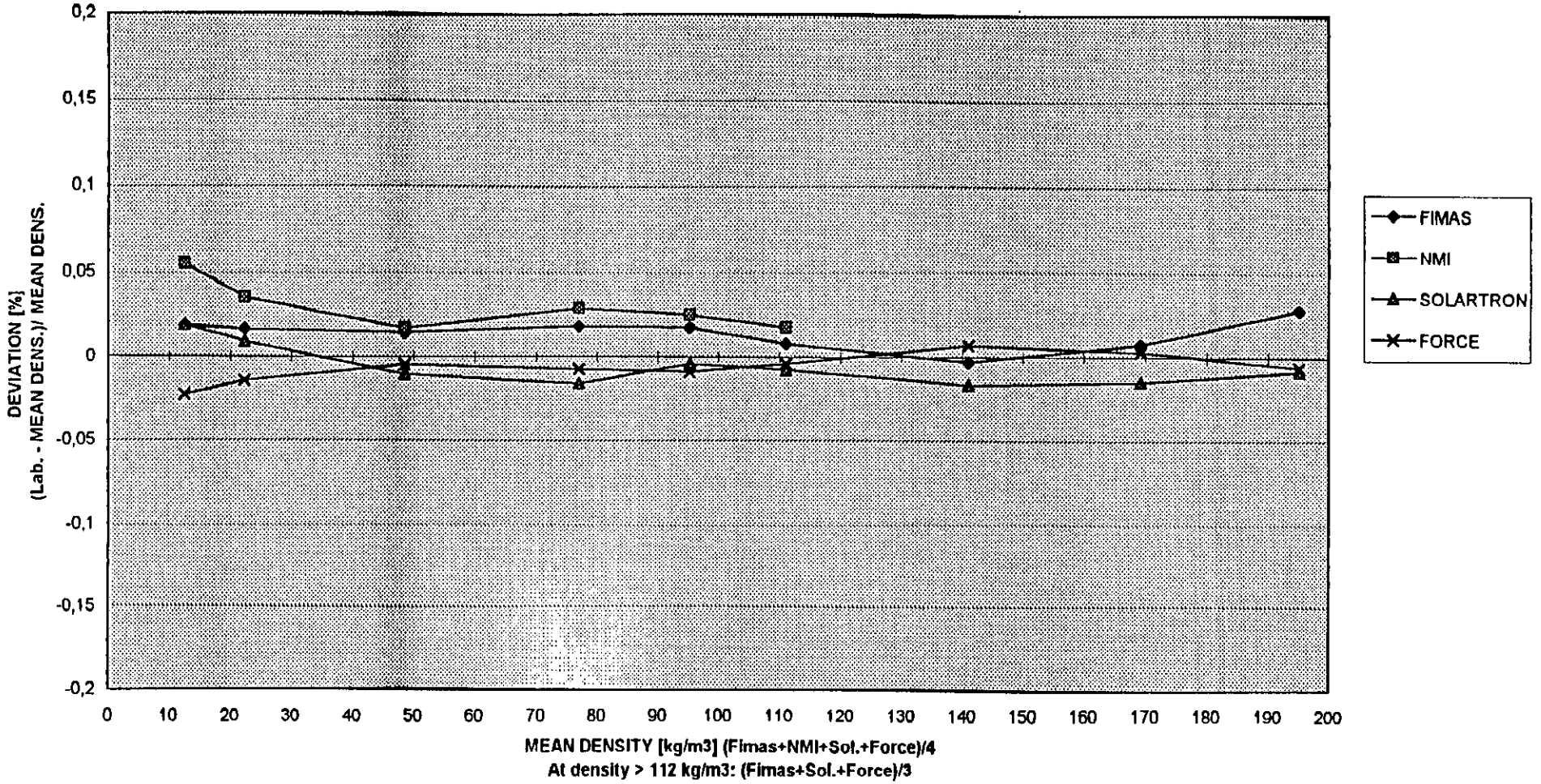

Figure 1: Comparison of the calibrations of the laboratories. Density Meter No. 120930 - Increasing pressure.

Table 4:

Comparison of the calibrations of the laboratories. Density Meter No. 120930 - Increasing pressure.

1	2	3	4	5	6	7	8	9	10	11	12	13
	FIMAS	NMI	SOLARTRON	FORCE	**MEAN VALUE**	FIMAS	NMI	SOL.	FORCE	Mean of	s-L	U-I
Period	Density	Density	Density	Density	**Density**	COL. 2-6/6	COL. 3-6/6	COL. 4-6/6	COL. 5-6/6	abs. val.		
microsec.	kg/m3	kg/m3	kg/m3	kg/m3	**kg/m3**	Dev. %	Dev. %	Dev. %	Dev. %	of dev. %	%	%
530	12,4873	12,4919	12,4873	12,4850	**12,4879**	0,018	0,055	0,018	-0,023	0,029	0,023	0,032
550	22,3131	22,3172	22,3115	22,3096	**22,3128**	0,016	0,034	0,009	-0,015	0,018	0,015	0,021
600	48,5306	48,5320	48,5187	48,5239	**48,5263**	0,014	0,017	-0,011	-0,005	0,012	0,013	0,018
650	77,0476	77,0558	77,0216	77,0340	**77,0398**	0,018	0,028	-0,016	-0,007	0,017	0,019	0,028
680	95,2831	95,2905	95,2627	95,2669	**95,2758**	0,017	0,025	-0,004	-0,009	0,014	0,014	0,020
705	111,1148	111,1251	111,0976	111,1063	**111,1110**	0,008	0,017	-0,008	-0,004	0,009	0,010	0,015
750	141,0613		141,0419	141,0659	**141,0564**	-0,003		-0,017	0,007	0,009	0,009	0,013
790	169,2724		169,2345	169,2601	**169,2557**	0,007		-0,015	0,003	0,008	0,011	0,016
825	195,1901		195,1195	195,1362	**195,1486**	0,028		-0,009	-0,006	0,014	0,019	0,027

	Nom. Range		CONSTANTS	FOR REGRESSSION CURVES (Density = Period*A*A +Period*B + C):			
	micro sec.		A	B	C		
FIMAS	525-565		-108,6503717	-0,02461343	0,0004776888	COL.:	Column
	565-654		-114,7926843	-0,00299635	0,0004586697	s-L:	Estimate for the between laboratory
	654-718		-115,0226488	-0,00323459	0,0004595702		variance. See [17]
	718-834		-109,5679945	-0,01814185	0,0004697523	U-I:	The uncertainty as evaluted from the inter-
							comparison results. U-I = Rep./2.
NMI	528-574		-110,5676202	-0,01747283	0,0004710576		Rep.: reproducibility limit[17]
	574-617		-117,1364620	0,00481016	0,0004521733		
	617-656		-124,7530588	0,02821584	0,0004342452		
	656-711		-116,6549303	0,00139393	0,0004563097		
SOLARTRON	524-600		-110,7913963	-0,01660134	0,0004701937		
	600-688		-108,3717026	-0,02335322	0,0004747287		
	688-831		-113,0017110	-0,00883064	0,0004634072		
FORCE	528-574		-109,4027523	-0,02177443	0,0004750025		
	574-616		-115,8077855	0,00040992	0,0004557938		
	616-710		-110,5563744	-0,01648012	0,0004693550		
	710-855		-115,3312565	-0,00274967	0,0004594834		

Decreasing pressure
The result of the comparison with decreasing pressure can be seen in figure 2, see page 9. The data basis for figure 2 can be seen in table 5, see page 10. The results for all three meters showed that all the laboratories deviate less than 0,030 % from the mean value in the whole range.

Uncertainty of the calibration of gas density meters evaluated from the results of the intercomparison.
The major aim of the intercomparison was to evaluate, if possible, the level of uncertainty of the calibration of gas density meters with nitrogen for the laboratories participating.

The uncertainty is a combination of the uncertainty of the data source plus the uncertainty of all the measured parameters of the laboratories. When applying the same data source the deviations between the laboratories are solely an expression of the differences in the measured parameters (pressure, temperature and periodic time) and the quality of the calibration gas.

An estimate for the uncertainty, U_I, for the results (the uncertainty of the data source not included) can be set up in a number of ways. The estimation of the uncertainty is here based on the reproducibility limit, Rep., of a standard measurement method, as calculated from ISO standard 5725[17].

Although the intercomparison was not performed to determine the uncertainty of a standard measurement method, the overall principle of calibration of gas density meters can be regarded as a standard method.

We have for the uncertainty:

$$U_I \approx \frac{Rep.}{2} \qquad 2)$$

The total uncertainty can then be expressed as:

$$U_\rho = \sqrt{U_I^{\,2} + U_T^{\,2}} \qquad 3)$$

where

Rep. = reproducibility limit [17]

U_ρ = the uncertainty of the gas density with a 95 % confidence level

U_I = the uncertainty as evaluted from the intercomparison results

U_T = the uncertainty of the source of data for nitrogen density

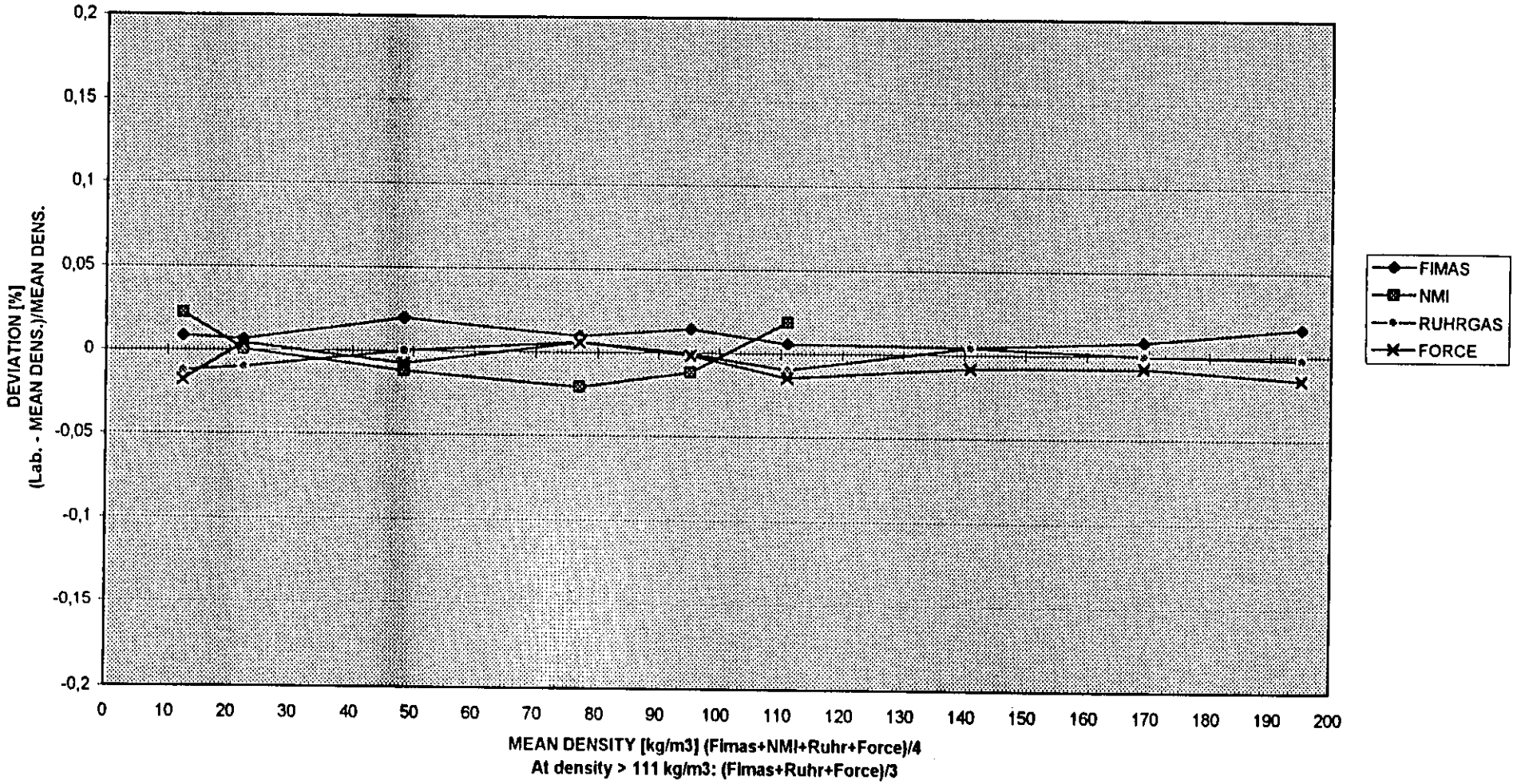

Figure 2: Comparison of the calibrations of the laboratories. Density Meter No. 120930 - Decreasing pressure.

Table 5:

Comparison of the calibrations of the laboratories. Density Meter No. 120930 - Decreasing pressure.

1	2	3	4	5	6	7	8	9	10	11	12	13
	FIMAS	NMI	RUHRGAS	FORCE	**MEAN VALUE**	FIMAS	NMI	RUHRGAS	FORCE	Mean of	s-L	U-I
Period	Density	Density	Density	Density	**Density**	COL. 2-6/6	COL. 3-6/6	COL. 4-6/6	COL. 5-6/6	abs. val.		
microsec.	kg/m3	kg/m3	kg/m3	kg/m3	**kg/m3**	Dev. %	Dev. %	Dev. %	Dev. %	of dev. %	%	%
530	12,4870	12,4887	12,4844	12,4837	**12,4860**	0,008	0,022	-0,012	-0,018	0,015	0,018	0,026
550	22,3113	22,3099	22,3076	22,3108	**22,3099**	0,006	0,000	-0,010	0,004	0,005	0,007	0,011
600	48,5256	48,5101	48,5160	48,5123	**48,5160**	0,020	-0,012	0,000	-0,008	0,010	0,014	0,020
650	77,0387	77,0154	77,0359	77,0356	**77,0314**	0,010	-0,021	0,006	0,005	0,010	0,014	0,020
680	95,2767	95,2520	95,2625	95,2614	**95,2631**	0,014	-0,012	-0,001	-0,002	0,007	0,010	0,015
705	111,1100	111,1246	111,0927	111,0875	**111,1037**	0,006	0,019	-0,010	-0,015	0,012	0,015	0,022
750	141,0541		141,0535	141,0360	**141,0479**	0,004		0,004	-0,008	0,006	0,007	0,011
790	169,2606		169,2458	169,2340	**169,2468**	0,008		-0,001	-0,008	0,005	0,008	0,011
825	195,1874		195,1503	195,1267	**195,1548**	0,017		-0,002	-0,014	0,011	0,016	0,022
	Nom. Range		CONSTANTS	FOR REGRESSSION CURVES (Density = Period*A*A + Period*B + C):								
	micro sec.		A	B	C							
FIMAS	525-565		-108,657599	-0,02451566	0,0004775289							
	565-654		-114,851556	-0,00275168	0,0004584115							
	654-765		-115,602164	-0,00163850	0,0004584624							
	688-833		-109,123322	-0,01951826	0,0004707633							
NMI	527-573		-109,727263	-0,02039582	0,0004735699							
	573-616		-117,786686	0,00745757	0,0004495063							
	616-656		-121,911561	0,01941692	0,0004409608							
	656-693		-94,982837	-0,06364729	0,0005050065							
	693-711		-125,149859	0,02453721	0,0004405729							
RUHRGAS	524-551		-107,137338	-0,03010463	0,0004826529							
	551-616		-112,625682	-0,01026705	0,0004647274							
	616-744		-111,681733	-0,01288908	0,0004664982							
	744-831		-108,520102	-0,02044000	0,0004709398							
FORCE	528-616		-111,863425	-0,01278293	0,0004667929							
	616-789		-112,774780	-0,00957348	0,0004639838							
	789-855		-126,308811	0,02393165	0,0004432572							

COL.: Column

s-L: Estimate for the between laboratory variance. See [17]

U-I: The uncertainty as evaluted from the inter-comparison results. U-I = Rep./2

Rep.: reproducibility limit[17]

In table 6 can be seen the largest uncertainty, U_ρ, of all the measurement points for all three density meters.

Table 6 Uncertainty of the calibration of gas density meters with nitrogen (95% confidence level) as evaluated from the results of the intercomparison.

	increasing pressure		decreasing pressure	
	1 MPa < p ≤12 MPa	pressures above 12 MPa	1 MPa < p ≤12 MPa	pressures above 12 MPa
U_I	±0,038 %	±0,027 %	±0,030 %	±0,022 %
U_T	±0,020 %	±0,050 %	±0,020 %	±0,050 %
U_ρ	±0,043 %	±0,056 %	±0,036 %	±0,055 %

Conclusion on the intercomparison

From the results of the intercomparison following main conclusions can be made:

- The calibration laboratories have an uncertainty that is less than ± 0,10 % to ± 0,15 % for a pure gas calibration when applying Wagner and Span[11] as the data source. All the laboratories could actually state an uncertainty of ± 0,05 % in the range below 12 MPa and ± 0,06 % above 12 MPa.

- Great care should be taken when choosing the data source for the density of the calibration gas, as this still is one of the major contributors to the uncertainty of the calibration of gas density meters. For calibrations performed with nitrogen the Wagner & Span data source[11] will give the least uncertainty.

THE GUIDELINE

Background

The natural gas industry has been growing steadily and the number of countries applying natural gas is also increasing. There has been a great deal of focus on the uncertainty of the determination of the amount of gas and thereby on the uncertainty of the determination of gas density.

The determination of the density of gas in the Nordic countries is mainly applied in the natural gas industry and here mainly in connection with metering the amount of energy for the purpose of settling accounts.

Natural gas is distributed to and/or from the Nordic countries to Europe and to Russia and to some extent between the Nordic countries themselves.

The vibrating element gas density meter is applied in three of the Nordic countries on an industrial level.

Check-up systems and low pressure systems are based on the determination of gas density by applying the real gas equation.

On the basis of this information a NORDTEST guideline was set up on how to determine gas density on an industrial level with following two methods:

a) applying a gas density meter with a vibrating element as sensor
b) applying the real gas equation.

In the NORDTEST guideline examples of the instrumentation of measuring systems are set up and the uncertainty for these examples is estimated.

ISO (International Organization for Standardization)
During the last 5 years one of the working groups of ISO (The International Organization for Standardization), TC193/SC2/WG1, has been working on a document which covers installation and maintenance of some of the instruments applied in gas measurement, e.g. vibrating element gas density meters, pressure transducers and resistance thermometers. The ISO document is now on a working draft status, ISO/WD 11793[18]. Although it will be a few years before the document is an ISO standard, the document gives good guidelines on many of the issues treated in the NORDTEST guideline and is referred to as often as possible.

Uncertainty calculation

The uncertainty in the NORDTEST guideline is based on BIPM recommendation INC-1(1980) that has resulted in WECC doc. 19-1990: Guidelines for the expression of uncertainty of Measurements in calibrations[19] and Guide to expression of uncertainty of measurement (ISO/TAG4/WG3) [20]. The BIPM recommendation INC-1 can be found in [20] annex A. The calculation of the uncertainty will follow [19] and [20] in general. To avoid large statistical calculations, some assumptions will be made. It is necessary to check if the assumptions are valid for the actual measuring system. If this is not the case [19] and [20] can give guidelines in how to proceed.

Terms such as random and systematic error sources are replaced by terms such as type A and type B uncertainty parameters. Type A parameters kan be measured and thereafter treated statistically. Type B parameters do not have enough documentation to perform a statistical analysis and the uncertainty has to be evaluated from prior knowledge, for example maximum and minimum value.

The uncertainty contributions from the two types of parameters are combined into an expression for the total uncertainty as seen in equation 5). This equation is valid if the parameters, x, are independent (not correlated).

$$\rho = f(x_1, x_2, \ldots, x_N) \qquad 4)$$

$$u_\rho = \sqrt{\sum_{i=1}^{N} \left(\frac{\partial f}{\partial x_i} \right)^2 \cdot \left(u_{\rho\text{-A}}{}^2(x_i) + u_{\rho\text{-B}}{}^2(x_i) \right)} \qquad 5)$$

$$U_\rho = k \cdot u_\rho \qquad 6)$$

U_ρ: expanded uncertainty of the density determination

u_ρ: combined standard uncertainty of the density determination

$u_{\rho\text{-A}}$: the standard uncertainty for parameters of type A

$u_{\rho\text{-B}}$: estimated approximations to the standard uncertainty for parameters of type B

k: coverage factor, for a 95 % confidence level: k=2

x_i: parameter

$\frac{\partial f}{\partial x_i}$: partial derivative here denoted sensitivity coefficient

Principles for determining gas density
The principles in how to determine gas density can be divided into following two groups:

a. on-line/in-line determination - continuous determination

a.1 continuous measurement of one primary parameter
- change in gascomposition a secondary effect

a.2 continuous measurement of several primary parameters
- change in gascomposition a primary effect

b. other determinations - non-continuous determination (often performed in laboratories).

The non continuous (laboratory) gas density determinations have an uncertainty that is less than the continuous density determinations, but the time and training necessary to apply the non-continuous methods do not render them practical for every day use for most industrial purposes. The non continuous methods are mainly applied to establish data from which equations of state can be derived for example for pure gases[21], [11]. Another application is check of continuous measuring systems [22].

Therefore the guideline deals only with the continuous determination.

Relation: $\rho = f(\tau, c, T, p)$
In the last 30 years a great deal of effort has been put into the development of a meter, from which the signal is primarily dependent upon density and only secondarily upon other parameters, such as pressure, temperature and gas composition. The meter is called a vibrating element gas density meter. The principle of this meter and its calibration can be seen on page 3.

In table 7 a list of the common instrumentation of measuring systems that apply gas density meters can be seen.

The guideline goes on to describe installation and maintenance and gives an example of the calculation of the uncertainty of the method.

Table 7: Commen instrumentation, $\rho = f(\tau,c,T,p)$

System	Instrumentation	Comments
a.1-a	density meter thermometer pressure transducer registration equipment	The pressure transducer is mainly included to be able to correct for the changes in gas composition through the determination of the velocity of sound.
a.1-b	density meter thermometer registration equipment	The gas composition is stable* and is measured at upstart.
a.1-c	density meter registration equipment	The gas composition and the temperature is stable* and are measured at upstart.

* The degree of stability that will result in a negligable influence on the density as determined by the density meter will differ depending on the type of density meter and even the density range. The gas composition and the gas temperature should regularily be checked to be sure that the system does remain stable.

The example chosen in the guideline corresponds to a.1-c and gives an uncertainty with a 95 % confidence level of ±0,20 %.

Relation: $\rho = p/(Z R_g T)$

The second method that is treated in the guideline is use of the gas density as determined from the real gas equation, equation 7).

$$\rho = \frac{p}{ZR_gT} \qquad 7)$$

ρ = density

p = pressure

T = temperature in Kelvin

Z = compression factor

R_g = gas consant; $R_g = \frac{R}{M}$

R = universal gas constant

M = molar mass

In table 8 can be seen the most common instrumentation when applying the real gas equation.

Table 8: Common Instrumentation, $\rho = p/(Z R_g T)$

System	Instrumentation	Comments
a.2-a	thermometer pressure transducer Z-meter gas analysis equipment-molar composition analysis registration equipment	Z is determined several times an hour. For more information about this meter see ISO WD 11793 [18].
a.2-b	thermometer pressure transducer gas analysis equipment-molar composition analysis registration equipment	The parameters, R_g and Z, can directly be calculated from the gas composition by applying recognized tables, e.g. ISO/DIS 12213 [23] part 2 for natural gas.
a.2-c	thermometer pressure transducer registration equipment	The gascomposition is stable and is measured by an external laboratory regularily. The parameters, R_g and Z, can directly be calculated from the gas composition by applying recognized tables, e.g. ISO/DIS 12213 [23] part 2 for natural gas.

The example chosen in the guideline corresponds to a.2-b and gives an uncertainty with a 95 % confidence level of ±0,23 %.

Acknowledgements
We would like to thank the laboratories for their participation in the intercomparison, especially following people: Mr. Jostein Eide and Mr. Atle Nordrehaug from FIMAS; Mr. Elskamp from NMI; Mr. Boeser and Mr. Boden from Ruhrgas and Mr.Norman Reed, Mr. Simon Wheeler and Mr. Andrew Matthews from Solartron.

We would also like to thank the NORDTEST project evaluation group listed in table 9, for giving support and guidance during the project.

Table 9: The project evaluation group

Country	Company	Name of participants
Denmark	Dangas A/S	Susanne Rasmussen
Denmark	Miljø- og Energiministeriet	Emil Sørensen
Finland	Gasum Oy	Jorma Rintamäki
Norway	Oljedirektoratet	Steinar Fosse
Norway	Statoil	Reidar Sakariassen
Sweden	Sydgas AB	Nils Widing

A special thanks to Dr. Manfred Jaeschke of Ruhrgas AG for commenting on the guideline at a short time notice.

References

1. M. Tambo, Tove Søgaard
   The Determination of gas density, part 1
   State of the art in the Nordic countries
   NORDTEST Technical report NT TECHN REPORT 353, NORDTEST,
   P.O.Box 116, FIN-02151

2. M. Tambo, Tove Søgaard
   The Determination of gas density, part 2
   Intercomparison: Calibration of gas density meters with nitrogen
   NORDTEST Technical report NT TECHN REPORT 354, NORDTEST,
   P.O.Box 116, FIN-02151

3. M. Tambo, Tove Søgaard
   The Determination of gas density, part 3
   A guideline to the determination of gas density
   NORDTEST Technical report NT TECHN REPORT 355, NORDTEST,
   P.O.Box 116, FIN-02151

4. P. Bates.
   Solartron 7812, Gas Density Transducer, Operating Manual.
   Solartron, Farnborough, October 1995.

5. Lars Rosenkilde and Marianne Tambo.
   Calibration and examination of gas density meters.
   1983-06-01, TR-projekt 133/360.81.368, UDC 531.75:662.767
   Dantest(now FORCE Institute).

6. Dr. M. Jaeschke, Dr.-Ing. X.Y. Guo, Dr. Ing.R. Kleinrahm,
   Prof. Dr.-Ing. W. Wagner
   A new accurate method for correcting the vos effect on vibrating gas density transducers
   Proceedings of the Int. Gas Research Conference in Cannes, 1995

7. J.W. Stansfeld.
   A new gas density meter with reduced velocity of sound effect.
   Schlumberger Industries(now Solartron), Transducer Division, Farnborough.

8. Dipl.-Ing- H. M. Hinze and Dr. M. Jaeshcke.
   Messung der dichte von erdgasen nach der wägemethode und mit betriebsdichteaufnehmern.
   VDI Reihe 6 Nr. 162, VDI-Verlag GmbH- Düsseldorf 1985

9. R.T. Jacobsen, et al
   Thermophysical properties of nitrogen from the fusion line to 3500 R (1944 K) for pressures to 150.000 psia (10342 x 10^5 N/m^3)
   NBS(now NIST) - National bureau of Standards, December 1973

10. International Union of Pure and Applied Chemistry, IUPAC.
Nitrogen, International thermodynamic tables of the fluid state-6.
Pergamon Press.

11. Wagner and R. Span.
Special Equations of State for Methane, Argon and Nitrogen for the Temperature Range from 270 to 350 K at Pressures up to 30 MPa.
International Journal of Thermophysics, Vol. 14, No. 4, July 1993.

12. L'Air Liquide, Division Scientifique.
Encyclopedie des gaz - l'Air Liquide - Azote- N_2.
Elsevier, Amsterdam , 1976

13. R.D.Goodwin
The thermophysical properties of methane, from 90 to 500 K at pressures to 700 bar
NBS - National bureau of Standards (Now NIST), April 1974

14. International Union of Pure and Applied Chemistry, IUPAC.
Methane, International thermodynamic tables of the fluid state - 5.
Pergamon Press.

15. International Union of Pure and Applied Chemistry, IUPAC.
Argon, International thermodynamic tables of the fluid state - 1.
Pergamon Press.

16. A.L. Gosman, R.D. McCarty, J.G. Hust.
Thermodynamic properties of argon- From the triple point to 300 K - At pressures to 1000 Atmospheres.
National Bureau of Standards(now NIST), March 1969.

17. International standard ISO 5725 parts 1,2,3,4 and 6.
Accuracy (trueness and precision) of measurement methods and results.
First edition 1994-12-15, International Organization for Standardization, (Geneva,Switzerland).

18. ISO Working Draft WD 11793
Natural gas - measurement of properties
Density , pressure, temperature and compression factor
ISO/TC193/SC2/WG1

19. Guidelines for the Expression of the Uncertainty of Measurement in Calibrations.
WECC (Western European Calibration Cooperation) Doc. 19-1990

20. Guide to the Expression of Uncertainty in Measurement (TAG 4)
First edition 1993, International Organization for Standardization,
ISBN 92-67-10188-9 Switzerland.

21. N. Pieperbeck, R. Kleinrahm, W.Wagner, M. Jaeschke
Results of (pressure, density, temperature) measurements on methane and on nitrogen in the temperature range from 273.15 K to 323.15 K at pressures up to 12 MPa using a new apparatus for accurate gas-density measurements.
M-2572, J. Chem. Thermodynamics 1991, 23, 175-194.

22. Gerhard Olbricht, Reiner Kleinrahm, Hans-Wilhelm Lösch, Wolfgang Wagner and Manfred Jaeschke
Entwiklung einer Transportablen Prüfeinrichtung für Betriebsdichteaufnehmer in Erdgasmessstrecken
GWF Gas-Erdgas 136 (1995) Nr. 2

23. International standard ISO/DIS 12213, part 1,2 and 3.
Natural gas - Calculation of Compression factor.
1994, International Organization for Standardization, (Geneva,Switzerland).

Annex 1 Address list of the laboratories participating in the intercomparison

FIMAS Calibrationcenter
P. O. Box 23
N-5363 Ågotnes
Norway
Att.: Jostein Eide
Tlf: 47 56 33 54 54
Fax: 47 56 33 46 70

FORCE Institute
Park Allé 345
2605 Brøndby
Denmark
Att.: Marianne Tambo/Tove Søgaard
Tlf.: 45 43 26 70 00
Fax: 45 43 26 70 11

Nederlands Meetinstituut
Hugo de Grootplein 1
Postbus 394
3300 AJ Dordrecht
The Netherlands
Att.: H. Elskamp
Tlf.: 31 78 633 23 32
Fax: 31 78 633 23 09

Ruhrgas Aktiengesellschaft
Betriebsstelle Essen-Altenessen
Gladbecker Strasse 404
D-45326 Essen
Germany
Att.: Hr. Boesen / Mr. Boden
Tlf.: 49 201 1 84 82 72
Fax: 49 201 1 84 83 93

Solartron Transducers
Victoria Road, Farnborough
Hampshire
GU14 7PW England
Att.: Simon Wheeler / Norman Reed
Tlf.: 44 1252 544 433
Fax: 44 1252 547 384

nordtest report

NT TECHN REPORT 355

Approved 1997-06

THE DETERMINATION OF GAS DENSITY - PART 3

A guideline to the determination of gas density

Marianne Tambo
Tove Søgaard

GENERAL

Nordtest was founded in 1973 by the Nordic Council of Ministers and since then Nordtest has been an active member of the international testing community. From the beginning Nordtest's activities have been focused upon development of Nordic test methods and Nordic cooperation concerning testing. However, European aspects have become more and more important for Nordtest, especially after the creation of the European Economic Area and after three Nordic countries becoming members of the European Union. The main part of the work is performed in the five Nordic countries, but there are also projects that involve participation from outside the Nordic countries. The importance of this cooperation is going to increase even more during the coming years. Here the main task is to actively take part in the development of international test methods and standards and ensure that they can be used in Nordic conditions.

As a result of its projects Nordtest is able to offer competence and expertise in the field of technical testing, a large Nordic network of experts, 500 recommended Nordic testing methods and over 350 published technical reports.

OBJECTIVES

Nordtest endeavours

- as the joint Nordic organisation in the field of technical testing, to promote viable industrial development and the international competitiveness of Nordic industry by furthering relevant and cost effective testing and measurement activity in the Nordic countries and by advancing Nordic interests in an international context, particularly within European testing.
- to ensure that the end users receive products which satisfy the requirements concerning safety, resource economy and good environment, and that they can be used under Nordic conditions.
- to remove technical barriers to trade and to ensure that problems which arise due to these are solved effectively, and endeavours to bring about mutual acceptance of test results.

PRINCIPAL AREAS OF OPERATION

Nordtest

- directs and finances joint research in testing technology and the development and implementation of test methods.
- coordinates and promotes Nordic cooperation and division of work in testing and promotes Nordic cooperation in research, testing, certification and standardisation.
- endeavours to bring about Nordic participation in European cooperation.
- functions as an information centre in technical testing in the Nordic countries.

ORGANISATION

The organisation of Nordtest comprises a board, a secretariat and several strategy and expert groups. The task of the strategy groups is to decide the strategic direction within their areas of responsibility. The expert groups are working in specific fields within the areas of responsibility of the strategy groups. Development work in testing technology takes place in the form of projects. The principal tasks of the expert groups are to look for and assign priority to suitable project proposals in their areas, supervise the progression of funded projects and participate in international cooperation. Project work may be multidisciplinary or product specific. The multidisciplinary work is carried out in close cooperation between the strategy and expert groups concerned.

The areas of responsibility of the strategy groups are selected with regard to the existence in theseareas of pronounced development needs in testing technology in relation to industry, end users, European directives, special Nordic conditions or wishes, or Nordic testing infrastructure.

The organisation presently comprises of the strategy groups **Biotechnology and Chemistry, Civil Engineering, Environment, Information Technology and Electronics, Materials Technology** and **Quality Assurance and Metrology** and the expert groups **Building Materials and Construction, Fire, Mechanical Building Services, Safety Critical Systems, Solid Waste, Sound and Vibration** and **Use of Materials.**

NT TECHN REPORT 355

Approved 1997-06

Authors:
Marianne Tambo
Tove Søgaard

NORDTEST project number: 1254-95

Institution: FORCE Institute

Title (English): -

Title (Original): THE DETERMINATION OF GAS DENSITY - PART 3: A guideline to the determination of gas density

Abstract:

This guideline is part 3 of the NORDTEST project: The determination of gas density.

NT TECHN REPORT 353
The determination of gas density - part 1
State of the art in the Nordic countries

NT TECHN REPORT 354
The determination of gas density - part 2
Intercomparison: Calibration of gas density meters with nitrogen

NT TECHN REPORT 355
The determination of gas density - part 3
A guideline to the determination of gas density

The guideline describe two measuring systems that determine gas density on an industrial level.

System 1) a gas density meter with a vibrating element as sensor.
System 2) the real gas equation.

The instrumentation, installation and maintenance are described with references to the relevant standards. To enable a common approach to the calculation of the determination of gas density, the guideline explains in general how to determine the uncertainty based on some of the latest principles for uncertainty estimation and illustrates this with some examples on the industrial level.

Technical Group: Strategy Group on Quality and Metrology

ISSN: 0283-7234 | **Language:** English | **Pages:** 29

Class (UDC): 53.088 | **Key words:** Gas density, Determination, Guideline

Distributed by:
NORDTEST
P.O.Box 116
FIN-02151 ESPOO
Finland

Publication code:

Table of Contents

1. Introduction

This guideline is part 3 of the NORDTEST project: The determination of gas density.

1) The determination of gas density - part 1
State of the art in the Nordic countries

2) The determination of gas density - part 2
Intercomparison: Calibration of gas density meters with nitrogen

3) The determination of gas density - part 3 (this report)
A guideline to the determination of gas density

The guideline describes two measuring systems that determine gas density on an industrial level including installation and maintenance of the measuring systems. As the uncertainty of the density determination is an important factor when choosing a measuring system and when settling disputes between buyers and sellers, there is given guidelines on how to calculate the uncertainty.

2. Background and aim

Density is defined as the mass of gas divided by its volume at specified conditions of pressure and temperature [1] and is given in kg/m^3. It is a combined parameter that normally is applied to obtain another property for example the mass or the volume. Gas density determination in the natural gas industry can be taken as an example. The end result of measuring systems for natural gas is how much energy has been used by the customer. To achieve this goal the amount of natural gas being consumed must be determined and that is often done by determining the density and the volume flow of the gas and then calculating the mass or the standard volume of the natural gas.

Today there is a need for the determination of gas density at all levels of obtainable uncertainty which can be from 0,02 % to 0,5 % depending on the choise of principle and instrumentation.

As there is a great number of ways to determine gas density, the seller and buyer of the gas product often chooses to measure the gas density with two different methods. This will often result in two different values for the gas density creating a dispute as to the correctness of each value. Although it is common knowledge that each density value has an uncertainty it often causes contractual disputes. The many different approaches to calculating the uncertainty is also cause for confusion.

This guideline will give an overview of the different principles that exist today to determine gas density and will go into details with two of the measuring systems that are applied on an industrial level. To enable a common approach to the calculation of the uncertainty of the determination of gas density, the guideline will continue to explain in general how to determine the uncertainty based on some of the latest principles for uncertainty estimation[4],[5] and will illustrate this with some examples on the industrial level.

2.1 ISO (International Organization for Standardization)

The International Organization for Standardization has a technical committee, TC193, natural gas and in this committee there has been produced several documents that will be referred to in this guideline. The documents have the status of draft international standards(DIS) and working draft standards (WD). During the last 5 years one of the working groups TC193/SC2/WG1 has been working on a document which covers installation and maintenance of some of the instruments that are treated in this guideline, e.g. vibrating element gas density meters, pressure transducers and resistance thermometers. The ISO document is now on a working draft status. Although it will be a few years before the document is an ISO standard the document gives good guidelines on many of the issues in this guideline and is referred to as: ISO WD 11793 [2].

3. Uncertainty calculation

The uncertainty in this guideline will be based on BIPM recommendation INC-1(1980) that has resulted in WECC doc. 19-1990: Guidelines for the expression of uncertainty of Measurements in calibrations[4] and Guide to expression of uncertainty of measurement (ISO/TAG4/WG3) [5]. The BIPM recommendation INC-1 can be found in [5] annex A. The calculation of the uncertainty will follow [4] and [5] in general. To avoid large statistical calculations, some assumptions will be made. It is necessary to check if the assumptions are valid for the actual measuring system. If this is not the case [4] and [5] can give guidelines in how to proceed.

Terms such as random and systematic error sources are replaced by terms such as type A and type B uncertainty parameters. Type A parameters kan be measured and thereafter treated statistically. Type B parameters do not have enough documentation to perform a statistical analysis and the uncertainty has to be evaluated from prior knowledge, for example maximum and minimum value.

The uncertainty contributions from the two types of parameters are combined into an expression for the total uncertainty as seen in equation 2). This equation is valid if the parameters, x, are independent (not correlated).

$$\rho = f(x_1, x_2, \ldots, x_N) \qquad 1)$$

$$u_\rho = \sqrt{\sum_{i=1}^{N} \left(\frac{\partial f}{\partial x_i} \right)^2 \left(u_{\rho\text{-}A}{}^2(x_i) + u_{\rho\text{-}B}{}^2(x_i) \right)} \qquad 2)$$

$$U_\rho = k \cdot u_\rho \qquad 3)$$

U_ρ: expanded uncertainty of the density determination

u_ρ: combined standard uncertainty of the density determination

$u_{\rho\text{-}A}$: the standard uncertainty for parameters of type A

$u_{\rho\text{-}B}$: estimated approximations to the standard uncertainty for parameters of type B

k: coverage factor, for a 95 % confidence level: k=2

x_i: parameter

$\frac{\partial f}{\partial x_i}$: partial derivative here denoted sensitivity coefficient

4. Principles for determining gas density

The principles in how to determine gas density can be divided into following two groups:

a. on-line/in-line determination - continuous determination

a.1 continuous measurement of one primary parameter
- change in gascomposition a secondary effect

a.2 continuous measurement of several primary parameters
- change in gascomposition a primary effect

b. other determinations - non-continuous determination (often performed in laboratories).

In table 1 can be seen some of the relations that apply for the determination of gas density.

Table 1: Fundamental relations

No.	Relation	Group	Common uncertainty level, %
1	$\rho_{(p,T)} = f(\tau, c, T, p)$	a1	0,1 - 0,5
2	$\rho_{(p,T)} = \frac{p}{Z(p,T) R_g T}$	a2	0,1 - 0,5
3	$\rho_{(p,T)} = \frac{m}{V_{(p,T)}}$	b	0,05 - 0,1
4	$\rho_{(p,T)} = \frac{\Delta F / g}{V_{s(p,T)}}$	b	0,02-0,05

As to be expected the non continuous (laboratory) gas density determinations have an uncertainty that is less than the continuous density determinations, but the time and training necessary to apply the non-continuous methods do not render them practical for every day use for most industrial purposes. The non continuous methods are mainly applied to establish data from which equations of state can be derived for example for pure gases[6], [7]. Another appliance is check of continuous measuring systems [8].

Therefore this guideline will in the following deal only with the continuous determinations.

5. $\rho = f(\tau, c, T, p)$

In the last 30 years a great deal of effort has been put into the development of a meter, from which the signal is primarily dependent upon density and only secondarily upon other parameters, such as pressure, temperature and gas composition. The meter is called a vibrating element gas density meter.

A vibrating element gas density meter consists of a measuring unit and an amplifier unit. The vibrating element is situated in the measuring unit and is activated at its natural frequency by the amplifier unit. The output signal is a frequency or a periodic time in the range 200 - 900 μseconds. Any change in the natural frequency will represent a density change in the gas that surrounds the vibrating element.

The relation between the density and the periodic time of the meter is obtained through calibration of the meter with a pure gas at one temperature and at several points along the meters measuring range. The calibration results (τ,ρ) are then fitted with a regression curve. The form of the regression curve varies from manufacturer to manufacturer and in equation 4) can be seen one type of curve. Corrections can be necessary to compensate for the differences between calibration conditions and actual conditions (e.g. different temperature and variation in gas composition). The correction for gas composition can be estimated from the velocity of sound in the actual gas as compared to the calibration gas. The manufacturer and the calibration laboratories will be able to furnish certificates that have the corrections incorporated or equations that can calculate the size of the corrections.

$$\rho = A\tau^2 + B\tau + C \qquad 4)$$

ρ: density of gas
τ: periodic time of the density meter
A,B,C: regression curve constants

5.1 Instrumentation and installation, $\rho = f(\tau,c,T,p)$

In principle the density meter is the only instrumentation necessary.

Often the pressure and temperature of a measuring site are regulated so that the deviations allowed only negligably influence the density as predicted by the density meter. The gas density can then be determined only with the gas density meter with a smaller addition to the uncertainty.

In other cases thermometers and pressure transducers are also included in the measuring system. The combinations of equipment listed in table 2 are the most commonly applied.

Table 2: Commen instrumentation, $\rho = f(\tau,c,T,p)$

System	Instrumentation	Comments
a.1-a	density meter thermometer pressure transducer registration equipment	The pressure transducer is mainly included to be able to correct for the changes in gas composition through the determination of the velocity of sound.
a.1-b	density meter thermometer registration equipment	The gas composition is stable* and is measured at upstart.
a.1-c	density meter registration equipment	The gas composition and the temperature is stable* and are measured at upstart.

* The degree of stability that will result in a negligable influence on the density as determined by the density meter will differ depending on the type of density meter and even the density range. The gas composition and the gas temperature should regularily be checked to be sure that the system does remain stable.

A flowcomputer is often applied as the registration equipment as the software in this equipment has been programmed with items such as the calibration constants of the meters. They are also built to register several parameters simultaneously. Some flowcomputers can calculate the velocity of sound based on the measurement of pressure and density and thereby determine the necessary correction to compensate for a variation in gas composition.

Before installation

The density meter must be calibrated before it can be applied to determine gas density. The calibration should be performed by a laboratory with traceability to international standards. The meter is calibrated with a reference gas such as pure nitrogen, argon or methane to obtain the relationsship between the signal of the instrument and the density of gas. The reason for applying these gases is the aknowledged data on these gases, e.g. [7]. The meter will have a characteristic temperature and gas composition offset (the latter is often called the velocity of sound offset). The size of these offsets are characteristic for each type of meter and normally the manufacturer of the meter has developed equations (empirically derived) to determine the size of the corrections. A number of the equations regarding the velocity of sound offset have been verified to be valid for a great number of gases, e.g. [9],[10],[11].

If the average composition of the actual gas is known, common practise is for the manufacturer of the gas density meters to issue an actual gas certificate where the calibration constants are valid for the actual gas. This is done by combining the density as determined by the pure gas calibration with the offset as determined empirically.

Pressure transducers and thermometers require calibration before installation. These sensors are so common that every country has laboratories that perform calibrations of these instruments with documented traceability to international standards.

The registration equipment should be chosen to suit the type of density meter and if relevant the type of pressure transducers and thermometers of the system and should also be checked/calibrated before installation.

Installation

The gas density meters should be installed according to the manufacturers guidelines. ISO WD 11793[2] and [12] gives more specific guidelines on installation, tests to be taken, calibration and verification. Here will be highlighted some of the areas where special care should be taken.

As the meters have to be demounted periodically for repair or recalibration, then the construction of the installation should take this into account.

Gas density meters are normally applied to measure gas density in pipelines and can be installed in several different manors with regard to the pipeline. These are treated in detail in ISO WD 11793[2]. The density meter receives a small sample of the gas continuously.

The flow through the density meter must be kept low enough to ensure that the pressure change from the main line is negligable but fast enough to represent the changes in gas composition.

Regardless of which form of installation is chosen, it is important to know what temperature and pressure the gas in the density meter will obtain. Even small differences from the actual temperature to the assumed temperature can cause large errors. For some natural gases ΔT of 3 K can correspond to an error in density of 1 %. Differences in pressure will have more influence on low pressure systems than high pressure systems

0,1 MPa in a 1 MPa system $\Rightarrow$ $\Delta\rho$ of appr. 10 %.

0,1 MPa in a 10 MPa system $\Rightarrow$ $\Delta\rho$ of appr. 1 %.

If the gas density meter is to be applied in connection with a volume flow meter to determine the amount of gas in kilograms, then great care must be taken to ensure that the gas density meter is installed, so the density at the same temperature and pressure as the volume flow meter can be determined. Often this will require either sufficient insulation of the density meter in connection with the pipeline or measurement of the temperature before and after the density meter. Some density meters have incorporated thermometers and these can be applied but care must be taken, as the thermometers are not directly in the gas but built into the foundation of the meter.

Regarding the pressure, it can be assumed that the pressure in the density meter is close to the pressure in the main pipeline, if the flow through the meter is small. On upstart of the measuring system the manufacturers gives guidelines on how to ensure a small pressure loss. The most efficient way would be to install flowmeters on the density meter outlet. In practise , though, this procedure is only applied to systems, that vent the gas to the atmosphere.

5.2 Maintenance, $\rho = f(\tau,c,T,p)$

The maintenance of a gas density meter is delt with in ISO WD 11793[2].

Shortly it can be said that if the density meter is operating on a gas that is free from dust and condensate and in temperature/pressure domains totally within the gaseous phase, then the meter has known to function well for several years. Even so it is recommended to calibrate the meter at least every 2 years. It is also recommended to set up an internal check (vacuum, air, or (p,T) measurements and the real gas equation) of the meter that can be performed several times a year, without demounting the meter, see [2].

If the meter is operating on gases that are not of above mentioned fine quality the vibrating element will slowly become contaminated and thereby show offsets from its calibration curve or instabilities. The meter will often return to normal after cleansing but it is recommended that a meter be recalibrated after having opened the meter and cleansed the vibrating element.

Taking apart the meter for cleansing should only be performed by welltrained personnel and in specially ventilated surroundings that ensure that no particle will settle on the vibrating element. Usually the laboratories that perform calibrations have rooms with special ventilation systems that ensure this. Manufacturers of the density meters of course also have these facilities.

By comparing the calibrations of the gas density meter (its history) the state of the meter can be determined. Comparisons can only be made if the meter has not been taken apart and cleansed before calibration. Shifts of around 0,10 % from calibration to calibration would indicate a need for demounting and cleansing the meter at least before the next calibration is performed.

Pressure and temperature sensors should be calibrated periodically, the interval depending on the type of instrument, and internal checks once a month are recommended.

The registration equipment should also be checked regularily. How often is dependent upon the type of equipment(6-12 months).

5.3Uncertainty, $\rho = f(\tau,c,T,p)$

In annex 3 the expanded uncertainty, U_ρ, is set up for one type of density meter system. The chosen density meter system has an uncertainty of $\pm 0{,}20$ %. The uncertainty for other combinations of equipment can be set up by following the guidelines in annex 2 and 3.

6. $\rho = p/(Z R_g T)$

The second method that will be treated is gas density as determined from the real gas equation, equation 5).

$$\rho = \frac{p}{ZR_gT} \qquad 5)$$

ρ = density

p = pressure

T = temperature in Kelvin

Z = compression factor

R_g = gas consant; $R_g = \frac{R}{M}$

R = universal gas constant

M = molar mass

6.1 Instrumentation and installation, $\rho = p/(Z R_g T)$

The instrumentation for this method varies greatly depending upon the desired accuracy.

In table 3 the most common intrumentation combinations are given.

Table 3: Common Instrumentation, $\rho = p/(Z R_g T)$

System	Instrumentation	Comments
a.2-a	thermometer pressure transducer Z-meter gas analysis equipment-molar composition analysis registration equipment	Z is determined several times an hour. For more information about this meter see ISO WD 11793 [2].
a.2-b	thermometer pressure transducer gas analysis equipment-molar composition analysis registration equipment	The parameters, R_g and Z, can directly be calculated from the gas composition by applying recognized tables, e.g. ISO/DIS 12213 [1] part 2 for natural gas.
a.2-c	thermometer pressure transducer registration equipment	The gascomposition is stable and is measured by an external laboratory regularily. The parameters, R_g and Z, can directly be calculated from the gas composition by applying recognized tables, e.g. ISO/DIS 12213 [1] part 2 for natural gas.

A flowcomputer is often applied for this registration as the software in this equipment has been programmed with items such as the calibration constants of the meters. They are also built to register several parameters simultaneously.

Before installation

Pressure transducers and thermometers can be obtained for all uncertainty levels. Great care should be taken to purchase the instruments that give the required uncertainty.

Pressure transducers and thermometers require calibration before installation. These sensors are so common that every country has laboratories that perform calibrations of these instruments with documented traceability to international standards.

The registration equipment should be chosen to suit the type of pressure transducers and thermometers of the system and should also be checked/calibrated before installation.

Installation

The equipment should be installed according to the manufacturers guidelines. ISO WD 11793 [2] gives more specific guidelines on pressure transducers of several types and of resistance thermometers. Here will shortly be listed some of the major items.

As the meters have to be demounted periodically for repair or recalibration, then the ease of demounting should be considered when building the installation.

It is important that the temperature and pressure are measured at the point where the density is to be determined. Regarding the temperature measurement the sensor is often placed in a pocket in the system. It is important that the temperature in the pocket actually represents the temperature in the gas line. This can be improved by having speciel thermoconductive oils in the pocket.

The gas analysis equipment usually measures on samples taken from the line and can therefore be placed at a different location than the other equipment. The sampling point should be the spot where the density is wished to be determined. The surroundings should correspond to the manufacturers guidelines. For more details on sampling please refer to ISO/DIS 10715 [13] and for more details on molar composition gas analysis please refer til ISO/DIS 6974 [14]. Most gas analysis equipment has to be calibrated with one or more reference gases [14] but this should be performed after installation of the equipment.

6.2 Maintenance, $\rho = p/(Z R_g T)$

Pressure and temperature sensors should be calibrated periodically, the interval depending upon the type of instrument, and internal checks once a month are recommended.

The registration equipment should also be checked regularily. How often is dependent upon the type of equipment(6-12 months).

The gas analysis equipment is normally calibrated and adjusted with the reference gas in connection with the daily use and large shifts in the setting of the analysis equipment would indicate a need for more extensive checks.

6.3 Uncertainty, $\rho = p/(Z R_g T)$

In annex 4 an example of a measuring system is set up. The the expanded uncertainty, U_ρ, has been calculated. The chosen system has an uncertainty of $\pm$ 0,23 %. The uncertainty for other combinations of equipment can be set up by following the guidelines in annex 2 and annex 4.

Aknowledgements

The authors would like to thank the NORDTEST project evaluation group listed in table 4, for giving support and guidance during the production of this document.

Table 4: The project evaluation group

Country	Company	Name of participants
Denmark	Dangas A/S	Susanne Rasmussen
Denmark	Miljø- og Energiministeriet	Emil Sørensen
Finland	Gasum Oy	Jorma Rintamäki
Norway	Oljedirektoratet	Steinar Fosse
Norway	Statoil	Reidar Sakariassen
Sweden	Sydgas AB	Nils Widing

We would also like to thank Dr. Manfred Jaeschke of Ruhrgas AG for commenting the document at a short time notice.

References

[1] International standard ISO/DIS 12213, part 1,2 and 3.
Natural gas - Calculation of Compression factor.
1994, International Organization for Standardization, (Geneva,Switzerland).

[2] ISO Working Draft WD 11793
Natural gas - measurement of properties
Density , pressure, temperature and compression factor
ISO/TC193/SC2/WG1.

[3] International vocabulary of basic and general terms in metrology (VIM).
Second edition 1993, International Organization for Standardization,
(Geneva,Switzerland).

[4] Guidelines for the Expression of the Uncertainty of Measurement in Calibrations.
WECC (Western European Calibration Cooperation) Doc. 19-1990.

[5] Guide to the Expression of Uncertainty in Measurement (TAG 4)
First edition 1993, International Organization for Standardization,
ISBN 92-67-10188-9 Switzerland.

[6] N. Pieperbeck, R. Kleinrahm, W.Wagner, M. Jaeschke
Results of (pressure, density, temperature) measurements on methane and on nitrogen in the temperature range from 273.15 K to 323.15 K at pressures up to 12 MPa using a new apparatus for accurate gas-density measurements.
M-2572, J. Chem. Thermodynamics 1991, 23, 175-194.

[7] W. Wagner and R. Span.
Special Equations of State for Methane, Argon and Nitrogen for the Temperature Range from 270 to 350 K at Pressures up to 30 MPa.
International Journal of Thermophysics, Vol. 14, No. 4, July 1993.

[8] Gerhard Olbricht, Reiner Kleinrahm, Hans-Wilhelm Lösch, Wolfgang Wagner and Manfred Jaeschke
Entwiklung einer Transportablen Prüfeinrichtung für Betriebsdichteaufnehmer in Erdgasmessstrecken
GWF Gas-Erdgas 136 (1995) Nr. 2

[9] Dipl.-Ing- H. M. Hinze and Dr. M. Jaeshcke.
Messung der dichte von erdgasen nach der wägemethode und mit betriebsdichte-aufnehmern.
VDI Reihe 6 Nr. 162, VDI-Verlag GmbH- Düsseldorf 1985

[10] Dr. M. Jaeschke, Dr.-Ing. X.Y. Guo, Dr. Ing.R. Kleinrahm, Prof. Dr.-Ing. W. Wagner
A new accurate method for correcting the vos effect on vibrating gas density transducers.
Proceedings of the Int. Gas Research Conference in Cannes, 1995

[11] Lars Rosenkilde and Marianne Tambo.
Calibration and examination of gas density meters.
1983-06-01, TR-projekt 133/360.81.368, UDC 531.75:662.767
Dantest(now FORCE Institute).

[12] Petroleum Measurement Manual, Part VII, Density, section 2, Continuous Density Measurement.
The Institute of Petroleum, London, nov. 1983.

[13] International standard ISO/DIS 10715
Natural gas - Sampling guideline
1994, International Organization for Standardization, (Geneva,Switzerland).

[14] International standard ISO/DIS 6974 part V.
Natural gas - Determination of composition with defined uncertainty by gas chromatography - Part 5: Determination of nitrogen, carbon dioxide and hydrogen carbons (C_1 up to C_5 and C_{6+}) for a laboratory and on-line process application.
1995, International Organization for Standardization, (Geneva,Switzerland).

Annex 1
Definitions, symbols and units

For the purpose of this technical report following defintions apply. Whenever possible the reference from where the definition is taken is given.

Related to gas density

Symbol	Name	Definition	Unit
ρ:	density of gas	The mass of gas divided by its volume at specified conditions of pressure and temperature [1].	kg/m^3
τ:	periodic time	The signal of the density meter [2].	µseconds
Δ:	Deviation	Deviation between two results.	result unit
B:	The barometric pressure	The pressure at atmosfæric conditions	Pa
c:	Velocity of sound	Sound velocity in a gas	m/s
m:	Mass	Mass of gas	kg
F:	Buoyant-force	Force exerted on a sinker[6],[7],[8]	kg m/s
f:	Function	f(x,z)	
g:	acceleration of free fall	Applied in the sinker method[6],[7],[8]	m/s
M:	Molar mass	The mass of one mole of gas	kg/mole
p:	Pressure	The absolute gas pressure	Pa
R:	Universal gas constant	R= 8,314510 J Mol^{-1} K^{-1}[1]	J Mol^{-1} K^{-1}
R_g:	Gas constant	The universal gas constant divided by the molar mass R/M	J kg^{-1} K^{-1}
Z:	Compression factor	$Z_{(p,T)} = Vm_{(p,T)}(real) / Vm_{(p,T)}(ideal)$, see ref. [1]	-
T:	Temperature	Thermodynamic temperature of the gas[1]	Kelvin
V:	Volume of gas	-	m^3
Vm:	Volume of gas pr. mole	-	m^3
V_S:	Volume of a sinker	The volume of the sinker applied in the sinker-method [6],[7],[8]	m^3

Definitions, symbols and units(continued)

Related to uncertainty

Symbol	Name	Definition	Unit
a_j:	upper/lower bound	[5] half-width of a rectangular distribution of possible values of input quantity x_i	input quantity
c_j:	constant	based on the probablity distribution	-
$\frac{\partial f}{\partial x}$:	sensitivity coefficient	partial derivative[5]	varies
k:	coverage factor	For a 95 % confidence level: k=2	-
s:	standard deviation	$\sqrt{\left(\sum_{i=1}^{n}\left(x_i - \bar{x}\right)^2 / (n-1)\right)}$	unit of property
u:	combined standard uncertainty	an estimated standard deviation that characterizes the dispersion of the values that could reasonably be attributed to the measurand[5]	unit of property
u_A:	standard uncertainty	the standard uncertainty for parameters of type A	unit of property
u_B:	standard uncertainty	estimated approximations to the standard uncertainty for parameters of type B	unit of property
U:	expanded uncertainty	the uncertainty of a property with a 95 % confidence level , see also [5] U=2u	unit of property
x:	parameter	-	varies
z:	parameter	-	varies

Annex 2 Combined standard uncertainty for the output of an instrument

When determining gas density several instruments can be applied.

- pressure transducers
- thermometers
- density meters
- gaschromatographs
- Z-meters

and also various registration equipment such as

- flow computers
- multimeters
- counters

To determine the expanded uncertainty of a measuring system one of the first steps is to estimate the contribution to the uncertainty from each of the instruments applied in the system.

This is done by estimating the combined standard uncertainty for the output, z_i, of each of the possible instruments. The combined standard uncertainty for each of the instruments will consist of uncertainty contributions from type A and type B components. Type A components can be measured and thereafter treated statistically. Type B components do not have enough documentation to perform a statistical analysis and the uncertainty has to be evaluated from prior knowledge, for example maximum and minimum value.

The standard uncertainty of type A components relevant for the output of an instrument are based upon repeated measurements and can be approximated by the experimental standard deviation of the mean output [5] as seen in equation 2.1.

$$u_{z-A} \approx s(\bar{z}) \qquad 2.1)$$

$$s^2(\bar{z}) = \frac{s^2(z_i)}{n} \qquad 2.2)$$

The standard uncertainty of type B components relevant for the output of an instrument are listed in table 2.1.

Table 2.1 Type B components

No.	Component description	a_j	c_j	$a_j \cdot c_j$
1	Calibration of the instrument			
2	Reading error during calibration			
3	Shift between calibrations			
4	Reading error during measurement			
5	Hysteresis effect			
6	Deviation from calibration conditions			
7	Installation effects.			

a_j: Half-width of a rectangular distribution of possible values of input quantity. $a = (a_+ - a_-)/2$[5]. Here the input quantity is each component. The component in row 1 is assumed to have a normal distribution but is for simplicity included in the table. The components in row 2-7 are assumed to have a rectangular distribution.

c_j: a constant based on the probability distribution of the value a. [5]

normal distribution: $c_j = 1$.

rectangular distribution: $c_j = 1/\sqrt{3}$

re 1: a_j from the calibration of the instrument is ½ of the uncertainty stated by the calibration laboratory, if the laboratory has stated an uncertainty at a 95 % confidence level.

re 2: a_j from the reading error when working with digital display instruments (registration equipment) can be set to 1/2 of the resolution.
For example: Pressure = 1,0005 MPa; resolution = 0,0001 MPa; a_j = 0,00005 MPa.

re 3: a_j for the shift between calibrations is based upon the knowledge of the history of the instrument. For every calibration (without repairs or adjustments) the new calibration results are compared to the former calibration results. The deviation between the two calibrations represents the shift. If the shift is too large the length of the recalibration period can be shortened and vice versa.
Example: calibration of a Pt-100 resistance thermometer at 20,00 °C

calibration date	1996-03-05	1997-03-05	shift, $2*a_j$
temperature as determined by the Pt-100.	20,05 °C	20,10 °C	0,05 °C

re 4: see re 2.

re 5: a_j for the hysteresis effect can be determined by the calibration laboratory. The laboratory will perform a calibration in steps from 0 to full span of the instrument and a second calibration from full span to 0 of the instrument. Any difference in the output of the instrument at the same calibration point for the 2 calibrations is an expression for the hysteresis effect and is equal to 2 a_j.

re 6: a_j for the deviation from the calibration conditions can be evaluated by the calibration laboratory or can in some cases be obtained as manufacturer information.
In some cases corrections are made and then a_j will be the interval in which the correction might lay.
For example: a gas density meter is calibrated at 20 °C with nitrogen and applied in natural gas at 5 °C. The reading of the density meter is corrected with the estimated offsets, resulting from the temperature and gas composition differences. a_j is then the error in the determination of the size of the offsets.

re 7: Installation can in itself cause errors and a_j must in each case be estimated. For example a thermometer placed in a pocket, will never completely obtain the temperature of the gas surrounding the pocket. The installation can though be made so that the error is negligable.

The standard uncertainty of type B components can then be estimated by equation 2.3).

$$u_{Z\,-B} = \sqrt{\sum\left(a_j \cdot c_j\right)^2} \qquad 2.3)$$

For the instrument the combined standard uncertainty can then be calculated from equation 2.4).

$$u_Z = \sqrt{\left(u_{Z-A}\right)^2 + \left(u_{Z\,-B}\right)^2} \qquad 2.4)$$

Annex 3 Calculation of the uncertainty of a gas density meter system ρ=f(τ, c,T,p)

The density is here determined using a vibrating element gas density meter.

$$\rho = \rho_{\text{density meter}} \qquad 3.1)$$

$$u_\rho = u_{\rho_{\text{density meter}}} \qquad 3.2)$$

Example

The gas is natural gas at following conditions:
(the natural gas data is taken from an example in [1])

p = 6 MPa

T = 290 K (t = 16,85 °C)

Z = 0,88006

R_g = 0,00049481 MJ/kmol K

ρ = 47,512 kg/m³

The gas composition is as listed in table 3.1

Table 3.1 Gascomposition

Component	Mole fraction	Uncertainty, mole fraction
CH_4	0,965	0,001
C2H6	0,018	0,001
C3H8	0,0045	0,0005
C4H10-i	0,001	0,0003
C4H10-n	0,001	0,0003
C5H12-i	0,0005	0,0001
C5H12-n	0,0003	0,0001
C6+	0,0007	0,0001
N2	0,003	0,001
CO2	0,006	0,001
Total	1	

The measuring system consists of the density meter and its registration equipment (table 2, system a.1-c). To simplify the example the density meter is calibrated with the registration equipment (a flowcomputer). In practise the instruments are calibrated separately and then the influence of the uncertainty of the input/output of the flowcomputer on the gas density should be included in this estimation. This can be done in the same manner as the combined standard uncertainty of the output of each instrument is estimated.

The combined standard uncertainty

$$u_\rho = u_{\rho_{\text{density meter}}} = \sqrt{\left(u_{\rho_{\text{density meter}}-A}\right)^2 + \left(u_{\rho_{\text{density meter}}-B}\right)^2}$$

$$u_\rho = \sqrt{(0{,}001)^2 + (0{,}0479)^2} = 0{,}048\ \text{kg/m}^3$$

The expanded uncertainty

$U_\rho = 2 \cdot u_\rho = 0{,}096\ \text{kg/m}^3$ **at 47,512 kg/m3 (290 K and 6 MPa)**

$U_\rho / \rho = 0{,}20\ \%$

In the following U_ρ is derived step by step.

The standard uncertainty of type A component is obtained by determining the density (at stable conditions) at the density of 47 kg/m^3 at least 10 times and deriving the standard deviation of the mean.

$$u_{\rho_{\text{density meter}}-A} \approx s\left(\overline{\rho_{\text{density meter}}}\right) = 0{,}001\ \text{kg/m}^3$$

The standard uncertainty of type B components

The type B components are listed in table 3.2. Each component is treated as in annex 2.

Table 3.2 Type B components

No.	Component description	a_j kg/m³	c_j	$a_j \cdot c_j$ kg/m³
1	Calibration of the instrument	0,047	1	0,047
2	Reading error during calibration	0,0005	$1/\sqrt{3}$	0,00029
3	Shift between calibrations	0,012	$1/\sqrt{3}$	0,0069
4	Reading error during measurement	0,0005	$1/\sqrt{3}$	0,00029
5	Hysteresis effect	0,0047	$1/\sqrt{3}$	0,0027
6	Deviation from calibration conditions	0,0047	$1/\sqrt{3}$	0,0027
7	Installation effects	0,008	$1/\sqrt{3}$	0,0046
$u_{\rho_{\text{density meter}}\text{-B}} = \sqrt{\sum \left(a_j \cdot c_j \right)^2}$				0,0479

re 1 calibration result is given with ± 0,2% with a 95% level of uncertainty ⇒ a = 0,047 kg/m³. The calibration is performed with nitrogen and an actual gas certificate is issued based on the above listed gas composition and 290 K. The density meter and the flowcomputer is calibrated as a unit. The flowcomputer has been checked/calibrated immediately before the calibration of the meter.

re 2 resolution: 0,001 kg/m³ ⇒ a = 0,0005 kg/m³

re 3 the shift between calibrations is in "clean" gases less than 0,05 % ⇒ a = 0,025 % ⇒ a = 0,012 kg/m³.

re 4 resolution: 0,001 kg/m³ ⇒ a = 0,0005 kg/m³

re 5 the density meter has a hysteresis less than 0,02 % ⇒ a = 0,01 % ⇒ a= 0,0047 kg/m³.

re 6 The density meter has a certificate for 290 K and the gas to be measured upon is at 290 K ± 2 K. The temperature sensitivity of the density meter is less than 0,01%/K⇒ a=0,0047 kg/m³. Because the gas composition varies very little the influence on the gas density is in this example negligable.

re 7 The difference in the temperature of the gas in the density meter and the gas in the pipeline is 0,1 K which corresponds to a density change of 0,016 kg/m³ ⇒ a = 0,008 kg/m³.

Annex 4 Calculation of the uncertainty of a real gas equation system $\rho=p/(ZR_gT)$

The density is here calculated from several measured parameters, see equation 4.1). The uncertainty can be calculated as seen in equation 4.2. This equation is the equation for noncorrelated parameters. It can be applied because the compression factor in most practicle situations can be assumed to be so constant, that the covariances of (p,Z), (T,Z) and (R_g,Z) are insignificant, see [5] section F 1.2.1. If the gascomposition, temperature or pressure of a measuring system should vary greatly then the estimation of the uncertainty should include the covariances and in [5] guidance is given on the estimation of these. Equations 4.3 to 4.4 give the sensitivity coefficients and when inserting these into equation 4.2 and dividing on both sides with ρ^2, then the relative uncertainty can be derived as in equation 4.5.

$$\rho=p/(ZR_gT) \qquad 4.1)$$

$$u_\rho^2 = \left(\left(\frac{\partial\rho}{\partial p}\right)^2 u_p^2 + \left(\frac{\partial\rho}{\partial T}\right)^2 u_T^2 + \left(\frac{\partial\rho}{\partial Z}\right)^2 u_Z^2 + \left(\frac{\partial\rho}{\partial R_g}\right)^2 u_{R_g}^2\right) \qquad 4.2)$$

$$\frac{\partial\rho}{\partial p} = \frac{1}{ZR_gT} \qquad \frac{\partial\rho}{\partial T} = -\frac{p}{ZR_gT^2} \qquad 4.3)$$

$$\frac{\partial\rho}{\partial R_g} = -\frac{p}{ZR_g^2T} \qquad \frac{\partial\rho}{\partial Z} = -\frac{p}{Z^2R_gT} \qquad 4.4)$$

$$\frac{u_\rho^2}{\rho^2} = \left(\left(\frac{u_p}{p}\right)^2 + \left(\frac{u_T}{T}\right)^2 + \left(\frac{u_Z}{Z}\right)^2 + \left(\frac{u_{R_g}}{R_g}\right)^2\right) \qquad 4.5)$$

Example

The gas is natural gas at following conditions:
(the natural gas data is taken from an example in [1])

p = 6 MPa
T = 290 K (t = 16,85 °C)

Z = 0,88006

R_g = 0,00049481 MJ/kmol K

ρ = 47,512 kg/m³

The gas composition is as listed in table 4.1

Table 4.1 Gas composition

Component	Mole fraction	Uncertainty, mole fraction
CH_4	0,965	0,001
C2H6	0,018	0,001
C3H8	0,0045	0,0005
C4H10-i	0,001	0,0003
C4H10-n	0,001	0,0003
C5H12-i	0,0005	0,0001
C5H12-n	0,0003	0,0001
C6+	0,0007	0,0001
N2	0,003	0,001
CO2	0,006	0,001
Total	1	

The measuring system consists of the instruments seen in table 4.2

Table 4.2 Measuring system

Instruments
Absolute pressure transducer
Pt-100 resistance thermometer
Flowcomputer
Gas chromatograph

To simplify the example the instruments are calibrated with the registration equipment (a flowcomputer). In practise the instruments are calibrated separately and then the influence of the uncertainty of the input/output of the flowcomputer on the output of each instrument should be estimated. This can be done in the same manner as the uncertainty of the output of each instrument is estimated.

The combined standard uncertainty

$$\frac{u_\rho^2}{\rho^2} = \left(\left(\frac{u_p}{p}\right)^2 + \left(\frac{u_T}{T}\right)^2 + \left(\frac{u_Z}{Z}\right)^2 + \left(\frac{u_{R_g}}{R_g}\right)^2 \right)$$

$$\frac{u_\rho}{\rho} = \sqrt{(2{,}7\cdot10^{-4})^2 + (3{,}2\cdot10^{-4})^2 + (7{,}6\cdot10^{-4})^2 + (7{,}5\cdot10^{-4})^2} = 11{,}5\cdot10^{-4}$$

(the relative uncertainties of the parameters are derived in the following)

$$u_\rho = 47{,}512\cdot11{,}5\cdot10^{-4} = 0{,}055\ \mathrm{kg/m^3}$$

The expanded uncertainty

$U_\rho = 2\cdot u_\rho = 0{,}11\ \mathrm{kg/m^3}$ **at 47,512 kg/m3 (290 K and 6 MPa)**

U_ρ/ρ = 0,23 %

In the following the relative combined standard uncertainties of the parameters are derived step by step.

u_p/p

$$u_p = \sqrt{(u_{p\text{-}A})^2 + (u_{p\text{-}B})^2}$$

The standard uncertainty of type A component is obtained by determining the pressure (at stable conditions) at the pressure of 6 MPa at least 10 times and deriving the standard deviation of the mean.

$u_{p\text{-}A} \approx s(\bar{p}) = 1{,}0$ kPa

The standard uncertainty of type B components

Table 4.3 Type B components u_p

No.	Component description	a_j kPa	c_j	$a_j \cdot c_j$ kPa
1	Calibration of the instrument	1	1	1
2	Reading error during calibration	0,5	$1/\sqrt{3}$	0,29
3	Shift between calibrations	1,0	$1/\sqrt{3}$	0,58
4	Reading error during measurement	0,5	$1/\sqrt{3}$	0,29
5	Hysteresis effect	0,5	$1/\sqrt{3}$	0,29
6	Deviation from calibration conditions	0,05	$1/\sqrt{3}$	0,03
7	Installation effects	≈ 0	$1/\sqrt{3}$	0
	$u_{p\text{-}B} = \sqrt{\sum \left(a_j \cdot c_j \right)^2}$			1,26

re 1 calibration result is given with the uncertainty of ± 2 kPa at a 95 % confidence level in the range 5-6 MPa ⇒ a= 1 kPa. The transducer and the flowcomputer is calibrated as a unit. The flowcomputer has been checked/calibrated immediately before the calibration of the transducer.

re 2 resolution 1 kPa (0,01 bar) ⇒ a = 0,5 kPa.

re 3 the shift between calibrations is less than 2 kPa ⇒ a = 1 kPa.

re 4 resolution 1 kPa (0,01 bar) ⇒ a = 0,5 kPa.

re 5 the hysteresis is less than 1 kPa ⇒ a = 0,5 kPa.

re 6 the temperature dependency of the transducer is given by the manufacturer to be less than 0,03 kPa / K. The transducer is calibrated at 293,15 K and the gas to be measured upon is at 290 K ⇒ a = 0,05 kPa.

re 7 The installation effects are estimated to be negligable (less than 0,01 kPa).

$$u_p = \sqrt{\left(u_{p\text{-}A}\right)^2 + \left(u_{p\text{-}B}\right)^2}$$

$$u_p = \sqrt{(1,0)^2 + (1,26)^2} = 1,61 \text{ kPa}$$

$$\frac{u_p}{p} = 1,61/6000 = 0,00027$$

u_T/T

$$u_T = \sqrt{(u_{T-A})^2 + (u_{T-B})^2}$$

The standard uncertainty of type A component is obtained by determining the temperature (at around 290 K) at least 10 times and deriving the standard deviation of the mean.

$$u_{T-A} \approx s(\overline{T}) = 0,02 \text{ K}$$

The standard uncertainty of type B components

Table 4.4 Type B component; u_T

No.	Component description	a_j K	c_j	$a_j \cdot c_j$ K
1	Calibration of the instrument	0,05	1	0,05
2	Reading error during calibration	0,05	$1/\sqrt{3}$	0,029
3	Shift between calibrations	0,1	$1/\sqrt{3}$	0,058
4	Reading error during measurement	0,05	$1/\sqrt{3}$	0,029
5	Hysteresis effect	≈0	$1/\sqrt{3}$	0
6	Deviation from calibration conditions	≈0	$1/\sqrt{3}$	0
7	Installation effects.	0,05	$1/\sqrt{3}$	0,029
	$u_{T-B} = \sqrt{\sum\left(a_j \cdot c_j\right)^2}$			0,092

re 1 calibration result is given with the uncertainty of ±0,1 K at a 95 % confidence level ⇒ a= 0,05 K. The thermometer and the flowcomputer are calibrated as a unit. The flowcomputer has been checked/calibrated immediately before the calibration of the thermometer.

re 2 resolution 0,1 K ⇒ a= 0,05 K.

re 3 the shift between calibrations is less than 0,2 K ⇒ a= 0,1 K.

re 4 resolution 0,1 K⇒ a= 0,05 K.

re 5 the hysteresis is negligable.

re 6 the thermometer is calibrated at ambient pressure and will be applied in 6 MPa, but the effect of this on the temperature measurement will be negligable.

re 7 the thermometer is situated in a pocket and even with thermal insulation of and thermal conductive oil in the pocket the difference between the temperature of the gas to the temperature measured has prior to upstart been determined to be around 0,1 K ⇒ a= 0,05 K.

$$u_T = \sqrt{(u_{T-A})^2 + (u_{T-B})^2}$$

$$u_T = \sqrt{(0,02)^2 + (0,092)^2} = 0,094 \text{ K}$$

$$\frac{u_T}{T} = 0,094/290 = 0,00032$$

u_Z/Z

Z is calculated from ISO/DIS 12213[1], part 2, applying the molar compositional analysis in table 4.1 obtained with a gaschromatographic analysis that has been performed at the upstart of the measuring system. The variations in gascomposition are very small.

The expanded uncertainty of Z is given in ISO/DIS 12213[1] as being a combination of the expanded uncertainty of the use of the calculation method and of the expanded uncertainty of the gas analysis. Use of the calculation method in this pressure, temperature range gives an uncertainty of ± 0,1 % at a 95 % confidence level. If the expanded uncertainty of the gasanalysis is as given in table 4.1 then according to ISO/DIS 12213[1] the influence of this on the compression factor is less than ± 0,1 %.

$$u_Z = \sqrt{(a_{\text{cal. method}} \; c_{\text{cal. method}})^2 + (a_{\text{analysis}} \; c_{\text{analysis}})^2}$$

$$a_{\text{cal. method}} = 0,05\ \%\ 0,88006 = 0,00044$$

$$c_{\text{cal. method}} = 1$$

$$a_{\text{analysis}} = 0,1\ \%\ 0,88006 = 0,00088$$

$$c_{\text{analysis}} = \frac{1}{\sqrt{3}}$$

$$u_Z = \sqrt{(0,00044)^2 + (0,00051)^2} = 6,7 \cdot 10^{-4}$$

$$\frac{u_Z}{Z} = \frac{6,7 \cdot 10^{-4}}{0,88006} = 7,6 \cdot 10^{-4}$$

u_{Rg}/Rg

R_g is calculated by applying the molar compositional analysis obtained from the gaschromatographic analysis, see table 4.1, that has been performed at the upstart of the measuring system. The expanded uncertainty of the determination is estimated to be ± 0, 13 % and as the variations in gascomposition are very small, no further contribution to the uncertainty of R_g is expected.

$$u_{R_g} = a_{R_g} \cdot c_{R_g}$$

$$a_{R_g} = 0,0013 \cdot 0,000495 = 6,435 \cdot 10^{-7}$$

$$c_{R_g} = \frac{1}{\sqrt{3}}$$

$$u_{R_g} = 3,72 \cdot 10^{-7}$$

$$\frac{u_{R_g}}{R_g} = \frac{3,72 \cdot 10^{-7}}{0,00049481} = 7,5 \cdot 10^{-4}$$

TECHNICAL REPORTS FROM THE STRATEGY GROUP ON QUALITY AND METROLOGY

48 Ohlon, R. Comments to the EUROLAB working document on quality systems. Espoo 1994. Nordtest, NT Techn Report 248. 66 p.

51 Steffen, B., Kallio, H. & Þorsteinsson, Freygarður, Editors, Traceable calibration and uncertainty of measurements and tests. Espoo 1994. Nordtest, NT Techn Report 251. 164 p.

52 Guðmundsson, Halldór & Rúnarsson, Tómas P., Traceable calibration and uncertainty of measurements in scanning electron microscopy. Espoo 1994. Nordtest, NT Techn Report 252. 48 p.

53 Lau, P., Pre-study for establishing a facility for calibration of liquid density meters. Borås 1994. Swedish National Testing and Research Institute, Report SP AR 1994:18. 26 p. (in Swedish)

84 Jensen, H. & Nielsen, L., Uncertainty of pH measurements. Espoo 1995. Nordtest, NT Techn Report 284. 22 p.

05 Calibration, Traceability and Uncertainty, Seminar in Espoo 1-2 November 1995. Espoo 1995. Nordtest, NT Techn Report 305. 154 p.

07 Ohlon, R., Schemes related to peer evaluation. Espoo 1995. Nordtest, NT Techn Report 307. 41 p.

08 Thun, R., Aunela-Tapola, L. & Tulenheimo, V., Quality assurance of industrial environmental performance. Espoo 1995. Nordtest, NT Techn Report 308. 71 p.

22 Ohlon, R., Preparation of contributions to development of harmonized standards. Borås 1996. Swedish National Testing and Research Institute, Report SP AR 1996:17. 39 p.

23 Elo, N., Kujala, S., Lindroos, V. & Tiittanen, K., Report format and signing of docments. Espoo 1996. Nordtest, NT Techn Report 323. 21 p.

24 Svensson, T., Digital filtering of data from measurements. Espoo 1996. Nordtest, NT Techn Report 324. 17 p.

32 Forstén, J., The different roles of organizations performing testing. Espoo 1996. Nordtest, NT Techn Report 332. 17 p.

51 Guðmundsson, H., Calibration and uncertainty of XRF measurements in the SEM. Espoo 1997. Nordtest, NT Techn Report 351. 42 p. NT Project No. 1280-96.

52 Rydler, K.-E. & Nilsson, H.,Transparency of national evaluation methods of accreditation in the field of electrical measurements. Espoo 1997. Nordtest, NT Techn Report 352. 61p. NT Project No. 1255-95.

53 Tambo, M. & Søgaard, T., The determination of gas density - part 1: State of the art in the Nordic countries. Espoo 1997. Nordtest, NT Techn Report 353. 19p. NT Project No. 1254-95.

54 Tambo, M. & Søgaard, T., The determination of gas density - part 2: Intercomparison — Calibration of gas density meters with nitrogen. Espoo 1997. Nordtest, NT Techn Report 354. 91 p. NT Project No. 1254-95.

55 Tambo, M. & Søgaard, T., The determination of gas density - part 3: A guideline to determination of gas density. Espoo 1997. Nordtest, NT Techn Report 355. 29 p. NT Project No. 1254-95.

NSFMW.97

North Sea FLOW Measurement Workshop

Paper 24: 4.4

DISTURBED FLOW PROFILES AND THEIR EFFECT ON GAS METER BEGAVIOUR

- SYSTEMATIC INVESTIGATIONS AND PRACTICAL CONCLUSIONS-

Authors:
Gudrun Wendt, Bodo Mickan, Rainer Kramer and Dietrich Dopheide
Physikalisch-Technische Bundesanstalt (PTB) Braunschweig, Germany

Organiser:
Norwegian Society of Chartered Engineers
Norwegian Society for Oil and Gas Measurement
Co-organiser:
National Engineering Laboratory, UK

DISTURBED FLOW PROFILES AND THEIR EFFECT ON GAS METER BEHAVIOUR

- SYSTEMATIC INVESTIGATIONS AND PRACTICAL CONCLUSIONS -

Gudrun Wendt

Bodo Mickan, Rainer Kramer, Dietrich Dopheide

Physikalisch-Technische Bundesanstalt (PTB) Braunschweig, Germany

Summary

Within the scope of an extensive PTB research project a special facility was built which allows the investigation of flow profiles downstream of several pipe geometries and flow straighteners. Modern and effective miniaturized semiconductor based laser Doppler techniques are used to measure the developing velocity profiles inside the pipe sections of interest. The corresponding reaction of turbine gas meters is determined with a high accuracy and repeatability using the PTB's flowrate standard facility with critical nozzles. Until now more than 150 different flow distributions have been investigated. The results are summarized in a flow profile catalogue which shows the high degree of systematics and generality of the work.

On the basis of these results it has become possible to achieve good transparency of the flow processes taking place in real gas pipe configurations and to explain the mechanism of the interaction between characterictic flow distributions and turbine meter performance.

The conclusions concerning the active conditioning of disturbed flows in particular allow optimized pipe lengths and flow conditioners to be recommended with a view to minimizing or eliminating the influence of flow disturbances on the flowmeter behaviour.

1 INTRODUCTION

It is a well-known fact in flow measurement that the behaviour of the measuring devices used can be affected very seriously by the flow conditions prevailing at their inlet pipe section. Different pipe configurations such as for instance bends, headers, pressure regulators, or changing diameters generate different distributions of the fluid's flow velocity and turbulence intensity. The concrete effect of these „disturbed" conditions on the measuring behaviour of a flowmeter installed downstream depends basically on the working principle of the meter itself. The resulting deviation in the meter reading can amount up to several percent.

The whole phenomenon of the so-called installation effects in flow measurement appears as a very complex and complicated problem: on the one hand the measuring practice shows a wide variety of pipe geometries and duct configurations, and on the other hand the different types of flowmeters react in very different kinds to the flow conditions at their inlet. That's why there are an actual need and a great interest in investigating and understanding the physics of the chain „pipe configuration - disturbed flow profile - change in flowmeter behaviour" with the final aim to find out effective methods and techniques to minimize the installation effects.

In the last few years many efforts were already made in this particular field of flow measurement. An analysis of the relevant publications shows that emphasis was placed predominantly on three aspects:

- Investigations into the concrete effects of special pipe configurations on the behaviour of special flowmeter types installed downstream (orifice metering installations [1-3], turbine meters [4,5], ultrasonic and electromagnetic flowmeters [6], or vortex flowmeters [7]).
  In some cases the measuring errors due to the flow disturbances tested are described as of a remarkable order of up to 5 % for orifice and turbine meters [8] or of up to 11 % for ultrasonic flowmeters [9].

- Study of the performance of different flow straighteners and conditioners such as perforated plates, tube-bundle, Zanker, or Etoile flow conditioners and of their efficiency for the reduction of flow disturbances and the establishment of nearly ideal flow conditions with well developed velocity and turbulence profiles.
  The respective publications describe the effect on both the flow profiles [10-12] and several complete flowmeter performances [13,14].

- Description of the methods for investigating the flow characteristics and their development downstream of the pipe configurations and flow conditioners to be investigated.
  In addition to the more conventional methods such as Pitot tubes [15] or hot film probes [14,16], laser methods are employed in a wide range of application, using, for example, Laser Doppler Anemometry (LDA) [4,10,17-18] or Particle Image Velocimetry (PIV) [19]. Recently the development of flow phenomena in pipes are studied by means of Computational Fluid Dynamics (CFD) [20,21] where a numerical simulation of the pipe flow gives, for example, obvious pictures of the complete velocity distributions in the pipe section of interest.

Most of the publications concerning the problems of flowmeter installation effects are, however, confined to the investigation of very individual cases: special pipe configurations, special flow distributions, and special flowmeter performances. A general systematic analysis of the whole interaction chain from certain pipe configurations through developing flow distributions to the resulting meter behaviour has been lacking. Therefore, a PTB research project sponsored by the DVGW (Deutscher Verein des Gas-und Wasserfachs) was initiated as a first step towards filling this gap. The main aims were:

- Experimental investigation of all practically relevant pipe geometries and flow phenomena developing downstream including the investigation of their decay, systematization and generalization of all data obtained

- Definition and quantification of flow characteristics describing the types of resulting perturbations such as swirl intensity, skewness, and asymmetry of the velocity profiles

- Determination of the deviations in the reading of various flowmeters (starting with turbine gas meters)

A solution of the installation effect problem is conceivable in two directions:

- Development of an empirical model to explain the metering effects and to predict, if possible, the expected shift in the meter reading

- Investigation of the efficiency of various types of flow conditioners and, if need be, development of optimized forms of conditioners in dependence on the perturbation and flowmeter typ

2 LDA DIAGNOSTIC FACILITY FOR INSTALLATION EFFECTS

At the first stage of the project the activities concentrated on the investigation of turbine gas meters working with air at atmospheric conditions. To carry out all experimental work mentioned above a special automated test facility was built.

This diagnostic facility takes advantage of two developments successfully pursued at the PTB in the last few years - first, the extensive research on laser techniques and the construction of efficient LDAs, and secondly, the use of critical nozzles for the establishment and measurement of the gas flow with a very high accuracy and reproducibility. It has thus become possible to combine the detailed knowledge of the flow characteristics inside the pipe infront of the flowmeter (including its inlet section) with the exact information about the behaviour of the flowmeter itself.

The LDA diagnostic facility (Figure 1) consists of the following main elements:

- the installation configurations to be investigated (for example, single or double bends, convergent or divergent sections, half plates, flow conditioners, various straight pipes up to 40 diameters in length, etc.)
- the optical test unit consisting of a two-component semiconductor LDA system to measure the flow profiles in the entire cross section of the pipe and a special pipe segment which allows the optical access to the flow inside the pipe
- the gas meter to be investigated
- the flowrate standard consisting of eight critical nozzles to determine the gas meter's dependence on the inlet flow profiles

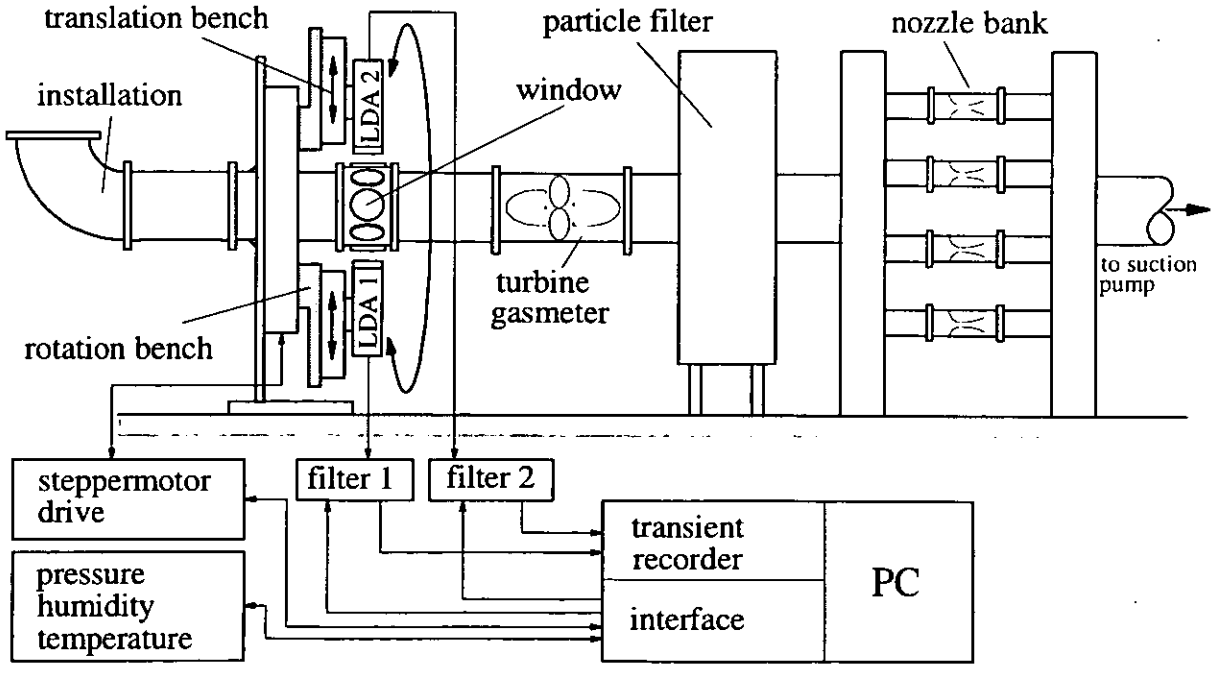

Fig. 1: Schematic view of the computer-controlled facility to investigate installation effects

This facility shows some specialities ensuring an uncomplicated and practice-related work. Free inlet and suction method for gas flow generation allow pipe configurations of any kind and size to be easily installed in a short time. This is, for example, an advantage over closed conduits as used in liquid or high pressure gas measurements. A second important characteristic of this facility is the large-scale simulation of the flow conditions actually encountered in industrial gas distribution and measuring systems. Most of the investigations in the past were carried out under ideal conditions using ideally fashioned pipework. In contrast to this, all pipe elements and devices used at PTB were taken from regular fabrication with common roughness characteristics and production tolerances. In this way it will be possible to transfer the test results directly to practical application.

The most important part of the facility is the LDA measuring unit. The connection to the piping is realized by a special pipe segment (Figure 2). Eight windows allow four different profiles rotated by 45 ° to be scanned. Inside the pipe, each window is made of a glass film to prevent changes in the diameter and to provide for a smooth inner contour of the pipe. The windows outside the pipe consist of plane glass plates to block pressure differences.

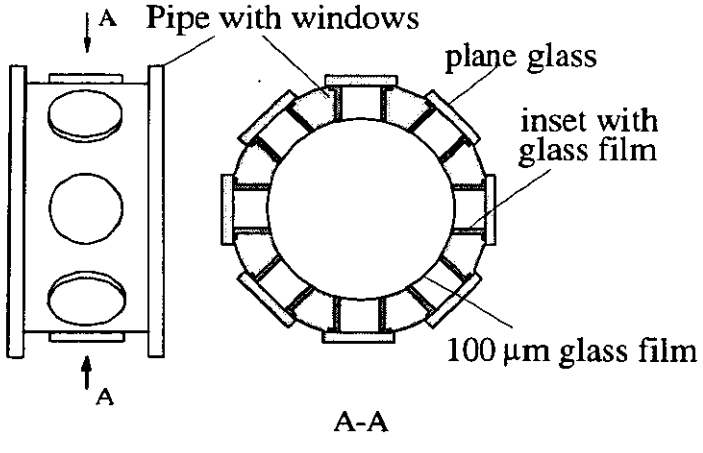

Fig. 2: Schematic view of the special pipe segment with outer glass windows and a smooth inner wall contour using thin glass films

Two separated LDAs for the two-dimensional measurement of the flow profiles are installed on a rotating mechanism and positioned face to face on both sides of the pipe segment described. Each miniature diode LDA is mounted on a precise linear traversing bench and can be operated by a remote control. A linear scan through the pipe diameter is easily done when moving tables are driven synchronously.

Remote control and automation of the facility covers the LDA acquisition system based on transient recorder plug cards for PC/AT, control of the positioning devices, setting of the flowrate, reading of the gas meter and acquisition of the state of flow, i.e. pressures, temperatures, humidity etc. The software extracts information relevant for the configuration of the set-up from parameter tables compiled by experience and it is able to perform complete velocity profile measurements completely automatically.

The main characteristics of the LDA test unit used for the experiments are:

Pipe diameter	DN 200
LDA-system	2 one-component semiconductor LDAs in forward scatter mode
Wavelength	780 nm and 830 nm
Colour splitting	optical filters
Velocity uncertainty	< 1 %
Acquisition	two channel transient recorder card, sample rate 100 Mhz
Number of sample points	1028 for each LDA and each measuring point

A particle filter installed downstream of the flowmeter to be tested protects the nozzle standard from deposition of seeding material necessary to produce scattering particles for the LDA.

The generation of a stable and well-known flowrate is realized by a nozzle bank consisting of eight critically nozzles with individual flowrates between 65 m^3/h and 2500 m^3/h, and a maximum flowrate of 5500 m^3/h when all nozzles are used in parallel. The uncertainty for the flowrate generation is less than 0,1 %, its reproducibility less than 0,01 %.

3 FLOW PROFILE MEASUREMENTS

Figure 3 shows the position of the velocity components used for the following presentation of the flow characteristics inside the optical test unit and the direction of the co-ordinate system. The two LDAs are measuring at an angle of + 45 degrees and - 45 degrees each with respect to the x-axis. Knowledge of these two components of the velocity vector allows the axial velocity component u and the tangential velocity component v to be evaluated as shown in this graphic.

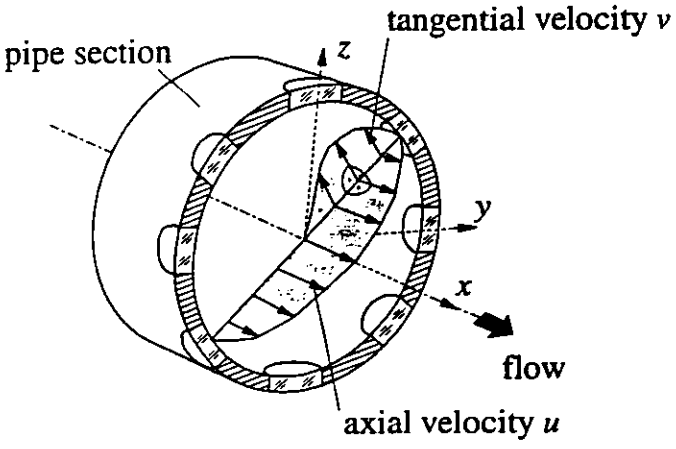

Fig. 3: Positions of the velocity components measured and the co-ordinate system used

In the following some typical pipe configurations (straight pipes of various lengths, single and double bends with constant and changing diameter) and the resulting velocity distributions are presented. They are selected from more than 100 different performances investigated and should give an idea about the kind and amount of data collected. In general, all configurations included in the experimental activities were investigated at various (normally four) flowrates and equipped at least with three different straight pipe

lengths (normally 2 D [1], 5 D, 10 D) between the perturbation exit and the flowmeter inlet. The configurations with double bends were measured in both symmetrical arrangements.

The velocity profile measurements were started with the determination of the undisturbed pipe flow conditions as a reference. For this purpose a straight pipe with different lenghts between 2 D and 40 D and free inlet flow was used. The resulting velocity distributions measured showed that a nearly fully developed turbulent velocity profile was obtained downstream of a straight pipe of 28 D long, see Figure 4. The distribution of the axial velocity components follows the theoretically predicted law, tangential velocity components are not visible. These profile parameters were assumed to be undisturbed and served as a basis for all comparisons described below.

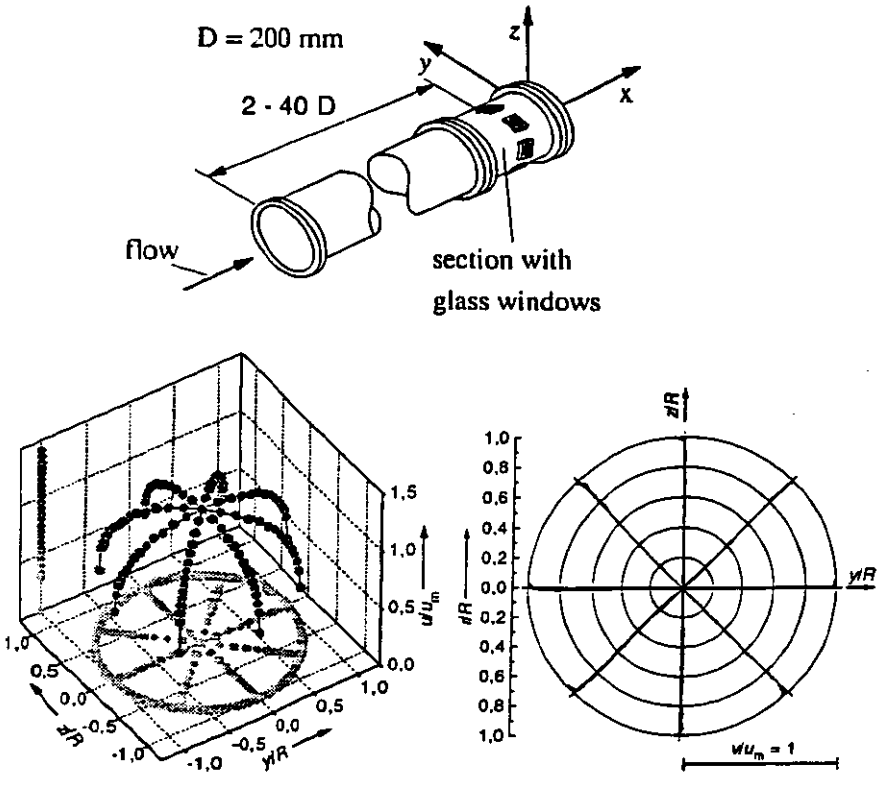

Fig. 4: Schematic view of the straight pipe investigated in different lengths and perspective plot of the axial components u (left picture) and the tangential components v (right picture) of the velocity distributions downstream of a straight pipe of 28 D in length.

Air flowrate Q = 1750 m^3/h; Reynolds number $Re = 1{,}9 \cdot 10^5$
All velocities shown are normalized with the mean axial flow velocity u_m. [2]

The first example (Figure 5) for disturbed flow conditions shows the axial and tangential components of the velocity distribution downstream of a single bend and straight pipe lengths of 2 D and 10 D. At the 2 D distance, the axial velocity profiles show a local minimum at the centre of the pipe and an elevation towards the pipe wall. The tangential velocity distribution at this 2 D distance is in good agreement with the theoretical model describing the generation of two secondary swirls for such a pipe configuration. These

[1] Usually, these straight pipe lengths are expressed in multiples of the inner pipe diameter D.

[2] All profiles treated in the following have been determined at the same flowrate and Reynolds number and are represented in the same graphic view.

disturbances decrease relatively quickly with increasing straight pipe length: At 10 *D* both the axial and the tangential distributions have a shape similar to that under undisturbed conditions. This assumption is supported considering the error shifts of a turbine meter G 1600 used for the described investigations compared with its reading at undisturbed flow conditions: + 0,48 % for the 2 *D* straight pipe between the bend and the meter, + 0,16 % for the 10 *D* straight pipe.

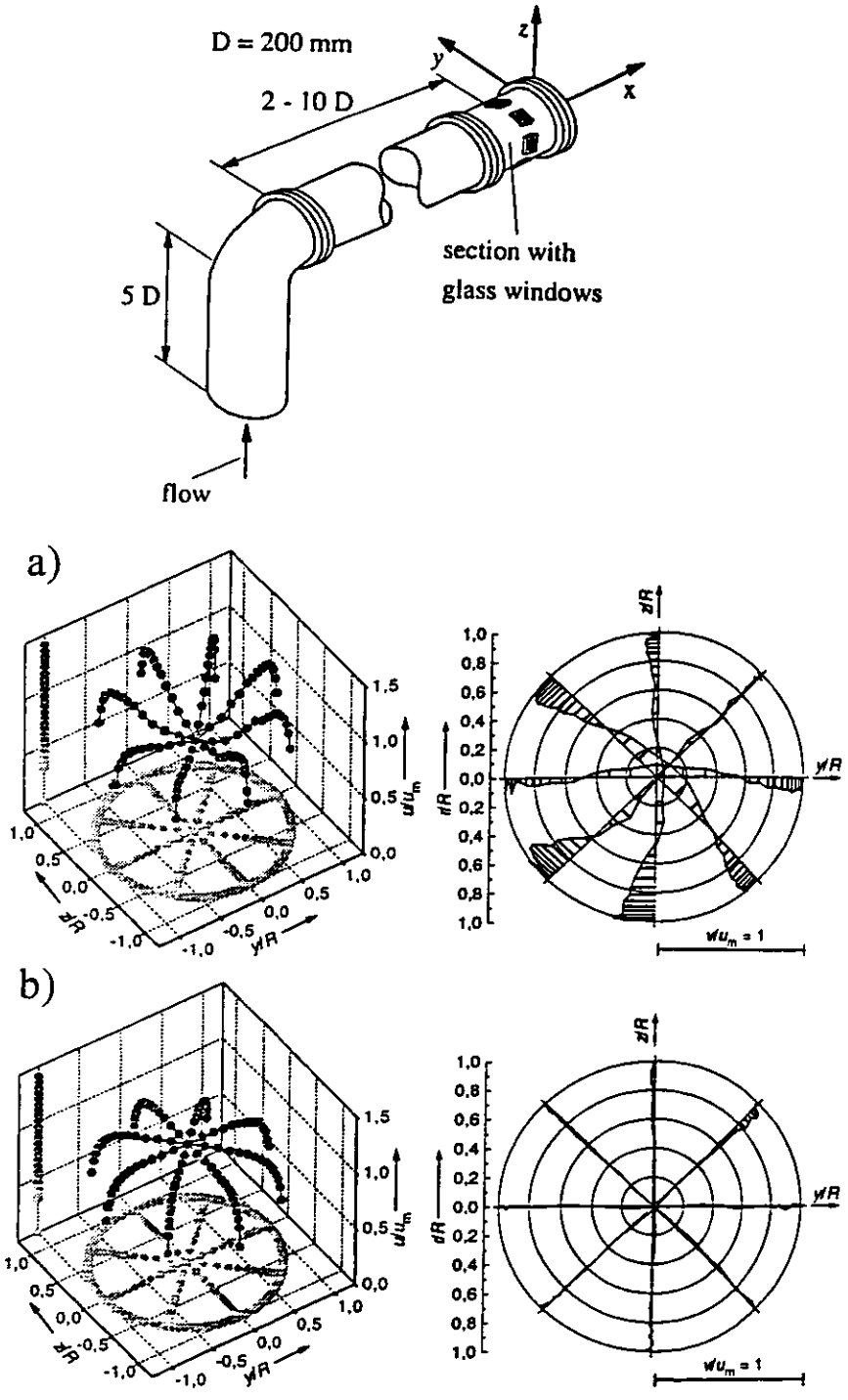

Fig. 5: Schematic view of the pipe configuration investigated and perspective plot of the axial components u (left pictures) and the tangential components v (right pictures) of the velocity distributions downstream of a single bend and a straight pipe of a) 2 D and b) 10 D

The next two figures show the flow characteristics for the same pipe configurations where the single bend has been replaced by a double bend with the diameter remaining unchanged (Figure 6) and a double bend in a reduced diameter, half pipe area plate between the bends and a diverging pipe section connected behind („high level perturbation" according to OIML R 32 [22] - Figure 7).

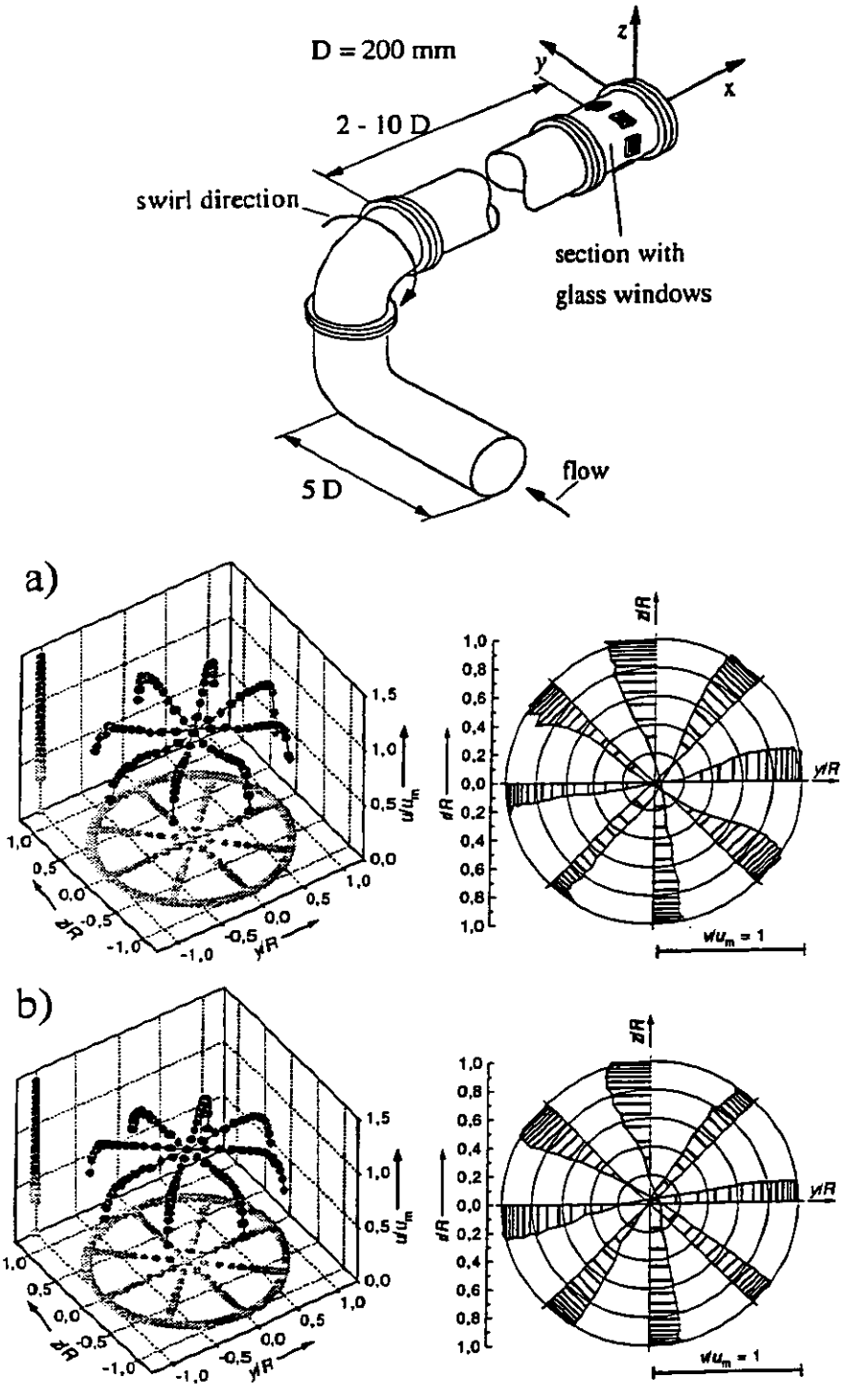

Fig. 6: Schematic view of the pipe configuration investigated and perspective plot of the axial components u (left pictures) and the tangential components v (right pictures) of the velocity distributions downstream of a double bend out of plane with unchanged diameter and a straight pipe of
a) 2 D and b) 10 D

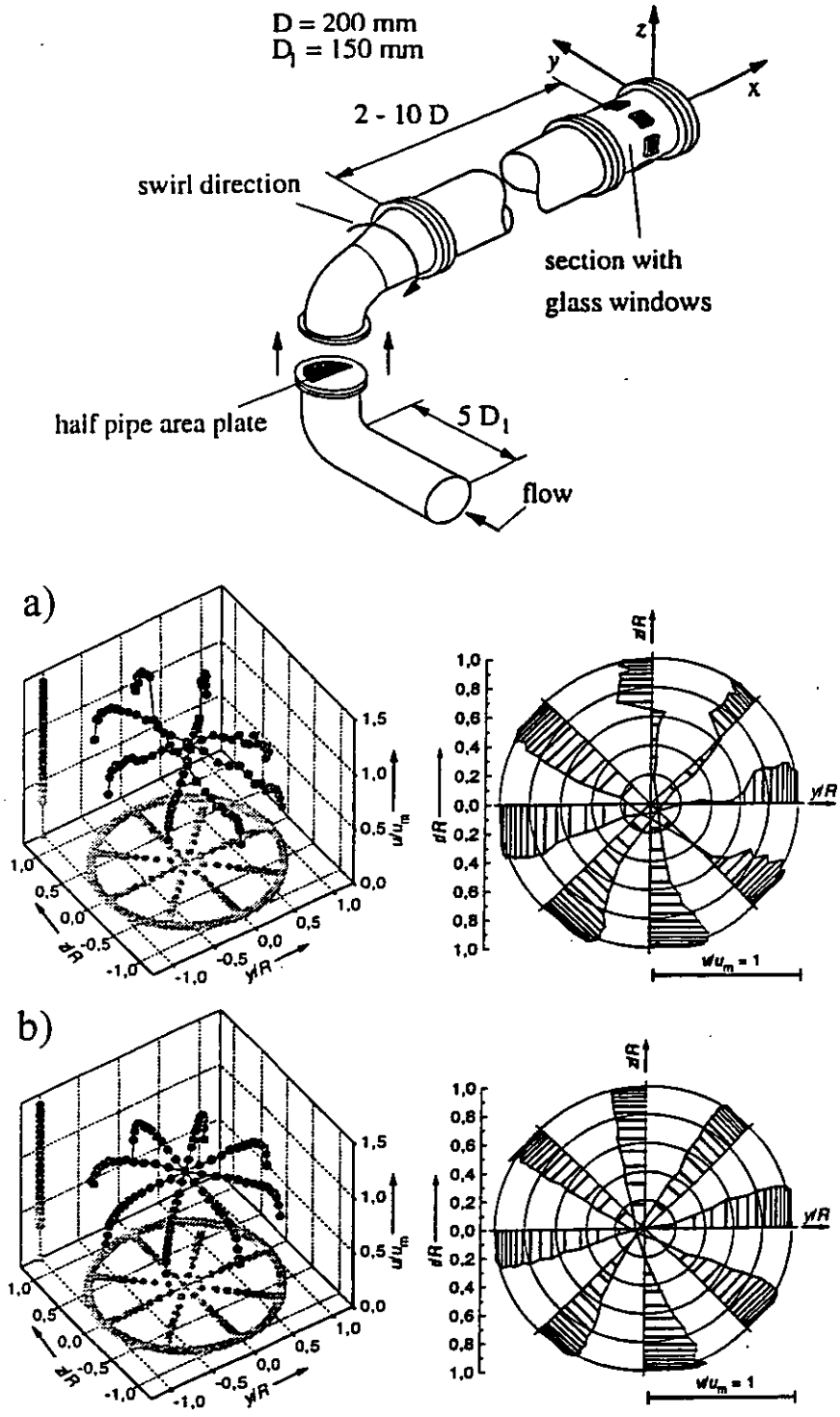

Fig. 7: Schematic view of the pipe configuration investigated and perspective plot of the axial components u (left pictures) and the tangential components v (right pictures) of the velocity distributions downstream of a double bend out of plane equipped with a half pipe area plate („high level perturbation" according to OIML R 32) and a straight pipe of
a) 2 D and b) 10 D

In both cases, the axial velocity profiles are not symmetrical, and the tangential components show swirls and secondary flows of high intensities. These tangential components v

reach values of up to more than 40 % of the mean axial velocity u_m. The conspicuously disturbed profiles (discontinuities in the axial and tangential profiles along two traverses) for the 2 *D* high level perturbation in Fig. 7 can be explained by the extremely high turbulence behind the half pipe area plate with reverse flows in the turbulent mixing zone and radial velocity components. Although a normalization of the axial velocity distributions towards the fully developed profile between the 2 *D* and 10 *D* distances is perceptible, the swirls continue to exist with nearly the same order of intensity at the 10 *D* distance.

A comparison of the turbine meter's error shifts for different straight pipe lengths between the perturbation and the meter inlet (Table 1) confirms the statement that a 10 *D* straight pipe is not long enough to effectively diminish the flow perturbations downstream of double bends out of plane.

Table 1: The error shift of a turbine gas meter G 1600 for different pipe configurations and straight pipes of different lengths upstream of the meter, compared with the undisturbed flow (volume flowrate Q = 1750 m³/h; $Re = 1{,}9 \cdot 10^5$)

	Error shift for straight pipe lengths of		
	2 D	**5 D**	**10 D**
Single bend (Fig. 5)	+ 0,48 %	+ 0,18 %	+ 0,16 %
Double bend out of plane (Fig. 6)	+ 1,13 %	+ 1,15 %	+ 0,88 %
High level perturbation (Fig. 7)	+ 1,37 %	+ 1,32 %	+ 1,08 %

In addition to the flow profiles, the turbulence intensity distributions were determined for all pipe geometries and flowrates investigated. Figure 8 shows some of them for the pipe configurations already described above (straight pipe, single bend, double bend out of plane and high level perturbation).

The turbulence intensity *Tu* was evaluated using the individual values of the axial and tangential velocity components u and v obtained during the profile investigations and assuming each of these individual values to be the sum of a time-averaged value ($\overline{u}$ or $\overline{v}$) and a instantaneous deviation (u' or v') from this averaged value

$$u = \overline{u} + u' \qquad \text{and} \qquad v = \overline{v} + v' \tag{1}$$

The equation to evaluate the turbulence intensity *Tu* reads as follows

$$Tu = \frac{\sqrt{s_u^2 + s_v^2}}{\sqrt{2} \cdot u_m} \tag{2}$$

where s_u^2 and s_v^2 are the variances of the axial and tangential velocity components u and v, respectively

$$s_u^2 = \overline{(u - \overline{u})^2} \qquad \text{and} \qquad s_v^2 = \overline{(v - \overline{v})^2} \tag{3}$$

and u_m is the mean axial velocity through the pipe.

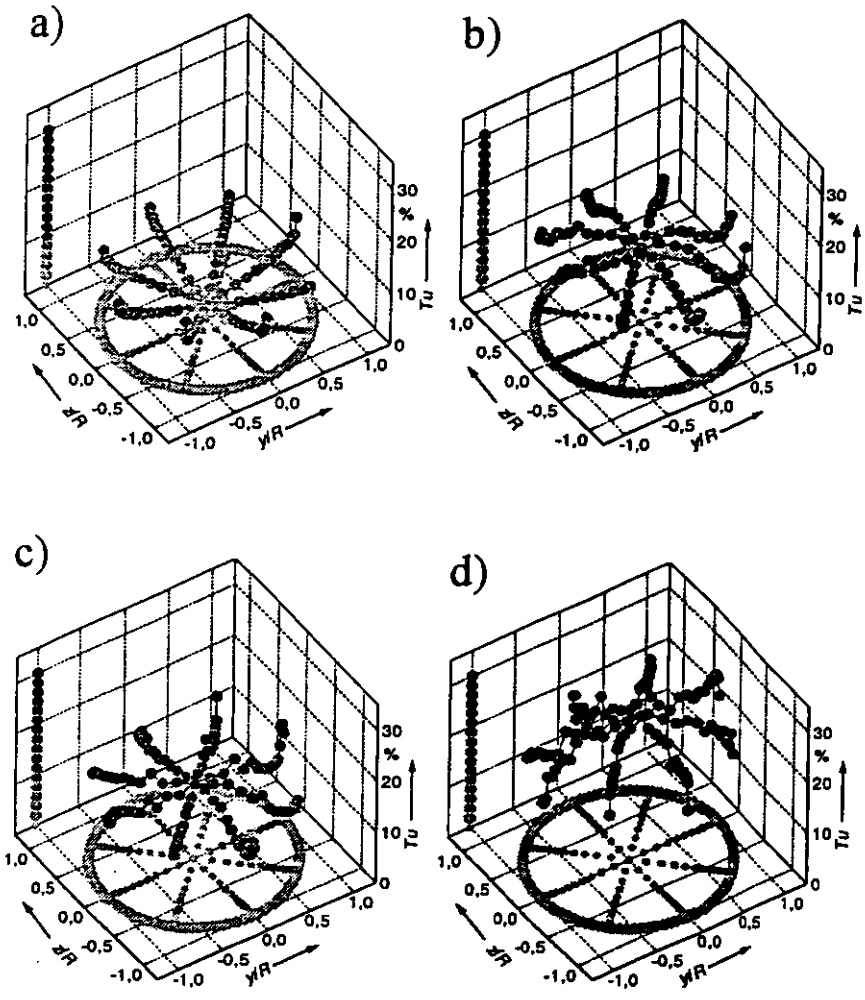

Fig.8: Measured turbulence intensity distributions for different pipe geometries
a) straight pipe of 28 D according to Fig. 4
b) single bend and 2 D straight pipe according to Fig. 5
c) double bend out of plane and 2 D straight pipe according to Fig. 6
d) high level perturbation and 2 D straight pipe according to Fig. 7

In the case of a straight pipe (Figure 8a) one recognizes a symmetrical degree of turbulence with a minimum in the centre of the pipe and higher turbulence intensities towards the wall as it is well known from literature. The turbulence intensity significantly increases in the core region when a single bend is applied (Figure 8b). A double bend out of plane as shown in Figure 8c provides for a much more asymmetrical turbulence distribution. The worst case is to be seen at the high level perturbation in Figure 8d where a very asymmetrical high level turbulence is to be observed.

The results of the investigations decribed in the previous chapter have led to important conclusions regarding the interaction chain between pipe geometries, developing flow distributions and the resulting behaviour of the flowmeter (namely the shift of the error curves). They have given a vivid picture of the processes taking place in the various pipe elements impressive investigated. Nevertheless, this knowledge is not enough to reach the

real goal - to improve flow measurements in general and, if possible, to avoid measurement mistakes at all.

There are two approaches to continuing the work making use of the experience and knowledge gained:

- first, to use suitable mechanical damping elements to influence the flow in such a way that, at the flowmeter inlet, the velocity profiles are nearly undisturbed and do not affect the meter reading. This method requires additional pipe installations (such as, for example, flow starighteners or conditioners), but it is independent of the flowmeter type;
- secondly, to try to describe mathematically the correlations found, to develop a corresponding model, and to predict and consider the changes in the flowmeter behaviour in dependence on the flowmeter type and the actual pipe configuration.

4 FLOW CONDITIONER INVESTIGATIONS

To prove that it is possible to provide for an efficient flow conditioning, another large series of experiments was carried out. Several types of flow straighteners and conditioners were investigated and evaluated with regard to their efficiency to reduce flow disturbances generated by the pipe configurations described above. Fig. 9 shows the most important types of flow conditioners examined: Etoile, Zanker, and tube-bundle conditioners as well as perforated plates of different kinds in various combinations (single, double, triple plates).

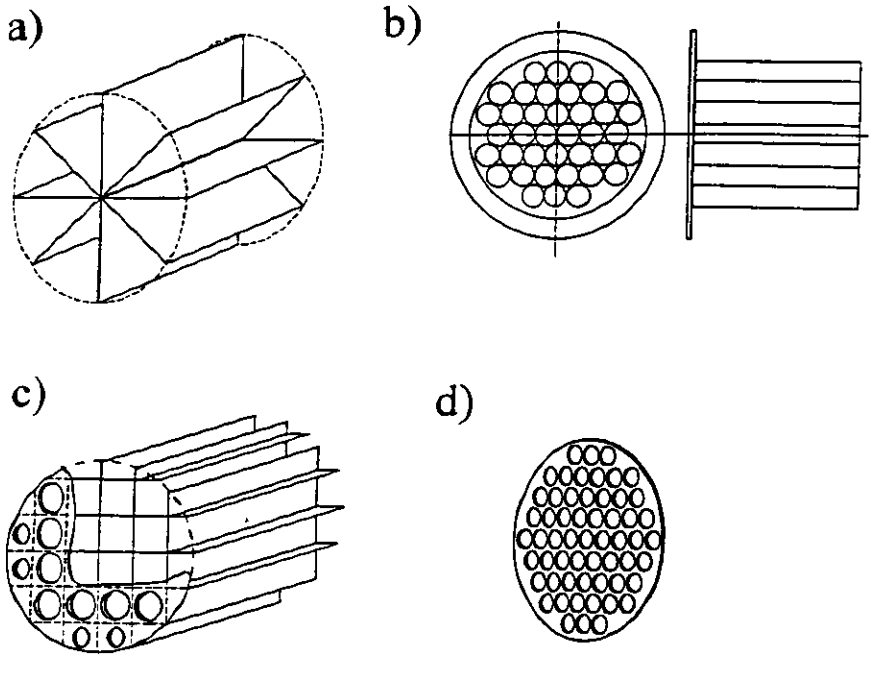

Fig. 9: Types of flow conditioners investigated
a) Etoile flow straightener
b) Tube-bundle flow straightener
c) Zanker flow conditioner
d) Single perforated plate

The following few examples are selected to discuss the most important results of the investigations. The experience gained in the experiments shows that the damping elements studied can be divided into two groups:

Flow straighteners

These devices are effective against the tangential velocity components in the flow and suppress the swirl in particular. The axial velocity components are nearly not affected "positively", in the majority of the investigations asymmetries and elevations of the profile are even intensified. Typical representatives of this group are the Etoile and the tube-bundle straighteners. Figure 10 shows the pipe configuration and the flow profiles of an Etoile straightener installed downstream of a double bend out of plane. The tangential velocity components are well removed, but the local minimum of the axial components is more strongly developed at the outlet of the straightener than at its inlet. The remaining error shift of the turbine meter installed downstream of this configuration still amounts + 0,28 % compared with meter's indication for the undisturbed flow. A very similar sitiuation can be observed when the Etoile is replaced by a tube-bundle straightener (see Figure 11).

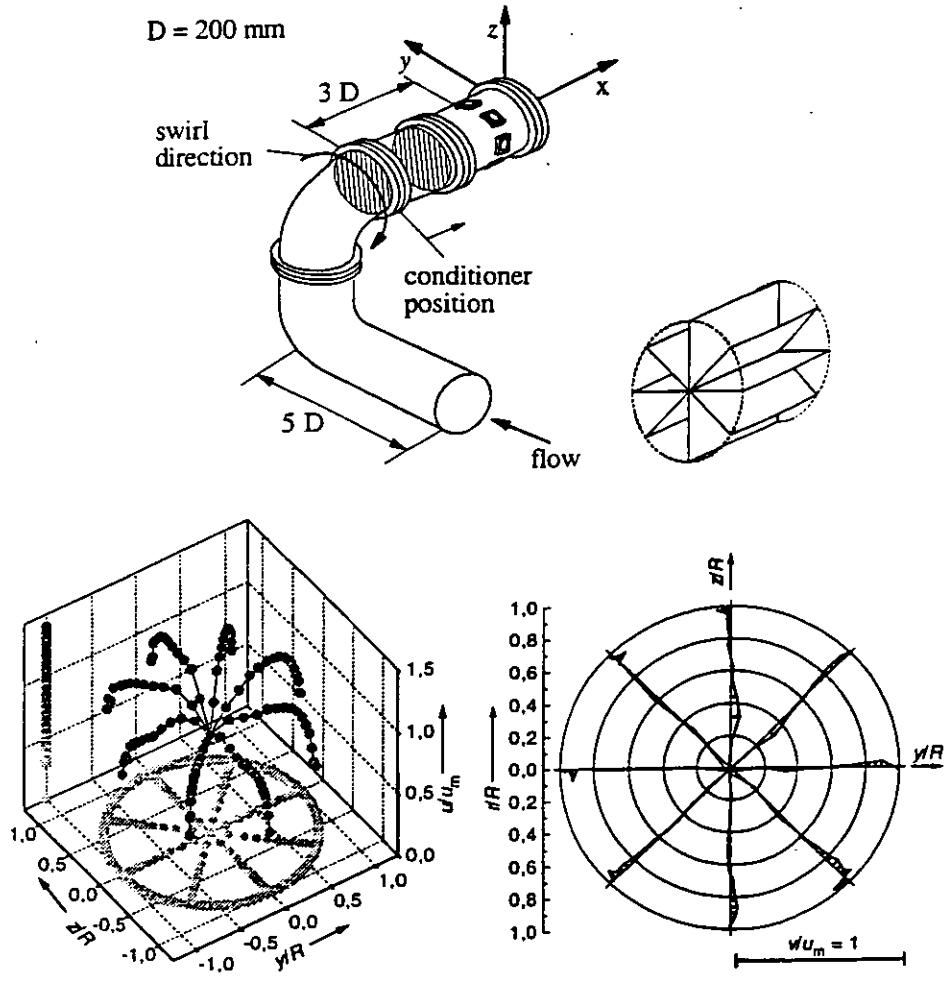

Fig. 10: Schematic view of the pipe configuration investigated and perspective plot of the axial components u (left picture) and the tangential components v (right picture) of the velocity distributions downstream of a double bend out of plane with unchanged diameter and an Etoile straightener directly behind the perturbation

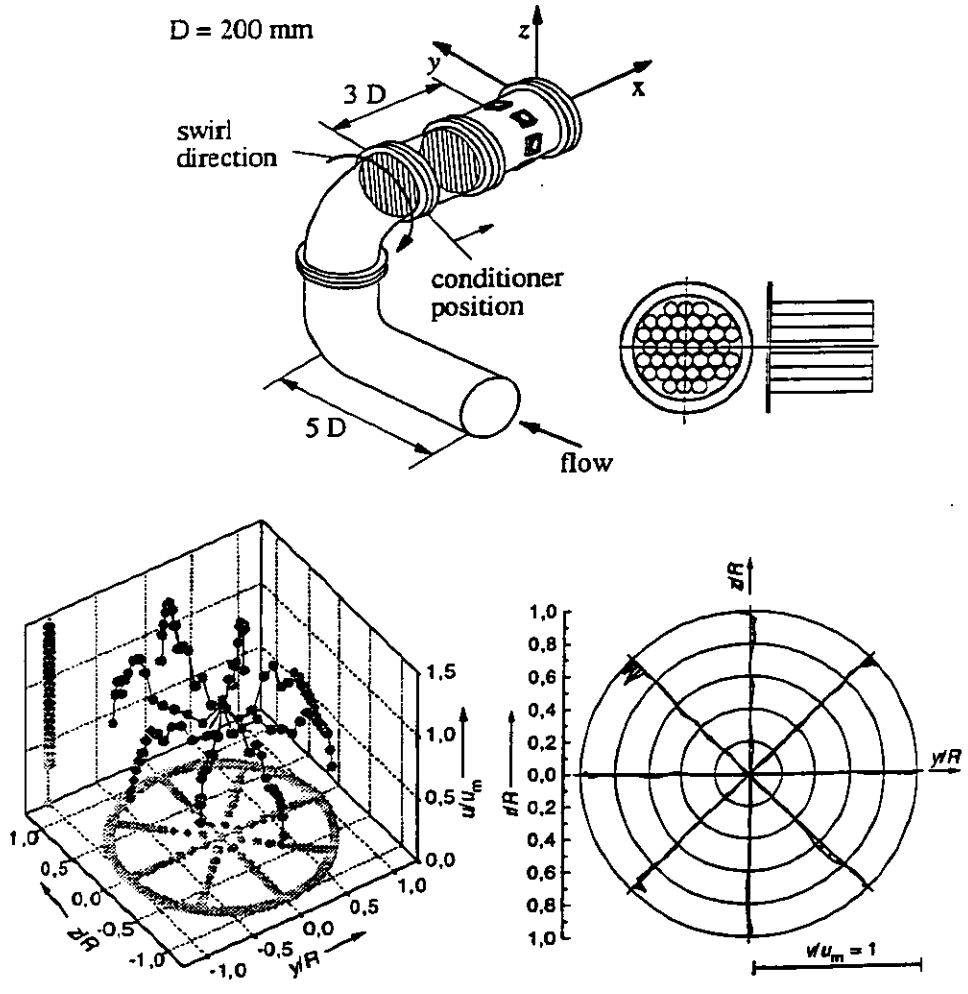

Fig. 11: Schematic view of the pipe configuration investigated and perspective plot of the axial components u (left picture) and the tangential components v (right picture) of the velocity distributions downstream of a double bend out of plane with unchanged diameter and a tube-bundle straightener directly behind the perturbation

Flow conditioners

Damping elements of the second type influence both the tangential and the axial velocity components of a disturbed flow. Zanker conditioners and perforated plates belong to this group. Figure 12 shows the axial and tangential velocity components of the flow downstream of a double bend out of plane and a Zanker conditioner. The velocity distribution obtained is very similar to that of an undisturbed flow. The remaining error shift of the turbine meter downstream of this configuration amounts to + 0,03 %, i.e. it lies clearly within the uncertainty of the flowrate standard (critical nozzles) used to investigate the meter behaviour.

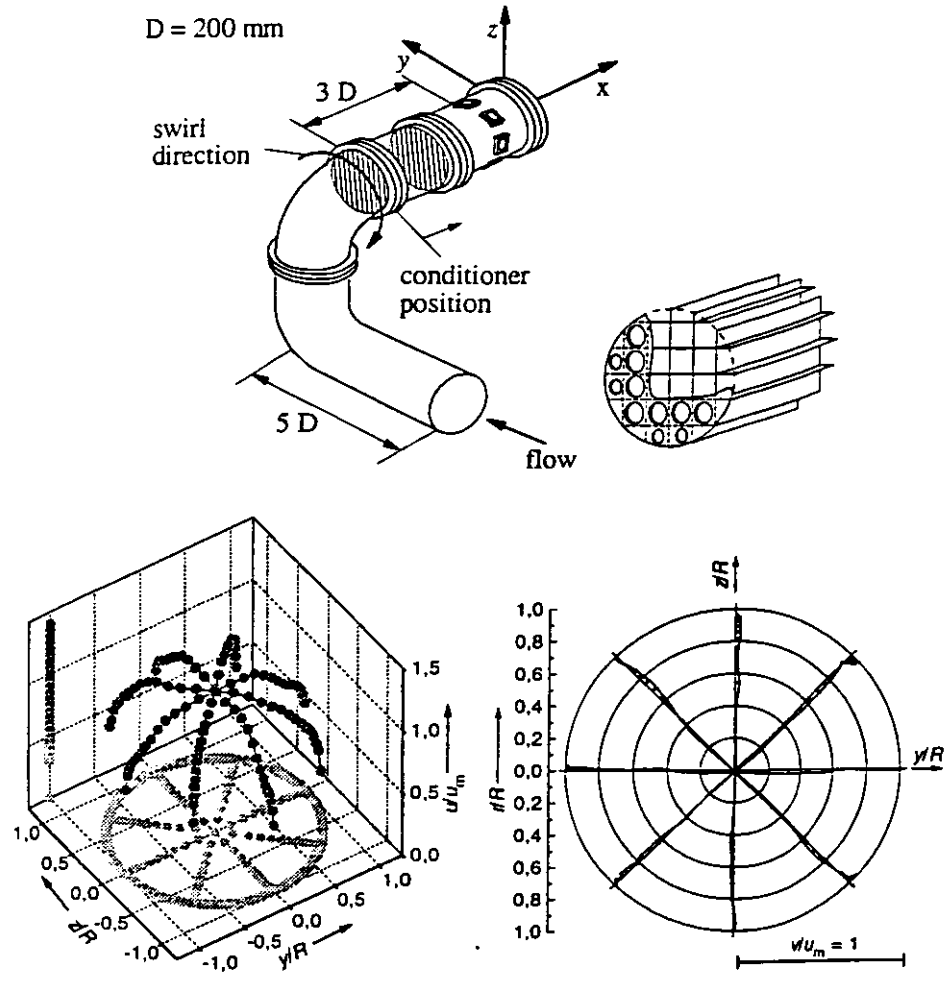

Fig. 12: Schematic view of the pipe configuration investigated and perspective plot of the axial components u (left picture) and the tangential components v (right picture) of the velocity distributions downstream of a double bend out of plane with unchanged diameter and a Zanker conditioner directly behind the perturbation

However, not only the type of the flow straightener/conditioner is of importance for reducing or removing flow disturbances downstream of unfavourable pipe geometries. The distance between the perturbation and the conditioner can also have a decisive influence on the result. This is why a lot of experiments were carried out to find the optimum geometrical arrangement of the various pipe and conditioner elements.

Figure 13 shows one example of such an investigation: A conventional perforated plate was installed directly downstream of a high level perturbation (Figure 13a) and 2 *D* behind the double bend's outlet (Figure 13b). The flow distributions were measured at a distance of 5 *D* downstream of the perturbation. The differences of both axial velocity distributions differ significantly. The 2 *D* distance between the plate and the perturbation shows a remarkable effect on the normalization of the axial velocity distribution, and this is confirmed by the error shifts of the turbine meter installed directly downstream of the configurations described: + 0,46 % for the configuration of Figure 13a) and + 0,12 % for the configuration of Figure 13b).

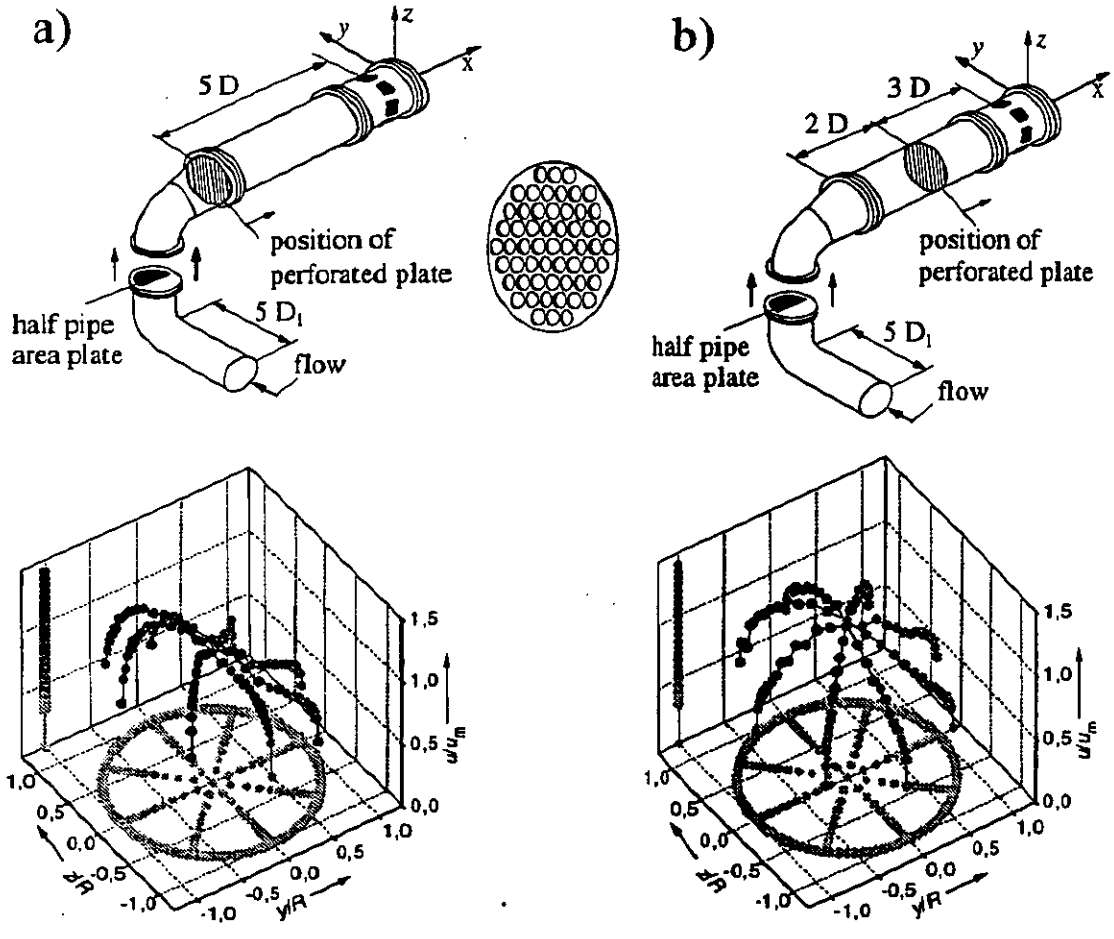

Fig. 13: Schematic view of the pipe configurations investigated and perspective plots of the respective axial components u of the velocity distributions downstream of a high level perturbation and a perforated plate
a) installed directly at the outlet of the double bend
b) installed at a position of 2 D behind the perturbation

More than 50 different conditioner configurations altogether were investigated and used to enlarge the existing flow profile catalogue. The results of these measurements allow well-aimed recommendations to be given for the use of optimum flow straightener/ conditioner configurations (if necessary, in combination with straight pipes of corresponding lengths), when the flow pattern downstream of a given pipe geometry is known.

5 CHARACTERIZATION OF DISTURBED FLOW PROFILES BY SPECIAL FLOW FIELD PARAMETERS

An analysis of the disturbed flow profiles investigated shows that there are three typical kinds of deviations of the profiles from the undisturbed case:

- *Swirl*

  This phenomenon can be described very easily looking at the tangential components of the velocity distributions (see, for example, Figures 6 and 7). Swirls are typical for all configurations with double bends out of plane. They can have a left-hand or a right-hand orientation in dependence on the position of the bends each to the other. Normally symmetrical configurations generate swirls of the same intensity, but with different directions of rotation. An example is shown in Figure 14.

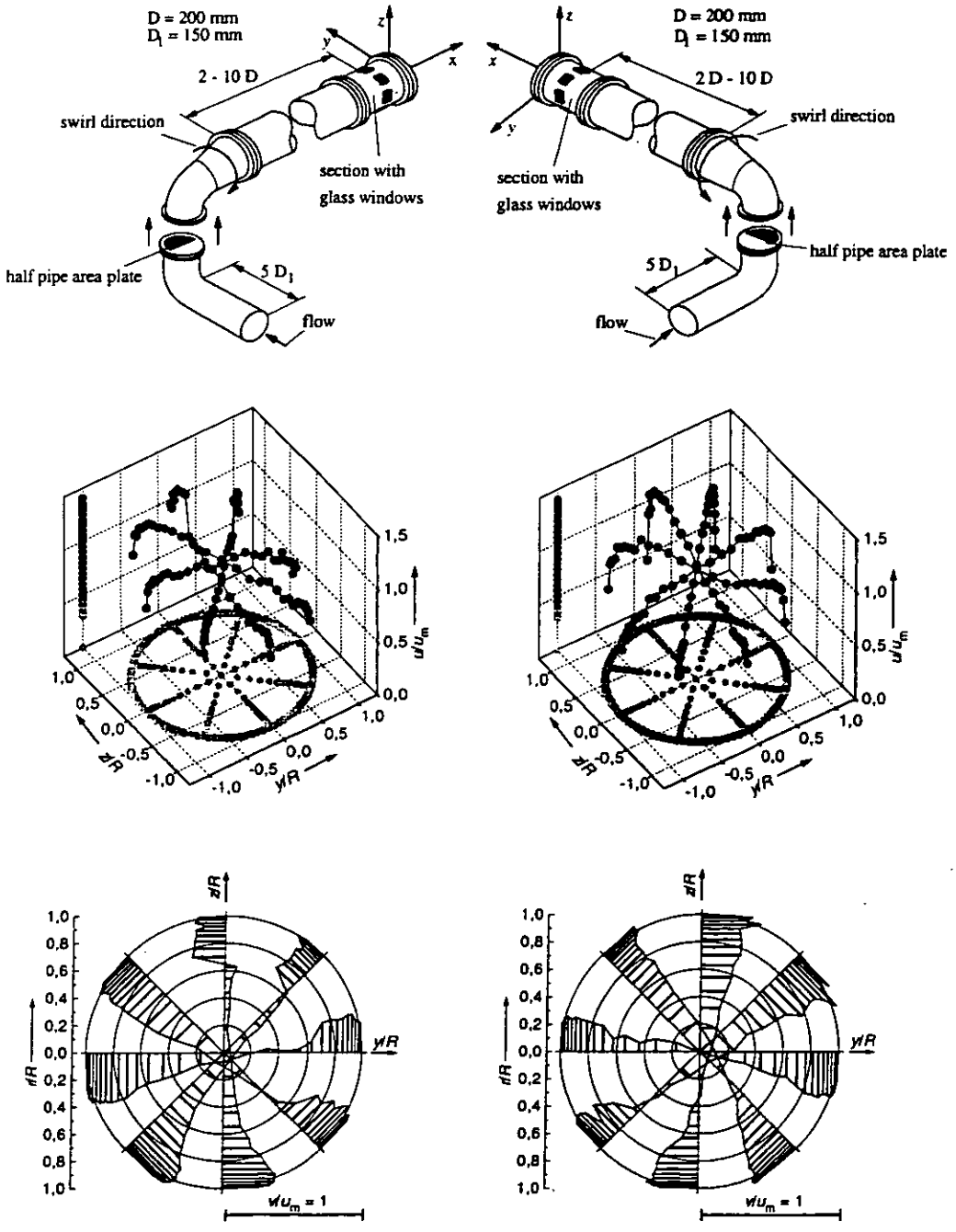

Fig. 14: Schematic view of the pipe configurations investigated and perspective plots of the respective axial components u and tangential components v of the velocity distributions downstream of a high level perturbation with right-hand and left-hand swirl and a straight pipe of 2 D in length

- *Asymmetry*

  If the distribution of the axial velocity component is not axisymmetric we speak about an asymmetry of the flow. Asymmetries can be observed downstream of any non-axisymmetric pipe configurations. Vivid examples for this kind of profil deformation are the axial velocity distributions in Figures 6a and 7a for the double bend configurations.

- *Flatness*

  Flatness is another kind of deformation of the axial velocity profil in a pipe flow. It characterizes (axisymmetric) deviations from the ideal shape of the axial flow profil. Respective examples are shown in Figure 5a (the single bend configuration) and Figure 10 (double bend configuration with Etoile flow straightener) where the velocity profiles have their maximum not at the centre of the pipe but an elevation towards the pipe wall.

To find out suitable parameters describing disturbed flow profiles, these three kinds of flow characteristics should be analyzed in relation to their effect on the flowmeter type to be investigated. According to the aims of the PTB project this analysis was started with turbine gas meters. Because turbine meters operate as integrators, the flow profile in front of the meter should be described by integrating flow field parameters.

Figure 15 shows the relations between the blades of a turbine wheel and the axial velocity of the gas flow.

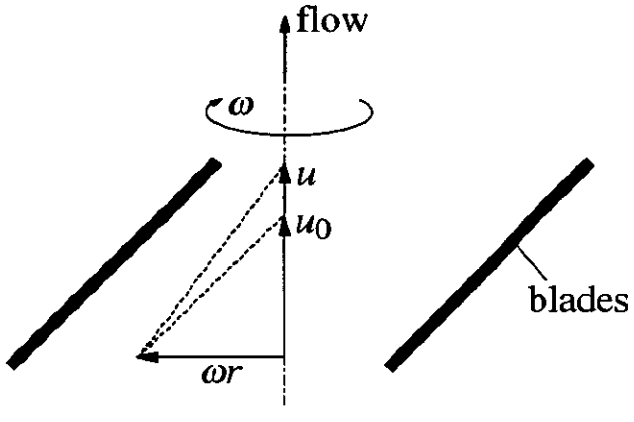

Fig. 15: Relations between the turbine wheel and the axial flow velocity u

In a coordinate system rotating with the blades, a certain axial velocity u_0 exists at which the flow is parallel to the blades. If the axial velocity is different, the flow will not be parallel to the blades and a force in the tangential direction will result, which is the first radial moment of the momentum flux. In the case of constant flowrate, at a specific rotating speed, the accelerating and decelerating forces at the turbine wheel are in balance. If the profile is changed (but not the flowrate), the force at the turbine wheel will also be changed and the wheel has to attain a different rotating speed before it comes to a new balance. Although the flowrate remains constant the rotating speed of the turbine wheel changes producing a change of the meter reading, e.g. an error shift. This interaction between flow

and turbine wheel leads to the assumption that the integral of the first radial moment of axial momentum fluxes is an effective flow field parameter for comparing the error shift of a turbine meter with the profile disturbances upstream of the meter. The definition of the axial momentum number is:

$$K_u = \frac{\iint_A \rho \cdot u^2 \cdot r \cdot dA}{\pi \cdot \rho \cdot u_m^2 \cdot R^3} \tag{4}$$

where u is the axial velocity, u_m is the bulk velocity, r is the radius coordinate, ρ is the gas density, A is the pipe cross-sectional area and R is the pipe radius.

A fully developed pipe flow has a certain momentum number K_{u0}. As only the difference between a disturbed flow and the undisturbed case is of interest, in the following the difference $\Delta K_u = K_u - K_{u0}$ will be used.

The same idea is also used to define the flow field parameter for the tangential velocity v. As shown in Figure 16, the gas flow with the axial velocity u is parallel to the wheel blades.

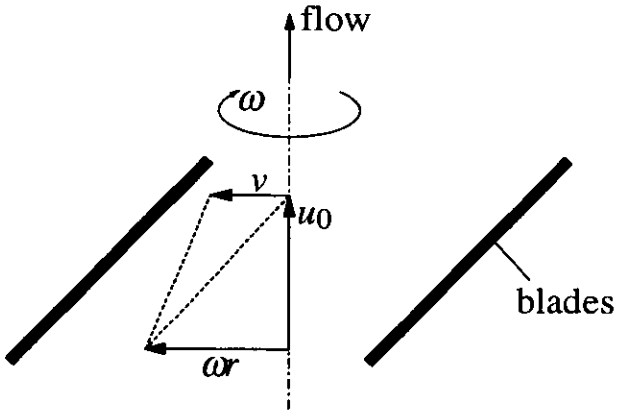

Fig. 16: Relations between the turbine wheel and the tangential flow velocity

If the flow contains an additional tangential component v, a force at the turbine wheel will again occur. The integrated first radial moment of tangential momentum fluxes, which is equal to the swirl number used by Kitoh [23] and Steenbergen [24] is therefore chosen to evaluate the force due to the tangential component. Following the considerations about K_u, the definition of the swirl number is:

$$K_v = \frac{\iint_A \rho \cdot u \cdot v \cdot r \cdot dA}{\pi \cdot \rho \cdot u_m^2 \cdot R^3} \tag{5}$$

The sign of the swirl number is related to the rotating direction of the swirl. Right-hand swirls have positive, left-hand swirls negative numbers.

Asymmetry is the third significant characteristic of the flow profiles. The distance of the centroid of the mass flow from the pipe axis is used to describe this asymmetry (Figure 17).

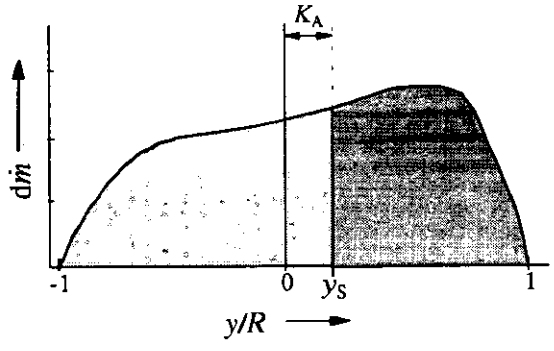

Fig. 17: Flow field parameter K_A for describing the asymmetry of the axial profile. K_A is the distance of the centroid (y_S) of the mass flow element $d\dot{m}$ from the pipe axis.

The respective flow field parameter - the non-dimensional asymmetry number K_A - is defined as follows:

$$K_A = \frac{\sqrt{\left(y_S^2 + z_S^2\right)}}{R}$$

$$y_S = \frac{\iint_A y \cdot d\dot{m}}{\dot{m}} \quad \text{and} \quad z_S = \frac{\iint_A z \cdot d\dot{m}}{\dot{m}} \tag{6}$$

where y, z are the coordinates of the pipe cross-section, y_S, z_S are the coordinates of the centroid, A is the area of the pipe cross-section, $d\dot{m}$ is the mass flow through a differential cross-sectional area and $\dot{m}$ is the mass flow.

6 AN EMPIRICAL MODEL TO EXPLAIN THE ERROR SHIFT OF TURBINE METERS

After defining the flow field parameters and quantifying the disturbances of the flow profiles it is now possible to compare these disturbances with the shift of the calibration curves (error shift) of gas meters applied downstream of the pertubation. In the PTB project four turbine meters were used for this investigation. Two of them were of the same geometry, so three geometries were tested. Table 2 gives a survey of the main characteristics of these turbine meters.

If disturbed profiles propel a turbine meter, the resulting error shift depends on the geometry of the meter inlet. An extensive study of this dependence was performed by Dijstel-

bergen et al. [25]. This study shows that the same perturbation can lead to opposite results only due to a change in the meter geometry.

Table 2: Geometrical characteristics of the turbine meters tested

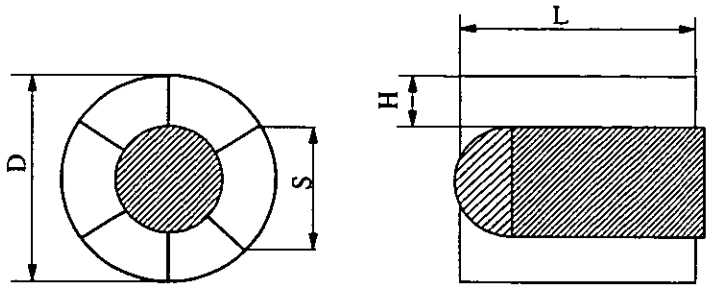

Turbine meter TM i	Number of vanes	D (mm)	S (mm)	H (mm)	L (mm)	Rotation of the turbine wheel
TM 1	6	200	104	45	90	right-turn
TM 2a and 2b	17	200	37	45	80-95	right-turn
TM 3	12	200	52	25	110	right-turn

The velocity profiles measured in front of the turbine meter have of course changed due to the inlet construction before the gas flow interacts with the turbine wheel. It is assumed that this change does not depend on the flowrate and can be described for every turbine meter by constant model parameters. This assumption and the sensitive comparison of the profile catalogue with the measured error shifts ΔE led to the simple model:

$$\Delta E_{\text{model}} = a_1 K_v (1 + a_2 K_A) + a_3 \Delta K_u \tag{7}$$

The model parameters a_1 to a_3 are characteristic for every turbine meter, and they have to be determined by regression from the flow field parameters and error shifts. The results for the four meters tested are given in Table 3.

Table 3: Values of the model parameters a_1 to a_3 in eq. (7) for the turbine meters tested

Turbine meter	a_1	a_2	a_3
TM 1	4,8	7,9	6,6
TM 2a and 2b	2,2	-7,2	3,0
TM 3	-0,18	130	5

The model can be validated by plotting the predicted error shifts ΔE_{model} versus the measured ΔE_{meas}. If the model matches well with reality, all points should lie close to the diagonal axis $y=x$ as can be seen in Figures 18 to 20.

The error shifts shown in these following figures were measured

- at different flowrates (25% q_{max} up to q_{max} of the turbine meters)
- downstream of different pipe configurations (straight pipes with free inlet, single bends, double bends out of plane)
- at different distances between perturbation and turbine meter.

In most cases shown, the difference between the measured and the predicted error shifts is smaller than 0,15%. It has to be emphasised that only part of the measured error shifts were used to determine the model parameters a_1 to a_3 for turbine meters TM1 and TM 2a. In addition to this, the model parameters for the meter TM 2b were derived directly from those of meter TM 2a which is of identical geometry (Fig. 19).

The model also allowed the error shift to be sufficiently predicted when meter TM 2b was used at 0 D downstream of a double bend out of plane although the profiles for this configuration were not measured. The values of the flow field parameters for a position directly behind the double bend (0-D-distance) were extrapolated from the values at the distances 2 D, 5 D and 10 D between the perturbation and the measuring position.

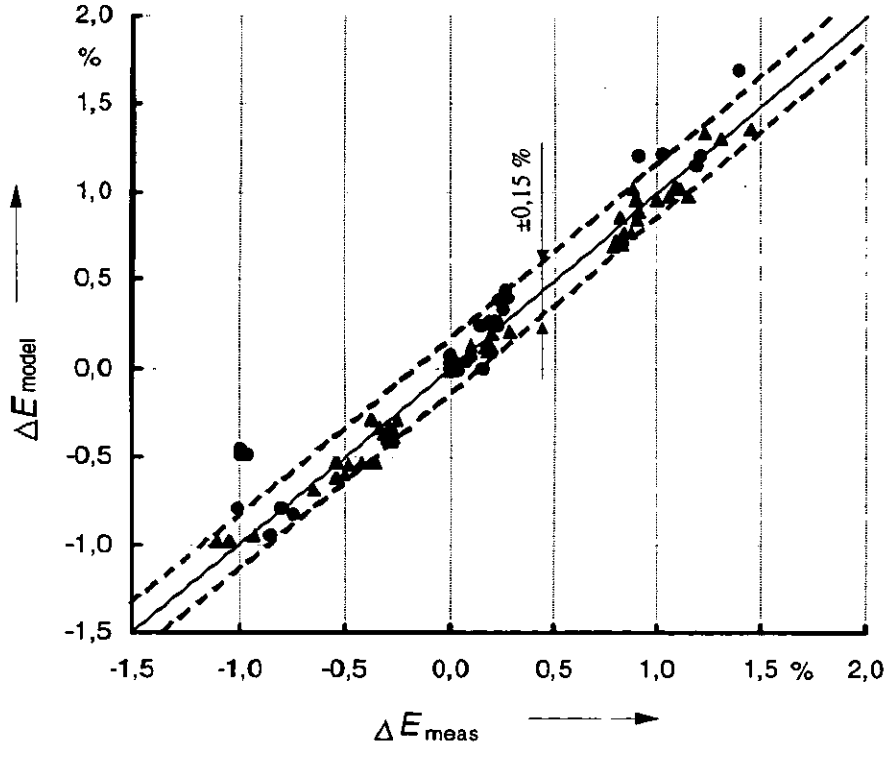

Fig. 18: Comparison of measured error shift ΔE_{meas} and predicted ΔE_{model} of turbine meter TM 1 according to eq. (7) and Table 3
▲ *measured results used for regression to determine the model parameters a_1 to a_3 in eq. (7)*
● *measured results not used for regression*

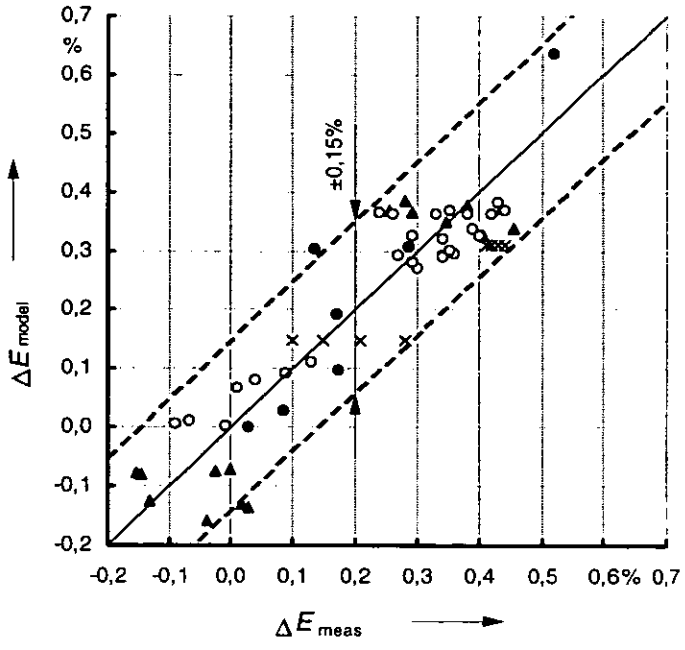

Fig. 19: Comparison between measured error shift ΔE_{meas} and predicted ΔE_{model} of turbine meters TM 2a and 2b according to eq. (7) and Table 3

- ▲ *results measured for TM 2a and used for regression to determine the model parameter a_1 to a_3 in eq. (7)*
- ● *results measured for TM 2a and not used for regression*
- o *results measured for TM 2b; the model parameters were taken directly from the meter TM 2a*
- × *results measured for TM 2b 0 D downstream of a double bend out of plane; the flow field parameters were extrapolated from the values at 2 D, 5 D, 10 D*

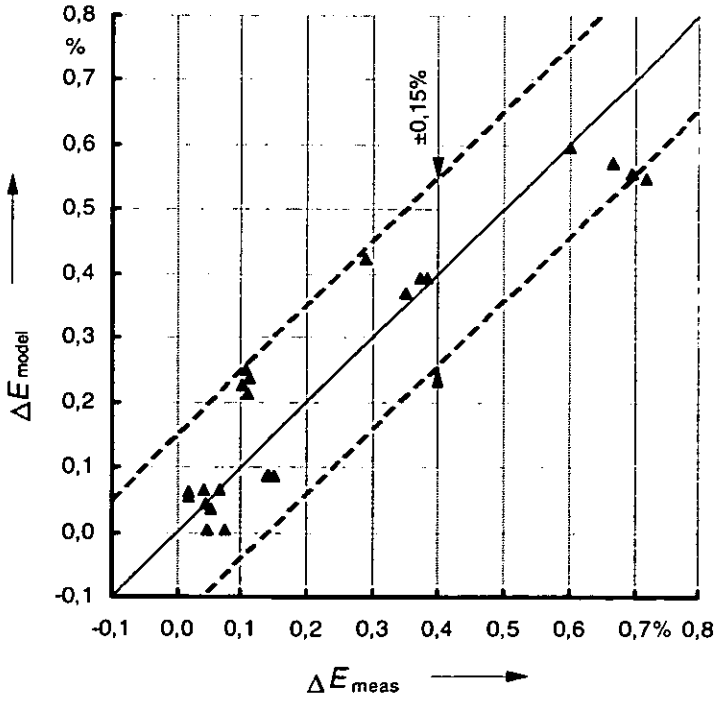

Fig. 20: Comparison between measured error shift ΔE_{meas} and predicted ΔE_{model} of turbine meter TM 3; according to eq. (7) and Table 3

When the uncertainty of 0,15% of the model is considered, the following points have to be kept in mind:

- The calibration curves of the turbine meters could be measured with an uncertainty of 0,08%; this is half the model uncertainty.
- The pipe configurations were used as recommended in the OIML R-32 [22]. That means that there is a $5D$ straight pipe with free inlet upstream of the bends. The flow profile $5\,D$ downstream of a free inlet depends on the conditions of the room, e.g. the distances from the pipe inlet to the ground or wall. Hence, the development downstream of the bends too, is not absolutely independent of the conditions of the test room and may differ in the different experimental setups.
- The accuracy of the numerical evaluation of the profiles is bounded by the limited number of measuring points.
- Sometimes there was a delay of several days between the measurements of the basic calibration curve and those of the calibration curve downstream of a special pipe configuration. A slight drift of the calibration curves between the measurements during this time cannot be excluded.

So it may be stated that the model is of sufficient quality to predict meter readings. It can explain the very different reaction of turbine meters to the same disturbed velocity profile and seperates the influence of flatness, swirl and asymmetry on the error shift. In addition, the model provides a new basis for evaluating the efficiency of flow conditioners. Both, the estimation of the error shift and the evaluation of flow conditioners, are of great interest and importance for practical use in industrial flow measurement as well as in flowmeter development and research.

7 REFERENCES

1 **Irving, S.J.:** The effects of bends on the discharge coefficient of orifice plates. In: Proceedings of the IMEKO-Conference on Flow Measurement of Fluids, FLOMEKO'78, Groningen, The Netherlands, Sept. 1978, 247-252

2 **Morrow, T.B.; Park, J.T.; McKee, R.J.:** Determination of installation effects for a 100 mm orifice meter using a sliding vane technique. J. Flow Meas. Instrum. **2** (1991), 14-20

3 **Morrison, G.L.; DeOtte, R.E. Jr.; Beam, E.J.:** Installation effects upon orifice flowmeters. J. Flow Meas. Instrum. **3** (1992), 89-94

4 **Mattingly, G.E.; Yeh, T.T.:** Elbow effects on pipe flow and selected flow meters. In: Proceedings of the 6th International Conference on Flow Measurement, FLOMEKO'93, Seoul, Korea, Oct. 1993, 61-79

5 **van der Kam, P.M.A.; van Dellen, K.:** The effect of double bends out of plane on turbine meters. J. Flow Meas. Instrum. **2** (1991), 61-68

6 **Halttunen, J.:** Installation effects on ultrasonic and electromagnetic flowmeters: a model-based approach. J. Flow Meas. Instrum. **1** (1990), 287-292

7 **Takamoto, M.; Utsumi, H.; Watanabe, N.; Terao, Y.:** Installation effects on vortex shedding flowmeters. J. Flow Meas. Instrum. **4** (1993), 277-285

8 **Brennan, J.A.; McFaddin, S.E.; Sindt, C.F.; Kothari, K.M.:** The influence of swirling flow on orifice and turbine flowmeter performance. J. Flow Meas. Instrum. **1** (1990), 5-8

9 **Heritage, J.E.:** The performance of transit time ultrasonic flowmeters under good and disturbed flow conditions. J. Flow Meas. Instrum. **1** (1990), 24-30

10 **Spearman, E.P.; Sattary, J.A.; Reader-Harris, M.J.:** Comparison of velocity profiles downstream of perforated plate flow conditioners. In: Proceedings of the 7th International Conference on Flow Measurement FLOMEKO'94, Glasgow, Scotland, June 1994

11 **Laws, E.M.; Ouazzane, A.K.:** A further study into the effect of length on the Zanker flow conditioner. J. Flow Meas. Instrum. **6** (1995), 217-224

12 **Laws, E.M.; Ouazzane, A.K.:** A preliminary study into the effect of length on the performance of the Etoile flow straightener. J. Flow Meas. Instrum. **6** (1995), 225-233

13 **Laws, E.M.; Ouazzane, A.K.:** A further study investigation into flow conditioner design yielding compact installations for orifice plate flow metering. J. Flow Meas. Instrum. **6** (1995), 187-199

14 **Stuart, J.W.; Park, J.T.; Morrow, T.B.:** Experimental results of an improved tube-bundle flow conditioner for orifice metering. In: Proceedings of the 7th International Conference on Flow Measurement FLOMEKO'94, Glasgow, Scotland, June 1994

15 **Harbrink, B.; Zirnig, W.; Hassenpflug, H.-U.; Kerber, W.; Zimmermann, H.:** The disturbance of flow through an orifice plate meter run by upstream header. In: VDI-Berichte 768, VDI-Verlag: Proceedings of the 5th International IMEKO-Conference on Flow Measurement FLOMEKO, Düsseldorf, Germany, Oct. 1989, 75-90

16 **Park, J.T.; Morrow, T.B.; Yeh, T.T.; Mattingly, G.E.:** Effect of velocity profile from tee and bundle flow conditioner on orifice meters. In: Proceedings of the International Gas Research Conference, Orlando, Florida, Vol. III, Nov. 1992, 223-234

17 **Wendt, G.; Kramer, R.; Dopheide, D.:** Einsatz eines miniaturisierten Laser-Doppler-Anemometers auf Halbleiterbasis für die Geschwindigkeitsprofilmessung in Gasleitungen. PTB-Mitt. **102**, 1992, 445-453

18 **Kramer, R.; Mickan, B.; Wendt, G.; Müller, H.; Dopheide, D.:** Automatisierte Messung von Strömungsprofilen im Einlauf von Gaszählern mit einem 2-Komponenten Halbleiter-LDA-System. In: Lasermethoden in der Strömungsmeßtechnik, 4. Fachtagung GALA e.V.; Verlag Shaker Aachen 1995, 31.1-31.6

19 **Schlüter, T.:** PIV-Messungen der Geschwindigkeitsverteilungen hinter verschiedenen Strömungsgleichrichtern (Dissertation). Shaker Verlag GmbH, Aachen 1996

20 **Sattary, J.A.; Reader-Harris, M.J.; Johnstone, L.A.:** Computation of flow through bends. In: Proceedings of the 14th North Sea Flow Measurement Workshop, Peebles, Scotland, 28-31 October 1996

21 **Hilgenstock, A.; Ernst, R.:** Analysis of installation effects by means of Computational Fluid Dynamics - CFD versus experiments? J. Flow Meas. Instrum. **7** (1996), 161-171

22 International Recommendation: Rotary piston gas meters and turbine gas meters. (OIML R-32); Edition 1989 (E)

23 **Kitoh, O.:** Experimental study of turbulent swirling flow in a straight pipe. In: Journal Fluid Mechanics **225** (1991), 445-479

24 **Morrow, T.B.; Park, J.T.; McKee, R.J.:** Determination of installation effects for a 100 mm orifice meter using a sliding vane technique. In: Flow Meas. Instr. **2** (1991)

25 **Dijstelbergen, H.H.; Bergervoet, J.T.M.:** Optimal straightening vanes for turbine meters. In: Proceeding of the 3rd International Symposium on Fluid Flow Measurement 1995, March 19-22, 1995; San Antonio, Texas

NSFMW.97

North Sea FLOW Measurement Workshop

Paper 25: 4·5

QUALITY ASSESSMENT OF GAS METERING STATIONS BY MEANS OF A PORTABLE AND RETRACHTABLE INSPECTION PROBE

Authors:
S. Larsen, J. Bosio and A.S. Sivertsen, Statoil/K-Lab, Norway

Organiser:
Norwegian Society of Chartered Engineers
Norwegian Society for Oil and Gas Measurement
Co-organiser:
National Engineering Laboratory, UK

15th North Sea Flow Measurement Workshop
Kristiansand, 28-30 October 1997

Quality assessment of gas metering stations by means of a portable and retractable inspection probe

by

Stein Larsen, Jan Bosio and Anne Synnøve Sivertsen

Statoil/K-Lab(*)

xxxxxxxxxxxx

ABSTRACT

The compliance of gas metering stations to design specifications has in general been limited to the comparison of as-built with the recommendations provided by accepted international standards, national regulations or recognised databases. A major objective of the design specifications is to ensure that the flow profile is fully developed at the location of the flow element (FE). Verification of the quality of a metering station can be conducted using provers or master meters for on site calibrations. A cheaper and more efficient method could be to perform measurement of the flow conditions in the metering stations by using an retractable inspection probe which could depict the flow inside the meter tube such as velocity profile and swirl angle.

K-Lab has over years contemplated such technology and has used and tested retractable inspection probes of different types. All of them use general Pitot measurement principles. The latest version of K-Lab's retractable inspection probe has been tested in different baseline configurations and Reynolds number at K-Lab. Reference configurations have been tubes with very long straight upstream lengths, immediately downstream of 90 degree bends in the same plane or in different planes. The test results show that the velocity profiles departing from fully developed flow and the presence of swirls are easily detectable.

The retractable inspection probe, described in this paper, has been built to be mounted in the meter tube through a conventional threaded pressure tapping through a 1" ball valve without depressurising the line. It can be mounted in pipes of different diameters and operated at pressures up to 150 bar, and is therefore a very flexible tool.

The paper presents the results obtained during tests at K-Lab and in a gas metering station at the Kårstø gas treatment plant.

Statoil / K-Lab, P.O.B. 308, N 5501 Haugesund, Norway
Tel.:(47) 52 77 21 85 Fax :(47) 52 77 22 10 E-mail:stla@statoil.no

Background

Quality assurance has become a key consideration in gas metering systems. Achieving continuous quality improvement in these systems calls for a comprehensive process of the kind depicted in figure 1. At any step in this process, the experience from the previous step is fed in with the aim of making an optimal choice. But those directly involved in or responsible for one of the phases must not forget that the activity they are pursuing is merely one link in a chain (ref.1).

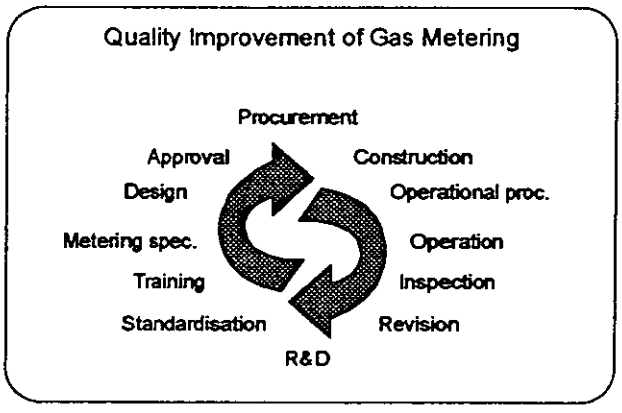

Figure 1

In the above process (fi.1) one of the key issues is *inspection*. Depending on the type of flowmeter which is used, different methods and procedures are recommended by the manufacturers or by the operational staff based upon their experience. This type of inspection generally addresses the instrument itself and its local environment, such as the secondary instrumentation, the pipe wall characteristics and the fluid properties. Except for laboratory applications, no practical devices have been developed to look inside the pipe and "watch" how the flowing fluid behave.

The test results and preliminary experience obtained by Statoil with its K-Lab probe are reported in the present paper.

Requirements of an inspection probe

Previous studies (ref.2) have shown that the departure from fully developed velocity profiles generates substantial errors in the discharge coefficient for orifice meters, as shown in figure 2.

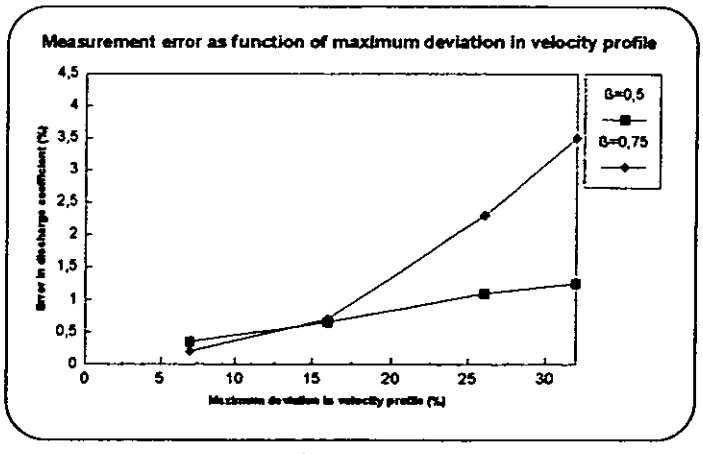

Figure 2

Statoil / K-Lab, P.O.B. 308, N 5501 Haugesund, Norway
Tel.:(47) 52 77 21 85 Fax :(47) 52 77 22 10 E-mail:stla@statoil.no

The inspection probe was therefore designed to meet the following requirements:

- portable
- sustain pressure up to 150 bar
- measure velocity profiles and swirl angles
- user friendly
- safe

Design of the inspection probe

The probe is a Cylinder Pitot (CP) originally designed and tested at Institute for Energy Technology and K-Lab from 1987 (ref.3). A new design based on the same principle, making the probe portable, was developed by Read Matre Instruments for K-Lab in 1996. The probe is shown in figure 3.

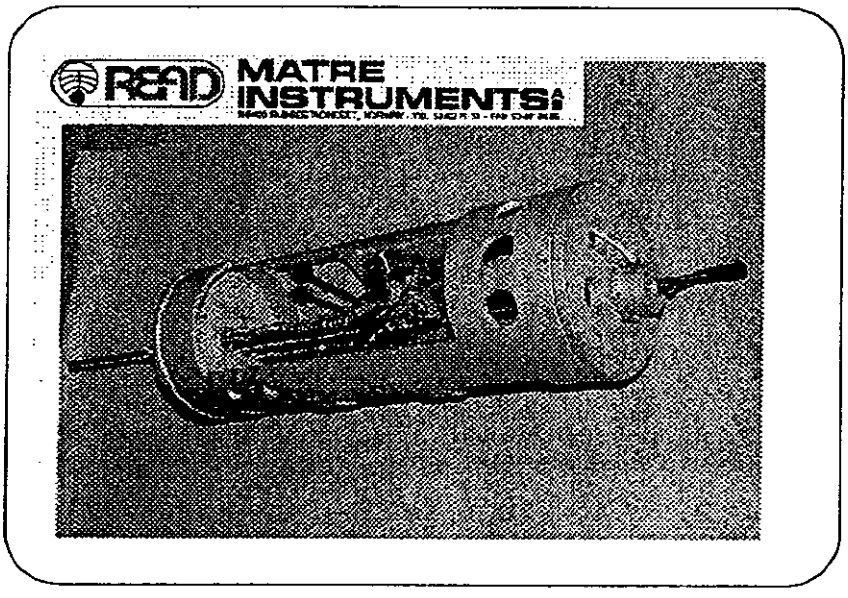

Figure 3

The CP probe is an aerodynamic sensor which is described in the literature to some extent (ref. 4 and 5). Its applications in fluid flow measurement in general, are only briefly described (ref.6). Recently such probes have been used in field tests (ref.7). The design used in the K-Lab probe applies specifications from reference 4.

The CP can be rotated and translated radially. The readings of the rotation angle and the radial position (on two separate rules), give the (ϕ, r) position of the CP inside the pipe.

To sustain the operating conditions which could be encountered in the field, the probe stem had an outer diameter of 12 mm to support flow induced vibrations. In practice, this means that the recommendations in ISO Standard 3977 was exceeded and a correction factor as recommended by the standard was applied (ref.8) for the flow calculations, taking into account the blockage of flow around the stem which influences the measurement of the static pressure.

Statoil / K-Lab, P.O.B. 308, N 5501 Haugesund, Norway
Tel.:(47) 52 77 21 85 Fax :(47) 52 77 22 10 E-mail:stla@statoil.no

How to use the probe

The K-Lab probe is built to be mounted in the meter tube through a conventional threaded pressure tapping and a 1" ball valve without depressurising the line. The tapping point has an inner diameter of approximately 12 mm. The probe is designed to be electrically connected to a computer which gives the (ϕ, r) position of the CP inside the pipe and the differential pressure between probe tip and the pipeline wall and also the differential pressure to calculate swirl angle.

The local mean velocity (U,r) is calculated from the differential pressure measured by the CP. The swirl angle is measured by rotating the probe until zero differential pressure is observed on the same differential pressure transmitters. The reading of the angle on the rule gives the degree of swirl.

K-Lab tests

The tests of the probe at K-Lab were carried out in the 6" test line, with more than 60D straight upstream pipe length and a K-Lab flow conditioner mounted at the upstream inlet of the straight pipe. The probe was installed vertically in the pipe.
The test conditions were as follow:

- *Pressure: 32bar - Average flowrate: 616 and 880 act.m³/h. - Re: respectively 3.48x10⁶ and 5.17x10⁶ - Results in figure 4 & 5*
- *Pressure: 72 bar - Average flowrate: 350 and 616 act.m³/h. - Re: respectively 4.5x10⁶ and 7.8x10⁶ - Results in figures 6 & 7*

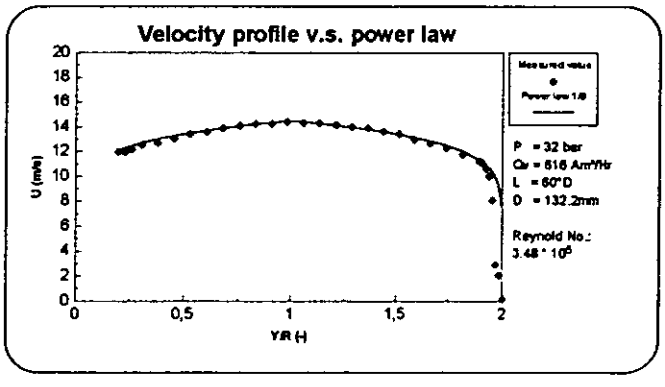

Figure 4

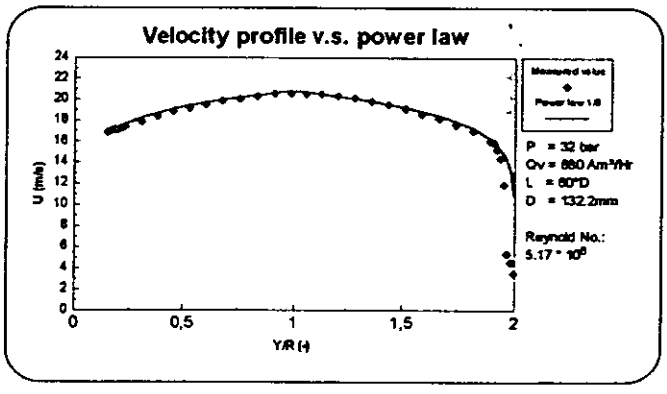

Figure 5

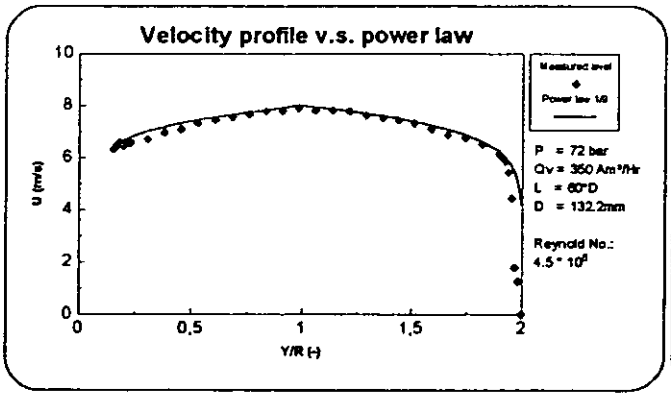

Figure 6

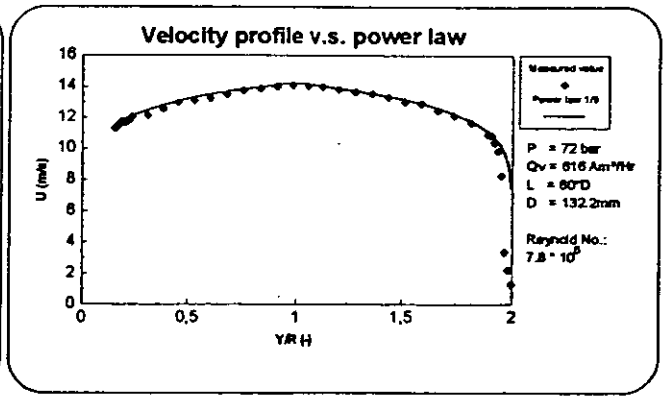

Figure 7

Statoil / K-Lab, P.O.B. 308, N 5501 Haugesund, Norway
Tel.:(47) 52 77 21 85 Fax :(47) 52 77 22 10 E-mail:stla@statoil.no

The results show that measured velocity profiles fit the 9th power law curve very closely, confirming fully developed flow (the 9th power law function has been chosen as reference (ref.2) as it produces representative velocity profiles for the Reynolds number range which is considered).

It was observed that the velocity measurements close to the walls were perturbed by the shape of the probe and by the tapping point used for insertion of the probe.

At the wall, opposite to the tapping point, the velocity measurements are stopped 10-15 mm from the wall due to flow induced perturbations occurring between the probe tip and the wall. On the other wall, at the tapping point, similar flow induced perturbations occur, much closer to the wall, due to the recirculation of flow in the annular space between the probe and the tapping.

Due to these wall effects, the comparison between the calculated flowrate, based on the integration of the measured velocity profiles and K-Lab reference flowmeters (sonic nozzles) was not representative. As an example, the accuracy claimed by industrial Pitot probes, not perturbed by such type of wall effects, is normally close to +\-5%.

Field tests

The field tests were performed in a 6" fuel gas metering station at the Kårstø gas treatment plant where the probe was installed horizontally, 8D downstreams of a senior orifice meter, the only position available for the test. The pipe inner diameter was 154.6 mm.

During the test, the plate was removed from the stream (senior fitting) and the straight pipe length upstream of the probe became 37D. Besides, opposite to the port where the probe was inserted, there was a tapping point for a densitometer. This allowed the probe to come much closer to the wall than in the K-Lab tests. However, coming close to the wall at both ends, the CP experienced similar type of flow induced disturbances as in the lab tests. No swirl was observed, except very close to the aperture of the tapping point of the densitometer.

The operating conditions during the field tests were as follow:

- *Pressure: 30 bar - Flowrate: 648 act.m³/h. - Re : 2.86 x10⁶ - Results in figure 8.*

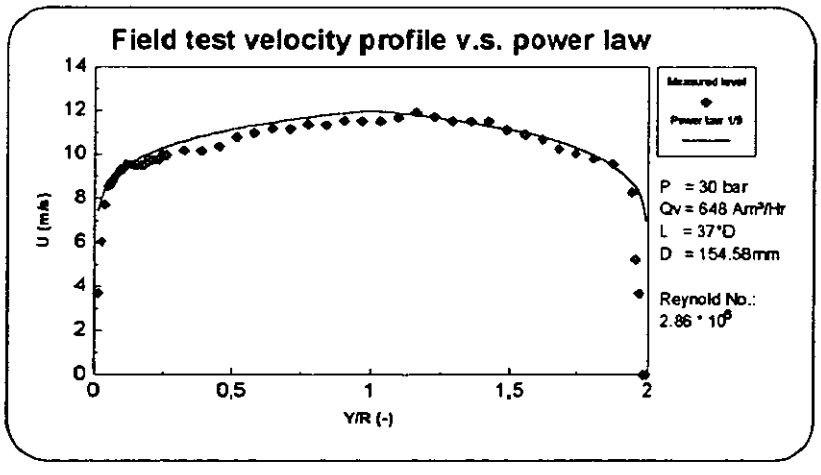

Figure 8

Statoil / K-Lab, P.O.B. 308, N 5501 Haugesund, Norway
Tel.:(47) 52 77 21 85 Fax :(47) 52 77 22 10 E-mail:stla@statoil.no

The results from these preliminary field tests show that the measured velocity profile fits the 9th power law curve in a fairly god manner.

How to use the information from the inspection probe

The probe has been designed to give a realistic picture of the flow profile and the degree of swirl in the meter tube, preferably at the position of the FE. However, in combination with available 3-dimensional CFD-calculations, the probe offers an efficient tool for the evaluation of the quality of metering stations in operation. Such analysis could tell the operator whether the meter run is within the required specifications or whether it needs to be improved, for instance by installing a flow conditioning device. The quality of the analysis depends on the position of insertion ports for the probe. When designing new metering stations it would be worthwhile to consider, from the beginning, tapping points for the insertion of an inspection probe at appropriate positions along the meter tube.

Conclusions

The preliminary results from the qualification tests conducted with the K-Lab inspection probe has documented:

- the velocity profiles and swirl angle measurements can be performed with the K-Lab probe. The probe ensures a good qualitative description of the existing profiles and swirls.
- that the probe is effectively portable. The probe can be lifted by one person. Two persons are required to conduct a field test which last approximately 2 to 3 hours, installation and dismounting included.
- the probe, in combination with CFD-simulations and flow conditoners, offers a performant package for the improvement of the quality of a gas metering station.
- additional tests are planned to confirm the preliminary results from the field tests. Special attention will be paid to improve the measurements close to the walls.

List of references

1. Challenges in Gas Metering Technology - J. Bosio, A.Erdal - International Energy Agency - Natural Gas Technologies: A driving Force for Market Development - Berlin 1-4 September 1996.
2. Short gas metering systems using K-Lab flow conditioners. P.L. Wilcox, T. Weberg, A.Erdal. 2nd International Flow Measurement Symposium, Calgary, Alberta, Canada, June 6-8, 1990.
3. Examination of the performance of three cylinder Pitot probes in swirling flow - D.Thomassen - Institute for Energy Technology - IFE/KR/F 87/171 - 1987 (Restricted)
4. Eigenschaften von Zylindersonden zur Strömungsmessung. Wuest, W. Zeitschrift für Instrumentkunde 71, 1963, Heft 7.

Statoil / K-Lab, P.O.B. 308, N 5501 Haugesund, Norway
Tel.:(47) 52 77 21 85 Fax :(47) 52 77 22 10 E-mail:stla@statoil.no

5. Cantilvered Pitot Cylinder. Winternitz F.A.L. The Engineer, May 27, 1955, pp 729-732
6. Pressure probes for fluid measurement. Chue S.H. Prog. Aerospace Sci., 1975, Vol. 16, No.2, pp.147-223.
7. Characterisation of swirling flow and its effects on orifice metering. Shen J.J.S., SPE Paper 22865, 66th SPE Conference, Dallas, TX, 1991.
8. International Standard Organisation. ISO 3966: Measurement of fluid flow in closed conduits using Pitot static tubes. 1977.

XXXXXXXXXXXXXXXXXXXXXXXXXXXXXXXX

Statoil / K-Lab, P.O.B. 308, N 5501 Haugesund, Norway
Tel.:(47) 52 77 21 85 Fax :(47) 52 77 22 10 E-mail:stla@statoil.no

NSFMW.97

North Sea FLOW Measurement Workshop

Paper ~~26~~: 4.6

COMPUTATION OF FLOW THROUGH VENTURI METERS

Authors:
Jane A. Sattery and Michael J. Reader-Harris, Flow Center NEL, U.K.

Organiser:
Norwegian Society of Chartered Engineers
Norwegian Society for Oil and Gas Measurement
Co-organiser:
National Engineering Laboratory, UK

COMPUTATION OF FLOW THROUGH VENTURI METERS

by

Jane A. Sattary and Michael J. Reader-Harris

Flow Centre
NEL
East Kilbride
Glasgow, G75 0QU, UK

SUMMARY

The computational fluid dynamics (CFD) work on Venturi meters reported in this paper was part of a large project for Shell Exploration and Production to investigate the application of Venturi meters to gas flow measurement. The majority of the experimental findings were reported in 'Unpredicted behaviour of Venturi flowmeters in gas at high Reynolds numbers' presented in the 1996 North Sea Flow Metering Workshop.

CFD has been used to model the flow through Venturi tubes and thereby gain understanding of how the discharge coefficient is affected by the vital parameters of diameter ratio, pipe Reynolds number and roughness. It has also been used to calculate the effect of manufacturing tolerance. The discharge coefficients obtained from the calibration of Venturi meters have been used to validate the CFD predictions The CFD results have also been compared with experimental results from the 1950s and 1960s with surprisingly good agreement.

This work forms the basis of further possible research using CFD on the effect of upstream and Venturi surface roughness on the performance of these meters. The knowledge gained on the effect of surface roughness may also be applicable to ultrasonic flowmeters.

1 INTRODUCTION

The oil and gas industry has in recent years shown a substantial interest in using Venturi meters as part of multiphase flow metering systems and particularly in wet gas metering applications. Much of this interest has stemmed from the basic understanding that Venturi flowmeters are rugged industrial devices which utilise a well established model of fluid flow to derive a fluid flowrate from a measurement of differential pressure. A high accuracy metering system for wet gas was described by Dickinson and Jamieson[1] in October 1993 and showed that use of this system rather than a conventional separation system could mean the difference between a marginal field being viable or not. The system utilized Venturis as the primary elements and used Murdock's[2] equation to correct for wet gas effects.

Shell Expro had an application for such a metering system which required an overall uncertainty close to that for gas fiscal metering systems. The installation would be operating at Reynolds numbers in the range 10^6 to 10^7, well above the upper range limit (10^6) stated in the Standard[3] for Venturi meters. Shell Expro accepted that the Venturi meters should be calibrated in liquid and gas to give baseline discharge coefficients. NEL was commissioned by Shell Expro to carry out the calibrations and also to carry out an independent parallel computer simulation study.

The Computational Fluid Dynamics (CFD) study was used to interpret and extend the experimental work: it examined the effect of changes in geometry, Reynolds number and roughness on the discharge coefficient of Venturi meters. The results of the simulations are presented in this paper. The CFD results are validated against the baseline calibrations carried out at NEL in water and also compare well with experimental and theoretical work on Venturi meters carried out in the 1950s and 1960s.

2 GEOMETRY AND SPECIFICATIONS

In the experimental programme the Venturi baseline calibrations in water were to be carried out first and so the computations were set up to simulate these calibrations as closely as possible so that direct baseline comparisons could be made.

Baseline cases similar to those in the experimental tests in water were computed for smooth Venturi tubes with pipe diameter, D = 154.04 mm and Reynolds number, $Re_D = 10^6$ for three different diameter ratios: $\beta = 0.4$, 0.6 and 0.75.

The Venturi tubes consisted of an entrance section of length 2D, a convergent section of included angle 21°, a throat section of length 1d, a divergent section of included angle 7.5° and an outlet section of length 2D. The pressure tapping holes were not modelled.

The radius of curvature on the intersection of the divergent section and the downstream section was always zero: the radius of curvature on all other corners was 5 mm (this is the smallest radius that could reasonably be obtained at the time).

The density, ρ, was specified as 10^3 kg/m^3 and the viscosity, μ, was 10^{-3} Pa s. The mass flowrate, q_m, was 120.4 kg/s giving a mean pipe velocity, $\bar{u}$, of 6.46 m/s.

3 BASELINE RESULTS

3.1 CFD Results

Figs 1 and 2 show the profiles along the length of the Venturi tube for $\beta = 0.4$ (on the graphs zero on the x-axis is at the Venturi tube inlet 2D upstream of the convergent section). Fig. 1 shows the velocity profiles along the length of the Venturi tube. The smooth profile is along the centreline with the peak at the throat. The mean velocity through the throat section was 40.37 m/s. The spiky profile is close to the wall: the discontinuities occur at the points adjacent to the corners of the Venturi tube. The maximum velocity at the intersection of the convergent and the throat section was 44.5 m/s.

Fig. 2 shows the static pressure profiles along the length of the Venturi tube: again the smooth profile is along the centreline and the spiked profile is along the wall; note that the static pressure is almost constant across the Venturi tube at the throat tapping, whereas at the corners it changes very substantially with radial position. The static pressure drops from 1.01019×10^5 Pa at the upstream wall tapping position to -7.18045×10^5 Pa at the throat tapping position giving a differential pressure of 8.19064×10^5 Pa.

The static pressure profiles are shown in detail in Fig. 3. The static pressure is at a minimum at the intersection of the convergent and throat section and is -1.04×10^6 Pa, 41 per cent lower than that at the throat. However, the positioning of the throat tapping is not critical since even at a distance of ¼d upstream of the throat tapping position the static pressure has decreased by only 1.2 per cent. The spike at each intersection did not just occur close to the wall: it persisted into the flow as shown by the three smoother profiles in Fig. 3; only at approximately 5 mm ($\approx$0.1d) from the wall did the static pressure adjacent to the corner equal that at the throat tapping.

3.2 Comparison With Experimental Results

The discharge coefficients obtained computationally, C_{CFD}, for the three diameter ratios were compared with those obtained experimentally, C_{EXP}, in water and are given in Table 1. The three Venturi tubes used in the water calibrations were manufactured to meet the requirements of BS EN ISO 5167-1[3]; also it should be noted that for $\beta = 0.4$ the maximum measured Reynolds number was less than 10^6. Table 1 also gives the percentage difference in discharge coefficient between computation and experiment, $\Delta C_{p.EXP}$, and between C_{CFD} and C given in BS EN ISO 5167-1, $\Delta C_{p.ISO}$.

TABLE 1

PERCENTAGE DIFFERENCE IN DISCHARGE COEFFICIENT

β	C_{CFD}	C_{EXP}	C_{ISO}	$\Delta C_{p,EXP}$	$\Delta C_{p,ISO}$
0.4	0.98463	0.9912	0.995	-0.66	-1.04
0.6	0.98618	0.9895	0.995	-0.34	-0.89
0.75	0.98637	0.9981	0.995	-1.18	-0.87

For a Classical Venturi tube with a machined convergent section the Standard specifies a discharge coefficient of 0.995 for all the diameter ratios. The agreement between computational and experimental results is surprisingly good, considering the discharge coefficients obtained from the Venturis in the experimental results differed within themselves by 0.9 per cent.

A major reason for the measured results always being higher than those computed is that the measurements are affected by the fact that the pressure tapping holes are sufficiently large that the measured static pressures are larger than those which would be obtained with a pressure transducer flush mounted on the wall. The measured differential pressure is smaller and the measured discharge coefficient larger than would be obtained in an experiment totally similar to the computational model. Further work is being done to quantify this effect.

3.3 Comparison With Earlier Experimental Work

The severe discontinuities in the pressure profile at the inlet and exit of the throat in the CFD results were observed some thirty years earlier experimentally by Lindley[4]. Lindley measured the wall pressure distribution along a Venturi with air as the working fluid. The results, Fig. 4, clearly show a strong adverse pressure gradient at the throat inlet which indicates the possibility of separation. The throat inlet section is shown in more detail by Lindley and reproduced in Figs 5 and 6 for throat Reynolds numbers, Re_d, below 3×10^5 and above 3×10^5 respectively. With the lower values of Re_d there is a clear flat spot downstream of the throat inlet. Lindley believed this was a clear indication of a separation bubble and subsequently proved the existence of a bubble at low values of Re_d by performing experiments with a perspex Venturi meter. However, this phenomenon was not seen at the higher values of Re_d shown in Fig. 6 and so Lindley concludes that no separation is expected to occur in this case. Lindley found similar results with water as the working fluid; there was evidence of separation but only for Re_d lower than about 2×10^5.

Following Lindley's conclusions no separation was expected for the baseline computations where Re_d ranged from 1.3×10^6 to 2.5×10^6. No flat spots were observed in the wall pressure profiles (Fig. 3) and there was no evidence of separation in any of the computations.

4 EFFECT OF COMPRESSIBLE FLOW

All baseline computations were carried out with incompressible flow specified in order to compare with the Venturi calibrations in water. When the Venturi meters were calibrated in high pressure gas in the next part of the experimental programme unexpected discharge coefficients were obtained; many of the discharge coefficients were greater than unity. An extensive investigation to determine the cause of this behaviour was undertaken by NEL and reported by Jamieson[5] in the 1996 North Sea Flow Metering Workshop. Prior to these results it was believed that for the computations the discharge coefficients would be identical for incompressible and compressible flows when computed at the same Reynolds number. To confirm this belief additional computations were performed to determine the effect of compressible flow at a similar Reynolds number to that of the calibrations in gas.

The incompressible flow computations were carried out with a structured mesh, however this technique was unsuitable for the computation of compressible flow through Venturis, therefore an unstructured grid was required to obtain a solution for compressible flows. Using the unstructured mesh a comparison was made between compressible and incompressible flow for $\beta = 0.4$, $Re_D = 2.66 \times 10^6$, $D = 154.04$ mm, $q_m = 5.8$ kg/s and at the inlet $\bar{u} = 12.68$ m/s, $\rho = 24.4$ kg/m^3 and $\mu = 1.7894 \times 10^{-5}$ Pa s.

For the compressible case the expansibility factor, ε, was calculated using the equation given in BS EN ISO 5167-1 for Venturi tubes:

$$\varepsilon = \left[\left(\frac{\kappa \tau^{2/\kappa}}{\kappa - 1} \right) \left(\frac{1 - \beta^4}{1 - \beta^4 \tau^{2/\kappa}} \right) \left(\frac{1 - \tau^{\left(\frac{\kappa-1}{\kappa}\right)}}{1 - \tau} \right) \right]^{1/2}$$

where τ is the ratio of the throat and upstream wall pressures at the points specified in the Standard, p_t / p_u, and κ is the isentropic exponent which for the ideal gas was computed as equal to the ratio of specific heat capacities, $\gamma = 1.4$. The numerical results are given in Table 2.

TABLE 2

COMPARISON OF COMPUTATIONS BETWEEN INCOMPRESSIBLE AND COMPRESSIBLE FLOW

	Incompressible	Compressible
C	0.98584	0.98699
ε	1.0	0.97783
p_u	2018222.35	2018815.58
p_l	1941433.40	1938852.10
Δp	76788.95	79963.48

The discharge coefficient in compressible flow only differs by 0.12 per cent from that computed for incompressible flow. It was therefore concluded that for the same Re_D the discharge coefficient would be almost the same for compressible or incompressible flow provided the maximum Mach number was always much less than 0.3.

To verify the unstructured mesh technique a comparison was made between the structured and unstructured mesh techniques for incompressible flow. There was a difference in discharge coefficient of only 0.05 per cent between the unstructured mesh at $Re_D = 2.66 \times 10^6$ and the structured mesh at the same Re_D obtained by interpolating between the values for $Re_D = 10^6$ and 4×10^6 (assuming a linear dependence on log Re_D).

5 EFFECT OF CHANGES IN GEOMETRY

5.1 Effect Of Increasing The Angle Of The Divergent Section

A study of the effect on the discharge coefficient of the angle of the divergent section was made by computing the discharge coefficient with included angles for the divergent section of 11° and 15° for $\beta = 0.4$ and 0.75. These were compared with those obtained for the baseline case (Table 1) which has an included angle of 7½°. For confirmation of the pattern the discharge coefficient for a divergent section of included angle 15° was obtained for $\beta = 0.6$. Table 3 gives the percentage change in discharge coefficient from the baseline for all the above computations. All the shifts were positive and less than 0.05 per cent.

TABLE 3

PERCENTAGE SHIFT IN DISCHARGE COEFFICIENT

β	$\alpha = 11°$	$\alpha = 15°$
0.4	0.05	0.05
0.6	-	0.02
0.75	0.04	0.02

The results show that an increase in the included angle from 7½° to 15° has an insignificant effect on the discharge coefficient.

5.2 Effect Of Increasing the Radii Of Curvature

A study of the effect on the discharge coefficient of increasing the radii of curvature at the intersections of the upstream pipe and the convergent, R_1, of the convergent section and the throat, R_2, and of the throat and the divergent section, R_3, was performed.

The baseline computations were performed with R_1, R_2, and R_3 = 5 mm; this was the minimum practicable radius of curvature possible at the time. The Venturi calibrations in water were performed on Venturis manufactured with a specified maximum radius of curvature tolerance of 1mm on all corners.

Computations were performed for Venturi tubes with the maximum radius of curvature permitted by BS EN ISO 5167-1 at a given intersection. For a classical Venturi tube with a machined convergent section the standard gives the following specification: $R_1 < 0.25D$ and R_2 and $R_3 < 0.25d$. Therefore, computations were performed for D = 154.04 mm, R_1 = 38.5 mm for all diameter ratios and R_2 and R_3 = 15.4 mm, 23.1 mm and 28.9 mm for β = 0.4, 0.6 and 0.75 respectively.

The result of these computations gave shifts in the discharge coefficient from the baseline case (Table 1) of less than ±0.025 per cent. However, where the maximum permissible radii of curvature were used the magnitude of the spikes at the intersections was reduced; for β = 0.4 the difference between the static pressure at the wall at intersection R_2 and that at the throat was 29 per cent, a reduction of 12 per cent from the geometry where the radii of curvature were all 5 mm.

6 EFFECT OF REYNOLDS NUMBER

Further computations were carried out for $Re_D = 2 \times 10^5$, 4×10^6 and 2×10^7 and β = 0.4, 0.6 and 0.75 to determine the effect of Reynolds number on discharge coefficient; the results are shown in Table 4, where $\Delta C_{P,b}$ is the percentage difference between C_{CFD} (given in Table 4 for each Re_D) and the baseline C_{CFD} (given in Table 1 for $Re_D = 10^6$).

TABLE 4

EFFECT OF REYNOLDS NUMBER ON DISCHARGE COEFFICIENT

Re_D	2×10^5		4×10^6		2×10^7	
β	C_{CFD}	$\Delta C_{P,b}$	C_{CFD}	$\Delta C_{P,b}$	C_{CFD}	$\Delta C_{P,b}$
0.4	0.98187	**-0.28**	0.98700	**0.24**	0.98864	**0.41**
0.6	0.98290	**-0.33**	0.98864	**0.25**	0.99061	**0.45**
0.75	0.98261	**-0.38**	0.98879	**0.25**	0.99078	**0.45**

On the basis of these computations it is clear that the discharge coefficient is a function of Reynolds number but that the term which describes the dependence on Reynolds number can be assumed not to be a function of β. More work is required to determine the exact functional relationship.

7 EFFECT OF ROUGHNESS

BS EN ISO 5167-1[3] specifies a maximum limit of upstream pipe roughness of $k_s/D \leq 10^{-3}$ (where k_s is the roughness height) on a length at least equal to 2D measured upstream from the classical Venturi tube. It also specifies that the roughness criterion R_a of the throat and that of the adjacent curvature shall be less than 10^{-5} d and that the divergent section is roughcast. For Venturi tubes with a machined convergent section it specifies that the entrance cylinder and the convergent section shall have a surface finish equal to that of the throat.

For the NEL calibrations the Venturi entrance cylinder, convergent section and throat had a specified maximum value for R_a of 0.4 μm for $\beta = 0.4$ and 0.8 μm for $\beta = 0.6$ and 0.75. On all other machined surfaces the value of R_a was 3.2 μm for all diameter ratios.

It was expected that the maximum shift in discharge coefficient would occur at the highest Reynolds number. Therefore, at $Re_D = 2 \times 10^7$, in addition to the computations with smooth walls, computations were performed for Venturi tubes of different roughnesses for $\beta = 0.75$ and $\beta = 0.4$. To verify this assumption one computation was performed for $Re_D = 1 \times 10^6$, $\beta = 0.75$, a smooth inlet, pipe roughness $R_a = 0.8$ μm for the 2D upstream of the convergent section, the convergent and the throat sections and $R_a = 3.2$ μm elsewhere; the shift in C was negligible.

7.1 Effect of Roughness for $\beta = 0.75$

For $\beta = 0.75$ and $Re_D = 2 \times 10^7$ seven roughness cases were computed.

The first case was computed with a smooth inlet and smooth Venturi tube and given in Table 4.

For the second case a rough upstream pipe was specified ($k_s/D = 5 \times 10^{-4}$). Over the 2D upstream of the entrance cylinder and throughout the Venturi tube smooth walls were specified. This gave a positive shift in discharge coefficient of 0.17 per cent.

The third case was an extreme case where the upstream pipework and the Venturi tube were rough ($k_s/D = 5 \times 10^{-4}$). This gave a shift in discharge coefficient of −1.17 per cent.

Cases 4 to 7 are shown in Fig. 7. The fourth case was a simulation of a typical Venturi tube (same roughness as in experimental tests) with a rough inlet (same as case 2) and gave no shift ($\Delta C = 0.01$ per cent) in discharge coefficient. The fifth case examined the effect of roughening the entrance section and the convergent section and for a rough inlet gave a shift in discharge coefficient of -0.35 per cent.

Since the effect of a rough inlet was to give a positive shift and the effect of a rough Venturi tube was to give a negative shift in discharge coefficient, the two effects can cancel each other out to some extent. Therefore, in order to determine a reasonable limit for roughness of the Venturi tube the worst case inlet profile is a smooth pipe. The last two cases were computed with a smooth inlet profile. The case where the Venturi tube had the same roughness as that of one of the Venturi tubes in the experiments (0.8 μm entrance, convergent and throat sections and 3.2 μm elsewhere) gave a shift in discharge coefficient of -0.21 per cent. This roughness of the Venturi tube is acceptable since with the smooth upstream pipe it is being used with the worst case inlet profile; the profile from a rougher pipe would have the effect of decreasing the magnitude of the shift and, as in case 4, an inlet pipe roughness of $k_s/D = 5 \times 10^{-4}$ gives no shift; this is the zero crossover point and an inlet pipe with a roughness greater than $k_s/D = 5 \times 10^{-4}$ would give a positive shift.

7.2 Effect of Roughness for $\beta = 0.4$

Three roughness cases were computed for $\beta = 0.4$ and $Re_D = 2 \times 10^7$; these are shown in Fig. 8 as cases 8, 9 and 10. The objective of computing these cases was to determine whether the maximum roughness limits in BS EN ISO 5167-1 for the critical sections of the Venturi tube are adequate. For $\beta = 0.4$ the maximum permissible roughness is $R_a = 0.6$ μm for the convergent and the throat sections. Case 8 with a rough inlet ($k_s/D = 5 \times 10^{-4}$) and smooth Venturi tube proved that the pipe roughness over the 2D upstream of the entrance cylinder has no effect on the discharge coefficient. Case 9 is the maximum permissible roughness for the convergent and the throat sections (i.e. Ra = 0.6 μm) and smooth elsewhere. This gave a shift in discharge coefficient of -0.30 per cent. Case 10 specified a rough convergent section and entrance cylinder only and smooth elsewhere; there was no change in discharge coefficient. These results show that the roughness limit for the convergent and for the upstream pipework is too small and for the throat it is too large.

7.3 Validation of Roughness Computations

Operational experience has shown that increasing Venturi flowmeter roughness decreases C. As Venturi roughness increases, the frictional losses and the measured pressure drop for the Venturi increase for a given flowrate and hence C is reduced. Theoretical analyses lead to the same conclusions. Increasing roughness causes the velocity gradient from the wall to reduce and hence the displacement thickness of the boundary layer to increase. Examination of Hall's equation[6], demonstrates that C will then be reduced.

These qualitative observations have been validated experimentally by several workers. Schlag[7] demonstrated this by artificially roughening the convergent cone of the Venturi and compared the calibration results before and after to discover that C had decreased. As part of the same programme, he investigated the effect of roughening the upstream pipe. The result was that increasing upstream roughness increased C. These results are shown in Fig. 9; the black dots correspond to a rough Venturi and the clear dots correspond to a smooth Venturi.

Hutton[8] conducted a series of experiments to investigate the effect of roughness on C: his results can be seen in Fig. 10. It can be seen that increasing Venturi roughness causes C to fall whereas increasing pipe roughness causes C to increase. Hutton concludes that if Venturi and upstream pipe are made of the same material, the Venturi roughness dominates and consequently C will fall with time as the system progressively rusts.

8 CONCLUSIONS - SPECIFIC

Baseline discharge coefficients have been computed for $\beta = 0.4$, 0.6 and 0.75 and D = 154.04 mm at a Reynolds number of 10^6. All computations showed unexpected spikes in all the profiles close to the pipe wall along the length of the Venturi tube. These spikes occurred at the intersections of the Venturi sections, in particular at the intersection of the conical convergent and the throat and at the intersection of the throat and the conical divergent sections. These spiky profiles do not just occur along the pipe wall but persist into the flow and decay with distance from the pipe wall; at the centreline all profiles are smooth and there are no spikes.

A comparison with a computation in compressible flow using an unstructured grid showed that there was no compressibility or mesh effect; the shift in discharge coefficient was insignificant and the same spiky profiles were present.

A change in the angle of the divergent section from an included angle of 7½° to 15° had no significant effect on the discharge coefficient.

A change in the radii of curvature at the most significant three intersections of the Venturi tube from 5 mm to the maximum permitted in BS EN ISO 5167-1 at a given intersection made no significant difference to the discharge coefficient.

Further Venturi tube discharge coefficients were computed for three values of β, 0.4, 0.6 and 0.75, at Reynolds numbers of 2×10^5, 4×10^6 and 2×10^7. These show that

the discharge coefficient is a function of Reynolds number but the term which describes the dependence can be assumed not to be a function of β.

The study of the effect of pipe roughness shows that discharge coefficients are only affected by pipe roughness at the higher Reynolds numbers. For a Venturi tube with $\beta = 0.75$ at $Re_D = 2 \times 10^7$ a rough ($k_s/D = 5 \times 10^{-4}$) inlet pipe has the effect of increasing the discharge coefficient, from the smooth inlet pipe case, by approximately 0.2 per cent. However, a Venturi tube with $R_a = 0.8$ μm and a smooth inlet pipe has the effect of decreasing the discharge coefficient, from the smooth Venturi tube case, by 0.2 per cent. For $\beta = 0.4$ and $Re_D = 2 \times 10^7$ there is no shift in discharge coefficient for a rough inlet pipe and smooth Venturi tube. The Venturi tube with $R_a = 0.6$ μm gives $\Delta C = -0.3$ per cent; this shift is entirely due to the rough throat.

9 CONCLUSIONS - GENERAL

This paper has shown that accurate simulations of flow through flowmeters are possible using CFD. The CFD results of flows through Venturi meters presented in this paper have been extensively verified using recent Venturi calibration data, detailed pressure profile data from the 1960's and surface roughness experiments from the 1950's.

The results showed that at high Reynolds numbers there was a small positive shift in discharge coefficient but nothing like the large shifts obtained when the Shell Venturi meters were calibrated at NEL in high pressure gas. However, the CFD acted as a useful tool in quickly eliminating suspected causes of the phenomenon: it showed that changes in geometry were probably not the cause. It also indicated that separation was probably not the mechanism by which the large shifts occurred. The only part of the Venturi that was not modelled were the pressure tappings, they appear to be the only possible geometrical cause of the problem. Also in the computations an ideal gas model was used and assumptions were made about expansibility. If the cause of the problem was flow related (as opposed to accoustic related) then these were the most likely causes.

The maximum roughness used for the CFD computations are the maximum limits specified in the Standard but further work needs to be done to determine if these are realistic for Venturis in service. The shifts reported in the literature are much larger than those found in the CFD work but the discharge coefficients were obtained from much rougher Venturis. Although roughness effects are understood qualitatively, to date nothing has been found in the literature that presents a general model quantifying the effect of age and roughness on discharge coefficients . This is not surprising as the issue is highly complex because of the vast array of roughening mechanisms and their possible effects on flow through the Venturi.

This work forms the basis of further possible research using CFD on the effect of upstream and Venturi surface roughness on the performance of these meters. The knowledge gained on the effect of surface roughness may also be applicable to ultrasonic flowmeters. The results of this work can also be used to improve the Standard for Venturi meters.

ACKNOWLEDGEMENT

The authors wish to thank Shell Exploration and Production for their kind permission to publish this paper. In particular they would like to thank Andy Jamieson for his continued support.

REFERENCES

1 DICKINSON and JAMIESON. High accuracy wet gas metering. North Sea Flow Metering Workshop, Bergen, Norway, Oct. 1993.

2 MURDOCK, J. W. Two phase flow measurement with orifices. Journal of Basic Engineering, Dec. 1962.

3 INTERNATIONAL ORGANIZATION FOR STANDARDIZATION. Measurement of fluid flow by means of orifice plates, nozzles and Venturi tubes inserted in circular cross-section conduits running full. BS EN ISO 5167-1, Geneva: International Organization for Standardization, 1991.

4 LINDLEY, D. Venturi meters and boundary layer effects. Ph.D. Thesis, University College of South Wales and Monmouthshire, Sept. 1966.

5 JAMIESON, A. W., JOHNSON, P. A., SPEARMAN, E. P., and SATTARY, J. A. Unpredicted behaviour of Venturi flowmeter in gas at high Reynolds numbers. North Sea Flow Measurement Workshop, Peebles 1996.

6 HALL, G. W. Application of boundary layer theory to explain some nozzle and Venturi flow peculiarities. Proc. Institute of Mechanical Engineers. London, Vol 173, No 36, pp 837, 1959.

7 SCHLAG, R. Survey of studies of classical Venturi meters at the University of Leige. Flow measurement in closed conduits. Proc. of a symposium held at the National Engineering Laboratory. Vol 1, Paper C2, Page 269, Sept. 1960.

8 HUTTON, S. P. The prediction of Venturi flowmeter coefficients and their variation with roughness and age. Proc. Instn. Civ. Engrs., Vol 3, Part 3, pp 216, 1954.

LIST OF FIGURES

3 Computed Pressure Profiles Along the Venturi in the Throat Region

4 Lindley (1966). Measured Pressure Profiles Along the Venturi Wall

5 Lindley (1966). Measured Pressure Profiles in the Region of the Intersection of the Convergent and Throat Sections for $Re_d < 300\ 000$.

6 Lindley (1966). Measured Pressure Profiles in the Region of the Intersection of the Convergent and Throat Sections for $Re_d > 300\ 000$.

7 Computed Effect of Roughness - Summary of Cases 4 to 7.

8 Computed Effect of Roughness - Summary of Cases 8 to 10.

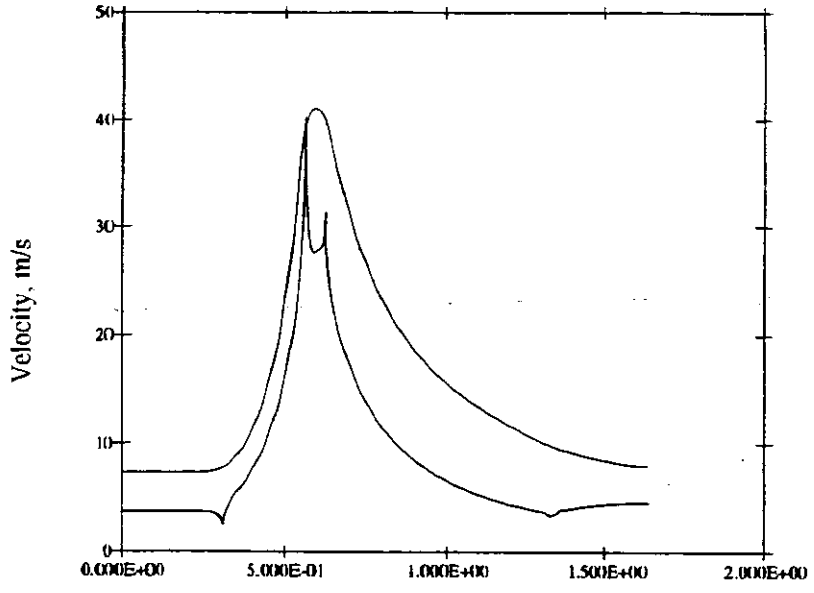

Fig. 1 Computed Velocity Profile Along with Venturi

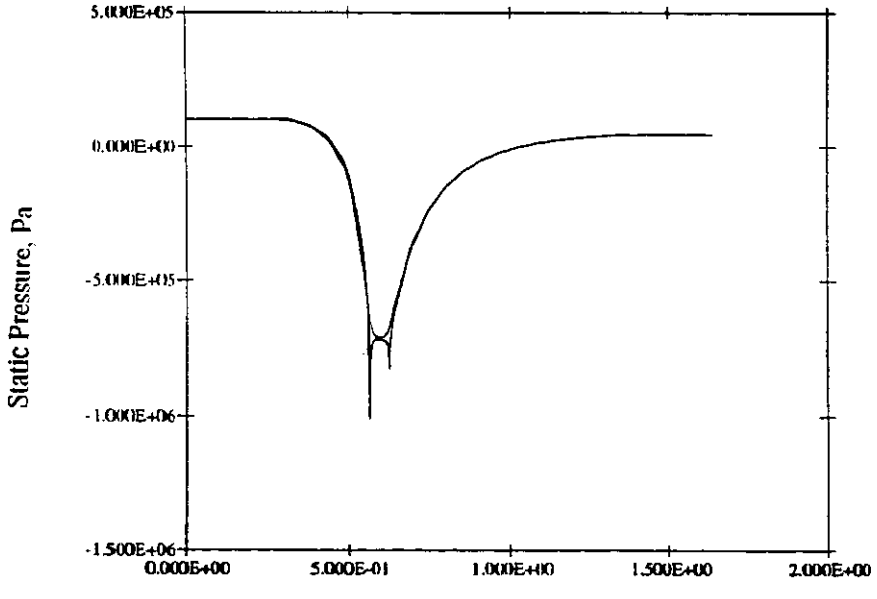

Fig. 2 Computed Pressure Profiles Along with Venturi

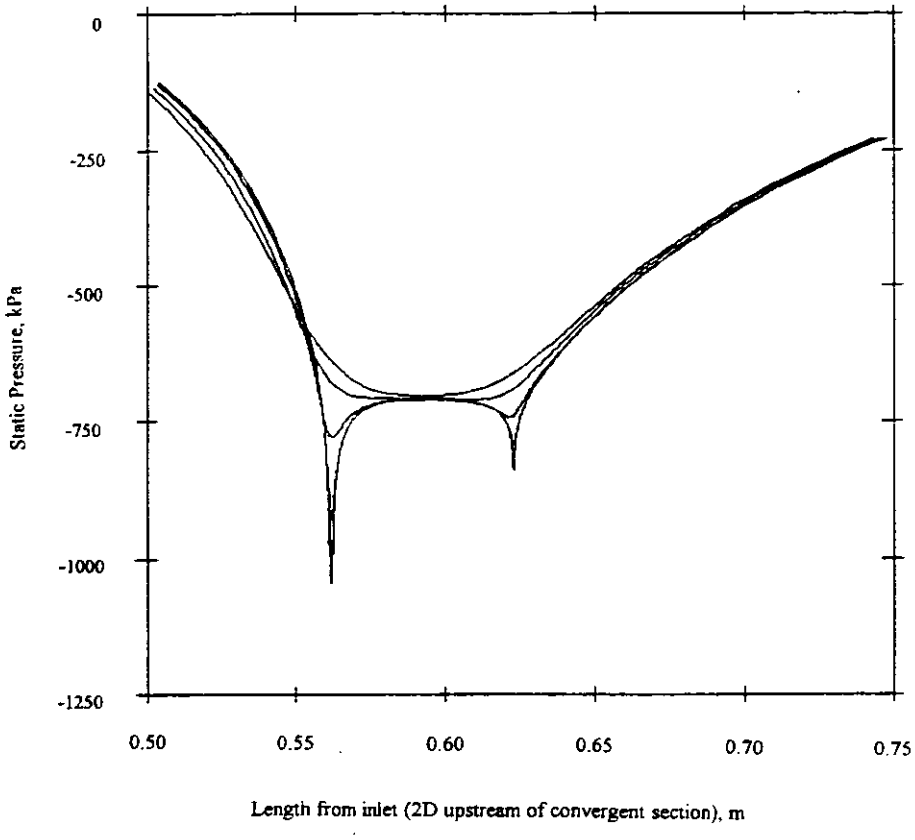

Fig. 3 Computed Pressure Profiles Along the Venturi in the Throat Region

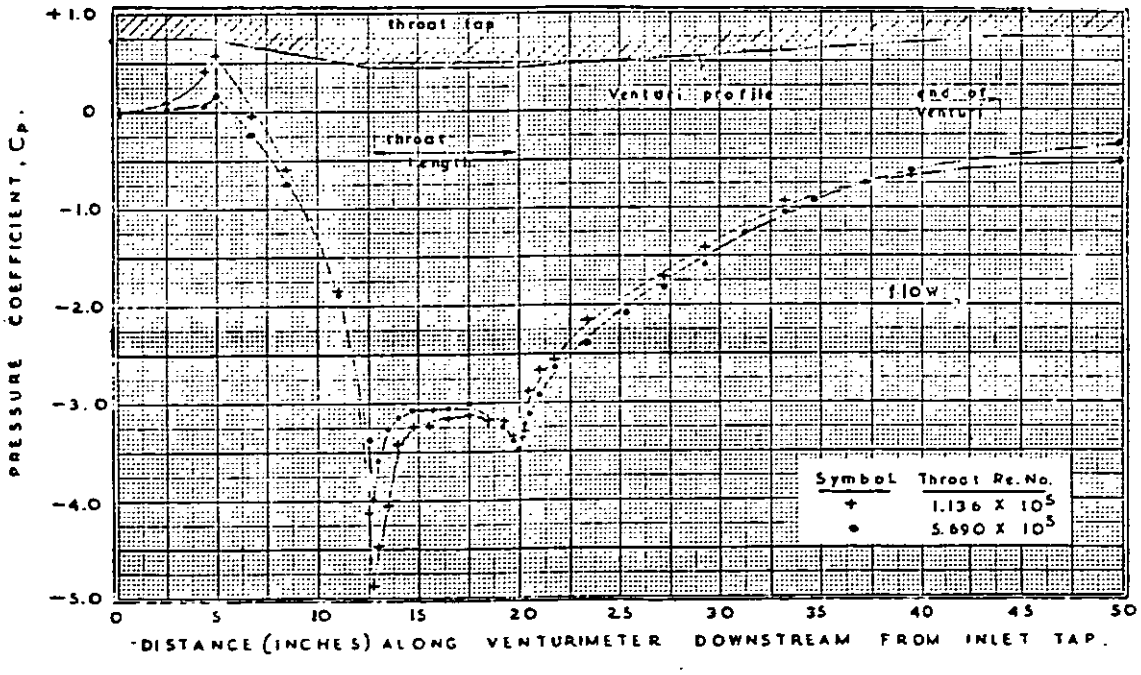

Fig. 4 Lindley (1966). Measured Pressure Profiles Along with Venturi Wall

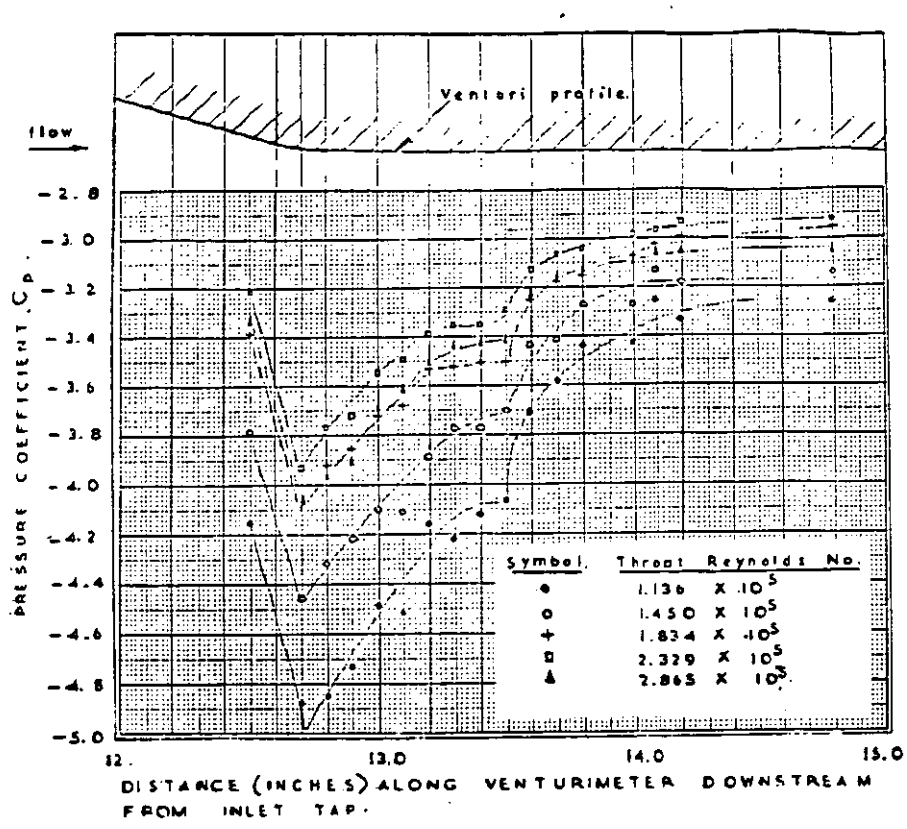

Fig. 5 Lindley (1966). Measured Pressure Profiles in the Region of the Intersection of the Convergent and Throat Sections for $Re_d < 300\,000$

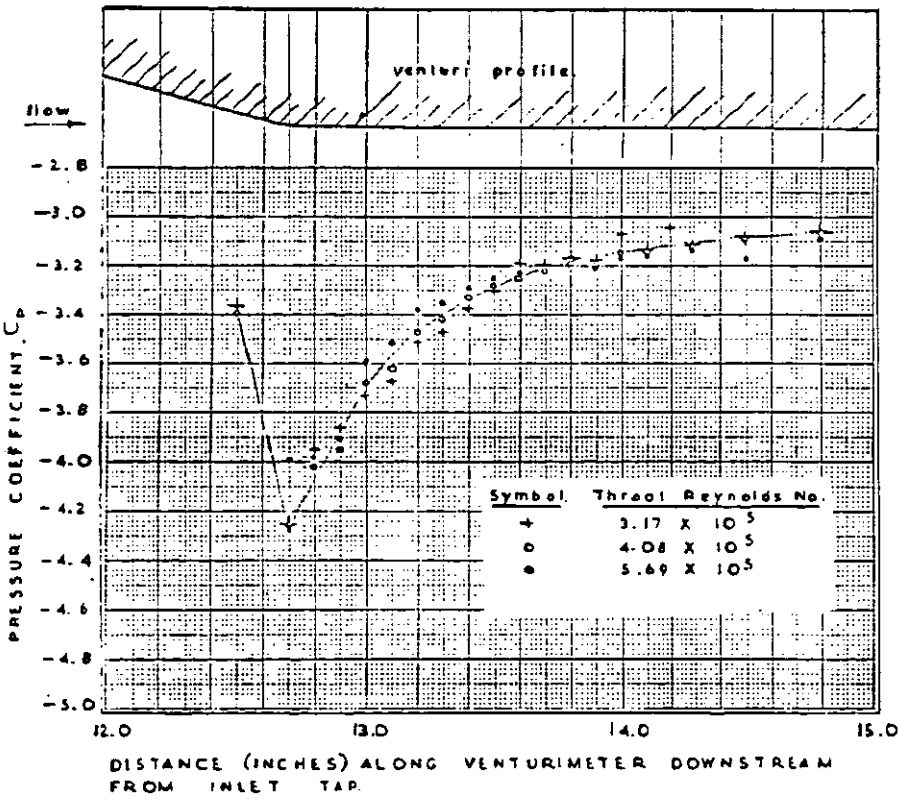

Fig. 6 Lindley (1966). Measured Pressure Profiles in the Region of the Intersection of the Convergent and Throat Sections for $Re_d > 300\,000$

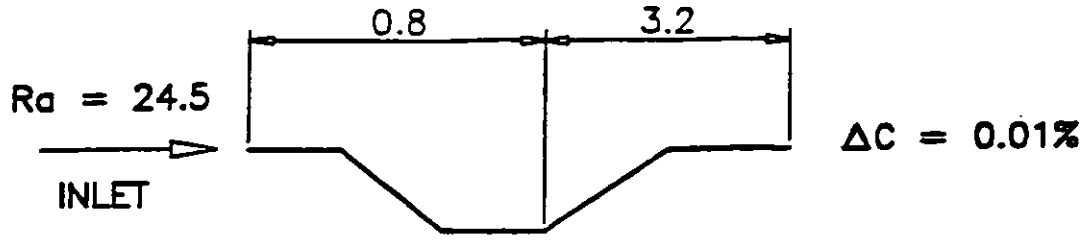

CASE 4: ROUGH INLET, VENTURI AS MANUFACTURED FOR EXPERIMENTS

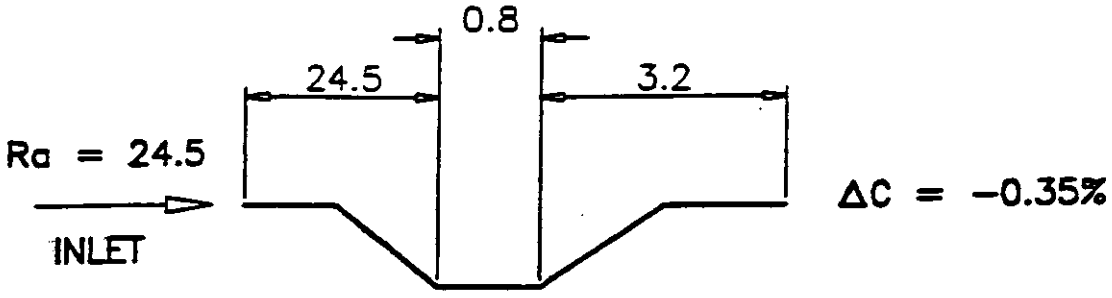

CASE 5: ROUGH INLET, ROUGH CONVERGENT SECTION

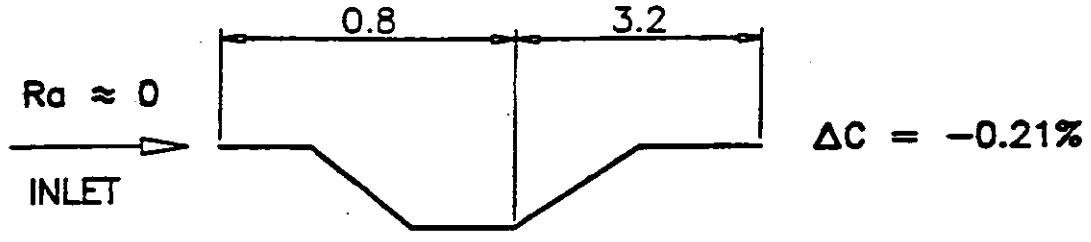

CASE 6: SMOOTH INLET, VENTURI AS MANUFACTURED FOR EXPERIMENTS

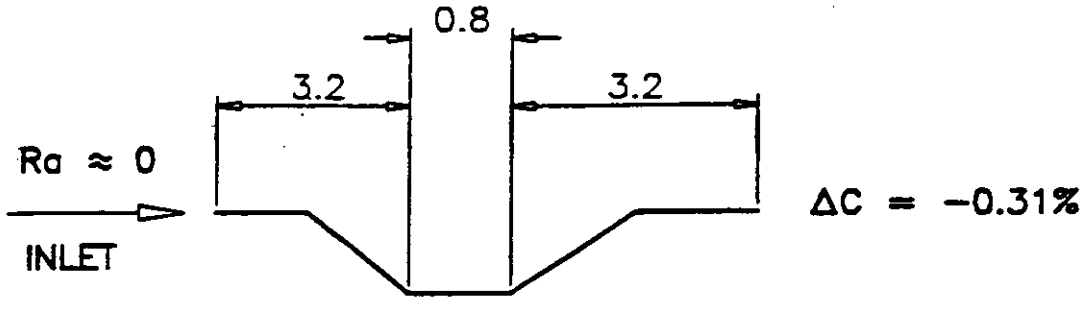

CASE 7: SMOOTH INLET, SLIGHTLY ROUGH CONVERGENT SECTION

Note: All values of Ra are in μm

Fig. 7 Computed Effect of Roughness - Summary of Cases 4 to 7

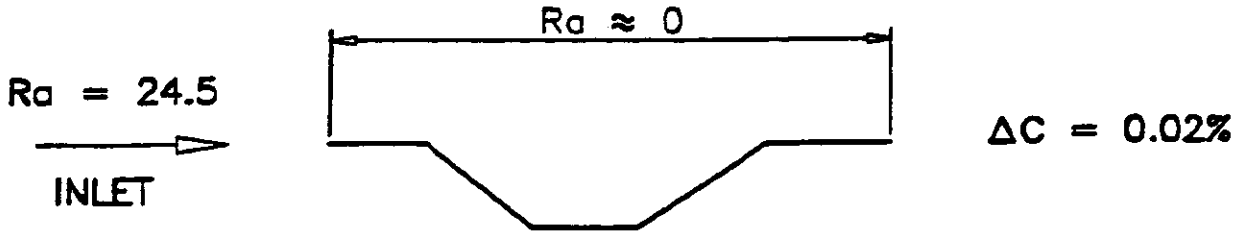

CASE 8: ROUGH INLET, SMOOTH VENTURI

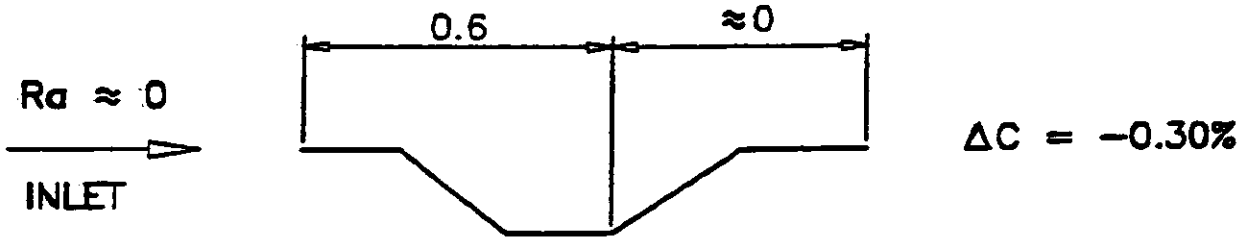

CASE 9: SMOOTH INLET, CONVERGENT & THROAT MAX IN ISO 5167

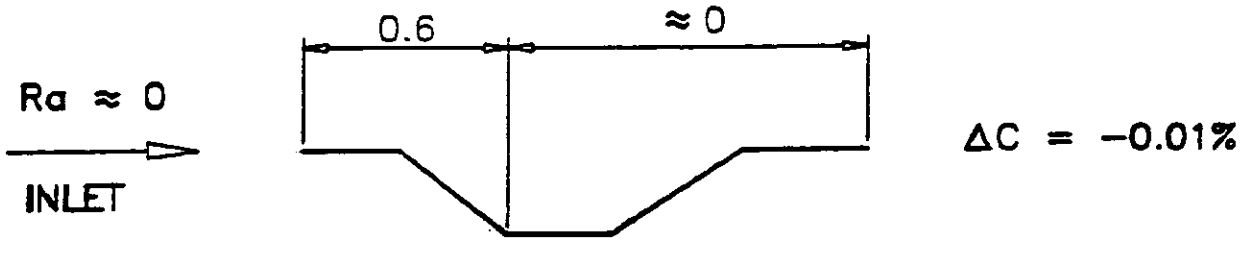

CASE 10: SMOOTH INLET, CONVERGENT ROUGH VENTURI SMOOTH

Note: All values of Ra are in μm

Fig. 8 Computed Effect of Roughness - Summary of Cases 8 to 10

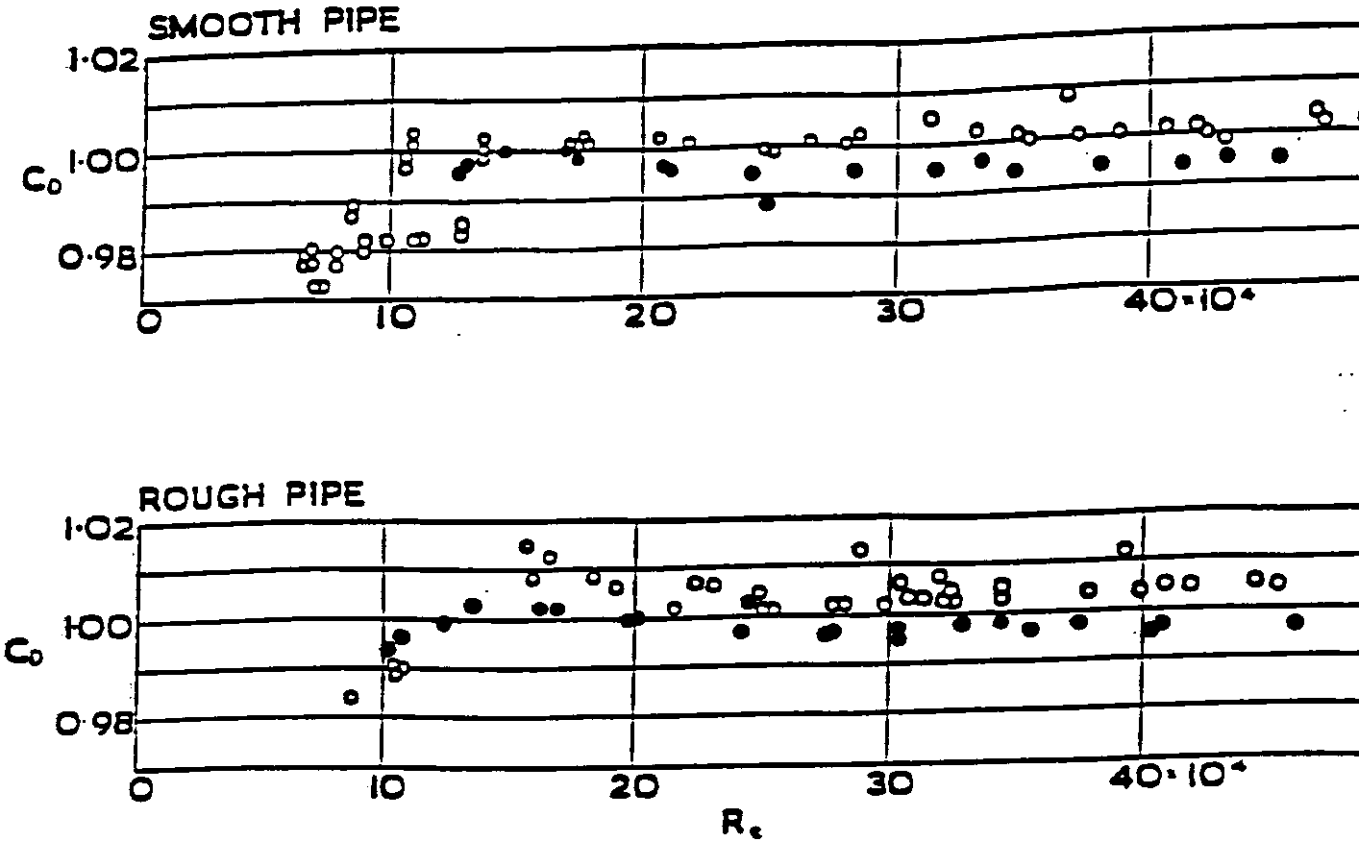

Fig. 9 Schlag (1960). Effect of roughness of convergent cone and upstream pipe

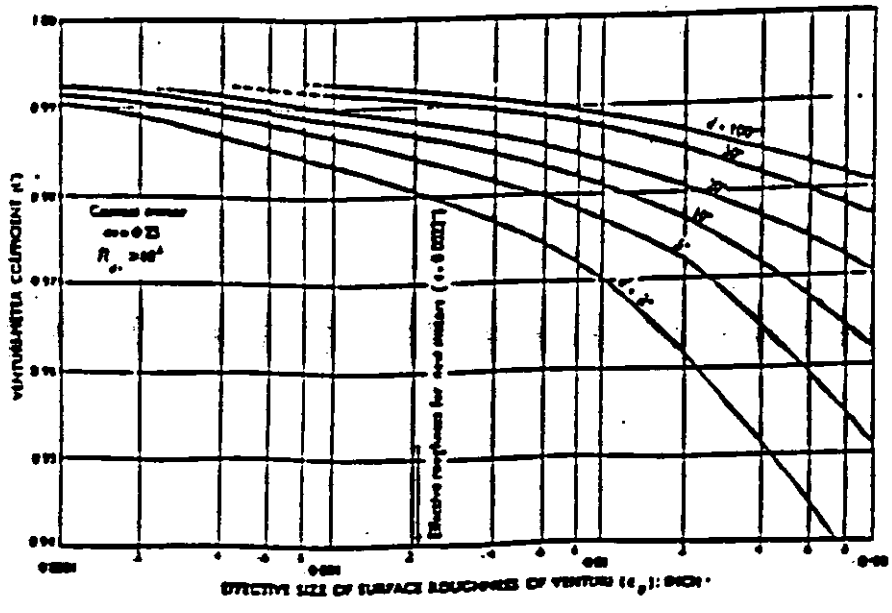

Fig. 10 Hutton (1954). Variation of C_d with surface roughness

NSFMW.97

North Sea FLOW Measurement Workshop

Paper ~~27~~: 5-1

WET GAS SAMPLING

Authors:
Thomas F. Welker, Welker Engineering Company, USA

Organiser:
Norwegian Society of Chartered Engineers
Norwegian Society for Oil and Gas Measurement
Co-organiser:
National Engineering Laboratory, UK

WET GAS SAMPLING

Thomas F. Welker
Welker Engineering Company
United States of America

The quality of gas has changed drastically in the past few years. Most gas is wet with hydrocarbons, water, and heavier contaminants that tend to condense if not handled properly. If a gas stream is contaminated with condensables, the sampling of that stream must be done in a manner that will ensure all of the components in the stream are introduced into the sample container as the composite.

The sampling and handling of wet gas is extremely difficult under ideal conditions. There are no ideal conditions in the real world. The problems related to offshore operations and other wet gas systems, as well as the transportation of the sample, are additional problems that must be overcome if the analysis is to mean anything to the producer and gatherer.

The sampling of wet gas systems is decidedly more difficult than sampling conventional dry gas systems.

Wet gas systems were generally going to result in the measurement of one heating value at the inlet of the pipe and a drastic reduction in the heating value of the gas at the outlet end of the system. This is caused by the fallout or accumulation of the heavier products that, at the inlet, may be in the vapor state in the pipeline; hence, the high gravity and high BTU. But, in fact, because of pressure and temperature variances, these liquids condense and form a liquid that is actually running down the pipe as a stream or is accumulated in drips to be blown from the system.

Gas is an extremely fragile product.

Everything that is done to it will affect its quality. This paper will cover the important aspects of collecting, transporting, and analyzing a representative gas sample. It will begin with where to take the sample and why, the sample probe and its design, sampling equipment and its design and operation, spot and composite sampling, right and wrong ways the industry uses sampling equipment. The transportation and analysis is an integral part of the final result. Your decisions are only as good as your samples. This paper will be the definitive word on wet gas sampling. The techniques and systems outlined will not only ensure a representative sample, but will ensure repeatability and a defensible system when followed to the letter.

With the advent of payment for natural gas by BTU, the popular concept is that, if liquid hydrocarbons are pushed into a pipeline, these liquid hydrocarbons can increase the BTU of the stream, and the gas will be worth more to the seller. This concept is not necessarily true, and free liquids will cause many more problems than we admit.

What is wet natural gas? A gas stream that contains hydrocarbons, water, or other liquid contaminants that will condense when the pressure or temperature change, is considered wet natural gas.

Where do these liquids come from?

Retrograde condensate is the most common liquid found in gas pipeline systems. This liquid comes from production of wet gas and/or condensate reservoirs. Retrograde condensation also comes from inadequate field processing and inadequate retention time in production separators. These liquids and others exacerbate measurement errors, change specific gravity, and create BTU problems.

Other liquids that present serious problems in the analysis, specific gravity, and BTU determination are liquids that end up in the pipeline because of operations abnormalities.

Methanol, odorant, corrosion inhibitors, and compressor oil, to name a few, create havoc in downstream systems. The most serious culprits, however, are compressor oil and valve grease & oil. These contaminants can and will end up in your sampling system and sample cylinders.

Liquids in gas pipeline systems create measurement errors, corrosion problems, as well as hydrate and pulsation problems.

With the obvious problems created by the liquids addressed, but not solved, how do you collect a representative gas sample from this flowing stream?

Wet gas, however, is always going to have aerosols entrained in the stream, and these aerosols must be taken as part of the products flowing down the line.

Since wet gas samples are going to contain aerosols, the location where the sample is taken must be chosen or built to ensure all of the components, both liquid and gas, are mixed in the line directly upstream of the sample probe.

The location of the sample probe must be directly downstream of the area where the contents of the line are mixed. This mixing is accomplished with special Komax static mixers.

Samples from wet gas systems taken downstream of Komax static mixers may be taken in horizontal or vertical lines.

A static mixer should be designed to create the dispersion and distribution desired without creating excessive pressure drop. The properly designed static mixer will do this over ranges from 1.5 feet per second and above.

The sampler spool will have the mixer installed with the sample point two pipe diameters downstream of the mixer. The sampler will be installed in a horizontal plane, so the products will flow down and out to the sample container.

Isokinetic Sample Pump

The sample pump must be designed specifically for the purpose of "grabbing" the sample and pumping that sample from the line regardless of flowing conditions (pressure or temperature) or product properties (viscosity, particulate content, or vapor pressure).

The isokinetic sample probe is designed specifically to trap a sample from the flowing stream and pump that sample into the container.

The inlet to the sample collection head should be large enough to inhibit the diversion of sample droplets. The sample head should be self-purging between strokes.

In order for this to be true, the sampling system must be installed properly, maintained in working order, and the sample must be subsequently handled properly.

The object of the composite sampling system is to gather representative "bites" or grabs of the gas moving by the sample point and inject those "bites" unchanged into a sample container for storage and transportation to an analyzing device.

The composite sampling system consists of the following items:

- Stream Conditioning (Komax static mixers)
- Isokinetic Sampling Pump
- Sample Timing System or Electronic Interface
- Sample Container

The composite sampler is normally used as a practical alternative to an on-line analyzer such as a calorimeter, therm titrator, or chromatograph. If instantaneous information is required, the on-line analyzer is the mechanism to use. If, however, the analysis and BTU can be sent from a lab at a later date, the composite sampler will provide as accurate, if not more accurate, information than the on-line analyzer.

It is understood that liquids cannot be removed from flowing gas streams; therefore, the sample will contain liquids or droplets that will condense. The sample that contains these condensables will be representative of the flowing stream. Two phase samples will not produce repeatable results in standard cylinders because the phases of the sample cannot

be controlled. The piston cylinder is the only container that can be used to ensure an accurate analysis of the collected sample. The sample may be kept in equilibrium in the piston cylinder.

Liquids in natural gas transmission and distribution systems are being ignored.

Because of economic considerations, or lack of knowledge, the liquids that are being generated at the wellhead are not being adequately removed to be able to move a clean, dry gas for transportation in the pipeline. Because of this, both the producer and gatherer experience losses and unaccounteds.

Is the sampling technique suitable to find liquids in the gas stream?

Liquid fallout – some hydrocarbons and water vapor may drop out under certain conditions of temperature and pressure. This liquid is equivalent to gaseous volume that is not accounted for. Water, CO_2, and liquid hydrocarbons knocked out at conditioning, treating, or processing plants should be properly accounted for.

The liquids in the metering and pipeline system create problems of lost efficiency, inaccurate measurement, hydrate problems, and inaccurate chart integration.

The study showed the increase in the specific gravity and BTU was not appreciable. The problems created by the liquids, however, were ever-present.

The removal of the liquids from the systems would have created increased revenues far greater than the BTU increase for the producer. The removal of the liquids from the system was found to be of a great benefit to the pipeline company in improved operations and measurement.

This wet gas problem is further compounded by the variation of cylinder pressures. It is important to note the pressure in the sample cylinder at the time the sample is taken. This pressure needs to be the same when the sample is run on the analytical device.

Excessive bleed during purge cycle is a means by which the BTU is also drastically affected. This excessive bleed or purge using gas from a standard cylinder will lower the pressure and allow heavies in the liquid state to vaporize and, therefore, affect the BTU by driving it up. The amount the BTU will be affected will be determined by the heavies in the cylinder and the decrease in pressure in the cylinder.

The sampler should be designed to pump all of the trapped sample into the container. Any product retained in the collection head because of clearances from pistons or inlet check valves will most certainly be heavier contaminants, such as water or natural gasoline, and oil.

Proportional-To-Flow Timing System

The wet gas sampling system, as with all multi-phase sampling systems, must be actuated proportional to the flowing stream. In order for the components in the sample container to be related to a specific volume of total products moving through the pipeline, the sampling system must be interfaced with the flow.

Sample Containers

The method of storing the collected sample is to employ a container that has a sliding piston. The use of the constant pressure sample container allows the sample to be stored and mixed without changing phase.

Since the sample container is normally going to have pressure higher than pipeline pressure on the piston above the product, the sampler must work independently of any associated conditions (pipeline pressure, ambient temperature, or precharge pressure on the cylinder).

To retain a collected sample in the same phase as it is in the pipeline, the light ends must be kept as part of the sample. If the light ends are retained, the BTU and specific gravity will not change. With proper pre-conditioning, the compositional analysis can be accurately determined.

To use the Constant Pressure Product Container (CPPC) as the sample container, the sampler will be required to capture the sample and pump that collected bite through the tubing and into the cylinder. The cylinder has a precharge gas on the back side of the piston to keep the sample in a single phase. The precharge gas is 50 to 100 psi above the pipeline pressure.

In order for the sample to be accurately analyzed, it must be kept in the same phase during collection and storage as in the pipeline.

The sample must be collected, stored, and transported in containers specifically designed for this function.

The transportable Constant Pressure (CP) sample container that is used must be capable of the phase control and must have the mixing capability to re-mix the contents of the container to a completely homogeneous mixture, and be D.O.T. Approved.

With gas, water, and hydrocarbon mixtures, the continued mixing of the contents during sample transfer from stationary container to transportation container or container into analytical devices or glassware cannot be stressed enough.

The sampling technique in spot sampling of wet gas is more sophisticated than normal dry gas.

Spot sampling wet gas should be done using the phase observation sight glass and piston cylinders with the phase control bleed plug in the precharge valve of the sample cylinder.

The sliding piston sample container should always be used in wet gas sampling.

By using the piston cylinder, the drawing of gas from the pipeline ensures the phase of the sample is always under control.

The piston cylinder also allows control of the gas as it is pushed into the analyzer. After the gas analysis has been done, the liquid phase can be measured and removed for further analysis.

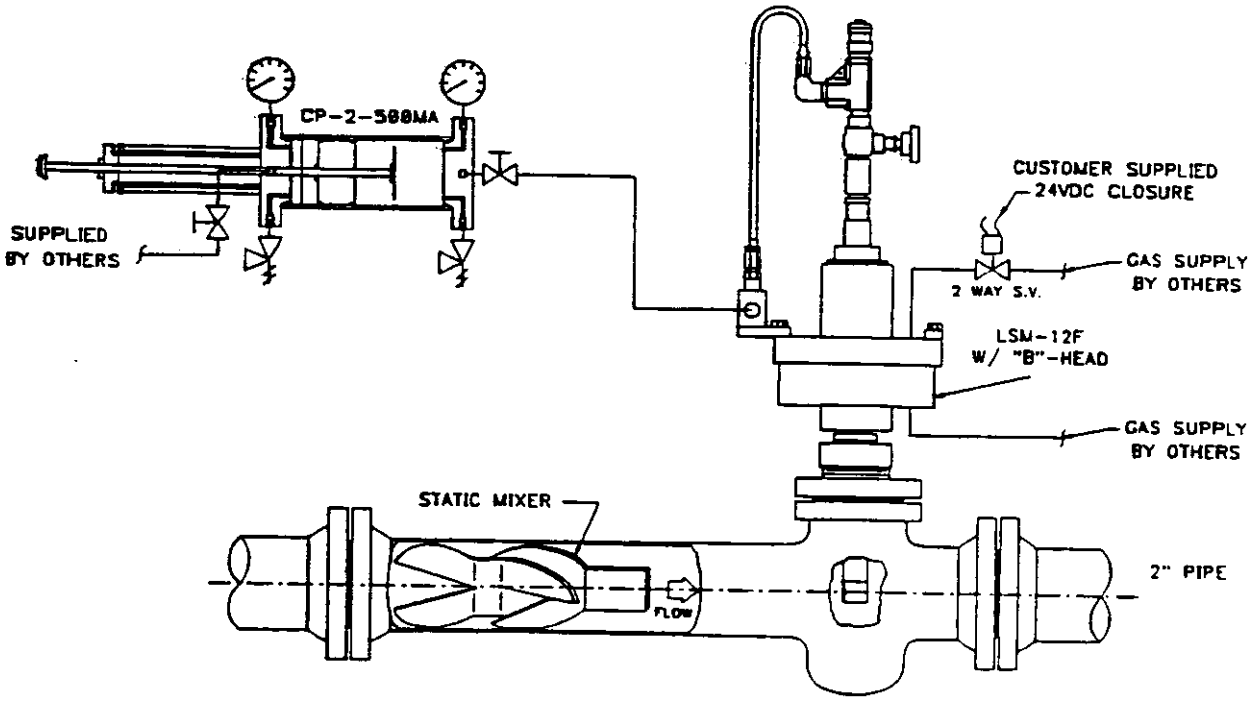

NSFMW.97

North Sea FLOW Measurement Workshop

Paper ~~28~~: 5·2

EVALUATION OF ON-LINE CHROMATOGRAPH PERFORMANCE

Authors:
Christopher J. Cowper and Richard P. Mounce, Effec Tech Ltd, U.K.

Organiser:
Norwegian Society of Chartered Engineers
Norwegian Society for Oil and Gas Measurement
Co-organiser:
National Engineering Laboratory, UK

EVALUATION OF ON-LINE CHROMATOGRAPH PERFORMANCE

Christopher J Cowper and Richard P Mounce

EffecTech Ltd., U.K.

SUMMARY

Gas Chromatography (GC) is very widely used for analysis of natural gas, with the most frequent use for the analytical data being the calculation of properties of the gas. Just as the composition data are used to calculate properties, so the uncertainty values associated with the composition data allow calculation of the uncertainty associated with the property. International Standard ISO 10723 [1] describes the procedures for estimation of composition uncertainty. This paper describes the use of ISO 10723, the range of results found, and the influence of these results on the calculated Calorific Value (CV) of natural gases. Similar calculations can be applied to other properties.

INTRODUCTION

Analysis of natural gas by gas chromatography is a well-established and mature technology. The most common configuration allows analysis of N_2, CO_2, C_1 to C_5 hydrocarbons individually, and a composite C_6+, representing all hydrocarbons of carbon number 6 and above. The particular chromatographic requirements of natural gas mean that the C_3 to C_5 hydrocarbons are separated on one column, which has a short pre-section from which C_6+ is backflushed, while the N_2, CO_2, C_1 and C_2 are stored in a separate column more suitable to their needs, and separated later in the analytical run. A further column may be introduced to allow separation and measurement of both O_2 and N_2. This is more common for laboratory-based analysers; on-line process instruments are very unlikely to be subject to air contamination.

Although the arrangement sounds complicated, the switching events occur under automatic control, and once set up, the chromatographic conditions are very stable. Analysis times are typically in the range 5 to 20 minutes. Other instrument configurations are available, including the use of a temperature-programmed capillary column for details of the higher hydrocarbons. For most properties, however, with the exception of hydrocarbon dewpoint and related calculations, analysis to C_6+ is sufficient.

PERFORMANCE EVALUATION

ISO 10723, "Natural gas - Performance evaluation for on-line analytical systems" was written so as not to be technique specific, other than to assume that the method of analysis produces composition data. Test gases are introduced, and the resulting data evaluated. To date, it has only been applied to gas chromatographs, but if a new and competitive analytical method emerges in the future, it should be equally applicable. Although the name suggests on-line systems, it can be and has been used successfully with laboratory analysers.

The evaluation procedure gives quantitative uncertainty values which will arise from the use of the analyser under defined conditions. It is assumed that the user has a set of requirements which the analyser is meant to satisfy. These should include

- The range of components to be analysed (normally decided before purchase).
- The range of compositions for each component.
- The allowable uncertainty for component measurement and/or calculated properties.

The procedure then covers the following topics in the context of the user's requirements:

- Is the instrument fit for purpose?
  - properly configured for natural gas analysis
  - measuring the range of components required
- Is it efficient?
  - separating components without them interfering with each other
  - completing the analysis in an acceptable time
- Is it precise?
  - capable of producing repeatable data when analysing a single gas
  - does repeatability vary with component concentration?
- Do bias errors arise from non-linear response?

The first two headings cover characteristics which are mainly answered by inspection, although whether it covers the concentration ranges required will arise from the testing. Error measurement is derived from the use of test gases.

Errors can be categorised as being either random or systematic (bias errors). Random errors arise because no system is capable of producing exactly the same data output when the same operations (analyses) are performed. In natural gas analysis by GC, typical causes of random errors include variations and spikes in the electrical supply, electrical interference from other equipment, changes in ambient conditions, particularly barometric pressure, and variations in operator procedure. Precision statements are the normal way of quantifying random error. Systematic errors can arise from improperly configured systems which fail to measure some components, from errors in the calibration gas being used, and from false assumptions about the nature of the instrument response characteristics. (This last cause is typically due to the assumption that the response/concentration relationship is a straight line through the origin, whereas in fact it follows a curve).

The procedure requires the use of seven test gases, so that each component is measured at seven different concentrations. These should cover a range slightly greater than that for which the analyser is required, and ideally be more or less equally spaced across that range. Given these requirements, the mixtures will have unusual compositions, and must be prepared according to the application. The gases need not contain all components, but should as a minimum contain N_2, CO_2, C_1, C_2, C_3 and C_4.

The test gases are each analysed several times, so as to get repeatability data at the different component concentrations. The analysis cycle time usually dictates how many repeats are possible at each level; all analyses should be completed during a single calibration interval,

typically a working day. With faster analysers, six to eight repeats can be achieved for each gas in half a day. More than this number of repeats is not really necessary.

Figure 1 illustrates a set of results for one component. The precision is evaluated from the scatter of results at each concentration, and the response curve is fitted to the mean values at each concentration.

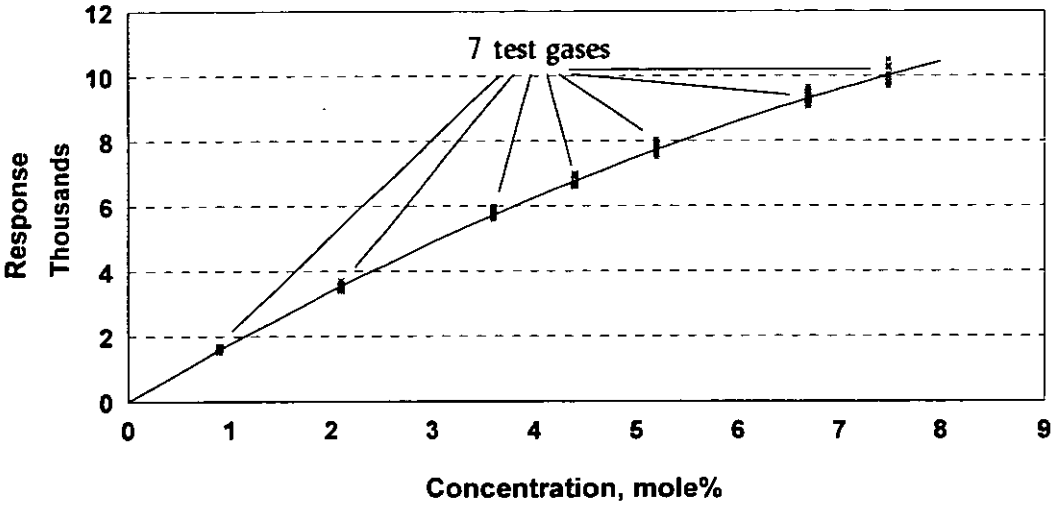

Figure 1. Use of test gases

The data are inspected for outliers before being subjected to regression analysis. This allows the precision for each component to be expressed either as a function of concentration or as a uniform value across the range, and the response curve to be expressed as a first-, second- or third-order polynomial.

PRECISION

Significance of Precision data

The standard deviation of a set of repeat data is easy to express, but by itself does not allow random error calculation which is meaningful. If we assume that:

- samples are measured by an analyser of known precision which uses a certified calibration mixture as a working standard on a day to day basis,
- the working standard has itself been measured against a primary, for example gravimetric, calibration standard, using an analyser with comparable precision to that used for sample measurement,
- both the primary and certified calibration mixtures are of similar composition to the sample, and
- the uncertainties associated with the composition of the primary calibration standard are small,

then we can create an error budget. The concentration, x_{iws}, of component i in the certified working standard is expressed as

$$x_{iws} = \frac{x_{ipr} \times A_{iws}}{A_{ipr}} \quad (1)$$

where x_{ipr} is the concentration of component i in the primary calibration standard
A_{iws} is the analyser response to component i in the working standard
A_{ipr} is the analyser response to component i in the primary calibration standard.

The concentration of component i in the sample, x_{isam}, is calculated as

$$x_{isam} = \frac{x_{iws} \times A_{isam}}{A_{iws}} \quad (2)$$

where A_{isam} is the analyser response to component i in the sample.

Combining these equations,

$$x_{isam} = \frac{x_{ipr} \times A_{iws} \times A_{isam}}{A_{ipr} \times A_{iws}} \quad (3)$$

Although A_{iws}, which appears in both the numerator and the denominator of equation (3), can be cancelled out when calculating the concentration, this is not permitted for statistical treatment of uncertainty. The uncertainty in x_{isam}, δx_{isam}, is expressed as

$$\frac{\delta x_{isam}}{x_{isam}} = \sqrt{\left(\frac{\delta x_{ipr}}{x_{ipr}}\right)^2 + 2 \times \left(\frac{\delta A_{iws}}{A_{iws}}\right)^2 + \left(\frac{\delta A_{isam}}{A_{isam}}\right)^2 + \left(\frac{\delta A_{ipr}}{A_{ipr}}\right)^2} \quad (4)$$

where δabc is the uncertainty in abc.

Equation 4 gives the random uncertainty for a component which has been analysed as described. According to ISO 6976 [2] the uncertainty on calculated CV, δH^0_{mix}, can be derived from the individual component uncertainties by

$$\delta H^0_{mix} = \sqrt{\sum_{i=1}^{N} \left[\delta x_i \times \left(H^0_i - H^0_{mix}\right)\right]^2} \quad (5)$$

Equation 5 sums the individual component uncertainties to give a CV uncertainty. Because it works this way, if the analytical requirement is to achieve a defined uncertainty on calculated CV, there is not a reverse route which will allow calculation of the component uncertainties from a required CV uncertainty. In the same way, a calculated CV alone does not allow the composition from which it was derived to be deduced.

Because a defined property uncertainty is a common requirement, we studied the precision data from a large number of process GCs to see if there is a useable relationship between property and component uncertainty. Figure 2 illustrates the data.

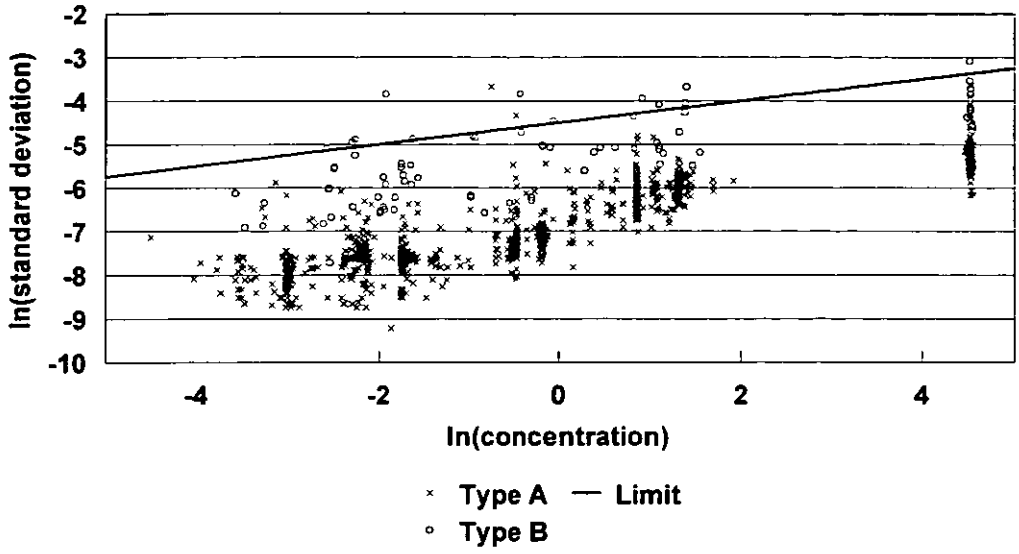

Figure 2. Relationship between standard deviation and concentration

When plotting standard deviations against concentration for different components which cover similar concentration ranges (for example N_2 and C_2), we found that concentration had more effect than the nature of the component. Their precision was linked more to the concentration, and broadly independent of what they were. Extending this to all components, expressed as natural logarithms to recognise the concentration differences, we found that the relationship extends over the entire component range. Furthermore, plotting data from instruments from two sources (Type A and B in Figure 2) shows that the precision of each type is different. Each shows a mean behaviour, expressed as

$$\ln(\text{standard deviation}) = A + B * \ln(\text{concentration})$$

with different coefficients A and B for each type.

It is possible to draw a line (Limit in Figure 2) which acts as a boundary to almost all the observations, and which has the equation

$$\ln(\text{standard deviation}) = -4.5 + 0.25 * \ln(\text{concentration}). \quad (6)$$

Applying these values to give an overall component uncertainty according to equation 4, and hence, for a series of typical natural gases, a CV uncertainty according to equation 5 gives values of slightly less than 0.1 MJ/m^3. In other words, if the requirement were for a method which would give a calculated CV with an uncertainty of 0.1 MJ/m^3, or approximately 0.25% relative, then any analyser where component standard deviations are shown to be below the limit value of equation 6 will satisfy the requirement.

Application of precision data

Since the composition and related uncertainties of a natural gas control the calculated CV and its uncertainty, respectively, it is of interest to study the effect of differing compositions and levels of precision. Five natural gas compositions were considered. One was a typical North Sea gas, and the other four were taken from an American Petroleum Institute group on

sampling [3]. These latter were formulated to represent CVs expressed in BTU of 800, 1000, 1250 and 1500. Such gases have wide compositional variations, and are chosen as deliberate extremes, to illustrate the effects.

Three levels of precision were considered. The best was taken from the mean values for Type A analysers illustrated in Figure 2. The boundary values from equation 6 were used for the "average" case, and the final values were taken from the worst case which we have encountered. The resulting CV uncertainties are listed in Table 1 and illustrated in Figure 3.

Table 1. CV uncertainty derived from component random errors

		Calorific Value uncertainty MJ/m^3		
	Calorific Value	Mean Type A	Limit	Worst case
North Sea gas	38.91	0.017	0.095	0.140
800 BTU gas	29.87	0.056	0.187	0.195
1000 BTU gas	37.36	0.012	0.081	0.114
1250 BTU gas	46.63	0.058	0.135	0.231
1500 BTU gas	55.98	0.187	0.242	0.372

From Table 1, it is clear that the best precision applies to the North Sea and 1000 BTU gases. For the other gases, the error increases according to how far their CVs differ from that of methane. The reason is implicit in equation 5. Gases with CVs close to that of methane tend to contain methane at the 90% level. In this case, the methane uncertainty makes very little contribution, as its CV is close to that of the mixture, and the sum of the contributing components is relatively small.

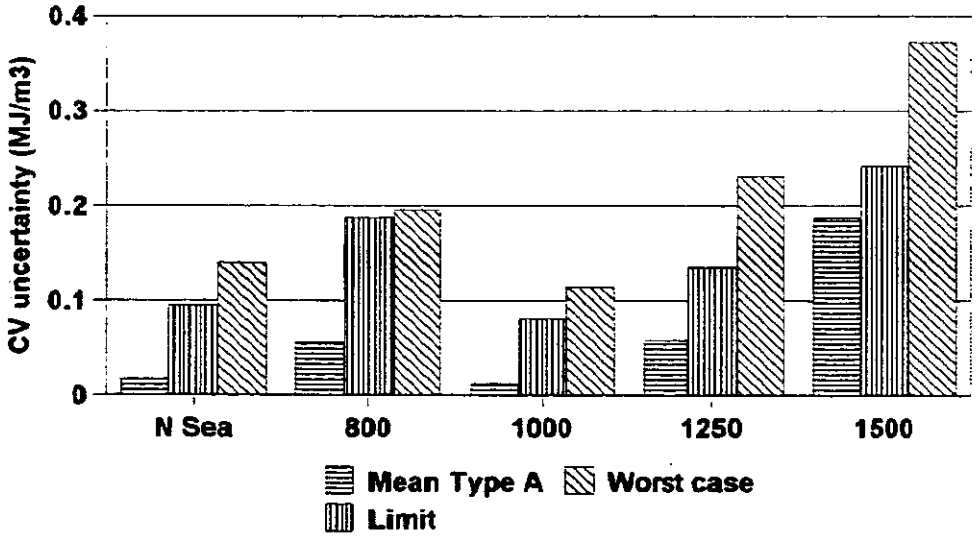

Figure 3. CV uncertainty derived from component random errors

With the best component precision (Mean Type A), there is a large difference in CV uncertainty according to composition (greater than a factor of 10). With the Limit precision,

only the high methane gases have CV uncertainty less than 0.1 MJ/m^3, and none of the gases in the Worst Case. These last figures would be good reason to reject an instrument. The Limit values can thus be seen to be appropriate for high methane gases, and if a CV uncertainty of 0.1 MJ/m^3 is required for other compositions, a more stringent component precision would be required.

BIAS ERRORS

Significance of bias errors

For the purpose of this paper, we assume that there is no bias error associated with the calibration gas, and that such error derives from deviations from response linearity, under circumstances where the data handling procedures assume that all components show fully linear response. It is possible, by multi-level calibration, to recognise and allow for non-linear response, but it is not the usual practice. We are only considering analyser response, because a faulty calibration gas is easily replaced, whereas an analyser is not.

Non-linearity of response is illustrated in Figure 4.

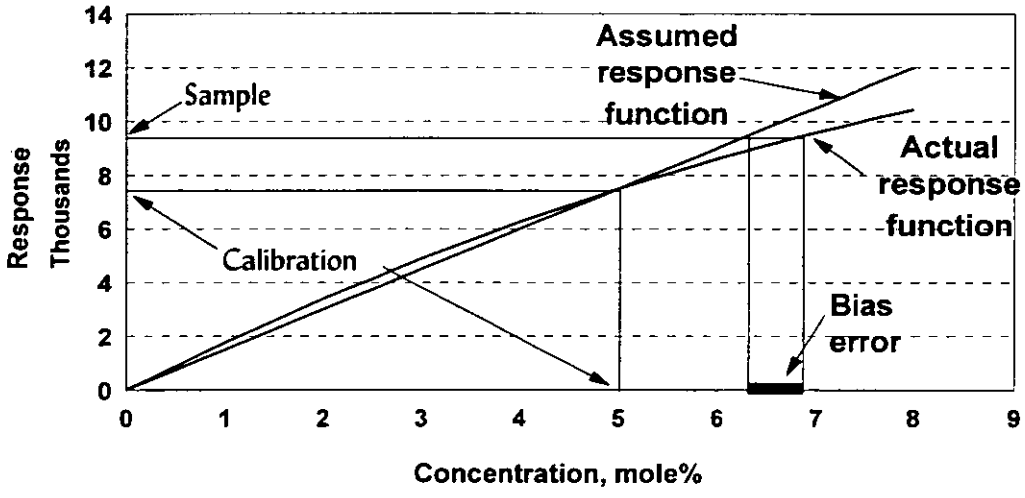

Figure 4. Bias error due to non-linearity

Bias errors only arise when the analyser is calibrated with a gas whose composition is significantly different from that of the sample. If they are effectively the same, or very similar, they will be using the same part of the response curve, and its shape does not matter, except that the response should increase with increasing component concentration. The circumstances described in the previous section, where the primary calibration gas, the certified daily calibration gas and the sample had very similar concentrations, would not give rise to significant bias error. We are not always so fortunate, however, and sample differences can cause problems.

The bias error for a component i depends upon the measured (f_i) and assumed (g_i) response functions, and upon the component concentrations in the calibration gas (x_{istd}) and the sample ($x_{isample}$), according to

$$\text{Error}_i = g_i^{-1} \times \left[\frac{g_i(x_{istd}) \times f_i(x_{isample})}{f_i(x_{istd})} \right] - x_{isample}$$

The error tends to zero as the function f_i and g_i converge, or as the concentrations x_{istd} and $x_{isample}$ converge. Bias errors are either positive or negative, as opposed to random errors, which define an uncertainty area about the "true" value. They can therefore reinforce or cancel each other's contribution to a property. Thus a positive bias error for nitrogen will reduce the resulting CV; a similar positive error for ethane will increase the CV, largely cancelling the effect of nitrogen.

Application of bias errors

The fact that bias errors are positive or negative means that it is more difficult to generalise about their effects. The following calculations use the same five compositions described above, with each being used in turn as calibration gas for analysis of the others. The measured response function is taken from the typical behaviour of a Type A analyser, and the assumed response function is complete linearity, i.e. a straight line through the origin. The resulting CV errors are listed in Table 2 and illustrated in Figures 5 and 6

. Table 2. CV bias derived from component bias errors

Calibration gas	Sample gas CV bias error - MJ/m^3				
	N. Sea gas	800 BTU	1000 BTU	1250 BTU	1500 BTU
N. Sea gas	0	0.540	-0.002	-0.112	-0.277
800 BTU	-0.014	0	-0.037	-0.018	-0.143
1000 BTU	0.005	0.556	0	-0.094	-0.275
1250 BTU	0.021	0.476	-0.003	0	-0.157
1500 BTU	0.021	0.385	-0.015	0.091	0

Figure 5 illustrates the CV bias as a function of the calibration gas, and Figure 6 as a function of the sample gas.

For the North Sea and the 1000 BTU gases, the bias error in each case is small when compared to a typical CV uncertainty requirement of 0.1 MJ/m^3. In such a case, the bias error is small enough to be ignored - it would be lost in the random uncertainty noise associated with the calculated CV. For the other gases, particularly the 800 and 1500 BTU gases, the bias error is significant and (probably) unacceptable. The solution in this case would be to choose an analyser with a more favourable response function, or, more simply, to choose a calibration gas closer in composition to, and hence better adapted for that type of sample.

It is interesting to note that the bias depends more upon the sample than upon the calibration gas. Figure 6 shows more closely consistent sets of bias errors when categorised according to the sample, and by far the lowest bias when the sample is a high methane gas. This can be explained intuitively. If the sample gas were pure methane, then the nature of the calibration

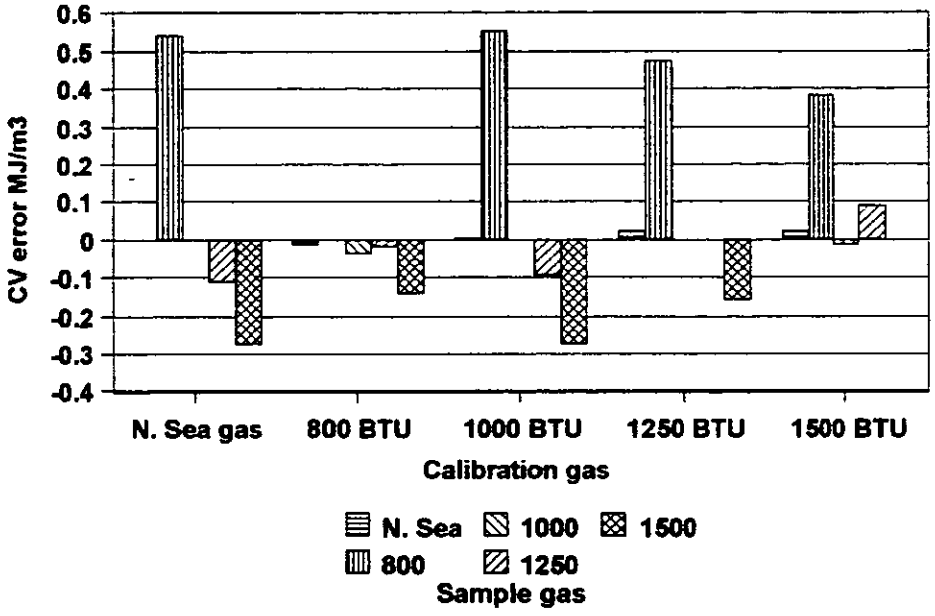

Figure 5. CV bias as a function of calibration gas

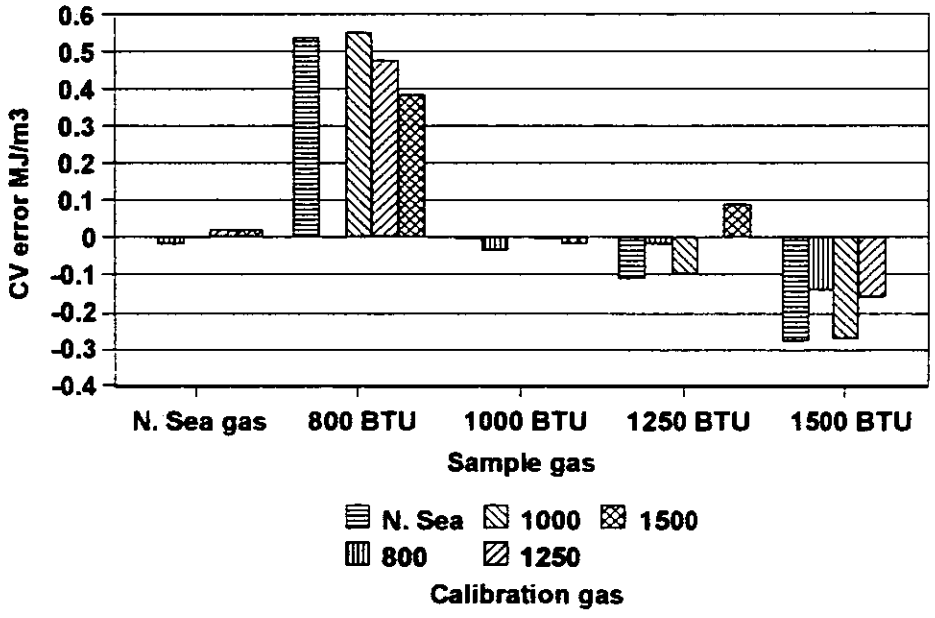

Figure 6. CV bias as a function of sample gas

gas is unimportant. Bias errors resulting from different calibration gas compositions would cause the measured methane in the sample to be different from 100%, but in the absence of any other measured components, normalisation would return the value to 100%. The further the sample composition deviates from pure methane, the greater the potential for bias errors to be significant.

It is unwise to generalise about the size of bias errors. If the North Sea gas is used as a calibration mixture for analysis of the 1500 BTU gas, the resulting bias error would be -0.277 MJ/m^3. If their roles were reversed, the bias would be 0.021 MJ/m^3.

ALTERNATIVE PROCEDURE

The use of seven test gases is not always practically convenient. Offshore operations are an obvious case in point. We have therefore considered and tested an alternative approach, using injection of a single gas at different pressures to simulate gases of different compositions. Figure 7 illustrates this approach.

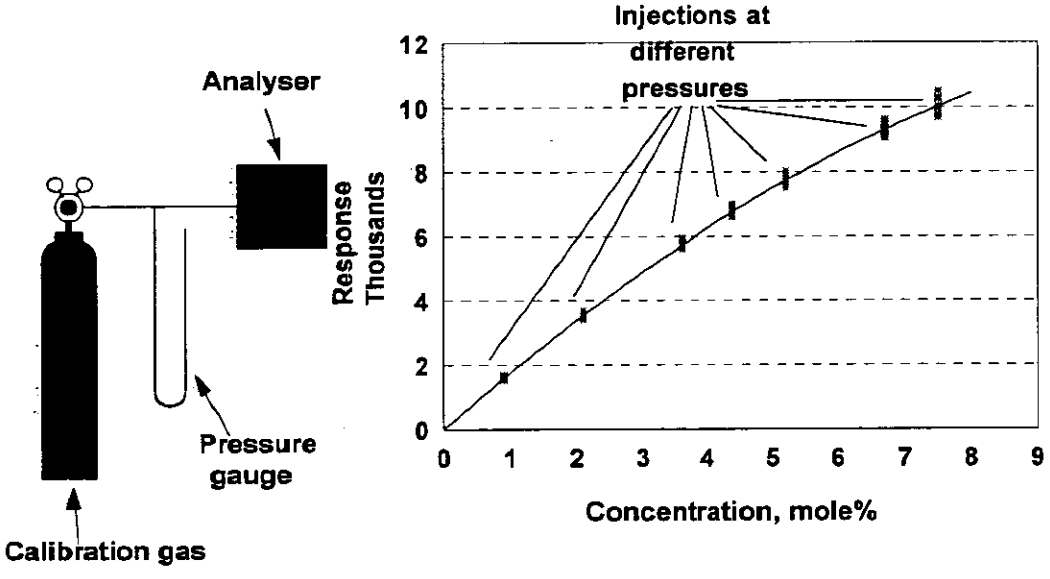

Figure 7. Variable pressure injection

The best choice for the single gas to be used is the existing calibration gas, which should have been chosen to be compatible with the expected sample compositions. Apart from convenience, an interesting feature is that the accuracy requirement for the test procedure is transferred from the seven test mixtures to the means of pressure measurement. Calculations show that the inherent accuracy of the evaluation procedure remains comparable, whichever procedure is followed.

CONCLUSIONS

ISO 10723 offers a procedure for natural gas analyser evaluation which quantifies the uncertainty of component measurement. The resulting data can be used directly, for product allocation, for example, or to compute properties such as CV, in which case the property uncertainty can be derived from the component data. Regular application of this procedure (for example, annually) would ensure that the user has an up to date certificate which describes the analyser's performance. With such a certificate, the user can confidently demonstrate that the analyser's contribution to, for example, fiscal metering is satisfactory.

An alternative approach, whereby instead of seven test gases, a single gas is used at a range of pressures, has been assessed and shown to be satisfactory.

REFERENCES.

1. ISO 10723 : 1995, Natural gas - Performance evaluation for on-line analytical systems, International Organisation for Standardisation, Geneva.

2. ISO 6976 : 1995, Natural gas - Calculation of calorific values, density, relative density and Wobbe index from composition, International Organisation for Standardisation, Geneva.

3. American Petroleum Institute, Committee on Gas Fluids Measurement, Chapter 14.1 (Natural Gas Sampling) Working Group.

NSFMW.97

North Sea FLOW Measurement Workshop

Paper 29: 5.3

MFI WATERCUT METER - A FISCAL METER

Authors:
Styrk Nordborg and Tone Kristin Børslid, Statoil, Norway
Magnus Hebenes, Multi-Fluid ASA, Norway

Organiser:
Norwegian Society of Chartered Engineers
Norwegian Society for Oil and Gas Measurement
Co-organiser:
National Engineering Laboratory, UK

MFI WATERCUT METER - A FISCAL METER

Authors:
Styrk Nordborg and Tone Kristin Børslid
Statoil, Norway
Magnus Hebnes
Multi-Fluid ASA, Norway

SUMMARY

Two MFI WaterCut Meters have since January 1996 been under testing at the Tordis oil metering station at Statoil's Gullfaks C platform. As a result of these test the Norwegian Petroleum Directorate (NPD) has given temporarily approval for fiscal use on Tordis throughout 1997.

The WaterCut Meters (WCM) are being tested with reference to the automatic sampling system. Conversion factors from laboratory to line conditions have been developed. Important issues for these test are long term stability and minimum down-time.

1 INTRODUCTION

Tordis is a subsea oil field located 12 km north-west of Statoil's Gullfaks C platform. Saga Petroleum operates Tordis remotely from Gullfaks C where the processing is done. Both produced oil and gas are measured to fiscal standards according to the NPD regulation and used for allocation.

The Tordis oil metering station is located after the 1st. stage separator. The temperature is 63 ^{0}C and pressure 70 bar. The oil contains 16 % to 18 % gas, but is stable at line conditions. The water content has during the test period varied from 0,1 to 22 %. Sand is also periodically present. The samplers does not handle these conditions well.

Long term stability and trouble free operations at high pressure and temperature conditions, are issues to be considered thoroughly. The accuracy of the MFI WaterCut Meter has been thoroughly tested under controllable conditions at the Mongstad Terminal [1]. The accuracy has also been tested at the BP Forties Field [2], but at considerable lower pressure than for the Tordis metering station .

The sampling and analysis procedures [3] [4] and sampler maintenance are time consuming both for operators and lab technicians. Using on-line measurement reduces the total operating costs.

2 WATERCUT METER INSTALLATION

The Tordis production is separated in two trains, A and B, each train having dedicated metering runs, sampler and MFI WaterCut Meters. The WaterCut Meters are located on the outlet headers, immediately before the in-line samplers.

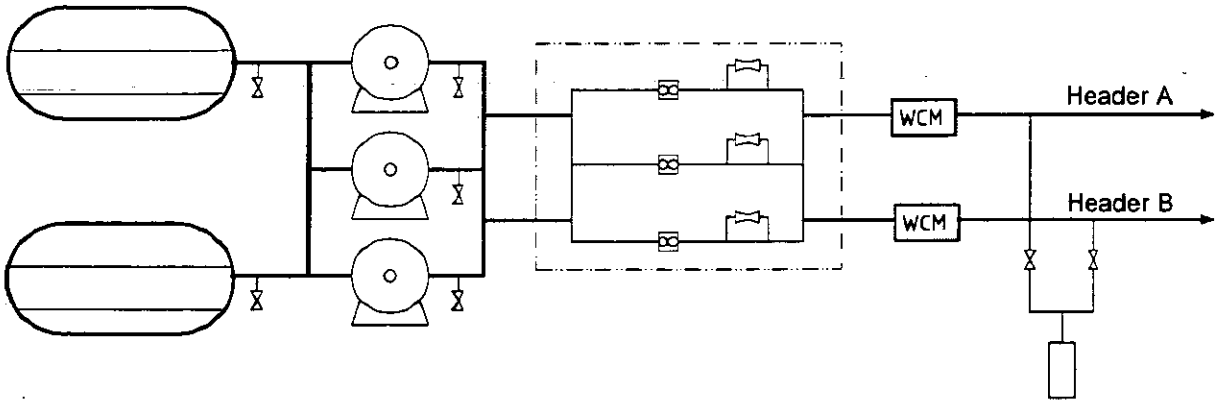

Figure 1. Installation

Both samplers are connected to the same sampling cylinder, sampling flow proportionally from separate production trains.

To get a representative sample from Tordis, both samplers must operate correctly. Tests at Tordis have shown high differences in grab samples. The volumes can vary from 0,8 ml to 1,2 ml. When two samplers with varying grab volumes, are sampling from different production train into one cylinder, the measurement uncertainty becomes high.

During 1996 the samplers were dismantled for repair 28 times, which gives us about 40 days without sampling. In agreement with the NPD the WaterCut Meters were used as back-up.

The two WaterCut Meters installed at the Tordis tie-in at the Gullfaks C platform are 6" full-bore monitors. The WaterCut Meters installed are LowCut models (0-20 % water range) and the AutoZero function is implemented.

The mixture density is measured by a Solatron densitometer interfaced to an Entelec main computer in a safe area. The mixture density from header A and B is transmitted to the WaterCut Meters on a RS422 link. As a result, all measurements and calculations performed in the WaterCut Meter are available and returned via the link to the Entelec main computer.

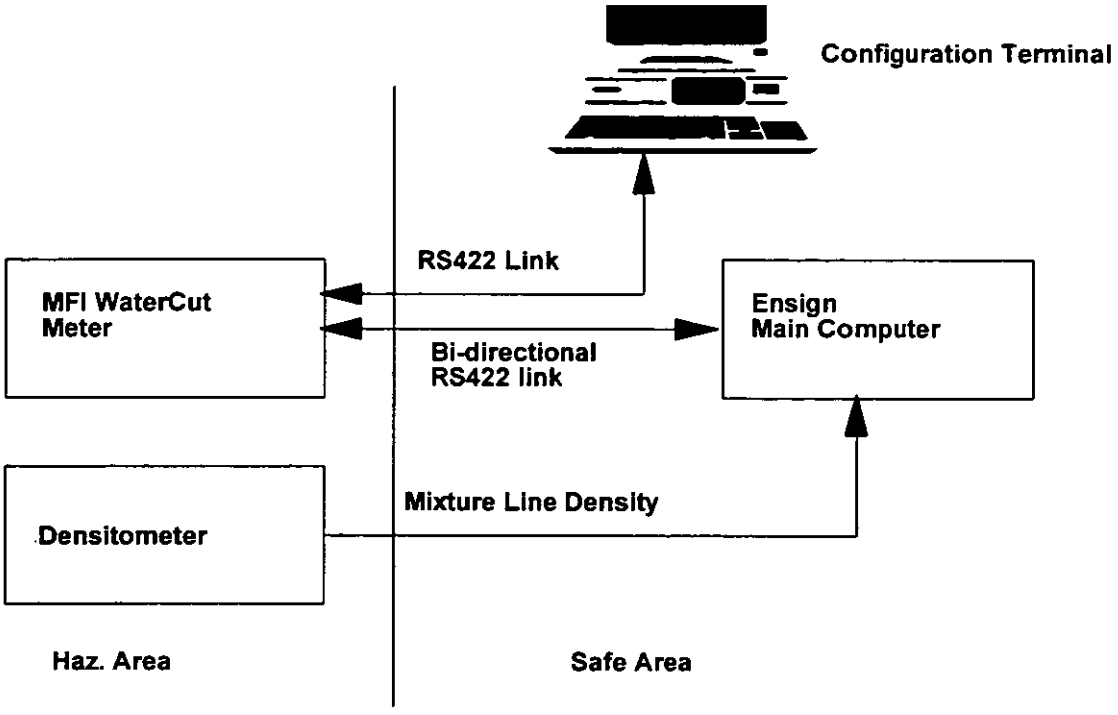

Figure 2. Block functional diagram

3 MEASUREMENT PRINCIPLE

3.1 MFI WaterCut Meter description

The MFI WaterCut Meter is a field instrument which determines the water content of mixtures of water and hydrocarbons by measuring the dielectric constants of the mixture. This basic method takes advantage of the large difference in the dielectric constants of hydrocarbon liquids and water respectively. The dielectric constant of water is far higher than that of oil. Thus, as the water content in a mixture increases, so does the mixture dielectric constant.

The WaterCut Meter uses the resonant cavity method to measure the mixture dielectric constant. A resonant cavity is a closed metal structure from which electromagnetic energy cannot escape. The WaterCut Meters are constructed such that the electromagnetic waves transmitted into a particular flowing mixture will, at a characteristic frequency (wavelength), resonate to produce a distinct peak amplitude. This peak corresponds directly to the water content of the mixture in that the characteristic resonant frequency is inversely proportional to the square root of the mixture's dielectric constants.

The resonant cavity method has long been a standard laboratory technique for measuring the dielectric constants of material samples.

3.2 Automatic Calibration (AutoZero)

The MFI WaterCut Meter uses an automatic calibration feature called the AutoZero function. With this feature the WaterCut Meter can continuously adjust its baseline calibration to minimise errors associated with changes in types of crude oil. Automatic calibration, therefore, significantly increases the accuracy of the Meter and reduces maintenance.

In operation the AutoZero function works as follows. First the WaterCut Meter determines the mixture density from the density input signal. Then it measures the raw dielectric constant of the mixture using the microwave sensor. Finally it shows a complex set of simultaneous equations to determine the correct Dry Oil Density and water content for the particular mixture.

4 CONVERSION FROM LAB TO LINE CONDITIONS

As the WaterCut meters are installed right after the 1st. stage separator, where the mixture has a high temperature and pressure, and a high gas content, conversion factors between lab and line conditions had to be developed for calibration purposes.

For Tordis oil which is stable at high line pressure, some of the oil will evaporate when a sample is taken for laboratory analysis. There is also volume change due to pressure and temperature changes. The shrinking factor, which is given as the volume ratio between the dry oil at line conditions and standard conditions, will include the evaporation as well as the PT corrections.

The water content found from the Karl Fisher titration method is given in weight percent pure water in relation to the weight of the sample mixture. This sample weight also includes the weight of salt.

In order to convert the Karl Fisher value to the corresponding volume percent water at line conditions, a determination of the evaporation is required.

Figure 3. Oil components

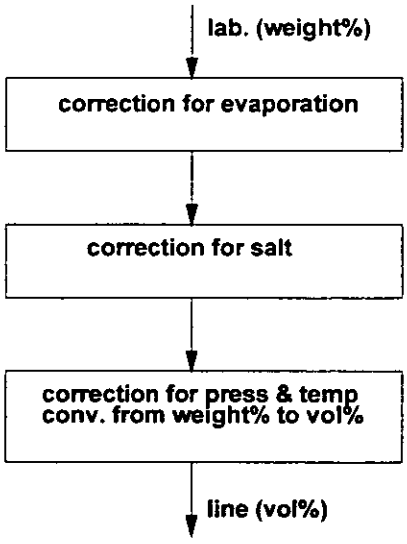

Figure 4. Conversion from lab to line conditions.

A simplified version of the upgraded Gullfaks C WaterCut Meters calibration calculations are shown below. New requirements are pressure, density of shrinked oil and shrinking factor as input parameters.

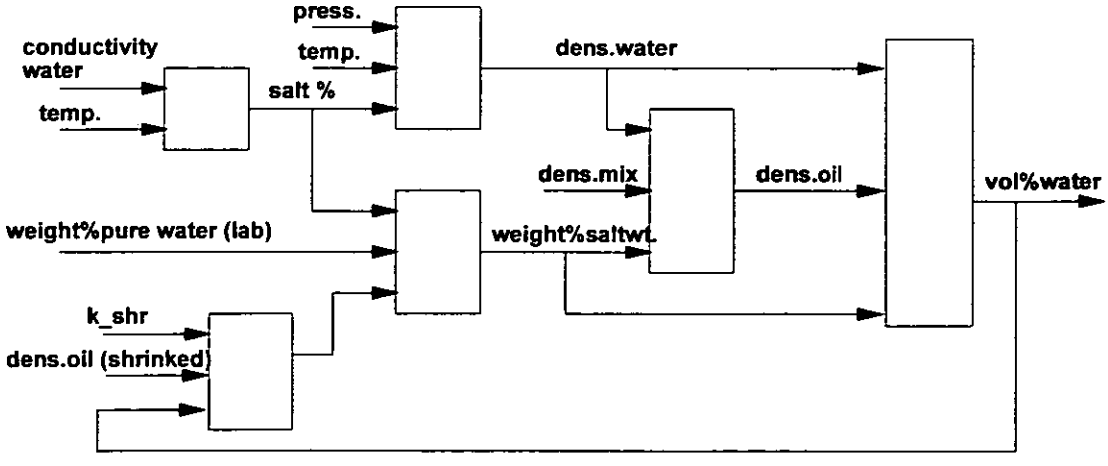

Figure 5. Simplified block diagram for calibration calculation.

5 TEST PROGRAM

A test program was started in January 1996. The initial idea was to compare spot samples with automatic measurements taken simultaneously at the WaterCut meter. However, as the spot samples were taken a considerable distance from the WaterCut meter, and the water content changed rapidly, it was not possible to get representative samples.

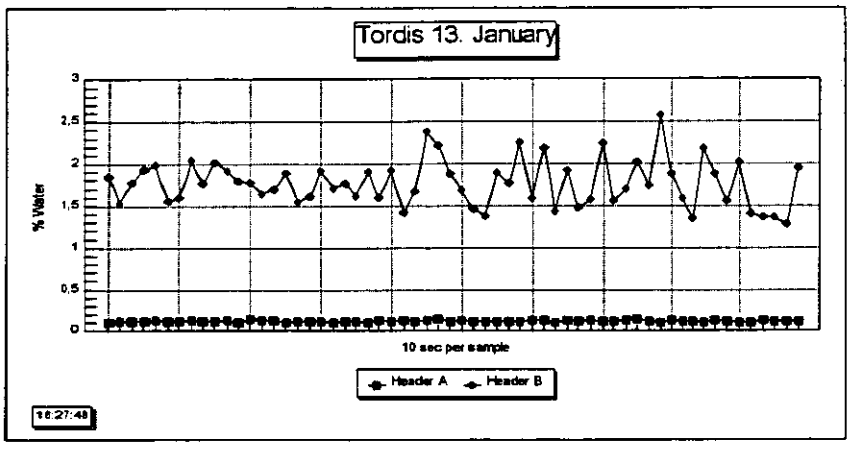

Figure 6. Changes in water fraction over a 10 minute period.

Figure 6 shows the water content on the B header varying from 1,3 % to 2,6 % through a 10 minutes period. Fig. 7 and 8 show a considerable difference between lab and on-line meter for water content above 1 %.

The WaterCut Meters were therefore tested separately with corresponding daily sampler as reference. An average of 24 hours from the WaterCut Meter was compared with the daily sample analysis.

6 TEST RESULTS

Results from January and February 1996 are presented below.

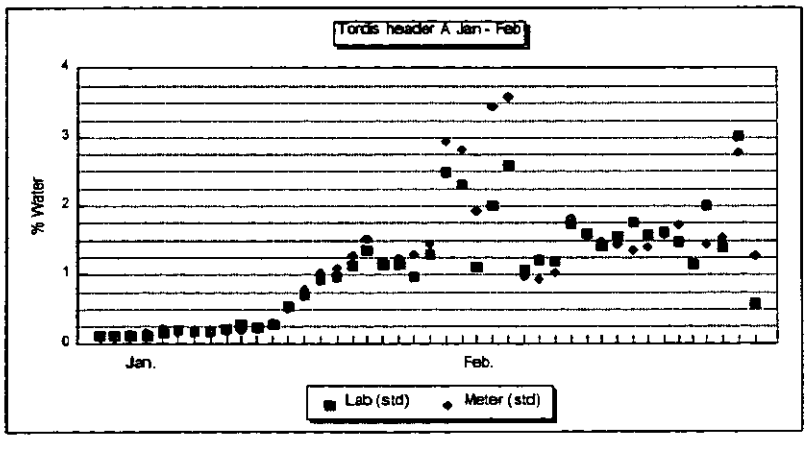

Figure 7. Spot samples compared to simultaneous readings from the WaterCut Meter

Both lab and meter values are converted to standard conditions. For water fractions below 1 % the sampling conditions were stable and the test show good agreement between spot samples and in-line meter. For water fractions above 1 % the deviation between reference and WaterCut Meter is explained by non-ideal reference conditions.

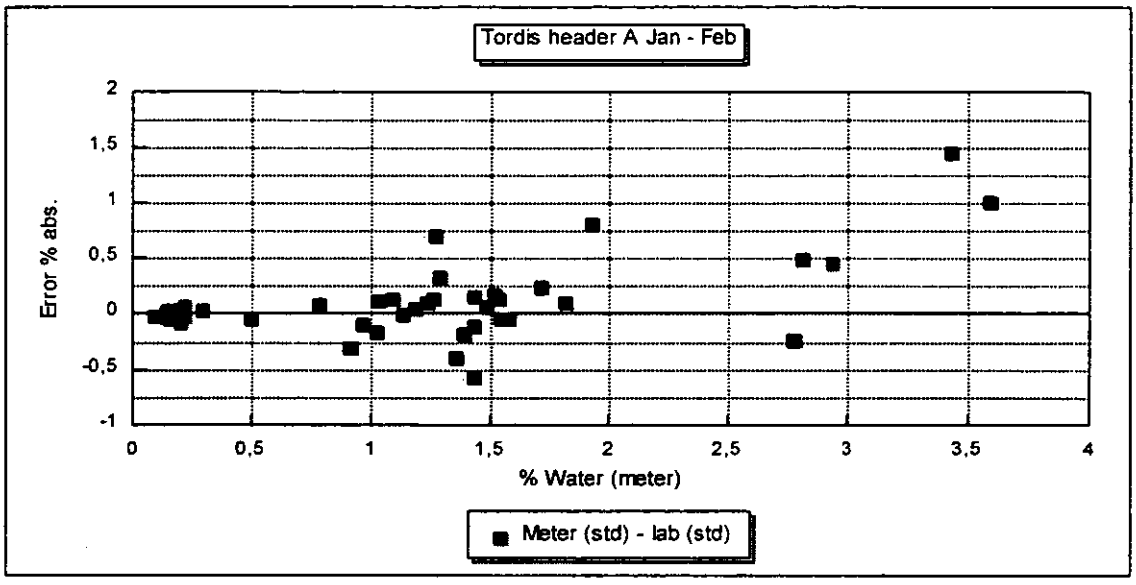

Figure 8, Deviation between spot samples and WaterCut Meter values in January and February.

Tests were done in May, September and November 1996 using the daily sampler as reference. During this period the water content varied from 0,5 % to 22 %. According to IP386, the Karl Fisher method can be used from 0,02 % to 5 %. For high water contents both Karl Fisher and centrifugal analysis were used. For high water contents the difference between lab and on-line values can be explained by the negative effect of emulsion breaker on the laboratory analysis.

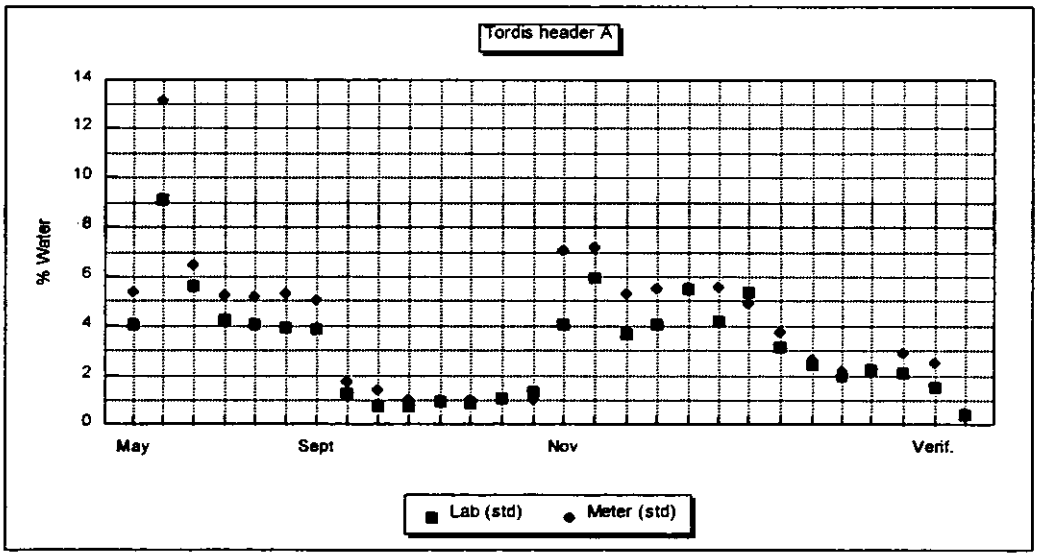

Figure 9. Daily samples and 24 hours flow weighted WaterCut Meter values, header A, included the following verification tests in -97.

For low water fractions the daily samples and the WaterCut Meter values correspond. The deviation increases with increasing water fraction. So does the uncertainty in the Karl Fisher analysis.

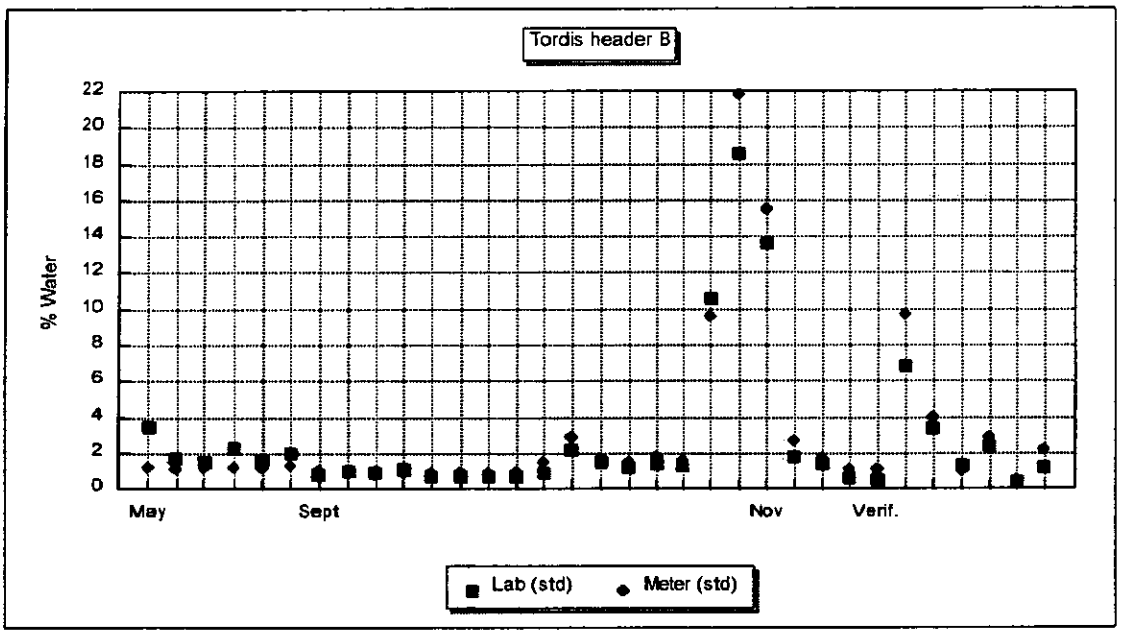

Figure 10, Daily samples and 24 hours flow weighted WaterCut Meter values, header B, included verification tests in -97.

The exceptionally high water contents at the end of September were due to separator problems. It gave us an unique opportunity to test the WaterCut Meter at the limit of its operational range. The WaterCut Meters measured the rapidly changing water contents without any difficulty.

7 CONCLUSION

The MFI WaterCut Meter has been successfully tested at the Tordis oil metering station. This has been a test site with highly non-ideal conditions. The WaterCut Meters have shown a significantly higher reliability and far less malfunctions than the automatic samplers. Long term stability and trouble free operation have been major issues in this test program. During the last one and a half years, the down-time of the WaterCut Meters has been neglibile.

Initial statistical work indicate good correlation between the MFI WaterCut Meter and traditional sampling also at Tordis operational conditions. The accuracy itself can not be fully verified under these conditions. However, the accuracy of the WaterCut Meters is previously tested under more ideal test conditions [1].

The NPD has temporarily approved the MFI WaterCut Meter as a fiscal water in oil monitor for use on Tordis. An application for permanent fiscal approval will be forwarded together with the results from the ongoing verification tests ultimo this year.

REFERENCES

1. OKLAND O., BERENTSEN H, OLSEN O.
   Testing water in oil monitors at the Mongstad Terminal,
   North Sea Measurement Workshop 1993

2. PURVEY R.
   Water In Oil: On-line measurement. The MFI WaterCut meter in offshore application
   North Sea Measurement Workshop 1994

3. INTERNATIONAL STANDARD - ISO 3171
   Petroleum liquids - Automatic pipeline sampling

4. STANDARD METHODS FOR ANALYSIS AND TESTING OF PETROLEUM AND RELATED PRODUCTS
   IP386/90 (ASTM D4928-89)
   Determination of water content of crude oil - Coulometric Karl Fisher method

5. MFI WATERCUT METER - INSTALLATION AND USER' S MANUAL
   Multi-Fluid ASA

NSFMW.97

North Sea FLOW Measurement Workshop

Paper 30: 6.1

CORIOLIS METER FOR LPG CUSTODY TRANSFER AT PETROBRAS

Authors:
Virgilio Antonio Rezende, Petrobas, Brazil
Cathy Apple, Micro Motion Inc. USA

Organiser:
Norwegian Society of Chartered Engineers
Norwegian Society for Oil and Gas Measurement
Co-organiser:
National Engineering Laboratory, UK

CORIOLIS METER FOR LPG CUSTODY TRANSFER AT PETROBRAS

Virgilio Antonio Rezende
Petrobras, Brazil
Cathy Apple
Micro Motion, Inc., USA

SUMMARY

Testing was conducted at Petrobras to evaluate the suitability of a Coriolis meter to measure the mass of LPG in a custody transfer application. The test results demonstrate that the Coriolis meter is capable of accurate volume and density measurement, which verifies the capability of the Coriolis meter to accurately measure mass. When the Coriolis meter tests began, some mistakes were made in zeroing the meter. From the proving results, one can clearly see the impact of not properly performing the Coriolis meter's zero calibration, and the improvement in measurement accuracy once the meter is properly zeroed. Presently, the Coriolis meter shows less variation than the turbine meter and densitometer, which are being used to measure mass.

INTRODUCTION

The standard Petrobras LPG mass measurement system consists of turbine meters, vibrating tube densitometers, and flow computers for performing mass calculations and totalizing. Petrobras became interested in using Coriolis meters for custody transfer LPG measurement because they provide significant advantages over conventional mechanical meters: low maintenance, low cost, and multivariable measurement. The Coriolis meter is unique in that it provides both a direct mass flow measurement, and an independent density measurement, from which the volumetric flow rate can also be determined. Since there are no petroleum standards currently available for Coriolis meters, Petrobras initiated a test program to evaluate the suitability of a Coriolis meter for the custody transfer measurement of LPG.

TEST SETUP AND PROCEDURES

The primary objective of the testing was to evaluate the ability of a Micro Motion model CMF300 Coriolis meter to measure the mass of LPG in a custody transfer application. A Brook's Compact Prover was used to evaluate meter flow measurement accuracy. This prover measures volume, and was not instrumented with a densitometer to determine the mass of the fluid measured by the prover. Since equipment was not available for mass proving, Petrobras decided to field prove the Coriolis meter's volume and density measurements. If the volume and density measurements are acceptable, the mass must also be acceptable, because the Coriolis meter volume is derived from the mass and density measurements. Because a Compact Prover was used, the Coriolis meter could not be tested at the normal delivery flow rate of $\approx$300 m^3/hr. Due to response time constraints, the Coriolis meter requires at least a 0.67 second prerun time prior to beginning to accumulate flow pulses. In order to meet this prerun requirement the Coriolis meter proving flow rate was limited to 210 m^3/hr or less. Inventory comparisons between the turbine meter and Coriolis meter were performed to

determine if a meter factor obtained for the Coriolis meter at an average flow rate of 170 m^3/hr would be valid at higher flow rates.

A secondary objective was to compare the performance of the Micro Motion CMF300 Coriolis meter to the existing measurement devices, the 6" Smith turbine meter, and the Dynatrol densitometer. A schematic of the field test facility employed at Petrobras' REPLAN refinery is shown in Figure 1.

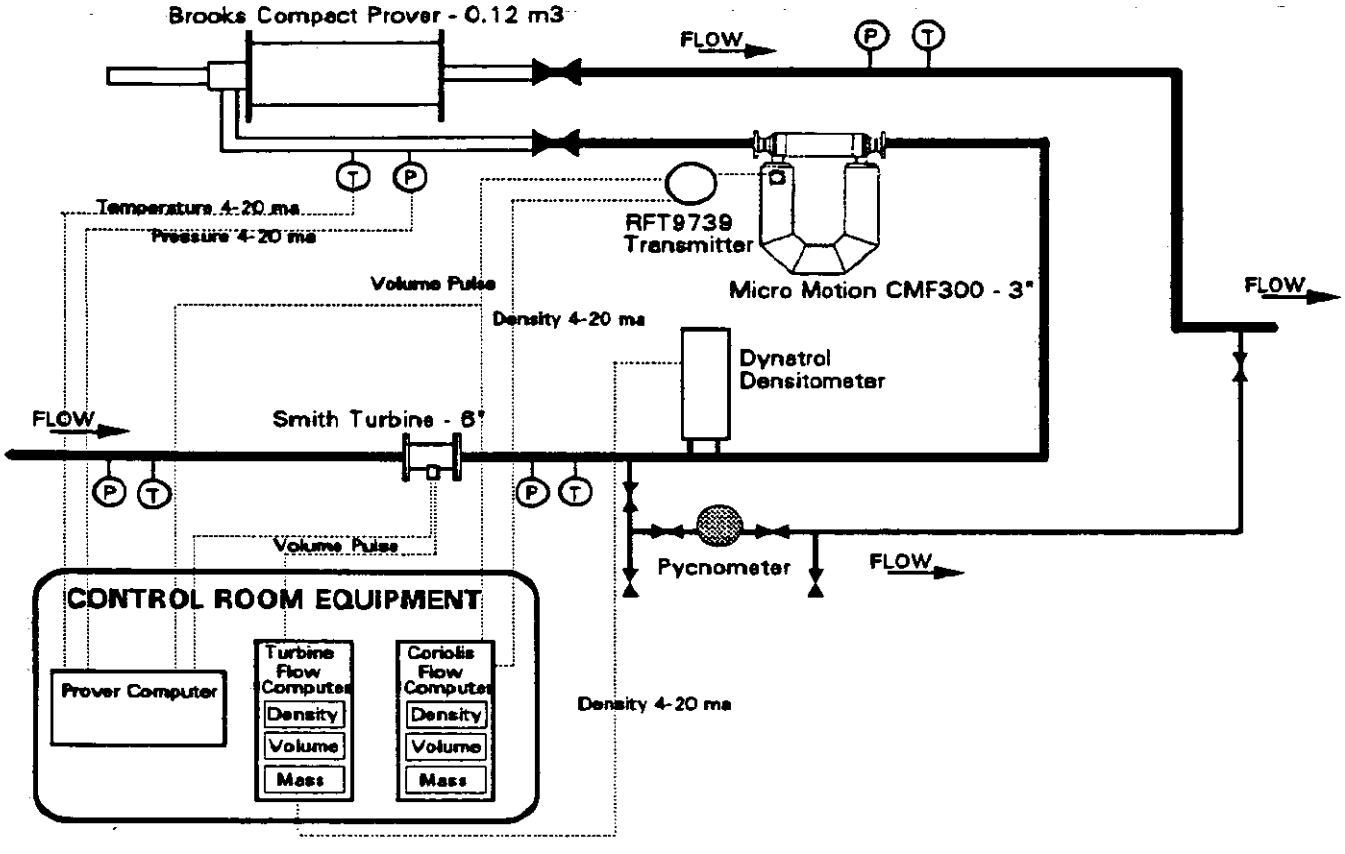

Figure 1. Petrobras REPLAN field measurement test facility

The volumetric flow measurement of the turbine and the Coriolis meter were proved against the 0.12 m^3 Brooks Compact Prover. Proving sessions were typically performed at least once per month for one year. For the turbine meter each proving consisted of 5 runs of 4 passes each. For the Coriolis meter 3 runs of 12 passes each were used. The meter factor was calculated by dividing the prover volume by the meter's measured volume. On average, 4-5 provings were performed for each proving session. The flow rate was usually varied between provings to evaluate the linearity of the meters. The prover computer would only accept one meter input, so the meters were not proved simultaneously.

The Dynatrol and the Coriolis meter's density measurements were proved with a pycnometer. The pycnometer is a pressure vessel of known volume and evacuated weight. Density is determined by weighing the filled vessel, and calculating density by dividing the mass of the product by the known volume. The pycnometer system was located at the Dynatrol. The procedure that was employed was to take the pycnometer sample and obtain the density measurements from the flow computers via radio transmission from the control room. The density indications from both the Dynatrol and the Coriolis meter were recorded simultaneously. The density factor is equal to the pycnometer density divided by the meter's density reading. The limitation with this method is that the Coriolis meter is located approximately 12 meters from the pycnometer, and the conditions at the meter will generally be slightly different than at the pycnometer - resulting in somewhat different densities at these two locations. The density difference between the pycnometer and the Coriolis meter does not remain constant because the pressure drop between the two locations changes with changing flow rate. The density of LPG is significantly affected by the operating pressure. The effect of pressure differences was not studied.

The inventory comparisons between the turbine and the Coriolis meter were very straightforward. After normal product deliveries to customers, the volume totals from the turbine and Coriolis meter were obtained from their respective flow computers. The Coriolis meter totals were compared to the turbine meter totals.

TEST RESULTS AND DISCUSSION

Volume Meter Factors

Table 1 shows the results of the volumetric provings from June 1995 to January 1996.

Table 1. Volume meter factor summary - June 1995 to January 1996

	CORIOLIS METER			TURBINE METER		
DATE	AVERAGE METER FACTOR	AVERAGE REPEAT. (%)	METER FACTOR VARIATION (%)	AVERAGE METER FACTOR	AVERAGE REPEAT. (%)	METER FACTOR VARIATION (%)
29-Jun-95	1.0112	0.018	0.186	0.9279	0.033	0.112
12-Jul-95	1.0122	0.020	0.210	0.9281	0.026	0.049
27-Jul-95	1.0121	0.035	0.254	0.9290	0.030	0.169
9-Aug-95	1.0110	0.031	0.157	0.9276	0.022	0.117
13-Sep-95	1.0111	0.039	0.279	0.9283	0.035	0.199
28-Sep-95	1.0112	0.031	0.167	0.9297	0.021	0.176
10-Oct-95	1.0123	0.032	0.527	0.9285	0.044	0.061
8-Dec-95	1.0107	0.036	0.064	0.9292	0.031	0.103
5-Jan-96	1.0140	0.031	0.129	0.9294	0.040	0.166
AVERAGE	1.0118	0.030	0.219	0.9286	0.031	0.128

As was stated previously, an average of 4-5 provings were performed each proving session. The first column of data presents the average meter factor obtained from these proving sessions. The second column of data is the average of the repeatabilities obtained for each proving. The criteria for acceptable repeatability is the meter factor variation between proving runs must be less than 0.05%. It can be seen that both the Coriolis meter (0.030%) and the turbine meter (0.031%) meet the repeatability criteria. The third column shows the variation between the maximum and minimum meter factors from each proving session. The Petrobras criteria is that the meter factor variation between provings must be less than ±0.15%. The variation between the average meter factors for the Coriolis meter fell within acceptable tolerances, except for January 5. However, the Coriolis meter showed excessive meter factor variation between the provings performed each session. Also, the average meter factor for the Coriolis meter (1.0118) indicated that it was reading low by approximately 1.2%. The meter factor should be much closer to 1.0000, for there to be agreement with the meter's factory calibration. It was felt that the Coriolis meter should perform better.

Upon consulting with Micro Motion, it was suggested that the Coriolis meter had not been properly zeroed. In order to validate this hypothesis, the meter factors for the Coriolis meter were plotted against flow rate, as shown in Figure 2.

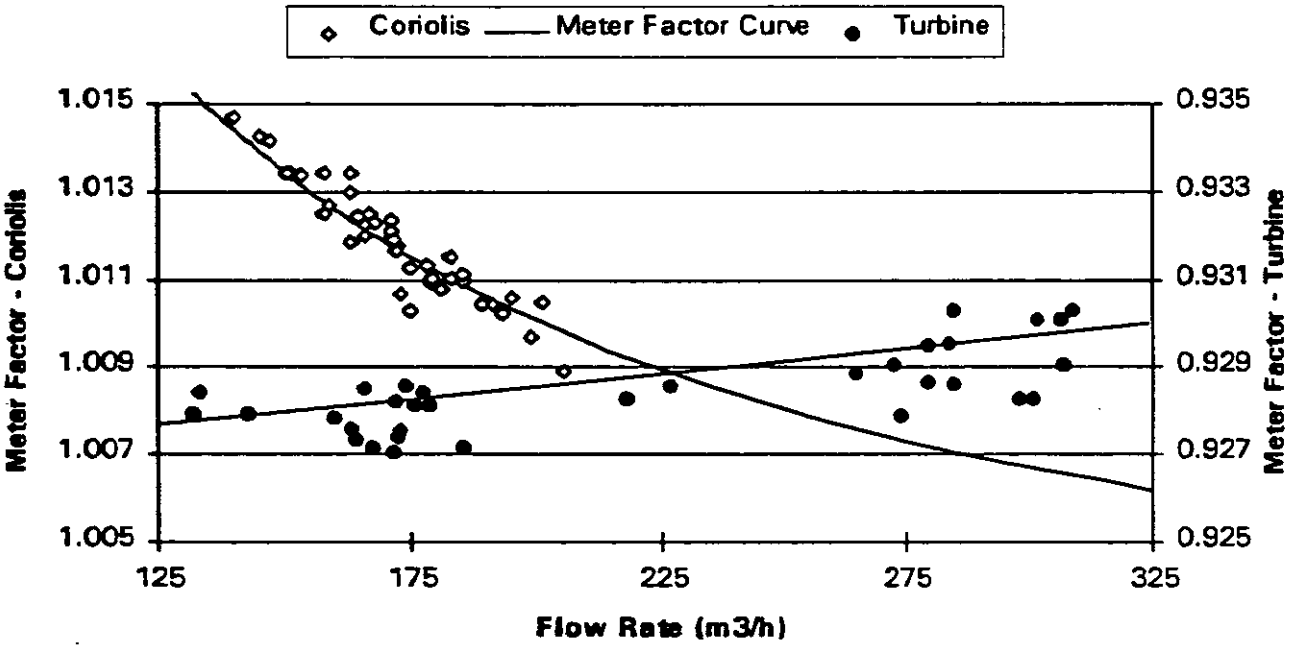

Figure 2. Coriolis and turbine meter factors versus flow rate (prior to rezeroing the Coriolis meter)

The data shows the characteristic trend of an improperly zeroed Coriolis meter. Probable causes of the improper zeroing of the Coriolis meter are: the meter was zeroed with a small amount of flow going through meter, or the meter was not zeroed when a new transmitter was installed. Micro Motion does not recommended routine meter rezeroing. However, they

advise occasional checking of the meter zero. Equation 1 is used to determine if the meter needs to be rezeroed.

$$\text{Flow Measurement Error } (\%) = \frac{\text{Flow rate indication with no flow}}{\text{Normal operating flow rate}} * 100 \qquad (1)$$

Flow is halted, then the meter's flow rate indication with no flow is recorded. Equation 1 is used to calculate the resulting error. If the error exceeds acceptable tolerances, the meter should be rezeroed.

The Coriolis meter was rezeroed on January 15, 1996. Figure 3 shows that rezeroing dramatically improved the linearity of the meter. In addition, rezeroing resulted in an average meter factor for the Coriolis meter of 0.9991. Therefore, the difference between the prover and the meter's factory calibration is only 0.09%.

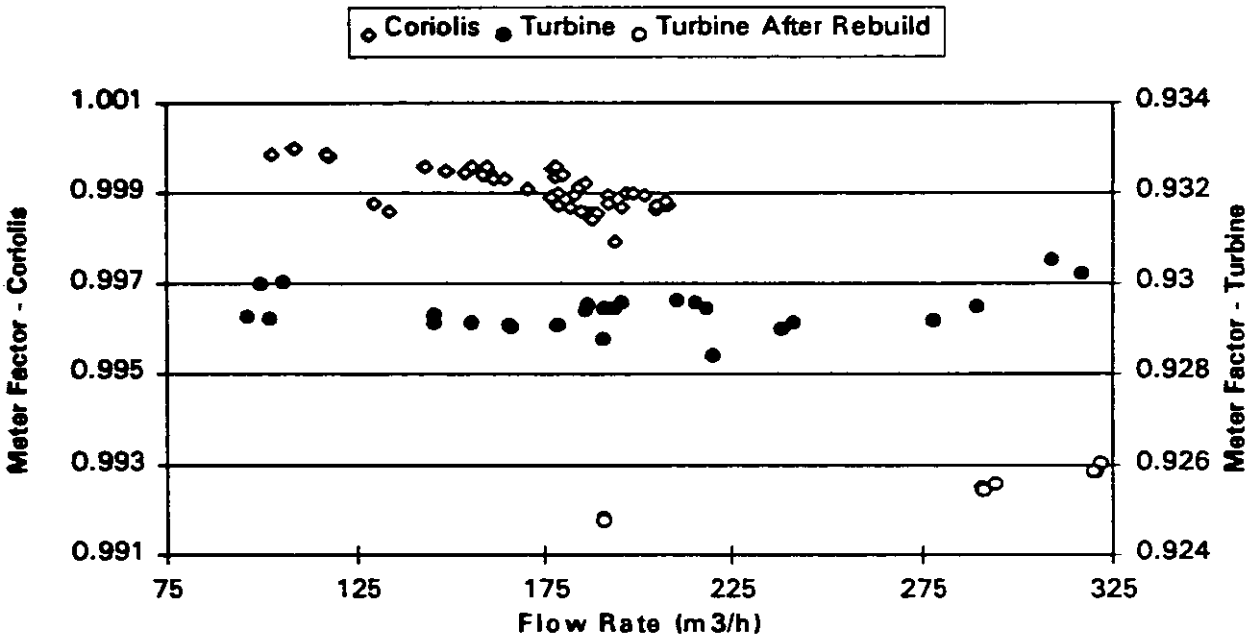

Figure 3. Coriolis and turbine meter factors versus flow rate (after rezeroing the Coriolis meter)

Table 2 presents the meter factor summary from January 1996 to May 1996. This table shows several interesting points. First, the average proving repeatabilities for both the turbine (0.036%) and the Coriolis meter (0.032%) are well within the 0.05% requirement. Second, the meter factor variation between provings improved tremendously for the Coriolis meter (average of 0.043%). Finally, a hole developed in the strainer upstream of the turbine meter, and some "dirty" LPG damaged the turbine meter. The turbine meter was rebuilt on May 14, 1996. The Coriolis meter was unaffected by exposure to the "dirty" LPG. In summary, once the Coriolis meter was zeroed properly its performance was excellent.

Table 2. Meter factor summary - January 1996 to June 1996

	CORIOLIS METER			TURBINE METER		
DATE	AVERAGE METER FACTOR	AVERAGE REPEAT. (%)	METER FACTOR VARIATION (%)	AVERAGE METER FACTOR	AVERAGE REPEAT. (%)	METER FACTOR VARIATION (%)
19-Jan-96	0.9988	0.026	0.054	No provings for turbine		
24-Jan-96	0.9988	0.034	0.046	0.9296	0.043	0.079
9-Feb-96	0.9991	0.026	0.031	0.9290	0.026	0.037
23-Feb-96	0.9999	0.013	0.019	0.9296	0.061	0.082
8-Mar-96	0.9988	0.056	0.055	0.9294	0.033	0.145
27-Mar-96	0.9985	0.032	0.107	0.9293	0.030	0.121
28-Mar-96	0.9986	0.044	0.038	0.9293	0.032	0.031
16-Apr-96	0.9995	0.029	0.008	0.9292	0.021	0.016
21-May-96	0.9995	0.021	0.028	0.9273[a]	0.027	0.119
22-May-96	0.9995	0.030	0.019	0.9263[a]	0.028	0.163
29-May-96	0.9988	0.044	0.029	0.9255[b]	0.024	0.122
AVERAGE	0.9991	0.032	0.043	0.9293[c]	0.035[c]	0.073[c]

(a) Turbine bearings replaced and rotor cleaned May 14, 1996. One pick-up was still bad.
(b) Turbine pickup repaired May 23, 1996.
(c) Averages do not include values after turbine was repaired on May 14, 1996.

Density Factors

The density factors for the Dynatrol and the Coriolis meter are presented in Figure 4. While there was some scatter in the density factors for the Coriolis meter, the overall average was 1.00002, which is outstanding.

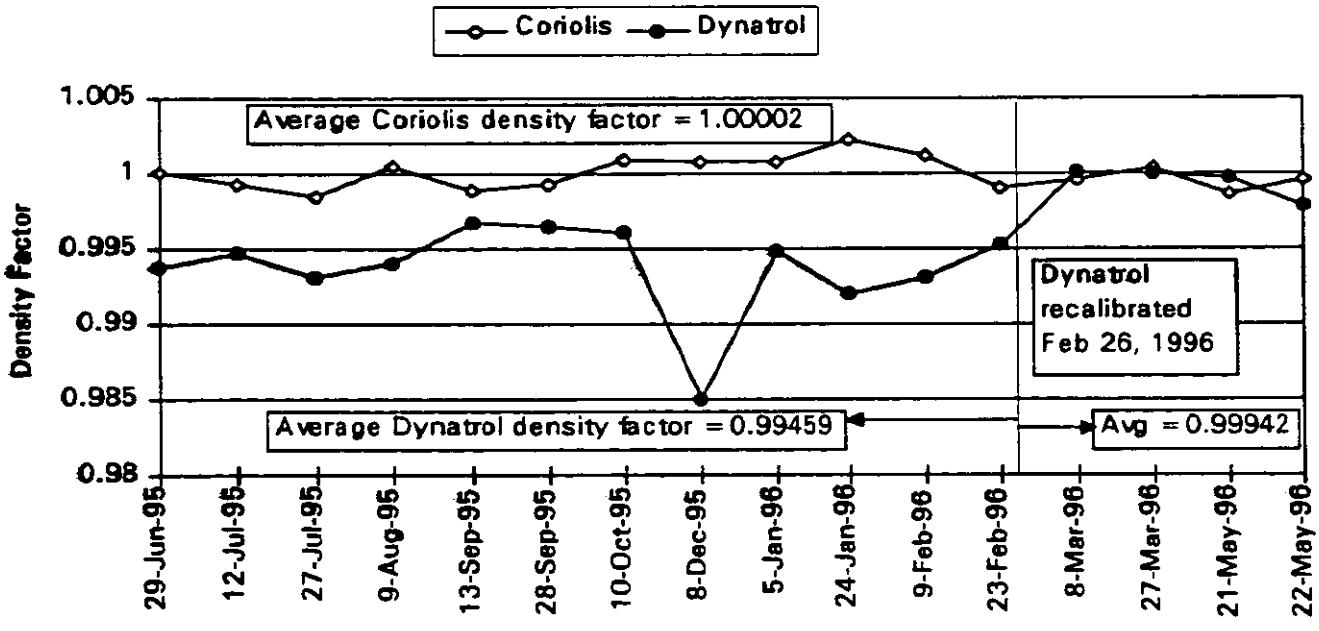

Figure 4. Density factors for Coriolis and Dynatrol density measurements

The scatter in the density factors for the Dynatrol were very similar to the Coriolis meter, except for an extreme point on Dec. 8, 1996. The repeatabilities for the density provings were fairly poor, the average repeatability for the Coriolis meter was 0.141%, and for the Dynatrol was 0.212%. The pycnometer proving procedure may not have been rigorous enough. In general, the density proving demonstrates the Coriolis meter's density measurement is very accurate and reliable.

Inventory Comparison

The gross volume inventory comparisons between the turbine and Coriolis meter are shown in Figure 5.

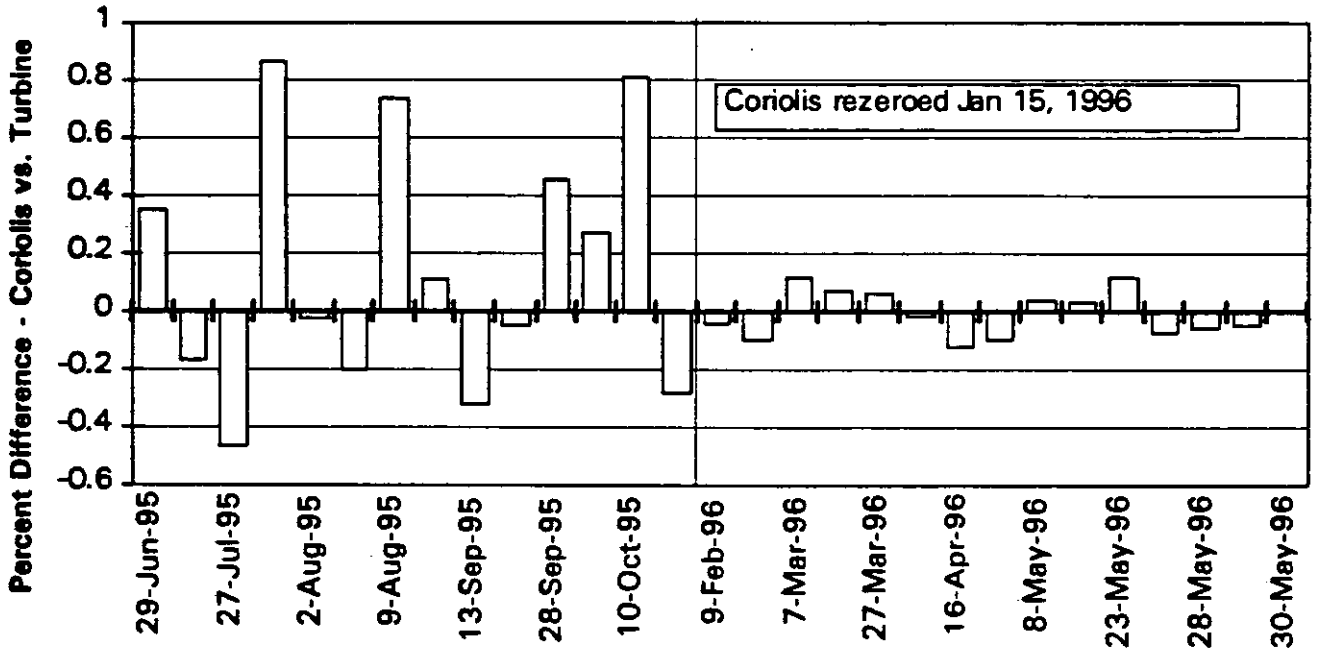

Figure 5. Inventory comparison between Coriolis and turbine meter measured volumes

The data prior to rezeroing the Coriolis meter is very disappointing. Six of the fourteen comparisons are outside of the Petrobras specification of 0.3% agreement between meters. These results are consistent with a zero offset in the Coriolis meter. The meter factor for the Coriolis meter that was programmed into the flow computer was 1.0117, based on an average flow rate of 170 m^3/h. However, the inventory comparisons were done at a variety of flow rates, up to 300 m^3/hr. Since the Coriolis meter was not properly zeroed, the meter factor determined at 170 m3/hr would not be applicable at other flow rates. For the remaining fifteen inventory comparisons after the meter was rezeroed, the greatest variation was 0.12%. These results demonstrate that if the Coriolis meter is properly zeroed, it can be proved at a low flow rate and be used to measure product at a higher flow rate.

REFERENCES

1. Rezende, Virgílio A., Introducing the Compact Prover in Brazil by Comparison Tests with a Conventional One. North Sea Flow Measurement Workshop. Lillehammer, Norway. October 1995.
2. Apple, Cathy, Use of Small Volume Provers to Verify Coriolis Flowmeter Performance. Korea Association of Standards and Testing Organizations - Flomeko'93. Seoul, Korea. October 1993.
3. American Petroleum Institute - Manual of Petroleum Measurement Standards. Chapter 14-Natural Gas Fluids Measurement, Section 6-Continuous Density Measurement. Second Edition, April 1991.

NSFMW.97

North Sea FLOW Measurement Workshop

Paper ~~31~~: 6.2

MASTER METER METHOD

Authors:
Philippe Dupuy, Faure Herman, France

Organiser:
Norwegian Society of Chartered Engineers
Norwegian Society for Oil and Gas Measurement
Co-organiser:
National Engineering Laboratory, UK

MASTER METER METHOD

Philippe DUPUY, FAURE HERMAN, France.

ABSTRACT

This paper was presented at the NEL, in London, on the dec., 11th, 1996. It reports the experience of FAURE HERMAN with master-meter prover and centralised calibration method, based on the use of the true helical bladed turbine meter, HELIFLU ™ TZN. This practice was originated on french pipelines networks, for products and crude oil, in the sixties.

FAURE HERMAN, FLUIDS MEASUREMENT

FAURE HERMAN is the manufacturer of the true helical bladed turbine meter, specialising in precision turbine meters for fiscal and high integrity applications.

We have considerable experience in the Oil and Gas industries, from exploration and production, transportation and refining. Most of the Major Oil Companies in the world have an item of our equipment on either export or allocation metering.

FAURE HERMAN is a medium-sized company and a division of the INTERTECHNIQUE group of France, with offices in UK, USA and Italy. The company conforms to ISO 9001 and is accredited by several international bureaus.

The main plant is in la Ferté-Bernard approximately 150 km south-west of Paris. It includes 3 fully certified and traceable pipe provers with the ability to attain up to 3,000 m^3/h on liquid, 2,500 m^3/h on gas. All the calibration for liquids are performed on hydrocarbons to cover viscosity ranges (0.6 - 400 cSt).

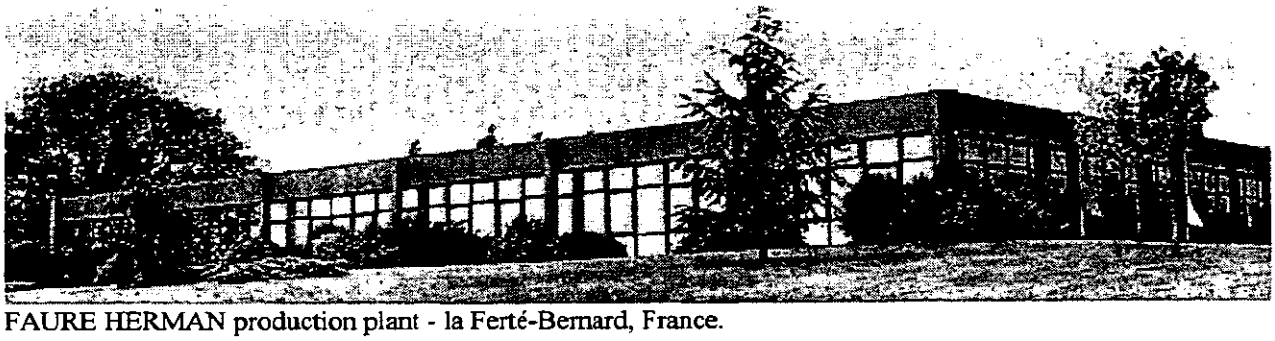

FAURE HERMAN production plant - la Ferté-Bernard, France.

MASTERY OF THE DUAL-BLADED TURBINE METER

The heart of FAURE HERMAN' success is the mastery of design and application of the helical bladed rotor, which is found in every FAURE HERMAN meter since 1953. The original concept was to provide a generic type of flowmeter, which was less effected by all usual influences, such as : changes in viscosity, temperature and pressure.

The main requirements are stability, durability and, above all, reliability in service. FAURE HERMAN now have over 8,000 units in service around the world on fiscal metering systems.

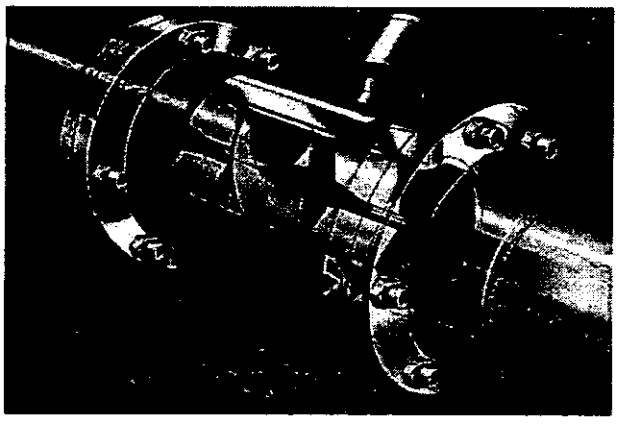

There has been extensive R & D over the years and we now have several designs of flowmeters suitable for most applications. Our current and most famous design is the HELIFLU ™ TZN.

The HELIFLU ™ TZN is an industrial version and is specifically aimed at the fiscal metering of hydrocarbon fluids, such as crude oils, condensates, refined products and LPG's..

The meter is designed to operate at extreme conditions and provides an alternative to traditional metering techniques.

The meter features :

- ⇒ High accuracy (better than ± 0.15%)
- ⇒ Repeatability (better than ± 0.02%)
- ⇒ Wide viscosity range (0.1 to 300 cSt +)
- ⇒ Long-term stability
- ⇒ Low pressure drop
- ⇒ Compact, low weight

Over the years, we have been asked to supply flowmeters for key monitoring points on various installation, where confidence had to be at the highest level. We have also provided alternative cost-effective solutions to traditional methods of metering, such as proving i.e. using our knowledge of the helical bladed devices as reference meters.

We have found that our HELIFLU ™ TZN unit out perform most turbine flowmeters currently available and that, in some cases, can perform as well as a traditional prover, i.e. returning linearity of better than ± 0.1% and repeatability better than ± 0.01%. This fact is most demonstrable on larger units.

FAURE HERMAN have been involved in numerous projects around the world, to provide alternative means of proving on metering systems. There are examples where master-meter provers have been employed to overcome some fundamental problems such as: cost, available space, location and level of local technical backup.

A direct comparison between master-meter provers using a HELIFLU ™ TZN and pipe provers is significant.

Typically :

⇒ a master meter prover costs approximately 40% less
⇒ the actual footprint tends to be at least half that of a pipe prover
⇒ it can be transported as a skid with greater ease, due to size
⇒ a system using HELIFLU ™ TZN meters can be re-sized
⇒ a master-meter prover tends to be more reliable, less to go wrong
⇒ proving time is reduced, can prove on line
⇒ the maintenance of the primary measuring element is extremely simple

EXPERIENCE OF METERING ONSHORE

In 1966, FAURE HERMAN embarked on a joint project with the Metrology Authorities of France, the major pipelines and oil company operating throughout the country. The aim was to install major pipelines, and generally to help the logistic of crude and refined hydrocarbons.

For this to happen, new procedures had to be developped, as well as cost-effective solutions of monitoring product in transit. All input and output points had to conform to the requirements of the French Department of Metrology.

This was achieved by the technique of centralised calibration and proved to be very successful, in many respects. Now virtually all the main operators involved in hydrocarbon transit rely on master-meter provers, i.e. it is now a standard practice.

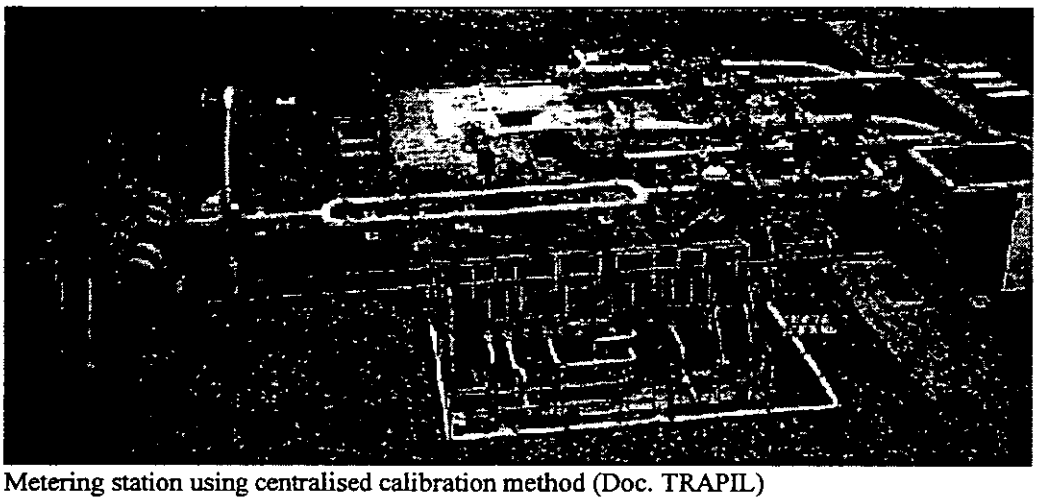

Metering station using centralised calibration method (Doc. TRAPIL)

In 1996, FAURE HERMAN supplied 3 skids for the metering stations of products pipelines, coming from the LEUNA 2000 refinery in former East-Germany, including master-meter provers. Each system has a capacity of 600 m^3/h and was approved by the German Authorities (PTB) for fiscal measurement.

EXPERIENCE OF METERING OFFSHORE

Recently, FAURE HERMAN completed a project in South-Eat Asia, where a metering system including a master-meter prover was installed on a FPSO. The aim was to reduce to a minimum the amount of deck space taken by the metering package.

The throughput was to be in the region of 3,000 m^3/h of condensate.

The use of a master-meter prover was ideal for this application, as in order to verify a throuput of 3,000 m^3/h with a traditional solution would have been involved the use of very large prover indeed. In this case, the saving was about 10 tons.

Metering unit on a FPSO

The problems associated with a prover of that size would have been the overall size, the amount of reinforcement to prevent torsional movement when service.

THE MASTER-METER PROVING METHOD

'' A master-meter is selected, maintained and operated to serve as a reference for the proving of another meter. A comparison of the two meter outputs is the basis of the master-meter proving method.''

These introductory words from the API (MPMS chapter 4, section 5), referring to the methodology, summarises briefly its basis, but do not provide complete answers. Some details rely on a site experience, validated or even amended by the local Metrology Authorities.

Therefore, FAURE HERMAN takes an active part in the API works, which should specify some elements. This is especially thecase for the definition of the number of test runs, the required accuracy, etc.

The procedure FAURE HERMAN is putting forward relies on draft proposals (MPMS chapter 12, section 2, part 4).

Metering with 3 streams and a master-meter.

THE ESSENTIALS OF THE METHOD

The use of the master-meter proving method requires :

⇒ accuracy and long-term repeatability of the HELIFLU ™ TZN turbine meter.

⇒ insensitivity of master-meter to viscosity and density variation.

⇒ re-calibration of the master-meter on proving facility (if a local station exists) or on the FAURE HERMAN calibration facilities, upto 3,000 m^3/h.

Nevertheless, the use of a centralised calibration method requires the availability of a spare meter during meter calibration and also the use of ''shuttle'' containers provided for transporting the meter in good conditions.

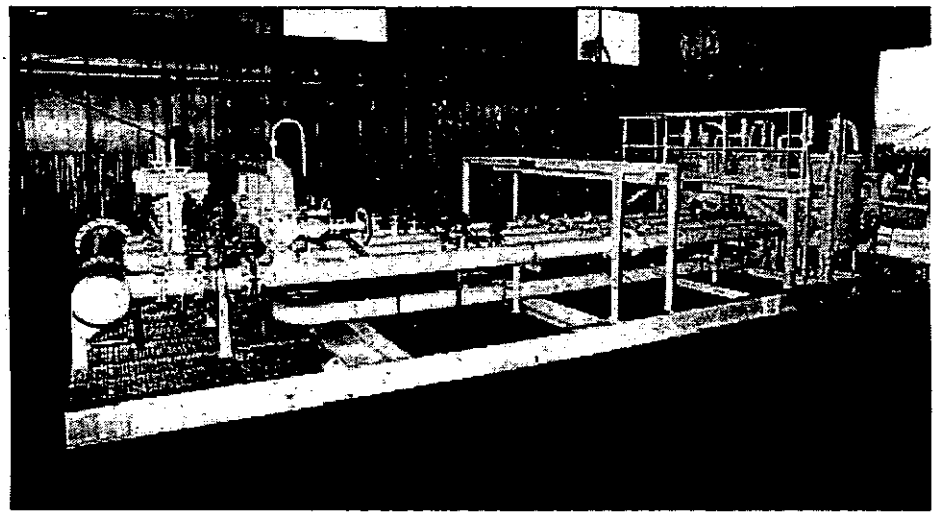

TECHNICAL OVERVIEW

Basic principle : pulse comparison

The method consists in installing in line a turbine flowmeter with a master turbine meter. When the liquid flows, the pulse counters of both meters are simultaneously triggered. When the last meter reaches a selected pulse amount, data are recorded.

To perform a prove with a sufficient accuracy, a high pulse number is used (API recommends a minimum of 10,000). To perform quickly the prove, the pulse interpolation method by double chronometry, in compliance with API requirements (chapter 4, section 6) may be used.

This basic principle shall be of course automated and carried out with a prove report. This report shall be validated by the local Metrology Authorities.

Prove report (to API)

A minimum of 5 tests are successively performed with the same meter. The system starts and stops automatically as soon as the pulse counter of one of the meters reaches 10,000 pulses. The data logging system stores all the values.

Then, the system checks :

⇒ if the repeatability of the Meter Factor calculated between line meter and master-meter is better than 0.02%.

⇒ if the average of the Meter Factor is different from the previous one.

With this information, some decision would be taken either manually or automatically.

If Δ between old MF and new MF is < 0.25% (*)	The new MF is introduced in the flow computer. The computer may perform a retroactive calculation on the previous volume.
If Δ between old MF and new MF is < 0.10%	The old MF is still valid. No value will be changed.
If Δ between old MF and new MF is > 0.25% (*)	The line meter will be removed and sent back to the centralised proving station.

(*) These values are not under any regulation. The company shall define this value with the local Metrology Authority. API chapter 13, section 2, will be helpful to establish statistics.

FREQUENCY OF OPERATION

The calibration frequency is mostly defined by the local Authorities. Experience of such a system involves a proving frequency reduction.

The common practice is to perform a prove once a day at the beginning of operation. Some operators have reduced the frequency of such proves to once a week.. In France, users and generally Metrology Authorities recommend to return the master-meter in a centralised proving station once a year.

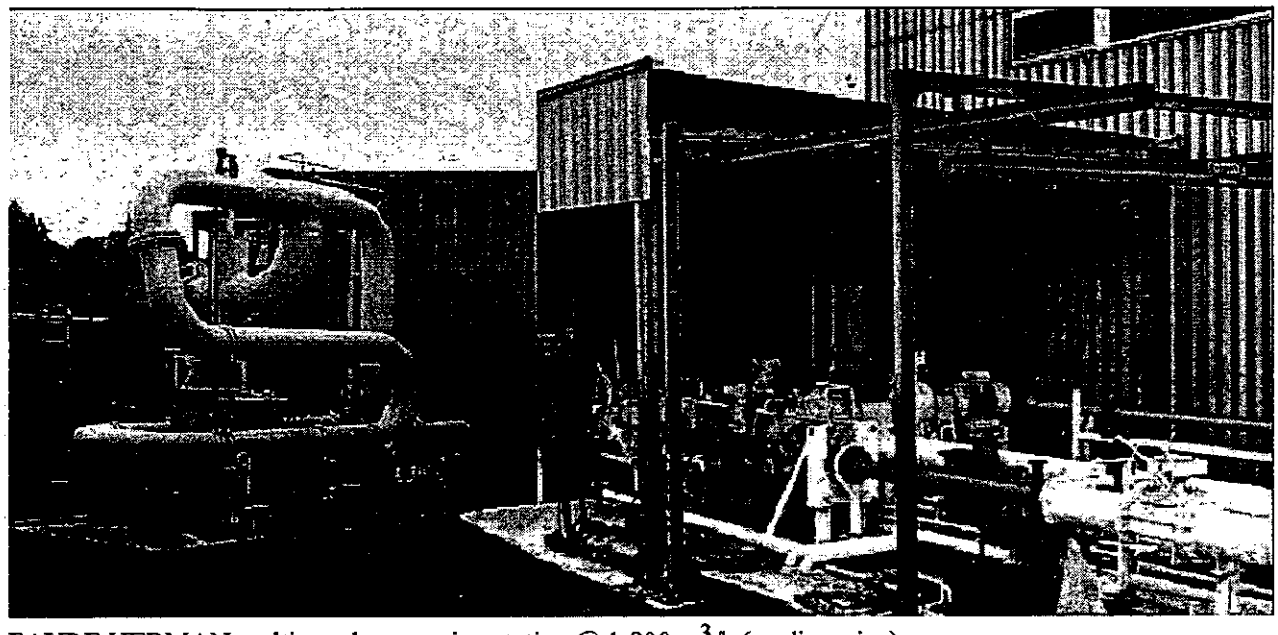

FAURE HERMAN multi-product proving station @ 1,000 m^3/h (medium size)

REFERENCES

1. Michel, C., Smith, P., Binet, P., ''Crude Oil Measurement on Floating Storage Vessel'', NEL, London, Dec. 11, 1996.

2. API, MPMS, chap. 4, section 5, 1988, reaffirmed oct. 1993 - ''Master Meter Prover''.

NSFMW.97

North Sea FLOW Measurement Workshop

Paper ~~32~~: 6·3

TESTRESULTS KROHNE 8" ULTRASONIC FLOWMETER

Authors:
Andrè H. Boer, Krohne Altometer, The Netherlands
Wim Volmer, Nmi Certin B.V., The Netherlands

Organiser:
Norwegian Society of Chartered Engineers
Norwegian Society for Oil and Gas Measurement
Co-organiser:
National Engineering Laboratory, UK

TESTRESULTS KROHNE 8" ULTRASONIC FLOWMETER

Authors:

Mr. André H. Boer
KROHNE Altometer, The Netherlands

Mr. Wim Volmer
NMi Certin B.V., The Netherlands

SUMMARY

A new development in the field of ultrasonic liquid flowmeasurements has resulted achieved with the multichannel liquid ultrasonic flowmeter; the first for use in maintenance-free custody transfer applications. Although ultrasonic flowmeters are used for standard applications in the oil industry for many years, this new development will have a big impact on custody transfer flow measurement. Not only because of the compactness, but also because of the low investment and operating cost of this flowmeter. This paper describes the system and the method of operation as well as practical experiences and achieved test results of this flowmeter.

PART I THEORY OF OPERATION

1. GENERAL BACKGROUND

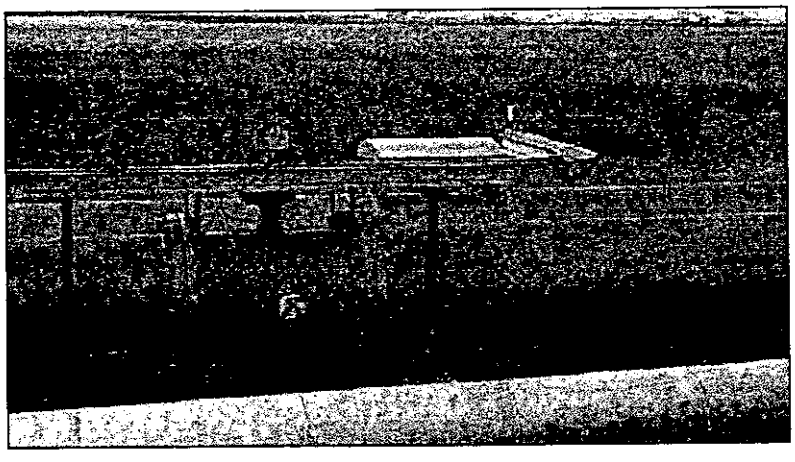

Figure 1: Double beam ultrasonic flowmeters in use in an pipeline sampling system

The development of a multichannel ultrasonic flowmeter was started some 3 years ago. It was based on the 15-year long existing practical experience in the field with single and dual beam ultrasonic flowmeters. Today many ultrasonic flowmeters (mainly dual beam technology) are used in a wide variety of applications in the oil industry.

Examples are applications in which ultrasonic flowmeters are used in batch representative sampling systems (see fig. 1) in (crude oil) blending applications or in pipeline transport. The experience gained in those applications was an important ingredient in the development of the multichannel ultrasonic flowmeter, which was aimed at reaching higher accuracies (linearity and repeatability) to within custody transfer specifications, even under rough process conditions and in a wide range of viscosities, densities, temperatures and pressures. In fact, when using such a multichannel flowmeter, a water calibration only should be sufficient to characterise the flowmeters behaviour also when used afterwards on other, higher viscous, liquids. How, in practical situations, this flowmeter performs is described in this paper.

2. SYSTEM AND THEORY OF OPERATION

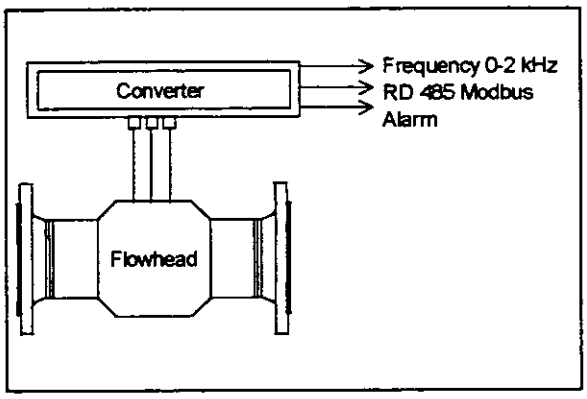

Figure 2: Total system

The newly developed ultrasonic multichannel flowmeter for custody transfer applications uses the well-known transit time, or time of flight, principle to measure the flow velocity. It consists of two main components. These are the flowmeter tube (flowhead) and the field mounted electronics (converter). The flowmeter system can be used like any other conventional flowmeter, i.e. pulses as output that represent a certain flow volume under operating conditions. Next to the flow information this system can also provide additional valuable status and process data. This will be discussed when dealing with the system layout in detail.

3. THE FLOWHEAD

The flowhead consists of a middle part made from a solid block of metal that holds the acoustic measurement paths. To this middle part an in- and outlet cone, with flanges, are welded. The flowmeters construction is symmetrical which means it can measure bi-directional flows. The cones play an important role in the shaping of non-axisymmetric flowprofiles, ensuring a symmetrical flowprofile inside the measurement section of the flowhead, which is also supported by earlier research (e.g. Teijema [1]). The angle of the cones is chosen such that a negligible pressure drop, identical to 2 m of straight pipe run, remains. With respect to the number and location of the measurement beams consideration was taken with respect to the requirements of insensitivity of flowprofile shape (transition from laminar to turbulent flowregimes, symmetricity), swirl and redundancy of information. This resulted in a flowhead with 5 measuring paths. With one measuring path in the centre and the other four two by two symmetrically aligned. Two paths of the five are turned by 90 degrees allowing for a swirl measurement.

4. THE FIELD MOUNTED CONVERTER

The field mounted converter consists firstly of the electronics for driving the sensors in the flowtube and secondly holds an electronic block that combines all data coming from the 5 individual measurements lines into an average volumetric flowrate, overall viscosity and status of the instrument. The driving of the sensors (10 in total, 2 per measurement line) is done in parallel. Each individual measurement line has its own driving electronics. Each driving electronics measures the flowvelocity for its measurement line every 40 msecs.

Thus consequently every 40 msecs 5 flowvelocities, representing the flowprofile, are sent to the supervisory electronic block for further processing. Next to the high measurement rate these 5 driving electronics also represent a certain redundancy. Comparison of the sonic velocities measured per measurement line (5 times) allows the supervisory system to detect failures of the driving electronics, when not already detected by the driving electronic itself.

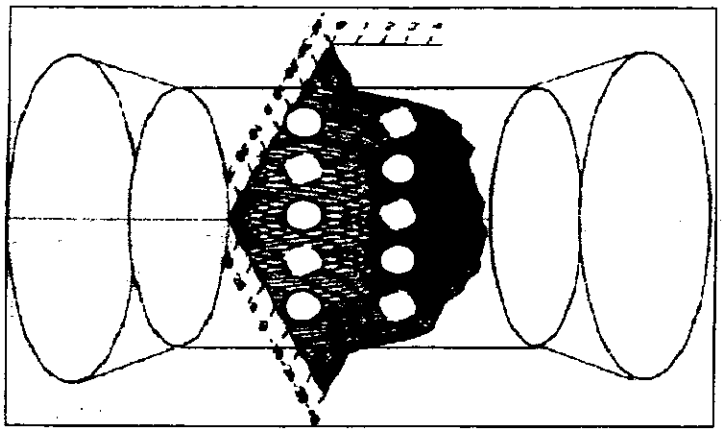

Figure 3: Flowhead with 5 measuring paths

Also checks on the shape of the flowprofile are performed. Should one, or even two, measuring paths fail then, using the redundant information, the correct value will be interpolated allowing the instrument to continue to measure. Additionally continuously the swirl component in the flow is measured and compensated for, when within tolerances. The outputs coming from this field mounted electronics are two phase shifted pulse outputs 0-2 kHz, a digital RS485 output with MODBUS protocol and status outputs. These outputs allow the ultrasonic multichannel flowmeter to be connected to many flowcomputers in use today.

5. PRACTICAL EXPERIENCE

During the development of this system a number of prototypes were constructed. Many tests were performed to investigate the behaviour of the flowmeter on non-symmetric flowprofiles, liquid viscosity change and temperature. During the development stage these in-house tests all showed very promising results upon which external tests were started. The fist test, still in operation, was installed October '95 at DOW Chemical Terneuzen.

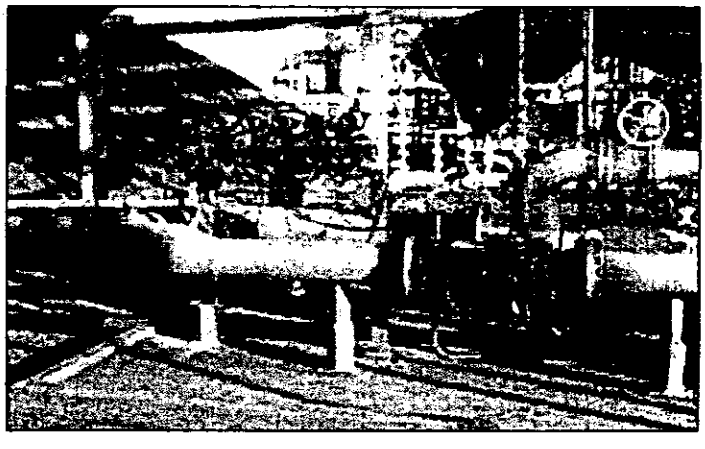

Figure 4: Dow Chemical Terneuzen

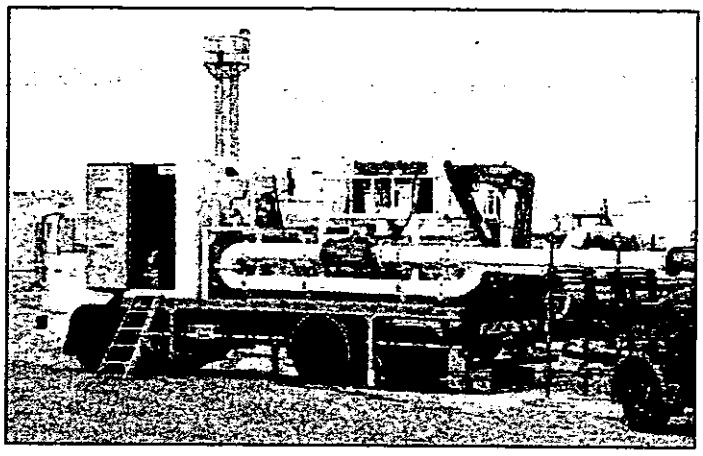

Figure 5: Nerefco Europoort

There cumene (viscosity 0.7 cSt.) is measured in a 10" pipeline ship loading application. The flowmeter is in operation since December 1995 and the flowmeter output is compared to the ship measurement. A second important set of measurements was obtained at Shell Pernis, where an 8" flowmeter was calibrated against a ball prover on liquids such as gasoline and naphtha. The results obtained here proved that the flowmeter could work well within the requirements set by the NPD.

With this as background a plan was devised to calibrate one flowmeter on water which would then be calibrated in the field on various hydrocarbons in a wide viscosity and temperature range. Since these tests were going to serve as input for the custody transfer type approval of this instrument the Dutch authorities, the NMI, were invited to witness all tests.

PART II TESTRESULTS

6. INTRODUCTION

In 1996 KROHNE Altometer contacted NMi to inquire about the legal requirements applicable to their ultrasonic flowmeter both in Norway and in The Netherlands. The purpose of this inquiry was to establish the possible necessity of changes in the construction and functionality of the meter, which at the time was still under development.

The legal requirements in Norway are stated in the NPD (Norwegian Petroleum Directorate); the legal requirements in the Netherlands are stated in the "Weights and Measures Act", which is very similar to OIML International Recommendation R117. When studying both documents, one can observe that if the device meets the requirements stated in the NPD, also compliance with OIML R117 is achieved.
In short this means:

- the meter accuracy has to better than ± 0.2 % for the complete flowrange ± 0.15 % for the flowrange is which the meter is intended to be used most
- the repeatability error has to be smaller than ± 0.2 %
- the correctness of datatransmission and calculations has to be guaranteed from the wetted parts to the BOL (Bill of Lading).

7. TESTREFERENCES

Depending on the application, compliance with several "legal" documents is mandatory for the US-meter. The requirements stated in OIML International Recommendation R117 usually cover National requirements applicable in many countries.

In Norway two sets of requirements are operational at present. The NPD has formulated a document, which applies for offshore measuring systems, including systems installed in pipelines that run from oil/gasrigs in the Northsea to refineries and factories on the mainland. Although harmonisation is in progress, there still are significant differences between OIML R117 "Measuring systems for liquids other than water" and "Regulations relating to fiscal measurement of oil and gas etc." issued by the Norwegian Petroleum Directorate.
The main differences are:

- Accuracy, repeatability and linearity requirements stated by NPD are stricter
- Accuracy, repeatability and linearity requirements stated by NPD apply to measuring device, without correction device
- According to NPD, all computerparts, which have a meteorological influence, must be provided in duplicate

Other, less significant, differences can be overcome by small adaptations in the testprocedures, thus achieving compliance with both R117 and the NPD-regulations.
See the Norwegian Petroleum Directive and OIML International Recommendation R117 for more detailed information.

8. TESTMETHOD

Unless otherwise stated all tests have been performed under the following conditions:

- measuring device mounted rigidly
- inlet: 20 D straight pipe
- outlet: 10 D straight pipe
- ambient conditions: varied
- testfluid(s):

Name	**Viscosity [cSt]**
Fuel oil	125 at 66 °C
Light cycle oil	1.5 at 70 °C
Water	1 at 8 °C

The accuracy of the meter has been determined at several (five or six) flowrates between the minimum and maximum flowrate. At each flowrate at least 5 measurements have been performed. All testequipment used, was certified.

9. TESTEQUIPMENT

In all of the accuracy tests performed thus far, a 24" Brooks compact prover has been used as a reference. During testing it turned out that the US-meter had an unexpectedly high repeatability value. In the near future extra tests will be carried out to establish the exact cause of this phenomenon.

At the moment the cause is thought to be one of the following:

- In contrast to conventional measurement principles, the US-meter picks up every change in liquid-conditions (pressure waves caused by opening and closing of valve) because of the high speed of the electronic processing of the measurement signals. How the sample-time, flowrate and pulse-interpolation interact is, at the moment, still to be found out.
- The way that the meter-pulses are generated.

Preliminary investigations show that a sufficiently high number of runs eliminates this problem. In future research the US-meter will be tested against a larger prover and a calibrated turbinemeter to eliminate the influence of typical compactprover properties. Tests on KROHNE Altometer's installation (testvolumes up to 10 m3), using water, show a repeatability error better than 0.05% on five consecutive measurements.

10. TEST SETUP

During the tests on Fuel oil and Light Cycle oil the testequipment was set up as given below.

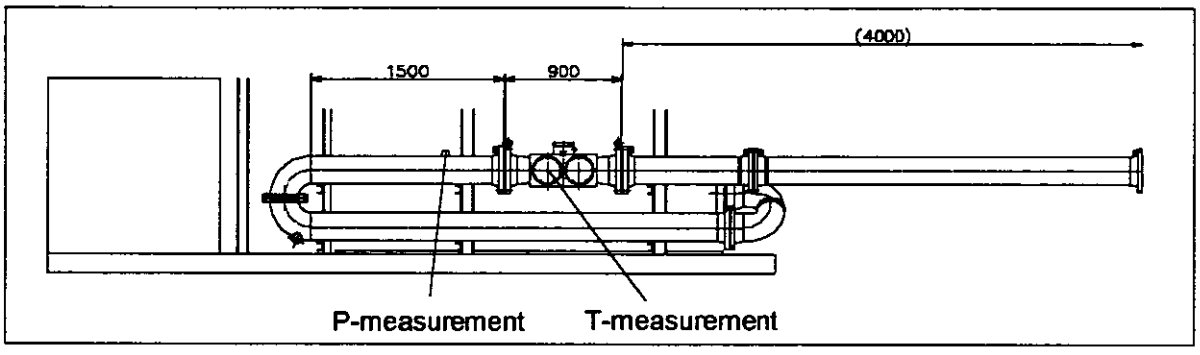

Figure 6: Testequipment

11. ACCURACY TESTS

OIML International Recommendation R117 and the NPD state the following values applicable to the accuracy tests on a measurement transducer installed in pipelines:

Document	Accuracy [%]	Repeatability [%]	Linearity [%]
OIML R117 (0.1 to 1 Qmax)	± 0.20	0.08	± 0.20 (*)
NPD (0.1 to 1 Qmax)	± 0.25	± 0.02	± 0.25
NPD(**)	± 0.15	± 0.02	± 0.15

(*) OIML R117 states that the measurement transducer meets this requirement, including a correction device.

(**) Flowrange in which the meter is commonly used

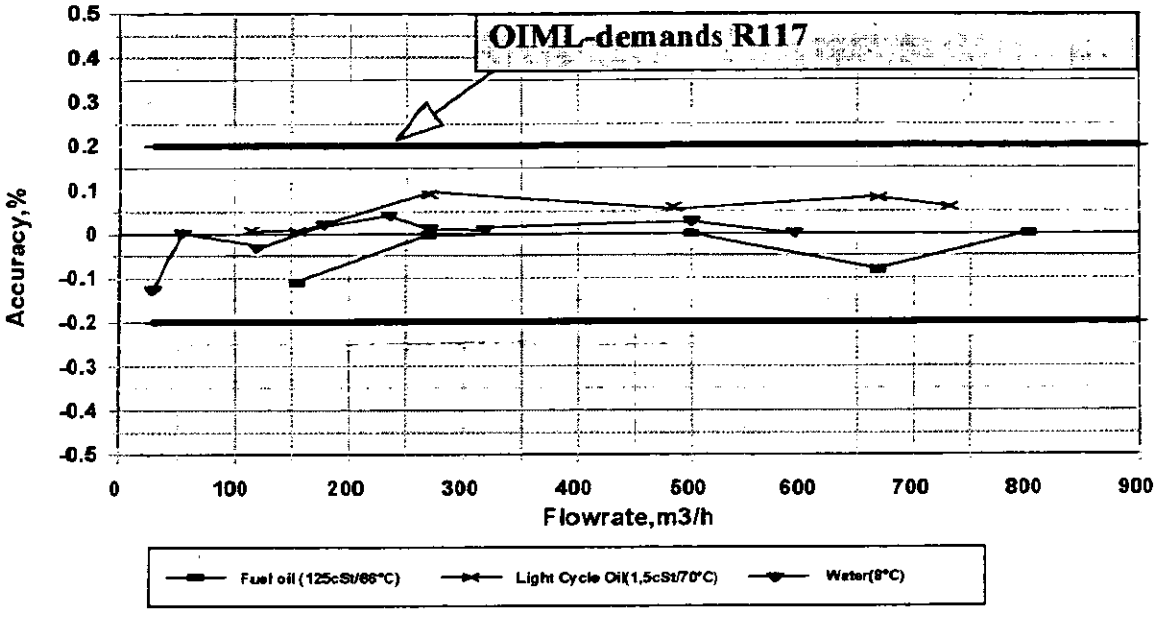

Figure 7: Testresults accuracy

During one test (1 run consisting of 84 strokes of the prover) the liquid-temperature did not vary by more than 0.2 °C and the liquid-pressure by no more than 0.15 bar. Because of the built in viscosity correction, as illustrated by Mr. André Boer, the meter characteristics prove to be almost independent of liquid-properties and flow profile. Even the transition from a turbulent to a laminar flowprofile has a negligible influence.

12. OTHER TESTS

Other tests that have been performed thus far are:

Description	Required by ...-regulations	Passed Yes/No
Dry heat	OIML / CE	
Cold	OIML / CE	
Damp heat	OIML / CE	
Power voltage variation	OIML / CE	Yes
Short time power reductions	OIML / CE	Yes
Bursts	OIML / CE	Yes
Electrostatic discharge	OIML / CE	Yes
Electromagnetic susceptibility	OIML / CE	Yes
Surges	CE	Yes
Emission	CE	

13. CONCLUSIONS

The KROHNE US-flowmeter meets the requirements applicable to the measurement of liquids for Custody Transfer purposes.

REFERENCES

[1] Teijema, J., "Nieuwe inzichten flowmeterinstallatie", Syllabus of workshop "Flowmeting : nu en morgen", KIVI/NIRIA/MRBT, Amsterdam, October 1990

NSFMW.97

North Sea FLOW Measurement Workshop

Paper ~~33~~: 6·4

FACTORS AFFECTING THE PERFORMANCE OF ULTRASONIC FLOWMETERS

Authors:
G.J. Brown, Flow Center, NEL, UK

Organiser:
Norwegian Society of Chartered Engineers
Norwegian Society for Oil and Gas Measurement
Co-organiser:
National Engineering Laboratory, UK

FACTORS AFFECTING THE PERFORMANCE OF ULTRASONIC FLOWMETERS

Gregor J Brown
Flow Centre, NEL
UK

SUMMARY

A programme of work is currently underway at NEL to investigate and characterise the performance of liquid ultrasonic meters over a wide range of conditions. This paper presents the results of laboratory evaluations in addition to the initial results of combined flow and flowmeter modelling.

Two-phase, oil/gas performance tests were conducted on commercially available meters of 4-inch nominal bore. Specific results have been selected to illustrate performance variations related to factors in meter design and operation.

Two-phase, oil/water performance tests with water-cuts of up to 15 % were also conducted on the above meters. These results are presented in their entirety. The results show deviations from single-phase performance which vary for each meter design.

Baseline calibration results for four commercially available clamp-on meters are presented. The results were obtained in good installation conditions on stainless steel pipes of 4-inch and 8-inch nominal bore. The results show different levels of accuracy associated with each meter and a general conformation with predicted behaviour.

The final section of the paper presents results obtained by a systematic numerical method of determining the flow profile sensitivity of various meter configurations. The results provide quantitative confirmation of the reduced sensitivity of multipath designs to variations in the velocity profile.

1 BACKGROUND

The use of ultrasonic technology for flow measurement in offshore applications has increased in the last few years. This is due to advances in the metering technology in addition to the force of economic pressure on field development strategies. Transit time ultrasonic flowmeters are now employed in a diverse range of gas flow applications from flare stack monitoring to sales gas custody transfer.

Liquid meters have, until recently, been used mainly in areas peripheral to the main product transfer. Now they are being considered for many more critical applications. One notable use is in custody transfer of processed crude from floating production storage and offloading (FPSO) vessels to shuttle tankers. In such applications the accuracy demands are higher than traditional ultrasonic meter usage with the

consequence that more consideration must be given to meter selection, configuration, calibration and installation in order to ensure best performance.

There is an increasing demand for continuous on-line flow measurement at intermediate stages in the production process stream. Many of these applications could be considered more demanding than custody transfer measurement, not in terms of accuracy, but in relation to installation and operating conditions. In these applications it may be necessary to trade accuracy against applicability. This will require a greater understanding of meter behaviour in 'non-standard' conditions.

2 INTRODUCTION

A programme of work is currently underway at NEL to investigate and characterise the performance of liquid ultrasonic meters over a wide range of conditions. The work was initiated in 1995 with the project *Ultrasonic Meters for Oil Flow Measurement*. The first stage results from the project were reported at last year's workshop [1]. The work has been continued in three further projects:

- Long-term evaluation of ultrasonic flowmeters
- Research into clamp-on ultrasonic meters
- Application of ultrasonic meters in non-standard flows

These projects have been specified to cover the following general application issues:

- Baseline performance in good installation and operating conditions
- Deviation from baseline performance due to meter installation downstream of flow disturbing pipe work configurations
- Behaviour in the presence of flow of more than one fluid component
- Performance and maintainability in the long-term

This paper details laboratory evaluation results from the second stage of the original project *Ultrasonic Meters for Oil Flow Measurement* and initial baseline results from the project *Research into Clamp-on Ultrasonic Meters*. In addition to the laboratory evaluation data, initial modelling results from the project *Application of Ultrasonic Meters in Non-Standard Flows* are presented.

3 THE METERS

Manufacturers of commercial transit time ultrasonic flowmeters have been invited to provide meters for inclusion in the laboratory evaluation tests of the programme. At present meters have been obtained from six different manufacturers covering a range of technological aspects both generic and proprietary.

Six meters were supplied in 1996 for the project *Ultrasonic Meters for Oil Flow Measurement*. Meter A was a single-beam clamp-on meter with 1 MHz transducers which were mounted in a horizontal diametric configuration on a 4 inch schedule 40 carbon steel spoolpiece provided by NEL. The design uses a digital correlation technique for the determination of the transit times and automatically corrects for profile effects on the basis of Reynolds number and bore roughness. Values of 20 cSt and of 0.21 mm were used for these parameters. The supplier of Meter A requested

that manufacturer and model details be omitted as the results did not conform with expectations.

Meters B_C, B_W, C and D were supplied by Panametrics, Ultraflux and Danfoss respectively. Meters B_C and B_W were both model XMT868 dual channel flow transmitters supplied with a single 4-inch schedule 40 carbon steel spoolpiece comprising both wetted and clamp-on transducer configurations. The meter supplied by Ultraflux was a model UF322-2 with two pairs of 1 MHz clamp-on transducers which were installed on a 4-inch schedule 40 stainless steel spoolpiece provided by NEL. Meters B_C, B_W and C each employed dual single-reflection diametric paths in perpendicular planes. Meter D was a 4 inch nominal bore Danfoss Sonoflow with the standard path configuration of two parallel mid-radius chords. More detailed description of meters A to D are provided in reference 2 along with the complete set of open results for each meter. The sixth meter included in the project was a Krohne Altometer UFM Multichannel for which the open test results have been previously described [1].

Meters E to H have been supplied by four different manufacturers for inclusion in the project *Research into Clamp-on Ultrasonic Meters*. In this paper they are described only by these nominal identifiers and by their transducer configurations. Meters E and F are dual-path meters which employed single-reflection diametric paths in perpendicular planes. Meters G and H are single-path meters for which the default path configuration employed was a horizontal diametric path with a single reflection. Further details of meters E to H will be given at a later date once the manufacturers have been given sufficient time to comment on the test results.

4 UNCERTAINTIES AND PERFORMANCE CHARACTERISTICS

The performance of transit time meters can be characterised by quantifying uncertainties in the determination of the transit time intervals and geometrical parameters of the meter tube. Assuming that the transit time difference measurement, Δt, is independent of the measurement of the upstream and downstream transit times, and that the product of these transit times can be approximated by the square of their mean, $\bar{t}$, the flowrate can be given by

$$q_v = k_h \frac{\pi D^2}{4} \frac{L^2 \Delta t}{2x\bar{t}^2} \tag{1}$$

where D is the diameter of the meter tube, L is acoustic path length in the flowing fluid, x is the axial projection of the path and k_h is the hydraulic or velocity distribution factor given by

$$k_h = \frac{\bar{v}_{actual}}{\bar{v}_{measured}} \tag{2}$$

By differentiation of equation 1 the sensitivity coefficients given in the following table are obtained.

Table 1 The Sensitivity Coefficients of Equation 1

$\delta_{kh} = \frac{\partial q_v}{\partial k_h}\frac{k_h}{q_v}$	$\delta_D = \frac{\partial q_v}{\partial D}\frac{D}{q_v}$	$\delta_L = \frac{\partial q_v}{\partial L}\frac{L}{q_v}$	$\delta_{\Delta t} = \frac{\partial q_v}{\partial \Delta t}\frac{\Delta t}{q_v}$	$\delta_x = \frac{\partial q_v}{\partial x}\frac{x}{q_v}$	$\delta_{\bar{t}} = \frac{\partial q_v}{\partial \bar{t}}\frac{\bar{t}}{q_v}$
1	2	2	1	-1	-2

Using the above table the uncertainty in the flowrate measurement can be determined by assigning a percentage uncertainty, E, to each of the parameters in equation 1 and substituting these into the equation

$$E_{qv} = \sqrt{(\delta_{kh}E_{kh})^2 + (\delta_D E_D)^2 + (\delta_L E_L)^2 + (\delta_{\Delta t}E_{\Delta t})^2 + (\delta_x E_x)^2 + (\delta_{\bar{t}}E_{\bar{t}})^2} \qquad (3)$$

An example follows for illustrative purposes.

4.1 Illustrative analysis

The uncertainties in D, L and x will be dependent on the methods by which they are established. A reasonable estimate of the uncertainty in D is 0.1% for measurement in the factory. The same figure could also apply for measurement of L and x. However in some cases, for example the case of transducers recessed in a well, the end points of L and x have no true physical definition, so a greater figure should be applied, say 0.2%. For in-situ, clamp-on measurement an uncertainty of a few millimetres is a reasonable assumption for pipe diameters up about 1 meter. L and x for clamp-on installations are derived from the measurement of $\bar{t}$ and D in addition to characteristic data relating to the transducers. To assume that the uncertainty in L or x is equal to the uncertainty in D would appear reasonable.

The relative uncertainty in Δt is dependent on the flow velocity. A simple estimate can be obtained by considering the timing clock resolution. Assuming a clock frequency of 100 MHz and ten thousand averaged measurements of the transit time difference interval we can ascribe an uncertainty of 0.05 nanoseconds for the timing resolution plus a zero-flow offset differential delay of 0.05 ns, giving a total figure of 0.1 ns. For clamp-on installations the signal-to-noise ratio is likely to be lower and poor alignment or coupling to the pipe wall may introduce a more significant differential delay so a figure of 0.5 nanoseconds could be applied.

The uncertainty in measurement of the transit time $\bar{t}$ is dependent upon the elimination of delays in transducers, electronics and recesses. If these are determined with reasonable accuracy we could assume a figure of 100 ns for the uncertainty in $\bar{t}$.

Taking the above figures the following 'dummy' curves of characteristic uncertainty versus velocity have been constructed for 4, 8 and 16 inch pipe sizes assuming a fluid sonic velocity of 1500 m/s and interrogation angles of 45 and 30 degrees for 'wetted' and 'clamp-on' configurations respectively.

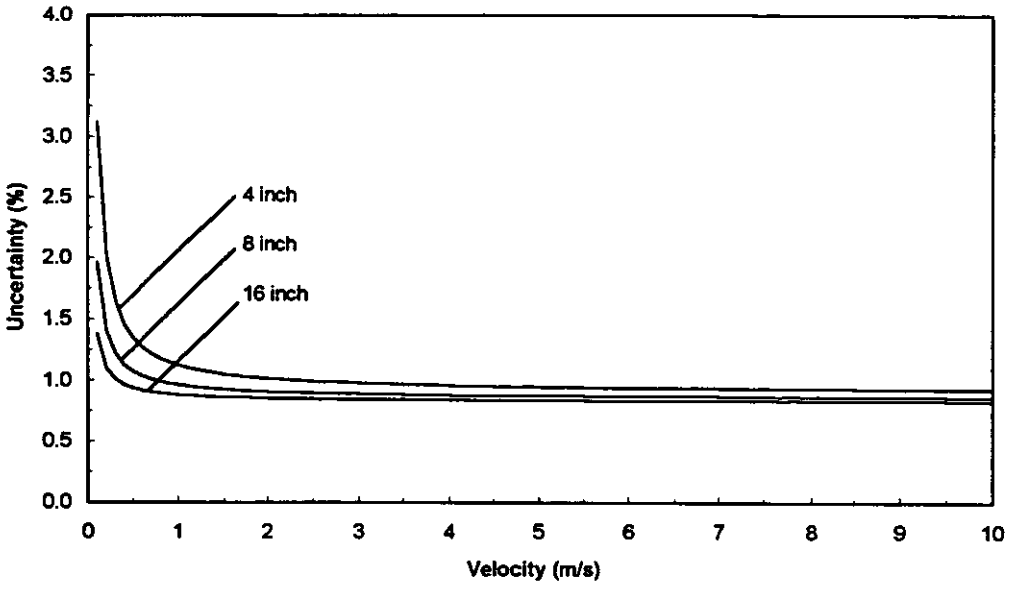

Figure 1 Illustrative performance curves (wetted assumptions)

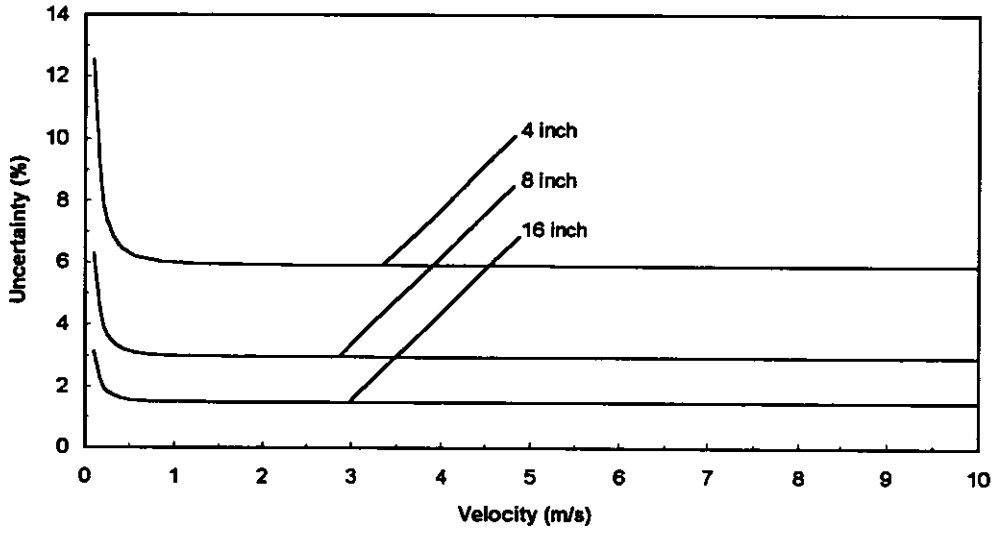

Figure 2 Illustrative performance curves (clamp-on assumptions)

Figures 1 & 2 illustrate two of the fundamental characteristics of the transit time measurement principle, i.e. increasing uncertainty as velocity is reduced and reducing uncertainty with increasing size. Not included in the above curves are the effects of the velocity distribution, attenuation, diffraction, noise etc.

4.2 Velocity Distribution Factors for Fully Developed Flow

In fully developed flows the velocity distribution factor, k_h, can be calculated as a function of Reynolds number and relative roughness, k/r. Figure 3 shows the turbulent flow k_h function derived by Fronek [3] for meters employing diametrical paths.

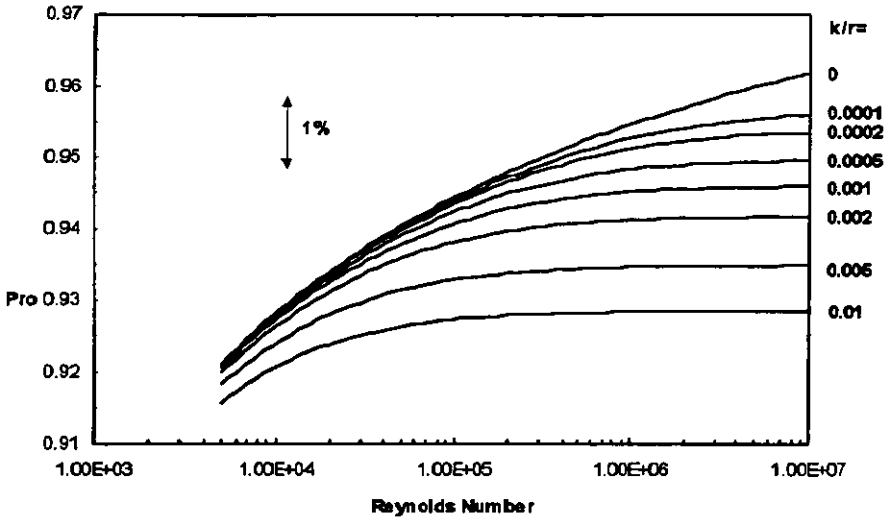

Figure 3 Diametric profile factor as a function of Reynolds number

In figure 4, the turbulent k_h factor is presented as a function of velocity for pipe diameters of 4, 6 and 16 inches, a constant roughness of 0.2 mm, and fluid viscosity of 1 and 5 cSt. From this figure we can see that non-linearity due to inaccuracy in k_h will be most significant at low velocities. The figure also illustrates that the linearity of the k_h function is relatively independent of the pipe size.

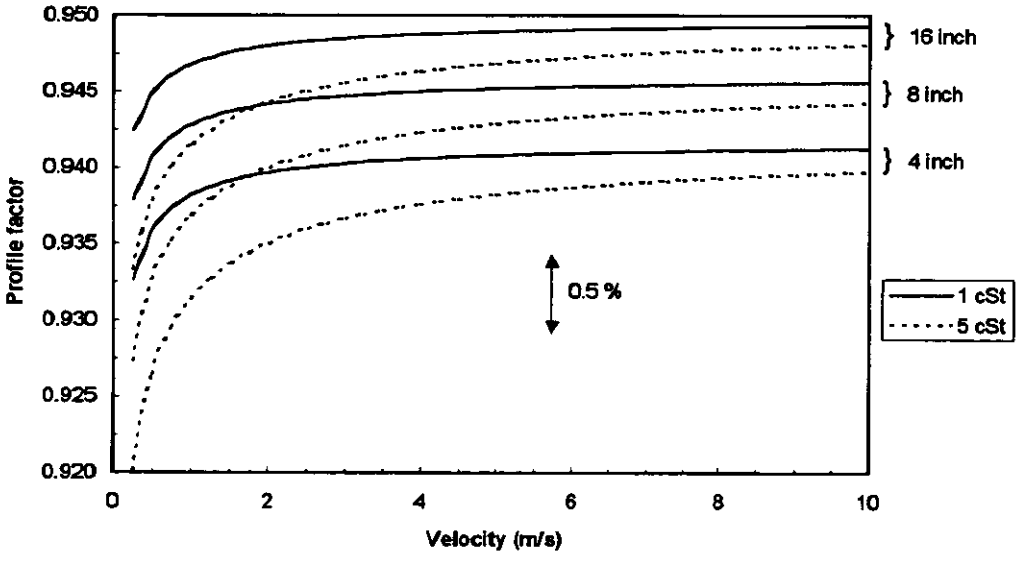

Figure 4 Diametric profile factor as a function of velocity

5 PERFORMANCE IN TWO-PHASE FLOW OF OIL AND GAS

The two-phase oil/gas tests reported here were conducted using a circuit of the main oil flow primary standard by introducing low flowrates of metered nitrogen into the test line on the downstream side of a reference positive displacement (PD) meter. The set-up is shown schematically in figure 5.

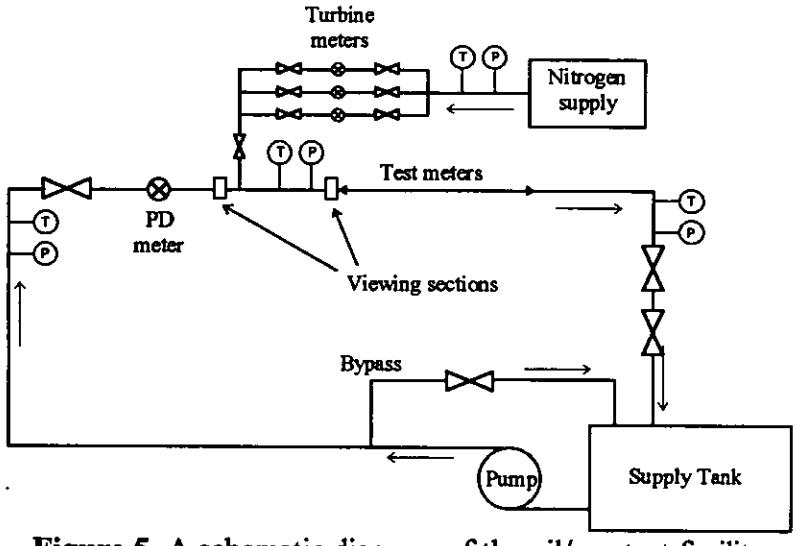

Figure 5 A schematic diagram of the oil/gas test facility

In general the performance of ultrasonic meters in flows of oil and gas is dependent on the gas distribution, the transducer locations and the signal detection and processing methods. The results of oil/gas tests have been presented previously in summary form [1]. Specific aspects of performance are studied here in greater detail.

5.1 Detection and processing of signals and measured parameters

Signal detection methods employed to determine the transit time intervals tend to be based on zero-crossing or correlation methods. For any given meter a choice of signal detection methods is generally not available, so that the detection method is chosen at the stage of meter selection. The degree of access to meter signal limits and fault response options varies from manufacturer to manufacturer and constrains the extent to which the meter behaviour may be tailored. For example, meter A has a 'low signal' parameter which can be set by the user to generate a fault response when the signal falls below the cut-off. Meter D's 'signal limit' settings are not adjustable whereas meters B_C & B_W has more than ten variable signal and flow parameter limit settings.

Figures 6 and 7 illustrate a difference in meter behaviour influenced by signal limit settings. For these results the mixture velocity was approximately 9 m/s and the gas was evenly distributed throughout the cross-section in the form of many sub-millimetre sized bubbles. The results of figure 6 show a deviation of approximately 0.5 to 1 % in the reading of meter B_C at 0.4 % gas volume fraction (GVF) and errors corresponding to a continuous fault occurrence at 0.8 % GVF when the output was forced to zero.

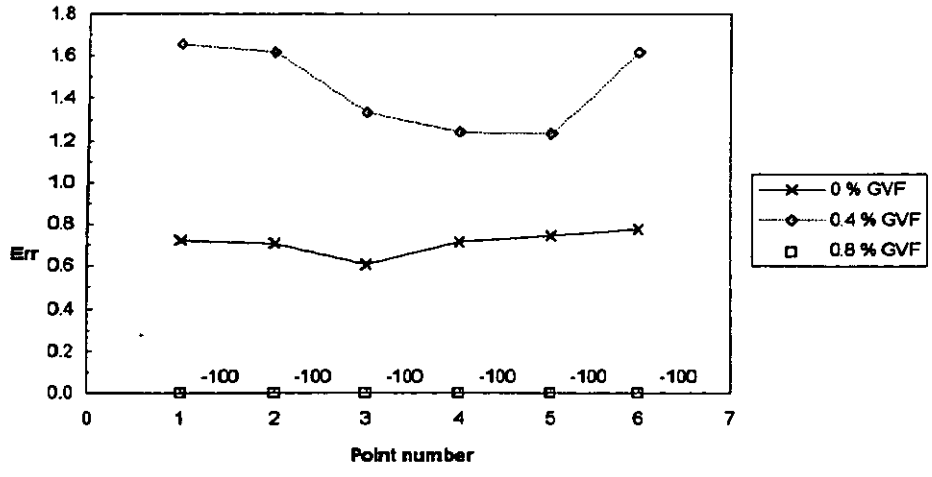

Figure 6 Oil/gas performance of meter B at a velocity of 9 m/s

Figure 7, however, shows a different response. At 0.4 % GVF the results lie within a few percent of the average 0 % gas result. At 0.8 % GVF the meter continued to output the flowrate although the magnitude of deviation from the 0 % gas results was increased to ±10 %.

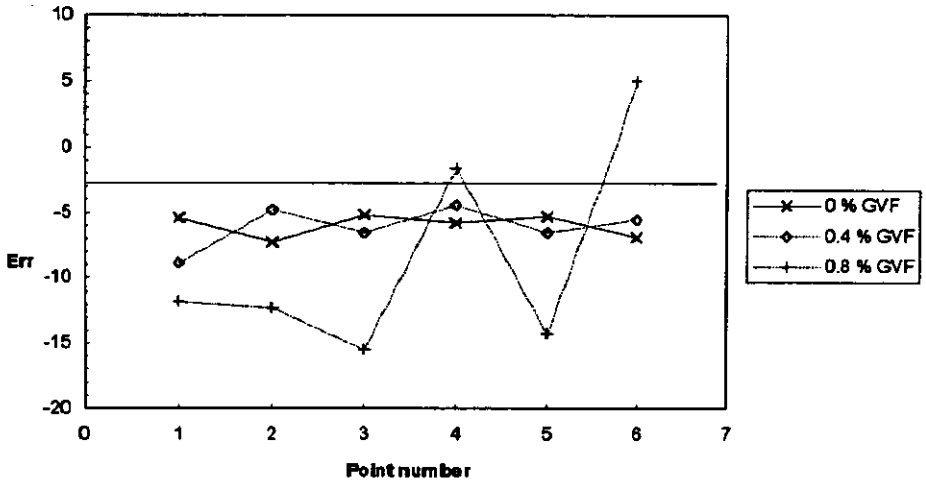

Figure 7 Oil/gas performance of meter A at a velocity of 9 m/s

Although meters A and B_C were supplied by different manufacturers and displayed some differences in basic characteristics (such as repeatability) they both employed correlation detection methods for the transit time measurement. The signal limit settings for meter B_C were set at default values (e.g. the signal low limit was set at 40 out of a possible range of -20 to 100) and the single limit setting of meter A was also set at its default, this taking the value 0 out of the possible range of 0 to 100. It can be considered then that by adjusting the signal parameters of Meter B_C its operating range may have been extended to include the 0.8 % GVF condition.

5.2 Void distribution and liquid velocity distribution

Figure 8 illustrates the influence of void distribution and liquid velocity distribution on meter D. The results shown here were obtained at a mixture velocity of approximately 4 m/s. At 0.75% GVF no fault indication was observed and the deviation was between approximately 3 and 5 %. At 1.5 % GVF intermittent faults and spurious high flowrate indications were observed which resulted in the high positive errors shown on the upper boundary of the graph shown in figure 8. At 4 % GVF signal fault conditions were indicated continuously but the magnitude of deviation was approximately the same as the 0.75 % GVF results.

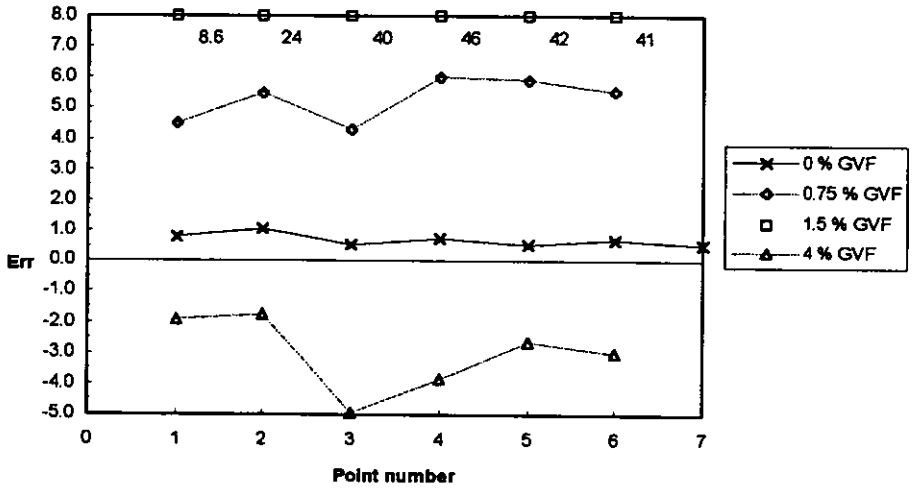

Figure 8 Oil/gas performance of meter D at a velocity of 4 m/s

This perhaps seemingly unusual behaviour can be explained qualitatively by considering the relation between the gas distribution and the position of the acoustic paths employed by the meter. As illustrated in figure 9 at the lowest gas fraction neither of the measurement paths are affected by the presence of the gas. At the second gas fraction the upper path is affected by the presence of the gas and spurious results are generated. At the highest gas fraction however, the amount of gas present in the upper chord has increased to such an extent that the measurement fails and the meter results are computed on the basis of the lower chord measurement only, which is free of gas.

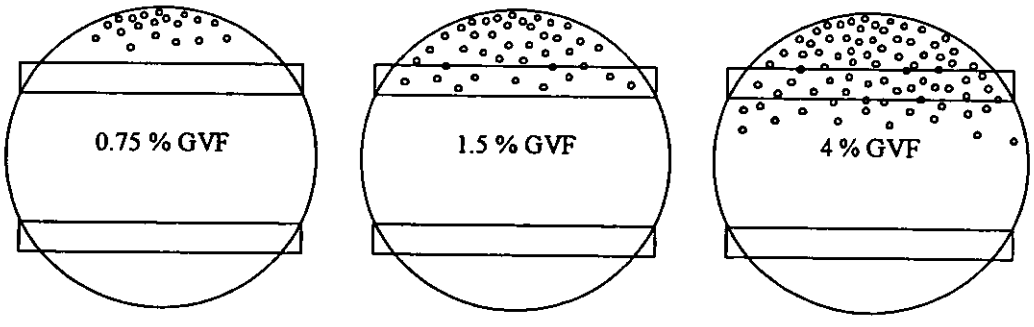

Figure 9 An illustration of the void distribution in meter D

The deviations at 0.75 and 4 % gas fractions show a bias due to the effect of the gas on the velocity distribution. Perhaps surprisingly, the deviations at 0.75 % GVF are, on average, greater in magnitude than those at 4 % GVF. It can be postulated therefore, that the performance of Meter D could be improved for two-phase, oil/gas horizontal flow by disabling the upper chord.

6 PERFORMANCE IN TWO-PHASE FLOW OF OIL AND WATER

The two-phase oil/water tests reported here were conducted in the multiphase calibration facility at NEL. A schematic diagram of the facility, as used for these tests, is shown in figure 10. The total reserve of oil and water is held in a vessel which acts as a combined storage tank and multiphase separator with water, oil and mixture compartments. The oil and water are drawn from each of the single-phase compartments and are delivered to the flow loop via calibrated reference meters. Also present in the system are sampling loops for the determination of background quantities of oil-in-water and water-in-oil. After the oil and water are allowed to co-mingle the fluids then flow to the test section along a 50m development length of straight pipe.

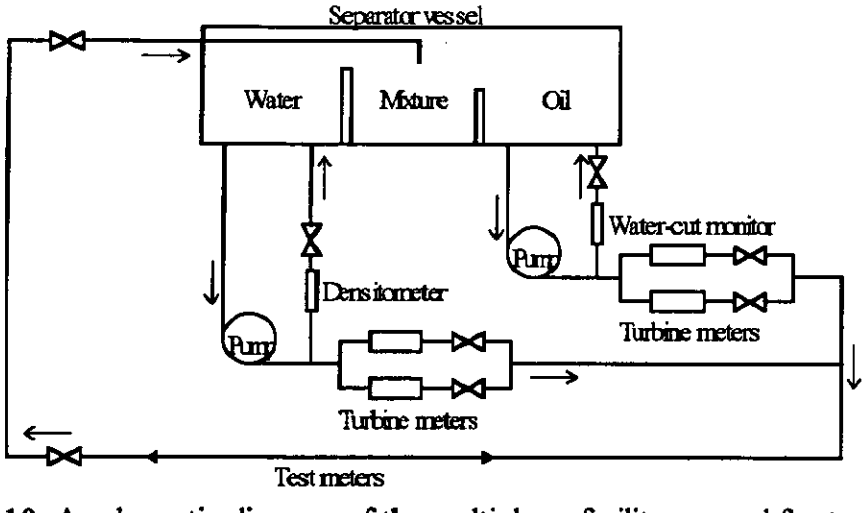

Figure 10 A schematic diagram of the multiphase facility as used for two-phase oil/water tests

The oil used in the facility was a crude-kerosene mix with approximate density and viscosity of 843 kg/m^3 and 7 cSt respectively at the test temperature of 35°C. The water used was a brine solution of density approximately 937 kg/m3 at the test temperature. The matrix of nominal test conditions is shown in Table 2.

Table 2 Nominal conditions for the oil/water tests

Nominal water-cut	Nominal flowrates (l/s)							
5 %	4	8	12	16	20	24	28	32
9 %	4	8	12	16	20	24	28	32
12 %	4	8	12	16	20	24	28	32
15 %	4	8	12	16	20	24	28	32

The results of the oil/water tests on meters A - D are shown in figures 11 to 16. Also shown for reference are the previously derived single-phase calibration results for oils of two viscosities. In general the results lie within a few percent of the oil calibrations at 3 and 30 cSt. Examining the characteristics in closer detail it can be seen that the deviations with respect to the single-phase calibrations are not consistent between the meters. These differences can be explained qualitatively by considering the influence of the physical aspects of the flow in relation to the measuring principle and the variations in meter design characteristics.

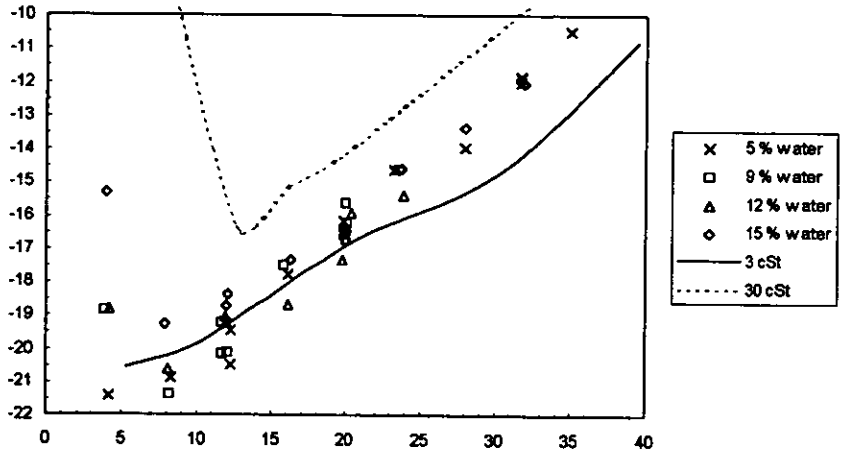

Figure 11 Oil/water performance of meter A

As the two fluids are immiscible the effect of gravity will produce a local fluid density profile which varies in the vertical direction. This will in turn influence the axial flow velocity profile and will also affect the ultrasonic propagation by means of refraction. The paths of meters A and D were orientated horizontally so it is expected that these results should show the influence of velocity profile but no strong influence of the density profile on the ultrasonic signal propagation. Both figure 11 and figure 12 show results which, considering the greater scatter shown, tend to lie within the envelope of the single-phase conditions. The greater scatter can be attributed to the scattering of the ultrasonic wave by water droplets which appear as local discontinuities in the acoustic impedance of the medium.

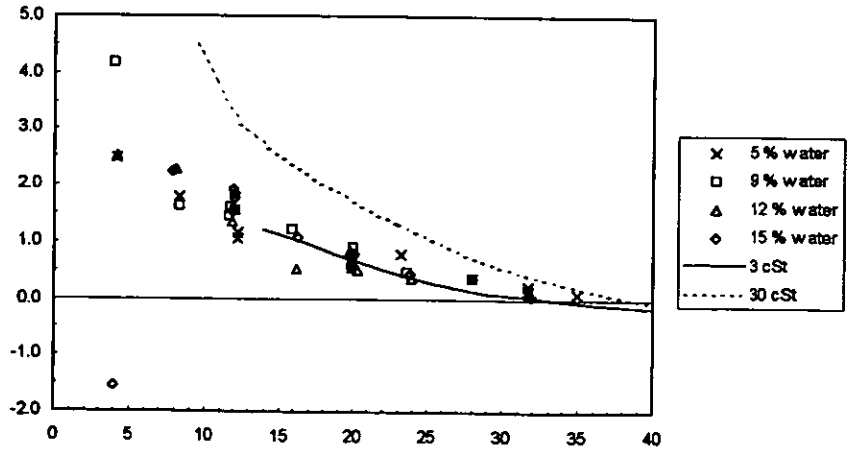

Figure 12 Oil/water performance of meter D

Note that the non-linearity displayed in figure 11 was considered to be the result of erroneous flow profile correction factors in the meter software for the Reynolds number range R_{eD} 6000 to R_{eD} 32,000.

The results for meters C, B_C & B_W presented in figures 13, 14 and 15 all show, in one form or another, behaviour which deviates from their single-phase performance.

The results of the oil/water tests conducted on meter C are shown in figure 13. The results at 9 and 12 % water-cut lie within the lines of the 3 and 30 cSt calibrations, however, the results at 5 % and 15 % water-cut show greater deviations. Especially remarkable are the 5 % results which show deviations of approximately -10 % from the 3 cSt calibration.

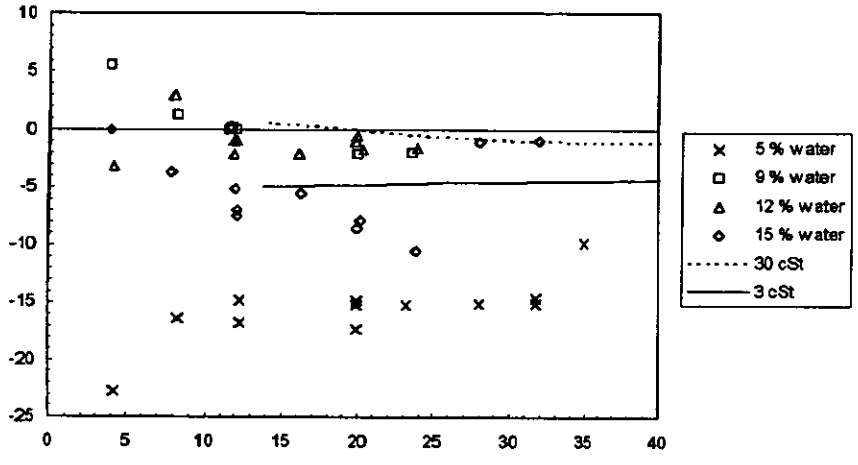

Figure 13 Oil/water performance of meter C

Figure 14 shows that the majority of results for meter B_W lie between the lines of the kerosene and velocite calibrations. When the spurious results shown of the lower limit of the graph were obtained, the meter was indicating a fault condition, but with no corresponding error message. It is interesting to note that the results produced during the fault condition correspond closely to 50 % of the actual flow, the implication being that the average flowrate is being computed from a valid measurement in one path and an indicated null in the other. The fault condition was eliminated by powering down the converter and occurred only once throughout the tests, so it would appear that the meter was subject to an internal error. However, it cannot be established conclusively that this fault was not caused by the two-phase conditions. Johannessen [4] also describes problematic results obtained in oil/water flow with a dual-path Panametrics meter, although the resulting deviations were of a lesser magnitude.

The results of the oil/gas tests on Meter B_C, the clamp-on configuration, show a similar trend to the wetted results. However all of the results above 20 l/s lie outside the envelope of the single-phase calibrations as shown in Figure 15.

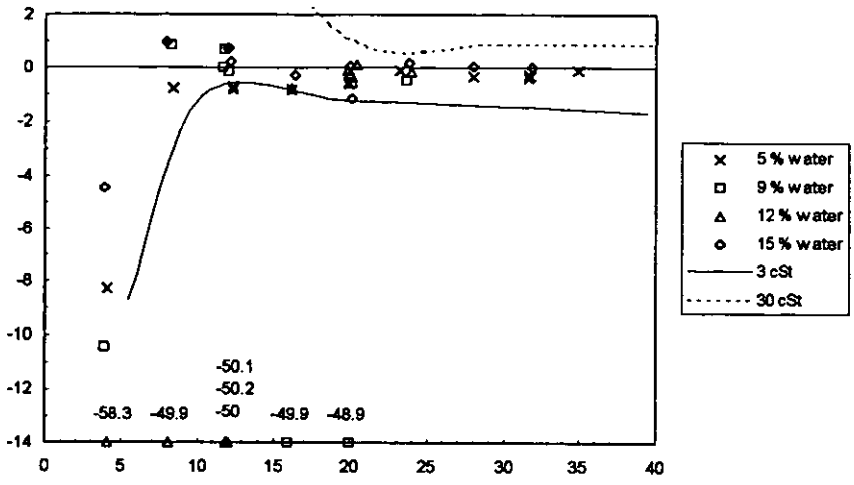

Figure 14 Oil/water performance of meter B_W

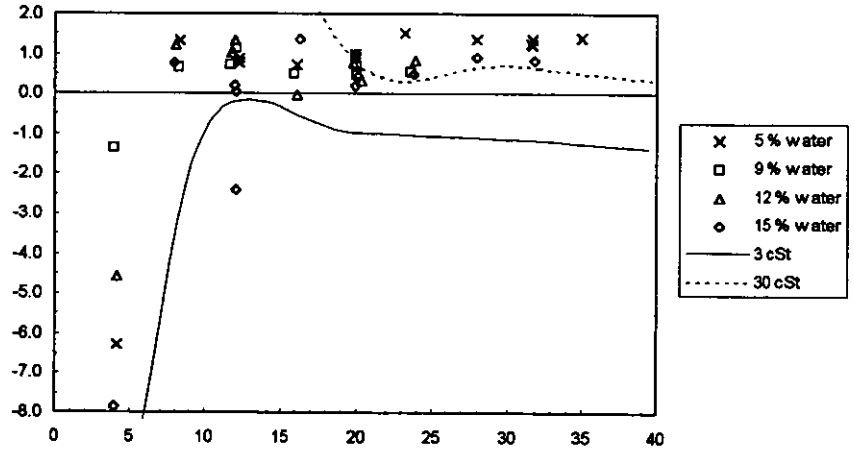

Figure 15 Oil/water performance of meter B_C

Meters B_W, B_C and C all employed dual diametric paths in perpendicular planes. As such each of the measurement paths has a component of length in the vertical direction. It can be considered that the performance of these meters was influenced by the density profile in the vertical direction in addition to the effects of the velocity profile and localised density variations.

If we assume that the large deviations exhibited by meter B_W are the result of an internal error (this is supported to some degree by the fact that 9 and 12% water results prior to and following the fault condition lie within the single-phase envelope) then the greatest deviations due to two-phase oil/water flow conditions were those of meter C. This performance can be related to the signal detection method employed by meter C, a zero-crossing detection method. It is generally accepted that zero-crossing detection methods are less robust than correlation detection methods when the ultrasonic waveform is subject to distortion or a reduction in signal-to-noise ratio.

7 BASELINE TESTS ON CLAMP-ON METERS

In this section preliminary results showing the performance of clamp-on meters in good installation conditions are presented. The results were obtained by gravimetric calibration in the water flow primary standard at NEL. The meters were installed on straight lengths of 4 and 8 inch nominal bore stainless steel pipework and were calibrated over a common velocity range. Upstream lengths of straight pipe were 65D and 45D for the 4-inch and 8-inch tests respectively.

For each of the meters common values were used for the pipe dimensions and default fluid property and pipe roughness parameters were input for dynamic profile correction. Automatic zero-setting procedures were followed according to the manufacturers instructions.

The behaviour of the meters generally conforms with the characteristics discussed in section 4. It should be noted that a relatively low velocity range was chosen for these tests in order to highlight variation in performance, and that, in most cases, the maximum velocity tested was around 50 % of the meter's range. Based on previous experience it is considered that observed performance can be extrapolated to higher velocities within the range of the meter. The results presented here have had a calibration factor applied and are discussed in terms of linearity and repeatability, not absolute error.

The 4-inch calibration results for meter E show a variation in meter factor of approximately 8 % over the range tested. For velocities of approximately 0.5 m/s and above the variation is less than 1%. The repeatability of the meter is better than 1 % for velocities lower than 1 m/s and better than 0.5 % for velocities above this limit.

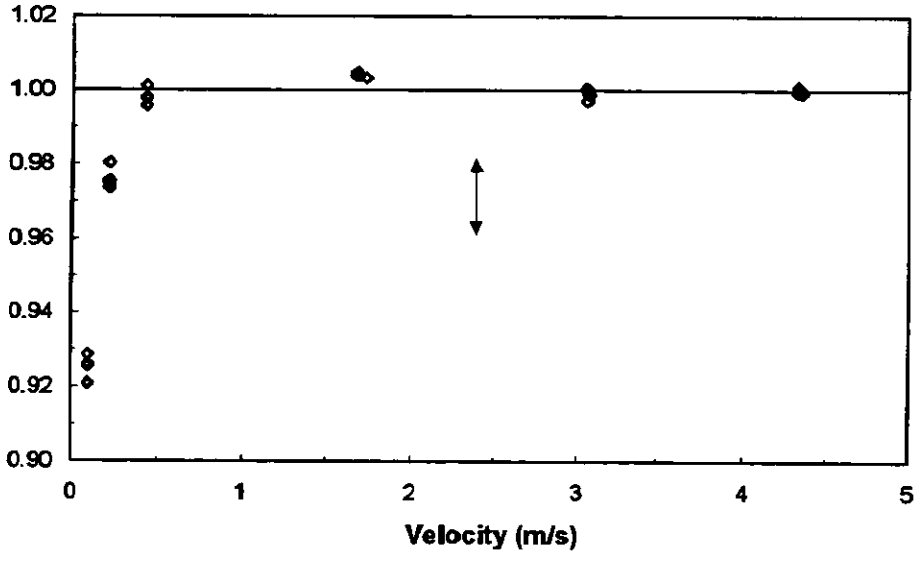

Figure 16 4-inch water calibration results for clamp-on meter E

The 8-inch calibration results for meter E show a variation in meter factor of approximately 6 % over the range tested. For velocities of approximately 0.5 m/s and above the variation is less than 1%. The repeatability of the meter is better than 0.8 % for velocities lower than 1 m/s and better than 0.4 % for velocities above this limit.

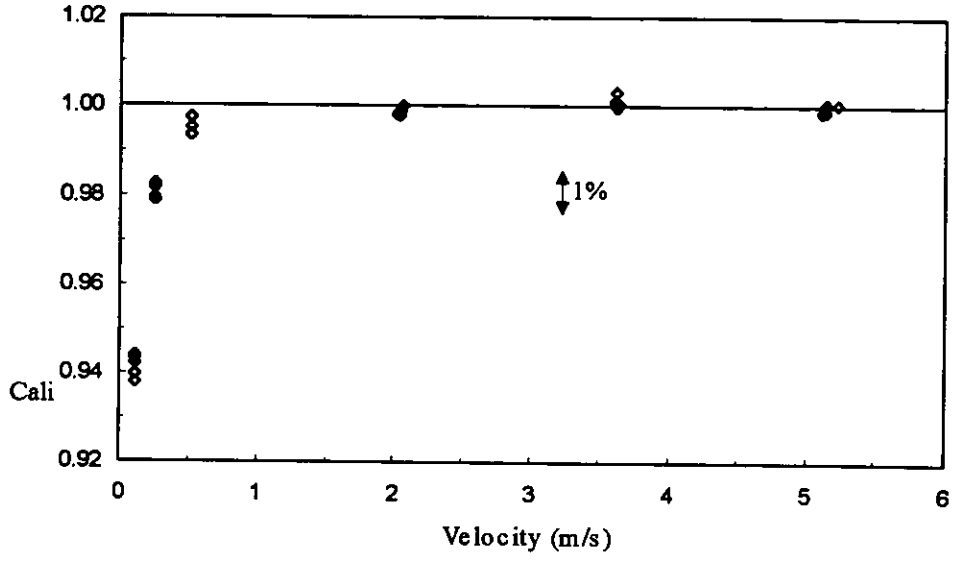

Figure 17 8-inch water calibration results for clamp-on meter E

The 4-inch calibration results for meter F show a variation in meter factor of approximately 10 % over the range tested. For velocities above 1 m/s the variation is less than 1 %. The repeatability of the meter is between approximately 1 and 2 % for velocities lower than 1 m/s and better than 1 % for velocities above this limit.

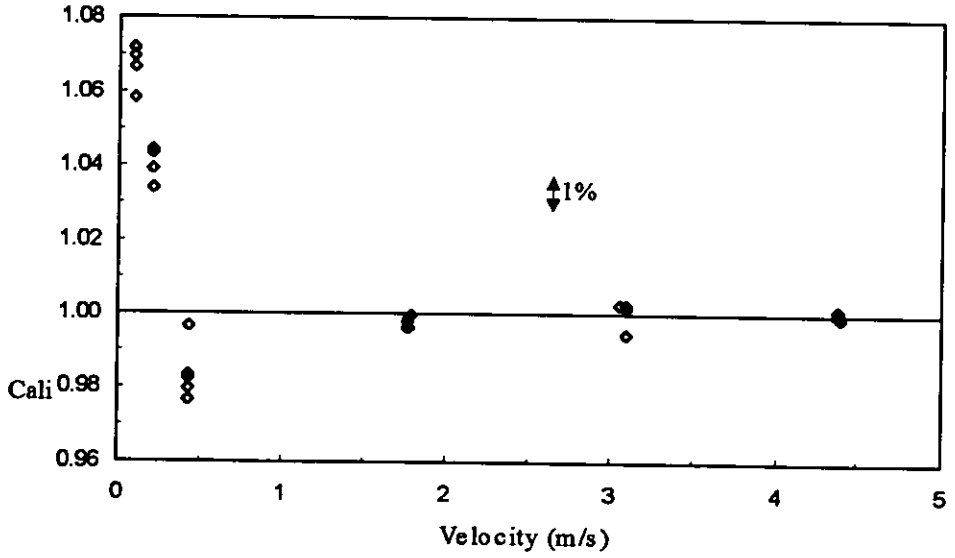

Figure 18 4-inch water calibration results for clamp-on meter F

The 8-inch calibration results for meter F show a variation in meter factor of approximately 2.5 % over the range tested. For velocities above 1 m/s the variation is less than 0.6 %. The repeatability of the meter is between approximately 1 and 3 % for velocities lower than 1 m/s and better than 0.7 % for velocities above this limit.

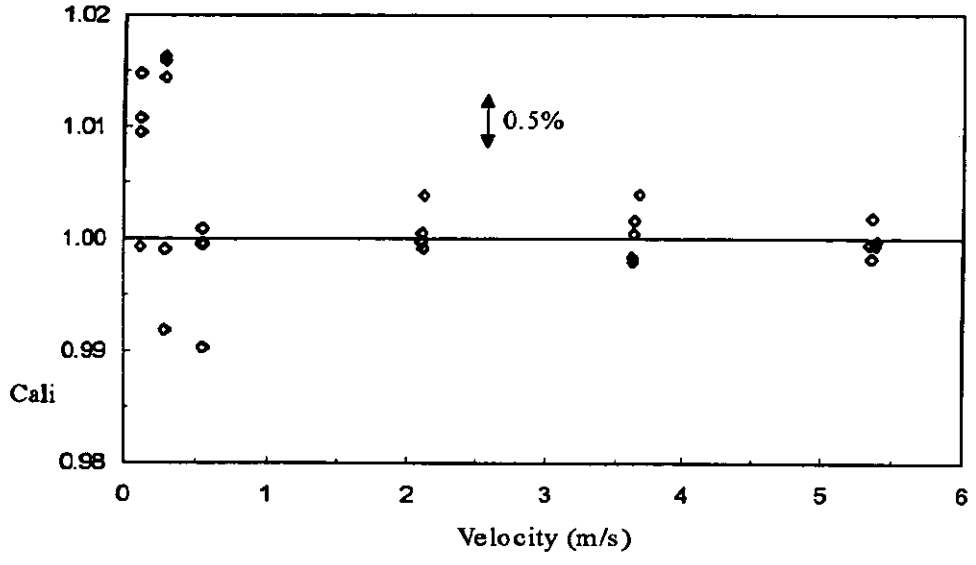

Figure 19 8-inch water calibration results for clamp-on meter F

The 4-inch calibration results for meter G show a variation in meter factor of approximately 65 % over the range tested. For velocities above 1 m/s the variation is approximately 8 %. The repeatability of the meter is between approximately 1.4 and 3.4 % for velocities above 1 m/s.

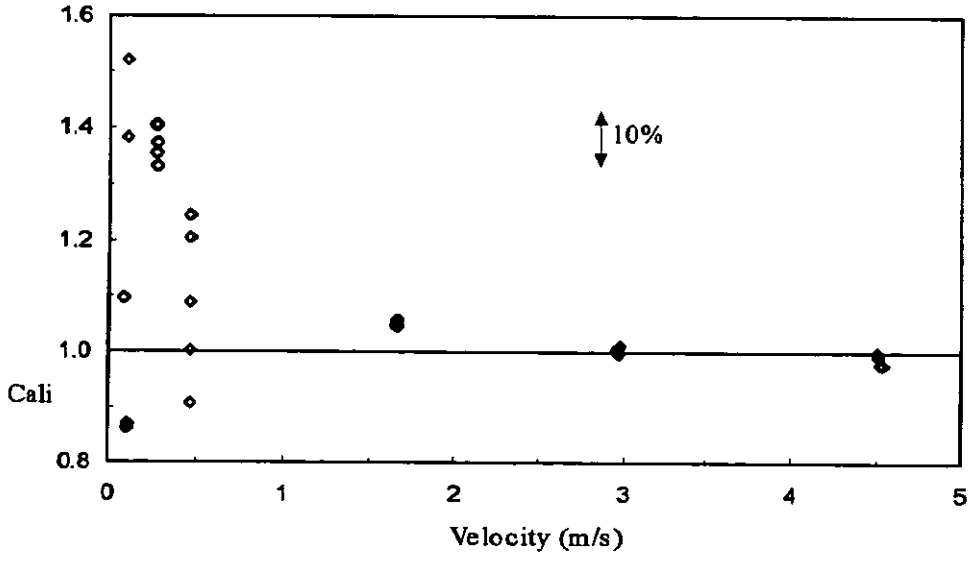

Figure 20 4-inch water calibration results for clamp-on meter G

The 8-inch calibration results for meter G show a variation in meter factor of approximately 21 % over the range tested. For velocities above 1 m/s the variation is approximately 1.2 %. The repeatability of the meter is better than 0.8 % for velocities above 1 m/s.

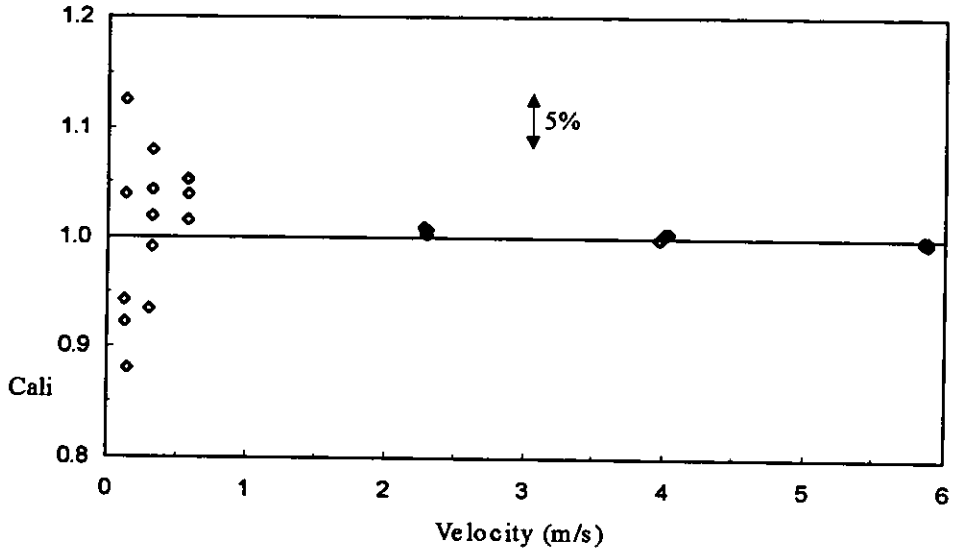

Figure 21 8-inch water calibration results for clamp-on meter G

The 4-inch calibration results for meter H show a variation in meter factor of approximately 30 % over the range tested. For velocities above 1 m/s the variation is approximately 5.5 %. The repeatability of the meter is between 1 and 2.5 % for velocities of approximately 0.5 m/s and above and is better than 7 % for velocities below this range.

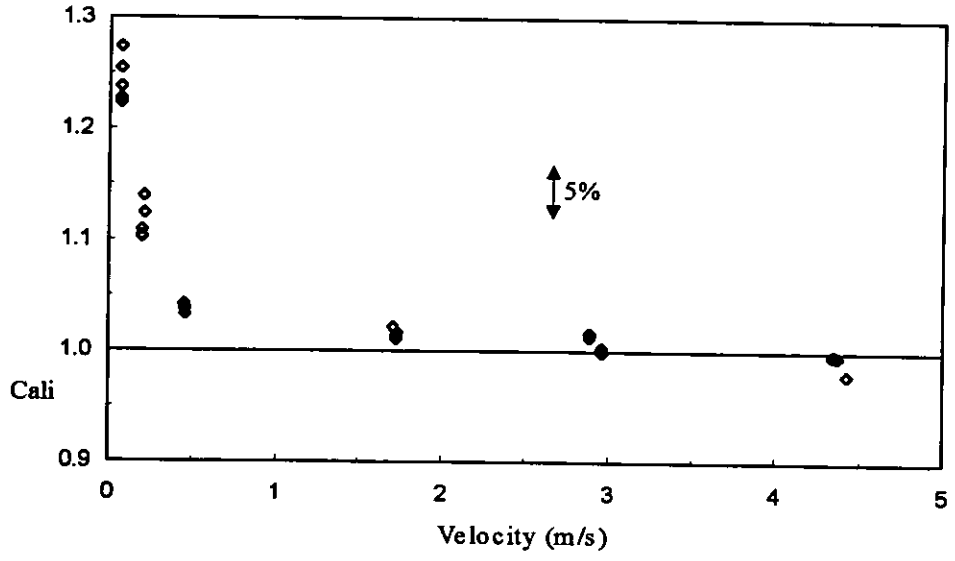

Figure 22 4-inch water calibration results for clamp-on meter H

The 8-inch calibration results for meter H show a variation in meter factor of approximately 24 % over the range tested. For velocities above 1 m/s the variation is less than 1.5 %. The repeatability of the meter is between 0.5 and 2 % for velocities above 0.25 m/s and is approximately 2.6 % for the tests at 0.15 m/s.

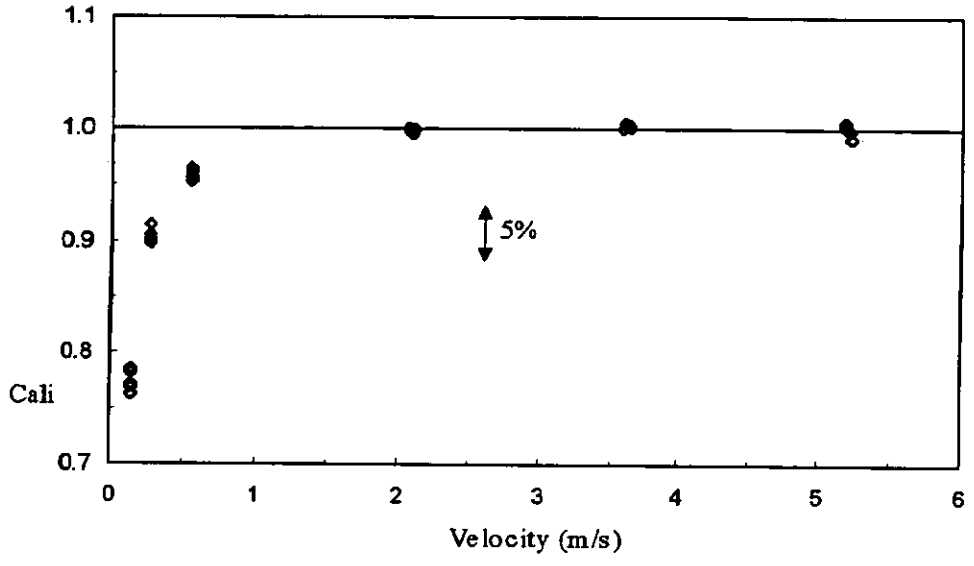

Figure 23 8-inch water calibration results for clamp-on meter H

8 THE INFLUENCE OF A DISTORTED VELOCITY PROFILE

The performance of ultrasonic meters in non-ideal installation conditions will be the cumulative effect of a number a number of factors. Two important factors are transverse velocity components (cross-flow and swirl) and distortions of the axial velocity profile. Other factors such as high turbulence intensity or acoustic noise at frequencies within the transducer bandwidth will also affect performance.

The influence of velocity profile distortion and swirl produced by upstream pipework is a major concern in offshore applications. Space and weight constraints are often prohibitive to the provision of long lengths of straight pipe. Flow conditioners or in-situ proving may be used but these methods are in conflict with two of the major incentives for using ultrasonic meters, i.e. reducing flow restriction and lowering operational costs.

The determination of installation effects by laboratory simulation of actual conditions is favoured as producing the most realistic results. A problem with this approach is that the resulting data is not easily applicable to differing pipework or meter configurations. Flow and flowmeter modelling has already proven to be useful in improving the understanding of measurement interaction mechanisms. It is also potentially useful for deriving quantitative information which could be used when installing a flowmeter.

The current work at NEL involves parallel model-based and experimental investigation of installation effects on transit time ultrasonic meters. The primary aim is to determine the potential of combining computational fluid dynamics (CFD) with a simple model of the flowmeter to determine the hydraulic calibration factor, k_h. To

enable this the simulated results will be compared with experimentally derived data for a range of configurations.

As a precursor to the CFD work numerical modelling has been carried out using mathematical velocity profiles formulated to depict real profiles encountered in practice. This approach is especially useful in the study of velocity profile effects as numerical calculations can be performed rapidly for various meter configurations. As the profiles can be integrated analytically, an exact reference can be determined against which the results can be compared. Results are given here for two velocity profiles and four meter configurations.

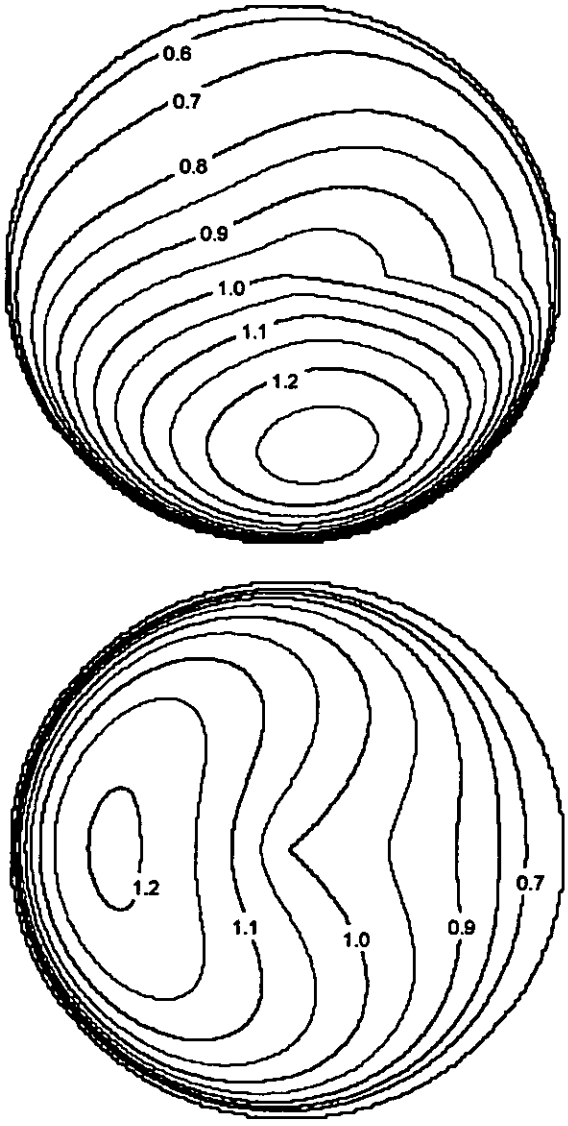

$$P6$$

$$u = (1-r)^{1/9} - \frac{r}{2\pi}(1-r)^{1/4}\,\theta \sin\theta$$

$$P9$$

$$u = (1-r)^{1/9} + \frac{2r}{\pi^5}(1-r)^{1/4}\,\theta^2(2\pi-\theta)^2$$

Figure 24 Contour plot representation of velocity profiles P6 & P9

The contour plots of figure 24 depict the profile functions P6 and P9 formulated by Salami [5] describing the ratio of local to central velocity, u, as a function of radial and angular location (r, θ). Using these functions k_h factors have been determined by numerical integration of the velocities along the measurement paths for each of the configurations given in Figure 25. For single diametric, orthogonal dual diametric and parallel dual mid-radius configurations the velocity determined by the meter is simply the average of the mean velocities determined on each path. For the 4-path arrangement the velocity determined by the meter is proportional to the sum of velocities which have been integrated and weighted according the rules of Gaussian quadrature [6].

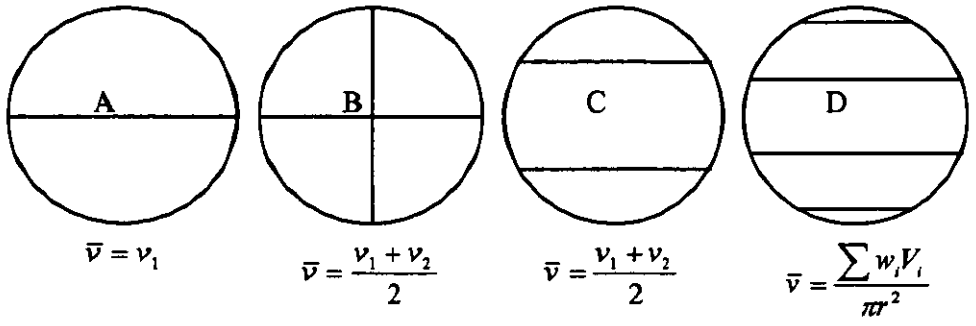

Figure 25 Meter configurations used in the numerical analysis

Figure 26 shows the k_h factor plotted against path orientation for the single diametric case. Also shown for reference are the k_h factors obtained using the power law profile with exponents of 1/6 and 1/10.

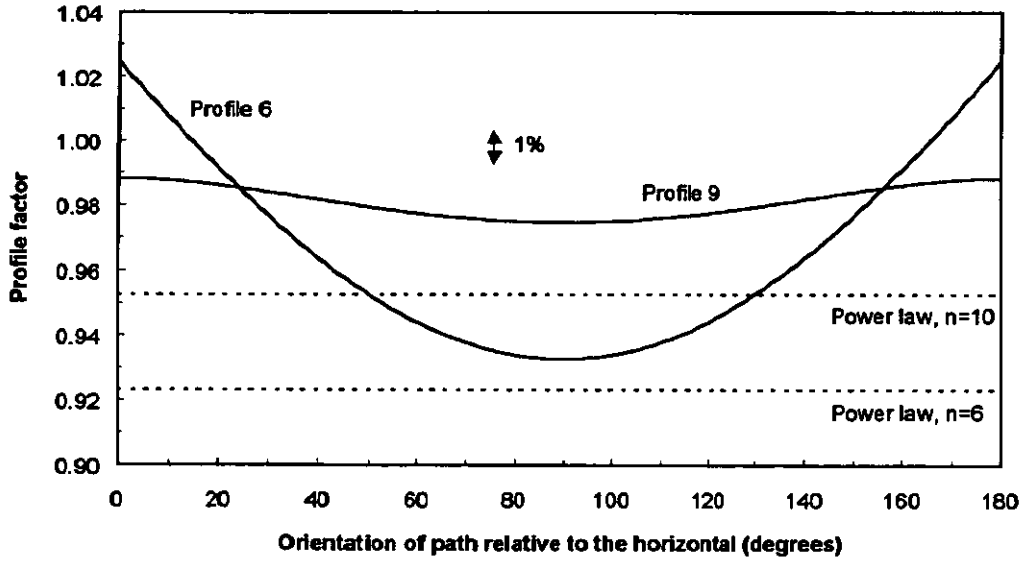

Figure 26 Profile factors for the single diameter path configuration

As can be seen from the figure the k_h factor for profile P6 varies significantly with orientation with a maximum installation effect of 7 - 10 % at an angle of 0°. For profile P9 the k_h factor varies less with orientation but is consistently about 2 to 6 % higher than for the powerlaw profiles.

Figure 27 shows the k_h factor plotted against beam orientation for the orthogonal dual diametric case. Again the k_h factors obtained using the power law profile are shown for reference. For both profiles the variation in k_h with orientation is reduced. For profile P9 the benefit of adding the second path is small. For profile P6 however the maxima have been reduced by about 4 % thus limiting the possible installation effect. However, there is now no orientation at which the k_h factor crosses into the powerlaw profile region.

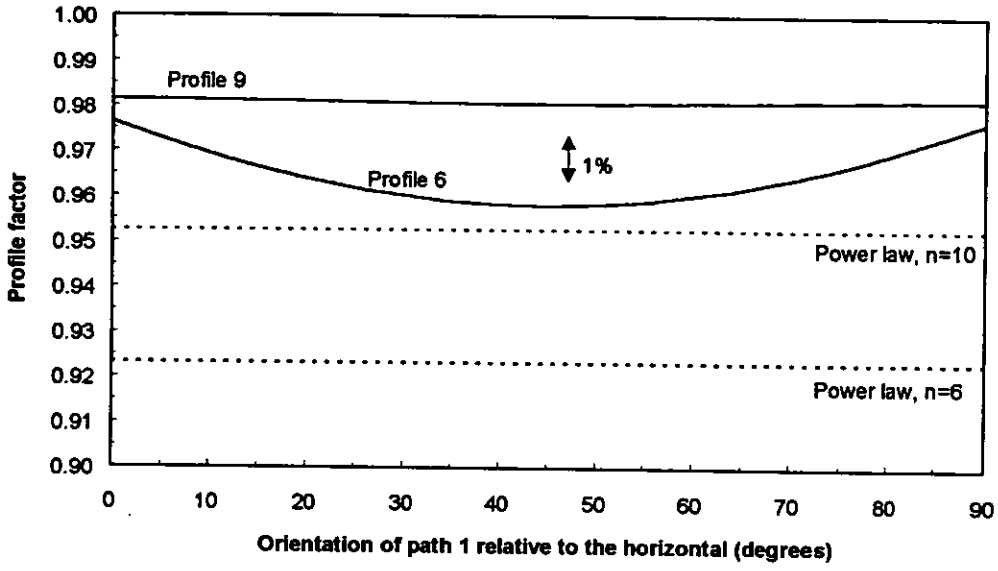

Figure 27 Profile factors for the dual diameter path configuration

Figure 28 shows the k_h factor plotted against path orientation for the parallel dual mid-radius configuration. Again the k_h factors obtained using the power law profile are shown for reference. In this case the deviation from the ideal k_h factor is within about 2 % for all orientations and for profile 6 the deviation is less than 0.5 % for over half of the angular range.

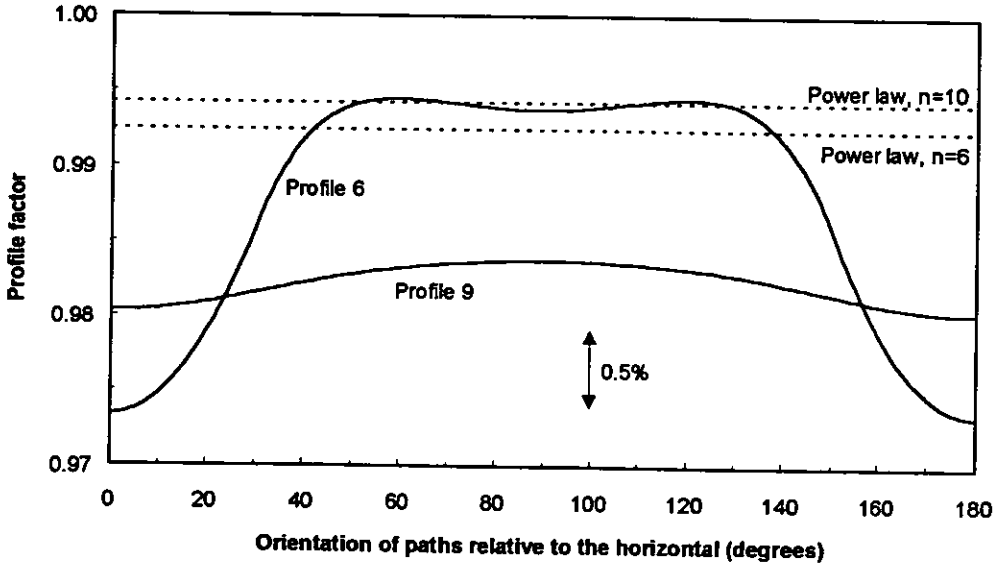

Figure 28 Profile factors for the dual mid radius path configuration

Figure 29 shows the k_h factor plotted against path orientation for the four-path Gaussian configuration. In this case the deviations from the powerlaw k_h factors are within 0.5 % for all but the extremes of profile 6.

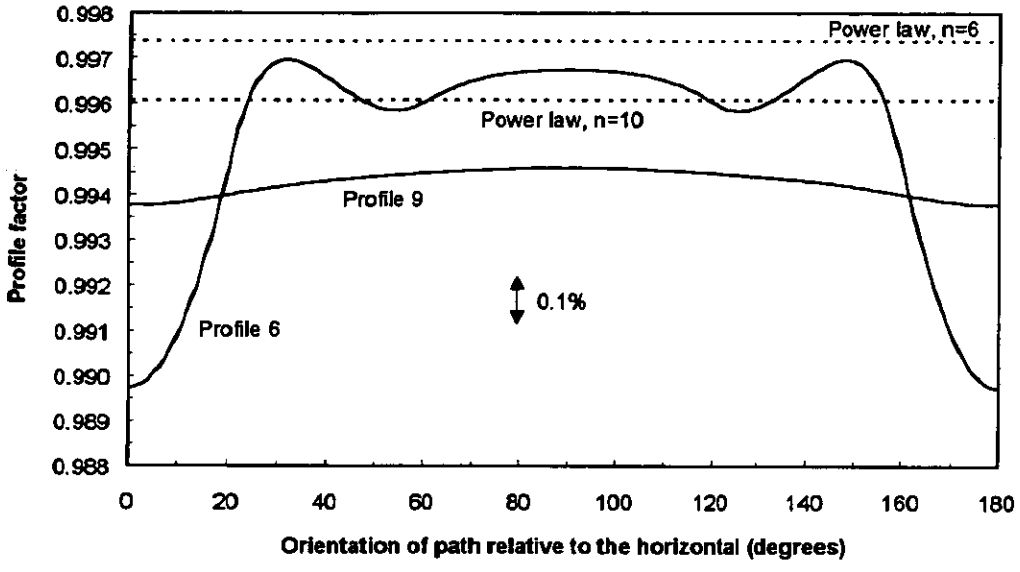

Figure 29 Profile factors for the Gaussian configuration

Summarising the above results in bar chart format (Figure 30) the reduction in sensitivity to distortions of the axial velocity profile realised by increasing the number of paths is clearly demonstrated. Indeed the Gaussian configuration (D) reduces the possible installation effect by more than a factor of 10. Figures 26 to 30 also illustrate that it is not only the number of paths which is important but also their location and orientation with respect to the velocity profile. For example orientating a single diameter path at 90° with respect to profile P6 produces a k_h factor which is in the range of values expected for fully developed flow.

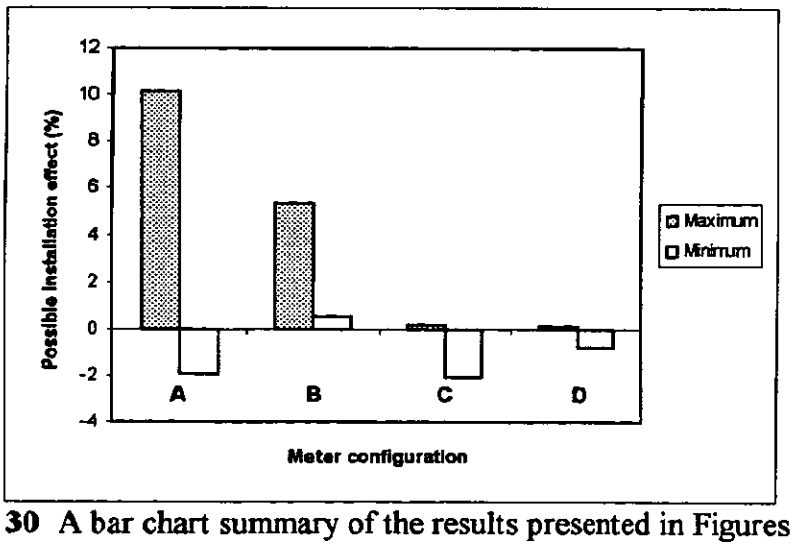

Figure 30 A bar chart summary of the results presented in Figures 26-29

Additional results have been obtained by this method for a wide range of profiles and meter configurations [7]. Further work will include the analysis of individual path velocities with respect to diagnosing distortions of the velocity profile.

9 DISCUSSION, CONCLUSIONS AND FURTHER WORK

The performance of transit time meters is adversely affected in the presence of two-phase flow. The effect on performance is dependent on the quantity, size, distribution and physical properties of the secondary component. As the acoustic impedance mismatch between oil and gas is much greater than that between oil and water, the effect of scattering and attenuation is significantly higher in oil/gas flow and thus this condition represents the greater problem.

Performance in oil/gas flow may be improved by adjusting signal parameters to accommodate a wider range of gas fractions. However, as the limiting gas fraction is approached the performance will suffer in terms of accuracy. Another way in which oil/gas performance may be improved is by operating the meter in a manner more suited to the flow pattern. For example in horizontal oil/gas flow disabling measurement chords which are in the upper half of the cross-section is likely to improve accuracy, especially at moderate velocities where gravitational separation of the phases is more distinct.

During the oil/water tests, meter signal quality was never reduced to such an extent that the ability of the meters to make transit time measurements was interrupted. However, large deviations were observed in two cases. In the first case, the deviations were thought to be related to errors in signal detection. This is related to the zero-crossing detection method employed by the meter, which is generally considered to be less robust than correlation detection methods. In the second case the occurrence of an internal error was suspected.

The clamp-on meter baseline calibration results show behaviour generally conforming with expected characteristics, i.e. repeatability and linearity improving with increasing velocity and pipe size. The results show that the zero-bias may be positive or negative and may change sign from one installation to another. Significant variations in the performance of the meters have been demonstrated. These results are currently under review by the meter manufacturers.

The numerical simulation of velocity profile effects demonstrates the relative sensitivity of various configurations encountered in practice. The results clearly show, in quantitative terms, the limitations of single and dual path configurations in relation to distortions of the axial velocity profile.

Ongoing and further work at NEL on ultrasonic flowmetering includes the following topics:

- Analysis of diagnostic capabilities of transit time meters in relation to two-phase and disturbed single-phase flows.

- Laboratory determination of installation effects on single and multipath ultrasonic liquid flowmeters

- CFD modelling of installation effects and comparison with experimental results
- Evaluation of transit time and reflective (e.g. Doppler) meters over a common range of two-phase flow conditions.
- Evaluation of clamp-on meter performance on a variety of pipe materials and in various flow conditions
- Long-term performance and maintainability tests on a selection of liquid ultrasonic meters

Completion of the current programme of work will result in a substantial database of ultrasonic flowmeter perfomance data and guidelines on use which, along with the cumulative result of other programmes, will assist in the development and successful deployment of ultrasonic flow measurement technology.

ACKNOWLEDGEMENTS

The work described in this paper was carried out as part of the Flow Programme, under the sponsorship of the DTI's National Measurement System Policy Unit. The author would also like to thank all those who have contributed to the projects in their many different ways.

REFERENCES

[1] BROWN, G. J., *Oil flow performance of ultrasonic meters* Proceedings of the North Sea Flow Measurement Workshop, Peebles, Scotland, 28-31 October 1996.

[2] BROWN, G. J., *Ultrasonic meters for oil flow measurement* NEL Report No: 169/96, April 1997.

[3] FRONEK, V., *Ultrasonic measurements of oil flow in a laminar flow-turbulent flow transition region* Flow Measurement of Fluids, Ed. Dijstelbergen, H. H., and Spencer, E.A., North-Holland Publ. Co., pp. 141-146, 1978

[4] JOHANNESSEN, A. A., *Evaluation of ultrasonic liquid flowmeters* Proceedings of the North Sea Flow Measurement Workshop, Bergen, Norway, 26 -28 October 1993.

[5] SALAMI, L. A., *Application of a computer to asymmetric flow measurement in circular pipes* Trans. Inst. M C 6(4), pp. 197-206, 1984.

[6] PANNELL, C. N., EVANS, W. A. B., and JACKSON, D. A. *A new integration technique for flowmeters with chordal paths* Flow Meas. Instrum., 1(4), pp. 216-224, 1990.

[7] BROWN, G. J., *The influence of asymmetric velocity profiles on ultrasonic transit time flow measurements* Manuscript in preparation.